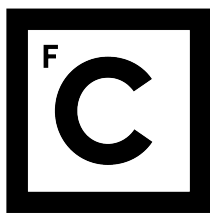


UNIVERSIDADE DE LISBOA  
FACULDADE DE CIÊNCIAS

UNIVERSIDADE FEDERAL DO  
RIO DE JANEIRO  
INSTITUTO DE GEOCIÊNCIAS



**Ciências**  
**ULisboa**



**Climate and vegetation dynamics and its impact on present and future fire  
regimes in Brazil**

*“Documento Definitivo”*

**Doutoramento em Ciências Geofísicas e da Geoinformação**

Meteorologia

**Programa de Pós-Graduação em Meteorologia**

Geofísica

Patrícia Santos Silva

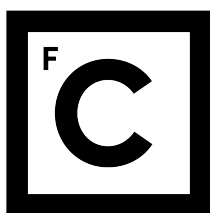
Tese orientada por:

Professor Doutor Carlos da Camara

Professora Doutora Renata Libonati

Documento especialmente elaborado para a obtenção do grau de doutor





**Ciências**  
**ULisboa**



**Climate and vegetation dynamics and its impact on present and future fire regimes in Brazil**

**Doutoramento em Ciências Geofísicas e da Geoinformação**  
Meteorologia  
**Programa de Pós-Graduação em Meteorologia**  
Geofísica

Patrícia Santos Silva

Tese orientada por:  
Professor Doutor Carlos da Camara  
Professora Doutora Renata Libonati

Júri:

Presidente:

- Miguel Centeno da Costa Ferreira Brito, Professor Associado com Agregação e Presidente do Departamento de Engenharia Geográfica, Geofísica e Energia da Faculdade de Ciências da Universidade de Lisboa

Vogais:

- Doutor José Ricardo de Almeida França, Professor Titular do Departamento de Meteorologia da Universidade Federal do Rio de Janeiro, Brasil
- Doutora Renata Libonati dos Santos, Professora Adjunta IV do Departamento de Meteorologia da Universidade Federal do Rio de Janeiro, Brasil (orientadora)
- Doutor Geraldo Alves Damasceno Junior, Professor Titular do Instituto de Biociências da Universidade Federal de Mato Grosso do Sul, Brasil
- Doutor Mário Jorge Modesto Gonzalez Pereira, Professor Auxiliar com Agregação da Escola de Ciências e Tecnologia da Universidade de Trás-os-Montes e Alto Douro
- Doutor João Manuel das Neves Silva, Professor Auxiliar do Instituto Superior de Agronomia da Universidade de Lisboa

Documento especialmente elaborado para a obtenção do grau de doutor  
Tese financiada pela Fundação para a Ciência e a Tecnologia (FCT) com a bolsa

SFRH/BD/146646/2019



# Acknowledgements

This thesis would not be possible without the continued support of my family. To my parents, Carlos and Helena, I extend my deepest thanks for providing all the tools and learning experiences that allowed me to be here, chasing a Doctoral degree. To my sister, Inês, thank you for all steady encouraging words and late night pep talks. You are my safe haven.

Equally important was the unwavering and relentless support of my dearest partner, Rafael, who stood by me on the deepest lows and upmost highs. You never gave up on me, even when I was ready to. You never hesitated to leap with me to the unknown, and all these marvelous adventures were only so because you were there. Thank you for being with me every step of the way, and I can only hope there are many more steps to go.

To my supervisors, Prof. Carlos da Camara and Prof.<sup>a</sup> Renata Libonati, for taking on this challenge with me. Thank you for all the opportunities you gave me, not only during this PhD programme, but along the 9 years we have been working together. I learned, and keep on learning, so much from you, and will do my best to make you proud from here onwards. Thank you for your support and for believing in me.

There are several people I would like to acknowledge, that contributed, not just to my academic progress, but to my personal betterment as well. Luiz Gustavo, for the continued friendship and for teaching me so much about fire in the Cerrado. Thank you for welcoming me in your home and showing me the beauty of Chapada dos Guimarães. Alexandre Enout and Cristina Cuiabália who, not only welcomed with open arms an unlikely academic challenge, but provided me with a one-in-a-lifetime opportunity to visit the RPPN Sesc Pantanal and explore this marvelous corner of Pantanal. I would also like to acknowledge Doug Kelley for the interesting conversations and collaborations.

To my colleagues and lab-mates at IDL, thank you for all the interesting conversations and support. A particular shout-out to Miguel Pinto, João Geirinhas, and Bárbara Mota.

Finally, I must acknowledge the outstanding legacy of Prof. Alberto Setzer, who left us much too soon. The first steps I took in research were partly based on his groundbreaking work in INPE, without which fire science in Brazil would be much impoverished. Although we only met once, I was left with a lasting mark.

I think it is only fitting that I end this Acknowledgements section with a remembrance of how much progress has been made in fire science over the last decades. This thesis stands on the shoulders of giants.

This work was supported by the Portuguese Foundation for Science and Technology (FCT) through the Doctoral grant SFRH/BD/146646/2019.

# Abstract

This thesis investigates regional fire patterns and their climatic and anthropogenic controls in the Brazilian savannas. The focus of this thesis is the Cerrado biome, and the main analysis consists in three stages: (i) including the fire component to the ecoregional map of the Cerrado through a classification that includes several fire parameters; (ii) analysing the climatic controls on regional burned areas; (iii) exploring the anthropogenic influence on regional fire dynamics. The first stage (i) explores the regional variability in fire behaviours in Cerrado, employing several satellite-derived datasets and fire attributes, such as extent, intensity, number, and size. This analysis reveals significant spatial heterogeneity in fire behaviour over the last two decades, namely in fire size. Then, the second stage (ii) explores if this geographical variability in fire behaviour is associated with distinct regional fire-climate dynamics using temperature and precipitation fields. Results show that extreme fire seasons are associated with both pre-conditioned and concurrent climate: early fire season burned areas are more influenced by pre-conditioned climate, whereas late-season fires depend heavily on concurrent weather patterns. Finally, stage (iii) further adds the anthropogenic component and tests the performance of fire-climate models in light of human land use, deforestation, and population patterns. A novel approach based on individual fire events is proposed and different fire-climate-human dynamics are found for smaller and larger fires. The findings of this thesis emphasize the regional variability in fire-climate-human relationships and suggest that a one-size-fits-all approach to fire management in the Cerrado may be insufficient. Moreover, due to the catastrophic 2020 Pantanal fire events, this thesis also explores fire and climate patterns in the region and the relationship between fire and heatwaves. Given the limited research on fire in the Pantanal wetlands, both these studies prove important contributions to fire science in the biome.

**Keywords:** fire-climate; statistical analysis; Cerrado; Pantanal; Brazil





# Resumo

Ao longo do século XXI, a ocorrência de grandes incêndios na vegetação tem captado a atenção da comunidade científica. Embora o fogo seja uma componente essencial do sistema terrestre, presente há 420 milhões de anos, a sua frequência e intensidade têm vindo a alterar-se. Atualmente, estima-se que grande parte dos ecossistemas mundiais tenha o seu regime histórico de fogo alterado, com consequências severas para o seu funcionamento e biodiversidade. A relação do fogo com o clima tem sido cada vez mais estudada a nível global e existe uma clara dinâmica entre estas duas componentes. Por outro lado, o fogo depende também da ação humana: de forma direta, como fonte de ignição e através da gestão da paisagem (afetando a quantidade, estado e continuidade do combustível disponível para arder); e indireta, ao modificar o clima. A presente tese de doutoramento pretende contribuir para o avanço destes temas na savana Brasileira, com especial foco no bioma Cerrado. Pretende-se avaliar os padrões de fogo regionais, assim como a sua relação com a componente climática e antrópica. O trabalho aqui apresentado divide-se em três linhas principais: (i) adicionar a componente do fogo ao mapa das ecoregiões do Cerrado; (ii) analisar qual a influência regional do clima no fogo; (iii) explorar qual a relação do fogo com atividades humanas.

Numa primeira instância (i) realizou-se uma análise inovadora de padrões de fogo regionais nas ecoregiões do Cerrado, com recurso a variados produtos derivados de satélite, incluindo áreas queimadas, potência radiativa, número e tamanho de cicatrizes. Esta análise pormenorizada das características regionais do fogo permitiu complementar o atual mapa das ecoregiões do Cerrado com informação relativa ao comportamento regional do fogo. Os resultados apontam para uma grande variabilidade espacial para todos estes atributos, com um claro gradiente norte-sul na incidência de fogo: ecoregiões localizadas a norte, nomeadamente na fronteira agrícola MATOPIBA, apresentam maiores áreas queimadas e tamanhos de fogo. Por outro lado, fogos intensos estão concentrados no Arco do Desmatamento e na fronteira com o bioma Caatinga. Usando informações de fogos individuais, estratificaram-se os fogos em quatro classes de tamanho de fogo: muito pequeno,

pequeno, médio, e grande. Verificou-se que os fogos grandes, não sendo frequentes, representam a maior parte da área queimada; fogos muito pequenos e pequenos, por outro lado, constituem a grande maioria dos fogos, mas representam uma porção pequena da área queimada total. Os resultados obtidos por tamanho de fogo sugerem ainda que os fatores influenciadores do fogo podem ser diferentes para cicatrizes de tamanhos distintos. Este trabalho contribui com a primeira análise de fogo regional no Cerrado usando vários atributos e com recurso a diferentes bases de dados. O uso de uma base de dados de fogos individuais permitiu melhor caracterizar o fogo regional, além de parâmetros mais genéricos como área queimada e potência radiativa. Ainda, ao adicionar a componente de fogo ao mapa das ecoregiões do Cerrado, podemos melhor interpretar estes padrões à luz dos diferentes contextos sócio-económicos regionais.

De seguida, considerando a grande variabilidade espacial no comportamento de fogo descoberta no passo anterior, pretendeu-se perceber como esta variabilidade estaria relacionada com o clima (ii). Primeiramente, mostrou-se que existe uma variedade geográfica no ciclo sazonal de temperatura e precipitação entre ecoregiões do Cerrado: a variação intra-anual de temperatura varia fortemente entre ecoregiões, com forte agregação geográfica; por outro lado, o ciclo sazonal de precipitação é semelhante em todo o Cerrado, com um período seco de Maio a Setembro. Para investigar como estas variáveis se relacionam com a ocorrência de fogo, avaliaram-se os padrões de temperatura e precipitação mensais para épocas de fogo (Agosto a Outubro) extremas. Em geral, épocas de fogo severas estão ligadas a condições quentes e secas em dois períodos: o outono austral (de Março a Maio) e durante os meses da época de fogo; por outro lado, épocas de fogo moderadas, estão associadas a condições frias e húmidas durante os mesmos períodos. Há, no entanto, alguma variabilidade espacial nestas relações entre ecoregiões, dado que nem todas apresentam relações significativas com ambos os períodos. De seguida, investigou-se se os diferentes meses da época de fogo (Agosto, Setembro e Outubro) teriam os mesmos controlos climáticos. Para tal, analisaram-se áreas queimadas extremas mensais para cada um destes meses. Em geral, os resultados indicam que as áreas queimadas de Agosto estão mais associadas às pré-condições durante o outono austral, enquanto que as áreas queimadas de Outubro apresentam fortes anomalias nas variáveis meteorológicas concorrentes. Esta discrepância na importância do clima antes e durante a época de fogo parece ser devido aos efeitos do clima na vegetação: no início da época de fogo, em Agosto, áreas

queimadas estão mais associadas às condições meteorológicas durante o outono austral, como proxy do estado da vegetação; por outro lado, no final da época de fogo, dado a exposição prolongada a condições quentes e de seca, a vegetação está seca e a ocorrência de fogo está ligada às condições meteorológicas atuais. Estes resultados informam diretamente políticas de manejo de combustível nas várias ecoregiões do Cerrado, e reforçam a necessidade de estudar os controles do fogo ao nível regional.

Considerando estas discrepâncias regionais na relação fogo-clima, investigou-se de seguida (iii) qual a relação do padrão de fogo com a presença humana no bioma. Para tal, usou-se informação de uso da terra antrópico, desmatamento e população, para analisar a distribuição geográfica das relações fogo-clima para diferentes tamanhos de fogo. Esta análise inovadora com base em cicatrizes individuais, pretende investigar se, para diferentes tamanhos de fogo, existem relações diferentes com o clima e com a atividade humana, como sugerido em estudos anteriores (i). Classificaram-se os fogos por ecoregião do Cerrado, em fogos extremos (top 5%) e moderados (restantes 95%). Ajustando modelos simples de regressão linear observou-se que o clima, avaliado através de um índice de risco de fogo, é um fator importante na variação anual de áreas queimadas para fogos extremos e moderados. A performance dos modelos varia de forma considerável entre ecoregiões, e a variância total explicada para o total de fogos é consideravelmente diferente daquela para fogos moderados/extremos. Alinhando estes modelos fogo-clima consoante a presença antrópica por ecoregião, observa-se um padrão espacial para os fogos moderados, onde ecoregiões com menos de 35%–37% de cobertura do solo antrópico; 37%–38% de desmatamento; e com população abaixo de  $\approx 800,000$  indivíduos, obtêm relações mais fracas com o clima. As ecoregiões com estas características de cobertura do solo antrópica e desmatamento estão localizadas no MATOPIBA. Isto indica que o clima não é o fator preponderante na variação anual de fogos moderados em ecoregiões onde está a ocorrer expansão antrópica e que, possivelmente, fatores socioeconómicos e políticos têm um papel fundamental. No caso de fogos extremos, não se observou nenhum padrão espacial relacionado com atividade humana. Este trabalho reflete no uso de fogos individuais no estudo dos seus potenciais controles, e em como estas relações podem ser diferentes dependendo das características individuais do evento.

Finalmente, o bioma Pantanal apresenta algumas semelhanças com o Cerrado, sendo também ele um bioma dependente do fogo com vastas áreas de formação savânica. Em

2020, o Pantanal viu uma das suas épocas de fogo mais destrutivas, com cerca de um terço do bioma afetado. Estes eventos tiveram vastas consequências, a nível ecológico, económico e de saúde pública, e trouxeram à luz a falta de conhecimento científico acerca do fogo na região. Assim, esta tese contribui para preencher essa lacuna com dois estudos no Pantanal: analisa os padrões de fogo e clima na maior Reserva Natural do Patrimônio Natural (RPPN) do país, a RPPN Sesc Pantanal; e relaciona a ocorrência de ondas de calor com área queimada no Pantanal trinacional (Brasil, Bolívia e Paraguai). No primeiro estudo, avaliou-se o desempenho de um produto de área queimada de alta resolução numa reserva natural, e analisaram-se os padrões climáticos dos últimos 40 anos. À luz dos eventos de 2020 no Pantanal, este estudo reflete sobre as políticas de manejo da paisagem e do fogo, e no uso e limitações de produtos de larga escala onde não existem outras fontes de dados disponíveis. O segundo estudo, procura relacionar a ocorrência de ondas de calor no Pantanal trinacional com áreas queimadas, e projectar vulnerabilidade futura. Usando um modelo estatístico, observa-se que a área queimada está fortemente relacionada com um índice de ondas de calor. Após validação e ajuste de 2 modelos regionais do clima (cada um forçado por 3 modelos globais), mostra-se que as temperaturas máximas e a ocorrência de ondas de calor irão aumentar no Pantanal sobre dois cenários distintos de alterações climáticas.

Deste modo esta tese contribui com novo conhecimento dos padrões regionais do fogo e os seus controlos climáticos e antrópicos no Cerrado, e ainda com dois estudos sobre padrões de fogo e clima no Pantanal. Todos os trabalhos aqui apresentados apresentam avanços consideráveis no conhecimento do comportamento do fogo nestes biomas que, comparando com outros ecossistemas mundiais, obtêm menor atenção da comunidade científica.

**Palavras-chave:** fogo-clima; análise estatística; Cerrado; Pantanal; Brasil

# Contents

<b>List of Figures</b>	<b>xiii</b>
<b>List of Tables</b>	<b>xxv</b>
<b>Acronyms</b>	<b>xxix</b>
<b>1 Introduction</b>	<b>1</b>
1.1 Fundamentals of fire science . . . . .	2
1.2 The role of fire in the Earth system . . . . .	4
1.2.1 Fire-vegetation feedbacks . . . . .	5
1.2.2 The human component . . . . .	7
1.3 Fire in Brazilian biomes . . . . .	10
1.3.1 Cerrado, the Brazilian savanna . . . . .	12
1.3.2 The Pantanal wetlands . . . . .	16
1.4 Objectives and Thesis Structure . . . . .	21
<b>2 Putting fire in the ecoregional map</b>	<b>25</b>
2.1 Introduction . . . . .	26
2.2 Data and methods . . . . .	28
2.2.1 Study area . . . . .	28
2.2.2 MODIS burned area, individual fire characteristics and fire radiative power products . . . . .	30
2.2.3 Statistical analysis . . . . .	31
2.2.4 Evaluating fire patterns by ecoregion . . . . .	32
2.3 Results . . . . .	32
2.3.1 Burned area patterns . . . . .	32

2.3.2	Fire intensity . . . . .	35
2.3.3	Fire size patterns . . . . .	37
2.3.4	Putting fire on the ecoregional map . . . . .	41
2.4	Discussion . . . . .	42
2.4.1	Understanding the patterns of fire variability . . . . .	42
2.4.2	Fire in the context of the ecoregional map and limitations . . . . .	47
2.5	Conclusion . . . . .	48
2.6	Supplementary Material . . . . .	50
<b>3</b>	<b>Understanding regional fire-climate dynamics</b>	<b>55</b>
3.1	Introduction . . . . .	56
3.2	Data . . . . .	58
3.3	Methods . . . . .	60
3.3.1	Composite analysis of extreme years . . . . .	60
3.3.2	Modelling regional fire-climate relationships . . . . .	61
3.4	Results . . . . .	62
3.4.1	Seasonal climate and burned area patterns . . . . .	62
3.4.2	Analysis of extreme fire seasons . . . . .	66
3.4.3	Analysis on a monthly basis for months of the fire season . . . . .	72
3.5	Discussion . . . . .	75
3.6	Conclusion . . . . .	83
3.7	Supplementary Material . . . . .	84
<b>4</b>	<b>The role of anthropogenic activity</b>	<b>85</b>
4.1	The case of the MATOPIBA region . . . . .	86
4.1.1	Introduction . . . . .	86
4.1.2	Methods . . . . .	87
4.1.3	Results and Discussion . . . . .	90
4.1.4	Conclusions . . . . .	97
4.2	Human activity influences regional fire-climate dynamics . . . . .	99
4.2.1	Introduction . . . . .	99
4.2.2	Data and methods . . . . .	102
4.2.3	Datasets and pre-processing . . . . .	102

4.2.4	Results . . . . .	106
4.2.5	Discussion . . . . .	109
4.2.6	Conclusions . . . . .	114
4.2.7	Supplementary Material . . . . .	117
<b>5</b>	<b>A slight detour through Pantanal</b>	<b>119</b>
5.1	Case study of the RPPN Sesc Pantanal . . . . .	120
5.1.1	Introduction . . . . .	120
5.1.2	Data and methods . . . . .	124
5.1.3	Results . . . . .	129
5.1.4	Discussion . . . . .	137
5.1.5	Conclusions . . . . .	141
5.1.6	Supplementary Material . . . . .	143
5.2	Synergy between heatwaves and fire in the Pantanal biome . . . . .	149
5.2.1	Introduction . . . . .	149
5.2.2	Data and methods . . . . .	151
5.2.3	Results . . . . .	155
5.2.4	Discussion . . . . .	163
5.2.5	Conclusion . . . . .	166
5.2.6	Supplementary Material . . . . .	168
<b>6</b>	<b>Final remarks</b>	<b>172</b>
6.1	Scientific outcomes . . . . .	174
	<b>References</b>	<b>178</b>
	<b>Annex A Silva et al. (2024a)</b>	<b>225</b>
	<b>Annex B Contribution to UNEP (2022)</b>	<b>245</b>
	<b>Annex C Libonati et al. (2022a)</b>	<b>255</b>
	<b>Annex D Libonati et al. (2022b)</b>	<b>275</b>





# List of Figures

- 1.1 A conceptual model describing the controls of fire across distinct spatial and temporal scales. Adapted from Araújo et al. (2024). . . . . 3
- 1.2 Landscape perspective of the multiple factors that influence, interact with, and are impacted by vegetation fire. Fires have numerous direct and indirect effects that impact the biosphere (including vegetation cover), geosphere (including soil erosion), hydrosphere (including fluvial sediment and nutrient transport), cryosphere (including soot fallout and changed albedo) and atmosphere (including smoke pollution). From Bowman et al. (2020). . . . . 4
- 1.3 Comparison of fire regimes under natural (lightning) and anthropogenic drivers in both fire-dependent (e.g., savanna) and fire-sensitive (e.g., rainforest) Brazilian ecosystems. From Pivello et al. (2021). . . . . 6
- 1.4 A wildfire is the result of a complex interaction of biological, meteorological, physical, and social factors that influence its likelihood, behaviour, duration, extent, and outcome (i.e., its severity or impact). Changes in many of these factors are increasing the risk of wildfire globally (e.g., climate change is increasing the frequency and severity of weather conducive to wildfire outbreaks, and changed demographics in high-risk regions are increasing the potential impacts of wildfires). From UNEP (2022). . . . . 8
- 1.5 Annual average active fire counts as detected by MODIS/AQUA sensor from 2003–2022 per South American country. The average of all countries in South America (SA) is represented in a solid black line. From Silva et al. (in press). . . . . 11

1.6	Brazilian vegetation types classified as fire-dependent, fire-sensitive and fire-independent, following Hardesty et al. (2005). Open vegetation types (grasslands, open savannas) are classified as fire-dependent; forests (rainforests, seasonal forests, woodland savanna) are classified as fire-sensitive, and xerophytic vegetation is classified as fire-independent. The inlay bars indicate the density of fire foci in 2020 for each fire sensitivity class. From Pivello et al. (2021). . . . .	12
1.7	A typical Cerrado landscape in Chapada dos Guimarães, Mato Grosso (MT), during the dry season. Photo taken by the author. . . . .	13
1.8	The inter-annual variability of burned area in Brazil from 2001–2019 is shown in grey and the corresponding percentage from the Cerrado biome is shown in red. All panels use the MODIS MCD64A1 500 meter product. From UNEP (2022). . . . .	16
1.9	A typical Pantanal landscape in the RPPN Sesc Pantanal, Mato Grosso (MT), during the dry season. Photo taken by the author. . . . .	17
1.10	Total 2020 burnt area in the Pantanal using the ALARMES 500m resolution product. Conservation units and Indigenous lands are shown in green and orange, respectively. The bottom left graph shows Pantanal’s average Daily Severity Rating (DSR) from January to August each year, estimated using the ERA5 reanalysis product (Libonati et al., 2020). DSR is a numeric rating of the difficulty of controlling fires. From UNEP (2022). . . . .	21
2.1	Cerrado distribution within Brazil (top left panel) with its 19 ecoregions with their names in alphabetical order. Land cover and land use information from the MapBiomias Collection 5 (MapBiomias, 2020; Souza et al., 2020) is shown for the year 2019. The Cerrado main agrobusiness frontier, MATOPIBA, is delimited in red, whereas the Amazonian Arc of Deforestation is striped brown. . . . .	29
2.2	a) Average normalized burned area (NBA) per year (dark grey bars) and dry season (light grey bars, representing months from June to October), with correspondent annual NBA variance (black whiskers); b) Ecoregion yearly contribution (%) to Cerrado’s total BA during the 2001–2019 period; c) Heatmap of average monthly normalized burned area (NBA, %). . . . .	34

2.3	Standardized anomaly of BA in each ecoregion of Cerrado from 2001 to 2019.	35
2.4	a) Fire Radiative Power (FRP values in MW) per ecoregion for the 2001–2019 period; colours represent the fire intensity classes (low: < 42 MW; moderate: 42–64 MW; and high: > 64 MW) and black diamonds the 99 <sup>th</sup> percentile of the FRP distribution. b) Monthly means of FRP values (MW) averaged over 2001–2019 for each ecoregion. . . . .	37
2.5	Spatial distribution of fire size classes (I: 0.21–1 km <sup>2</sup> ; II: 1–10 km <sup>2</sup> ; III: 10–50 km <sup>2</sup> and IV: > 50 km <sup>2</sup> ) and all classes (Total), derived from GFA over the period of 2003–2018. . . . .	38
2.6	Frequency (%) of the number of fire scars (bottom bars) and the corresponding total BA (top bars) over the 2003–2018 period according to fire size class (I: 0.21–1 km <sup>2</sup> ; II: 1–10 km <sup>2</sup> ; III: 10–50 km <sup>2</sup> and IV: > 50 km <sup>2</sup> ). . . . .	39
2.7	Distribution of burn date (in julian day) according to fire size class (I: 0.21–1 km <sup>2</sup> ; II: 1–10 km <sup>2</sup> ; III: 10–50 km <sup>2</sup> and IV: > 50 km <sup>2</sup> ) for each ecoregion, considering the period from 2003 to 2018. Dry season between June and October is shaded in grey. . . . .	40
2.8	Cerrado ecoregional map updated with main fire characteristics in each ecoregion. Spatial distributions of each fire characteristic are illustrated in Supplementary Material: Figure 2.11. A description of each fire class (represented in the colour bar) is provided in the Supplementary Material: Table 2.2. Plus and minus signs denote respectively, increasing and decreasing BA trends during the 2001–2019 period. . . . .	42
2.9	Trends of a) Burned area (NBA, %), b) Fire intensity (FRP, MW) and burned area per fire scar size (NBA, %) for the classes: c) I (0.21–1 km <sup>2</sup> ), d) II (1–10 km <sup>2</sup> ), e) III (10–50 km <sup>2</sup> ) and f) IV (> 50 km <sup>2</sup> ) classes. NBA and FRP trends are estimated for the 2001–2019 period, whereas burned area fire size trends from 2003 to 2018. Dotted cells mean statistical significance at the 5% level (see Methods). . . . .	50
2.10	Interannual variability of yearly burned area (BA, km <sup>2</sup> , black lines) and Fire Radiative Power (FRP, GW, grey lines) from 2001 to 2019. Values in the top right corner show coefficient of determination from simple linear regression between the two products. . . . .	51

2.11	Spatial distribution of a) Burned Area, b) Fire scar sizes and c) Fire intensity, that lead to Figure 2.8. Burned area and Fire intensity classes (a and b) are based on first and third quartiles (low: below the 25 <sup>th</sup> percentile; high: above the 75 <sup>th</sup> percentile; moderate: between the 25 <sup>th</sup> and 75 <sup>th</sup> percentiles); and the Fire scar size which most contributed to the total burned area (middle panel) was stratified in: small scars and medium-large (big) scars. . . . .	51
3.1	Cerrado’s location within Brazil (dark grey) and South America (light grey). The transition zone between the Cerrado and Amazon biomes, the Arc of Deforestation, is hatched and MATOPIBA, defined here as the intersection of states Maranhão, Tocantins, Piauí and Bahia, with Cerrado, is marked by a solid black line. Cerrado’s 19 ecoregions (Sano et al., 2019) are shown and numbered, with the respective names listed in the column on the right. Cerrado’s ecoregions are further categorized into 5 classes based on their geographical location within Cerrado: north (red); orange (central-west); yellow (central-east); west (light blue); and south (dark blue). Finally, ecoregions not considered in this study are numbered but shown in dark grey. . . . .	59
3.2	Seasonal cycles of burned area (left-hand axis in black pertaining to the grey bars, km <sup>2</sup> ), precipitation (right-hand axis in blue pertaining to the blue curve, mm) and temperature (right-hand axis in red pertaining to the red curve, °C) for the evaluated ecoregions. Values represent an average of monthly burned area and precipitation(temperature) totals(averages) over the 2001–2023 period. The . . . . .	63
3.3	share of fire season (ASO) burned areas in yearly burned areas in shown in the top right of each panel, and ecoregions are categorized geographically, according to Figure 3.1: north, central-west, central-east, west, and south; and the corresponding category is shown in the top right corner of each subplot. . . . .	64
3.3	Interannual variability of yearly (dashed curves) and fire season (grey bars) burned areas per ecoregion. Coloured bars represent years of severe (red) and mild (green) fire seasons, defined as those . . . . .	65

3.4	above(below) percentile 75(25) of the 2001–2023 time series. Values for the 25 <sup>th</sup> and 75 <sup>th</sup> percentiles are show below the title of each panel, and ecoregions are categorized geographically, according to Figure 3.1: north; central-west; central-east; west; and south; the corresponding category is shown in the top right corner of each subplot. . . . .	66
3.4	Monthly anomalies of temperature (left-hand panel; red; °C) and precipitation (right-hand panel; blue; mm) for composites of severe (solid curves) and mild (dashed curves) years in Cerrado’s ecoregions. Severe(mild) years are defined as those where fire season burned areas exceed(fall behind) the 75 <sup>th</sup> (25 <sup>th</sup> ) percentile of fire season burned areas over the 2001–2023 period. Two noteworthy 3-month periods are highlighted: the austral autumn (March, April, and May - MAM; light grey); and the fire season (August, September, and October - ASO; dark grey). . . . .	67
3.5	Seasonal anomalies of temperature and precipitation for composites of extreme years along Cerrado’s ecoregions for pre-conditions (autumn - MAM) and the concurrent conditions (fire season - ASO). Colours(numbers) represent standardized(absolute) anomalies of temperature (T, °C) and precipitation (P, mm). Anomalies are in respect to seasonal averaged temperatures and aggregated precipitation over the considered periods. Ecoregions are categorized geographically, according to Figure 3.1: north, central-west (Central-W), central-east (Central-E), west, and south. . . . .	69
3.6	Standardized anomalies of temperature and precipitation along Cerrado’s ecoregions for composites of extreme monthly burned areas in August (top row), September (middle row), and October (bottom row). Standardized anomalies for both climate variables were computed for the austral autumn (MAM; left-hand plots) and the corresponding month (either August, September, or October; right-hand plots). Red(blue) lines represent positive(negative) standardized anomalies, while flame(dot) symbols pertain to composites of severe(mild) burned areas. Ecoregions are categorized geographically, according to Figure 3.1: north, central-west (Central-W), central-east (Central-E), west, and south. . . . .	73

3.7	Severe (red) and mild (green) fire years defined as those above and below the 75 <sup>th</sup> and 25 <sup>th</sup> percentile of burned areas over the 2001–2023 period, respectively. Each subplot represents the severe and mild fire years estimated using: fire season (ASO) burned areas; burned areas during the month of August; burned areas during the month of September; and burned areas during the month of October. . . . .	84
4.1	Spatial distribution of the 41 microregions from MATOPIBA in the Cerrado biome. . . . .	88
4.2	Burned area (km <sup>2</sup> ) in MATOPIBA (dark grey) and Cerrado (light grey) for the dry season from 2001 to 2018. Numbers above dark grey bars reflect the percentage of burned area in MATOPIBA in regards to that of Cerrado's in each year. . . . .	91
4.3	Coefficient of determination values between SBA and CL/LU (upper/lower figure) for MATOPIBA from 2001 to 2018/2017, respectively. Values close to 1(0) indicate a high(low) relation between SBA and CL/LU. The filled(empty) circles represent significance below the 5(10)% level. . . . .	93
4.4	Trends of SBA, CL and LU for the study region over 2001–2018. Warmer(cooler) colors represent an upward(downward) trend and filled(empty) circles represent significance below the 5(10)% level. . . . .	95
4.5	Spatial variability of the climatic and anthropogenic variables employed in this study. From left to right: average fire season DSR over 2003–2018 (shades of blue); average fractions of anthropogenic land use (%) over 2003–2018 (shades of orange); average deforested fraction (%) over 2003–2018 (shades of green); and average populace (people) over 2003–2018 (shades of grey). . . . .	104
4.6	Contribution of each fire class to total burned area (%). Mild(extreme) fires are shown in yellow(red) and the associated values are shown in black(white). The 95 <sup>th</sup> percentile (P95) of fire size are listed at the right-hand side of the plot. . . . .	106

4.7	Comparing the coefficients of determination ( $R^2$ ; %) of each regional fire-climate model for both mild and extreme classes of fire, and their corresponding anthropogenic characteristics, namely: average fraction of anthropogenic land use over 2003–2018 (%); average deforested fraction over 2003–2018 (%); and the decimal logarithmic of average populace over the 2003–2018 period. Ecoregions located in the MATOPIBA and Arc of Deforestation regions are shown in yellow markers, and crosses represent non-significant fire-climate models (with p-values below the 5% level). . . . .	108
4.8	Results of the threshold analysis for mild fires by means of the Kruskal-Wallis test statistic, for each anthropogenic variable. From left to right: average fraction of anthropogenic land use over 2003–2018 (%); average deforested fraction over 2003–2018 (%); and the decimal logarithmic of average populace over the 2003–2018 period. For simplicity, we chose the threshold value of 36% in the case of anthropogenic land use (where it ranged between 35%–37%; Supplementary Material: Table 4.2), and 37% in the case of deforested fraction (ranging from 37%–38%; Supplementary Material: Table 4.3). Boxplots represent the distribution of ecoregions below and above the threshold value, and the p-value for the Kruskal-Wallis test is shown in green. . . . .	109
5.1	Map of the RPPN Sesc Pantanal with land cover information for 2021 (MapBiomass, 2023), along with its location within the Brazilian Pantanal (pink) and Brazil/South America (light/dark grey) in the lower right panel.	125
5.2	Year to year mapping of burned areas by the <i>AQM-LS</i> product from 2000 to 2021. Commission errors are shown in purple, and hits ( <i>AQM-LS<sub>val</sub></i> ) are shown in red. Years with a white X in red background highlight years where the validation found no burned areas, and the red circles highlight very small burned areas. . . . .	130
5.3	a) Interannual variability of burned area from 2000–2021 as estimated by the validated <i>AQM-LS</i> product ( <i>AQM-LS<sub>val</sub></i> ). b) The number of times a pixel was burnt over the time series (2000–2021). . . . .	132
5.4	Land cover types of burned areas using the validated <i>AQM-LS</i> product ( <i>AQM-LS<sub>val</sub></i> ) from 2000 to 2021. . . . .	133

5.5	Seasonal cycles of: a) surface temperature ( $^{\circ}\text{C}$ , red); b) relative humidity (% , orange); c) precipitation (mm, blue); d) wind speed (km/h, green); and e) fire danger index Daily Severity Rating (DSR) (dimensionless, purples). Lighter to darker colours represent a decadal mean from 1980–1989 to 2010–2019, and the average for the last 2 years (2020–2021). Black lines are the average over the time series, from 1980 to 2021. Grey shaded areas represent the months from July to October. . . . .	134
5.6	Interannual variability from 1980 to 2021 for: a) temperature ( $^{\circ}\text{C}$ , reds); b) relative humidity (% , oranges); c) precipitation (mm, blue); d) wind speed (km/h, greens); and e) fire danger index DSR (adimensional, purples). Darker shades represent the extremes, evaluated as percentiles 90 for temperature, wind speed and DSR; and percentile 10 for relative humidity. Dashed lines represent significant trends (below the 5% confidence level), and the trend slope is shown on the graph with the corresponding colour. Non-significant trends are not shown. . . . .	136
5.7	Examples of misclassification by the <i>AQM-LS</i> product, due to spectral confusion from temporal changes. (a) Clouds in 2000, as through Landsat-7 imagery on June 2 <sup>nd</sup> with the <i>AQM-LS</i> product superimposed in orange. (b) Paths in 2011, as seen through (1) Landsat-5 imagery on February 1 <sup>st</sup> and (2) Landsat-5 imagery on August 12 <sup>th</sup> with the <i>AQM-LS</i> product superimposed in orange. (c) Water bodies and seasonally flooded areas in 2011, as seen through (1) Landsat-5 imagery on February 1 <sup>st</sup> , (2) Landsat-5 imagery on August 12 <sup>th</sup> , and (3) Landsat-5 imagery on August 12 <sup>th</sup> with the <i>AQM-LS</i> product superimposed in orange. Landsat imagery appears in colour composition (RGB) which combines the reflectance spectral bands of short-wave infrared (SWIR, in Red), near-infrared (NIR, in Green) and red (in Blue). . . . .	143



5.8	The case of the year 2003. The RPPN Sesc Pantanal is illustrated in the bottom left corner, and the section that is shown in top panels is highlighted in green. (a) Raw Landsat-7 imagery for October 1 <sup>st</sup> 2003 in colour composition (RGB) which combines the reflectance spectral bands of short-wave infrared (SWIR, in Red), near-infrared (NIR, in Green) and red (in Blue). (b) as (a) but with the validated <i>AQM-LS</i> product ( <i>AQM-LS<sub>val</sub></i> ) superimposed in red. . . . .	144
5.9	Seasonal cycles from 1980 to 2021 for: temperature (°C, top left), relative humidity (% , top right), total precipitation (mm, bottom left) and wind speed (km/h, bottom right). Grey curves represent years 1980 to 2019, shades getting darker as the years progress; and the red and yellow curves represent 2020 and 2021, respectively. Temperature, relative humidity and wind speed, are monthly averages, whereas precipitation is accumulated over the entire month. . . . .	145
5.10	Interannual variability from 1980 to 2021 of total yearly precipitation (top panel) and total summer precipitation (bottom panel). Summer is defined as December of the previous year, and January and February from the current year (e.g. the 1980 summer total is the sum of precipitation from December 1979 and January and February from 1980). Dotted lines represent trends, estimated using the Mann-Kendall non-parametric test, and, if significant below the 5% level, the trend slope is printed on the graph. . . . .	145
5.11	Interannual values of yearly burned area as estimated using the validated <i>AQM-LS</i> product ( <i>AQM-LS<sub>val</sub></i> , grey bars in both top and bottom panels corresponding to the right y-axis), and yearly averages of the Daily Severity Rating (DSR, bottom panel, red curve corresponding to the left y-axis), from 2000 to 2021. Grey box in both plots shows the resulting linear regression models, using the fire danger indexes as predictors of interannual burned area, and the corresponding coefficient of determination ( $R^2$ ). . . . .	146

5.12	The Pantanal biome with land cover information for 2019 from the Copernicus Global Land Service (Buchhorn et al., 2020). (b) Pantanal’s monthly averages of burned area (gray bars) as estimated by the MCD64A1 Collection 6 product over 2002–2020, and seasonal precipitation (blue line) and heatwave incidence (orange line) patterns in ERA5 reanalysis for the period 1981–2020. . . . .	152
5.13	Interannual variability of annual burned area (light gray bars) and fire season burned area (August to October; dark gray bars), using the MODIS MCD64A1 product, and the percentage of Pantanal under heatwave ( $\%Pantanal_{HW}$ ) over the dry season (April to October; orange bars), from 2002 to 2020. (b) Relationship between $\%Pantanal_{HW}$ over the dry season and the fire season burned area, estimated using ERA5 reanalysis, from 2002 to 2020, evaluated using a simple linear regression model. Black line indicates the resulting regression line and on the bottom right corner is the corresponding equation and goodness-of-fit ( $R^2$ ). . . . .	156
5.14	(a) Taylor diagram of raw CORDEX-CORE historical simulations compared to ERA5. Tmax monthly mean (circles) and monthly P90 (triangles) during dry season months (April–October) over Pantanal for the period 1981–2005, for each simulation (color range) and for the ensemble mean (gray). All Pearson correlation coefficients presented here are statistically significant at the 99.9% level. (b) Tmax distribution over Pantanal for dry season months of the historical period in ERA5 (purple), CORDEX-CORE original (gray) and CORDEX-CORE after bias correction (light gray). . . . .	158
5.15	Average difference on Tmax over the Pantanal region for April to October between the historical period and three projected RCP8.5 periods (2026–2050 as short term; 2051–2075 as mid term; and 2076–2099 as long term), for the six CORDEX-CORE simulations considered and the ensemble mean (rightmost panel). All data is from the bias-corrected simulations. . . . .	159
5.16	Same as Figure 4 for RCP2.6. . . . .	160

5.17	Percentage of Pantanal under heatwave from 1981 to 2099. Evolution for historical (black line), RCP2.6 (blue line), and RCP8.5 (red line) bias-corrected CORDEX-CORE runs. The gray, blue and red shaded regions show the maximum range between individual model runs. Solid lines represent the ensemble mean and those that are thicker show a smoothed time series for better visualization. The smoothing is performed by applying a Savitzky–Golay filter with a window length of 19 years and a polynomial order 5. . . . .	161
5.18	Yearly average of Tmax (left) and P90 Tmax (right) over Pantanal during the 1981–2099 period, in ERA5 (solid purple line), and for CORDEX-CORE RCP scenarios ensemble means before (dashed blue and red lines) and after (solid blue and red lines) bias correction. For CORDEX-CORE corrected, ensemble means are shown in solid lines, and the minimum and maximum of each single realization is shown in shades for the bias corrected time series. . . . .	169
5.19	Distribution of hourly Tmax in ERA5 (purple bars) and in the ensemble of CORDEX-CORE historical runs before (black line) and after (gray bars) bias correction. Period 1981–2005. . . . .	170
5.20	Leave-One-Out Cross-Validation (LOOCV) scheme performed from 2002 to 2020: observed burned area values (from MODIS MCD64A1) are shown in a solid black line, whereas the LOOCV predicted values for burned area are shown in a dashed black line. The resulting coefficient of determination from the observed and the predicted burned area values is also shown in red.	170



# List of Tables

- 2.1 Area of each ecoregion (Area, km<sup>2</sup>), and average and standard deviations of natural (Natural landcover, %) and anthropogenic (Anthropogenic landcover, %) landcover over the 2001–2018 period, estimated using the MapBiomass Collection 4.1 product (MapBiomass, 2020; Souza et al., 2020). Last column shows correspondent total burned area (BA, km<sup>2</sup>) using the MCD64A1 product from 2001 to 2019. . . . . 52
- 2.2 Description of each obtained fire class as described in Methods, using a 3-letter sequence (first column); long description of sequence (second column); criteria used to describe such sequence (third column); and lastly, ecoregions belonging to each sequence and its trends (fourth column). Percentiles are represented by p25 (25<sup>th</sup> percentile) and p75 (75<sup>th</sup> percentile). . . . . 53
- 3.1 Bivariate linear models of annual fire season (ASO) burned areas using temperature and precipitation. Goodness-of-fit is evaluated through the Adjusted R<sup>2</sup> (%). Coefficients  $\beta_1$  and  $\beta_2$  correspond to the regression coefficients associated with concurrent conditions of the fire season (ASO) and pre-conditions during autumn (MAM), respectively, and are accompanied by the associated significance, where \* denotes significant relationships below the 5% level and \*\* denotes relationships below the 10% level. The intercept of the regression is shown as  $\beta_0$ , and the Variance Inflation Factor (VIF) for both predictors is depicted as well. Ecoregions are categorized geographically, according to Figure 3.1: north, central-west (Central-W), central-east (Central-E), west, and south. . . . . 71

3.2	Bivariate linear models to predict annual burned areas for each month of the fire season (either August, September, or October) using pre-conditions during autumn (MAM) and concurrent conditions (either August, September, or October) of temperature or precipitation. Goodness-of-fit is evaluated through the Adjusted $R^2$ (%). Coefficients $\beta_1$ and $\beta_2$ correspond to the regression coefficients associated with concurrent conditions (either during August, September, or October) and pre-conditions during autumn (MAM), respectively, and are accompanied by the associated significance, where * denotes significant relationships below the 5% level and ** denotes relationships below the 10% level. The intercept of the regression is shown as $\beta_0$ , and the Variance Inflation Factor (VIF) for both predictors is depicted as well. Ecoregions are categorized geographically, according to Figure 3.1: north, central-west (Central-W), central-east (Central-E), west, and south. . . . .	76
3.3	As in Table 3.2 but for September. . . . .	77
3.4	As in Table 3.2 but for October. . . . .	78
4.1	Goodness of fit (as evaluated through the coefficients of determination – $R^2$ ) of simple regression models using fire season averaged DSR to predict interannual burned areas of mild, extreme, and total fire events during the fire season, for each of the 19 ecoregions of Cerrado. . . . .	107
4.2	Results of the iterative analysis to find a threshold value for average fraction of anthropogenic land use over 2003–2018 (%), in which two groups of ecoregions have statistically different strengths of the fire-climate relationship, for the mild and extreme fire classes. For each threshold value, the Kruskal-Wallis (KW) test statistic and associated p-value are shown, along with the number of ecoregions that are below ( $N <$ ) or above ( $N \geq$ ) the threshold. Threshold values that yielded significant results below the 5% level are highlighted in grey, and those chosen as the best threshold values are in bold. For more information on selection criteria see Methods. . . . .	117
4.3	As Table 4.2 but regarding the average deforested fraction over 2003–2018 (%). . . . .	118

4.4	As Table 4.2 but regarding the decimal logarithm of average populace over the 2003–2018 period. There is one additional column that converts the threshold value back to population: “Threshold (people)” . . . . .	118
5.1	Comparison of the <i>AQM-LS</i> product ( <i>AQM-LS</i> ) and its validated version ( <i>AQM-LS<sub>val</sub></i> ), both values in thousands of hectares (ha). Column “ <i>AQM-LS</i> – <i>AQM-LS<sub>val</sub></i> ” shows the absolute difference, in thousands of ha, and “Difference to <i>AQM-LS</i> (%)” shows the relative difference from <i>AQM-LS<sub>val</sub></i> to <i>AQM-LS</i> , estimated as $(AQM-LS - AQM-LS_{val})/AQM-LS \times 100$ . . . . .	147
5.2	RCM considered in this study: runs for the South American domain at $0.22^\circ \times 0.22^\circ$ spatial resolution (SAM-22) available within the CORDEX-CORE (Giorgi et al., 2022). . . . .	153
5.3	Future evolution of heatwave index ( $\%Pantanal_{HW}$ ) under RCP2.6 and RCP8.5 scenarios for three time periods: short-term from 2026 to 2050; mid-term from 2051 to 2075; and long-term from 2076 to 2099. For comparison, we further show values for the historical run from 1981 to 2005. Average values are calculated as ensemble mean from all RCM realizations. Std corresponds to the standard deviation, over time, of the ensemble mean for the considered period. Values between parentheses indicate relative change compared to the historical value. The presence of a trend is evaluated through the Mann–Kendall test at a 5% significance level. Upwards arrows indicate a significant positive trend. The average inter-model spread corresponds to the average, over each period, of the difference between the highest and lowest individual member values every year. . . . .	162
5.4	Kolmogorov-Smirnov test p-values against Mielke beta-kappa distribution for Tmax in ERA5 and the historical CORDEX-CORE simulations, for months April through October during the period 1981–2005. . . . .	168





# Acronyms

**AMO** Atlantic Multidecadal Oscillation. 44

**BA** Burned Area. 27, 28, 30–34, 36–38, 41, 42, 44–49, 88

**BUI** Build-up Index. 89

**CDF** Cumulative Distribution Function. 154, 155

**CFWIS** Canadian Fire Weather Index System. 103

**CMIP** Coupled Model Intercomparison Project. 165

**CORDEX** COordinated Regional Downscaling EXperiment. 23, 165

**CORDEX-CORE** COordinated Regional Climate Downscaling EXperiment-COMmon  
Regional Experiment. 151, 152, 154, 157, 158, 160, 164–166, 168

**DC** Drought Code. 89

**DMC** Duff Moisture Code. 89

**DSR** Daily Severity Rating. 89, 90, 103, 104, 106, 112, 127

**ECMWF** European Centre for Medium-Range Weather Forecasts. 60, 89, 126, 151

**ENSO** El Niño-Southern Oscillation. 163

**ESGF** Earth System Grid Federation. 152

**FFMC** Fine Fuel Moisture Code. 89

**FRP** Fire radiative power. 30–32, 35, 36, 43, 45

**FWI** Fire Weather Index. 89, 90, 127

**GCM** Global Climate Model. 152, 158

**GFA** Global Fire Atlas. 30, 31, 102, 113, 114

**GFED** Global Fire Emissions Database. 46

**GIS** Geographic Information System. 127

**IBGE** Instituto Brasileiro de Geografia e Estatística (Brazilian Institute of Statistics and Geography). 11, 87

**IFM** Integrated Fire Management. 47, 173

**IOD** Indian Ocean Dipole. 163

**ISI** Initial Spread Index. 89

**ITCZ** Atlantic Intertropical Convergence Zone. 138

**KS** Kolmogorov-Smirnov. 168

**LASA/UFRJ** Laboratório de Aplicações de Satélites Ambientais do Departamento de Meteorologia da Universidade Federal do Rio de Janeiro. 126, 177

**LULC** Land Use and Land Cover. 103

**MATOPIBA** confluence of states Maranhão – MA, Tocantins – TO, Piauí – PI, and Bahia – BA. 13, 14, 26, 29, 34, 44, 45, 47–49, 86–88, 90–94, 97–99, 101, 108, 110, 174

**MJO** Madden–Julian Oscillation. 163

**MODIS** Moderate Resolution Imaging Spectroradiometer. 30, 31, 59, 88, 102, 151

**NASA** National Atmospheric Space Agency. 30, 88, 89, 151

**NBA** Normalized Burned Area. 31–33, 40, 48

**NIR** Near-Infrared. 127

**PREVFOGO** National Center for the Prevention and Fighting of Forest Fires. 47

**QDM** Quantile Delta Mapping. 154, 155, 158, 164, 165, 168

**RCM** Regional Climate Model. 152, 154, 158, 164–166

**RCP** Representative Concentration Pathways. 152, 154, 158, 163, 168

**RGB** Red, Green and Blue. 127

**RPPN** Reserva Particular do Patrimônio Natural. 120, 174

**SBA** Satellite Burned Area. 88, 90–94, 96–98

**Sesc** Serviço Social do Comércio. 124

**SWIR** Short-Wave Infrared. 127

**UNESCO** United Nations Educational, Scientific and Cultural Organization. 19, 121

**UPRB** Upper Paraguay River Basin. 17–19

**USA** United States of America. 46

**VPD** Vapour Pressure Deficit. 101



# Chapter 1

## Introduction

*This chapter is partly based on the following book chapters:*

- *Silva, P. S., Libonati, R., Schmidt, I. B., Nogueira, J., and DaCamara, C. C. (2024a). Climate Change and Fire: The Case of Cerrado, the Brazilian Savanna. In Mishra, M., de Lucena, A. J., and Maharaj, B., editors, Climate Change and Regional Socio-Economic Systems in the Global South, chapter 6, pages 87–105. Springer Nature Singapore, 1st edition*
- *Silva, P. S., Libonati, R., Marengo, J., Costa, M. C., Alves, L., and Schmidt, I. (in press). Fire in the Anthropocene. In Vânia Pivelo and Alessandra Tomaselli Fidelis, editor, Fire in South American ecosystems, chapter 13. Springer Nature*

## 1.1 Fundamentals of fire science

Fire has been a natural disturbance in the Earth system for over 420 million years (Bowman et al., 2009), and its environmental controls have long been subject to study. In general, it is widely recognized that fire requires biomass available to burn, atmospheric conditions conducive to combustion, and an ignition source (Moritz et al., 2012). However, fire activity affects natural terrestrial systems in a wide range of spatial and temporal scales (Moritz et al., 2005): from local (e.g. individual plants) to global (e.g. by shaping vegetation and biome distribution) scales; and from a single fire event to its effect on evolutionary time scales (e.g. by influencing species distribution and abundance).

Fire science has evolved substantially over the last few decades marked, for instance, by the emergence of remote sensing, automatic detection, and increased modelling capabilities. This allowed a better assessment of fire activity, but also of the environmental controls of fire that act at distinct spatial and temporal scales. Fire triangles are a common starting point for conceptualizing these interactions, and Figure 1.1 illustrates a widely accepted conceptual model that describes the controls of fire activity across multiple spatial and temporal scales (Moritz et al., 2005; Higuera, 2015).

At the local scale, the fire-fundamentals are illustrated based on the interaction between oxygen, heat, and fuel. When the occurrence of all these drivers evolves into a fire event, its behaviour is no longer describable solely by oxygen, heat and fuel. The fire behaviour triangle illustrates the main factors that influence fire behaviour, particularly its speed, direction, duration, and flame characteristics (UNEP, 2022): topography (slope, aspect, elevation), weather (mainly through temperature, precipitation, relative humidity and wind) and fuel (vegetation type and condition, amount, continuity, extent, among other factors). The link between fire and weather is long and widely known (Schroeder et al., 1970), and when meteorological conditions favour the occurrence and spread of fire, it is commonly referred to as fire weather (Schroeder et al., 1970; Quilcaille et al., 2023). Fire weather conditions generally include, but are not limited to, high temperatures and wind speeds, associated with low relative humidity and precipitation. Fuel is also present in the traditional fire triangle, where it represents any material that is capable of burning, however, for fire behaviour, the type of vegetation, its patchiness, and dryness, among others, become detrimental to understanding the evolution of a fire event.

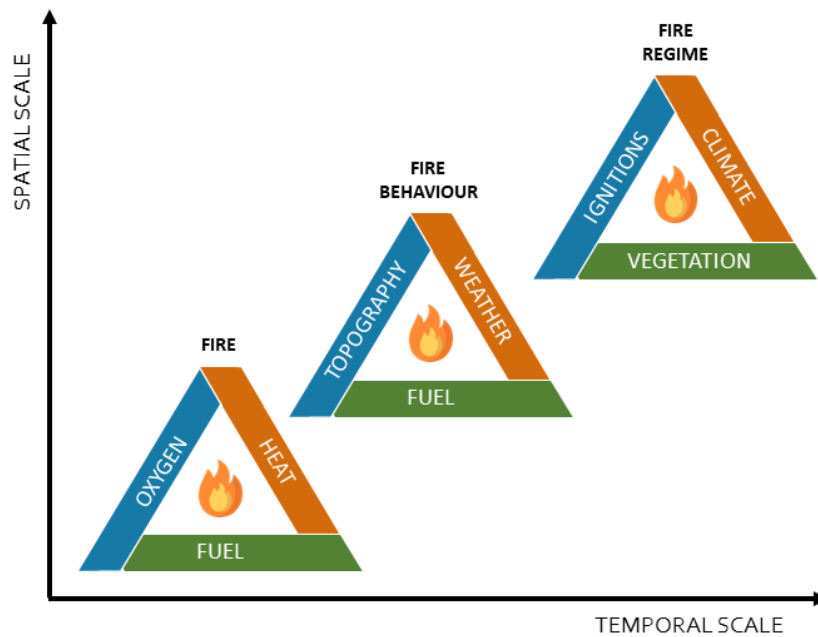


Figure 1.1: A conceptual model describing the controls of fire across distinct spatial and temporal scales. Adapted from Araújo et al. (2024).

Lastly, in ecosystems where fire is an important ecological component, there is a broad level of stability in its parameters, commonly referred to as the “fire regime”: the “characteristic pattern of fire established over time and space” (UNEP, 2022). Although there is no formal definition, the fire regime comprises a set of parameters used to describe historical fire patterns, including ignition sources, frequency, intensity (the amount of energy released during the fire), extent (burned area), seasonality and heterogeneity (patchiness). Fire regimes are defined on large spatial (ecosystem or landscape) and temporal (decades to centuries) scales and are influenced by ignition sources (source, seasonality, density, location and timing), vegetation (productivity, flammability, and distribution), and climate (including moisture content, length and severity of the dry season, extreme wind patterns) (Figure 1.1).

Although these definitions are employed worldwide, each ecosystem has its own relationships with fire. With increasing anthropogenic presence in ecosystems and the remarkable influence of humans on fire activity (e.g. by increased ignitions, landscape management, or climate change), the human component has to be incorporated in the controls and drivers of fire activity and there is a need to better assess the interactions between these variables. In the next section, we will delve on the impacts of fire activity in ecosystems worldwide and how humans are influencing and shaping these dynamics.

## 1.2 The role of fire in the Earth system

Fire is an essential feature of the Earth system that influences global ecosystem patterns and processes, such as climate, vegetation, biogeochemical cycles, and human activity, and also feedbacks to them in multiple ways (Figure 1.2).

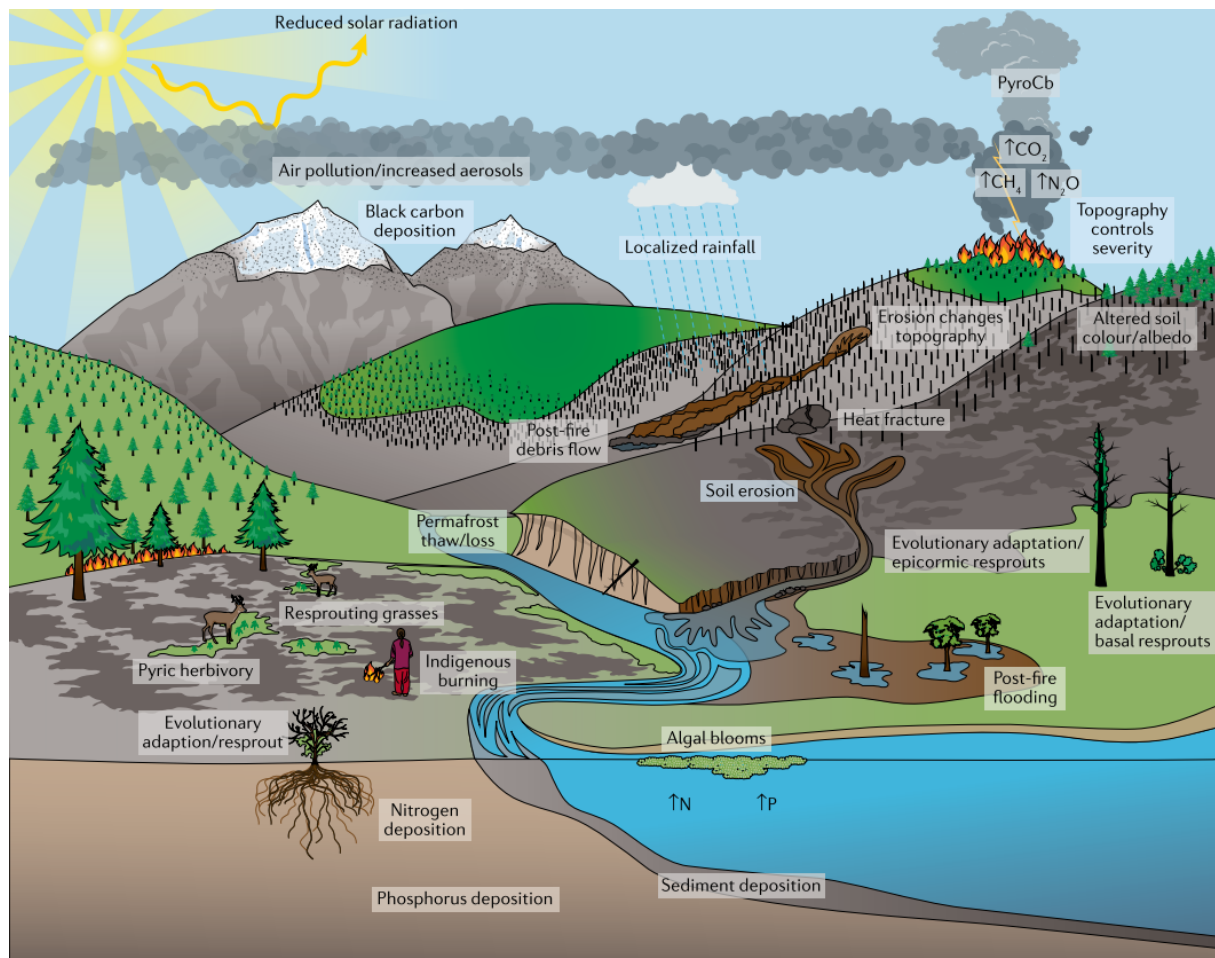


Figure 1.2: Landscape perspective of the multiple factors that influence, interact with, and are impacted by vegetation fire. Fires have numerous direct and indirect effects that impact the biosphere (including vegetation cover), geosphere (including soil erosion), hydrosphere (including fluvial sediment and nutrient transport), cryosphere (including soot fallout and changed albedo) and atmosphere (including smoke pollution). From Bowman et al. (2020).

For instance, fire modifies the Earth's radiative balance by emitting large quantities of greenhouse gases and aerosols into the atmosphere, changing its composition and how it interacts with solar radiation (Bowman et al., 2020): greenhouse gases trap infrared radiation and increase the greenhouse effect, whereas aerosols reduce transmission of solar energy to the surface. The occurrence of extreme fires can generate deep, smoke-infused thunderstorms, known as pyrocumulonimbus (PyroCb: Figure 1.2), further inject-



ing aerosols into the atmosphere and impacting radiation budgets (Peterson et al., 2018). These storms positively feedback with fire by increasing lightning strikes and igniting new fires (McRae et al., 2015). Moreover, high amounts of black carbon in smoke influence the Earth system by inhibiting rainfall (Rosenfeld, 1999), and the transport and eventual fallout of black carbon to the cryosphere reduces albedo and increases snow and ice melt (Thomas et al., 2017; Skiles et al., 2018).

### 1.2.1 Fire-vegetation feedbacks

Fire shapes ecological communities worldwide influencing vegetation distribution, structure and composition. In a world without fire, considering climate as the sole determinant of global vegetation, Bond et al. (2005) found that closed forests, which currently cover a quarter of the globe, would double in size. It has been proposed that fire–tree cover feedbacks maintain savanna and forest as alternative stable states, as fire sustains savannas where climate favours forests by limiting tree cover and maintaining open canopies which, in turn, creates favourable conditions for further fire activity (Staver et al., 2011).

However, fire can either be a beneficial or damaging disturbance depending on the ecosystem. While those with little or no evolutionary exposure to fire will likely see negative effects, ecosystems with a history of fire experience selective pressures that cull and shape the species pool and the environment in line with the fire regime (UNEP, 2022). Global ecosystems may then be classified through their relationship with fire and its evolutionary role (Hardesty et al., 2005):

- **Fire-sensitive** ecosystems are those where species have not evolved with the presence of fire. While fire may play a secondary role in maintaining natural ecosystem processes and structure, they are not able to respond positively or rebound after fire. They represent 22% of ecosystems on Earth and include, for example, mangroves and many tropical and subtropical broadleaf forests.
- **Fire-independent** ecosystems represent 15% of Earth, and are those that naturally lack sufficient fuel or ignition sources to sustain fire, and thus fire is not considered an evolutionary force. Examples are tundras and deserts.
- In **fire-dependent** ecosystems, fire is a fundamental disturbance, sustaining native fauna and flora while occurring at the natural bounds set by seasonal climates, fuel

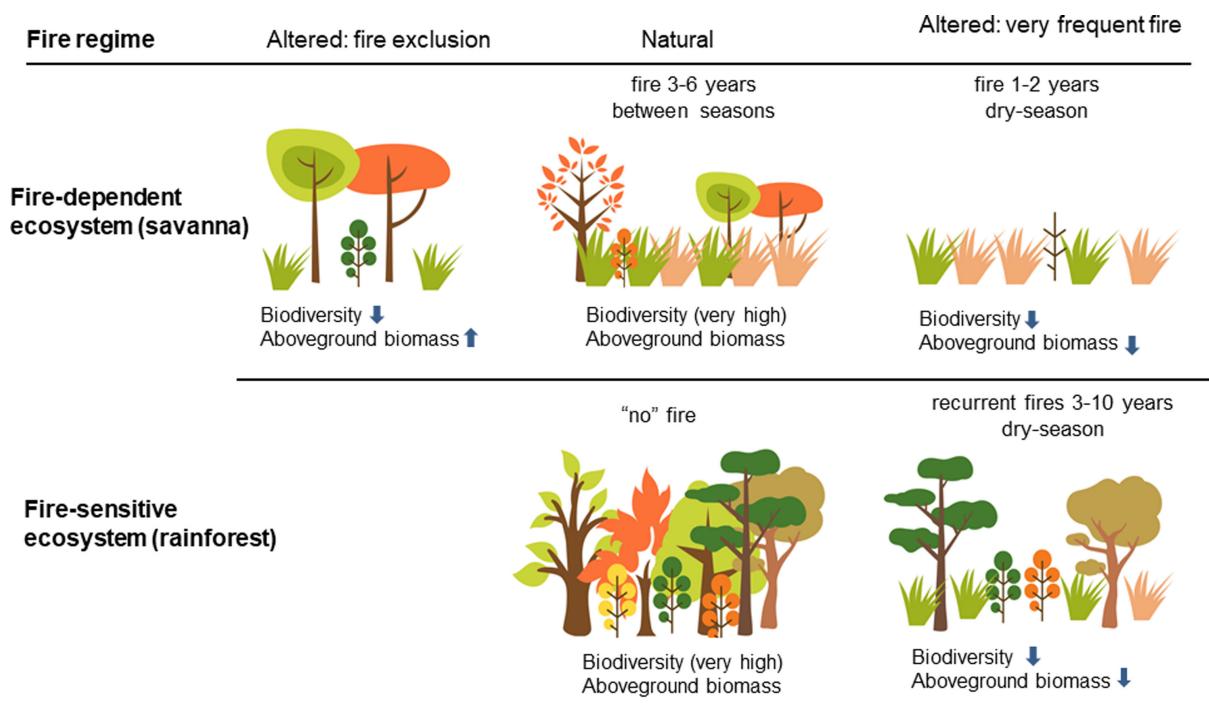


Figure 1.3: Comparison of fire regimes under natural (lightning) and anthropogenic drivers in both fire-dependent (e.g., savanna) and fire-sensitive (e.g., rainforest) Brazilian ecosystems. From Pivello et al. (2021).

accumulation, ignitions and other natural factors (Hardesty et al., 2005). These natural fires are often triggered by lightning and incandescent fallout from volcanic eruptions (Glikson, 2013). Species in fire-dependent ecosystems have evolved with fire and developed adaptations, such as thick barks, fire stimulated recruitment, crown sprouting or below-ground reserve structures (Bowman et al., 2009). The vast majority of ecosystems on Earth are fire-dependent (55%), including grasslands, savannas, boreal, and Mediterranean forests.

In general, in fire-dependent ecosystems, the occurrence of fire tends to favour grasses and herbaceous plants over woody species, promoting open environments. Conversely, fire-sensitive ecosystems that do not see frequent fire support longer-lived species and adaptations to fire will be rare (Figure 1.3).

However, altered fire regimes can considerably disturb these natural dynamics (Figure 1.3). In fire-dependent ecosystems, species are not simply adapted to fire but instead to a set of environmental conditions that encompass the fire regime that, when altered, may severely disrupt ecosystem services. For instance, high fire frequency favours herbaceous plants that are fire-adapted and more resilient, to the detriment of woody species, which

leads to lower biodiversity and decreased aboveground biomass (Pivello et al., 2021). Conversely, fire exclusion causes woody encroachment and an increase in aboveground biomass, associated with acute biodiversity loss (Figure 1.3; Rosan et al., 2019; Abreu et al., 2017). Additionally, altered fire regimes in fire-dependent ecosystems increase the exposure and vulnerability of adjacent ecosystems that are not adapted to fire, such as seasonally flooded forests (Bilbao et al., 2020).

In fire-sensitive ecosystems, where the fire return interval is estimated to be in the hundreds or even thousands of years (Kauffman and Uhl, 1990), increased fire frequency leads to high tree mortality and extensive damage to roots (Figure 1.3). In general, this leads to an increasingly open environment that promotes fuel drying, which in turn makes the forest even more susceptible to fires (Pivello et al., 2021).

In short, fire plays an important role in maintaining biodiversity in fire-dependent ecosystems, where many plants, animals, and ecosystems depend on particular temporal and spatial patterns of fire (Kelly et al., 2020), and is detrimental to ecosystem services and biodiversity in fire-sensitive ecosystems.

### **1.2.2 The human component**

Humans have shaped patterns of global burning for millennia (Bowman et al., 2020). Initially, fire was used for warmth, cooking and hunting (Glikson, 2013). More recently, as the transition from subsistence to industrial economies unfolded, forests turned into agricultural or pastoral landscapes through the use of fire (Bowman et al., 2009), and with increased landscape fragmentation the use of fire became utilitarian, for uses such as crop enhancement, charcoal production, and smelting activities (Gillson et al., 2019). Humans now directly influence fire regimes by modifying landscapes and fuel loads, by suppressing natural ignitions whilst also being an ignition source, and indirectly by affecting the climate (Figure 1.4).

## Factors and conditions influencing wildfire occurrence

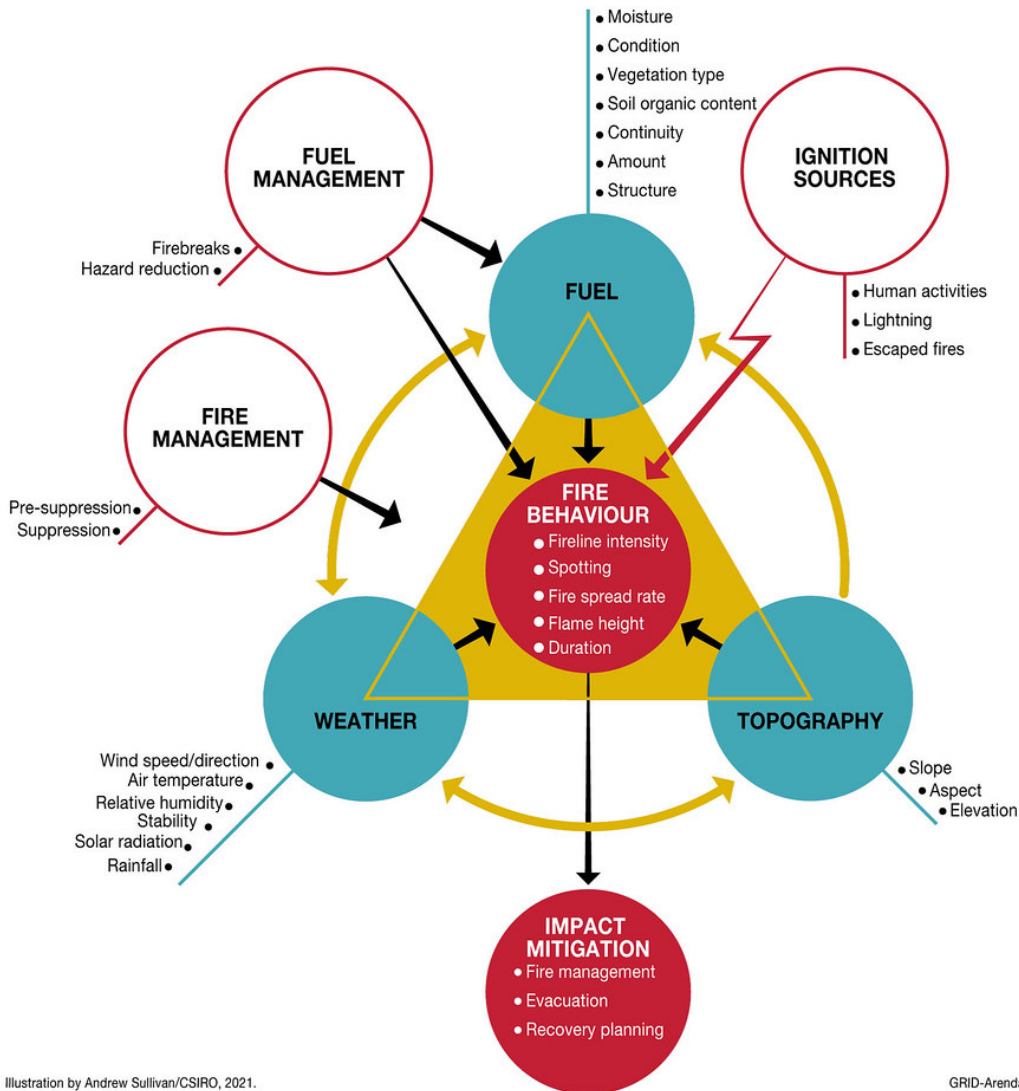


Figure 1.4: A wildfire is the result of a complex interaction of biological, meteorological, physical, and social factors that influence its likelihood, behaviour, duration, extent, and outcome (i.e., its severity or impact). Changes in many of these factors are increasing the risk of wildfire globally (e.g., climate change is increasing the frequency and severity of weather conducive to wildfire outbreaks, and changed demographics in high-risk regions are increasing the potential impacts of wildfires). From UNEP (2022).

The beginning of the 20<sup>th</sup> century saw a decrease in global fire activity, mostly due to fire suppression and elimination and highly modified and fragmented landscapes (Mouillot and Field, 2005). In many fire-prone ecosystems, fire suppression and elimination has homogenised and simplified landscapes, eroding their ability to recover from disturbance, and setting the stage for larger and more intense fires (Gillson et al., 2019). Accordingly, the latter half of the 20<sup>th</sup> century is marked by an increase in global burned areas that are not spatially homogeneous, with regional fire regimes showing great differences in the

magnitude and direction of change (Mouillot and Field, 2005). Many ecosystems where fire is historically absent or rare have burned recently, such as the Amazon rainforest (Barlow et al., 2019). Tropical forests, in particular, saw an exponential increase in biomass burning over the last few decades due to deforestation associated with agricultural expansion (Mouillot and Field, 2005).

Additionally, anthropogenic climate change has led to increases in fire weather conditions worldwide (Jones et al., 2022; Liu et al., 2022; Touma et al., 2021), driven mainly by alterations in temperature and precipitation patterns. The last decades have been marked by lengthened fire seasons (Jolly et al., 2015; Richardson et al., 2022) and an increasing trend in global extreme fire weather (Jain et al., 2021). In turn, extended and severe fire seasons contribute to higher levels of atmospheric aerosol concentrations, triggering feedback mechanisms between fire and climate (Bevan et al., 2009; Cox et al., 2008).

Despite generalized aggravated fire danger due to climate change, the beginning of the 21<sup>st</sup> century saw a decrease in global burned areas, due to the substantial decrease in fire activity over savanna and grassland ecosystems because of agricultural expansion and intensification (Andela et al., 2017). In line with other studies (e.g. Jones et al., 2022; Slyphard et al., 2017; Kelley et al., 2019), this illustrates that the relationship between fire and climate may be altered or even superseded by human activities. Nevertheless, the strong association and feedback mechanisms between anomalous fire weather and extreme fire behaviour suggest that anthropogenic climate change will impact future fire regimes (Bowman et al., 2020; Flannigan et al., 2013). Indeed, future climate change is projected to change global fire patterns (Moritz et al., 2012; Pechony and Shindell, 2010), associated with the expansion of fire-prone areas worldwide (Senande-Rivera et al., 2022) and a continued increase in fire weather conditions (Clarke et al., 2022; Abatzoglou et al., 2019).

Alongside socioeconomic and environmental changes, anthropogenic climate change has also contributed to a rise in extreme fires worldwide (Liu et al., 2022; UNEP, 2022). Wildfires, defined as “unusual or extraordinary free-burning vegetation fires with negative impacts,” have a synergic relationship with climate change in which they are mutually exacerbating: meteorological conditions favourable to wildfires are increasing over many regions of the globe, while wildfires further contribute to climate change by emit-

ting massive amounts of greenhouse gases to the atmosphere and accelerating ecosystem degradation (UNEP, 2022). Wildfires have been shown to be closely linked to extreme fire weather conditions and future projections point to an increase in days conducive to wildfire events by 20% to 50% in many fire-prone landscapes (Bowman et al., 2017). It is also expected that wildfires will become longer and more intense in the future (Quilcaille et al., 2023).

Over the last decades, fires have also been a substantial source of carbon dioxide, releasing 2.2 Pg of carbon per year in the period of 1997 to 2016, representing almost a quarter of global carbon emissions from fossil fuel combustion (van der Werf et al., 2017). Around a fifth of this value is due to deforestation and agricultural practices (van der Werf et al., 2017), estimated to contribute up to 19% of the total increased radiative forcing since pre-industrial times (Bowman et al., 2009). While vegetation fires may see some of the carbon re-captured due to post-fire recovery, permanent deforestation or burning of organic deposits - such as peatlands - are net sources of carbon to the atmosphere (Bowman et al., 2020), further contributing to the previously mentioned feedback mechanism between climate and fires.

Accordingly, anthropogenic activity influences fire over multiple temporal and spatial scales. Considering the fire behaviour and regime triangles (Figure 1.1), humans now directly or indirectly influence all its components by altering the amount, type, and connectivity of fuel, the frequency of ignitions, and disrupting climate patterns. Currently, there are very few environments that are not influenced by anthropogenic fires: around 93% of fire-sensitive ecosystems and 77% of fire-dependent ecosystems worldwide show altered fire regimes where fire is thought to be occurring beyond natural bounds (Hardisty et al., 2005). Changes in historical fire activity threaten biodiversity worldwide, particularly savannas, grasslands, shrublands and forests (Kelly et al., 2020). Moreover, as climate changes and ecological thresholds are crossed, the relative dominance of species will alter, both responding to and driving changes in fire conditions (Gillson et al., 2019).

### **1.3 Fire in Brazilian biomes**

In the global context, Brazil is a major fire hotspot, along with northern Australia, central and southern Africa, and Eurasia (Bowman et al., 2020). Amongst South American

countries, Brazil is by far the largest contributor to the sub-continent’s total fire count, representing around 57% of annual fires (Figure 1.5). Brazil is also the most affected country in terms of total burned areas, with an annual average of 34.5 Mha over the 2001–2019 period, which represents roughly 4% of its territory (Bilbao et al., 2020). Over the last decade, Brazil has experienced unprecedented wildfires (e.g. Libonati et al., 2020; Silveira et al., 2020) with severe impacts on animal populations (e.g. Tomas et al., 2021) and public health (e.g. Machado-Silva et al., 2020).

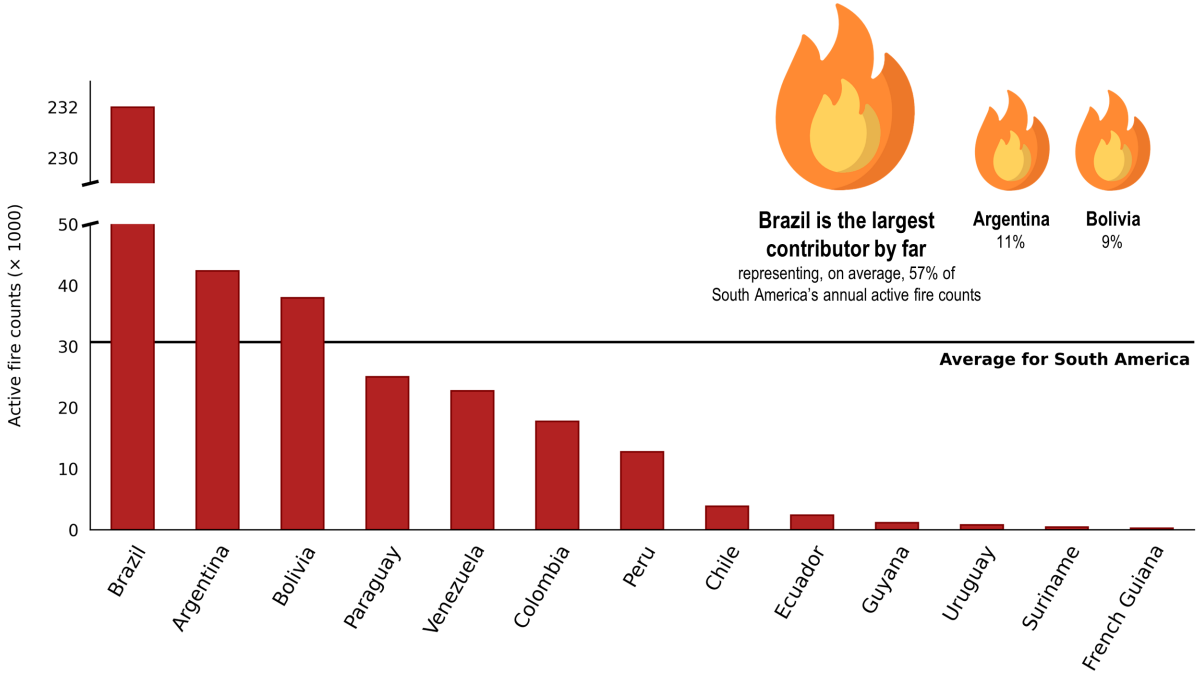


Figure 1.5: Annual average active fire counts as detected by MODIS/AQUA sensor from 2003–2022 per South American country. The average of all countries in South America (SA) is represented in a solid black line. From Silva et al. (in press).

Nevertheless, the impacts of fire in Brazilian ecosystems differ greatly. Brazil is home to several unique ecosystems, including some of the most important phytogeographical domains in South America (Dionizio et al., 2018). There are six Brazilian biomes, as defined by Instituto Brasileiro de Geografia e Estatística (IBGE): the Amazon rainforest; the savannas of Cerrado; the Atlantic Forest; the semi-arid lands of Caatinga; the Pantanal wetlands; and Pampa. These ecosystems have very distinct relationships with fire (Figure 1.6): Cerrado, Pantanal and Pampa are fire-dependent; the Amazon and the Atlantic Forest are fire-sensitive; and Caatinga is fire-independent. Accordingly, the occurrence of fire will have a very different impact and role in each of these ecosystems, and these

differences are to be kept in mind when studying fire activity in Brazil.

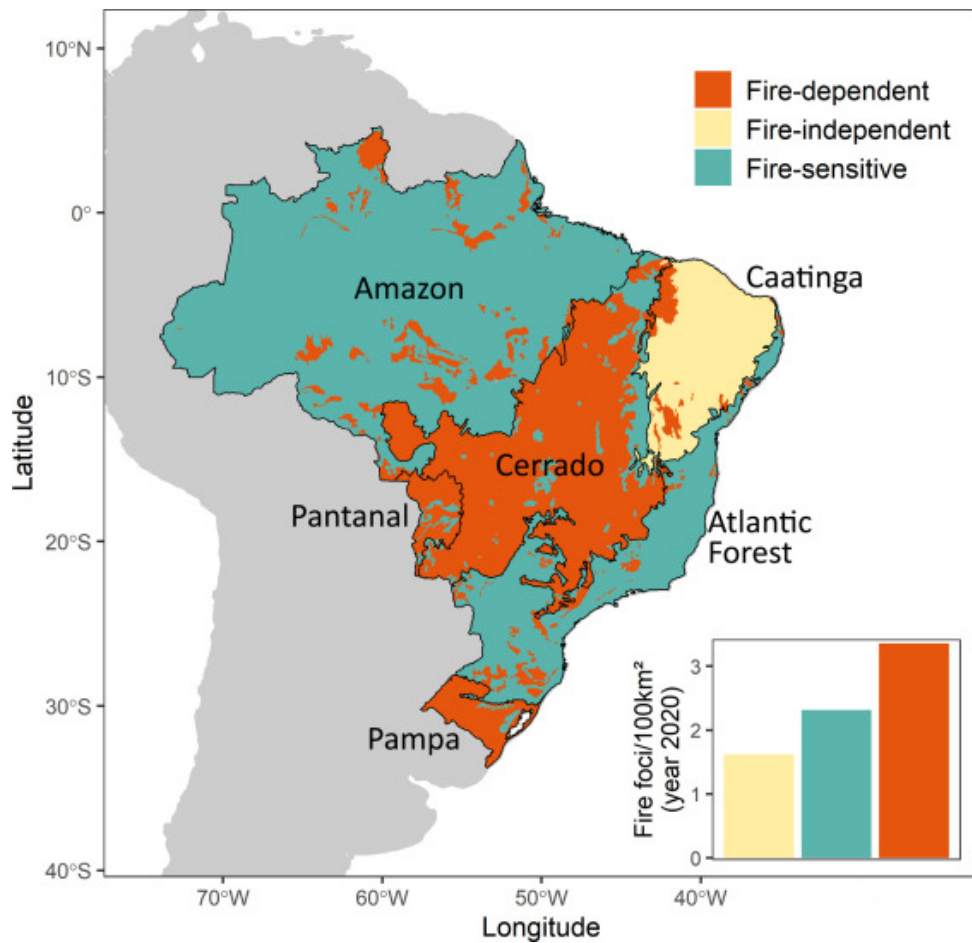


Figure 1.6: Brazilian vegetation types classified as fire-dependent, fire-sensitive and fire-independent, following Hardesty et al. (2005). Open vegetation types (grasslands, open savannas) are classified as fire-dependent; forests (rainforests, seasonal forests, woodland savanna) are classified as fire-sensitive, and xerophytic vegetation is classified as fire-independent. The inlay bars indicate the density of fire foci in 2020 for each fire sensitivity class. From Pivello et al. (2021).

### 1.3.1 Cerrado, the Brazilian savanna

Cerrado is the second largest biome in South America covering around 2 million km<sup>2</sup> in central Brazil (Figure 1.7). Cerrado is a highly heterogeneous landscape with 11 main phytophysiological types (Ribeiro and Walter, 2008): grasslands (campo sujo, campo limpo, campo rupestre); savanna formations (*cerrado sensu stricto*, parque de cerrado, palmeiral, vereda); and forest formations (mata ciliar, mata de galeria, mata seca, cerrado). Cerrado is also the most floristically diverse savanna in the world (Myers et al., 2000; Klink and Machado, 2005) with over 13,137 plant species, on par with the 13,214 plant species reported for the Amazon region (Overbeck et al., 2015). A high degree of



endemism has been observed for plants and animals of Cerrado (Silva and Bates, 2002) with around 4,800 species of plants and vertebrates unique to the biome (Strassburg et al., 2016).



Figure 1.7: A typical Cerrado landscape in Chapada dos Guimarães, Mato Grosso (MT), during the dry season. Photo taken by the author.

Climate in Cerrado is markedly seasonal with an extended dry season from May to September (Pivello, 2011) and, according to the Köppen climate classification, the prevailing climate type is tropical seasonal (Aw) supporting a dry winter and rainy summer (da Silva Junior et al., 2020). However, Cerrado is already showing significant changes from its historical record. Since 1961, maximum and minimum temperatures have increased by 2.2–4.0 °C and 2.4–2.8 °C, respectively, and relative humidity has decreased by about 15% (Hofmann et al., 2021). The MATOPIBA region (the confluence of states Maranhão – MA, Tocantins – TO, Piauí – PI, and Bahia – BA) shows temperature increases at a rate of 0.3 °C per decade since 1981, with a warming rate of 0.45 °C per decade after the turn of the 21<sup>st</sup> century, associated with decreasing rainfall, an increase in dry day frequency, and drought (Marengo et al., 2022).

Additionally, recent studies point to a very degraded biome. Around 46% of Cerrado’s native vegetation cover has been lost and only 19.8% remains undisturbed (Strassburg et al., 2017). Despite falling annual deforestation rates since the 2000s (Lapola et al.,

2014), around 93,000 km<sup>2</sup> of natural vegetation cover have been converted into agricultural lands from 2002 to 2009, an indication that current deforestation rates are still high and increasingly leading to landscape fragmentation and loss of ecosystem function (Overbeck et al., 2015). Southern Cerrado has most of its territory now deprived of native vegetation as a result of historical land conversion into agriculture and pasture lands since the 1960s (Sano et al., 2020). Continuous stretches of intact and undisturbed Cerrado are mostly located within the transitional area between Cerrado and the Amazon, commonly referred to as the Arc of Deforestation (Marques et al., 2020), or within Brazil's latest agricultural frontier, the MATOPIBA. Both these regions have seen high conversion rates over the last few decades and, during 2013–2017, the mean deforestation rate in MATOPIBA was 241% higher than any other region in the biome (Trigueiro et al., 2020). Land conversion in Cerrado is mainly associated with human activities as a result of the dramatic changes in land use promoted by large-scale agriculture (soybean, rice, corn, and cotton monocultures), livestock ranging, and mineral extraction (Overbeck et al., 2015; Klink and Machado, 2005).

Heavily contrasting with its neighbouring biome, the Amazon, less than 7% of Cerrado's present cover is under legal protection (Soares-Filho et al., 2014). Unlike the rainforest, Cerrado does not have a Soy Moratorium (Soterroni et al., 2019), and there is also no well-established and routinized deforestation surveillance program (Lapola et al., 2014). Over the last decades, the ongoing economic development has been at the expense of native cover and associated ecosystem services, including fire, severely disturbing and threatening Cerrado's unique landscapes.

### **1.3.1.1 Fire in Cerrado**

As discussed above, Cerrado is considered a fire-dependent biome (Hardesty et al., 2005), where fire has been a frequent and natural disturbance for millions of years (Mistry, 1998; Simon et al., 2009). Fire is thus a key component in defining the biome's physiognomy and structure, influencing species abundance and diversity (Simon et al., 2009; Simon and Pennington, 2012). Many species from Cerrado grasslands and savannas are fire-resistant, which makes this biome very resilient to fire activity (Pivello, 2011): several plant species have belowground woody organs that promote quick leaf and flower sprout after fire; Cerrado's typical twisted trees and shrubs have developed thick bark layers and fruit walls

that protect their tissues and seeds from high temperatures; and belowground biomass is at least two times higher than aboveground biomass. Fire further contributes to trait variability in plants (Hoffmann et al., 2012a; de L. Dantas et al., 2013) and affects their reproductive success by influencing seed germination and flowering (Fidelis and Blanco, 2014; Fidelis et al., 2022). It modifies competition among trees and herbaceous plants such as grasses, shrubs, and lianas (Dionizio et al., 2018) and affects nutrient cycling (Nardoto et al., 2006). Frequently burned sites in Cerrado tend to become grassy and open, as most trees are killed or maintained in short stature by fire and ash deposition brings nutrients to the surface soil (Pivello, 2011). Consequently, along with rain seasonality and soil features, fire acts as one of the vegetation determinants in Cerrado (Lehmann et al., 2014).

In Cerrado, lightning-induced ignitions primarily occur during the transition period between the rainy and dry seasons (Ramos-Neto and Pivello, 2000; Schumacher et al., 2022), producing low-intensity fires constrained by soil and fuel moisture (Ramos-Neto and Pivello, 2000; Alvarado et al., 2020), that trigger a positive feedback loop by favouring the growth of grass species that is not to the detriment of tree species (Hoffmann et al., 2012a). However, the vast majority of ignitions in the Cerrado are anthropogenic, leading to larger and more intense fires that trigger changes to the floristic composition and community structure of tree-shrub vegetation, favouring fire-resistant species and negatively impacting fire-sensitive species (de Azevedo et al., 2020). Anthropogenic ignitions prevail in the dry season and for a variety of reasons: in areas with native vegetation cover, fire is usually used as an inexpensive tool to clean up deforested or degraded areas (da Silva Junior et al., 2020), whereas in small-scale agricultural areas, fire serves a diversity of purposes, such as the management of species and landscapes, cattle raising upon native or exotic pasturelands, and subsistence agriculture (Schmidt et al., 2007; Eloy et al., 2019).

On par with savannas worldwide (Shlisky et al., 2008; Archibald, 2016), human influence has been disrupting fire regimes in Cerrado. Cerrado is responsible for more than half of Brazil's annual burned areas (Figure 1.8), burning vast areas every year (de Araújo et al., 2012; Bilbao et al., 2020) that mostly affect the native vegetation remnants (Oliveira et al., 2022). Recent estimates show that around 3.4% of the biome burns annually (Alencar et al., 2022), and, alongside the Amazon rainforest, Cerrado has the largest number of fires country-wide (Pivello et al., 2021; da Silva Junior et al., 2020).

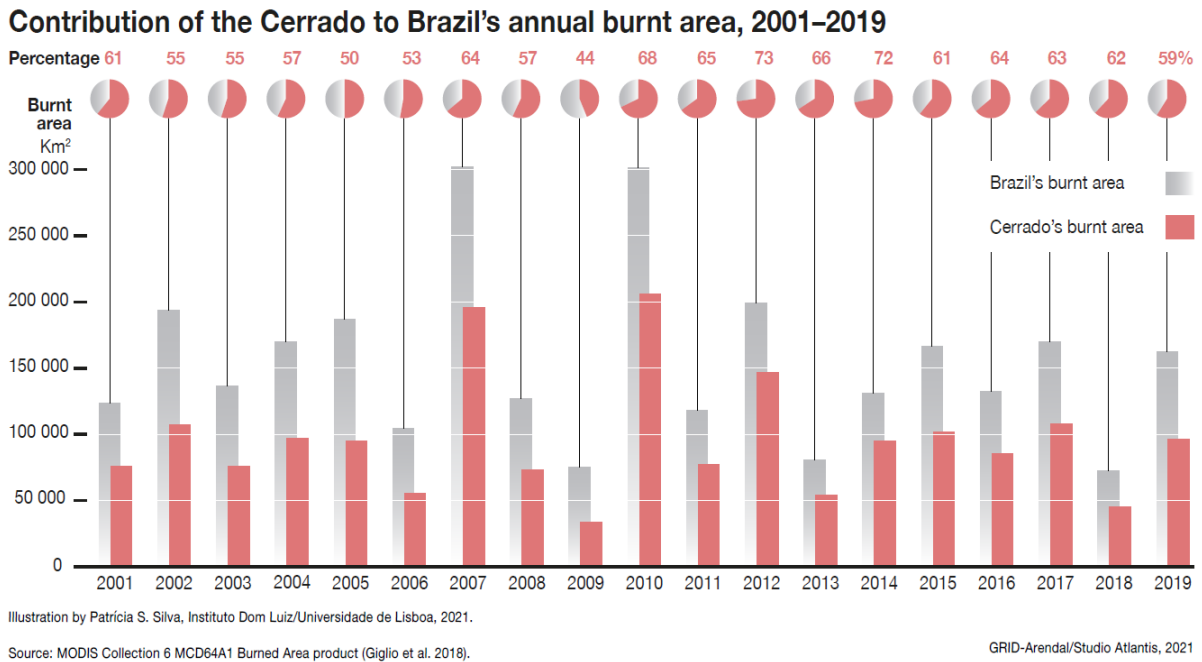


Figure 1.8: The inter-annual variability of burned area in Brazil from 2001–2019 is shown in grey and the corresponding percentage from the Cerrado biome is shown in red. All panels use the MODIS MCD64A1 500 meter product. From UNEP (2022).

Alterations in Cerrado’s historical fire regime severely weakened the biome by limiting regeneration capabilities (Santana et al., 2020; Rosan et al., 2019) and compromise Brazil’s pledges to the Paris Agreement (da Silva Junior et al., 2020). In the period of 1999 to 2018, Cerrado was responsible for emitting more than 2,500 Tg of carbon to the atmosphere, second only to the Amazon, and these rates are not expected to decrease (da Silva Junior et al., 2020). Moreover, a reduction in the biomass of fire-sensitive species may transform Cerrado from a carbon sink into a source of carbon emissions (de Azevedo et al., 2020). According to a study covering the period from 2005 to 2016, ozone emissions have also been rising in Cerrado, reducing air quality and increasing regional health risks (Pope et al., 2020).

### 1.3.2 The Pantanal wetlands

The Pantanal biome covers 179,300 km<sup>2</sup> across Brazil (78%), Bolivia (18%) and Paraguay (4%), and is considered the largest continuous stretch of wetlands in the world (Tomas et al., 2019). In Brazil, Pantanal is located within the states of Mato Grosso (MT; 35%) and Mato Grosso do Sul (MS; 65%).

As the name suggests, Pantanal is a periodically flooded savanna located in the Upper

Paraguay River Basin (UPRB) comprising around 41% of its territory (Junk et al., 2014). Pantanal is characterized by an ever-changing boundary between land and water, where vast areas change seasonally from terrestrial to aquatic systems (Figure 1.9; Alho and Silva, 2012). Its landscape consists of a mosaic of floodable and non-floodable savannas, grasslands, forests, open woodlands, and temporary or permanent aquatic habitats (Tomas et al., 2019). This allows for a high biodiversity (Tomas et al., 2019; Junk et al., 2011), where animals thrive with minimal competition due to a mismatch in the production of food and other ecological resources (Alho and Silva, 2012).



Figure 1.9: A typical Pantanal landscape in the RPPN Sesc Pantanal, Mato Grosso (MT), during the dry season. Photo taken by the author.

Pantanal is highly dependent on the highlands of Cerrado due to its river sources, and the flood pulse in Pantanal is heavily influenced by the Amazon rain regime on the northern Paraguay River and thus spreads from north to south, reaching the southern regions later in the dry season (Guerra et al., 2020; Bergier et al., 2018). The biome has well-defined dry and wet seasons: rainfall occurs in the austral summer (November to March), producing a seasonal flood pulse (Tomas et al., 2019). During summer, concurrent with the rainy season, the rivers overflow their banks and flood the lowlands, inundating around 70% of the floodplain that remains flooded for around 4 to 8 months per year (Marengo et al., 2015). Over the dry season, the Paraguay and Paraná rivers withdraw into their banks,

partially draining the lowlands (Marengo et al., 2015).

However, in par with worldwide trends, the climatic patterns of Pantanal have been changing. Current temperature trends in the biome are four times greater than the average global warming (Libonati et al., 2022a), leading to the increased occurrence of extreme heat events (Marengo et al., 2021a; Libonati et al., 2022a). Precipitation patterns are altered, soil moisture is decreasing (Marques et al., 2021), and drought periods are becoming more frequent, such as the event from 1961/1962 to 1971/1972 (Alho and Silva, 2012), or the historical drought affecting Pantanal since 2019 (Marengo et al., 2021b). Since 1960, there is also a marked increase in the number of days without precipitation, and a decrease in the available surface water during the dry season (Lázaro et al., 2020).

Moreover, Pantanal's landscape has been changing rapidly. The native vegetation of the plateau has been extensively replaced by mechanized agriculture since the 1970s, with a predominance of grain monoculture (soybean, maize, and cotton) and sugarcane for the production of biofuels (Guerra et al., 2020). Much like the Arc of Deforestation, Pantanal also shows an "arc" with an increased probability of native vegetation loss: this arc of vegetation starts on the plateaus of Cerrado and Amazon and continues inwards towards the lowlands of Pantanal, across the transitional areas between biomes and comprising non-flooded areas suitable for agriculture (Guerra et al., 2020). These transitional areas are also those where anthropogenic expansion has been happening in previous years, showing a clear pattern of agricultural expansion into non-flooding areas. The seasonally flooded grasslands of Pantanal are used as pastures for cattle raising, an activity that has been going on for two and a half centuries and represents the main economy in the region (Damasceno-Junior, 2021). There are around 3,000 ranches in the Brazilian Pantanal, but the numbers for Bolivia and Paraguay are not known (Tomas et al., 2019). In Brazil, the states encompassing the UPRB, Mato Grosso do Sul and Mato Grosso, are the main cattle producers in the country (respectively, producing 10% and 14% of the Brazilian herd; Guerra et al., 2020).

Pantanal lacks protective legislation and law formulation is often undermined or weakened given the strong influence of the politically powerful agribusiness sector (Schulz et al., 2019). The Brazilian Pantanal is mostly comprised of private lands, around 93% of its area, and only a very small part is protected (Tomas et al., 2019): strictly protected areas

cover around 14,800 km<sup>2</sup> (5.71% of the biome); and private protected areas cover around 3,046 km<sup>2</sup> (1.7%). In the UPRB there are two UNESCO Biosphere Reserves containing protected and managed areas: the Pantanal Biosphere Reserve in Brazil (UNESCO, 2024b) and the El Chaco Biosphere Reserve in Paraguay (UNESCO, 2024).

### 1.3.2.1 Fire in Pantanal

As pointed out above, Pantanal is considered a fire-dependent biome, where both flood and fire act as ecological filters, and the ecosystem is resilient if their historical patterns do not change (Pivello et al., 2021; de Oliveira et al., 2014). Although the interaction between flood and fire is not yet fully understood, they affect the structure of riparian forests in Pantanal by regulating the abundance and composition of species (de Oliveira et al., 2014; de Sá Arruda et al., 2016). For instance, the occurrence of monodominant vegetation types, such as the “Paratudal”, has been linked to the synergy between flood and fire (Manrique-Pineda et al., 2021; Pott et al., 2011). Species along the riparian forests of Pantanal have developed adaptations to both flood and fire (Junk, 2013), and have been shown to maintain high functional diversity (de Oliveira et al., 2014).

Natural ignitions in the Pantanal occur between the dry and wet seasons, caused by lightning strikes (Pivello et al., 2021). However, a recent study has found that 83.3% of burned areas in Pantanal are caused by humans and that natural-caused fire scars accounted for only 5% of total fire events (Menezes et al., 2022). Fire is used as an inexpensive management tool for cattle raising in natural grasslands and savannas in Pantanal: during the austral winter (which coincides with the dry season) fire is traditionally used to remove dead plant parts and kill pests, control shrubs, and promote resprouting of tough grasses before the rainy season (Alho and Silva, 2012; Damasceno-Junior, 2021). Accordingly, where natural fires used to occur every 3–6 years, anthropogenic fires now increased fire activity by 2–3 fold (Pivello et al., 2021). These anthropogenic fires often start in grasslands, but due to favorable meteorological conditions spread to neighboring savannas and forests (Alho and Silva, 2012).

From 2002 to 2010, Pantanal was the third Brazilian biome with the largest burned areas (around 6%), behind Cerrado (73%) and the Amazon rainforest (14%; de Araújo et al., 2012). In relative terms to its total area, Pantanal has the largest percentage of burned areas over the 2001–2019 period (45%), of which 16.5% are considered wildfires

that mostly occur in native vegetation remnants (Oliveira et al., 2022). Over the last two decades, most fires occurred in grasslands and, while larger fires often occur in grasslands and forests, smaller fires affect mostly croplands (Correa et al., 2022).

In 2020, Pantanal saw one of its most destructive fire seasons to date (Figure 1.10; Libonati et al., 2020). Studies found that the 2020 fires were an interplay of extreme and extraordinary meteorological conditions (Libonati et al., 2022a) and negligent use of fire (Mataveli et al., 2021). Around a third of the biome was burnt (Libonati et al., 2020), and these fires represent a 376% increase compared to the average annual burned area of the last two decades (Garcia et al., 2021). The 2020 forest fires were responsible for almost half of Pantanal's carbon loss in 2020 (Barbosa et al., 2022).



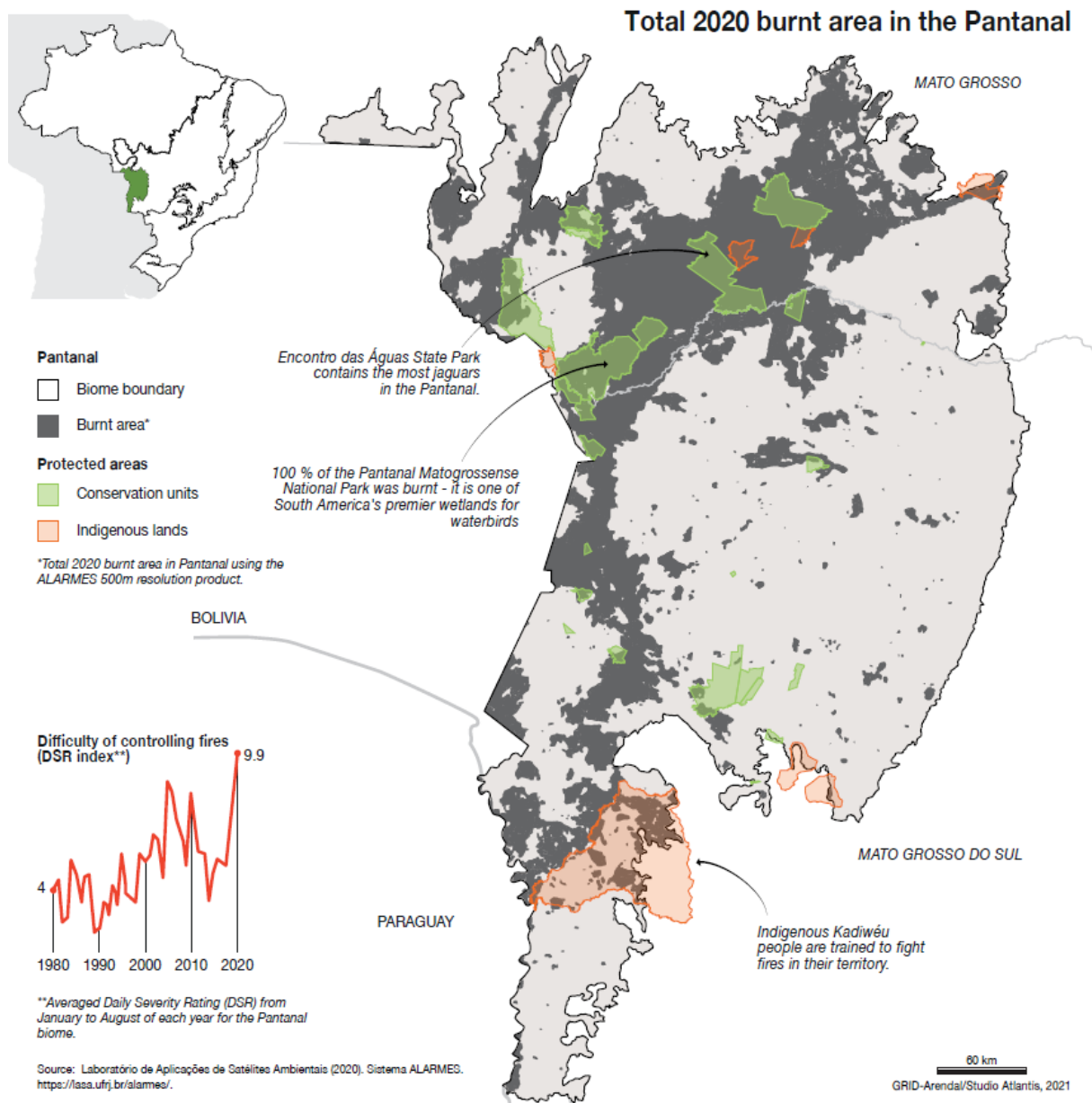


Figure 1.10: Total 2020 burnt area in the Pantanal using the ALARMES 500m resolution product. Conservation units and Indigenous lands are shown in green and orange, respectively. The bottom left graph shows Pantanal's average Daily Severity Rating (DSR) from January to August each year, estimated using the ERA5 reanalysis product (Libonati et al., 2020). DSR is a numeric rating of the difficulty of controlling fires. From UNEP (2022).

## 1.4 Objectives and Thesis Structure

The initially defined purpose of this thesis was to evaluate fire and its drivers within the Brazilian savannas. The main focus was accordingly the Cerrado biome, and the main objectives were:

- to assess regional fire behaviour in the Brazilian Cerrado, considering several com-

ponents of fire activity (such as extent, intensity, and individual fire scars).

- to shed light on the regional climatic and anthropogenic drivers of fire in Cerrado, their interactions and mediating factors.

However, coinciding with the start of my doctoral programme, the summer of 2020 saw a record-breaking fire season break out in the Pantanal. The magnitude and severity of these events prompted the academic community to turn its attention to the region, in an effort to provide much-needed information about its fire regimes and drivers. This was well within the scope of my doctoral research, as I was performing similar analysis for the neighbouring Cerrado biome. As such, part of this thesis also focuses on fire activity in the flooded savannas of Pantanal, and its two other objectives are:

- to evaluate fire occurrence in a protected area of Pantanal severely hit by the 2020 fires, and reflect on associated fire management strategies.
- to study the influence of heatwaves on burned areas in tri-national Pantanal, and provide future outlooks.

The structure of this thesis is as follows:

- **Chapter 1** presents several concepts that will be employed throughout this thesis, highlighting the role of fire as an essential Earth system disturbance, and provides a literature review on fire in Brazilian biomes, focusing on the Cerrado and Pantanal.
- **Chapter 2** addresses the regional diversity in fire behaviour in the Cerrado and completes the biome's ecoregional map with information on regional fire characteristics. It is based on a scientific article published in the *Journal of Environmental Management*.
- **Chapter 3** investigates the regional climatic controls of fire activity within Cerrado's ecoregions. These results are new and have not been published elsewhere.
- **Chapter 4** presents two different studies that evaluated regional fire drivers in Cerrado, including the anthropogenic component.
  - **Section 4.1** showcases the case study of the MATOPIBA region, Brazil's current agricultural frontier. This section is based on a conference proceeding published in *IEEE Xplore*, which was awarded the Third Best Paper award in

the LAGIRS 2020 Student Paper Competition.

- **Section 4.2** employs an individual fire event dataset to further study the regional strength of the fire-climate relationship along anthropogenic geographical gradients for different fire sizes. These results are new and have not been published elsewhere.
- In **Chapter 5** we shift focus from the Cerrado to the Pantanal biome.
  - **Section 5.1** shows the case study of the RPPN Sesc Pantanal, the largest privately held natural reserve in Brazil. This section is based on a scientific article published in Environmental Science and Policy, and the European Geosciences Union (EGU) also awarded the Roland Schlich Travel Grant for this study.
  - **Section 5.2** explores the synergy between fire and heatwaves in Pantanal. It is based on a scientific article published in Journal of Environmental Management, product of the CORDEX Central America and South America Online Paper-Writing Workshop on Regional Climate Modeling.
- Finally, **Chapter 6** concludes the main findings of this thesis and deliverables.



## Chapter 2

# Putting fire in the ecoregional map

*This chapter is based in the following scientific article: Silva, P. S., Nogueira, J., Rodrigues, J. A., Santos, F. L., Pereira, J. M., DaCamara, C. C., Daldegan, G. A., Pereira, A. A., Peres, L. F., Schmidt, I. B., and Libonati, R. (2021). Putting fire on the map of Brazilian savanna ecoregions. Journal of Environmental Management, 296:113098*

The Brazilian savanna (Cerrado) is considered the most floristically diverse savanna in the world, home to more than seven thousand species. The region is a mosaic of savannas, grasslands and forests whose unique biophysical and landscape attributes are on the basis of a recent ecoregional map, paving the way to improved region-based strategies for land management actions. However, as a fire-prone ecosystem, Cerrado owes much of its distribution and ecological properties to the fire regime and contributes to an important parcel of South America burned area. Accordingly, any attempt to use ecoregion geography as a guide for management strategies should take fire into account, as an essential variable. The main aim of this study is to complement the ecoregional map of the Cerrado with information related to the fire component. Using remotely sensed information, we identify patterns and trends of fire frequency, intensity, seasonality, extent and scar size, and combine this information for each ecoregion, relying on a simple classification that summarizes the main fire characteristics over the last two decades. Results show a marked north-south fire activity gradient, with increased contributions from MATOPIBA, the latest agricultural frontier. Five ecoregions alone account for two thirds of yearly burned area. More intense fires are found in the Arc of Deforestation and eastern ecoregions, while ecoregions in MATOPIBA display decreasing fire intensity. An innovative analysis of fire scars stratified by size class shows that infrequent large fires are responsible for the majority of burned area. These large fires display positive trends over many ecoregions, whereas smaller fires, albeit more frequent, have been decreasing in number. The final fire classification scheme shows well defined spatially-aggregated groups, where trends are found to be the key factor to evaluate fire within their regional contexts. Results presented here provide new insights to improve fire management strategies under a changing climate.

## 2.1 Introduction

Fire is recognized as an essential component of the Earth system. Around 40% of the world's land surface, including grasslands, savannas, Mediterranean shrublands and boreal forests, owe their distribution and ecological properties to the fire regime (Bond et al., 2005). In recent decades, many aspects of the natural fire regime, such as frequency, extent and seasonality, have been extensively modified by human activity. Meaningful

advances in Earth observation technology in recent decades have allowed the compilation of long-term fire datasets with reasonable spatial resolution and improved accuracy (Giglio et al., 2016). Newly developed tools and methodologies allow distinguishing individual fire events (Archibald and Roy, 2009; Balch et al., 2020; Oom et al., 2016) based on burn date, and provide accurate information on burning location and duration (Andela et al., 2019), fire shape complexity, orientation and elongation (Laurent et al., 2018; Nogueira et al., 2017b), and other fire characteristics related to fire patch size (Artés et al., 2019; Campagnolo et al., 2019; Hantson et al., 2015).

The Cerrado is the largest contributor to Brazil's annual burned area (BA) (Silva et al., 2019) and represents an important parcel of South America and even global BA (Bowman et al., 2020; Lizundia-Loiola et al., 2020). Recent studies highlight that Cerrado has strong spatial variability in BA (Campagnolo et al., 2021; Rodrigues et al., 2019; Santos et al., 2020), hinting that unique fire patterns may emerge within the biome, based on distinct landscape structure (Magalhães et al., 2020; Song et al., 2018), regional climate (Marinho et al., 2020; Mistry, 1998; Ratter, 1997) and fire policies (Durigan, 2020; Schmidt and Eloy, 2020). Contemporary fire patterns in Cerrado have been well documented based on field records (Alvarado et al., 2017; Coutinho, 1990; Gomes et al., 2018; Stradic et al., 2018; Ramos-Neto and Pivello, 2000; Rissi et al., 2017). However, in situ studies, given their limited geographical range, may present limited potential for biome-wide extrapolation (de Arruda et al., 2018). A remote sensing approach fills this gap and allows the characterization of fire attributes within Cerrado with larger spatial coverage and temporal homogeneity compared to in situ methods (Chuvieco et al., 2008). Using satellite-derived datasets, various studies have striven to characterize fire activity in Cerrado (de Araújo et al., 2012; de Oliveira-Júnior et al., 2021; Mataveli et al., 2018; Rodrigues et al., 2019), allowing an increased understanding of existing fire patterns and behaviour.

A recent study partitioned Cerrado into 19 ecoregions, reflecting the environmental heterogeneity within the biome (Sano et al., 2019). These regions were classified based on physical characteristics (elevation, rainfall, and soil), patterns of human occupation (land use and land cover), and level of biodiversity conservation (conservation units and indigenous lands). The resulting classification allows the analysis of 19 unique ecoregions in terms of biophysical characteristics, protected areas, environmental liability, and priori-

ties for biodiversity conservation, paving the way to improved region-based strategies for land management actions (Figure 2.1). However, this classification did not consider fire activity, an undeniably important feature in Cerrado, as recognized by the authors of that study.

Relying on the most up-to-date satellite-derived datasets of BA, fire size, fire duration and fire intensity for 2001–2019, we mapped fire characteristics for each ecoregion of Cerrado. Fire was characterized by means of seasonal and interannual variability of the fire features, as well as their anomalies, frequency, and trends. Finally, as a guide to management and conservation policies, we produced a new Cerrado fire classification and map, based on BA, fire scar size, and fire intensity.

## **2.2 Data and methods**

### **2.2.1 Study area**

Despite being the most floristically diverse savanna in the world (Klink and Machado, 2005), with less than 3% of its original extent currently under strict protection (Ferreira et al., 2020), Cerrado (Figure 2.1) rarely reaches a high level of attention within the international community, especially when compared to its northern neighbour, the Amazon forest (Colli et al., 2020). The Cerrado is the second largest biome in Brazil, covering around 2 million km<sup>2</sup> (MMA, 2020). It has enormous importance for species conservation and the provision of ecosystem services, spanning three of the largest watersheds in South America and contributing to 43% of Brazil’s surface water outside the Amazon (Strassburg et al., 2017). It is one of the most important global biodiversity hotspots (Klink and Machado, 2005; Overbeck et al., 2015), and relies on fire to shape its vegetation distribution, ecosystem functioning and ensure species survival (Abreu et al., 2017; do Couto de Miranda et al., 2014; Durigan, 2020; Ribeiro and Walter, 1998). It is a mosaic of soil types and topographic settings, resulting in a variety of water dynamics and different plant communities, including fire-resistant open grasslands and savannas, and fire-sensitive riparian forests (Ribeiro and Walter, 1998). As in all savannas, the Cerrado has high intra-annual variability in precipitation (Ratter, 1997), and a well-defined dry season in winter, generally from May to October (de Araújo et al., 2012; Grimm, 2011;



Silva et al., 2019). Here, we define the dry season as lasting from June to October, while May is a transitional month with very little fire activity.

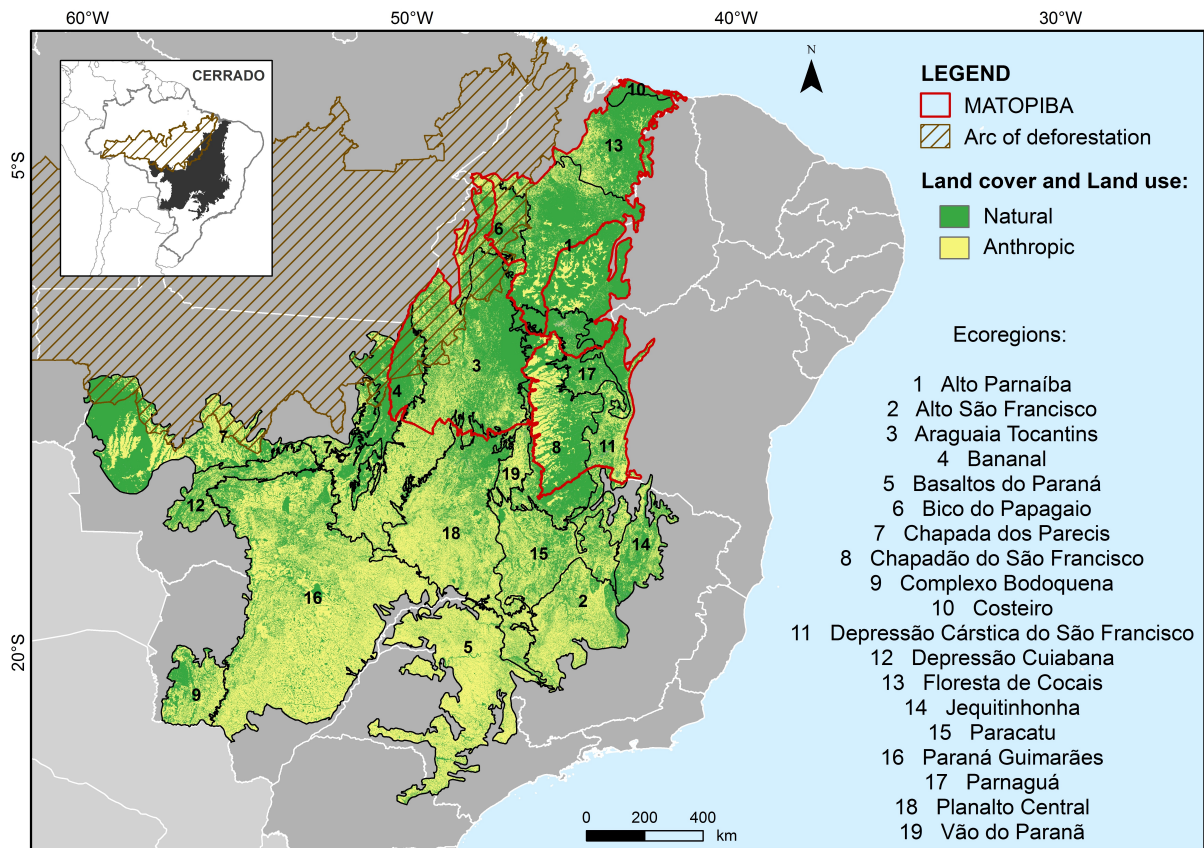


Figure 2.1: Cerrado distribution within Brazil (top left panel) with its 19 ecoregions with their names in alphabetical order. Land cover and land use information from the MapBiomas Collection 5 (MapBiomas, 2020; Souza et al., 2020) is shown for the year 2019. The Cerrado main agrobusiness frontier, MATOPIBA, is delimited in red, whereas the Amazonian Arc of Deforestation is striped brown.

The Cerrado has been severely disrupted, with land conversion occurring mostly since the 1960's in the southern portion of the region. Since the 2010's, the newest agricultural frontier is concentrated in northern Cerrado, particularly in MATOPIBA (Figure 2.1), the territory encompassing the states of Maranhão-MA, Tocantins-TO, Piauí-PI and Bahia-BA (Silva et al., 2020; Trigueiro et al., 2020). Eastern MATOPIBA partly overlaps the Cerrado-Amazon transition region, the so-called Arc of Deforestation (Figure 2.1). Characterized by uncontrolled deforestation and land conversion to industrial agriculture (Marques et al., 2020), the Arc of Deforestation is the world's largest savanna-forest interface.

## 2.2.2 MODIS burned area, individual fire characteristics and fire radiative power products

We used three satellite-derived datasets; the MCD64A1 collection 6 burned area product (Giglio et al., 2018), the Global Fire Atlas database (Andela et al., 2019), and the MCD14ML collection 6 fire radiative power product (Giglio et al., 2016).

Developed by the National Atmospheric Space Agency (NASA), MCD64A1 is a monthly BA product derived from the MODIS (Moderate Resolution Imaging Spectroradiometer) sensors aboard the Terra and Aqua satellites, at 500 m spatial resolution (Giglio et al., 2018). Maps of BA in geographic projection (WGS 1984) covering the period 2001 to 2019 were obtained using the MODIS Reprojection Tool from NASA (Dwyer and Schmidt, 2006) to reproject the adjacent non-overlapping tiles of  $10^\circ$  by  $10^\circ$  (at the equator) with global sinusoidal projection.

The Global Fire Atlas (GFA) is a global fire database derived from MCD64A1 collection 6 that provides individual fire characteristics, such as timing (day of burn) and location of ignition points, fire size ( $\text{km}^2$ ), fire duration (days), daily expansion ( $\text{km}^2.\text{day}^{-1}$ ), fire line length (km) and speed ( $\text{km}.\text{day}^{-1}$ ), and direction of fire spread (Andela et al., 2019). GFA classifies the individual events from daily MODIS data, based on a fire persistence threshold that determines how long a fire may take to spread from one 500 m grid cell into the next and to distinguish individual fires that are adjacent, but that occurred at different times in the same fire season. This threshold is presented as the final and initial date in the product. We obtained gridded 500 m layers over the study region from 2003 to 2018 to estimate fire size and day of burn.

Fire radiative power (FRP) is a measure of the instantaneous release of combustion energy and has been used as an effective estimator of the fire intensity (Laurent et al., 2019; Sperling et al., 2020). We use FRP data derived from NASA's MODIS Aqua + Terra Thermal Anomalies/Fire locations (collection 6) standard quality product (MCD14ML). For 2001 to 2019, we downloaded data in shapefile format from the Fire Information for Resource Management System (FIRMS, 2020). In order to minimize false alarms, only pixels with confidence level above 50%, and of type 0 (presumed vegetation fires) are analysed.

Limitations of the datasets are related to uncertainties associated with satellite-derived fire products. In the Cerrado, uncertainties in the MCD64A1 product are large over the southern portion, consistent with small and fragmented fire scars associated with pasture and croplands, whereas uncertainties in the north are generally small due to the predominance of larger fires patches (Campagnolo et al., 2021; Rodrigues et al., 2019). Moreover, the GFA database considers individual fire events greater than 21 ha, the minimum fire size detected by MODIS sensors (Giglio et al., 2018) limiting the estimates of fire size smaller than this threshold. However, the advantage of MODIS data for mapping individual fire sizes is the daily temporal resolution, since the 16-day Landsat return interval is often not enough to individualize scars with separate ignitions that eventually coalesce into a single, large BA. This is a very common situation in savanna and grassland landscapes (Andela et al., 2019; Sá et al., 2003). Finally, the MODIS FRP product is limited by detection above the threshold of 9–11 MW (Schroeder et al., 2010). However, very low FRP occurs mainly away from the diurnal peak of fire activity in Cerrado (between 15 and 18 hours local time) (Giglio, 2007), thus the effect of MODIS FRP detection limit on the assessment of total landscape-scale FRP is negligible (Sperling et al., 2020).

### 2.2.3 Statistical analysis

We considered the total accumulated monthly and annual BA ( $\text{km}^2$ ) for each of the 19 ecoregions (Figure 2.1). Following the approach of Sousa et al. (2015), we also estimated the monthly Normalized Burned Area (NBA) for each ecoregion, defined as the ratio between the total amount of BA ( $\text{km}^2$ ) in each ecoregion and its respective total area ( $\text{km}^2$ ) (Table 2.1, 2<sup>nd</sup> column). We also evaluated interannual BA variability, using standardized anomalies based on the reference 19-year period (from 2001 to 2019). Based on previous works (Pereira et al., 2017; Santos et al., 2020), single fire events from GFA were categorized into four classes according to fire scar size: I (0.21–1  $\text{km}^2$ ), II (1–10  $\text{km}^2$ ), III (10–50  $\text{km}^2$ ), and IV (> 50  $\text{km}^2$ ). For each class of scar size, we calculated the respective total number of fire events (N scars), BA ( $\text{km}^2$ ), and the distribution of the burn day (day of year) of each individual fire event.

We also analysed interannual trends in BA, fire intensity and fire size through slopes of linear regression for the study period. Given the short length of the time series, slopes

were estimated using the Theil-Sen robust regression (Sen, 1968; Theil, 1950), and trend significance was assessed with the two-tailed Mann-Kendall non-parametric test (Gilbert, 1987; Kendall, 1975; Mann, 1945).

## 2.2.4 Evaluating fire patterns by ecoregion

For each of the 19 ecoregions, we evaluated satellite-derived historical fire data to identify similar fire patterns among ecoregions, considering the characteristics of the BA, fire intensity and fire size. We stratified the NBA and FRP values according to percentiles 25 (p25) and 75 (p75) for ecoregion's annual averages over the 2001–2019 period. Then, for each ecoregion, the BA totals for each scar size class were aggregated, and the size class with the largest contribution was chosen as the main contributor to the ecoregion's total BA.

Results from the above-described stratification were then represented by letters, leading to a 3-letter combination coding each ecoregion characteristics in terms of burned area (NBA), fire scar size, and fire intensity (FRP), respectively. The first uppercase letter distinguishes among ecoregions of low (L, < p25), moderate (M, between p25 and p75), and high (H, > p75) BA. The second lowercase letter indicates the scar type that most contributed to the total BA: small scars (s, 0.21–10 km<sup>2</sup>) and big scars (b, > 10 km<sup>2</sup>). The third lowercase letter denotes fire intensity characteristics, namely low (l, < p25), moderate (m, between p25 and p75) and high (h, > p75). Finally, positive (+) or negative (-) signs are added to indicate increasing and decreasing trends of BA over the 2001–2019 period, as estimated from the MCD64A1 product. A schematic description of the classification is provided in Supplementary Material: Table 2.2.

## 2.3 Results

### 2.3.1 Burned area patterns

Four ecoregions burn, on average, more than 8% of their area each year (Figure 2.2a). In particular, the yearly BA in Bananal is twice that of the remaining ecoregions, with at least 24% of its area burning annually (equivalent to 16,114 km<sup>2</sup> per year), mostly during the dry season (23.4%). The highest five out of 19 ecoregions account for, on average,

67.4% of yearly BA in Cerrado, which translates to 81,522 km<sup>2</sup> per year (Figure 2.2b). Conversely, the lowest five ecoregions just account for 2.7% of the yearly BA on average, about 3,305 km<sup>2</sup> per year. Spatial patterns of average yearly contributions to the total BA in Cerrado (Figure 2.2b) show higher yearly contributions in the central-northern region and lower values in the south. Accordingly, ecoregions with BA classified as high (i.e. > p75, with NBA > 8%) are located in central and northern Cerrado, those classified with BA as low (i.e. < p25, with NBA < 2.3%) concentrate in the eastern and south-eastern Cerrado, and the remaining ecoregions, classified as moderate, occur mostly in the southern part (Supplementary Material: Figure 2.11a). There is a marked spatial contrast in central-eastern Cerrado, where several ecoregions with high BA occur side by side with others with BA classified as low.

The dry season (June to October) accounts for more than 90% of the annual BA in all ecoregions in 2001–2019 (Figure 2.2a), except Chapadão do São Francisco (89.6%), Costeiro (85.9%), Jequitinhonha (85.2%), Paraná Guimarães (85.1%), Basaltos do Paraná (82.3%), Chapada dos Parecis (78.2%) and Floresta de Cocais (73.6%). The months of August to October account for at least 64% of the BA, but six ecoregions (Alto de São Francisco, Paracatu, Complexo Bodoquena, Paraná Guimarães, Jequitinhonha and Depressão Cárstica de São Francisco) show an even shorter window with most fire activity occurring within a 2-month period (Figure 2.2c). The case of Alto Parnaíba is worth noting since, although 90.2% of the BA occurs during the dry season, there is a secondary peak in March (Figure 2.2c). A similar pattern is observed in Chapada dos Parecis, where BA is also recorded earlier in the year, from February to March.

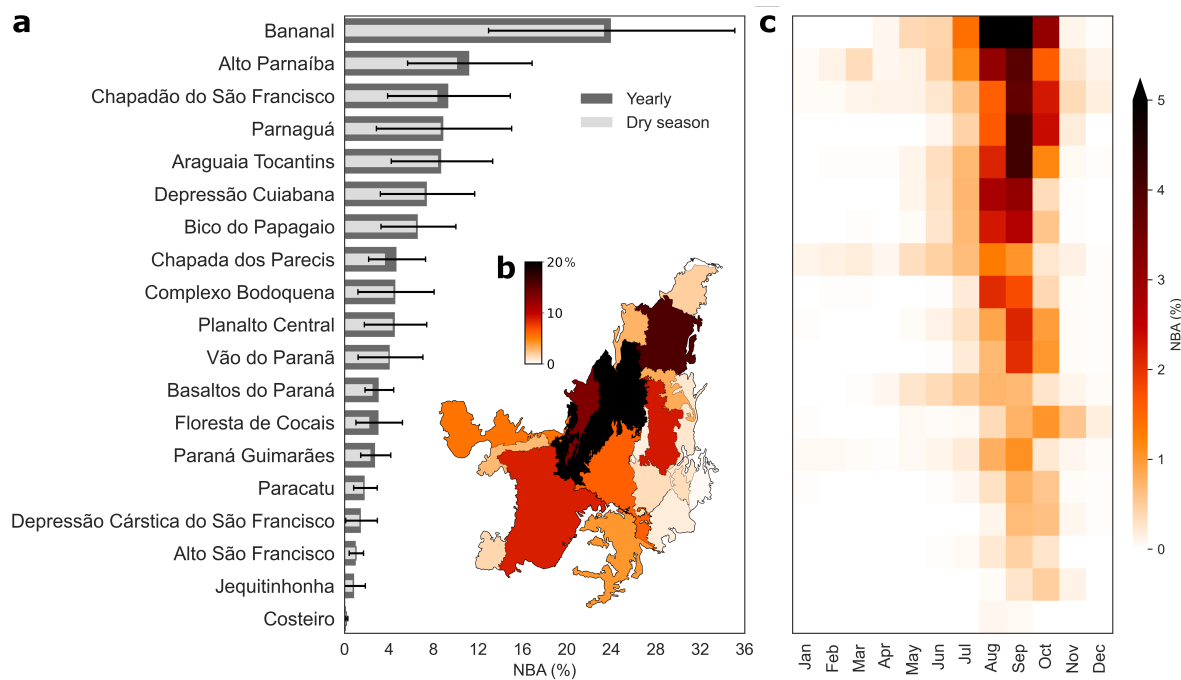


Figure 2.2: a) Average normalized burned area (NBA) per year (dark grey bars) and dry season (light grey bars, representing months from June to October), with correspondent annual NBA variance (black whiskers); b) Ecoregion yearly contribution (%) to Cerrado's total BA during the 2001–2019 period; c) Heatmap of average monthly normalized burned area (NBA, %).

In 2001–2019 (Figure 2.3), most ecoregions display positive BA anomalies in 2007 and 2010 (18 and 14 ecoregions, respectively). The former was the most severe fire year for the biome, and only Costeiro did not show a positive anomaly, consistent with very low annual BA. Although not as widespread as in 2007, 2010 shows comparatively high anomaly values in the western Cerrado and recorded the highest anomaly in Paraná Guimarães. The year 2012 displays high positive anomalies in the ecoregions that encompass MATOPIBA. Conversely, many ecoregions show negative anomalies in 2009 and 2018 (11 ecoregions in both years), mostly over the central Cerrado.

Burned area trends show an overall decrease in most ecoregions (Supplementary Material: Figure 2.9a), significant at the 5% level for Basaltos do Paraná, Chapada dos Parecis, Depressão Cuiabana and Costeiro. All ecoregions in the Arc of Deforestation display non-significant negative trends, except for Bananal and Floresta de Cocais, with non-significant positive trends, which were also found in Planalto Central and Alto Parnaíba.

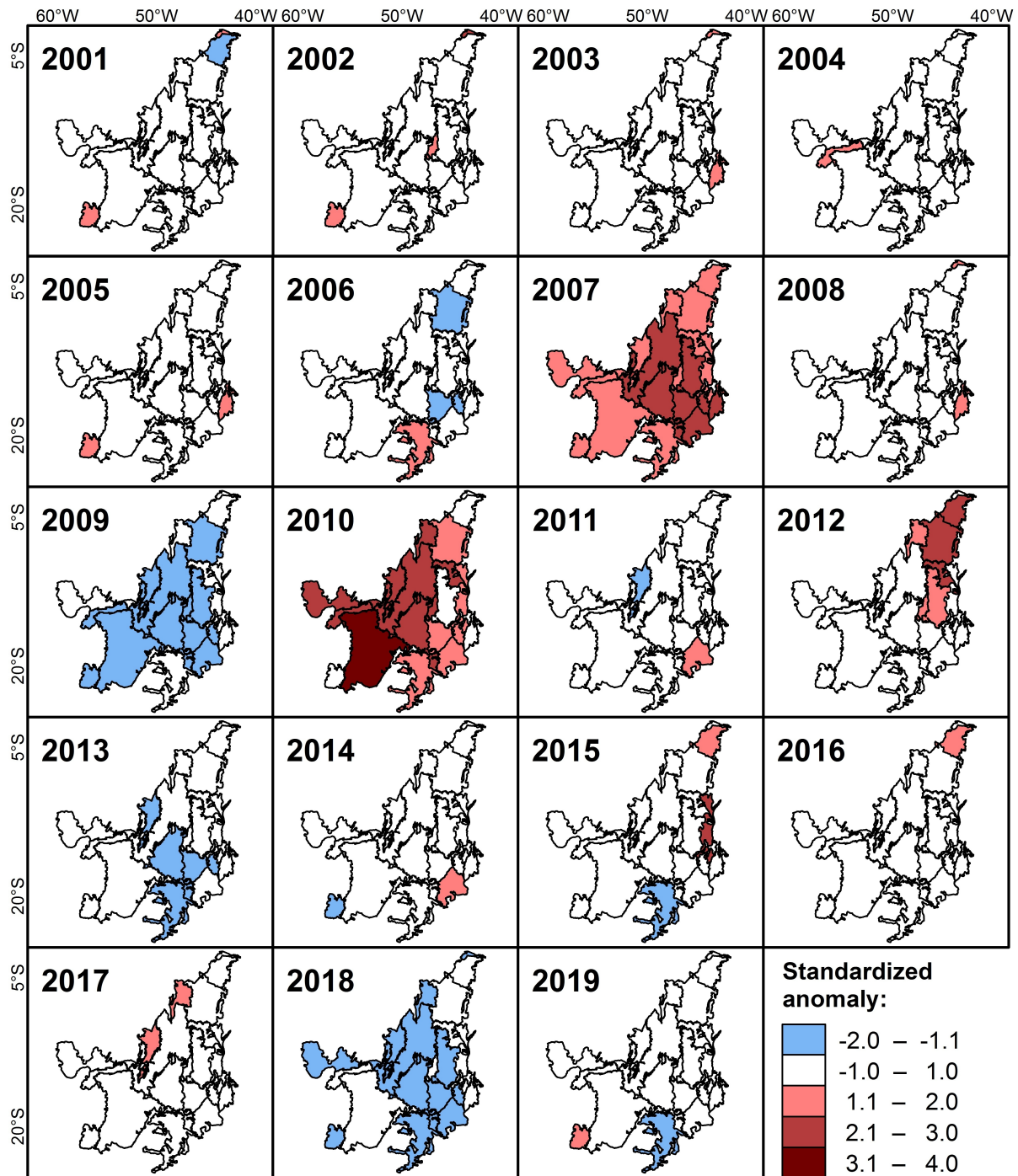


Figure 2.3: Standardized anomaly of BA in each ecoregion of Cerrado from 2001 to 2019.

### 2.3.2 Fire intensity

Ecoregions present large spatial heterogeneity in fire intensity (Figure 2.4). The five regions classified with high fire intensity (i.e.  $> p_{75}$ , with FRP  $> 63.7$  MW) border other biomes, with Chapadão do São Francisco, Parnaaguá and Depressão Cárstica do São Francisco being located in the border with the Caatinga biome, and Chapada dos

Parecis and Bananal in the border with Amazonia (Figure 2.4a, Supplementary Material: Figure 2.11c). Chapada dos Parecis recorded the maximum value of fire intensity in a single event, reaching 11,334 MW in September 2003. Conversely, ecoregions with low fire intensity (i.e. < p25, with FRP < 42 MW) occur in Alto São Francisco, Planalto Central, Vão do Paranã, Costeiro, and Complexo Bodoquena (Figure 2.4a). The heavy tails in FRP distributions in most regions show that a great majority of fires are predominantly of low intensity.

Most ecoregions show marked seasonality in fire intensity (Figure 2.4b), with higher values towards the end of the dry season (in September and October). Alto Parnaíba and Chapada dos Parecis recorded BA values at the beginning of the year, which were not detected as active fires by the FRP product, suggesting that those relatively large BA correspond to fires with very low intensity.

Fire intensity trends show significant increase over Basaltos do Paraná, Paracatu, Paraná Guimarães and Planalto Central (Supplementary Material: Figure 2.9b). Northern ecoregions (Alto Parnaíba, Costeiro and Floresta de Cocais) show a decreasing FRP over 2001–2019. Interannual variability (Supplementary Material: Figure 2.10) displays a peak in total annual FRP in 2007 and 2010 for many ecoregions, namely Araguaia Tocantins and Bananal, further confirming the two years as extremely severe for these ecoregions. Yearly FRP values closely track those of BA, with very high coefficients of determination ( $R^2 > 0.8$ ) in the vast majority (14) of ecoregions.



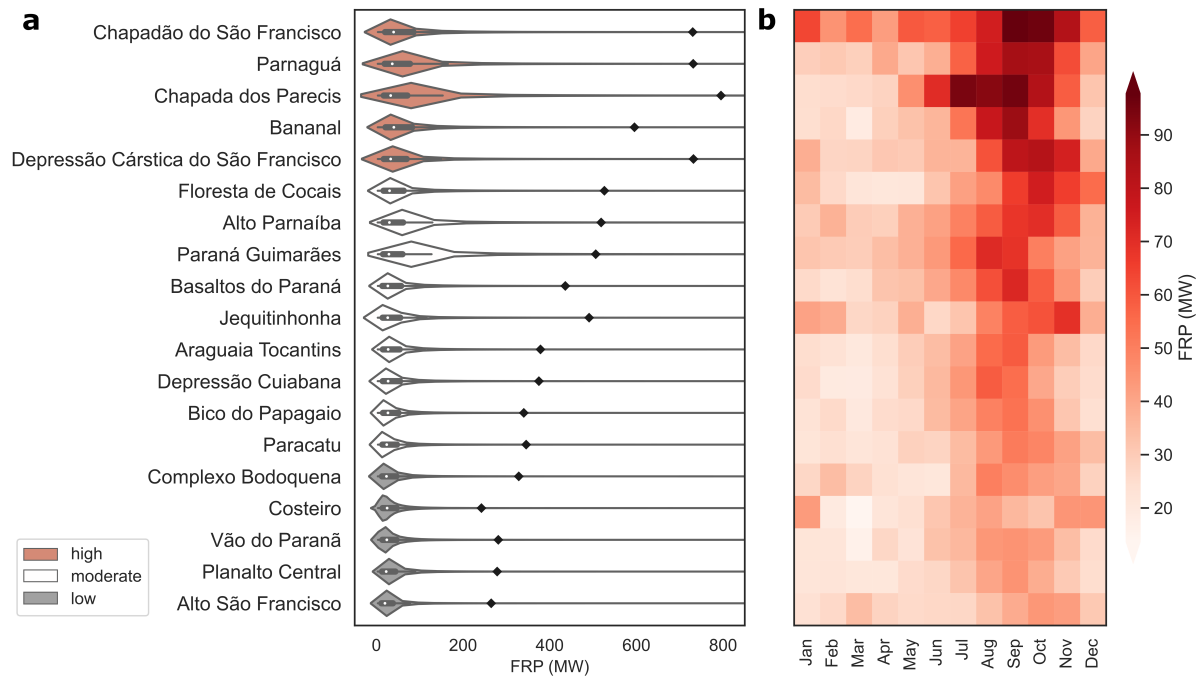


Figure 2.4: a) Fire Radiative Power (FRP values in MW) per ecoregion for the 2001–2019 period; colours represent the fire intensity classes (low: < 42 MW; moderate: 42–64 MW; and high: > 64 MW) and black diamonds the 99<sup>th</sup> percentile of the FRP distribution. b) Monthly means of FRP values (MW) averaged over 2001–2019 for each ecoregion.

### 2.3.3 Fire size patterns

Big scars (> 10 km<sup>2</sup>) occur mainly in northern ecoregions (Figure 2.5) and represent 20% (class III) and 10% (class IV) of the total number of fire scars, respectively. Although infrequent, they account for almost 90% of the total BA in the Cerrado. Conversely, small scars (< 10 km<sup>2</sup>) are very common over the biome, and are much more evenly spread out over most ecoregions (Figure 2.5); however their contribution to the biome total BA is small (10%).

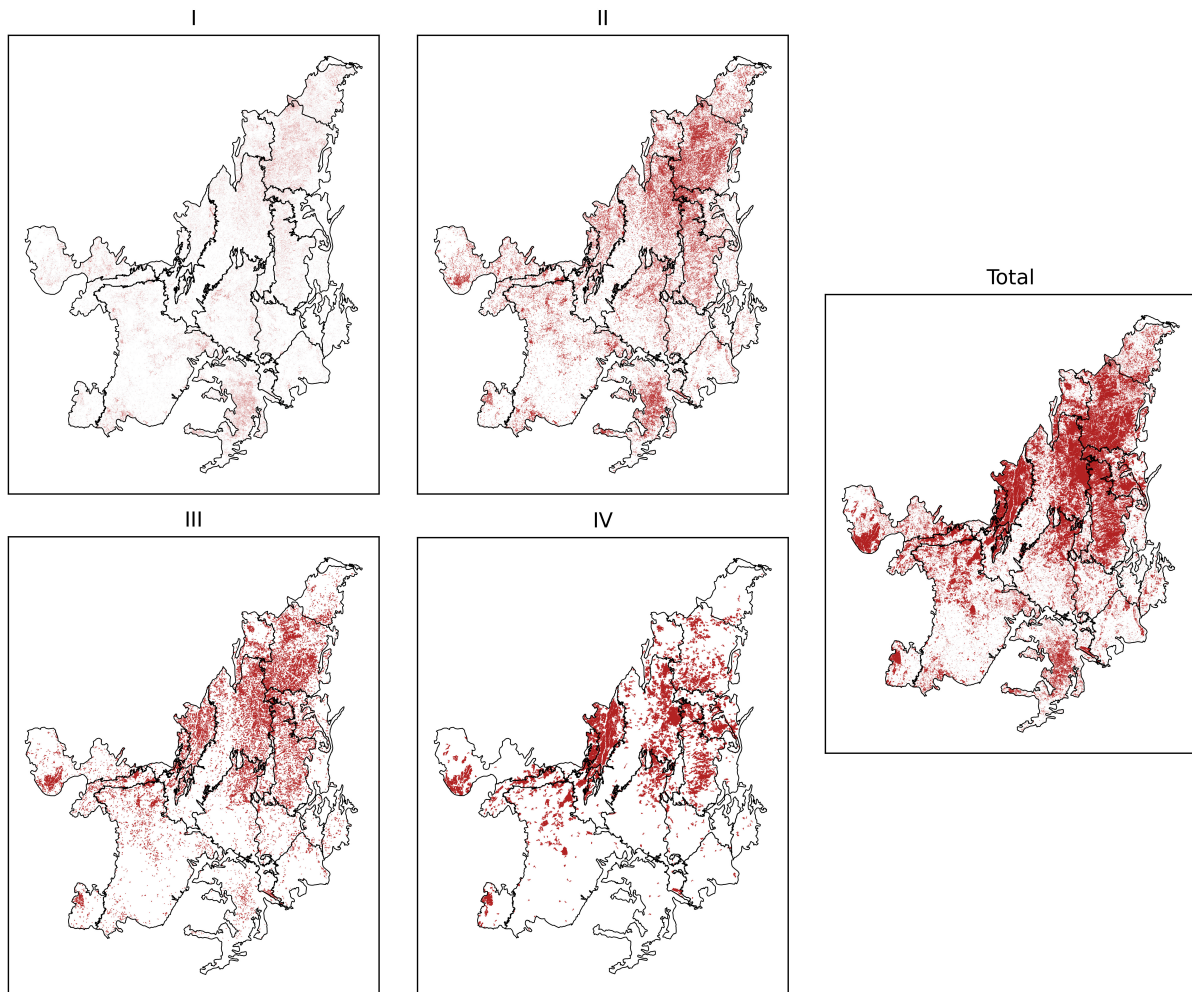


Figure 2.5: Spatial distribution of fire size classes (I: 0.21–1 km<sup>2</sup>; II: 1–10 km<sup>2</sup>; III: 10–50 km<sup>2</sup> and IV: > 50 km<sup>2</sup>) and all classes (Total), derived from GFA over the period of 2003–2018.

All ecoregions show that more than 80% of their scars belong to the small class (Figure 2.6). At least half of the total BA in ecoregions results from big scars. The exceptions are Floresta dos Cocais, Basaltos do Paraná and Costeiro that, along with Alto São Francisco, show a higher frequency of small scars that have a larger contribution to their total BA. By contrast, class IV scars represent more than 50% of the total BA in Araguaia Tocantins, Depressão Cuiabana, Complexo Bodoquena, Bananal and Depressão Cárstica do São Francisco. These regions burn extensively every year (Figure 2.2a), suggesting that a very small number of big events is responsible for most of the Cerrado BA, a typical pattern for fire-prone environments (Campagnolo et al., 2021; Oom et al., 2016). The biggest disparity was found in Bananal, where 7% of the class IV scars account for 70% of its total BA. In turn, Basaltos do Paraná, Planalto Central and Chapada dos Parecis have many scars, but contribute much less to the total BA in the Cerrado.



Figure 2.6: Frequency (%) of the number of fire scars (bottom bars) and the corresponding total BA (top bars) over the 2003–2018 period according to fire size class (I: 0.21–1 km<sup>2</sup>; II: 1–10 km<sup>2</sup>; III: 10–50 km<sup>2</sup> and IV: > 50 km<sup>2</sup>).

There are considerable differences in fire seasonality when evaluating by fire size (Figure 2.7). Overall, during the study period most fires occur in the dry season, and infrequent big fires show much less scattering than the remaining classes, concentrating mostly in August and September. Fires in classes I, II and III start to occur before the start of the dry season. This is particularly pronounced in Chapada dos Parecis, Basaltos do Paraná and, to a lesser extent, in Paraná Guimarães, where there is a marked contrast between large scars and the remaining size classes. In many ecoregions (Alto Parnaíba, Chapada dos Parecis, Chapadão do São Francisco, Depressão Cárstica do São Francisco, Floresta de Cocais, Paraná Guimarães and Planalto Central) small fires keep occurring after the end of the dry season.

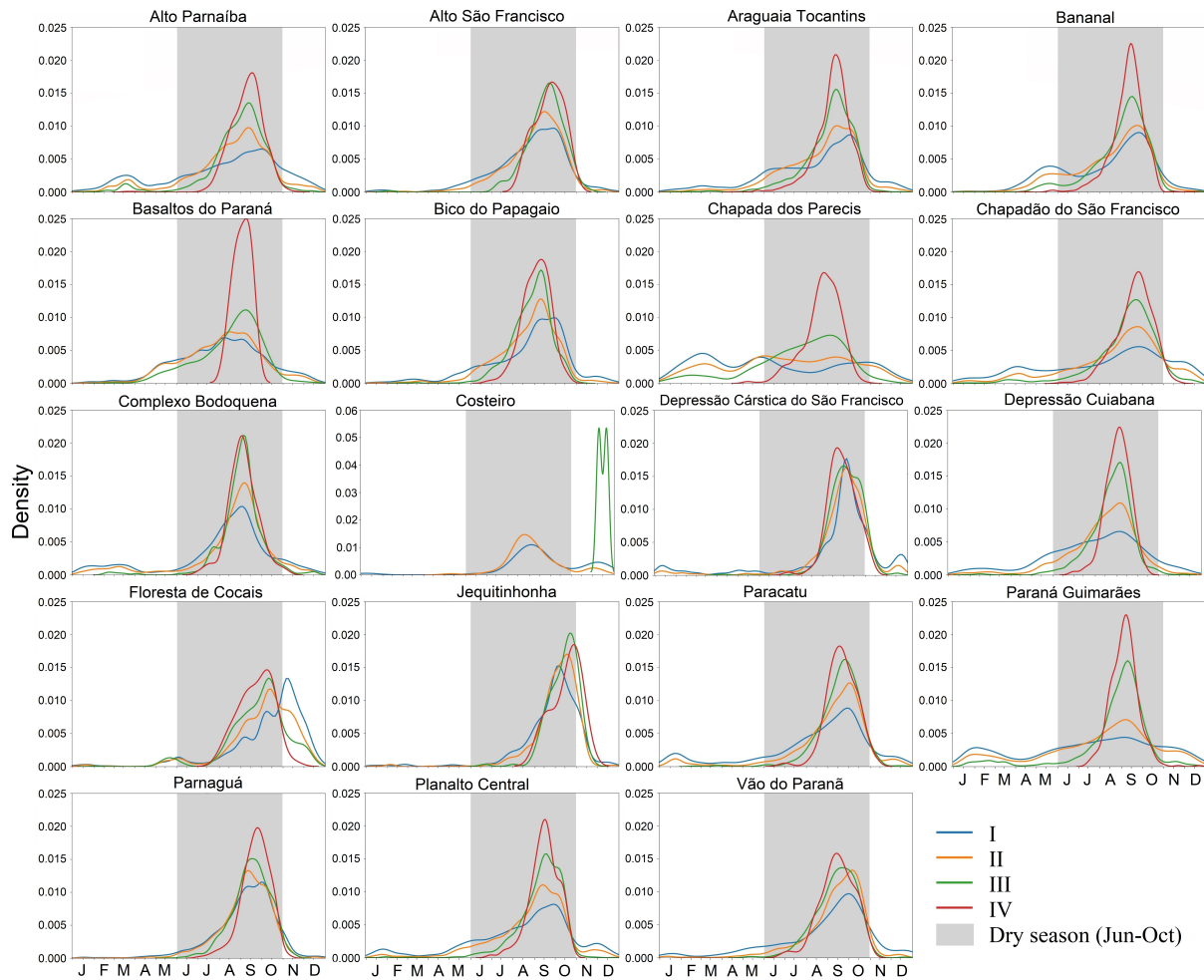


Figure 2.7: Distribution of burn date (in julian day) according to fire size class (I: 0.21–1 km<sup>2</sup>; II: 1–10 km<sup>2</sup>; III: 10–50 km<sup>2</sup> and IV: > 50 km<sup>2</sup>) for each ecoregion, considering the period from 2003 to 2018. Dry season between June and October is shaded in grey.

When stratified by scar size (Supplementary Material: Figure 2.9c-f), NBA rates of change and spatial patterns of trends deviate markedly from the total NBA (Figure 2.9a). Annual NBA trends of class I fire patches show that almost all ecoregions display a decreasing rate, except for Complexo da Bodoquena. Class II fires show significant negative trends in Basaltos do Paraná, Chapada dos Parecís, Chapadão do São Francisco, Costeiro and Jequitinhonha. In turn, classes III and IV fire trends are positive over the central and north-western ecoregions, albeit non-significant. The most pronounced increase in NBA for class IV fire patches is seen over the Bananal ecoregion, while the highest positive rates of change for class III patches occur in Alto Parnaíba.

### 2.3.4 Putting fire on the ecoregional map

As described in Methods, the ecoregions were classified according to characteristics in the BA (Low, Moderate, High), fire size scar (small and big), and fire intensity (low, moderate, high). As shown in Figure 2.8 and described in Supplementary Material: Table 2.2, when the different characteristics were assigned to the ecoregions, we obtained the following nine fire classes: Hbh, Hbm, Msm, Mbh, Mbm, Mbl, Lbh, Lbm, and Lsl.

Results show well-defined groups of similar fire characteristics over Cerrado (Figure 2.8). Ecoregions classified as Hbh and Hbm are spatially aggregated over central-northern Cerrado. However, these ecoregions present distinct BA trends: although classified as Hbm, Alto Parnaíba and Araguaia Tocantins show opposite trends; and a similar contrast is observed in ecoregions classified as Hbh with Bananal presenting a positive trend and negative trends being displayed by Chapadão do São Francisco and Parnaguá. The contrast of Depressão Cárstica do São Francisco, the only ecoregion classified as Lbh, with the neighbouring Hbh ecoregions is worth being noted in what respects to BA even though they share similar characteristics in scar size and fire intensity. Ecoregions with low BA (Lbh, Lbm and Lsl) are also spatially aggregated in eastern Cerrado. The same does not happen with ecoregions of medium BA (Msm, Mbh, Mbm and Mbl), with patches spreading mostly over southern and south-western Cerrado and two ecoregions located in the northern part.

### **Burned area**

H: High  
M: Moderate  
L: Low

### **Fire scar size**

b: big  
s: small

### **Fire intensity**

h: high  
m: moderate  
l: low

### **Burned area trend**

+: positive  
-: negative

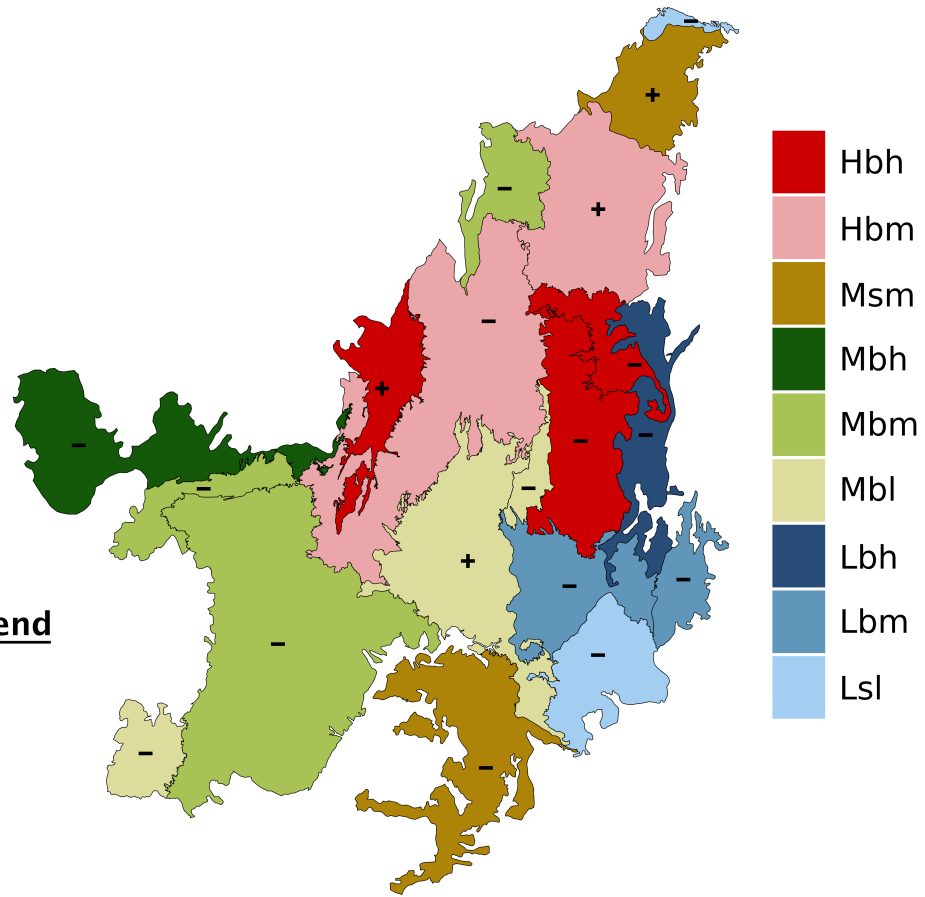


Figure 2.8: Cerrado ecoregional map updated with main fire characteristics in each ecoregion. Spatial distributions of each fire characteristic are illustrated in Supplementary Material: Figure 2.11. A description of each fire class (represented in the colour bar) is provided in the Supplementary Material: Table 2.2. Plus and minus signs denote respectively, increasing and decreasing BA trends during the 2001–2019 period.

## **2.4 Discussion**

### **2.4.1 Understanding the patterns of fire variability**

The spatial heterogeneity of fire patterns within the Cerrado translate into considerable regional disparities in BA, fire intensity and distribution of fire size classes. Other parameters, such as fire seasonality, are consistent throughout the biome. The vast majority of ecoregions show increased fire activity and intensity from June to October, covering the Cerrado dry season (de Araújo et al., 2012; Silva et al., 2019). Although ignitions by lightning take place mainly at the transition between rainy and dry season (Ramos-Neto and Pivello, 2000), most ignitions are anthropogenic and fire is used mainly during the dry season for a variety of reasons, such as the management of species (Schmidt et al., 2007)

and landscapes, cattle raising upon native or exotic pasturelands, subsistence and industrial agriculture (Eloy et al., 2019). The annual cycle of fire intensity is controlled by fuel availability (Oliveira et al., 2015; Wooster et al., 2005). In Cerrado, the growing period preceding the dry season tends to modulate the fire activity by affecting the accumulation of fine fuels (Krawchuk and Moritz, 2011) and, especially, fuel moisture (Nogueira et al., 2017a; Alvarado et al., 2020), which are also influenced by the hydrological regime, fire return interval and extent of area burned (Oliveira et al., 2021). Rate of fire spread is limited by high fuel moisture in the rainy season and early-dry season, and therefore fire intensity is low and fire size is small. Throughout the dry season, the fuel becomes drier and more intense fires potentially will spread more widely, depending on the landscape fragmentation level (Pyne et al., 1996). This explains the marked peak in fire intensity at the end of the dry season, in September and October, which extend into November. High FRP values towards the end of the dry season are consistent with a significant increase in fuel curing, leading to higher fire intensity, extent and severity in open savannas (Rissi et al., 2017; Rodrigues et al., 2021; dos Santos et al., 2021). These late dry season wildfires commonly affect fire-sensitive vegetation, such as riparian forests, with high severity and negative impacts (Flores et al., 2020). However, the relationship between fire size and FRP in savannas and grasslands is complex, depending on the spatial fuel continuity, fuel load, fire season and moisture content (Laurent et al., 2019). Most active fires display low intensity, regardless of land cover and use and, therefore, location parameters of the FRP distribution, such as the mean or the median, are not adequate to characterize the different fire intensity distributions, differences only becoming apparent in the high quantiles (Hernandez et al., 2015; Luo et al., 2017; Oliveira et al., 2015), which better reflect heterogeneity in land use and land cover, landscape fragmentation, and land management across ecoregions (Libonati et al., 2021). In addition, when evaluating the distribution of burn dates by fire scar size (Figure 2.7), significant differences in seasonal cycles emerge between those classified as big (classes III and IV) and small (classes I and II) scars. Big scars (namely, class IV) have a narrow window of occurrence when compared to that of small scars, more evenly spread out during the year, in many cases preceding or continuing after the dry season. This behaviour is consistent throughout ecoregions and entails that major fire events in Cerrado are fairly concentrated in a 2–3 month period within the dry season.

Fire activity in Cerrado also displays marked interannual variability associated with large-scale patterns of atmospheric variability. As the year with most extensive burning in the biome over the last two decades, 2007 is characterized by a severe drought induced by a La Niña event (de Araújo et al., 2012). In 2010, a strong positive phase of the Atlantic Multidecadal Oscillation (AMO) induced record drought conditions over the eastern and southern Amazonia, and adjacent western Cerrado ecoregions (Andreoli et al., 2017) that reflected in high values of BA in almost all ecoregions. The extensive burning in 2012 in north-eastern ecoregions (Silva et al., 2020) is also in line with an extreme drought (Cunha et al., 2019; Jimenez et al., 2019; Marengo et al., 2013) which may have been aggravated by increased deforestation rates and incentives for land conversion resulting from changes to the Brazilian Forest Code that also took place in this year (federal law 12.651/2012). Conversely, the negative anomalies of BA in 2009 are associated to severe flooding, which occurred in western and central Amazonia and the adjacent Cerrado (Marengo et al., 2012), and the global BA minimum since 1997 that was recorded in 2018 (Blunden and Arndt, 2019) relates to the wet conditions induced by the weak La Niña/neutral pattern early in the year. However, years such as these, marked by increased precipitation and flood events, lead to higher biomass production and thus to a higher availability of fuel to burn in the following years (Schmidt and Eloy, 2020).

Large BA totals are found in parts of MATOPIBA, where most of the Cerrado native vegetation remains. This region has been experiencing high rates of deforestation and land conversion to agriculture and pasture (Spera et al., 2016), in which fire is widely used as an inexpensive and effective tool (Reddington et al., 2015; Zalles et al., 2019). Currently, 48% of Brazil's total soybean production comes from the Cerrado, and almost a quarter of this production area is located in MATOPIBA, mainly in the plateaus of the Chapadão do São Francisco and Alto Parnaíba (Santos et al., 2020). Unlike in Amazon where the Soy Moratorium between producers and the government prohibits the buying of soybean grown on recently deforested lands (Soterroni et al., 2019), the last undisturbed remnants of MATOPIBA are not protected by a consistent agreement but are indeed the target of governmental incentives for deforestation (Pitta and Vega, 2017). Within the study period, around 10% of the area of these two ecoregions burned annually (Figure 2.2a) and an increase in fire activity and ecosystem disturbance is expected with further agricultural expansion in MATOPIBA (Soterroni et al., 2019). For instance, Depressão Cárstica do



São Francisco, Chapadão do São Francisco and Parnaíba, three eastern ecoregions partly located in MATOPIBA, also show high fire intensities, and are considered at risk of very extensive land conversion between 2021 and 2050 (Soterroni et al., 2019). Partly located in MATOPIBA, Araguaia Tocantins is the highest contributing ecoregion to the Cerrado total BA (Figure 2.2b). This ecoregion encompasses both the Xerente Indigenous Land, Jalapão State Park and most of the Serra Geral do Tocantins protected area, lands that had high fire activity until the implementation of a pilot project for integrated fire management in 2015 (de Moraes Falleiro et al., 2016; Schmidt et al., 2016), and preliminary results point to a change of spatial fire patterns in some conservation units (Mistry et al., 2019). However, the fire management program is restricted to protected areas, possibly limiting its impacts on fire patterns at the regional level. With low fire intensity and negligible BA that averages about 18 km<sup>2</sup> per year in the study period, Costeiro is an exception to the overall ecological and economical context of MATOPIBA (Supplementary Material: Table 2.1). This ecoregion is covered by sand dunes and low density of vegetation, which virtually does not burn (Françoso et al., 2015).

With intense fires and particularly high fire incidence, and with large extents of its area burning annually, Bananal is practically all within the Araguaia National Park and Indigenous Land. This ecoregion has the highest percentage of protected areas (46.3%) and of extremely high priority areas (26.8%) of all Cerrado ecoregions (Sano et al., 2019), an important feature since fire occurrence in these areas involves a complex dynamics of ownership land conflicts. Chapada dos Parecis, an ecoregion located within the Arc of Deforestation has recurrent, intense fires and displays the maximum recorded value of fire intensity in a single event. This ecoregion has high spatial discrepancies with large extents of savanna and forest in its western region (Gomes et al., 2018) and high anthropogenic use in the eastern region (Marques et al., 2020), especially due to soybean expansion in Mato Grosso state. Chapada dos Parecis and Alto Parnaíba show significant fire activity in March, most likely related to soil preparation for planting crops. Given that these fires occur during the Cerrado wet season (November to May), the scarce fuel after vegetation conversion and high relative humidity do not allow high intensity fires.

A very distinct picture is found in most of the southern ecoregions, with lower contributions to the BA in the Cerrado, smaller scars with low FRP values, associated with extensive areas of agriculture and pastures. Basaltos do Paraná and Paraná Guimarães

show predominantly small fire scars: these are heavily deforested ecoregions where fire is mainly used for agricultural management. Large fire scars in these ecoregions are found within Indigenous Lands (Daldegan et al., 2019), where extensive areas of native vegetation remain and fire is traditionally used for many practices, including for hunting, for stimulating fructification, for managing biomass accumulation in grasslands, among others (de Moraes Falleiro et al., 2016). Paraná Guimarães has not been subject to recent agricultural expansion, as it has been widely explored by farmers since the 1960s (Sano et al., 2020), given its highly fertile soils. Similarly, Basaltos do Paraná is a traditional agricultural region where fire is still used for cropland management, especially in already consolidated and historical lands producing sugarcane, soybean and maize (de Andrade et al., 2020; Loarie et al., 2011). Sugarcane production in this ecoregion has been expanding prompted by the biofuels market (Loarie et al., 2011). Many ecoregions in the southern Cerrado show negative BA trends, but increasing fire intensity, suggesting that agricultural activities historically developed in these regions have replaced the native vegetation with croplands and planted pastures, which tend to have small but intense fires in highly fragmented landscapes, unsuitable to the spread of large fires (Magalhães et al., 2020).

Recent advances in agricultural expansion may explain negative BA trends over most ecoregions (Supplementary Material: Figure 2.9a). Fire activity tied to deforestation was high in earlier years. Later, controlled use of fire in agricultural landscapes led to a decrease in BA (de Oliveira et al., 2017; Eloy et al., 2019). Human activity was pinpointed as a driver of long-term global trends in BA (Andela et al., 2019), and similar trends due to land use change were found in the USA, Indonesia, and Australia (Bird et al., 2016; Field et al., 2016; Grégoire et al., 2013; Syphard et al., 2017; Taylor et al., 2016). Our results are also in line with those obtained using data derived from the Global Fire Emissions Database (GFED), where BA is found to be increasing over the north-eastern Cerrado and decreasing in the south (Andela et al., 2017; Chen et al., 2013; Forkel et al., 2019). However, BA trends vary substantially when the analysis is stratified by fire scar size. The observed distinct trends among fire size classes depend on regional underlying controls, such as local climate, population density, urban-rural interface, and fire management practices (Forkel et al., 2019; Hantson et al., 2015). Large scars occur mainly in northern ecoregions and in transitional areas between biomes, marked by high deforestation rates

and land conversion, such as the Arc of Deforestation and MATOPIBA. In the northern ecoregions, the landscape is less fragmented and land clearing has intensified since 2002 as croplands expanded to MATOPIBA.

It may be argued that ecoregional differences in fire size and fire seasonality patterns should be also viewed in light of the recent paradigm shift from a no-fire policy (Durigan and Ratter, 2016) to an Integrated Fire Management program (IFM), that is occurring in the Cerrado (Schmidt et al., 2018). However, according to the National Center for the Prevention and Fighting of Forest Fires - PREVFOGO, less than 125,000 km<sup>2</sup> are under IFM, therefore these changes are likely not enough to generate changes in fire patterns in any of the ecoregions.

#### **2.4.2 Fire in the context of the ecoregional map and limitations**

The proposed stratification of ecoregions into fire classes is especially pertinent, given the number and substantial variability of ecosystem types within Cerrado. The nine distinct combinations of fire characteristics obtained, namely Hbm, Hbh, Mbm, Mbh, Mbl, Msm, Lbm, Lbh and Lsl, reflect the natural constraints in the types of fire patterns present (Archibald et al., 2013). Large extensions of BA (Hbm, Hbh) are distributed over central-northern ecoregions, which currently concentrate most of the remnants of native Cerrado vegetation, and have been under high anthropogenic pressure (Alencar et al., 2020). Systematic fire activity, as seen in these regions during 2001–2019, may severely disrupt ecosystem functions. Conversely, ecoregions with low amounts of BA (Lbm, Lbh and Lsl) are located along the eastern and south-eastern portions of the biome, which have been historically occupied for longer periods. South-eastern ecoregions have considerably less native vegetation cover, a high level of landscape fragmentation and less land susceptible to burn (Souza et al., 2020). In the central-eastern Cerrado several ecoregions featuring high values of BA are side by side with others displaying low values, under very distinct regional contexts: Depressão Cárstica de São Francisco (Lbh) concentrates small landholder parcels dedicated to cattle ranching and subsistence farming and has distinct socio-economics characteristics compared to Chapadão do São Francisco (Hbh), an ecoregion dominated by commodity-driven and large-scale farms (IMAFLOA, 2018). Ecoregions with moderate BA (Mbm, Mbh, Mbl and Msm) have relatively more recent economic development (da Rosa et al., 2016) and exhibit high deforestation rates

from 2000 to 2008 (PPCDAm and PPCerrado, 2020). Basaltos do Paraná is an exception to that pattern, given that it is a traditional agricultural region with high landscape fragmentation that prevents the spread of large fires. Interestingly, Basaltos do Paraná and Floresta de Cocais, which have very distinct regional contexts, share the same fire classification (Msm). However, Floresta de Cocais is characterized by medium NBA values and an increasing BA trend, because it is an area of agricultural expansion in MATOPIBA (de Araújo et al., 2019).

It's worth noting that when evaluating fire activity within ecoregions, we are driving our classification by biophysical parameters that ensure similar ecosystem types, and not by clusters of similar fire characteristics. This assumes homogeneity within ecoregions that vary significantly in size, and may mask patterns within. Sano's ecoregions have been defined based on rainfall patterns, topography and land cover, variables that have been shown to closely relate to fire activity (Libonati et al., 2015; Silva et al., 2019; Pausas and Ribeiro, 2013; Bowman et al., 2020), and thus we believe the assumption of similar fire features within ecoregions to be reasonable. Nevertheless, a proper evaluation of these drivers and of regional fire regimes in Cerrado would require that fire features drive the classification, which may or may not correspond to the ecoregional map. This, however, is beyond the scope of this work where the main goal was to assess fire in the context of predefined Cerrado ecoregions.

## 2.5 Conclusion

We stratified the temporal and spatial characteristics of fire patterns in the ecoregions of Cerrado into nine classes of fire activity and added this information to the ecoregional map of Cerrado. Information includes the main components of fire activity, namely BA, fire intensity and fire size in regions with homogeneous biophysical and anthropogenic characteristics. An innovative approach classifying fire scars into distinct size classes revealed a diversity of fire patterns previously masked by generalized analysis, providing crucial and novel insights into the regional understanding of fire activity. By highlighting the differences in fire activity among the ecoregions and per fire size, our approach will be of use for decision-makers when planning locally-sensitive fire management and emergency actions, and when designing strategies to reduce emissions without compromising local

biodiversity.

Although restricted to a period of 19 years due to satellite data availability, our analysis provides critical insights into regional fire activity in the Cerrado biome, at a time when both climate and land use are steadily changing. This is a crucial aspect, since fire activity in the Cerrado is closely linked to regional climate patterns (Libonati et al., 2015; Silva et al., 2019), and the biome is expected to become drier (Blázquez and Silvina, 2020) and warmer (Feron et al., 2019), further promoting conditions favourable to increased fire activity (Page et al., 2017). Fire seasons are also expected to expand (Flannigan et al., 2013) and fire danger may reach critical values much more frequently (Silva et al., 2016). Under these scenarios, disruptions in the historical fire regime may lead to an increase in BA over the Cerrado (Silva et al., 2019), with substantial and possibly irreversible consequences, including changes in ecological community composition (Krawchuk et al., 2009) and biome distribution (Lapola et al., 2009; Oyama and Nobre, 2003).

Considering ongoing and expected future agricultural expansion, particularly in MATOPIBA, consistent and robust environmental strategies are urgently needed to prevent further degradation of the Cerrado (Lahsen et al., 2016) and ensure the protection of native vegetation remnants (Soterroni et al., 2019). Thus, since neither climate nor the socioeconomic conditions in the Cerrado biome are expected to remain stable in the future, fire patterns are very likely to continue changing. Further research on realistic and adequate representation of fire patterns at a regional level is necessary to improve understanding of how the Cerrado ecosystems may respond to future changes.

## 2.6 Supplementary Material

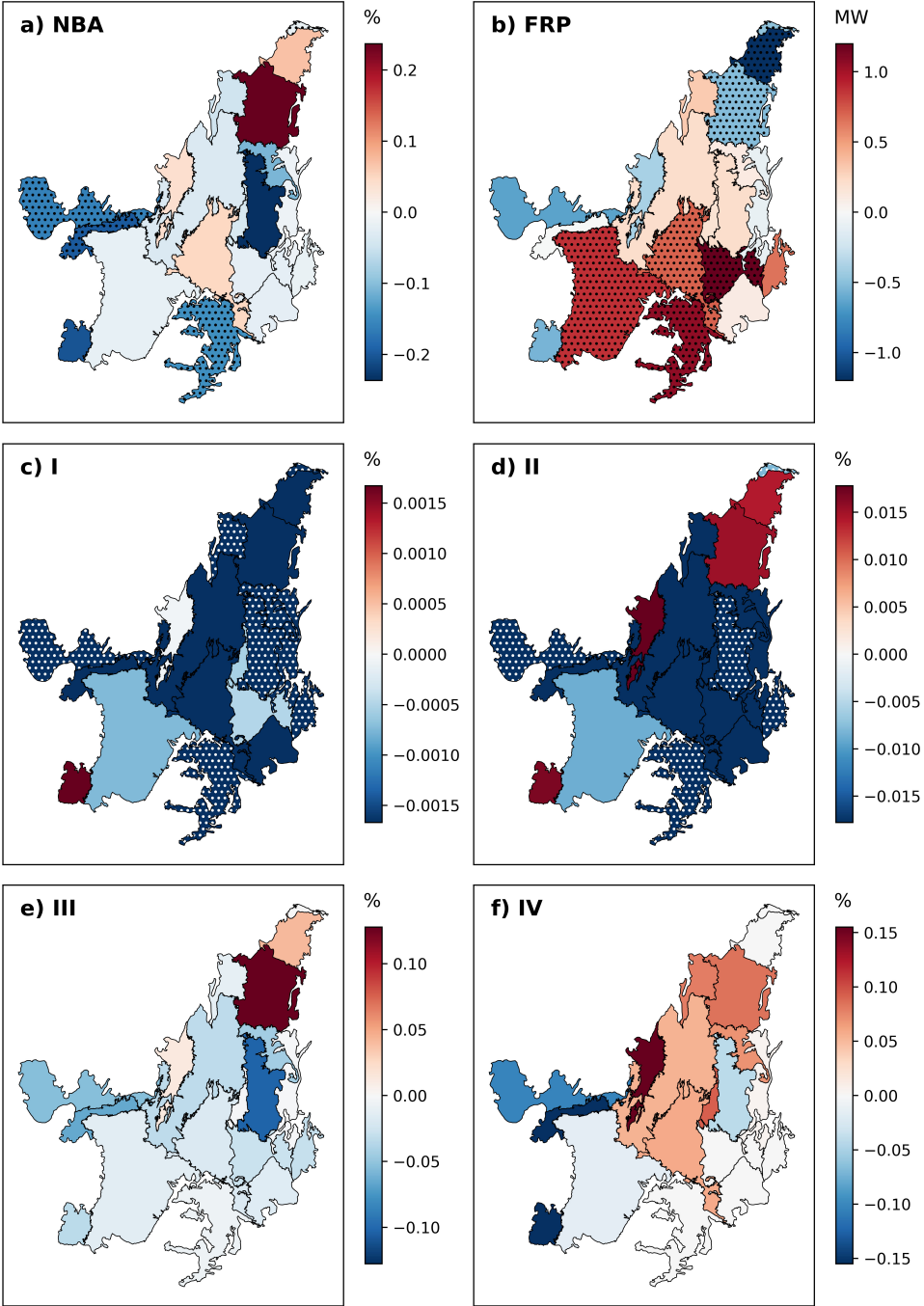


Figure 2.9: Trends of a) Burned area (NBA, %), b) Fire intensity (FRP, MW) and burned area per fire scar size (NBA, %) for the classes: c) I (0.21–1 km<sup>2</sup>), d) II (1–10 km<sup>2</sup>), e) III (10–50 km<sup>2</sup>) and f) IV (> 50 km<sup>2</sup>) classes. NBA and FRP trends are estimated for the 2001–2019 period, whereas burned area fire size trends from 2003 to 2018. Dotted cells mean statistical significance at the 5% level (see Methods).

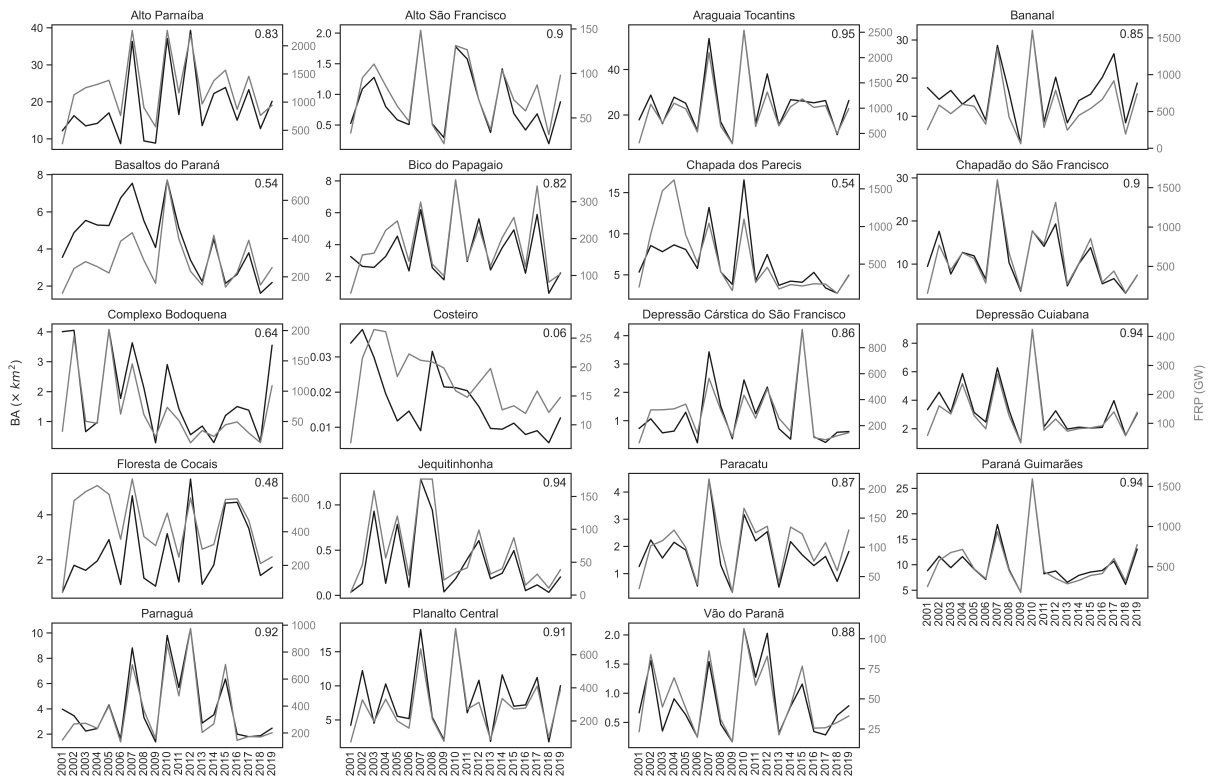


Figure 2.10: Interannual variability of yearly burned area (BA, km<sup>2</sup>, black lines) and Fire Radiative Power (FRP, GW, grey lines) from 2001 to 2019. Values in the top right corner show coefficient of determination from simple linear regression between the two products.

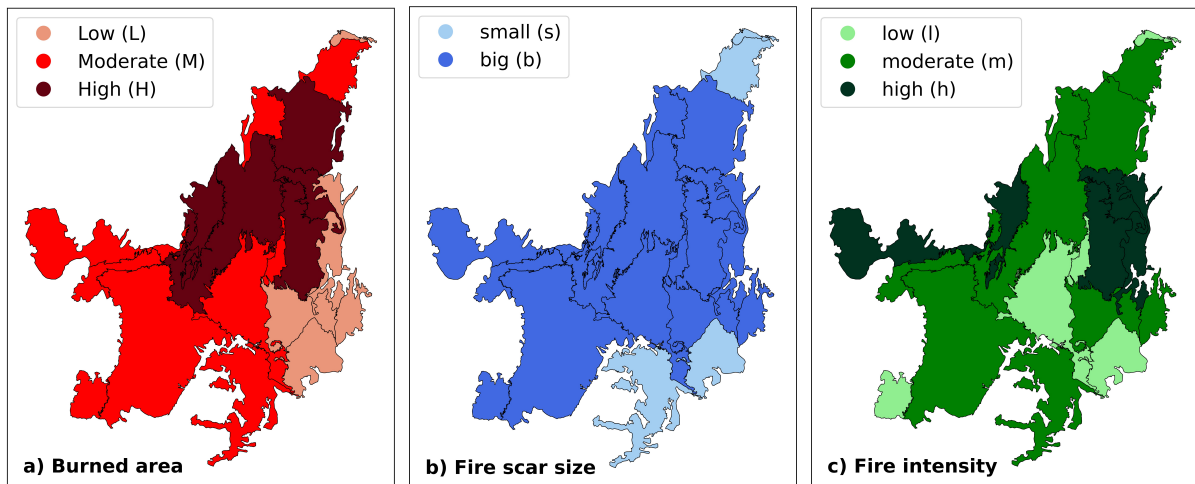


Figure 2.11: Spatial distribution of a) Burned Area, b) Fire scar sizes and c) Fire intensity, that lead to Figure 2.8. Burned area and Fire intensity classes (a and b) are based on first and third quartiles (low: below the 25<sup>th</sup> percentile; high: above the 75<sup>th</sup> percentile; moderate: between the 25<sup>th</sup> and 75<sup>th</sup> percentiles); and the Fire scar size which most contributed to the total burned area (middle panel) was stratified in: small scars and medium-large (big) scars.

Table 2.1: Area of each ecoregion (Area, km<sup>2</sup>), and average and standard deviations of natural (Natural landcover, %) and anthropogenic (Anthropogenic landcover, %) landcover over the 2001–2018 period, estimated using the MapBiomas Collection 4.1 product (MapBiomas, 2020; Souza et al., 2020). Last column shows correspondent total burned area (BA, km<sup>2</sup>) using the MCD64A1 product from 2001 to 2019.

<b>Ecoregion</b>	<b>Area (km<sup>2</sup>)</b>	<b>Natural landcover (%)</b>	<b>Anthropogenic landcover (%)</b>	<b>BA (km<sup>2</sup>)</b>
Alto Parnaíba	167,985	87.8 ± 4.2	12.2 ± 4.2	360,071
Alto São Francisco	81,664	39.5 ± 1.3	60.5 ± 1.3	16,535
Araguaia Tocantins	285,579	64.0 ± 2.9	36.0 ± 2.9	475,711
Bananal	67,140	87.7 ± 1.8	12.3 ± 1.8	306,606
Basaltos do Paraná	140,313	20.2 ± 0.6	79.8 ± 0.6	83,680
Bico do Papagaio	53,855	71.8 ± 3.7	28.2 ± 3.7	68,128
Chapada dos Parecis	137,047	66.1 ± 2.7	33.9 ± 2.7	123,222
Chapadão do São Francisco	118,630	76.7 ± 5.1	23.3 ± 5.1	211,848
Complexo Bodoquena	40,372	51.7 ± 1.9	48.3 ± 1.9	35,543
Costeiro	8,858	86.3 ± 0.6	13.7 ± 0.6	333
Depressão Cárstica do São Francisco	78,406	64.2 ± 1.8	35.8 ± 1.8	22,842
Depressão Cuiabana	45,179	65.6 ± 3.5	34.4 ± 3.5	64,127
Floresta de Cocais	74,808	85.6 ± 3.8	14.4 ± 3.8	44,282
Jequitinhonha	39,182	67.4 ± 3.0	32.6 ± 3.0	6,878
Paracatu	93,626	52.2 ± 2.3	47.8 ± 2.3	33,418
Paraná Guimarães	364,524	32.5 ± 0.9	67.5 ± 0.9	194,674
Parnaguá	46,003	90.5 ± 1.1	9.5 ± 1.1	78,248
Planalto Central	175,622	44.2 ± 1.1	55.8 ± 1.1	153,349
Vão do Paranã	20,615	46.9 ± 3.7	53.1 ± 3.7	16,201



Table 2.2: Description of each obtained fire class as described in Methods, using a 3-letter sequence (first column); long description of sequence (second column); criteria used to describe such sequence (third column); and lastly, ecoregions belonging to each sequence and its trends (fourth column). Percentiles are represented by p25 (25<sup>th</sup> percentile) and p75 (75<sup>th</sup> percentile).

Type	Description	Criterion	Ecoregion (trends in BA)
<b>H High burned area ecoregion</b>			
<b>Hbm</b>	High burned area, big scars and moderate fire intensity	NBA > p75; scars > 10 km <sup>2</sup> ; p25 < FRP < p75	Alto Parnaíba (+) Araguaia Tocantins (-)
	High burned area, big scars and high fire intensity	NBA > p75 ; scars > 10 km <sup>2</sup> ; FRP > p75	Bananal (+) Chapadão do São Francisco (-) Parnaguá (-)
<b>M Moderate burned area ecoregion</b>			
<b>Mbm</b>	Moderate burned area, big scars and moderate fire intensity	p25 < NBA < p75; scars > 10 km <sup>2</sup> ; p25 < FRP < p75	Bico do Papagaio (-) Depressão Cuiabana (-) Paraná Guimarães (-)
	Moderate burned area, big scars and high fire intensity	p25 < NBA < p75; scars > 10 km <sup>2</sup> ; FRP > p75	Chapada dos Parecis (-)
<b>Mbl</b>	Moderate burned area, big scars and low fire intensity	p25 < NBA < p75; scars > 10 km <sup>2</sup> ; FRP < p25	Complexo Bodoquena (-) Planalto Central (+) Vão do Paranã (-)
	Moderate burned area, small scars and moderate fire intensity	p25 < NBA < p75; scars < 10 km <sup>2</sup> ; p25 < FRP < p75	Basaltos do Paraná (-) Floresta de Cocais (+)
<b>L Low burned area ecoregion</b>			
<b>Lbm</b>	Low burned area, big scars and moderate fire intensity	NBA < p25; scars > 10 km <sup>2</sup> ; p25 < FRP < p75	Jequitinhonha (-) Paracatu (-)
	Low burned area, big scars and high fire intensity	NBA < p25; scars > 10 km <sup>2</sup> ; FRP > p75	Depressão Cárstica do São Francisco (-)
<b>Lsl</b>	Low burned area, small scars and low fire intensity	NBA < p25; scars < 10 km <sup>2</sup> ; FRP < p25	Alto São Francisco (-) Costeiro (-)

## **Author contribution**

PSS, JAR, RL and CCD conceived and designed the study; PSS, JAR and FLMS performed the data analysis; PSS, RL, JAR and FLMS analysed the data; PSS, JN and RL wrote the paper; JMCP, CCD, GAD, AAP, LFP, IBS, JN and RL contributed to discussion; all authors revised the paper.

## Chapter 3

# Understanding regional fire-climate dynamics

Fire activity in the Brazilian savanna (Cerrado) is heavily constrained by climate, however the climate modes that lead to extreme fire seasons are not yet well understood. Climate conditions during the fire season determine fire weather, but climate patterns prior to the fire season months may also modulate fuel availability and condition. In the context of a changing climate, understanding the climatic patterns that lead to extreme fire events, and their mediating factors, is crucial to build resilient landscapes and inform decision-making. Studies worldwide have shown that these fire-climate dynamics vary significantly per ecosystem and in this study, we propose to uncover the nature of these relationships for Cerrado. We evaluate the regional temperature and precipitation patterns that lead to severe and mild fire seasons in the ecoregions of Cerrado. We identify two periods that show contrasting behaviours in both extremes: the concurrent climate conditions during the fire season months (August to October) and pre-conditions during the austral autumn (March to May). Albeit with noteworthy regional discrepancies, in general we find that severe fire seasons are preceded by hot and dry conditions during the austral autumn, and associated with hot and dry conditions during the fire season months. Mild fire seasons see the opposite pattern, with colder and wetter conditions both during and prior to the fire season. We further investigate the climate modes that lead to extreme fire activity in each month of the fire season and find that, over most ecoregions, early fire season burned areas are influenced by pre-conditions during the austral autumn, whereas late fire season burned areas rely on concurrent favourable meteorological conditions. These results contribute to the understanding of the regional fire-climate dynamics of the second largest biome in South America, and provide a starting point for possible regional fire outlooks. We further provide regionally tailored information that, considering recent Brazilian policies, may prove useful for fire management.

### **3.1 Introduction**

Climate is one of the main drivers of fire activity worldwide (Jones et al., 2022; Bedia et al., 2015). Weather conditions favourable to fire, commonly referred to as fire weather conditions, generally include high air temperatures, low soil moisture and air humidity, accompanied by strong winds, that provide appropriate conditions for fires to occur and spread (IPCC, 2021; Aldersley et al., 2011). The single or concurrent occurrence of

extreme events, such as droughts and heatwaves (Zscheischler and Seneviratne, 2017), is also linked with severe fire seasons, such as the Pantanal 2020 fires (Libonati et al., 2022b,a) or the Australian 2019/2020 bushfires (Abram et al., 2021; Squire et al., 2021). Additionally, climate modulates fuel amount and availability through direct and indirect effects on vegetation (Pausas and Ribeiro, 2013; Krawchuk and Moritz, 2011).

Within the Brazilian Cerrado, fire is a crucial feature. This savanna-like landscape covers 2 million km<sup>2</sup>, and is the largest contributor to Brazil's and South America's annual burned area (UNEP, 2022; Bilbao et al., 2020). As a fire-dependent biome, Cerrado relies on its natural fire regime to maintain the ecosystem's functioning and structure (Pivello et al., 2021) and has been shown to sustain high pyrodiversity (Silva et al., 2021). Biome-wide studies point out that interannual burned area variability in Cerrado can be explained through precipitation (Libonati et al., 2015) and fire danger indexes (Li et al., 2021b; Silva et al., 2019; Nogueira et al., 2017a). However, this may not be the case at the smaller scales, as local studies have found that the drivers of fire highly depend on regional context. Large fires in Cerrado have been associated with high wind speeds and compound hot-dry conditions, with considerable discrepancies in the importance of these drivers regionally (Li et al., 2021a; Libonati et al., 2022a). For instance, the vapour pressure deficit (VPD) is the main driver of fire spread and fire intensity in Cerrado's grasslands, forests and savanna regions, whereas fine fuels influence combustion rates and carbon emissions (Gomes et al., 2020). In turn, burned areas in mountainous regions of Cerrado, have been shown to be sparsely correlated with concurrent precipitation but better explained by drought during the dry season (Alvarado et al., 2017). Similarly, Conciani et al. (2021) found that, for three protected areas within Cerrado, precipitation did not explain the interannual variability of burned areas but, when considering human factors such as land use management and agropastoral activities, the variance explained increased substantially.

These relationships become increasingly complex when considering regions with high anthropogenic activity, such as the Arc of Deforestation and Brazil's latest agricultural frontier, MATOPIBA, the confluence of states Maranhão (MA), Tocantins (TO), Piauí (PI), and Bahia (BA). In the Upper Xingu basin, stretching across both the Amazon and Cerrado biomes, the concurrence of air dryness and low precipitation drives fire occurrence (Ribeiro et al., 2022). In the state of Tocantins, de Andrade et al. (2021) have shown that

burned areas are positively correlated with the duration of the dry season and negatively correlated with total rainfall, while Santana et al. (2020) pointed out that the synergies between fire recurrence in the Araguaia National Park and biophysical variables, including the enhanced vegetation index (EVI), gross primary production (GPP), and land surface temperature (LST), strongly depend on land cover type. Silva et al. (2020) found that, while a fire danger index explains 52% of interannual variability of the total burned area in MATOPIBA, the relationship between the fire danger index and regional burned area varied greatly when considering MATOPIBA's 41 microregions.

Accordingly, while helpful, large-scale assessments of fire-climate relationships mask distinct regional patterns. Indeed, worldwide, fire-climate dynamics have been shown to highly depend on geographical location (Zubkova et al., 2019; Syphard et al., 2017). Although the currently available literature on the drivers of fire in Cerrado hints at complex relationships between climate and fire activity with high geographical variation, a comprehensive study on the regional climate controls of fire activity is lacking for the Cerrado biome. In this study, we provide a novel assessment of regional fire-climate relationships considering Cerrado's ecoregions. We first assess the climatic conditions that lead to extreme fire seasons, and then dive on the specific climate modes that influence each month of the fire season.

## **3.2 Data**

### **2.1 Study area**

We partition Cerrado into 19 ecoregions as proposed by Sano et al. (2019) (Figure 3.1). These ecoregions are unique in terms of landscape characteristics and were defined based on their physical attributes (elevation, rainfall, and soil), land use types, land cover classes and conservation status (protected areas and indigenous territories). Silva et al. (2021) studied fire behaviours within each ecoregion using several fire parameters (e.g. burned area, fire intensity, and size of individual fire events), and further updated the ecoregional map with regional fire characteristics. For the purposes of this study, we only considered ecoregions that burn regularly. As such, the five ecoregions classified as low-burned areas in Silva et al. (2021), namely: Alto São Francisco, Depressão Cárstica do São Francisco,

Jequitinhonha, Paracatu, and Costeiro, were not considered in the present study.

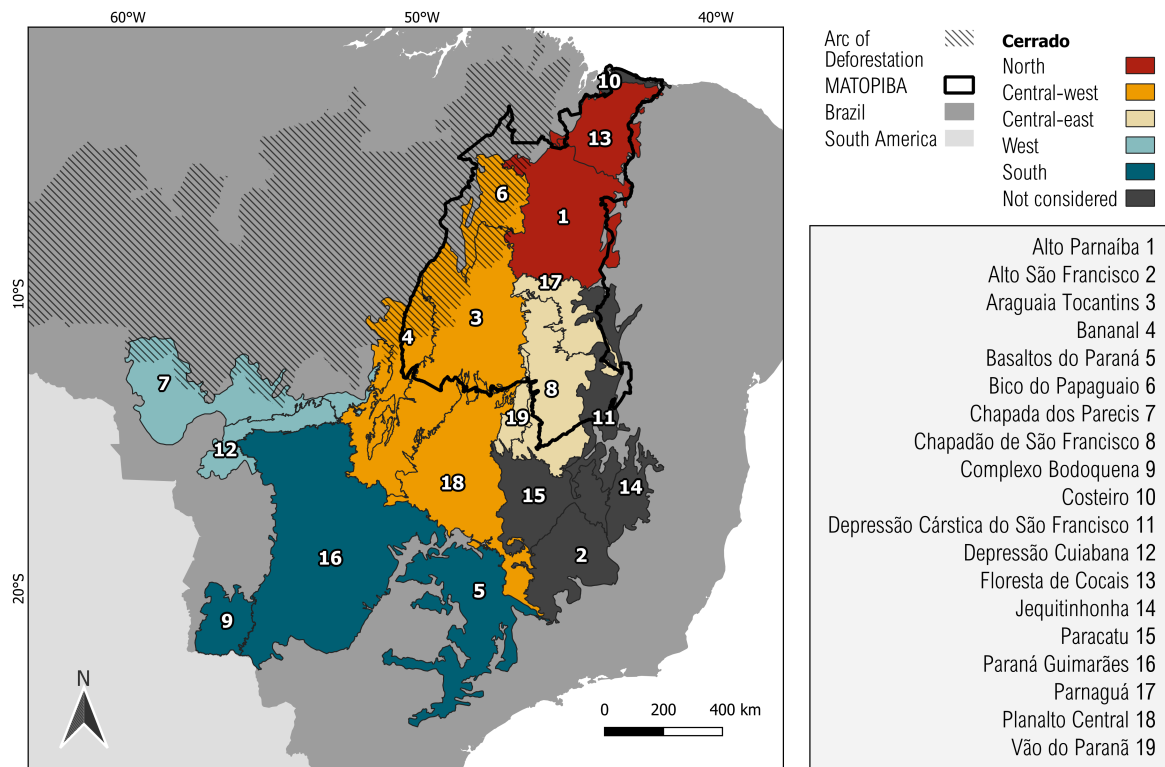


Figure 3.1: Cerrado’s location within Brazil (dark grey) and South America (light grey). The transition zone between the Cerrado and Amazon biomes, the Arc of Deforestation, is hatched and MATOPIBA, defined here as the intersection of states Maranhão, Tocantins, Piauí and Bahia, with Cerrado, is marked by a solid black line. Cerrado’s 19 ecoregions (Sano et al., 2019) are shown and numbered, with the respective names listed in the column on the right. Cerrado’s ecoregions are further categorized into 5 classes based on their geographical location within Cerrado: north (red); orange (central-west); yellow (central-east); west (light blue); and south (dark blue). Finally, ecoregions not considered in this study are numbered but shown in dark grey.

## 2.2 Datasets and pre-processing

Burned area was obtained from the Moderate Resolution Imaging Spectroradiometer (MODIS) MCD64A1 Collection 6.1 product (Giglio et al., 2018), for the 2001–2023 period. Using the Fuoco server from the University of Maryland, the Win05–07 tiles were merged to obtain data for South America. Data were then reassigned to a binary classification according to unburnt/burnt pixels. Monthly and yearly sums of burned areas at 500-meter spatial resolution were computed over each ecoregion. The MODIS MCD64A1 product is known to perform well over the Brazilian savanna, but uncertainties are larger in southern Cerrado due to the prevalence of smaller and scattered fire scars (Campagnolo

et al., 2021; Rodrigues et al., 2019).

Daily surface temperature and hourly total precipitation were downloaded from the European Centre for Medium-Range Weather Forecasts' (ECMWF) ERA5 reanalysis (Hersbach et al., 2020), at a  $0.25^\circ \times 0.25^\circ$  spatial resolution for the 2001–2023 period. Daily precipitation totals were computed. All data was masked per each ecoregion and spatial means were computed.

## 3.3 Methods

### 3.3.1 Composite analysis of extreme years

The fire season in Cerrado is fairly constant throughout ecoregions, with most annual burned area occurring during the austral summer from August to October (Silva et al., 2021), thus the annual fire regime is heavily constrained by fires in this period. As such, this study focuses on extreme fire seasons, defined as the months of August, September, and October (ASO).

To analyse the climatic conditions that lead to extreme fire season years, we followed the approach proposed by Pereira et al. (2013). We obtained, for each ecoregion, the top(bottom) burned area years, defined as those above(below) the 75<sup>th</sup>(25<sup>th</sup>) percentile of fire season burned areas over 2001–2023, henceforth referred to as severe(mild) fire years. Severe and mild fire years per ecoregion are shown in Supplementary Material: Figure 3.7.

A composite analysis was performed to compare climatic conditions associated to severe and mild years. Composites consist of monthly averages over the years that define the severe and mild classes, per ecoregion, and composite anomalies are computed by subtracting the monthly average of the full time series (2001–2023). This analysis allowed to pinpoint two 3-month period that may, to some extent, influence burned areas during the fire season: pre-conditions during the austral autumn (defined as March, April, and May; MAM); and the concurrent conditions of the fire season (ASO). Seasonal means(accumulated values) of temperature(precipitation) were estimated for these two periods, and composite anomalies computed in a similar manner to that previously explained. Standardized anomalies were also estimated by further dividing the composite



anomalies by the corresponding standard deviation.

A similar procedure was employed to study the climatic conditions associated with severe/mild fire years per month of the fire season (ASO). For each month (August, September, and October), severe and mild fire years were defined in the same way as previously described for the fire season: by means of the 75<sup>th</sup> (severe) and 25<sup>th</sup> (mild) percentile of the 2001–2023 time series (shown in Supplementary Material: Figure 3.7). We further compute seasonal means (sums) of temperature (precipitation) during the austral autumn (MAM) to assess the influence of pre-conditioned climate on severe/mild burned areas of each month of the fire season, and use the corresponding monthly mean (sum) of temperature (precipitation) to evaluate the influence of concurrent climate conditions.

### 3.3.2 Modelling regional fire-climate relationships

We investigated the regional relationship between fire and climate in each ecoregion through linear models that predict burned area (BA):

$$BA = \beta_0 + \beta_1 \times C_1 + \beta_2 \times C_2 + \varepsilon \quad (3.1)$$

where  $\varepsilon$  is the error of the regression, BA is the predictand,  $C_1$  and  $C_2$  are the two predictors (standardized values of either temperature or precipitation), that respectively represent concurrent conditions during the fire season (ASO) and pre-conditions during the austral autumn (MAM), and  $\beta_0$ ,  $\beta_1$ , and  $\beta_2$  are the regression coefficients. The significance of each predictor was evaluated through the corresponding p-values and considered significant if below the 5% confidence level. The adjusted coefficient of determination ( $R^2$ ) provided the total variance explained by the model. Regression models given by Equation 3.1 were also used to predict annual values of burned area in each individual month of the fire season (months of August, September, and October). The Variance Inflation Factor (VIF) was computed to measure multicollinearity amongst predictors, with VIF values above 5 requiring re-assessment of predictors (Montgomery et al., 2012).

## 3.4 Results

### 3.4.1 Seasonal climate and burned area patterns

Temperature and precipitation patterns vary considerably within ecoregions according to the vast latitudinal extent of the Cerrado (Figure 3.2). Nevertheless, while the annual cycle of precipitation is somewhat similar throughout the Cerrado, there are very distinct regional temperature patterns.

With the exception of Planalto Central, northern (Alto Parnaíba and Floresta de Cocais) and central-western (Araguaia Tocantins, Bananal, and Bico do Papagaio) ecoregions have unimodal annual cycles of temperature, growing steadily from April to September, when the annual maxima are reached. On the other hand, Planalto Central (north), much like central-eastern ecoregions (Chapadão do São Francisco, Parnaguá, and Vão do Paranã), experiences abrupt temperature increases from July onwards, reaching the annual maxima around September. These ecoregions, along with Depressão Cuiabana (west), also show a bimodal temperature distribution, with a secondary peak around April and May. Chapada dos Parecis (west), shows a steady increase in monthly temperatures from February onwards, peaking in September, and followed by an abrupt drop from October to January. Lastly, southern ecoregions present a unimodal cycle that is substantially different from that of northern and central-western ecoregions, with annual maxima from September to March, and a sudden drop in monthly temperatures from April to August.

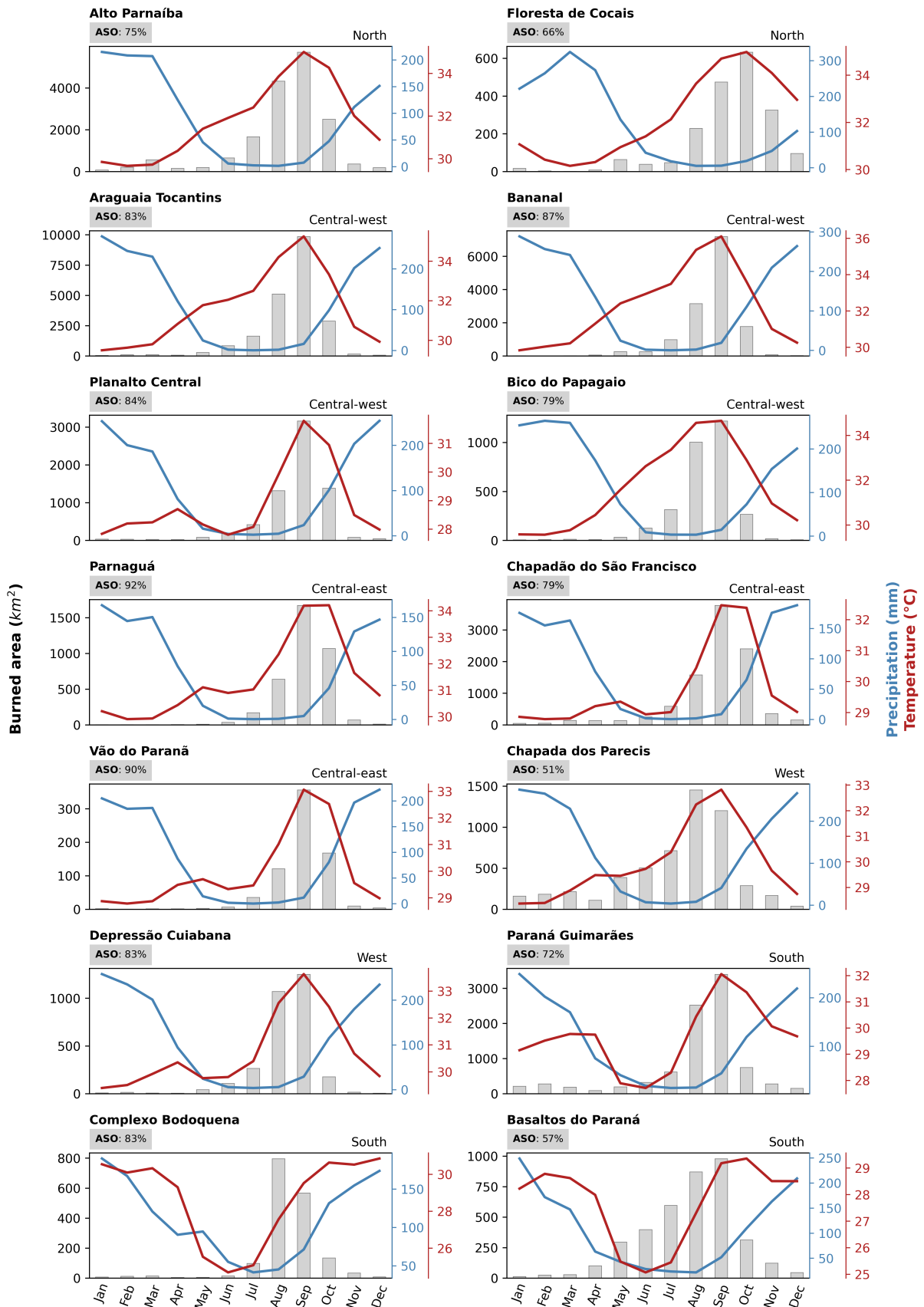


Figure 3.2: Seasonal cycles of burned area (left-hand axis in black pertaining to the grey bars, km<sup>2</sup>), precipitation (right-hand axis in blue pertaining to the blue curve, mm) and temperature (right-hand axis in red pertaining to the red curve, °C) for the evaluated ecoregions. Values represent an average of monthly burned area and precipitation(temperature) totals(averages) over the 2001–2023 period. The

Figure 3.2 (*cont.*): share of fire season (ASO) burned areas in yearly burned areas in shown in the top right of each panel, and ecoregions are categorized geographically, according to Figure 3.1: north, central-west, central-east, west, and south; and the corresponding category is shown in the top right corner of each subplot.

Albeit with slight spatial discrepancies, in general Cerrado shows a marked dry season that spans from May to September. With the exception of southern ecoregions (Basaltos do Paraná, Paraná Guimarães, and Complexo Bodoquena) that see rainfall throughout the entire year, the austral winter months of June, July, and August, have virtually zero precipitation. Nevertheless, Floresta de Cocais, the northernmost ecoregion, shows a different annual precipitation cycle as its dry season seems to start later in August and last until November, peaking during March.

In general, the majority of burned areas occur during the months of August, September, and October (ASO). The fire season represents 51% to 92% of annual burned areas in Cerrado's ecoregions. With the exception of Basaltos do Paraná (57%) and Chapada dos Parecis (51%), fire season (ASO) burned areas represent at least two-thirds of annual burned areas. Peaks in burned area occur in September for all ecoregions, with the exceptions of Complexo Bodoquena and Chapada dos Parecis, which see a peak in burned area one month earlier in August, and Bico do Papagaio, which sees a burned area peak one month later in October.

We then evaluated the interannual variability of yearly and fire season amounts of burned area per ecoregion. Severe and mild years based on fire season burned areas are highlighted in Figure 3.3. Although extreme years vary greatly amongst ecoregions, there are noteworthy temporal and spatial patterns. The years 2007 and 2010 are marked as severe for all ecoregions considered, except for 2010 in Complexo Bodoquena. Ecoregions located in northern and central Cerrado (namely, Alto Parnaíba, Araguaia Tocantins, Bananal, Bico do Papagaio, Chapadão do São Francisco, Floresta de Cocais, Parnaguá, Planalto Central, and Vão do Paraná) all show 2012 as a severe year, whereas central-eastern ecoregions (Chapadão do São Francisco, Parnaguá, and Vão do Paraná) have 2010, 2011 and 2012 in common as severe fire years.

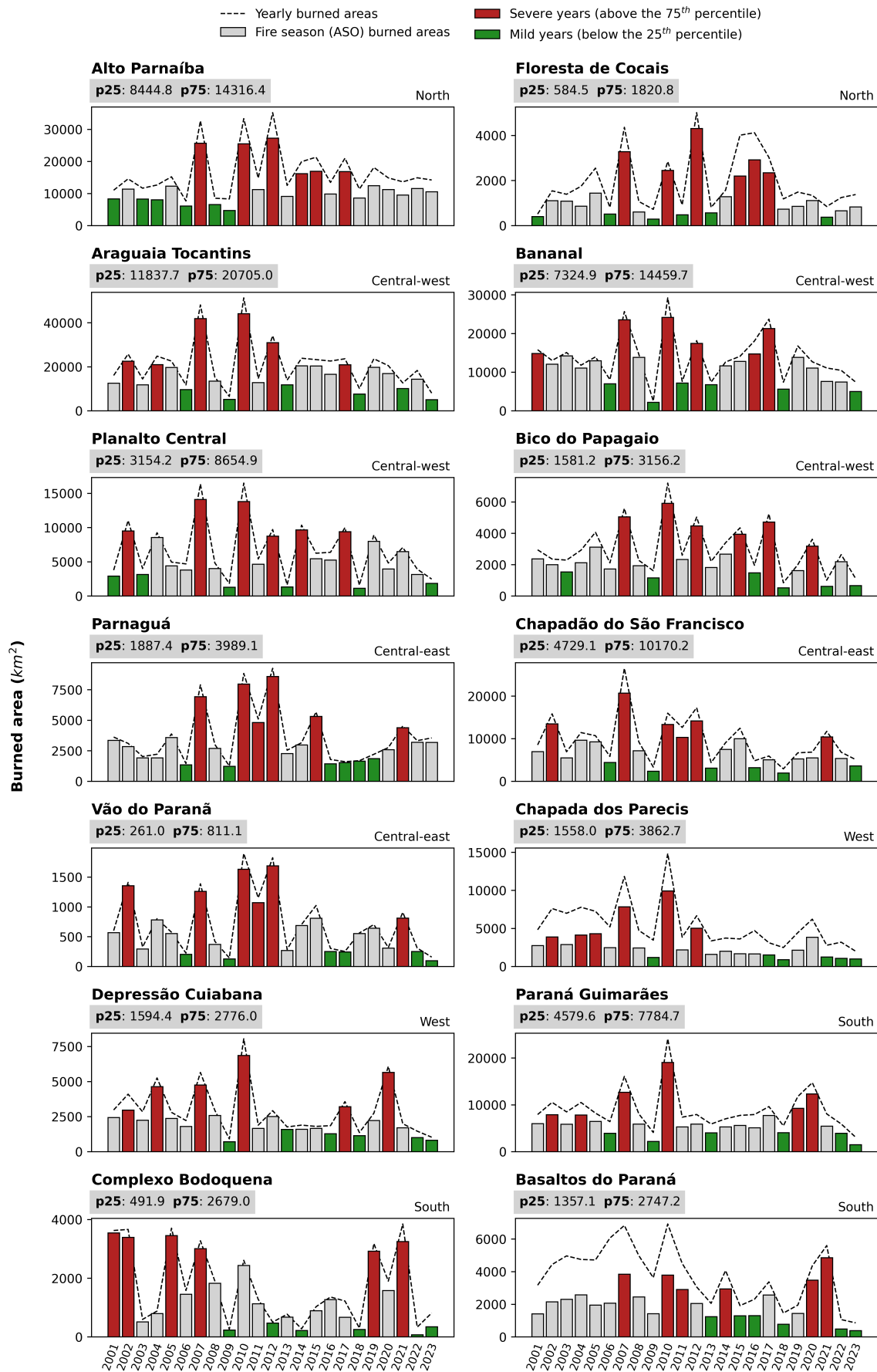


Figure 3.3: Interannual variability of yearly (dashed curves) and fire season (grey bars) burned areas per ecoregion. Coloured bars represent years of severe (red) and mild (green) fire seasons, defined as those

Figure 3.3 (*cont.*): above(below) percentile 75(25) of the 2001–2023 time series. Values for the 25<sup>th</sup> and 75<sup>th</sup> percentiles are show below the title of each panel, and ecoregions are categorized geographically, according to Figure 3.1: north; central-west; central-east; west; and south; the corresponding category is shown in the top right corner of each subplot.

## 3.4.2 Analysis of extreme fire seasons

### 3.4.2.1 Monthly anomalies

Monthly anomalies for extreme fire-year composites find contrasting patterns in temperature and precipitation during severe and mild fire seasons (Figure 3.4). Nevertheless, there are very distinct seasonal patterns amongst Cerrado’s ecoregions.

Northern ecoregions (Alto Parnaíba and Floresta de Cocais) show systematic positive(negative) temperature anomalies throughout most of the year for severe(mild) fire seasons. Precipitation differs substantially for severe and mild fire seasons during autumn (MAM), and slightly by the end of the fire season (ASO) in October. During most of the fire season (ASO) precipitation anomalies are similar for both severe and mild fire years.

Central-western ecoregions (Araguaia Tocantins, Bananal, Planalto Central, and Bico do Papagaio) have two marked periods with contrasting temperature anomalies for severe and mild fire seasons: in autumn (MAM), and in the months of September and October, where positive(negative) temperature anomalies are found for severe(mild) fire seasons. During autumn (MAM) precipitation anomalies are also largely different between severe and mild fire seasons, and then again by the end of the fire season (ASO) in October. As with northern ecoregions, the onset of the fire season (ASO) in August and September is marked by very similar rainfall conditions during both severe and mild fire seasons. The described patterns are less pronounced in Bico do Papagaio than in the remaining central-western ecoregions.

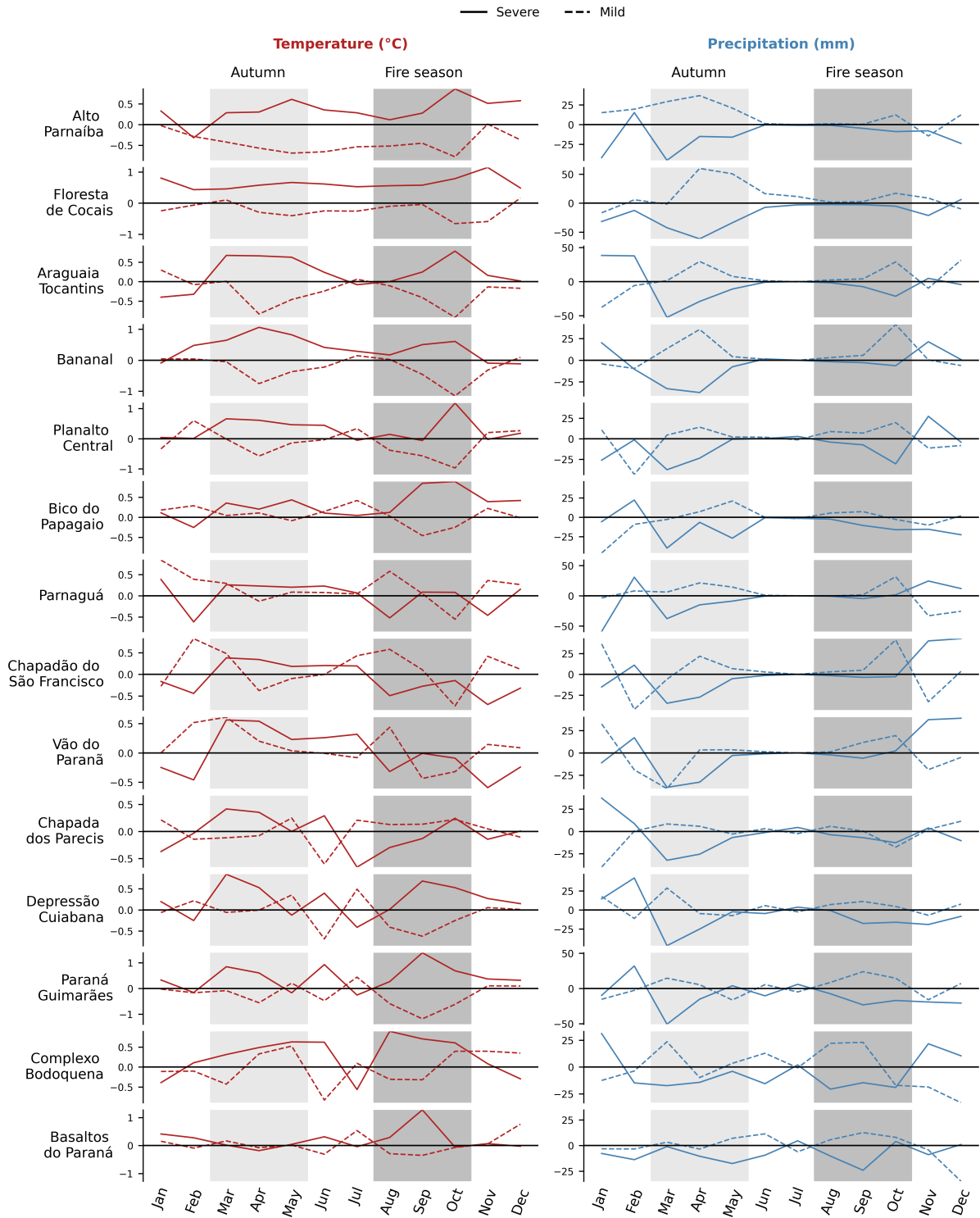


Figure 3.4: Monthly anomalies of temperature (left-hand panel; red; °C) and precipitation (right-hand panel; blue; mm) for composites of severe (solid curves) and mild (dashed curves) years in Cerrado's ecoregions. Severe(mild) years are defined as those where fire season burned areas exceed(fall behind) the 75<sup>th</sup>(25<sup>th</sup>) percentile of fire season burned areas over the 2001–2023 period. Two noteworthy 3-month periods are highlighted: the austral autumn (March, April, and May - MAM; light grey); and the fire season (August, September, and October - ASO; dark grey).

Conversely, central-eastern ecoregions (Parnaguá, Chapadão do São Francisco, and Vão

do Paraná) do not show considerable differences in temperature values between severe and mild fire seasons, except during February, August, and November, when mild(severe) fire seasons are marked by positive(negative) temperature anomalies. Patterns in precipitation anomalies are not as clear as in previous ecoregions, with not-so-well-defined positive(negative) precipitation anomalies for mild(severe) fire seasons in autumn and during the month of October. Nonetheless, there is a pattern in the final months of the year, during the months of November and December, where severe(mild) fire seasons are associated with positive(negative) precipitation anomalies.

Western ecoregions (Chapada dos Parecis and Depressão Cuiabana) show similar behaviour for temperature anomalies during autumn (MAM), when severe(mild) fire seasons show positive(negative) temperature anomalies, but a very distinct behaviour during the fire season (ASO): while Depressão Cuiabana shows contrasting behaviours of positive(negative) temperature anomalies during severe(mild) fire seasons, Chapada dos Parecis has no discernible pattern. In the case of precipitation, anomalies for both severe and mild fire seasons are similar along the two western ecoregions: no contrasting anomalies throughout the years for composites of severe and mild fire seasons, except during early autumn (MAM) in March.

Lastly, southern ecoregions (Paraná Guimarães, Complexo Bodoquena, and Basaltos do Paraná) present very distinct temperature anomaly patterns. Complexo Bodoquena and Basaltos do Paraná only show considerable differences between severe and mild fire seasons during August and September, whereas Paraná Guimarães has a similar behaviour as western ecoregions: contrasting temperature anomalies during autumn (MAM) and the entirety of the fire season months (ASO). The fire season months (ASO) are marked by positive(negative) precipitation anomalies for mild(severe) fire seasons, and Complexo Bodoquena and Basaltos do Paraná also show the same behaviour in precipitation anomalies for March.

### **3.4.2.2 Anomalies prior and during the fire season**

The previous analysis allowed to pinpoint two distinct 3-month periods where, in general, there are contrasting temperature and precipitation anomalies for severe and mild fire seasons: the austral autumn (MAM) representing pre-conditions; and the concurrent conditions of the fire season (ASO). Figure 3.5 summarizes the temperature and



precipitation anomalies during both these periods for severe and mild fire seasons.

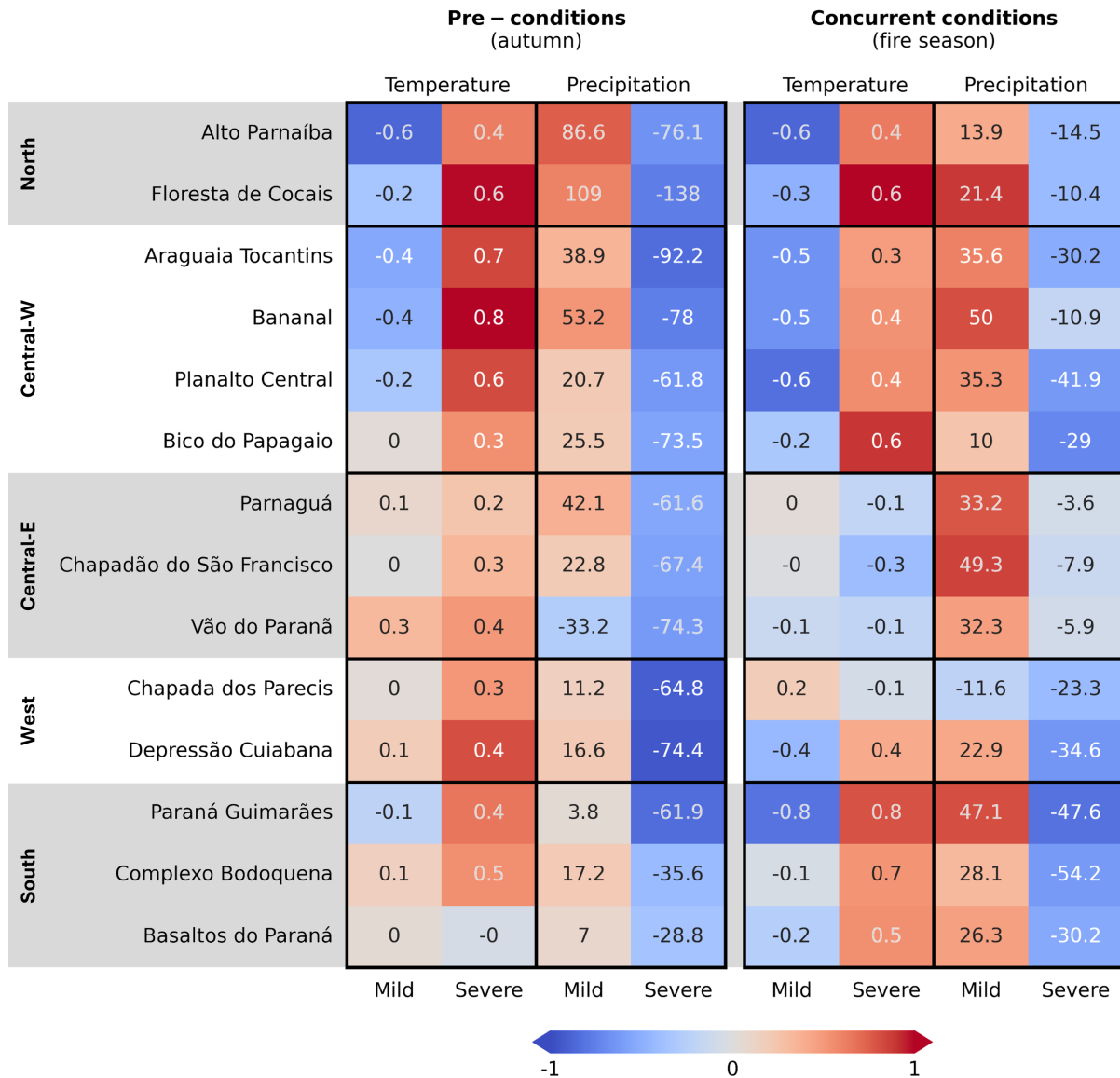


Figure 3.5: Seasonal anomalies of temperature and precipitation for composites of extreme years along Cerrado’s ecoregions for pre-conditions (autumn - MAM) and the concurrent conditions (fire season - ASO). Colours(numbers) represent standardized(absolute) anomalies of temperature (T, °C) and precipitation (P, mm). Anomalies are in respect to seasonal averaged temperatures and aggregated precipitation over the considered periods. Ecoregions are categorized geographically, according to Figure 3.1: north, central-west (Central-W), central-east (Central-E), west, and south.

During autumn (MAM), with the exception of Bico do Papagaio, all northern and central-western ecoregions show very distinct temperature anomalies, where severe(mild) fire seasons are marked by positive(negative) temperature anomalies. The remaining ecoregions show very low standardized temperature anomalies of the same signal, with the exception of the southern ecoregion Paraná Guimarães. Standardized temperature anomalies are

higher in central-western ecoregions, namely Araguaia Tocantins, Bananal, and Planalto Central, along with Floresta de Cocais located in northern Cerrado, and Depressão Cuiabana located in western Cerrado. Conversely, all ecoregions have contrasting behaviours in precipitation anomalies: severe(mild) fire seasons are associated with negative(positive) precipitation anomalies. Vão do Paranã is the sole exception, with negative precipitation anomalies for both severe and mild fire seasons. Standardized anomalies are higher in western ecoregions, and Paraná Guimarães.

During the fire season (ASO), there are contrasting temperature and precipitation patterns for northern, central-western, and southern ecoregions: severe(mild) fire seasons are associated with positive(negative) temperature anomalies and negative(positive) precipitation anomalies. On the other hand, central-eastern ecoregions have very low standardized and absolute temperature anomalies during this period and often of the same signal. Regarding precipitation, central-eastern ecoregions show contrasting anomalies, with negative(positive) anomalies for severe(mild) fire seasons, where standardized anomalies for mild fire seasons are relatively high and standardized anomalies for severe fire seasons are very low. In the case of western ecoregions, Chapada dos Parecis and Depressão Cuiabana have very distinct climate patterns during the fire season (ASO): Chapada dos Parecis has very low standardized anomalies for both temperature and precipitation, and negative precipitation anomalies for both severe and mild fire seasons; on the other hand, Depressão Cuiabana has contrasting patterns for both temperature and precipitation, where severe(mild) fire seasons are associated with positive(negative) temperature anomalies and negative(positive) precipitation anomalies.

### 3.4.2.3 Fire-climate models

The strength of the relationship between yearly values of temperature and precipitation and yearly fire season burned areas is assessed by fitting bivariate linear models using temperature or precipitation values over the austral autumn (MAM) and the fire season (ASO) as predictors of annual fire season burned areas (Table 3.1).

The strength of these relationships varies greatly along Cerrado's ecoregions, with adjusted  $R^2$  values ranging from 5% to 60% for temperature and from 7% to 41% for precipitation. In general, temperature models perform best for northern and central-western ecoregions, whereas precipitation models achieve higher coefficients of determination for northern and

Table 3.1: Bivariate linear models of annual fire season (ASO) burned areas using temperature and precipitation. Goodness-of-fit is evaluated through the Adjusted  $R^2$  (%). Coefficients  $\beta_1$  and  $\beta_2$  correspond to the regression coefficients associated with concurrent conditions of the fire season (ASO) and pre-conditions during autumn (MAM), respectively, and are accompanied by the associated significance, where \* denotes significant relationships below the 5% level and \*\* denotes relationships below the 10% level. The intercept of the regression is shown as  $\beta_0$ , and the Variance Inflation Factor (VIF) for both predictors is depicted as well. Ecoregions are categorized geographically, according to Figure 3.1: north, central-west (Central-W), central-east (Central-E), west, and south.

	Temperature					Precipitation					
	Adjusted $R^2$	$\beta_1$	$\beta_2$	$\beta_0$	VIF	Adjusted $R^2$	$\beta_1$	$\beta_2$	$\beta_0$	VIF	
<b>North</b>	Alto Parnaíba	31	572	3152 *	12533	1.3	35	-1241	-3166 *	12533	1.1
	Floresta de Cocais	60	674 *	213	1334	1.9	41	-340 **	-559 *	1334	1.0
<b>Central-W</b>	Araguaia Tocantins	35	2683	4457 *	17829	1.1	21	-2055	-3267	17829	1.3
	Bananal	43	2613 *	1871 **	12104	1.2	22	-1883	-1395	12104	1.1
	Planalto Central	47	1713 *	1639 *	5853	1.0	24	-1431 **	-710	5853	1.2
	Bico do Papagaio	25	622 **	191	2488	1.2	19	-356	-498	2488	1.0
	Parnaguá	9	-399	632	3374	1.1	14	-90	-739	3374	1.4
<b>Central-E</b>	Chapadão do São Francisco	5	-697	914	7752	1.1	17	-1300	-783	7752	1.5
	Vão do Paraná	8	19	132	645	1.0	7	-61	-83	645	1.3
	Chapada dos Parecís	15	74	843 **	2942	1.0	35	-251	-1228 *	2942	1.1
<b>West</b>	Depressão Cuiabana	14	379	427	2496	1.0	39	-362	-830 *	2496	1.1
	Paraná Guimarães	19	1451 **	691	6667	1.0	27	-1272	-1222	6667	1.1
<b>South</b>	Complexo Bodoquena	11	329	255	1497	1.0	32	-604 *	-596 *	1497	1.1
	Basaltos do Paraná	13	404	-109	2162	1.0	18	-419 **	-180	2162	1.0

western ecoregions.

In the case of temperature models, pre-conditions during autumn (MAM) are significant for only three ecoregions: Alto Parnaíba (north), Araguaia Tocantins (central-west), and Planalto Central (central-west). Additionally, concurrent conditions during the fire season (ASO) are significant in three ecoregions: Floresta de Cocais (north), Bananal (central-west), and Planalto Central (central-west). Planalto Central is thus the sole ecoregion where both predictors are significant but, as seen by the standardized regression coefficients, pre-conditions during autumn (MAM) have a slightly larger impact in yearly burned areas than concurrent temperatures during the fire season (ASO).

For precipitation models, all northern and western ecoregions, along with Complexo Bodoquena, show that pre-conditions in autumn (MAM) are significant when modelling yearly fire season burned areas. Conversely, only Complexo Bodoquena (south) achieves significance for concurrent rainfall during the fire season (ASO) and both predictors seem to translate in a similar amount of yearly burned area.

### **3.4.3 Analysis on a monthly basis for months of the fire season**

#### **3.4.3.1 Anomalies prior and during the fire season months**

Given the lack of significance of pre-conditions during autumn (MAM) in modelling yearly fire season burned areas, and the contrasting patterns found for this period in the composite analysis, we investigated whether evaluating the entirety of the fire season could mask distinct monthly controls. Accordingly, we performed the same analysis, but using instead severe and mild composites of: August burned areas; September burned areas; and October burned areas. We then evaluate temperature and precipitation for pre-conditions during autumn (MAM) and the concurrent conditions of each month. Figure 3.6 shows temperature and precipitation anomalies for pre-conditions during autumn (MAM) and concurrent conditions of each month (either August, September, or October) for composites of severe and mild years of each month of the fire season (either August, September, or October; see Methods).

Severe(mild) Augusts are in general associated with positive(negative) temperature anomalies and negative(positive) precipitation anomalies during autumn (MAM). Only four ecoregions show no contrast during autumn (MAM) between severe and mild Au-

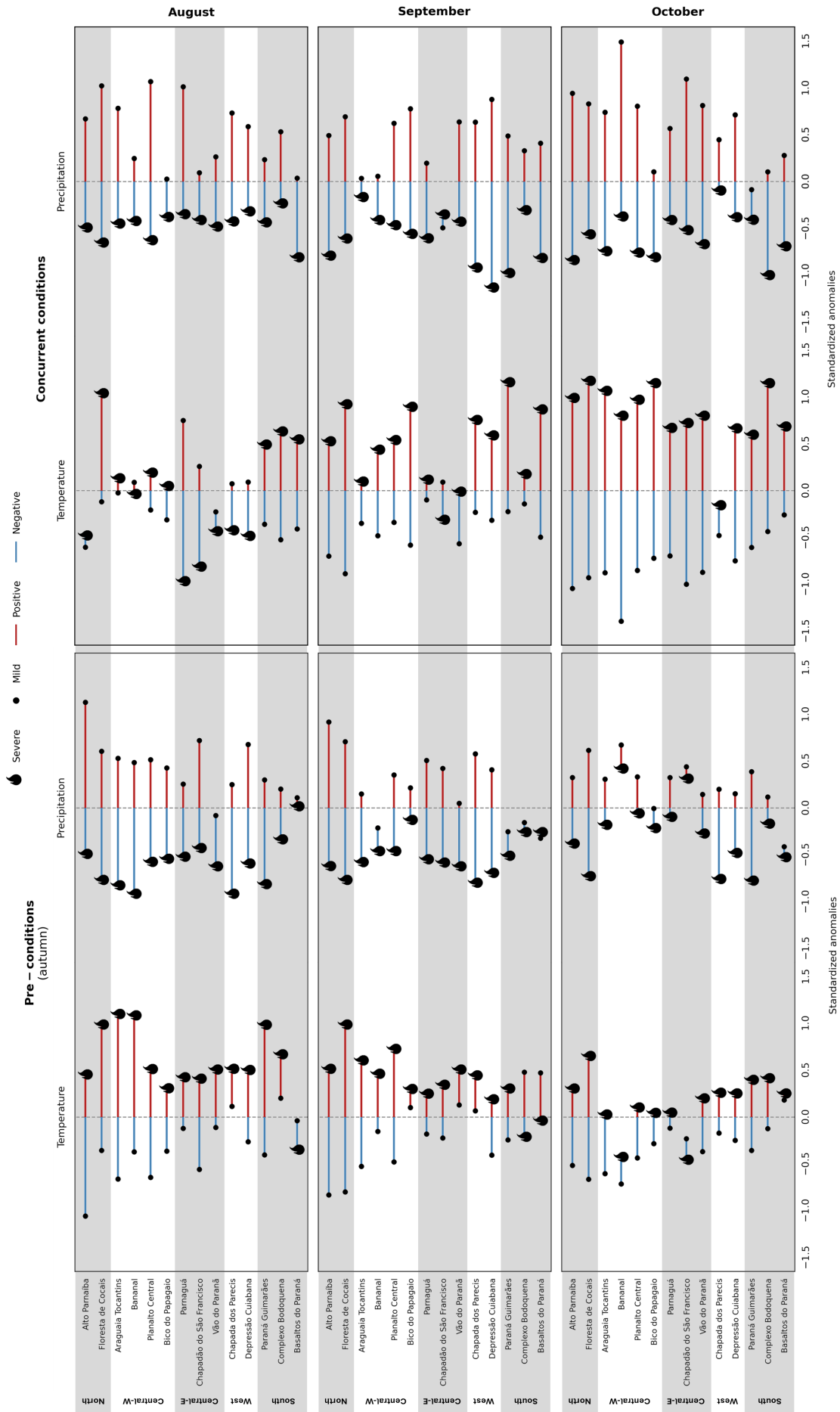


Figure 3.6: Standardized anomalies of temperature and precipitation along Cerrado's ecoregions for composites of extreme monthly burned areas in August (top row), September (middle row), and October (bottom row). Standardized anomalies for both climate variables were computed for the austral autumn (MAM; left-hand plots) and the corresponding month (either August, September, or October; right-hand plots). Red (blue) lines represent positive(negative) standardized anomalies, while flame(dot) symbols pertain to composites of severe(mild) burned areas. Ecoregions are categorized geographically, according to Figure 3.1: north, central-west (Central-W), central-east (Central-E), west, and south.

gusts, namely: Chapada dos Parecis (west), Complexo Bodoquena (south), and Basaltos do Paraná (south), in the case of temperature; and Vão do Paranã (central-east) and Basaltos do Paraná (south), in the case of precipitation. Severe(mild) Augusts are also associated with concurrent negative(positive) rainfall anomalies. Concurrent temperature anomalies do not present a consistent behavior, with only southern and central-western ecoregions (excepting Planalto Central), and Floresta de Cocais (north), showing positive(negative) temperature anomalies for severe(mild) Augusts. The remaining ecoregions either show the opposite pattern with negative(positive) temperature anomalies for severe(mild) Augusts or there is no contrasting behaviour between August extremes.

In general, severe(mild) Septembers are marked by positive(negative) temperature and negative(positive) precipitation anomalies, during both autumn (MAM) and September. Nevertheless, in autumn (MAM), two southern ecoregions show the opposite temperature pattern, and three other ecoregions, namely Bico do Papagaio (central-west), Vão do Paranã (central-east), and Chapada dos Parecis (west), show no contrasting temperature pattern for both severe and mild Septembers. Likewise, Bananal (central-west) and all southern ecoregions show no contrasting precipitation anomalies for severe and mild Septembers during autumn (MAM). When looking at concurrent temperature and precipitation anomalies, only Chapadão do São Francisco (central-east) shows a distinct pattern, with opposite temperature patterns and no diverging behaviour for severe and mild September in precipitation anomalies.

Lastly, severe and mild Octobers are associated with strong and contrasting concurrent anomalies in both temperature and precipitation. Only Chapada dos Parecis (west) and Paraná Guimarães (south) have no contrasting temperature and precipitation patterns, respectively. Both concurrent temperature and precipitation anomalies seem to be more pronounced for northern and central (both west and east) ecoregions. On the other hand, severe and mild Octobers obtain much lower temperature and precipitation anomalies during autumn (MAM) and three ecoregions do not show contrasting patterns for either climate variable. Nevertheless, the northern and western ecoregions, along with Vão do Paranã (central-east), Paraná Guimarães (south), and Complexo Bodoquena (south), show positive(negative) temperature anomalies and negative(positive) precipitation anomalies for severe(mild) Octobers.

### 3.4.3.2 Fire-climate models

Similarly to the analysis for extreme fire seasons, we further fit bivariate linear models that consider the pre-conditions during autumn (MAM) and the concurrent conditions of the evaluated month, for both temperature and precipitation, as predictor of yearly burned areas in each of the months of the fire season: August, September and October (Table 3.2, 3.3 and 3.4, respectively).

Models fitted for October burned areas using temperature as predictor achieve coefficients of determination that range from 15% to 70%. Concurrent temperatures in October are significant for all ecoregions excepting Chapada dos Parecis (west), whereas pre-conditions during autumn (MAM) are not significant for any of the evaluated ecoregions. In the case of precipitation models for October, in which explained variance ranges from 14% to 50%, 4(8) ecoregions show significance for (pre-)concurrent conditions.

Conversely, for temperature models of August and September burned areas, the explained variance is generally lower than that obtained for October burned areas, ranging from 7% to 58% and 4% to 51%, respectively. Nevertheless, in the case of August(September), 5(4) ecoregions show pre-conditions during autumn (MAM) as a significant predictor, and 4(6) ecoregions obtain the same result for concurrent conditions during August(September). Considering precipitation, models fitted for August(September) show coefficients of determination ranging from 8% to 46%(12% to 59%), and show significant regression coefficients for pre-conditions over 7(4) ecoregions, whereas 3(7) show concurrent rainfall in August(September) as significant.

## 3.5 Discussion

Seasonal precipitation patterns are similar throughout the Cerrado biome, with a marked dry season that peaks during the austral winter from June to August. There are, however, very distinct regional temperature patterns. In agreement with previous studies (Silva et al., 2021), our findings indicate that the vast majority of yearly burned areas occur within a 3-month period from August to October, which has often been considered as Cerrado's fire season. Throughout the vast majority of ecoregions, the fire season coincides with peaks in temperature, and with the transition from the austral winter (June, July,

Table 3.2: Bivariate linear models to predict annual burned areas for each month of the fire season (either August, September, or October) using pre-conditions during autumn (MAM) and concurrent conditions (either August, September, or October) of temperature or precipitation. Goodness-of-fit is evaluated through the Adjusted  $R^2$  (%). Coefficients  $\beta_1$  and  $\beta_2$  correspond to the regression coefficients associated with concurrent conditions (either during August, September, or October) and pre-conditions during autumn (MAM), respectively, and are accompanied by the associated significance, where \* denotes significant relationships below the 5% level and \*\* denotes relationships below the 10% level. The intercept of the regression is shown as  $\beta_0$ , and the Variance Inflation Factor (VIF) for both predictors is depicted as well. Ecoregions are categorized geographically, according to Figure 3.1: north, central-west (Central-W), central-east (Central-E), west, and south.

		August									
		Temperature			Precipitation						
	Adjusted $R^2$	$\beta_1$	$\beta_2$	$\beta_0$	VIF	Adjusted $R^2$	$\beta_1$	$\beta_2$	$\beta_0$	VIF	
North	Alto Parnaíba	47	-1765 *	2470 *	4322	1.5	39	-920 **	-1617 *	4322	1.0
	Floresta de Cocais	36	188 **	35	228	2.3	29	-115	-135 **	228	1.0
Central-W	Araguaia Tocantins	55	-886 **	2500 *	5106	1.1	46	-1242 *	-1600 *	5106	1.0
	Bananal	52	-491	1740 *	3151	1.2	28	-469	-1022 *	3151	1.0
	Planalto Central	34	104	513 *	1314	1.0	30	-360 **	-317 **	1314	1.0
	Bico do Papagaio	10	-154	231	1003	1.5	22	-145	-247 **	1003	1.0
Central-E	Parnaçuá	58	-420 *	245 *	637	1.0	16	-149	-186	637	1.0
	Chapadão do São Francisco	34	-648 *	422 **	1575	1.0	26	-409	-529 *	1575	1.0
	Vão do Paraná	7	-15	30	121	1.0	8	-21	-29	121	1.0
West	Chapada dos Parecis	15	-136	373	1454	1.0	36	-350 **	-485 *	1454	1.0
	Depressão Cuiabana	3	-57	30	1071	1.0	29	-154 **	-140 **	1071	1.0
	Paraná Guimarães	8	164	301	2524	1.0	31	-486 *	-544 *	2524	1.0
South	Complexo Bodoquena	25	404 *	254	795	1.0	29	-441 *	-463 *	795	1.2
	Basaltos do Paraná	16	157 **	-61	871	1.0	17	-172 **	14	871	1.0



Table 3.3: As in Table 3.2 but for September.

		September											
		Temperature						Precipitation					
		Adjusted R <sup>2</sup>	$\beta_1$	$\beta_2$	$\beta_0$	VIF	Adjusted R <sup>2</sup>	$\beta_1$	$\beta_2$	$\beta_0$	VIF		
<b>North</b>	Alto Parnaíba	30	382	1409 *	5709 *	1.1	50	-1531 *	-1585 *	5709	1.0		
	Floresta de Cocais	51	138	204 *	474	1.7	50	-225 *	-215 *	474	1.0		
<b>Central-W</b>	Araguaia Tocantins	35	2232 **	2546 *	9845 *	1.0	23	-2033	-1944	9845	1.0		
	Bananal	33	1765 *	959	7185	1.1	18	-1234	-941	7185	1.0		
	Planalto Central	49	1065 *	1164 *	3158 *	1.0	22	-827 **	-485	3158	1.1		
	Bico do Papagaio	43	585 *	40	1219	1.2	26	-420 *	-232	1219	1.0		
	Parnaguá	6	67	276	1670	1.0	39	-608 *	-665 *	1670	1.1		
<b>Central-E</b>	Chapadão do São Francisco	4	-318	377	3774	1.0	20	-824	-930	3774	1.0		
	Vão do Paranã	12	64	88	356	1.0	18	-106 **	-55	356	1.0		
<b>West</b>	Chapada dos Parecis	21	295	299	1201	1.1	47	-370 **	-486 *	1201	1.2		
	Depressão Cuiabana	28	544 *	243	1250	1.0	59	-720 *	-361 **	1250	1.1		
<b>South</b>	Paraná Guimarães	34	1414 *	418	3398	1.0	34	-1284 *	-467	3398	1.1		
	Complexo Bodoquena	8	124	-31	567	1.0	12	-145	-53	567	1.0		
	Basaltos do Paraná	37	437 *	26	979	1.0	31	-350 *	-148	979	1.0		

Table 3.4: As in Table 3.2 but for October.

		October					October				
		Temperature			Precipitation		Precipitation				
		Adjusted R <sup>2</sup>	$\beta_1$	$\beta_2$	$\beta_0$	VIF	Adjusted R <sup>2</sup>	$\beta_1$	$\beta_2$	$\beta_0$	VIF
North	Alto Paranaíba	70	1106 *	46	2502	1.1	49	-849 *	-220	2502	1.1
	Floresta de Cocais	51	347 *	44	632	1.3	34	-187 **	-216 *	632	1.0
Central-W	Araguaia Tocantins	60	1846 *	-328	2878	1.1	35	-1512 *	459	2878	1.3
	Bananal	53	1042 *	-406 **	1768	1.1	29	-797 *	408	1768	1.1
	Planalto Central	47	972 *	60	1382	1.0	31	-829 *	85	1382	1.2
	Bico do Papagaio	62	207 *	-1	266	1.1	16	-81	-59	266	1.0
Central-E	Parnaçuá	33	431 *	-90	1067	1.2	14	-280	21	1067	1.5
	Chapadão do São Francisco	51	1162 *	-427	2403	1.1	50	-1352 *	662 *	2403	1.6
	Vão do Paraná	41	86 *	9	168	1.1	31	-86 *	21	168	1.4
West	Chapada dos Parecis	15	22	87	287	1.0	30	-16	-131 *	287	1.0
	Depressão Cuiabana	32	135 *	71	176	1.0	33	-63	-142 *	176	1.0
	Paraná Guimarães	33	316 *	74	745	1.0	22	-148	-205	745	1.1
South	Complexo Bodoquena	28	99 *	44	134	1.0	33	-135 *	-79 **	134	1.2
	Basaltos do Paraná	27	133 *	0	312	1.2	30	-123 *	-57	312	1.0

and August) to spring (September, October, and November), which marks the start of the first rains in September and October. On the other hand, the months immediately prior to the fire season, June and July, are marked by the virtual absence of rainfall, with the exception of the southern ecoregions and the northernmost ecoregion (Floresta de Cocais). This slight mismatch between the fire season and the peak of the dry season in Cerrado has been reported previously (Silva et al., 2019; Alvarado et al., 2017).

This diversity in seasonal climate over Cerrado hints at distinct regional climate-fire relationships. An analysis of temperature and precipitation anomalies during severe and mild fire seasons provided an initial assessment of these regional interactions. Indeed, climate patterns during severe and mild fire seasons vary considerably along Cerrado's ecoregions, with similar patterns often aligning geographically. This spatial agreement might be due to a similar climate, but also that contiguous ecoregions may share the same extreme years. Precipitation patterns during extreme years are much more similar along Cerrado's ecoregions than those of temperature. Severe and mild fire seasons generally see large and contrasting precipitation anomalies during the austral autumn (March, May, and April). In the case of temperature anomalies, northern ecoregions show contrasting anomalies for extreme fire seasons throughout the entire year, while central-western ecoregions have two separate 3-month periods where discrepancies between severe and mild fire seasons are more pronounced: pre-conditions during the austral autumn and the concurrent conditions of the fire season. Central-eastern and western ecoregions present no clear distinction in temperature anomalies between severe and mild fire seasons throughout the year, with the exception of Depressão Cuiabana. Lastly, southern ecoregions show differences in temperature anomalies during the fire season only.

Nevertheless, most ecoregions show contrasting behaviours between severe and mild fire seasons to some extent during two distinct 3-month periods: the austral autumn from March to May; and the fire season months from August to October. Severe fire seasons show negative precipitation anomalies during the austral autumn in all ecoregions, which contrasts with positive anomalies during mild fire seasons. In the case of northern and central-western ecoregions, where 3 of the highest burning ecoregions are located (Alto Parnaíba, Araguaia Tocantins, and Bananal), temperature anomalies are also consistently high in this period during severe fire seasons. The austral autumn coincides with the growing season over most of Cerrado (Arantes et al., 2016), and it has been reported for

several regions (e.g. Abram et al., 2021; Pereira et al., 2013) that hot and dry conditions during the growing season impact vegetation growth and health, resulting in dry fuel loads that, when exposed to favourable fire weather during the fire season, are more susceptible to burn.

However, these results for extreme fire seasons mask distinct monthly dynamics. In general, burned areas during the early fire season in August are much more constrained by pre-conditions of temperature and precipitation during the austral autumn, whereas late fire season burned areas in October rely on concurrent favourable climate conditions. This dynamic may be explained by the mediator effect of vegetation. In August, fuel moisture levels are generally high (Ramos-Neto and Pivello, 2000), hindering the occurrence of large burned areas even with favourable concurrent fire weather conditions; however, if fuel conditions deteriorate due to exposure to hot and dry weather during the growing season, it will be more susceptible to burning. On the other hand, by the end of the fire season vegetation stress is, in general, quite high due to several months of prolonged hot and dry conditions. September and October usually see the first rains, and their occurrence seems to be determinant for extreme burned areas during these months. These results are in line with previous assessments suggesting that fire activity in Cerrado is moisture-dependent (Alvarado et al., 2017), and that seasonal fire activity increases with a rapid drying of grasses or herbaceous fuel (Nogueira et al., 2017a).

The importance of climate conditions during the austral autumn in preconditioning fuel dryness during the fire season months provides an opportunity for early warning of burned areas in August. In the case of high-burning ecoregions, such as Alto Parnaíba, Araguaia Tocantins, and Bananal, bivariate models show that both temperature and precipitation during the austral autumn influence the interannual variability of early fire season burned areas in August. The other two ecoregions that make up the top 5 high burning ecoregions in Cerrado (Silva et al., 2021), Parnaguá and Chapadão do São Francisco, also show importance for temperature and precipitation during the austral autumn, respectively. This means that monitoring climate conditions during the autumn months may provide a useful outlook for early fire season burned areas, as a measure of the fuel dryness during the fire season. On the other hand, results also show that for all ecoregions, and for both temperature and precipitation, the months immediately prior to the fire season (June and July) do not seem to be relevant to either severe or mild fire seasons. In the context of fire

management, this assessment may assist in scheduling and defining the proper time and place for prescribed burning, a technique that is increasingly used to manage fuel loads in Cerrado landscapes (Schmidt et al., 2018). Controlled burns for agriculture also benefit from this outlook, as many large fires in Cerrado are agricultural burns that, often due to fire weather and stressed vegetation conditions, escalate to uncontrolled wildfires.

When looking at fire season burned areas, we find high regional variability in the explained variance of fire-climate models using either temperature or precipitation. However, when looking at bivariate models per month of the fire season, we find that August-burned areas are often linked with climate conditions prior to the fire season, whereas October-burned areas are associated with concurrent conditions. September seems to be a transitional month, where both pre-conditioned and concurrent climate may play a role. The primary aim of using bivariate models in this study was to explore relationships between regional fire activity and climate variables during and prior to the fire season. However, the very low coefficients of determination obtained with either temperature or precipitation, suggest that these variables may not be suitable for predictive purposes. Nevertheless, previous biome-wide studies found that precipitation can successfully model fire in Cerrado (Libonati et al., 2015; Mataveli et al., 2018). Given that the top 5 ecoregions contribute to, on average, 68% of Cerrado's yearly burned areas (Silva et al., 2021), it may be that, when fitting models to total burned areas in the biome, these models mostly reflect the fire-climate relationships within the highest burning ecoregions. In this study, the best-performing models are indeed those of the highest burning ecoregions, such as Araguaia Tocantins and Bananal. Furthermore, several other studies have shown that meteorological fire danger indices are successful in predicting interannual burned areas in Cerrado (Silva et al., 2019; Nogueira et al., 2017a). These complex indices take into account several other meteorological variables (such as relative humidity and wind speed), and mathematically reflect the influence of climate on several components of fire activity, such as fuel combustibility and fire spread. Additionally, the fact that both temperature and precipitation models perform worst when predicting August and September burned areas, in comparison to October burned areas, may reflect the importance of the mediating factors during these months (such as vegetation availability and condition, as previously hypothesized) and that they must be considered as well in modelling efforts.

Understanding the climatic drivers of burned areas in the biome, and their mediating

factors, is crucial in light of ongoing and future climate change: there has been a steady increase in temperatures over the last 40 years in Cerrado (Marengo et al., 2022; Hofmann et al., 2021), and less rainfall during the dry season (Blázquez and Silvina, 2020; Zappa et al., 2021). As the highest contributor to Brazil’s annual burned areas (UNEP, 2022), Cerrado is also responsible for a large portion of greenhouse gas (GHG) emissions. In the period of 1999 to 2018, Cerrado was responsible for emitting more than 2,500 Tg of carbon to the atmosphere, second only to the Amazon, and these rates are not expected to decrease (da Silva Junior et al., 2020). Brazil is amongst the largest carbon emitters worldwide (UNEP, 2023) and plays a crucial role in combating climate change. On October 2023, Brazil made the first adjustment of its Nationally Determined Contribution (NDC) to the Paris Agreement, pledging to cut GHG emissions by half in 2030 and achieve carbon neutrality by 2050. Lowering fire emissions in Cerrado is a crucial step to achieve these goals, that must be achieved through appropriate fire management policies. With this study, we hope to provide regionally tailored information to assist in drafting these policies and inform decision-making.

Moreover, as shown for biomes worldwide, while climate acts as an enabler of fire, it does not preclude the importance of other bioclimatic and human controls (Jones et al., 2022). Over South America, in particular, the prevalence of anthropogenic burning now dominates extensive regions across the continent, not only altering natural fire regimes in fire-prone regions such as Cerrado, but also inducing fires in fire-sensitive ecosystems (Libonati et al., 2021; Pereira et al., 2022). Ignitions in Cerrado are predominately anthropogenic (Schumacher et al., 2022), often associated with agricultural, land conversion, or traditional practices (Eloy et al., 2019; Durigan and Ratter, 2016). Moreover, socio-economic factors vary greatly amongst Cerrado’s ecoregions: southern Cerrado is characterized by severely altered landscapes and agricultural lands; while its northern region holds the last remnants of native vegetation cover and has high deforestation rates over the last few decades (Sano et al., 2019; Trigueiro et al., 2020). Relationships between land use and fire in Cerrado have been shown to be quite complex and highly dependable on regional context (Silva et al., 2020), and may, to a certain extent, explain the high regional variability of climate’s influence on burned areas found in this study. As such, next steps in evaluating regional drivers of fire in Cerrado should include the anthropogenic component.

## 3.6 Conclusion

Fire weather is considered to be the dominant control in burned areas worldwide (Jones et al., 2022) and in this study, we provide a first assessment of regional fire-climate dynamics throughout the Brazilian Cerrado. We analyse the climatic conditions (as evaluated through temperature and precipitation) that lead to severe and mild fire seasons in Cerrado’s ecoregions. Results show that there is high variability within the biome, but ecoregions with similar patterns align geographically. In general, we find contrasting behaviours in both temperature and precipitation for severe and mild fire season during two distinct 3-month periods: the pre-conditions during the austral autumn; and the concurrent conditions of the fire season. Ecoregions that burn the most show the largest contrasting behaviours during these periods and are also those for which bivariate models of temperature or precipitation perform best in predicting annual fire season burned areas.

We further assess the influence of pre-conditions during the austral autumn and concurrent conditions during the fire season in severe and mild years for each of the fire season months. For many ecoregions, we find that early fire season burned areas are constrained by pre-conditions during the austral autumn, whereas late fire season burned areas are linked to concurrent climate conditions. Severe(mild) burned areas in August are associated with hot and dry(cold and wet) conditions during the austral autumn, and severe(mild) burned areas in October are associated with hot and dry(cold and wet) concurrent conditions. September is an intermediate month, seemingly influenced by both pre-conditions and concurrent climate.

We hypothesize that the mediating effect of vegetation plays a crucial role in explaining these patterns. Hot and dry conditions during the growing season affect vegetation health and lead to highly curated fuel loads that are more susceptible to burning during the fire season. Moreover, these results provide important information for fire management strategies, as we show that fire season months have different climatic constraints. Monitoring meteorological conditions during the austral autumn may provide useful outlooks for early fire season burned areas, while late fire season burned areas require a closer monitoring on concurrent meteorological conditions. Understanding the importance and dynamics of the mediating effect of vegetation in the fire-climate relationship is thus essential to bet-

ter inform fire management in the Cerrado biome. As a severely disturbed biome that is subject to high anthropogenic pressure, future assessments of regional drivers in Cerrado should also consider the human influence on fire activity.

### 3.7 Supplementary Material

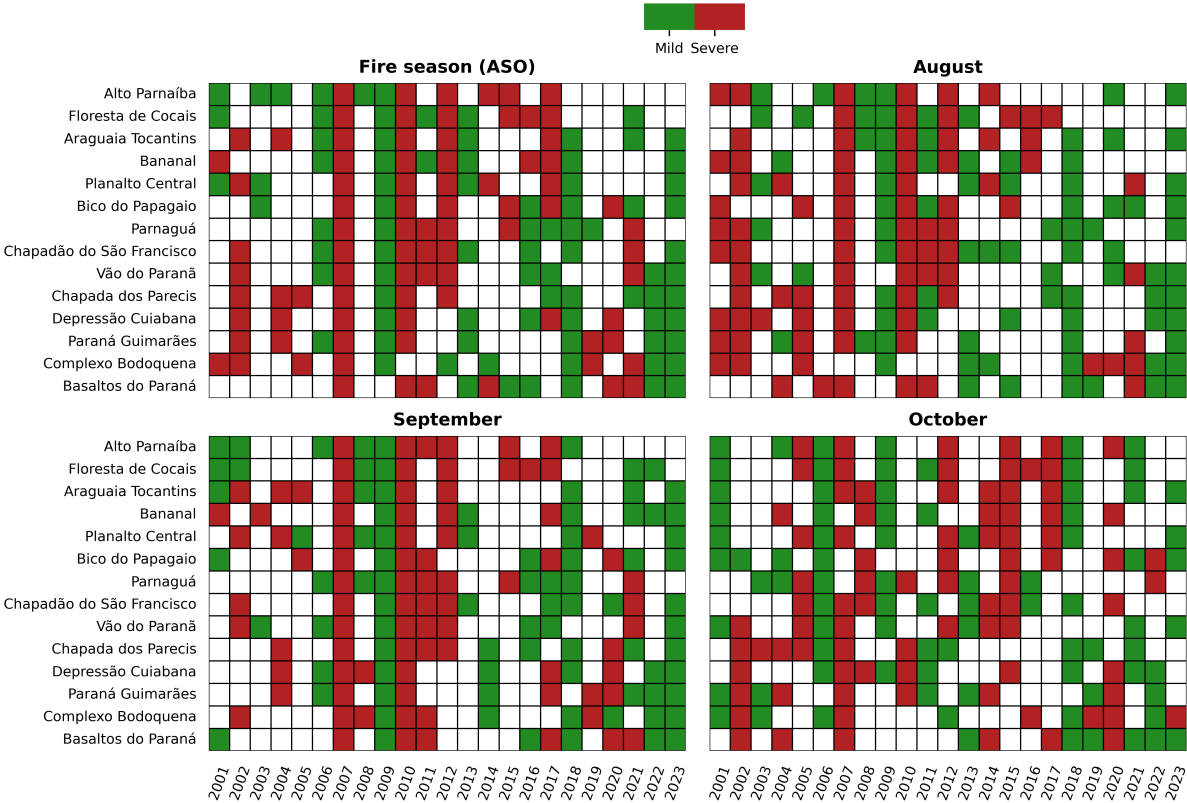


Figure 3.7: Severe (red) and mild (green) fire years defined as those above and below the 75<sup>th</sup> and 25<sup>th</sup> percentile of burned areas over the 2001–2023 period, respectively. Each subplot represents the severe and mild fire years estimated using: fire season (ASO) burned areas; burned areas during the month of August; burned areas during the month of September; and burned areas during the month of October.



## Chapter 4

# The role of anthropogenic activity

## 4.1 The case of the MATOPIBA region

*This section is based in the following conference proceeding: Silva, P., Rodrigues, J., Santos, F., Pereira, A., Nogueira, J., DaCamara, C., and Libonati, R. (2020). Drivers Of Burned Area Patterns In Cerrado: The Case Of Matopiba Region. 2020 IEEE Latin American GRSS & ISPRS Remote Sensing Conference (LAGIRS)*

The Brazilian savanna (Cerrado) is one of the most important biodiversity hotspots in the world. Being a fire-dependent biome, its structure and vegetation dynamics are shaped by and rely on the natural occurring fire regime. Over the last decades, Cerrado has been increasingly threatened by accelerated land cover changes, namely the uncontrolled and intense use of fire for land expansion. This is particularly seen in Brazil's new agricultural frontier in northeastern Cerrado: the MATOPIBA region. Changes in MATOPIBA's fire regime resulting from this rapid expansion are still poorly understood. Here we use satellite-derived datasets to analyze burned area patterns in MATOPIBA over the last 18 years, at the microregions level. We further evaluate the role of climate and land use in spatial and temporal burned area variability and assess their trends in the last two decades. Results show an increased contribution of MATOPIBA to Cerrado's total burned area over the last few years: Maranhão and Tocantins present the highest values of total burned area with some microregions burning more than twice its area over the study period. Climate is shown to play a relevant role in MATOPIBA's fire activity, explaining 52% of the interannual variance, whereas land use and burned area were found to have more complex interactions that are highly dependent on the regional context. Lastly, climate and land use drivers are found to have an overall increasing trend over the last two decades, whereas burned area trends show much heterogeneity within MATOPIBA.

### 4.1.1 Introduction

Fire events are complex disturbances that influence vegetation dynamics, biodiversity and ecosystem services, particularly in fire-dependent biomes such as the Brazilian savannas (Cerrado) (Hardesty et al., 2005). Cerrado is one of the most important global biodiversity hotspots and is increasingly threatened partly due to a lack of a consistent fire policy (Durigan and Ratter, 2016). This fire-prone biome relies on fire to shape its vegetation

distribution and composition and burns regularly constrained to the annual and seasonal climatological conditions. Nevertheless, changes in the fire regime consequent of future aggravation of climate conditions might lead to irreversible damage.

While climate has been shown to strongly influence fire activity in Cerrado (Silva et al., 2019; Hoffmann et al., 2012b), anthropogenic action plays a preponderant role: over the last decades, most human-induced ignitions have been found to be due to increases in land use management, expansion for livestock and agriculture (Song et al., 2018). The uncontrolled and intense use of fire has contributed to accelerate land cover changes (Lapola et al., 2014) and to disrupt natural spatial patterns of fire events in this biome. The role of human activity is particularly relevant in Brazil's new agricultural frontier, the northern region of Cerrado known as MATOPIBA (de Miranda et al., 2014).

Satellite-derived datasets have proven a useful tool to understand changes in the fire regimes, particularly in Brazil where field records are costly and irregular. These datasets provide long-term burned area information with reasonable spatial resolution, improved accuracy, higher spatial coverage and temporal homogeneity. They allow a comprehensive characterization of systematic spatial and temporal burned area patterns, improving the understanding of fire activity in Cerrado (Rodrigues et al., 2019; Nogueira et al., 2017a; Libonati et al., 2015).

Here, we explored the burned area patterns in Cerrado over the last 18 years, in the context of regional climate variations and anthropogenic drivers. Land use and a purely climate-driven fire danger index are evaluated as drivers of spatial burned area patterns. We focused on the MATOPIBA region, given its importance as the new agricultural frontier, and perform our study at the microregions level, as defined by the Brazilian Institute of Statistics and Geography (IBGE). Understanding regional fire regimes can provide useful information to trigger appropriate fire management and policy decisions.

## **4.1.2 Methods**

### **4.1.2.1 Study area**

Our study area is the MATOPIBA region, considered here the IBGE's microregions that compose the Maranhão (MA), Tocantins (TO), Piauí (PI) and Bahia (BA) states that are included in the geographical extension of Cerrado. IBGE's microregions are groups of

municipalities with common geographical characteristics (IBGE, 1990). In our analysis, MATOPIBA contains 41 microregions in a  $0.25^\circ$  regular grid by nearest-neighbor interpolation, totalizing  $709,508 \text{ km}^2$  of extension (Figure 4.1), which represents 35% of Cerrado biome.

Although the agricultural frontier in MATOPIBA exists since the 1980's, it began to rapidly expand after the agri-food crisis of 2007/2008 (Pereira and Pauli, 2016). This region is highly sought by businesses given the cheap labor, inefficient supervision and arable land. The main cultures are corn, soybean, and cotton (Sano et al., 2010).

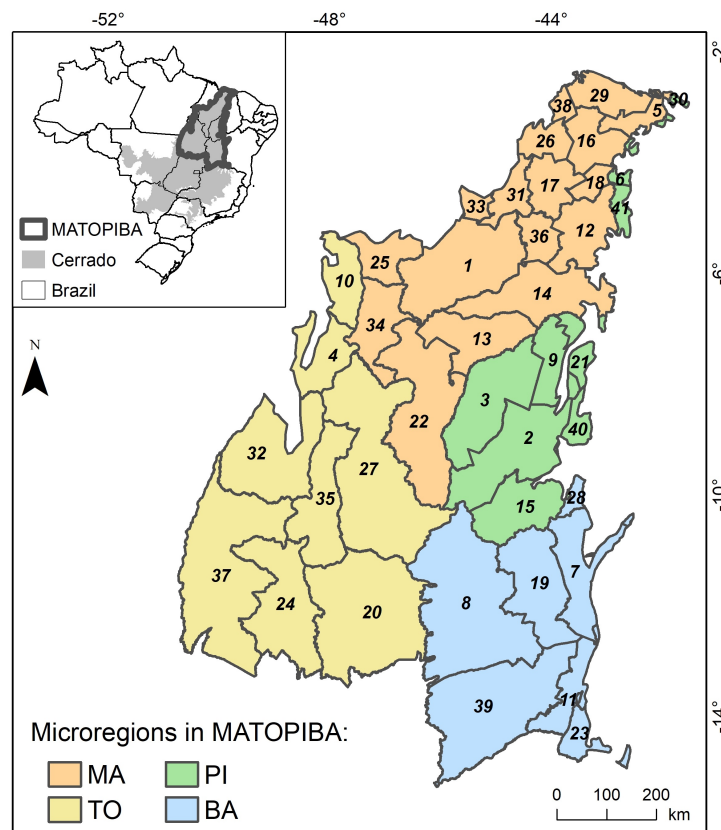


Figure 4.1: Spatial distribution of the 41 microregions from MATOPIBA in the Cerrado biome.

#### 4.1.2.2 MCD64 satellite burned area (SBA) product

We used the MCD64A1 Burned Area BA version (collection 6, C6) product (Giglio et al., 2018) derived from MODIS sensors developed by the National Atmospheric Space Agency (NASA). The algorithm of the C6 is based on multiple stages, using time series composites and conditional thresholds (Giglio et al., 2018) to estimate the monthly SBA at 500m of spatial resolution from 2000 to present. The adjacent non-overlapping tiles of 10 degrees

square (at the equator) for the study area were downloaded in HDF4 file format. Tiles of the Burn Date layers were mosaicked and remapped using the Modis Reprojection Tool from NASA (Dwyer and Schmidt, 2006). This product was already validated in the Cerrado biome and has been shown to accurately identify burned areas, particularly in northern Cerrado (Rodrigues et al., 2019).

#### **4.1.2.3 Datasets of drivers on SBA patterns**

As drivers, we evaluated land use (LU) and climate (CL) effects. LU was evaluated using Mapbiomas v.3.1 (MapBiomas, 2019), a dataset developed by a collaborative network of experts in Brazilian biomes. Mapbiomas uses a machine learning method (Random Forest) to perform a pixel by pixel classification based on an annual mosaic from Landsat satellite images at 30m spatial resolution with a median value in each year. The training of this algorithm uses balanced samples and in post-classificatory images, temporal, spatial, frequency and gap filling filters are applied (MapBiomas, 2019). LU is divided in six classes (Farming, Pasture, Agriculture, Annual and Perennial Crop, Semi-Perennial Crop and Mosaic of Agriculture and Pasture), and data was downloaded in GeoTIFF format and stored in WGS84 datum from 2001 to 2017.

To account for the effects of CL, we used the Canadian Forest Fire Weather Index (FWI) System (van Wagner, 1987). The FWI system consists of six components that account for the effects of fuel moisture and wind on fire behavior and has been shown to be highly adaptable and accurately replicate fire danger conditions in diverse ecosystems around the world (Pinto et al., 2018; Taylor et al., 2016). The first three FWI components are fuel moisture codes: the Fine Fuel Moisture Code (FFMC), the Duff Moisture Code (DMC), and the Drought Code (DC). High values indicate dry fuels and only DC has memory. The remaining three components are: the Initial Spread Index (ISI), the Build-up Index (BUI) and the Fire Weather Index (FWI), which are fire behavior indices whose values rise as the fire danger increases. They represent, respectively, the rate of fire spread, the fuel available for combustion and the frontal fire intensity. FWI components are estimated with daily values at 18 UTC of air temperature, air relative humidity, wind speed, and previous 24-hour precipitation. Meteorological data from the European Centre for Medium-Range Weather Forecasts' (ECMWF) ERA5 reanalysis product (C3S, 2017) were employed.

In this study, we use the Daily Severity Rating (DSR), an extension of the FWI system,

consisting of a numeric rating that indicates the difficulty to control fires, more accurately reflecting the expected efforts required for fire suppression. Computation of DSR requires applying a power relation emphasizing higher FWI values. Silva et al. (2019) showed that 71% of the interannual variability of SBA in Cerrado can be explained using the DSR.

#### **4.1.2.4 Statistical analysis**

Accumulated monthly SBA values were estimated for each microregion to evaluate the trends of interannual SBA and drivers over the 2001–2018 period. As proposed in previous works (Rodrigues et al., 2019; Nogueira et al., 2017a) we analyzed SBA in Cerrado’s dry season: June, July, August, September, and October (JJASO), when there is highest fire incidence in this biome.

Relationships between interannual SBA and anthropogenic drivers were evaluated through the determination coefficient and corresponding p-value from simple linear regression.

For the trend analysis, we used the non-parametric Theil-Sen regression (Theil, 1950; Sen, 1968), a robust estimator insensitive to outliers with a breakdown point of about 29.3% in regards to that of simple linear regression. The statistical significance of the trends was evaluated by the two-tailed Mann-Kendall non-parametric test (Mann, 1945; Kendall, 1975). The test assumes that when no trend is present, the observations are not serially correlated over time. Hence, we detrended each time series by subtracting its corresponding Theil-Sen regression equation and evaluated for autocorrelation between ranks (Hamed and Rao, 1998). The modified Mann-Kendall test accounts for the effects of serial correlation in data and was applied to the detrended time series that showed to be serially correlated.

### **4.1.3 Results and Discussion**

#### **4.1.3.1 Temporal and spatial distribution of SBA**

Over the last 18 years, MATOPIBA accounted for approximately 58% of burned area in the Cerrado biome (Figure 4.2), a significant amount considering that MATOPIBA accounts for 35% of this biome’s area. Its contribution is relatively constant: around half of Cerrado’s total SBA. The SBA in MATOPIBA was lowest at the beginning of the century ( $\approx 53\%$ ) compared to that of the last few years ( $\approx 61\%$ ), hinting at increased

importance in Cerrado’s total burned area.

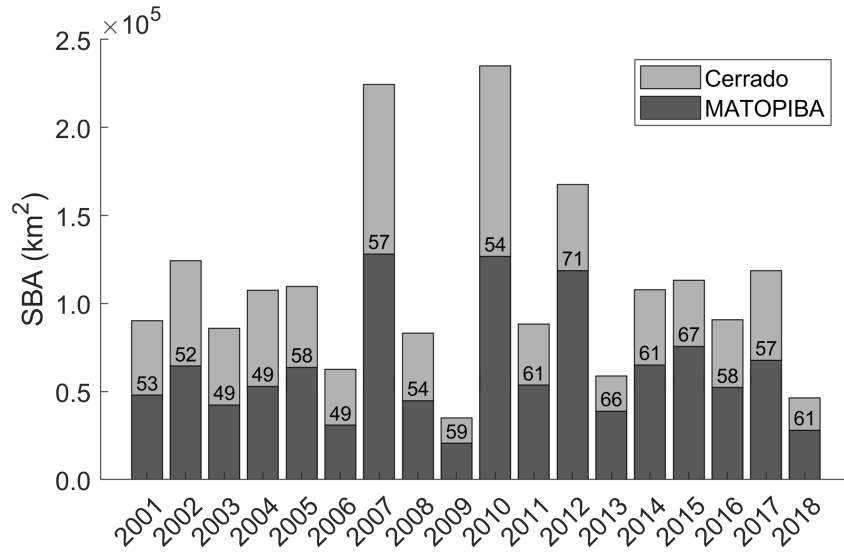


Figure 4.2: Burned area (km<sup>2</sup>) in MATOPIBA (dark grey) and Cerrado (light grey) for the dry season from 2001 to 2018. Numbers above dark grey bars reflect the percentage of burned area in MATOPIBA in regards to that of Cerrado’s in each year.

The highest contribution ( $\approx 71\%$ ) of MATOPIBA to the total burned area in Cerrado was observed in 2012, whereas the lowest ( $\approx 49\%$ ) were in the years 2003, 2004 and 2006 (Figure 4.2). Its highest SBA values are in the years 2007, 2010 and 2012, coinciding with those of Cerrado. These were years of drought events in Brazil: the dry season months of 2007 saw anomalous precipitation values, below the average for Cerrado (Mataveli et al., 2018); a similar case was found for 2010 (Mataveli et al., 2018; Marengo et al., 2017), a year also known for a widespread drought in the Amazon rainforest (Marengo et al., 2011); lastly, northeast Brazil was also found to be in severe drought in 2012 (Marengo et al., 2013). Drought-fire interactions are often associated with major fire activity events (Brando et al., 2014), and several studies have pinpointed the inverse relationship between burned area and precipitation in Cerrado (Nogueira et al., 2017a; Libonati et al., 2015), where seasonal fire activity increases with a rapid drying of fuel.

The highest SBA counts are represented by microregions localized in the Tocantins (TO) state, accounting for, on average, 50% of MATOPIBA’s total burned area over the 18 years. The remaining microregions in the other states account for approximately 23% (MA), 13% (PI) and 14% (BA) of total burned area in MATOPIBA. There are six microregions that burned more than twice its area over the 18 years, all within the 15 largest

microregions of MATOPIBA (with over 20,000 km<sup>2</sup>). Of these, only Alto Parnaíba Piauiense/PI(3) is not located in TO or MA. Jalapão/TO(27) achieved the highest SBA value, burning more than thrice its area (332%) over the study period, a concerning figure, given that it is the largest microregion in MATOPIBA (with 53,507 km<sup>2</sup>).

#### **4.1.3.2 Drivers of spatial burned area patterns**

To assess the influence of CL and LU in spatial SBA trends, we evaluated coefficients of determination derived from simple linear regression (Figure 4.3). The linear relationship of SBA and CL is that of positive slope for all microregions, meaning that when CL increases, SBA increases as well. CL significantly explains on average 52% of MATOPIBA's interannual variance (p-value below 0.001) and more than 25% in most microregions (25 out of 41). Furthermore, CL explains at least half the interannual variance in six microregions and, of these, only Rio Formoso/TO(37) is amongst those with the highest burned area. The remaining five microregions with the highest burned area values, identified in the previous section, have coefficients of determination in the range 6%–22%, suggesting that climate is not the main driver in these microregions but rather an aggravating factor.



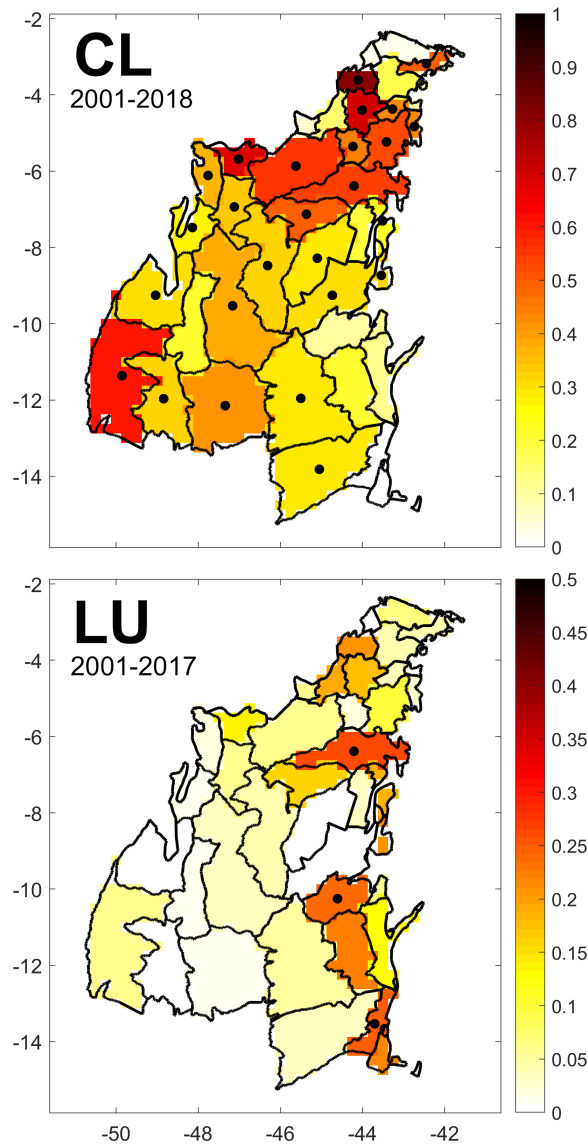


Figure 4.3: Coefficient of determination values between SBA and CL/LU (upper/lower figure) for MATOPIBA from 2001 to 2018/2017, respectively. Values close to 1(0) indicate a high(low) relation between SBA and CL/LU. The filled(empty) circles represent significance below the 5(10)% level.

Microregions presenting higher correlation with CL are mostly located in the northern region of MATOPIBA, where the larger areas of native vegetation (savanna) are located and might have not yet been disrupted by anthropogenic activity. Low values obtained for the coefficients of determination might suggest that MATOPIBA is shifting from a climate-controlled historical fire season to a disturbed regime.

On the other hand, SBA and LU present different relationships depending on microregion, resulting in an overall non-significant low coefficient of determination for MATOPIBA (1.4% with a p-value of 0.65). The relationship between SBA and LU is much more

complex than that of SBA and CL, as it is highly dependable on the type of land use change. The use of fire to expand the agricultural frontier has been characterized by two stages: the use of fire to clear native vegetation into arable land, in which case burned area increases; and the use of controlled and seasonal fire in the harvest season and to clear the agricultural fields, in which case burned area decreases. Accordingly, when performing simple linear regression using LU as a predictor of burned area, distinct signals were found. All microregions in BA obtained a negative slope, indicating an inverse relationship: the higher the land use, the lower the SBA; which is in accordance with BA being a heavily deforested state with most of its area used for agriculture. Oppositely, microregions in MA presented mostly positive slopes, confirming the clearing of native vegetation discussed previously, and subsequent higher burned areas. However, the vast majority of these relationships are not significant at the 5/10% level. LU only explains more than 25% of the variance in two microregions, significantly at the 5% level: Bom Jesus da Lapa/BA(11) and Chapadas do Alto Itapecuru/MA(14). Chapadas do Extremo Sul Piauiense/PI(15) closely follows with  $R^2 = 0.24$ , equally significant at the 5% level. Moreover, when looking at Chapadas do Alto Itapecuru/MA(14), CL explains 54% and LU explains 27%, suggesting that this region is heavily influenced by these two drivers.

The remaining of MATOPIBA, although substantially influenced by CL and, in the case of some microregions, LU as well, might be also constrained to other drivers not studied here. We hypothesize that population density, urban area, fuel availability and topography might play a significant role in SBA variability as well as fire management and environmental policies.

#### **4.1.3.3 Trends of spatial burned area patterns**

Opposite SBA trends are found within MATOPIBA (Figure 4.4, top figure): MA presents an overall significant positive trend, whereas BA shows a negative trend; the remaining states (TO and PI) show contrasting patterns within their borders. Consequently, when analyzing SBA trends for the entirety of the MATOPIBA no conclusion can be drawn, which is not the case for both the CL and LU drivers (Figure 4.4, middle and bottom figures) that present significant positive trends in the region below the 5% significance level.

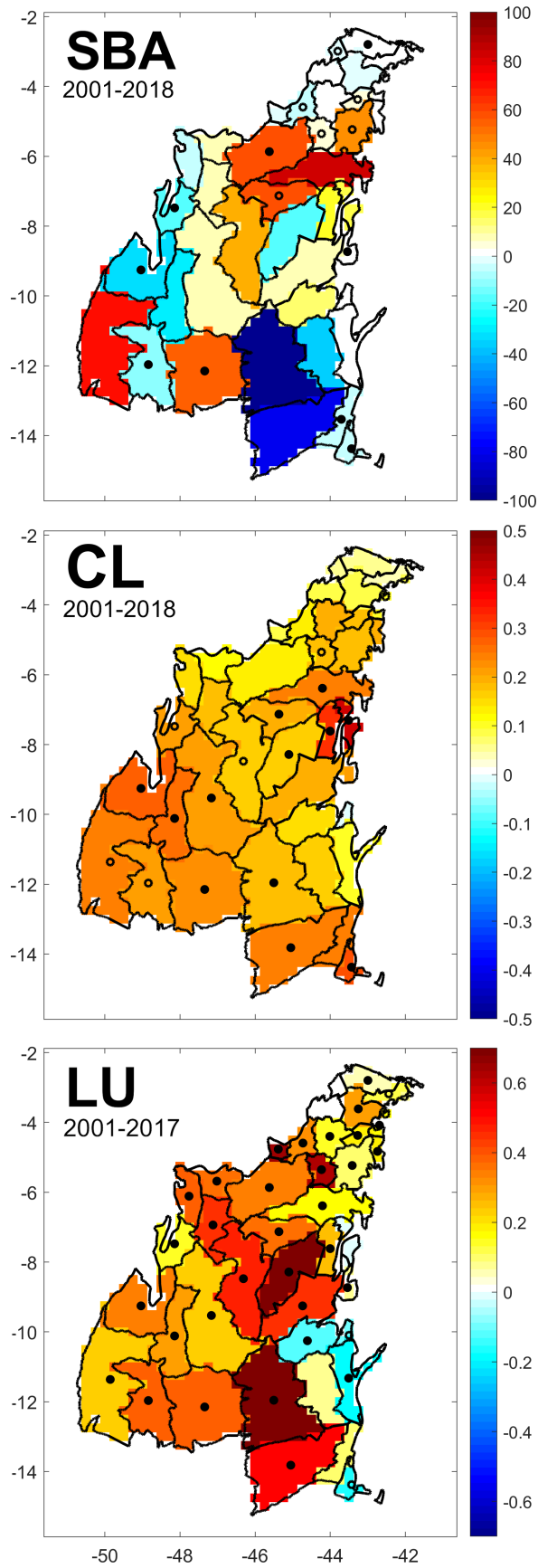


Figure 4.4: Trends of SBA, CL and LU for the study region over 2001–2018. Warmer(cooler) colors represent an upward(downward) trend and filled(empty) circles represent significance below the 5(10)% level.

When evaluating at the state level the only state presenting a significant SBA trend was MA, with a positive trend over the last 18 years (p-value of 0.003). Accordingly, significant positive SBA trends are found within central MA, consistent with significant positive LU trends: amongst the four states, Maranhão presents the highest amount of Cerrado's native vegetation and it has been increasingly cleared over the study period for agricultural purposes. Southern MA and western PI show predominantly non-significant positive trends, which is consistent with increased agricultural expansion over the study period (Bolfe et al., 2017).

Northwestern TO, limiting the Cerrado and Amazon biomes, presents predominantly negative SBA trends and significant positive LU trends. This region is part of the Arc of Deforestation, an area characterized by historical deforestation and, accordingly, these microregions were, at the beginning of our study period, mostly deforested. Although our results show a continued agricultural expansion over the 2001–2018 period, fire activity in these microregions is controlled and used mainly for agricultural practices, consistent with the negative trends of SBA.

Although mostly not statistically significant, BA shows decreasing SBA trends. This region has also seen substantial agricultural expansion over the last few years: data from GITE – EMBRAPA shows that Barreiras/BA(8) and Santa Maria da Vitoria/BA(39) were amongst the microregions with the highest production of cotton, corn and soy in 2012 (Pereira and Pauli, 2016). However, when looking at LU trends, significant negative trends are found in eastern BA microregions. These microregions are in the transition between the Cerrado and Caatinga biomes, the latter is a semiarid ecosystem characterized by a long dry season. Given its longer period without rain, along with disadvantageous topography, the expansion of agricultural land use in Caatinga is difficult (Mingoti et al., 2014). It's worth noting that these microregions in BA showing significant decreasing trends, along with Chapadas do Extremo Sul Piauiense/PI(15), show minor variations along the 18 years of data (decreases of the normalized burned area around 0.1%–1.4%). Moreover, excluding Guanambi/BA(23), they do not have high LU percentages (average over the 17 years: range 3%–14%).

Overall, microregions that present significant LU positive trends above 0.45 are amongst those with the highest deforestation rates (Garcia and Filho, 2018) but also those with

highest growth and concentration of annual cropland area in this century (Lorensini et al., 2015), that have been previously subject to human-driven change.

Lastly, CL presents positive trends for all microregions, some of them significant at the 5/10% level (17 out of 41). This indicates fire danger (and thus climate conditions favorable for fire activity) has been increasing over the last 18 years. This is in agreement with the analysis of increased temperature and decreased precipitation and moisture over the last decades for Brazil (de Barros Soares et al., 2017). Furthermore, when looking at historical data from 1989 onwards these trends not only obtain higher absolute values, as all microregions in MATOPIBA present significant values below the 5% level, except for northern MA. A positive CL trend reflects changes in meteorological parameters (namely increased temperature and lower relative humidity) that might have profound effects on the seasonality of fire activity and vegetation phenology. This takes special relevance in light of future projections for the Brazilian Cerrado that show increased fire danger under several climate change scenarios for the 21<sup>st</sup> century (Silva et al., 2019), suggesting that this historical positive CL trend over Cerrado will most likely be kept.

#### **4.1.4 Conclusions**

MATOPIBA's importance in the context of fire activity in Cerrado is not to be disregarded as we found that this region represents more than half the annual burned area of the Brazilian savanna. Maranhão and Tocantins states have the highest contributions to this value, contributing to 73% of MATOPIBA's total burned area over 2001–2018. Burned area totals also showed that some microregions burned more than twice its area over the study period.

SBA was found to be significantly constrained by climate and we hypothesize that anthropogenic drivers (including those not evaluated in this work, such as urban areas, deforestation, fuel availability, fire management, environmental policies and population density) play a substantial role in short term SBA trends. It's worth emphasizing that climate provides conditions for burning, but fire events are always dependent on ignition, which in Brazil is known to be almost certainly human. Land use did not prove to be a relevant factor in the vast majority of MATOPIBA, which leads us to conclude that the human-driven component of burned area must be further evaluated. This driver was

also found to be very complex to analyze its influence on burned area given the high dependence on the regional context.

Overall trends in MATOPIBA of CL and LU have been of increase over the 2001–2018 period; SBA, however, presented very distinct trends within the study region. Although constrained to administrative areas, this study provides useful information to characterize each microregion and contribute for improved and more adequate policy measures.

## 4.2 Human activity influences regional fire-climate dynamics

Favourable meteorological conditions are crucial for fire to occur and spread, and climate has a modulating effect on fuel availability and condition. Human activity is also hypothesised to play a considerable role in fire activity in the Brazilian savannas (Cerrado), given its socio-economic context. However, how anthropogenic activity factors into fire-climate dynamics is still poorly understood. Here, we explore how anthropogenic activity, evaluated through land use, deforestation, and population, influences regional fire-climate relationships. We employ a novel approach based on individual fire scars and stratify fires into two classes: mild fires, which correspond to the vast majority of fires (95%); and extreme fires that, albeit infrequent (top 5%), contribute to a large portion of total burned area. We find that the performance of fire-climate models varies significantly per ecoregion and fire size, suggesting different driving factors. Indeed, in the case of mild fires, fire-climate models perform worst in ecoregions with fractions of anthropogenic land use below  $\approx 36\%$ , deforested fraction below  $\approx 37\%$ , and population above  $\approx 800,000$  people. These ecoregions are, incidentally, those located in the Arc of Deforestation and MATOPIBA. On the other hand, in ecoregions with a larger anthropogenic footprint, fire-climate models perform best. These results suggest that, in the case of mild fires, climate may not be the main driver of interannual variability in areas of anthropogenic expansion. In the case of extreme fires, we find no clear patterns between the strength of regional fire-climate relationship with anthropogenic variables, suggesting that climate may be the main environmental control. These results pave the way to a better understanding of the regional fire-climate-human relationships in Cerrado, and show that these relationships depend on individual fire characteristics. This study reinforces the need to consider individual fires when studying fire drivers, and reflect on the scale on which these controls act.

### 4.2.1 Introduction

Anthropogenic activity is changing fire regimes worldwide (Pereira et al., 2022; Bowman et al., 2020). Recent declines in global burned area have been attributed to human activity (Andela et al., 2017; Lasslop and Kloster, 2017) and, in some regions, human influence on

fire regimes might even override the relationship between fire and climate (Jones et al., 2022; Syphard et al., 2017; Aldersley et al., 2011). Anthropogenic activity influences fire in a variety of ways, both directly and indirectly impacting several aspects of fire regimes (Bowman et al., 2011; Kelly et al., 2023; Keeley and Pausas, 2019). Across vast areas of the globe, humans are now the primary ignition source, altering the amount and seasonality of fires (Ganteaume and Syphard, 2018; Balch et al., 2017; Archibald, 2016). These human-ignited fires have been shown to increase extreme fire behaviour and severely impact ecosystem functioning (Hantson et al., 2022; Archibald, 2016). Humans also affect fire extent and intensity through land management by modifying vegetation structure and composition which influences fuel combustibility and continuity. Moreover, anthropogenic climate change is disturbing weather patterns and worsening fire weather conditions worldwide (Richardson et al., 2022; Jain et al., 2021; Abatzoglou et al., 2019). These recent human-driven changes in climate have been linked to increases in the length of fire season (Jolly et al., 2015) and are projected to contribute to extreme fire weather over the 21<sup>st</sup> century (Touma et al., 2021).

Nevertheless, the manner in which humans impact fire activity varies considerably around the globe. For instance, it has been shown that human activity in temperate regions leads to less fires, whereas in tropical ecosystems human presence enhances fire activity (Lasslop and Kloster, 2017). In the tropical savannas of Brazil — Cerrado — fire is a crucial feature. This savanna-like biome is the largest contributor to Brazil’s annual burned area (UNEP, 2022; Mataveli et al., 2018) and, as a fire-dependent biome, it relies on its natural fire regime to maintain the ecosystem’s functioning and structure (Pivello et al., 2021). However, climate change together with the recent drastic changes to its landscape (Schmidt and Eloy, 2020; Strassburg et al., 2017), have disrupted the historical fire regime, leading to high pyrodiversity (Kelly et al., 2023) and very distinct regional fire behaviours (Silva et al., 2021). There is also a severe north-south contrast on total burned area trends (Andela et al., 2017; Silva et al., 2021; Jones et al., 2022) and, while the number of smaller fires seems to be decreasing, larger fires are increasing (Silva et al., 2021).

These regional variations in fire activity hint at distinct regional drivers of fire activity. While several studies have highlighted the role of climate (Li et al., 2021b; Silva et al., 2019; Nogueira et al., 2017a), studying the human constraints of fire activity in Cerrado is



much more complex. Spanning 2 million km<sup>2</sup>, Cerrado has very diverse landscapes where human presence and influence vary significantly. Cerrado harbours the last agricultural frontier of Brazil - MATOPIBA (the confluence of states, Maranhão - MA, Tocantins - TO, Piauí - PI, and Bahia - BA), where there is active deforestation (Trigueiro et al., 2020), and most of the native vegetation of Cerrado remains (Strassburg et al., 2017). Within MATOPIBA, relationships between anthropic land use and fire were found to be very complex, and often altogether opposite, due to interactions between fire with deforestation and agriculture (Silva et al., 2020). There is also emerging evidence that regions with high landscape fragmentation and agricultural fraction are linked with lower burned areas (Rosan et al., 2022; Rodrigues et al., 2019), whereas larger burned areas occur where native vegetation cover remains (Silva et al., 2021; Campagnolo et al., 2021). Ribeiro et al. (2024) further found that burned areas in the Amazon-Cerrado transition, commonly referred to as the Arc of Deforestation, are linked to changes in land use, particularly forest and savanna conversion to agriculture and pasture.

The direct assessment of human influence on fire activity is lacking in Cerrado, with only a few studies evaluating these relationships locally (e.g. Conciani et al., 2021). More recently, Segura-Garcia et al. (2024) showed that human presence shapes the relationship between climate and burned areas in the natural vegetation of Cerrado. They found that, for grid cells with high anthropogenic land use, there is little to no influence of climate in natural burned areas, whereas where anthropogenic land use was lower than 40%, increased temperature and vapour pressure deficit (VPD) led to larger burned areas. Additionally, global studies also provide preliminary insights on how humans may influence fire within Cerrado. Population density seems to be negatively correlated with burned areas over the biome (Jones et al., 2022; Forkel et al., 2019), and Andela et al. (2017) found that livestock density and cropland fraction are also negatively correlated with burned areas. Kelley et al. (2019) showed that fires in tropical savannas have the highest sensitivity to human suppression and ignitions, and Forkel et al. (2019) found that land cover is one of the most important predictors of burned areas in Cerrado.

However, it has been suggested that metrics that are often employed to study fire, such as total burned areas or fire severity, fail to capture human impacts that are essential to a better understanding of human-fire interactions (Shuman et al., 2022). Alternatively, individual fire data derived from remote sensed pixel-level burned area has recently emerged

as an important source of information (e.g. Andela et al., 2019; Laurent et al., 2018; Artés et al., 2019). These datasets contribute to a better understanding of fire patterns and provide crucial information (such as fire count, size, and spread) to assess the driving factors that influence fire activity worldwide (e.g. Hantson et al., 2015; Andela et al., 2022). In the case of Cerrado, previous works revealed very distinct spatial and temporal patterns for different fire size across the region (Silva et al., 2021; Campagnolo et al., 2021; Rodrigues et al., 2019; Santos et al., 2021). In particular, these works hypothesize that spatial variability in the occurrence of distinct fire sizes may be linked to both climate and human activity: while the prevalence of smaller fires in the historical agricultural frontier may be associated to agricultural practices, larger fires within the areas of ongoing agricultural expansion occur alongside high rates of deforestation and land conversion.

Here, we build on this evidence, and propose a paradigm shift from traditional analysis of driving factors that influence fire activity in Cerrado. We question whether fires of different size have distinct relationships with climate and anthropogenic activity. To do so, we evaluate regional climatic and anthropogenic drivers of fire in Cerrado’s ecoregions using individual fire events, instead of total burned area. For each ecoregion, we classify individual fires as mild and extreme, and assess the influence of climate (as evaluated based on a meteorological fire danger index) and anthropogenic drivers (namely land use, deforestation, and population) on each class during the 2001–2023 period.

## **4.2.2 Data and methods**

### **4.2.2.1 Study area**

We partition Cerrado into 19 ecoregions as proposed by Sano et al. (2019). These ecoregions are unique in terms of landscape characteristics and were defined based on their physical attributes (elevation, rainfall, and soil), land use types, land cover classes and conservation status (protected areas and indigenous territories).

### **4.2.3 Datasets and pre-processing**

Information on individual fire events was obtained from the Global Fire Atlas (GFA) from January 2003 to November 2018 (Andela et al., 2019). GFA derives individual fire characteristics from the MODIS MCD64A1 Collection 6 burned area product (Giglio et al.,

2018), including timing (day of burn) and location of ignition points, fire size ( $\text{km}^2$ ), fire duration (days), daily expansion ( $\text{km}^2 \cdot \text{day}^{-1}$ ), fire line length (km) and speed ( $\text{km} \cdot \text{day}^{-1}$ ), and direction of fire spread. For the purposes of this study, we restricted to individual fire size.

Climate was characterized through a meteorological fire danger index based on the Canadian Fire Weather Index System (CFWIS; Figure 4.5). CFWIS relies on daily values of temperature, relative humidity, wind speed, and daily precipitation to estimate 7 sub-indices that describe different characteristics of fire occurrence and behaviour (van Wagner, 1987). Based on CFWIS, the Daily Severity Rating (DSR) is a numerical representation of the difficulty of controlling fires that reflects the expected effort required for fire suppression. DSR has been shown to adequately describe burned areas in Cerrado before (Silva et al., 2019). Data was obtained from the Copernicus Emergency Management Service available in Copernicus' Climate Data Store (Copernicus Climate Change Service, 2019). This global dataset uses meteorological fields from historical simulations of the ERA5 reanalysis to compute CFWIS's indices from 1940 onwards, in a regular  $0.25^\circ \times 0.25^\circ$  grid (Vitolo et al., 2020). We use daily DSR data from the consolidated dataset and system version 4.1 for the 2003–2018 period.

Anthropogenic land use was evaluated using the MapBiomas Collection 7 product, a Brazilian platform of annual land use and land cover (LULC) mapping (Figure 4.5; MapBiomas, 2023). We obtained yearly maps from 2003 to 2018 and selected landcover classes associated with anthropic use, namely: Pasture, Soybean, Sugar cane, Rice, Cotton, Other Temporary Crops, Coffee, Citrus, Other Perennial Crops, Forest Plantation, Mosaic of Uses, Urban Area, Mining, and Aquaculture. For each ecoregion, we then obtained the anthropogenic land use fraction per year of the time series.

Deforestation rates were obtained from the PRODES project (Figure 4.5; INPE, 2024) available through the Terrabrasilis platform (Assis et al., 2019). The PRODES product results of visual interpretation of satellite imagery at 30-meter resolution and considers deforestation to be suppression of native vegetation cover, regardless of future use. PRODES has bi-annual data from 2002 to 2012, and yearly deforestation rates from 2013 to 2023. The year 2000 aggregates total deforested area up to this point in time. We used total deforested areas by 2000 and the annual rates to estimate the deforested fraction of

each ecoregion for all available years from 2003–2018.

Finally, to account for population we rely on annual official population estimates per county between 2003 and 2018 (Figure 4.5; IBGE, 2019). We aggregated all counties within each ecoregion.

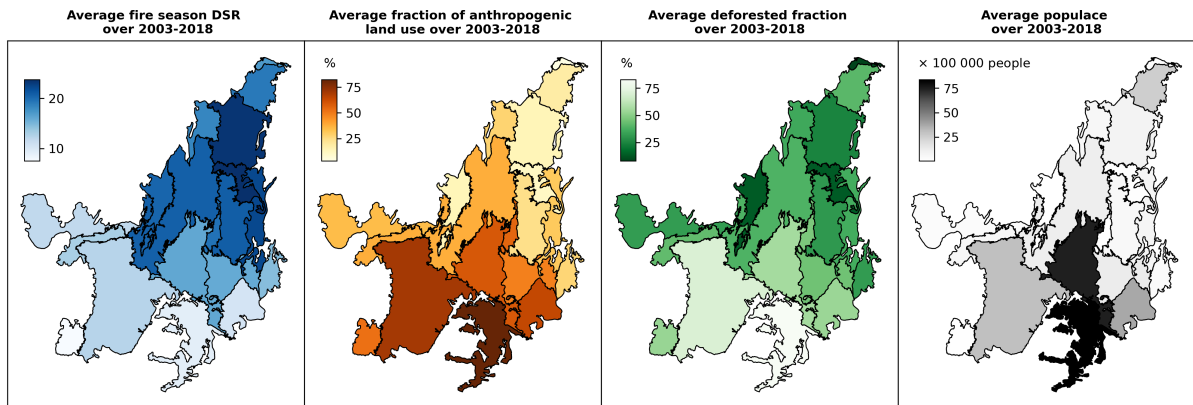


Figure 4.5: Spatial variability of the climatic and anthropogenic variables employed in this study. From left to right: average fire season DSR over 2003–2018 (shades of blue); average fractions of anthropogenic land use (%) over 2003–2018 (shades of orange); average deforested fraction (%) over 2003–2018 (shades of green); and average populace (people) over 2003–2018 (shades of grey).

#### 4.2.3.1 Methods

##### Classes of fire size

Silva et al. (2019) found that the DSR successfully models annual burned areas during the fire season (defined as August to October) in Cerrado. We use this as a starting point to study regional fire-climate relationships within the biome, and thus this study focuses only on fire season fires. Accordingly, for each year from 2003 to 2018, individual fire events were filtered to those occurring only in months of August, September, and October.

Then, fire season fires were stratified into two classes based on a threshold of fire size: mild fires, defined as individual fire events with burned areas below the threshold; and extreme fires, defined as individual fire events with burned area equal or greater than the threshold. The chosen threshold was the 95<sup>th</sup> percentile of fire size considering all fire season fires over the 2003–2018 period.

##### Fire-climate models

By means of simple linear regression, the fire season averaged DSR is used as a predictor of the annual fire season burned areas per class over the 2003–2018 period. As the distribution of burned areas is often right skewed, yearly totals are log-transformed using the decimal logarithm. As an example, in the case of mild fires, the predictand is the decimal logarithm of total yearly burned area from all mild fires from 2003 to 2018. Goodness-of-fit is assessed through the coefficient of determination ( $R^2$ ) and relationships are considered significant if below the 5% level.

### **Anthropogenic component**

Following methods proposed in Syphard et al. (2017), we attempt to explain the regional variation in the strength of fire-climate relationships using anthropogenic variables. To do so, for each ecoregion and each fire class (mild and extreme), we compared the variance explained ( $R^2$ ) by the fire-climate models with the following anthropogenic characteristics: average fraction of anthropogenic land use over the 2003–2018 period (%); average deforested fraction over the 2003–2018 period (%); and total population. In the case of population, data was considerably right skewed and was log-transformed using again the decimal logarithm.

We further employed the non-parametric Kruskal-Wallis test by ranks (Kruskal and Wallis, 1952), to find a threshold value on which two independent samples are statistically different. In the context of this paper, we wanted to test whether there were any two groups of ecoregions that are significantly different based on the strength of their fire-model relationship. These two groups are defined with a threshold value from the anthropogenic variables, i.e., a threshold value for anthropogenic land use, deforestation, and population. We iteratively tested threshold values of each anthropogenic variable considering the full range of possible values and defined a minimum sample size of 5 (i.e., each group defined by the threshold needs to have at least 5 ecoregions, but the two groups may have a different sample size). The Kruskal-Wallis test then determines whether these two groups originate from the same distribution. For each anthropogenic variable, we selected the threshold value associated with a p-value below 0.05. If there is more than a single significant threshold value, we selected firstly based on the lowest p-value, then by the sample size of each group: we preferred groups with similar sample sizes.

## 4.2.4 Results

Extreme fires account for more than 50% of total burned areas during the fire season in 10 out of 19 ecoregions over the 2003–2018 period (Figure 4.6). The highest values are found in Chapada dos Parecis and Complexo Bodoquena, where extreme fires represent on average 69% and 66% of total fire season burned areas, respectively. On the other hand, Costeiro and Basaltos do Paraná show the lowest contribution of extreme fires with 29% and 34%, respectively. Nevertheless, the extent of extreme fires varies significantly amongst ecoregions. For instance, in the case of Costeiro extreme fires are those above 3.6 km<sup>2</sup>, which greatly contrasts with extreme fires in Bananal which extend above 106.8 km<sup>2</sup>.

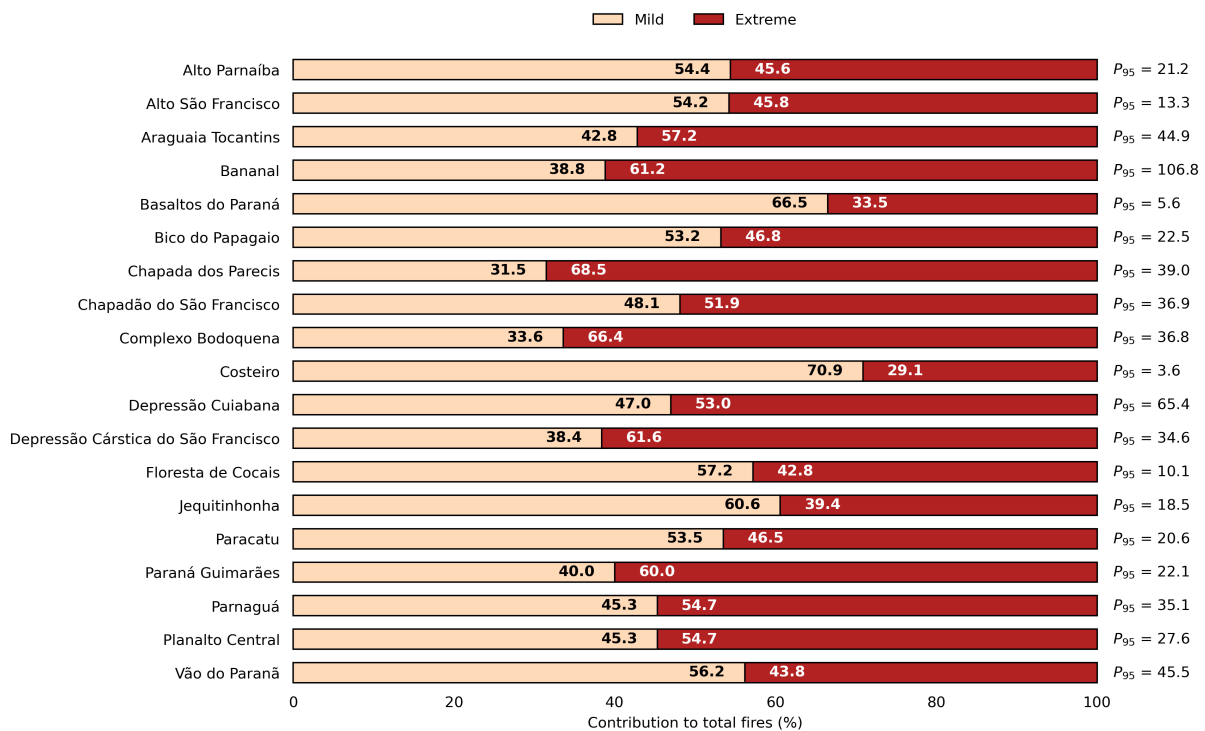


Figure 4.6: Contribution of each fire class to total burned area (%). Mild(extreme) fires are shown in yellow(red) and the associated values are shown in black(white). The 95<sup>th</sup> percentile (P<sub>95</sub>) of fire size are listed at the right-hand side of the plot.

We find that there is high spatial variability in the strength of the fire-climate relationship, as evaluated through simple linear regression using fire season averaged DSR to predict the interannual variability of mild and extreme fires during the fire season (Table 4.1). Variance explained ranges from 0% to 79% in the case of mild fires, and 5% to 75% in the case of extreme fires. Nevertheless, the vast majority of ecoregions present a

significant (below the 5% significance level) relationship, with only 3 and 5 ecoregions showing non-significant regression coefficients for mild and extreme fires, respectively. Complexo Bodoquena, Costeiro, and Jequitinhonha, have non-significant relationships for both mild and extreme fires; Depressão Cárstica do São Francisco presents a significant relationship for mild fires but non-significant for extreme fires, and Vão do Paranã shows the opposite result. Some ecoregions have considerably lower coefficients of determination for mild than extreme fires: Bananal, Basaltos do Paraná, Bico do Papagaio, Chapada dos Parecis, and Chapadão do São Francisco.

Table 4.1: Goodness of fit (as evaluated through the coefficients of determination –  $R^2$ ) of simple regression models using fire season averaged DSR to predict interannual burned areas of mild, extreme, and total fire events during the fire season, for each of the 19 ecoregions of Cerrado.

	Mild	Extreme	Total
Alto Parnaíba	<b>51.8</b>	<b>51.2</b>	<b>53.6</b>
Alto São Francisco	<b>45.0</b>	<b>31.6</b>	<b>38.2</b>
Araguaia Tocantins	<b>55.8</b>	<b>59.1</b>	<b>60.8</b>
Bananal	<b>27.7</b>	<b>58.1</b>	<b>57.6</b>
Basaltos do Paraná	<b>44.4</b>	<b>75.5</b>	<b>64.9</b>
Bico do Papagaio	<b>50.3</b>	<b>71.0</b>	<b>67.9</b>
Chapada dos Parecis	<b>25.1</b>	<b>71.2</b>	<b>65.8</b>
Chapadão do São Francisco	<b>26.6</b>	<b>48.5</b>	<b>42.3</b>
Complexo Bodoquena	16.7	8.2	24.2
Costeiro	0.0	13.9	1.1
Depressão Cárstica do São Francisco	<b>28.1</b>	6.1	<b>25.1</b>
Depressão Cuiabana	<b>54.0</b>	<b>51.9</b>	<b>70.1</b>
Floresta de Cocais	<b>55.6</b>	<b>43.4</b>	<b>53.9</b>
Jequitinhonha	24.0	5.1	<b>27.9</b>
Paracatu	<b>59.3</b>	<b>44.1</b>	<b>61.9</b>
Paraná Guimarães	<b>79.2</b>	<b>73.6</b>	<b>76.1</b>
Parnaguá	<b>37.5</b>	<b>35.3</b>	<b>38.2</b>
Planalto Central	<b>67.3</b>	<b>58.4</b>	<b>66.7</b>
Vão do Paraná	<b>43.9</b>	24.2	<b>53.6</b>

We then associated the regional fire-climate coefficients of Table 4.1 with their corresponding anthropogenic characteristics, namely: the average fraction of anthropogenic land use and deforestation during the 2003–2018 period, and decimal logarithm of aver-

age population during the same period (Figure 4.7). In the case of mild fires, ecoregions with larger anthropogenic land use, deforestation, and population, seem to show larger variance explained by climate. On the other hand, ecoregions with a lesser anthropogenic footprint, present lower coefficients of determination of the fire-climate models. Ecoregions within MATOPIBA and the Arc of Deforestation appear clustered, as they have the lowest amounts of anthropogenic land use and deforestation. Regarding population, the relationship between the variance explained by fire-climate models and the decimal logarithm of population appears linear. Accordingly, the impact of population increase in the strength of fire-climate relationships decreases as population values rise.

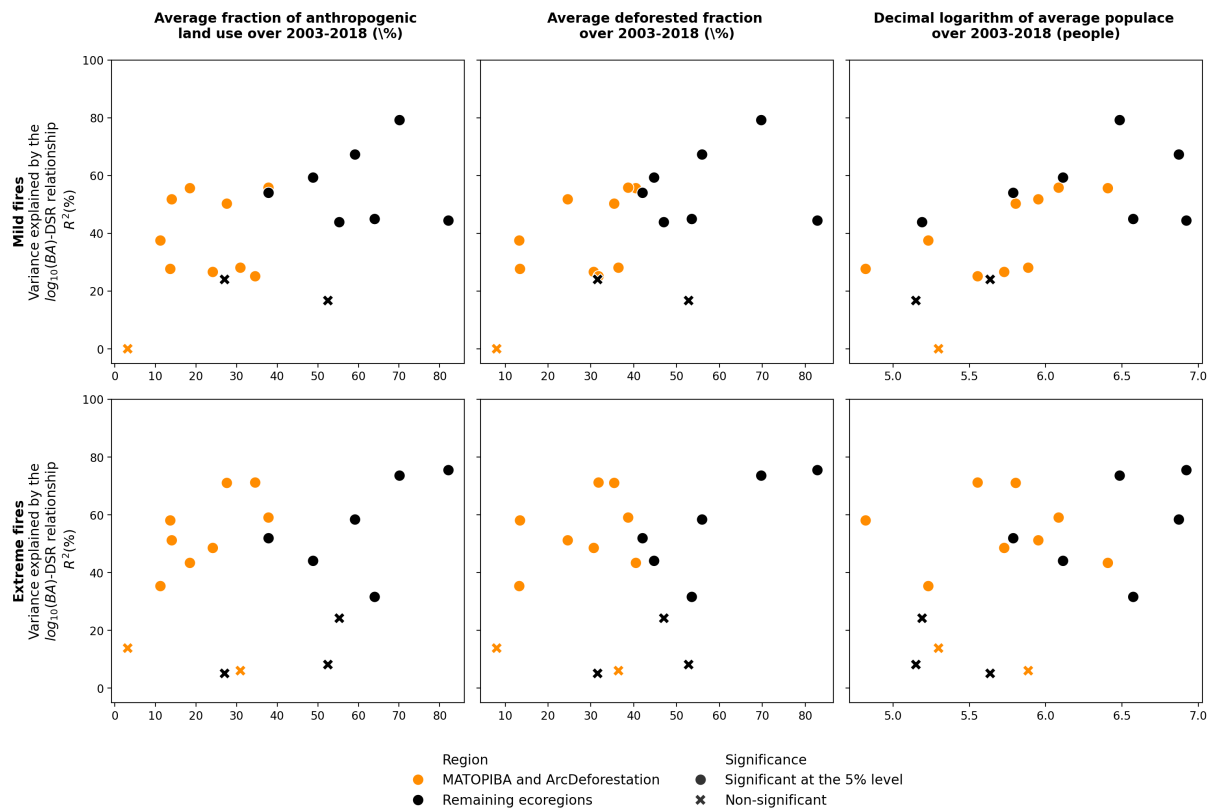


Figure 4.7: Comparing the coefficients of determination ( $R^2$ ; %) of each regional fire-climate model for both mild and extreme classes of fire, and their corresponding anthropogenic characteristics, namely: average fraction of anthropogenic land use over 2003–2018 (%); average deforested fraction over 2003–2018 (%); and the decimal logarithmic of average populace over the 2003–2018 period. Ecoregions located in the MATOPIBA and Arc of Deforestation regions are shown in yellow markers, and crosses represent non-significant fire-climate models (with p-values below the 5% level).

In the case of extreme fires, no patterns are evident. The strength of fire-climate relationships does not seem to be linked to any of the anthropogenic variables considered. This is confirmed when looking for threshold values of anthropogenic variables that significantly



differentiate between two groups of ecoregions, based on the strength of their fire-climate relationship (Supplementary Material: Tables 4.2, 4.3 and 4.4). We find that extreme fires do not show significant threshold values for any anthropogenic variables, whereas mild fires do (Figure 4.8). Ecoregions below the 35%–37% threshold of anthropogenic land use show weaker fire-climate relationships, while the opposite stands for ecoregions above the threshold value. For deforestation, ecoregions with a deforested fraction below 37%–38% have less variance explained by climate than those above that threshold. Finally, ecoregions with population higher(lower) than  $\approx 800,000$  people have stronger(weaker) fire-climate relationships.

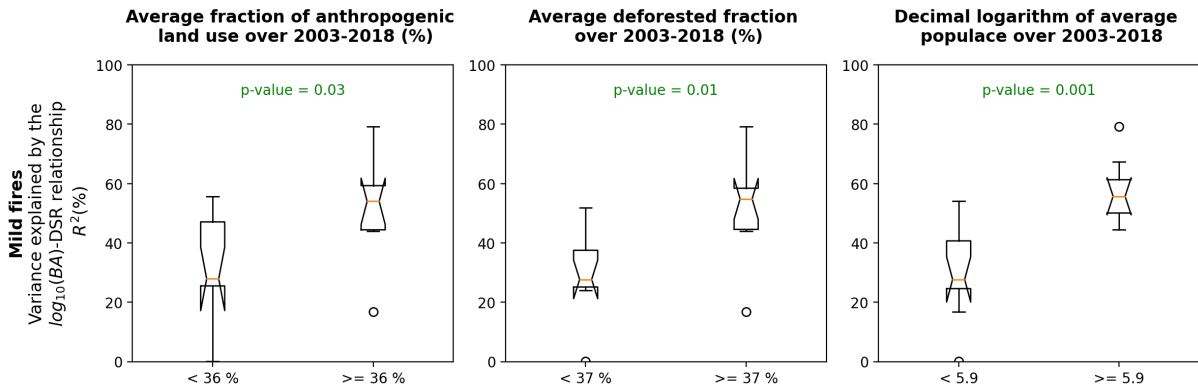


Figure 4.8: Results of the threshold analysis for mild fires by means of the Kruskal-Wallis test statistic, for each anthropogenic variable. From left to right: average fraction of anthropogenic land use over 2003–2018 (%); average deforested fraction over 2003–2018 (%); and the decimal logarithmic of average populace over the 2003–2018 period. For simplicity, we chose the threshold value of 36% in the case of anthropogenic land use (where it ranged between 35%–37%; Supplementary Material: Table 4.2), and 37% in the case of deforested fraction (ranging from 37%–38%; Supplementary Material: Table 4.3). Boxplots represent the distribution of ecoregions below and above the threshold value, and the p-value for the Kruskal-Wallis test is shown in green.

## 4.2.5 Discussion

The influence of climate on mild and extreme fires varies considerably amongst ecoregions. Considering only significant model results (below the 5% significance level), we find high geographical variation in the strength of the fire-climate relationship, ranging from 25.1% to 79.2% and 31.6% to 75.5%, for mild and extreme fires, respectively.

### 4.2.5.1 Mild fires

This variation in the strength of the fire-climate relationship for mild fires is associated with anthropogenic variables. Ecoregions with less anthropogenic land use, deforested

areas, and population have weaker fire-climate relationships. On the other hand, in ecoregions where human presence is more prominent, the variance explained by climate is higher.

In the case of anthropogenic land use and deforestation, there is a clear clustering of ecoregions located within the agricultural frontiers of MATOPIBA and the Arc of Deforestation. These ecoregions are characterized by weaker fire-climate models compared to the remaining ecoregions, which entails that climate is not the main driver of mild fires. In the case of population, albeit there is no geographical clustering, there is a seemingly linear relationship between the variance explained by climate and the decimal logarithm of total population. This suggests a non-linear relationship between population and the strength of climate in explaining interannual burned areas. This is not unexpected, as the non-linear relationship between population and fire activity has been documented elsewhere: for instance, in Africa, it has been found that human ignitions increase linearly with population density up to a threshold, from which ignition number decreases as humans start to live in closer proximity to each other (Archibald, 2016). We also find that for population values below  $\approx 800,000$  people, fire-climate models perform worse.

These results are to be analyzed within the current and historical socioeconomic context of Cerrado. Fires in Cerrado are predominately of human origin (Schumacher et al., 2022). However, how humans use fire varies considerably along its 19 ecoregions. Ecoregions located within MATOPIBA and the Arc of Deforestation contain the last remnants of native vegetation, and are areas of ongoing agricultural expansion, marked by high deforestation rates (Trigueiro et al., 2020). Here, fire is often used as an inexpensive tool to clean up deforested or degraded areas (Schmidt and Eloy, 2020), and these deforestation fires are typically small (Andela et al., 2022). Conversely, the remaining ecoregions of Cerrado are located in the southern part of the biome, the historical agricultural frontier during the 1960s (Sano et al., 2020), which is now a highly fragmented landscape covered by agricultural and pasture lands, and mostly deprived of native vegetation cover (Trigueiro et al., 2020). In small-scale agricultural areas of Cerrado, fire serves a diversity of purposes, such as the management of species and landscapes, cattle raising upon native or exotic pasturelands, and subsistence agriculture (Eloy et al., 2019; Moura et al., 2019). The vast majority of fires in these ecoregions are small due to land fragmentation and lack of fuel continuity, and seem to be decreasing over the last two decades (Silva et al., 2021).

Indeed, recent declines in burned areas over savanna ecosystems, including the Cerrado, have been attributed to agricultural expansion and intensification, where shifts to more capital-intensive agriculture led to fewer and smaller fires (Andela et al., 2017).

It is possible that, in ecoregions where there is ongoing anthropogenic expansion, fire-climate models perform worse because the interannual variability in mild fires is not so much influenced by meteorological fire danger, as by socioeconomic and political factors. On the other hand, in ecoregions that have been exposed to human pressure for far longer, and are not subject to ongoing land use transition, meteorological fire danger may play a more critical role in the interannual variability of burned areas.

These results may seem to contrast with those of Segura-Garcia et al. (2024), where the authors found that in areas of higher human presence, the climate had little to no effect on natural burned areas. However, two key differences are worth pointing out: while Segura-Garcia et al. (2024) evaluated total burned areas in natural vegetation, in the present study we do not differentiate between fires occurring in natural or anthropic areas and instead classify by fire size. By considering all fires, we are considering added dynamics between fire and human activity, such as using fire for agricultural management in pastures and croplands. We build on this previous study with the novel information that regional fire-climate relationships and their interaction with anthropogenic activity in Cerrado differ based on fire size.

#### **4.2.5.2 Extreme fires**

In the case of extreme fires, the variation in the fire-climate relationship was not associated with any of the anthropogenic variables considered in this study and, for some ecoregions, the coefficient of determination of the fire-climate relationship was higher than that obtained for mild fires. The occurrence of extreme fires in Cerrado (Li et al., 2021a) and worldwide (e.g. Libonati et al., 2022b; Ramos et al., 2023; Deb et al., 2020; Wang et al., 2015) has been linked to severe fire weather and extreme, often compounded, meteorological events (such as drought and heatwaves). The role of favourable meteorological conditions on extreme and unusual fires has been well documented (UNEP, 2022), and is a necessary condition for large fires by directly influencing fire spread and indirectly impacting fuel amount and condition. Nonetheless, most extreme fires in Cerrado are a result of human-ignited fires, either for agricultural purposes or deforestation, that spread

to neighbouring areas and turn into uncontrolled wildfires (Schmidt and Eloy, 2020).

We also find that the extent of extreme fires seems constrained by land fragmentation. Results show relatively smaller extreme fire sizes in ecoregions with the largest amount of anthropic land use, such as Basaltos do Paraná (5.6 km<sup>2</sup>), Alto São Francisco (13.3 km<sup>2</sup>), and Paraná Guimarães (22.1 km<sup>2</sup>). On the other hand, several ecoregions with low anthropic land use show similar extents for extreme fires, such as Floresta de Cocais (10.1 km<sup>2</sup>), Alto Parnaíba (21.2 km<sup>2</sup>), and Bico do Papagaio (22.5 km<sup>2</sup>). In this case, there is high fuel continuity, which implies land fragmentation is not a limiting factor for large fires.

In accordance with previous studies (Silva et al., 2021), we also find that a small number of total fires is responsible for the vast majority of burned areas within Cerrado. During the fire season, the top 5% of fires correspond to at least 29% of burned areas over the study period, and in 10 ecoregions they amount to more than 50% of total burned areas. In Chapada dos Parecis and Complexo Bodoquena, ecoregions bordering the Amazon and Pantanal, respectively, the top 5% of fire events are responsible for more than 66% of burned areas. These extreme fires consume large extents, spreading through both fire-dependent and fire-sensitive vegetation and severely impacting the ecosystem (Durigan and Ratter, 2016; Schmidt et al., 2018).

#### **4.2.5.3 Implications**

Previous studies have relied on total burned areas to explain and quantify controls of fire activity worldwide (e.g. Andela et al., 2017; Jones et al., 2022). In environments dominated by large fires, that constitute the vast majority of burned areas, such as the Cerrado, we argue that this approach mainly reflects the drivers of infrequent and extreme fire events. Our results show that when fitting simple regression models to total burned areas, regardless of fire size, the goodness-of-fit changes significantly compared to that obtained for mild and extreme fires only (Table 4.1). Accordingly, using total burned areas to study the climatic controls of fire may mask distinct dynamics that are dependent on individual fire characteristics.

Additionally, biome-wide results for Cerrado showed that the DSR explains 71% of the interannual variability of burned areas (Silva et al., 2019). Here, we find overall weaker fire-

climate models using the same predictor, and the strength of the model varies significantly by ecoregion and by class of fire (Table 4.1). Given the high spatial heterogeneity in fire behaviour within Cerrado (Silva et al., 2021), it is expected that the controlling factors of fire activity also vary. Indeed, the influence of climate in annual burned areas varies considerably amongst Cerrado's 19 ecoregions and depends on fire size, reflecting distinct socioeconomic contexts. However, it may also be that different drivers act on different spatial scales: human influence on fire activity may be better captured at smaller spatial scales (e.g. local to regional), than that of climate, which may perform best at larger spatial scales (e.g. ecosystem to global).

For this reason, when assessing anthropogenic drivers, the use of an individual fire database, such as the GFA employed in this study, provides an opportunity to further explore fire-human relationships. Previous studies have used similar databases of individual fire events to classify fires based on their individual attributes and underlying human and natural controls (e.g. Andela et al., 2022). Such a classification is lacking for the Cerrado. Still, our results provide an initial assessment of climatic and anthropogenic drivers based on individual fire attributes that hint at distinct anthropogenic controls based on fire size. These results have important implications for fire management, as it is essential that fire management policies consider the human factor, and its regionally diverse interactions with fire. Given that the majority of ignitions in Cerrado are human, increased public awareness and public policies are needed to reduce the number of human-started wild-fires. Likewise, given the undeniable importance of climate in modelling burned areas in Cerrado, fire policies must also be drafted in light of ongoing changes in climate and the projected increases in meteorological fire danger (Silva et al., 2016).

Assessing regional fire and its bioclimatic and human controls is essential to inform the next generation of fire models. Although the majority of global fire models now include the human component to a certain extent (Rabin et al., 2017), the relationship between fire and humans is often simplistic and generically applied throughout the globe (Ford et al., 2021). However, interactions between humans and fire are very diverse and highly dependent on regional context (Jones et al., 2022; Kelley et al., 2019). Studies have highlighted the need to assess regional interactions between fire and its bioclimatic and socioeconomic controls to improve predictive fire models (Andela et al., 2017; Forkel et al.,

2019).

These relationships are heterogeneous over space and time and require regular reassessment as human impacts on the ecosystem evolve driven, for example, by politics, economy, or climate change. Indeed, future predictions point to very distinct burned area trends driven by changing climatic and socioeconomic patterns (Wu et al., 2021). Further studies are also needed to assess the role of anthropogenic activity directly on regional fires in Cerrado. Although the present study hints at possible regional human influence in the case of mild fire events, we do not directly compare or evaluate the relationship between fire and anthropogenic variables (e.g. through a linear regression model, as employed for fire-climate models). The reason is that the anthropogenic variables considered here (namely, land use, deforestation, and population) have very strong trends throughout the time series, making any linear modelling approach inappropriate.

Moreover, the lack of a national fire database with attribution of ignition sources is a major hindering factor to studying anthropogenic drivers of fire occurrence in the Brazilian Cerrado. Global satellite-derived estimates can help fill some of these gaps, and products on individual fire events, such as the GFA employed in this study, further allow fire events to be classified based on their individual attributes and tested for different controls of fire activity. However, these products are limited to the last two decades, and are also known to underestimate small fires (Ramo et al., 2021; Boschetti et al., 2019; Randerson et al., 2012) that, in Cerrado, possibly constitute the vast majority of fire events (Silva et al., 2021). Improved national intelligence, along with satellite-derived products with a longer time series and thinner spatial resolutions, are thus essential to better study and inform on the historical and current fire drivers in the Brazilian Cerrado.

#### **4.2.6 Conclusions**

This study provides a novel assessment of the climatic and anthropogenic drivers of regional fire activity in Cerrado's ecoregions. Using information on individual fires, we classify fires into mild and extreme fire events. We find that the definition of extreme event varies regionally, ranging from events extending 3.6 km<sup>2</sup> to 106.8 km<sup>2</sup>. Albeit in smaller numbers, these extreme fires are responsible for the majority of burned areas over most ecoregions. The strength of the fire-climate relationships shows high geographical

variation and in many cases it is stronger for extreme fires. Fire-climate models perform worse for mild fires in areas of anthropogenic expansion, entailing that climate is not the main driver of fire in these regions. On the other hand, extreme fires seem to be constrained mainly by climatic conditions and show no geographical gradient with any of the anthropogenic variables considered in this study.

Our results highlight that fire in Cerrado has very distinct regional controls and further show how these relationships may differ based on individual fire size. We reflect on the need to consider the distinct spatial scales at which fire drivers act, and move away from a single driver perspective. We provide the first analysis of fire-climate-human relationships in Cerrado based on individual fire attributes, and illustrate how the use of total burned areas to study drivers of fire may mask distinct fire-climate-human dynamics that rely on more detailed information. This is especially true in biomes as large as the Cerrado, with a large variety of regional fire dynamics and diverse socioeconomic contexts.

Understanding how anthropogenic activities can directly or indirectly influence fire activity at the regional level is crucial, not only to support decision-making in fire management but also to improve fire modelling efforts.





## 4.2.7 Supplementary Material

Table 4.2: Results of the iterative analysis to find a threshold value for average fraction of anthropogenic land use over 2003–2018 (%), in which two groups of ecoregions have statistically different strengths of the fire-climate relationship, for the mild and extreme fire classes. For each threshold value, the Kruskal-Wallis (KW) test statistic and associated p-value are shown, along with the number of ecoregions that are below ( $N <$ ) or above ( $N \geq$ ) the threshold. Threshold values that yielded significant results below the 5% level are highlighted in grey, and those chosen as the best threshold values are in bold. For more information on selection criteria see Methods.

Threshold	Mild				Extreme			
	KW statistic	KW p-value	N ecoregions < threshold	N ecoregions $\geq$ threshold	KW statistic	KW p-value	N ecoregions < threshold	N ecoregions $\geq$ threshold
19	0.42	0.52	5	14	0.42	0.52	5	14
20	0.42	0.52	5	14	0.42	0.52	5	14
21	0.42	0.52	5	14	0.42	0.52	5	14
22	0.42	0.52	5	14	0.42	0.52	5	14
23	0.42	0.52	5	14	0.42	0.52	5	14
24	0.42	0.52	5	14	0.42	0.52	5	14
25	1.11	0.29	6	13	0.38	0.54	6	13
26	1.11	0.29	6	13	0.38	0.54	6	13
27	1.11	0.29	6	13	0.38	0.54	6	13
28	1.97	0.16	8	11	0.68	0.41	8	11
29	1.97	0.16	8	11	0.68	0.41	8	11
30	1.97	0.16	8	11	0.68	0.41	8	11
31	2.67	0.10	9	10	2.16	0.14	9	10
32	2.67	0.10	9	10	2.16	0.14	9	10
33	2.67	0.10	9	10	2.16	0.14	9	10
34	2.67	0.10	9	10	2.16	0.14	9	10
35	<b>4.51</b>	<b>0.03</b>	<b>10</b>	<b>9</b>	0.81	0.37	10	9
36	<b>4.51</b>	<b>0.03</b>	<b>10</b>	<b>9</b>	0.81	0.37	10	9
37	<b>4.51</b>	<b>0.03</b>	<b>10</b>	<b>9</b>	0.81	0.37	10	9
38	1.83	0.18	12	7	0.11	0.74	12	7
39	1.83	0.18	12	7	0.11	0.74	12	7
40	1.83	0.18	12	7	0.11	0.74	12	7
41	1.83	0.18	12	7	0.11	0.74	12	7
42	1.83	0.18	12	7	0.11	0.74	12	7
43	1.83	0.18	12	7	0.11	0.74	12	7
44	1.83	0.18	12	7	0.11	0.74	12	7
45	1.83	0.18	12	7	0.11	0.74	12	7
46	1.83	0.18	12	7	0.11	0.74	12	7
47	1.83	0.18	12	7	0.11	0.74	12	7
48	1.83	0.18	12	7	0.11	0.74	12	7
49	0.62	0.43	13	6	0.19	0.66	13	6
50	0.62	0.43	13	6	0.19	0.66	13	6
51	0.62	0.43	13	6	0.19	0.66	13	6
52	0.62	0.43	13	6	0.19	0.66	13	6
53	2.48	0.12	14	5	1.23	0.27	14	5
54	2.48	0.12	14	5	1.23	0.27	14	5
55	2.48	0.12	14	5	1.23	0.27	14	5

Table 4.3: As Table 4.2 but regarding the average deforested fraction over 2003–2018 (%).

Threshold	Mild				Extreme			
	KW statistic	KW p-value	N ecoregions < threshold	N ecoregions ≥ threshold	KW statistic	KW p-value	N ecoregions < threshold	N ecoregions ≥ threshold
31	2.48	0.116	5	14	0.21	0.64	5	14
32	6.43	0.011	7	12	0.35	0.55	7	12
33	6.43	0.011	7	12	0.35	0.55	7	12
34	6.43	0.011	7	12	0.35	0.55	7	12
35	6.43	0.011	7	12	0.35	0.55	7	12
36	5.35	0.021	8	11	0.01	0.93	8	11
37	<b>6.41</b>	<b>0.011</b>	<b>9</b>	<b>10</b>	0.54	0.46	9	10
38	<b>6.41</b>	<b>0.011</b>	<b>9</b>	<b>10</b>	0.54	0.46	9	10
39	4.17	0.041	10	9	0.11	0.74	10	9
40	4.17	0.041	10	9	0.11	0.74	10	9
41	2.73	0.099	11	8	0.25	0.62	11	8
42	2.73	0.099	11	8	0.25	0.62	11	8
43	1.83	0.176	12	7	0.11	0.74	12	7
44	1.83	0.176	12	7	0.11	0.74	12	7
45	0.62	0.430	13	6	0.19	0.66	13	6
46	0.62	0.430	13	6	0.19	0.66	13	6
47	0.62	0.430	13	6	0.19	0.66	13	6
48	0.86	0.355	14	5	0.86	0.35	14	5
49	0.86	0.355	14	5	0.86	0.35	14	5
50	0.86	0.355	14	5	0.86	0.35	14	5
51	0.86	0.355	14	5	0.86	0.35	14	5
52	0.86	0.355	14	5	0.86	0.35	14	5

Table 4.4: As Table 4.2 but regarding the decimal logarithm of average populace over the 2003–2018 period. There is one additional column that converts the threshold value back to population: “Threshold (people)”.

Threshold	Threshold (people)	Mild				Extreme			
		KW statistic	KW p-value	N ecoregions < threshold	N ecoregions ≥ threshold	KW statistic	KW p-value	N ecoregions < threshold	N ecoregions ≥ threshold
5.3	199526	4.94	0.026	5	14	2.78	0.10	5	14
5.4	251189	4.94	0.026	5	14	2.78	0.10	5	14
5.5	316228	4.94	0.026	5	14	2.78	0.10	5	14
5.6	398107	6.92	0.009	6	13	0.93	0.33	6	13
5.7	501187	9.78	0.002	7	12	2.86	0.09	7	12
5.8	630957	9.63	0.002	9	10	2.16	0.14	9	10
5.9	794328	<b>10.37</b>	<b>0.001</b>	<b>11</b>	<b>8</b>	2.73	0.10	11	8
6	1000000	9.26	0.002	12	7	2.58	0.11	12	7
6.1	1258925	6.92	0.009	13	6	1.51	0.22	13	6
6.2	1584893	4.53	0.033	14	5	1.93	0.16	14	5
6.3	1995262	4.53	0.033	14	5	1.93	0.16	14	5
6.4	2511886	4.53	0.033	14	5	1.93	0.16	14	5

## Chapter 5

### A slight detour through Pantanal

## 5.1 Case study of the RPPN Sesc Pantanal

*This section is based on the following scientific article: Silva, P. S., Rodrigues, J. A., Nogueira, J., Moura, L. C., Enout, A., Cuiabália, C., DaCamara, C. C., Pereira, A. A., and Libonati, R. (2024b). Joining forces to fight wildfires: Science and management in a protected area of Pantanal, Brazil. Environmental Science & Policy, 159:103818*

In 2020, the world’s largest continuous stretch of wetlands, the Pantanal in South America, recorded its most catastrophic fire season of the last two decades, resulting in severe economic, ecological and health consequences. Regional environmental institutions and communities are taking measures to protect their unique ecosystem, as is the case of the Reserva Particular do Patrimônio Natural (RPPN) Sesc Pantanal, a national protected area. The reserve was severely affected by the 2020 wildfires and is now en route to recover and intensify prevention strategies. Here, we employ a state-of-the-art satellite-derived burned area dataset and a global climate reanalysis product to map and assess the incidence and vulnerability of this reserve to its most concerning disturbance: wildfires. We validated the remote-sensed burned area product and found that the product successfully maps the years with higher fire activity. Then, we studied historical occurrences of burned areas within the reserve. The results show large burned areas are uncommon, and highlight the year 2020 as an outlier, when around 65% of the reserve was burned. Climate trends over the last four decades show increasing temperatures and wind speed, and decreasing relative humidity and precipitation. Fire weather is thus steadily rising, bearing favourable conditions for fire activity over the most critical months of the year. This study provides useful information for fire management decisions within the largest privately held natural reserve in Brazil, and further allows the assessment of the applicability and limitations of large-scale and state-of-the-art products to inform decision-making within protected areas.

### 5.1.1 Introduction

Pantanal is the largest continuous stretch of wetlands in the world, characterised by an ever-changing boundary between land and water, where many regions change seasonally from terrestrial to aquatic systems Alho and Silva (2012). In Brazilian territory, the

Pantanal biome covers the Brazilian states of Mato Grosso do Sul and Mato Grosso, and it is surrounded by the Cerrado and Amazon biomes, where spring-fed rivers and headwaters are located (Guerra et al., 2020). The Pantanal captures water from the surrounding plateaus during the rainy season, and then drains it slowly to the lower sections of the Paraguay river, creating a complex drainage network (Ivory et al., 2019). Its landscape consists of a mosaic of floodable and non-floodable grasslands, forests, open woodlands, and temporary or permanent aquatic macrohabitats (Cunha et al., 2021; Tomas et al., 2019). This allows for high biodiversity (Tomas et al., 2019). In 2000, the “Pantanal Conservation Area” was inscribed on UNESCO’s World Heritage list (UNESCO, 2024b), and around 25,156,000 ha were deemed as an UNESCO Biosphere Reserve (UNESCO, 2024a). These sites are home to nearly 3 million people, and the Pantanal Biosphere Reserve is one of the largest biosphere reserves in the world (UNESCO, 2023).

Pantanal is also considered a fire-dependent biome, where fire influences species type, abundance, and ecological functioning and processes (Pivello et al., 2021). Fire promotes seed germination for some species (Pott and Pott, 2004) and, along with the flood pulse, it allows the existence of several monodominant vegetation types (Manrique-Pineda et al., 2021; Pott et al., 2011). Accordingly, both fire and flood act as ecological filters that, among other factors, shape the structure of plant communities in tropical wetlands and floodable savannas, in such a way that this neotropical savanna wetland system is resilient as long as its natural patterns and periodicities of flooding and burning are maintained (de Sá Arruda et al., 2016; de Oliveira et al., 2014). Lightning strikes may sometimes originate fire in the Pantanal region, however this natural source is infrequent and more likely to happen during the summer period, from December to February (Menezes et al., 2022). The vast majority of fires in Pantanal are associated with anthropogenic ignitions (Menezes et al., 2022).

In 2020, severe wildfires threatened the delicate balance of Pantanal’s wetlands. Around a third of the biome was burned (Libonati et al., 2020), killing at least 17 million vertebrates (Tomas et al., 2021). The severity of these wildfires has been linked to several environmental and socioeconomic factors, including: severe drought; location of the fire corridor in the Paraguay River flood zone; firefighters’ constraints; insufficient wildfire prevention strategies; and budget reductions in public environmental agencies (Garcia et al., 2021). More than a third of these wildfires occurred in areas previously unburnt

or where burning is not usual (Barbosa et al., 2022; Garcia et al., 2021; Libonati et al., 2022b), and mostly over natural vegetation (Correa et al., 2022). They particularly affected forested regions, contributing the most (47%) to the total carbon loss of the 2020 Pantanal wildfires (Barbosa et al., 2022).

The 2020 wildfires have also been shown to be closely linked with atypical meteorological conditions (Libonati et al., 2022b; Marques et al., 2021), particularly a prolonged and severe drought (Marengo et al., 2021b; Thielen et al., 2020). Fire danger levels in 2020 reached unseen values over the last 40 years and large burned areas occurred simultaneously with compounded drought and heatwave events (Libonati et al., 2022b). Climate change has been occurring fast in the Pantanal, with temperatures rising steadily over the last four decades (Libonati et al., 2022b; Marques et al., 2021), along with increased evapotranspiration rates (Marques et al., 2021). Soil moisture has been decreasing (Marques et al., 2021) and the number of days without precipitation has substantially increased, while the water mass during the drought season decreases (Geirinhas et al., 2023; Lázaro et al., 2020). The extent of wildfires in Pantanal has been linked to the occurrence of heatwaves (Silva et al., 2022) that are rising together with extreme hot conditions (Libonati et al., 2022b; Marengo et al., 2021b). Expected future changes in climate might provide even more favourable conditions for wildfires to occur (Ribeiro et al., 2022; Marengo et al., 2016).

In light of ongoing and future climate change, and motivated by the events of 2020, the academic community has been making efforts to further understand and characterise historical fire and climate patterns in Pantanal. Likewise, protected areas within the biome are already being adapted and measures are being taken to prevent such events from happening again. Over the last decades, most protected areas in Pantanal followed a zero-fire policy due to the perceived negative consequences of any type of fire on the native vegetation. However, the wildfires of 2020 put the effectiveness of the zero-fire policy into question (Garcia et al., 2021). Part of the answer might lie in the neighbouring biome, the Cerrado, where a broad approach dedicated to the use of fire to manage rural and traditional territories was introduced in some protected areas in 2014, known as Integrated Fire Management (IFM) (Schmidt et al., 2016). The successful results generated with the IFM implementation led the federal public authorities, responsible for Brazilian protected areas, to expand and recommend this approach to other areas with

recurrent fire issues (Schmidt et al., 2018). The IFM aims to change harmful fire regimes (frequent, high intensity wildfires that burn large areas in the peak of the dry season) to the ones that benefit at the same time environmental conservation and socioeconomic needs, by accounting for cultural and scientific knowledge and technical experience (Myers, 2006).

However, the lack of long-term reliable data in Pantanal hinders these assessments and the ensuing decision-making. There are very few long-term meteorological stations in Pantanal, and these are mainly located in the southernmost regions (Hofmann et al., 2010). This provides an opportunity to explore reanalysis products which provide observation-based estimates of meteorological fields, around the globe, with a common spatial and temporal resolution. Similarly, the systematic quantification of burned areas is only possible due to recent advances in remote sensing techniques and burned area mapping by satellite information.

Although satellite-derived products provide a means to obtain spatially and temporally consistent burned area data, their applicability and usefulness in fire management highly depend on the time and spatial scales at which these products operate. Quick and real-time management decisions rely on near-real time estimates that, until a few years ago (de Aplicações de Satélites Ambientais do Departamento de Meteorologia da UFRJ, 2024), could only be provided for Pantanal through active fire products (e.g. FIRMS). On the other hand, long-term fire dynamics can be easily assessed through satellite-derived burned area products. Although great strides have been made over the last decades to improve satellite-derived burned area estimates, the automatic detection of burned areas remains complex due to the wide spatial and spectral diversity of burned patches (Bastarrika et al., 2011). In general, most satellite-derived burned area products develop algorithms to reduce false alarms (commission errors) while increasing the detection of burned patches (omission errors). Balancing and reducing commission and omission errors becomes challenging as strict detection criteria may lead to lower commission errors but may fail to detect fires, while the opposite would occur with less strict detection criteria (Boschetti et al., 2004). Accordingly, global products often employ algorithms that consider a wide range of burning conditions and thus have distinct commission and omission errors in different landscapes (Rodrigues et al., 2019). On the other hand, algorithms that are developed for a specific site or ecosystem may provide more accurate estimates,

albeit at the expense of applicability in other regions (Campagnolo et al., 2021).

Here, we employed a burned area product specifically developed for Brazilian biomes and a state-of-the-art global reanalysis dataset to study fire and climate within a privately held natural reserve in Pantanal: the Reserva Particular do Patrimônio Natural (RPPN) Sesc Pantanal. First, we validated the satellite-derived burned area dataset to the study region. Then, we used the validated data to evaluate historical fire activity within the reserve and further evaluated climate trends to understand current and future vulnerability to climate change. Lastly, these results were interpreted in light of past and current fire management within the RPPN Sesc Pantanal, along with ongoing and future challenges.

## **5.1.2 Data and methods**

### **5.1.2.1 Study area**

Located in northern Pantanal, the RPPN Sesc Pantanal is managed by the Serviço Social do Comércio (Sesc, a Commercial Service Institution), covering slightly less than 108,000 ha. Created on July 4<sup>th</sup>, 1997, in the municipality of Barão de Melgaço, in Mato Grosso state, this reserve has been dedicated to preserving and restoring its biodiversity and ecosystems over the last 20 years. The maintenance of the RPPN Sesc Pantanal ensures the availability of water and its quality and supports high levels of biodiversity. Since 2000 it has been included as part of Pantanal's Biosphere Reserve and 3 years later it became a Ramsar site adhering to its Convention on Wetlands, an intergovernmental treaty signed in 1971 that provides the framework for the conservation and the wise use of wetlands and their resources (Ramsar, 2023).

The western and eastern parts of the reserve are bordered by the Cuiabá and São Lourenço rivers respectively, and the southern region shares a border with the Indigenous Land of Perigara (Figure 5.1). The surroundings of the RPPN Sesc Pantanal are mostly occupied by cattle ranches and the district of São Pedro de Joselândia with a population of around 2,000 people dispersed in rural properties.



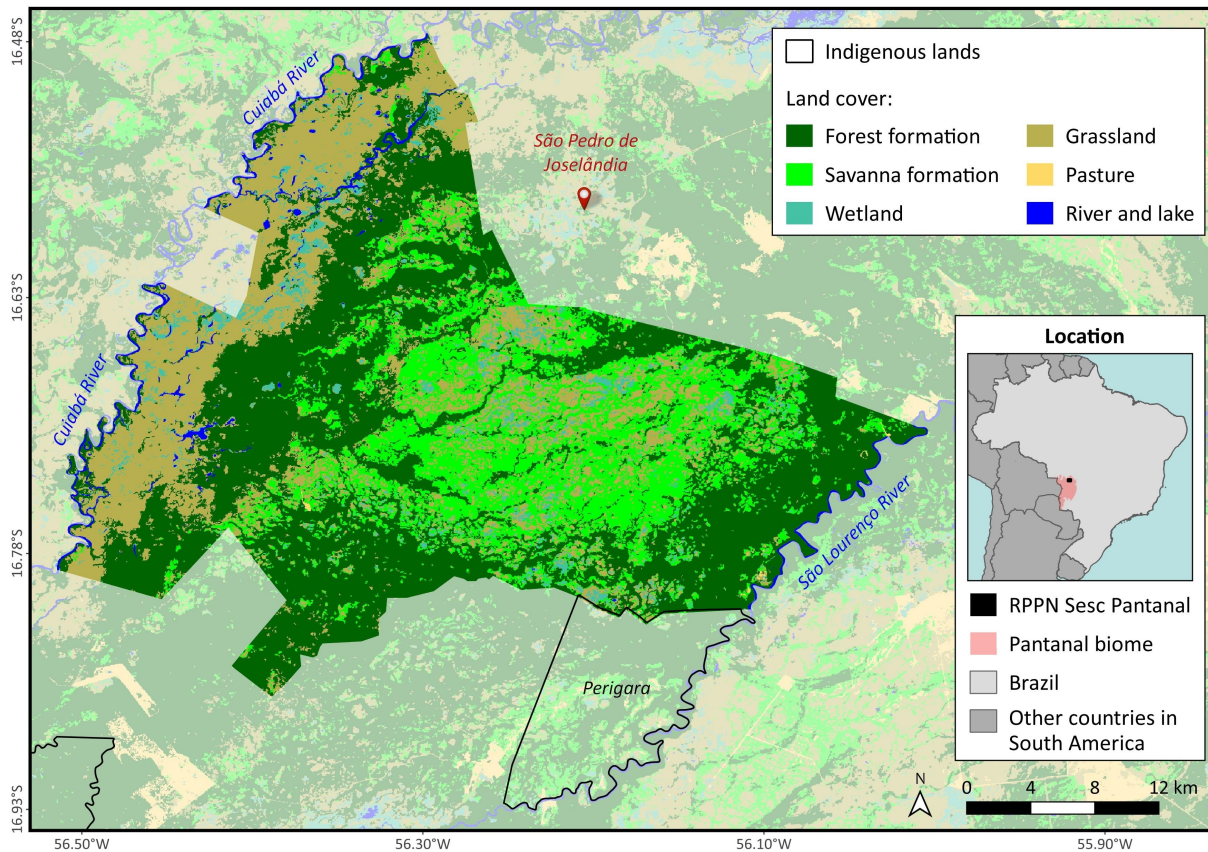


Figure 5.1: Map of the RPPN Sesc Pantanal with land cover information for 2021 (MapBiomas, 2023), along with its location within the Brazilian Pantanal (pink) and Brazil/South America (light/dark grey) in the lower right panel.

Hofmann et al. (2010) provided an extensive characterization of climate within the RPPN Sesc Pantanal. According to the Köppen climate classification, they defined climate in the reserve as “Aw” (Tropical savanna climate with dry-winter characteristics), marked by a pronounced dry season in the winter. Rainfall occurs during the summer, with annual totals varying between 1,000 and 1,600 mm. The reserve’s territory is periodically flooded in almost its entirety during the rainy season (December to April), due to the accumulation of rainfall in the region and on headwaters of rivers within the Alto Paraguai basin. It also features very high temperatures with monthly means above 22 °C and an average annual temperature of around 26.5 °C.

The reserve has a wide variety of vegetation types and has recently been described with 13 macrohabitats (Cunha et al., 2021), including both fire-sensitive and fire-dependent formations (Pivello, 2011). All the environments within the reserve are preserved and free of anthropogenic disturbance for more than 20 years (Brandão et al., 2011).

### 5.1.2.2 Datasets and pre-processing

Burned area data was obtained from the *AQM-LS* V1 product (Pereira et al., 2021) covering the 2000–2021 period. The *AQM-LS* product is a joint effort of LASA/UFRJ and Instituto Federal de Educação, Ciência e Tecnologia do Sul de Minas (IFSULDEMINAS). Derived from multi-temporal composite satellite imagery, namely Landsat missions, at 30 m spatial resolution, this algorithm also uses machine learning and active fire data to map yearly burned areas. Here, we employed one of the first versions of the *AQM-LS* extended to the Pantanal biome.

For validation, Landsat imagery from the U.S. Geological Survey was accessed from Google Earth Engine (GEE). All imagery was collected for Level 2, Collection 2, and Tier 1, for Landsat missions 5, 7, and 8, spanning from 2000 to 2021.

Land cover information was obtained from the MapBiomias Collection 7 product (MapBiomias, 2023). MapBiomias Collection 7 mapped 27 classes of land use and land cover annually over all Brazilian biomes from 1985 to 2021. It relies on a random forest algorithm applied to Landsat satellite imagery, with a spatial resolution of 30 m (Souza et al., 2020). We used the 2000–2021 period, to match the range of the burned area satellite-derived product. Moreover, for the purposes of this study, all pixels within the “River, Lake and Ocean” class (ID 33) were removed.

To evaluate the current climate, we studied climatic variables often used in fire danger assessment to represent distinct components of fire occurrence, frequency, and behaviour, namely: temperature, precipitation, relative humidity, and wind speeds (IPCC, 2022; UNEP, 2022). To do so, we used ERA5, the state-of-the-art reanalysis product from the European Centre for Medium-Range Weather Forecasts (ECMWF; Hersbach et al., 2020). ERA5 runs from 1959 to the present, with hourly output, and describes the Earth in a regular  $0.25^\circ \times 0.25^\circ$  grid which corresponds to, approximately,  $25km \times 25km$ . For this analysis we used the following meteorological parameters taken at 16:00 UTC (which corresponds to 12:00 local standard time, as per methods used in the Canadian Forest Fire Weather Index system; van Wagner, 1987) from 1980 to 2021: 2-metre temperature, 2-metre dew point temperature, and the u and v components of 10-metre wind. Hourly fields of total precipitation were also downloaded and accumulated into daily totals. Surface and dew-point temperatures are used to estimate relative humidity by means of

the August–Roche–Magnus formula (Lawrence, 2005). Finally, wind  $u$  and  $v$  components were also converted to wind speed (ECMWF, 2024). Amongst several reanalysis products, ERA5 has shown increased accuracy in simulating wind speeds in Brazil (Siefert et al., 2021). Data for all variables was masked to the shapefile of the RPPN Sesc Pantanal, and all grid points that touched the reserve’s polygon were used.

ERA5’s fire danger product based on the Canadian Forest Fire Weather Index (FWI) System (van Wagner, 1987), was also employed (Vitolo et al., 2020). The FWI system uses daily values of temperature, relative humidity, wind speed and daily precipitation to estimate seven indices that describe different components/constraints of fire. Here, we used the Daily Severity Rating (DSR), a numerical representation of the difficulty of controlling fires computed using the FWI index, that more accurately reflects the expected effort required for fire suppression. The FWI system is a highly adaptable fire danger index system, widely used to characterise meteorological fire danger worldwide (e.g. Quilcaille et al., 2023; IPCC, 2022; Jain et al., 2021; Abatzoglou et al., 2019). Both FWI and DSR have been used to study fire in Brazilian biomes (Li et al., 2021b; Silva et al., 2019), including Pantanal (Libonati et al., 2020, 2022b; Martins et al., 2022). Similarly to meteorological fields from the ERA5 reanalysis, DSR data was also masked to the shapefile of the RPPN Sesc Pantanal, including all grid points that touched the polygon.

### 5.1.2.3 Validation of the burned area product

To validate the *AQM-LS* product within our study area, we visually inspected multi-temporal Landsat imagery using Geographic Information System (GIS) technology, particularly QGIS version 3.22.6 with GEE plugin integration. Visual inspection is often employed in validation studies (e.g. Bowman et al., 2003), algorithm development (e.g. Pinto et al., 2021; Daldegan et al., 2014), and operational purposes (Bastarrika et al., 2011). For each year, we compared the yearly *AQM-LS* burned area map with Landsat imagery from January 1 to December 31 in colour composition (red, green and blue; RGB). The combination of the reflectance spectral bands of short-wave infrared (SWIR, in Red), near-infrared (NIR, Green), and red (Blue), allowed the visual identification of vegetation fire scars by contrasting fire events (shades of red) with the unburned vegetation (shades of green). This colour composition has been shown to allow an easy

interpretation of burned areas (Pinto et al., 2021; Pereira et al., 1999). By overlaying the *AQM-LS* burned area map with the Landsat imagery in RGB, we investigated the spatial and temporal agreement/discordance between these products. Commission errors (i.e. false alarms) were manually removed from the raw *AQM-LS* mapping, henceforth referred to as the validated version (*AQM-LS<sub>val</sub>*).

#### 5.1.2.4 Analysis of burned land cover

To assess the land cover types that corresponded to burned areas in *AQM-LS<sub>val</sub>*, we simply overlapped and intercompared pixel to pixel these products in the same raster format, as they have the same spatial (30 m) and temporal (yearly) resolution. We then assigned the correspondent land cover classification to each burned pixel in the *AQM-LS<sub>val</sub>* product.

#### 5.1.2.5 Statistical analysis

To evaluate interannual climate patterns we focused on the period from July to October, when most wildfires occur in Pantanal (Damasceno-Junior, 2021). Averages were computed in the case of temperature, relative humidity, wind speed, and the fire danger index (DSR), and precipitation was aggregated over these months. Climate extremes were evaluated through the 90<sup>th</sup> percentile of temperature, wind speed, and DSR, and the 10<sup>th</sup> percentile for relative humidity.

Trends in burned area and climate variables were evaluated using the non-parametric Theil-Sen regression (Sen, 1968; Theil, 1950), a robust estimator insensitive to outliers with a breakdown point of about 29.3% compared to simple linear regression. The statistical significance of the trends was evaluated by the two-tailed Mann-Kendall non-parametric test at the 5% significance level (Kendall, 1975; Mann, 1945).

Lastly, the relationship between interannual burned area and the fire danger index was estimated through simple linear regression, and goodness of fit evaluated by the coefficient of determination ( $R^2$ ).

### 5.1.3 Results

#### 5.1.3.1 Validation of the burned area product

We found that there are considerable differences between the raw *AQM-LS* product and Landsat imagery. The *AQM-LS* algorithm showed commission errors for almost all years of the time series, leading to an overestimation of burned areas within the RPPN Sesc Pantanal (Figure 5.2).

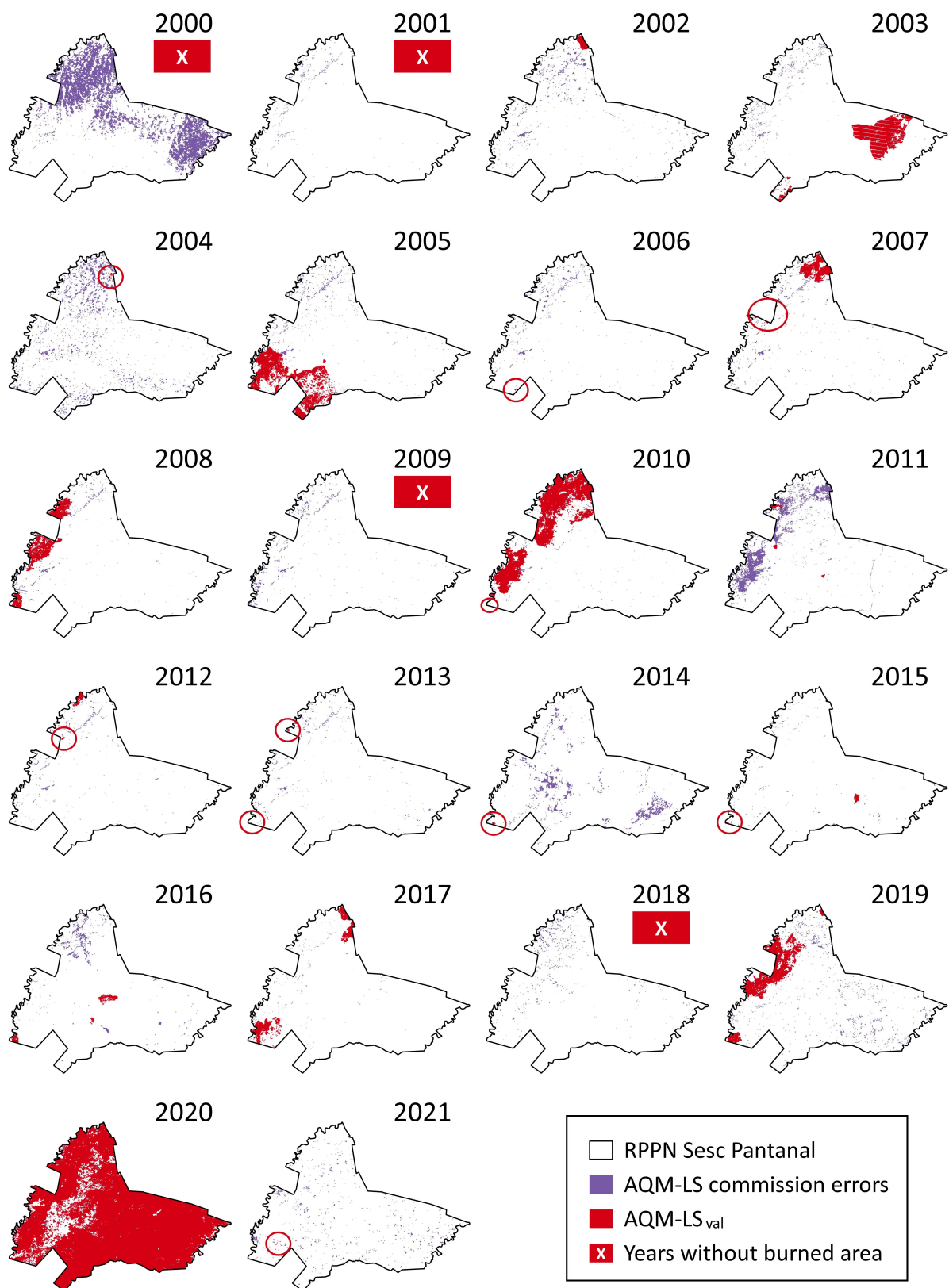


Figure 5.2: Year to year mapping of burned areas by the *AQM-LS* product from 2000 to 2021. Commission errors are shown in purple, and hits (*AQM-LS<sub>val</sub>*) are shown in red. Years with a white X in red background highlight years where the validation found no burned areas, and the red circles highlight very small burned areas.

Years with higher burned areas were found to be properly mapped (Supplementary Material: Table 5.1), in which the difference between the validated ( $AQM-LS_{val}$ ) and raw  $AQM-LS$  products range from 0% to 9% (2003, 2005, 2010, 2019, and 2020). On the other hand, differences reached 100% in four years (2000, 2001, 2009, and 2018), in which all mapped burned areas were commission errors, and another six years had commission errors above 94% (2004, 2006, 2011, 2013, 2014, and 2021). Nevertheless, these high relative differences between the raw and validated products correspond to small burned areas, ranging from 100 to 2,900 ha. Only the year 2000 was particularly anomalous as the  $AQM-LS$  product assigned 12,330 ha of burned areas, where there were none.

Commission errors were often due to misclassification of clouds, water bodies, seasonally flooded areas, and paths (Supplementary Material: Figure 5.7). It is also worth noting the case of 2003 (Supplementary Material: Figure 5.8), where there are clear missing gaps in data, both in the  $AQM-LS$  mapping and in Landsat imagery used for the visual validation, due to the failure of the Scan Line Corrector in Landsat-7 from June 1<sup>st</sup> 2003 onwards (USGS, 2024).

### 5.1.3.2 Historical fire characterization

Using  $AQM-LS_{val}$ , we characterised historical fire activity within the RPPN Sesc Pantanal. As in the entirety of the Pantanal biome (Libonati et al., 2022b), 2020 recorded severe wildfire events, with more than 70,000 ha of burned area (around 65% of the reserve's area), severely contrasting with the previous years (2000–2019) when there was an average of 1,685 ha burned per year (Figure 5.3a). Unlike previous years, the wildfires advanced towards the centre of the reserve and 70% of the total burned area in 2020 had not been burned before (over the 2000–2019 period).

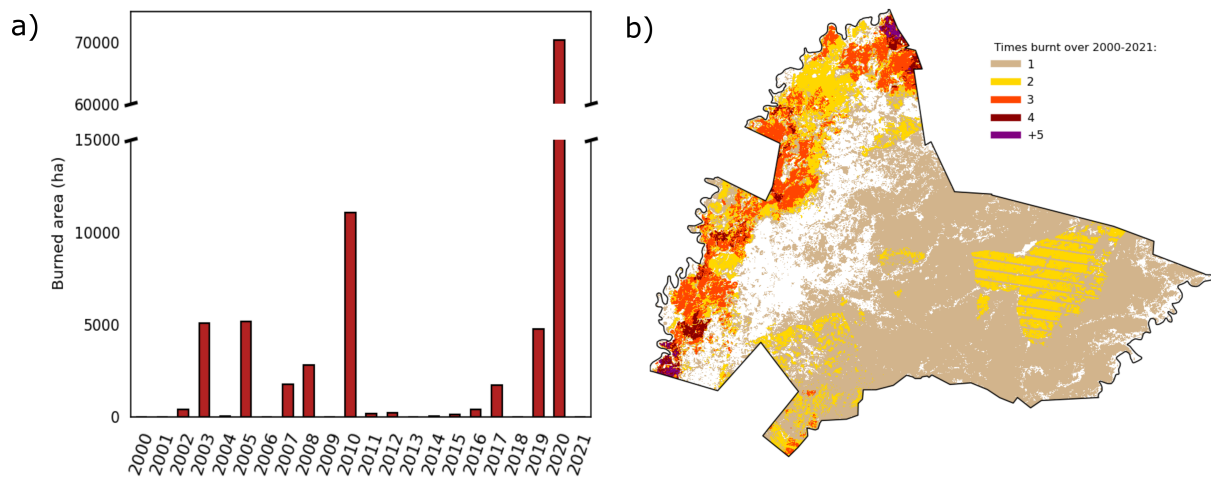


Figure 5.3: a) Interannual variability of burned area from 2000–2021 as estimated by the validated *AQM-LS* product (*AQM-LS<sub>val</sub>*). b) The number of times a pixel was burnt over the time series (2000–2021).

Before 2020, only in 2010, the reserve burned over 10,000 ha, and the most extreme events were found to be those burning above 2,004 ha (the 75<sup>th</sup> percentile). Over 22 years of data, no burned area trend was found. Most areas were hit only once (69% of the total burned area), most of which occurred in 2020 (Figure 5.3b). A smaller percentage of areas burned two (20%) or three (9%) times over the 2000–2021 period, and only 2% burned more than four times. Around 33% of the reserve seems never to have burned over the last 22 years.

Recurring burned areas are located in the western region (Figure 5.3b), near the Cuiabá river and on the frontier with adjacent territories. These regions are classified as grasslands by the MapBiomas product in 2021 (Figure 5.1), but it is worth noting that the MapBiomas product alternatively considers this region as grasslands and wetlands (depending on the year). Accordingly, when analysing burned areas by land cover type throughout 2000–2019 (Figure 5.4), most burned areas occurred in grasslands and wetland formations corresponding to this western region. Wetlands and grasslands corresponded to approximately 50.8% and 27.3% of the total burned areas over this period, followed by savannas and forests (12.9% and 8.4%, respectively). The year of 2020, however, changed this pattern: most burned areas occurred in forested areas (37.4%), followed by grasslands (29.7%) and savanna formations (27.2%). The years of 2005 and 2010 also burned a larger portion of forest, with 1,165 ha (22.6% of the total annual burned area) and 632 ha (5.8%), respectively. Lastly, in 2003, a large stretch of burned savanna, around 2,966



ha (58.3%), exceeded the areas burned of grasslands, with slightly more than 1,802 ha (35.4%).

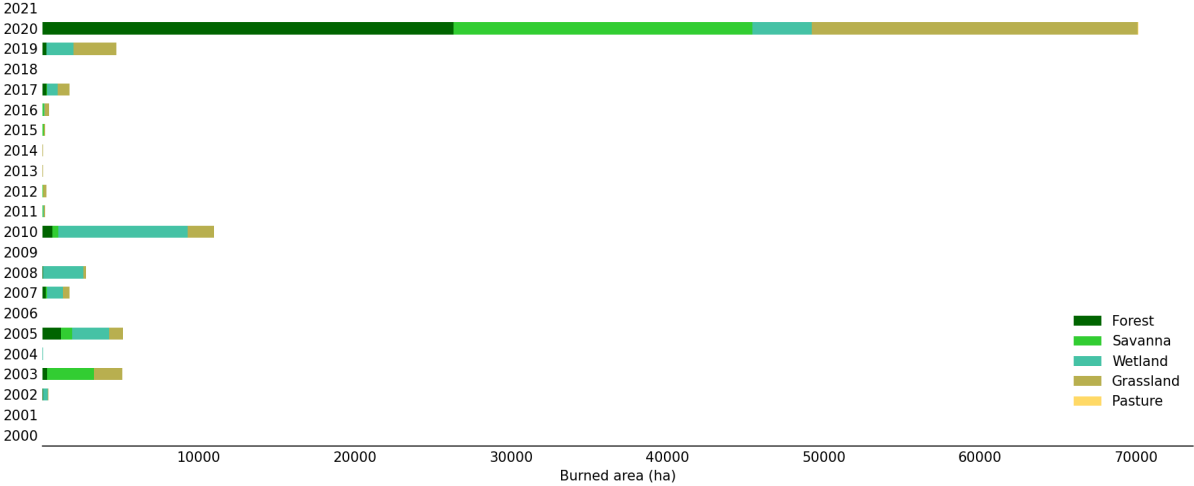


Figure 5.4: Land cover types of burned areas using the validated *AQM-LS* product (*AQM-LS<sub>val</sub>*) from 2000 to 2021.

### 5.1.3.3 Climate

Regional climate within the RPPN Sesc Pantanal was characterised using reanalysis data. Considering the average over the last 40 years, higher temperatures were found from August to October, preceded by the lowest temperature values from May to July (Figure 5.5a). There was little variation in absolute temperatures, with temperatures ranging from 30–31 °C during the austral summer months (henceforth defined as December, January and February) and 29–32 °C in austral winter (henceforth defined as June, July and August). Conversely, relative humidity had higher variability (Figure 5.5b): lower values from July to September ranging from 43% to 48%, and summer months from 68% to 71%. The reserve also showed a marked rainfall seasonality (Figure 5.5c), with a dry season from April to October, reaching minimum rainfall values from June to August (below 16 mm/month). Summer months represented, on average, 51% of total annual precipitation, and the average annual precipitation over the last 40 years was around 1,459 mm. Finally, the months with the highest wind speeds occurred from July to September with 9.2–9.5 km/h (Figure 5.5d).

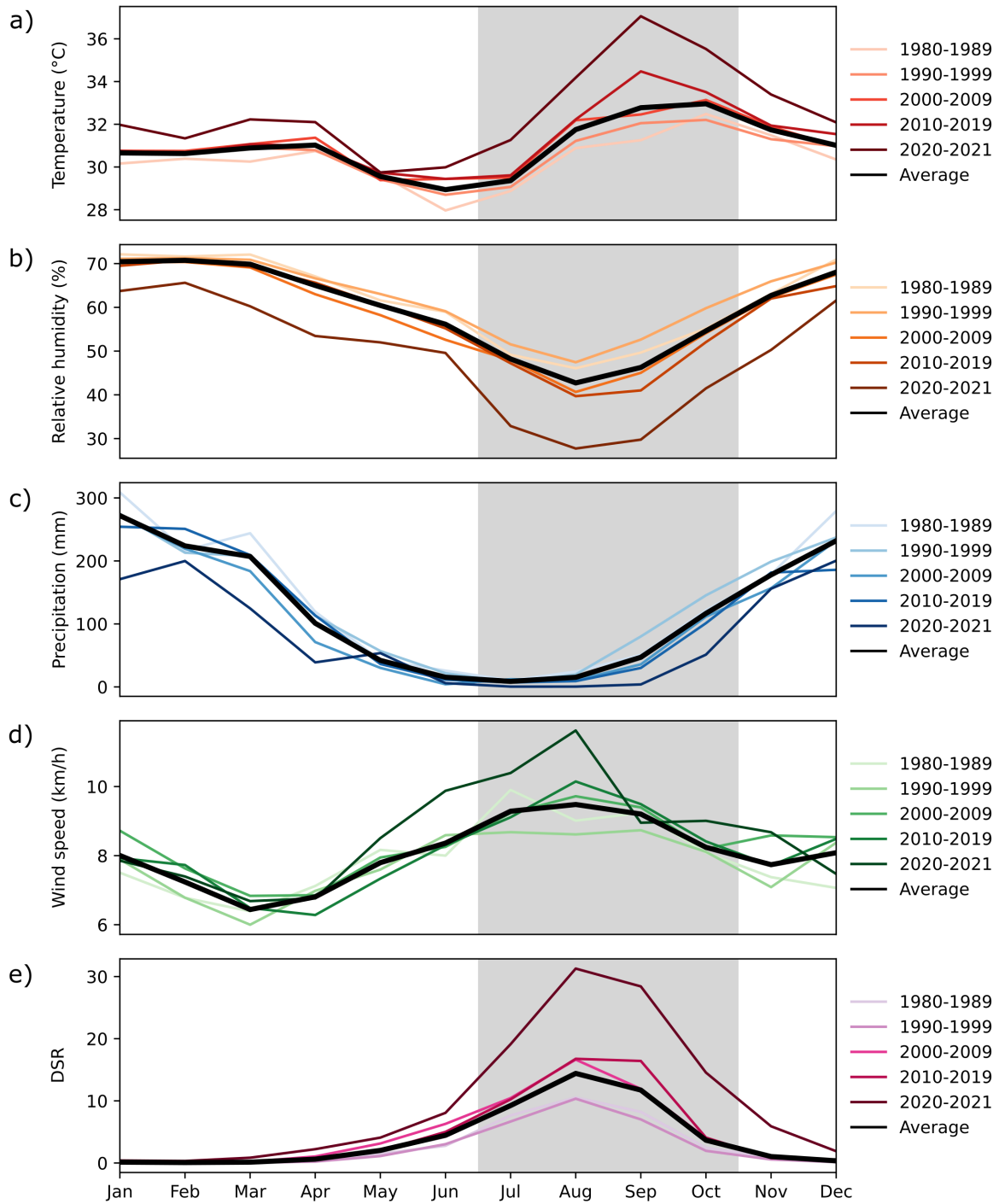


Figure 5.5: Seasonal cycles of: a) surface temperature ( $^{\circ}\text{C}$ , red); b) relative humidity ( $\%$ , orange); c) precipitation (mm, blue); d) wind speed (km/h, green); and e) fire danger index Daily Severity Rating (DSR) (dimensionless, purples). Lighter to darker colours represent a decadal mean from 1980–1989 to 2010–2019, and the average for the last 2 years (2020–2021). Black lines are the average over the time series, from 1980 to 2021. Grey shaded areas represent the months from July to October.

However, we found that seasonal patterns seem to be changing (Figure 5.5). Although the seasonality of temperature does not appear to be altered, its magnitude is higher the closer it is to the 21<sup>st</sup> century (Figure 5.5a). Values from 2020–2021 were well above

those of the previous decade (2010–2019), and when looking at seasonal cycles per year (Supplementary Material: Figure 5.9), both years achieved unprecedented temperature values in September and 2020 continued with record values up to November. Similarly, relative humidity values from the 1980–1999 period were systematically higher than the following 20 years (2000–2020), particularly from the months of August to October (Figure 5.5b). Both 2020 and 2021 achieved unseen lower relative humidity values from August to September, and 2020 reached minimum values over most of the months (Supplementary Material: Figure 5.9).

The later months of the dry season show decreasing precipitation over the last decades, with 2020–2021 having remarkably less rainfall in September and October than the climatological mean (Figure 5.5c). Although wind speed patterns were not as easily interpreted, it is worth pointing out that wind speeds during the 2020–2021 period were also systematically higher than the climatological mean for months May to August (Figure 5.5d).

The 4-month period from July to September coincides with yearly maximum temperatures and wind speed, lowest values of relative humidity, and the end of the dry season. Accordingly, fire danger achieved higher values from July to September, and reached its maximum in August. Consistent with climatic trends, the DSR was found to be systematically increasing over the last decades, and the 2020–2021 period achieved much higher values than the climatological mean (Figure 5.5e).

Moreover, meteorological conditions favourable to fire seem to be increasing since 1980, particularly in the critical months from July to September (Figure 5.6). Average temperatures and wind speeds were found to be steadily rising (at a rate of 0.76 °C and 0.18 km/h per decade; Figures 5.6a and 5.6d), while relative humidity and precipitation showed decreasing trends (lowering 2.74% and 33.1 mm per decade, respectively; Figures 5.6b and 5.6c). Accordingly, DSR was also substantially increasing at a rate of 22.8 per decade (Figure 5.6e). The year of 2020 showed unprecedented fire danger values over the time series, when DSR reached a maximum of 25. In contrast, there was a slight decrease in DSR values during 2021 (21).

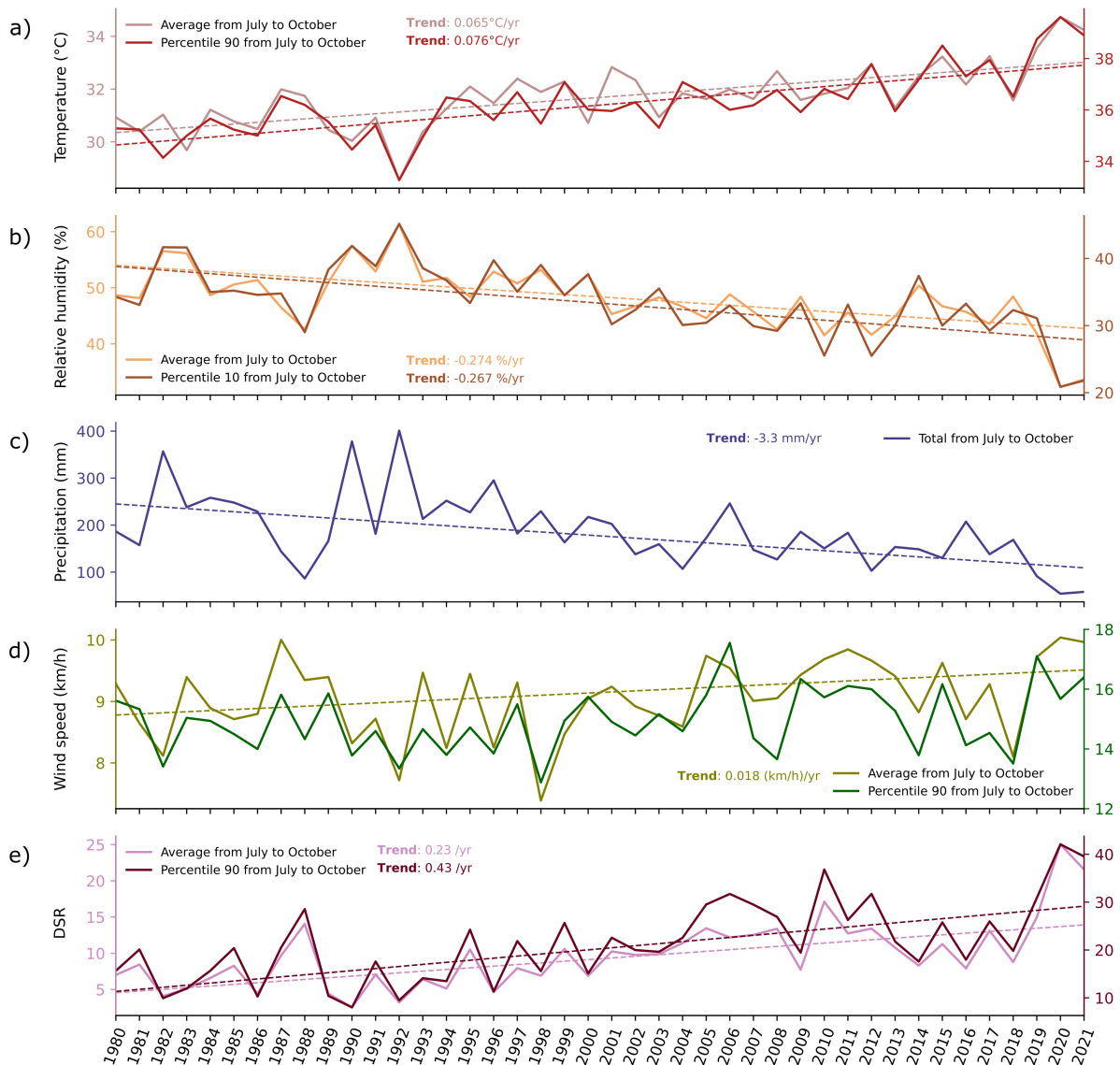


Figure 5.6: Interannual variability from 1980 to 2021 for: a) temperature ( $^{\circ}\text{C}$ , reds); b) relative humidity (% , oranges); c) precipitation (mm, blue); d) wind speed (km/h, greens); and e) fire danger index DSR (adimensional, purples). Darker shades represent the extremes, evaluated as percentiles 90 for temperature, wind speed and DSR; and percentile 10 for relative humidity. Dashed lines represent significant trends (below the 5% confidence level), and the trend slope is shown on the graph with the corresponding colour. Non-significant trends are not shown.

The average of annual precipitation has also been decreasing at an alarming rate of -99.7 mm/decade (Supplementary Material: Figure 5.10). The average value for the last 10 years (2012–2021), around 1,297 mm, was significantly lower than the climatological mean (1,459 mm). Even when looking at the wet season, particularly the summer months, responsible for most of the yearly rainfall, there was also a decreasing trend of -47.3 mm/decade.

Temperature extremes seem to be increasing more than average, at a rate of 0.76  $^{\circ}\text{C}$  per

decade (Figure 5.6a). The 10% lowest relative humidity values also showed a decreasing trend in the July–October period, at a rate of 2.67% per decade (Figure 5.6b). Lastly, wind speed showed no significant trends for extreme values (Figure 5.6d).

There seems to be little correlation between the fire danger index and burned area. A simple linear regression model using averaged values of DSR from July to October as predictor of interannual burned areas ( $AQM-LS_{val}$ ) resulted in a coefficient of determination of 0.48 (Supplementary Material: Figure 5.11).

## 5.1.4 Discussion

### 5.1.4.1 Using remote sensed burned areas to study fire activity

We found that the  $AQM-LS$  algorithm sometimes failed to distinguish between burned and unburned areas within the RPPN Sesc Pantanal, and often assigned wrong classifications. This led to an overestimation of burned areas, which is most conspicuous in years that, according to visual inspection, showed little to no fire activity. On the other hand, years with large burned areas were well-mapped by the  $AQM-LS$  product. Compared to other remote sensed burned area products derived from Landsat imagery that rely on change detection approaches based on pairs of images, the  $AQM-LS$  product has significantly reduced omission errors (Pereira et al., 2021). Nevertheless, in contrast with the automatic detection by the  $AQM-LS$  product and visual inspection, the RPPN Sesc Pantanal managers and firefighters report that almost the entirety of the reserve burned in 2020. The  $AQM-LS$  marked a large stretch of forested regions as unburned, known as the fire-sensitive “Cambarazal” (Sesc, 2023), where lower temperatures and higher relative humidity usually hinder the occurrence and spread of fires (Hofmann et al., 2010). It is not surprising that fires in forested regions are largely undetected, as it is widely known that satellite-derived burned area products have difficulty in detecting understory fires, as the tree canopy obscures the burning underneath (Morton et al., 2013). It is also worth noting that mapping burned areas in the tropics presents a greater challenge as the ephemeral character of the signal is easily scattered by the wind, rain, or hidden by re-growth (Pereira et al., 2021; Pereira, 2003).

#### 5.1.4.2 Understanding fire patterns

The *AQM-LS<sub>val</sub>* product provided a reliable 20-year history of fire dynamics within the reserve. In general, large fires are not common within the reserve. Apart from 2020, only 2003, 2005, 2010 and 2019, burned considerable areas. Amongst these, the years of 2005 and 2010 were marked by reduced rainfall during the austral summer due to an anomalous northward position of the Atlantic Intertropical Convergence Zone (ITCZ; Marengo et al., 2021b), which may have led to drier, and thus more susceptible to burning, biomass during the austral winter.

Burned area estimates from the last two decades showed how extreme and unprecedented the 2020 wildfires were, with six times more burned area than the previous record year (2010). Records from the RPPN Sesc Pantanal management detail that these wildfires began in a rural area at the northern border on August 2<sup>nd</sup>, but soon there were multiple ignition sources and fire-lines coming from different directions towards the reserve. The fire-fighting efforts focused on infrastructure and the main roads that worked as firebreaks and fire-free corridors for animals to escape. Despite all efforts, it was estimated that thousands of vertebrates were killed (Crawshaw et al., 2020). Most of the area burned in 2020 had not burned over the last two decades, which, associated with non-existent fuel management actions, allowed the accumulation of biomass susceptible to burning.

In general, higher fire incidence was found near the reserve's limits, particularly along the northern and western border. This region is marked in the land cover product as wetlands and grasslands, but it represents the main flooded areas within the reserve, consisting of three macrohabitats (Sesc, 2023): clean and natural field (“Campo limpo natural” in portuguese); flooded shrubland (“Arbustais inundados”); and riparian forest (“Floresta ribeirinha do rio Cuiabá”). As a RPPN, no anthropogenic fire is allowed within its limits and, accordingly, the wildfires that affect the reserve often start in the surrounding regions and move towards the RPPN's area. It is common for rural populations in this region to use fire to stimulate pasture regrowth, clean areas, burn the garbage, for slash and burn agriculture, hunt (indigenous hunting) and celebrate (cultural celebrations or rituals) (Ibama, 2018; Sesc, 2023). Mainly these fires are conducted as controlled burns, but sometimes they are carried out without due care, under risky fire weather and environmental conditions, and without safety measures, facilitating its spread and generating

wildfires. Apart from the natural fires, other anthropogenic sources have been reported for the RPPN's region, such as electrical wiring ruptures (due to poor maintenance), vehicle accidents, and burning to clean the vegetation on the side of the road (Sesc, 2023). The combination of these anthropogenic fire sources, fuel loads available in large extensions with extremely dry periods, significantly increases the risk of wildfires.

#### **5.1.4.3 Fire in the context of a changing climate**

A state-of-the-art reanalysis product allowed an assessment of historical trends in meteorological variables and fire weather. Although there is no in-situ data to compare or validate ERA5's estimates, we found that precipitation estimates are in agreement with a previous study in the RPPN (Hofmann et al., 2010), and in line with the surrounding regions (Ivory et al., 2019; Marengo et al., 2015).

Over the last decades, monthly fire danger has been systematically increasing, particularly from July to September. Along with October, these months are considered Pantanal's fire season, where the vast majority of fires occur (Damasceno-Junior, 2021; Libonati et al., 2022b). Compared with September, October showed a considerable decrease in fire danger due to increased rainfall and relative humidity. Nevertheless, concurrent with high temperatures and wind speeds, fuel loads are extremely dry by the end of the dry season and highly susceptible to burning, which may lead to large burned areas in September and October, as seen in the case of the 2020 Pantanal fires (Libonati et al., 2022b). Additionally, the dry season seems to be expanding, with systematically lower rainfall values for September and October over the last 22 years. Associated with increased temperatures and decreased relative humidity, fire weather conditions last longer every year, in line with reports from the RPPN Sesc Pantanal management team.

In par with Pantanal, the reserve is experiencing changes in climate patterns, with increasing conditions favourable to wildfire occurrence over the last four decades. These climate change trends in Pantanal, and by extent the reserve, will likely persist in the future (Llopart et al., 2020; Marengo et al., 2015), associated with higher frequency and extent of extreme events such as heatwaves or droughts (Ribeiro et al., 2022; Reboita et al., 2021a; Silva et al., 2022; Thielen et al., 2020). However, climate may not be the main driver of fire within the RPPN, as a fire danger index explained slightly less than 50% of interannual burned areas. A relevant example is the case of the year 2021, when

fire danger was very high, including a record in temperatures for September and in relative humidity in July, but there were virtually no burned areas. This is to be expected as fire in the reserve is mainly anthropogenic (Neves, 2015) and, although favourable meteorological conditions are a necessary condition for large wildfires to occur, they alone are not sufficient. Along with climate, several other factors might weigh in the occurrence and spread of fire, such as fuel amount and conditions, ignition sources, and fire management.

#### **5.1.4.4 Implications for fire management**

Before the creation of the reserve in 1997, the area of the reserve was used for cattle breeding and controlled burns were commonly applied (Brandão et al., 2011). In its central area (Figure 5.1), a savanna-like formation called “Campos de murundu”, where the cattle grazed, had the largest areas burned every other year in September and October (corresponding to less than 5% of the reserve’s area, except for 1993 when almost 20% was burned) (Sesc, 2023). However, after the creation of the RPPN no controlled burn was carried out, as the RPPN Sesc Pantanal followed a zero-fire policy. Preventive measures focused only on environmental education, social mobilisation, and capacity building. Throughout protected areas in Brazil, it has been shown that since its implementation, the zero-fire policy has increased large wildfire events, as the unmanaged vegetation expressively built-up fuel loads (Moura et al., 2019).

After the 2020 Pantanal wildfires, the need to change fire management and policy in the biome became readily apparent. Strategies and initiatives were quickly introduced, such as the creation of many community, volunteer and private fire brigades, and the development of management plans like the IFM. In 2021, the first experimental prescribed burns were applied in three small areas in the reserve to help managers better understand fire behaviour and severity. Associated with increased research efforts, such as the present study, this knowledge expansion combined with fire management needs, led to the decision to implement the IFM approach in the reserve. As well as continuing the RPPN’s previous preventive efforts, the IFM requires continued work on maintaining firebreaks, implementing prescribed burns, suppression of wildfires, and collaborative work with the reserve’s neighbours, interested organisations and researchers (Sesc, 2023). Accordingly, joint efforts were made with the collaboration of community leaders, scientists, the Military Fire Department and other civil society organisations (SOS Pantanal, Mupan, and



Funatura) to build capacity in the surrounding communities, install modern fire monitoring equipment to detect ignition sources, recover fire sensitive forests that were burned in 2020, and invest in fire-related research in the reserve (Sesc, 2023).

It is expected that the implementation of IFM within the reserve will change several aspects of its fire regime, particularly through prescribed burns that aim to control fuel loads prior to the critical wildfire season. As prescribed burns are undertaken in strategic and fire-adapted areas at the beginning of the dry or rainy season, the frequency and seasonality of fires will change, while the occurrence and extent of wildfires are expected to decrease (Ribeiro and Pereira, 2023; Santos et al., 2021). These changes in fire activity will require a continuous assessment of its effect within the reserve's 13 macrohabitats. Understanding the optimal frequency, timing, and extent of prescribed burns, the amount and seasonality of fine fuels that need managing, and impacts on biodiversity, are some of the key research questions to be addressed.

### **5.1.5 Conclusions**

This study provides an historical characterization of fire and climate within the largest privately held protected area in northern Pantanal: the RPPN Sesc Pantanal. We validated a Brazilian burned area product, and found large commission errors, mainly due to clouds, water bodies, flooded areas, and roads, leading to overestimating burned areas within the reserve. On the other hand, the automatic algorithm properly mapped years with large burned areas, albeit with omission errors in 2020. The validated dataset allowed a better assessment of fire activity in the reserve over the last two decades. We found that large burned areas are not common within the reserve, and most burned areas occurred in its western region near the Cuiabá river. Most of these burned areas were due to wildfires that started outside of the confines of the reserve but spread inwards, severely damaging its ecosystems. The most extreme year within the time series was 2020, in par with the rest of the Pantanal biome, where most of the reserve burned and forested regions were particularly affected.

We also showed that changes in climate are occurring within the reserve, mirroring trends for the Pantanal biome. Fire weather conditions seem to have lasted longer every year and steadily increased over the last 40 years. These trends reinforce the importance of

developing an integrated adaptive fire management in the reserve that preserves the microclimate, the environment, and its biodiversity to avoid extreme wildfires, such as those observed in 2020. An appropriate IFM for the region is only possible through interaction between various actors (firefighters, local agents, surrounding communities), adequate investment in firefighting equipment and infrastructure, environmental education to reduce ignition sources and reinforce the ecological value of the reserve, and local knowledge of the areas that are most vulnerable to fire for an efficient environmental management.

Finally, we found that, while satellite-derived burned area and reanalysis products provide useful information relevant to decision-making in the RPPN Sesc Pantanal, combining these products with local knowledge and expertise is crucial. Remote sensed burned area products have developed rapidly over the last decades due to better instruments and algorithms, but still show limitation. In particular, for smaller areas, such as protected areas, where a high spatial resolution is required, these products still show high commission errors, per our case in the RPPN Sesc Pantanal, and require visual interpretation by a skilled interpreter to yield accurate and precise results. On the other hand, reanalysis products also allow the assessment of climate where in-situ measurements and long-term datasets are not available or reliable.

This study provides tailored information for fire management decisions within the RPPN Sesc Pantanal, using methods that may be easily replicated and employed to study other protected areas worldwide. Our findings further highlight the role of fire management policies in wildfire occurrence and prevention, and align with recent studies for the Pantanal (Ribeiro and Pereira, 2023; Garcia et al., 2021) and worldwide (UNEP, 2022; Stoof and Kettridge, 2022; Rego et al., 2021) on the introduction of an integrated fire management approach as a possible solution.

## 5.1.6 Supplementary Material

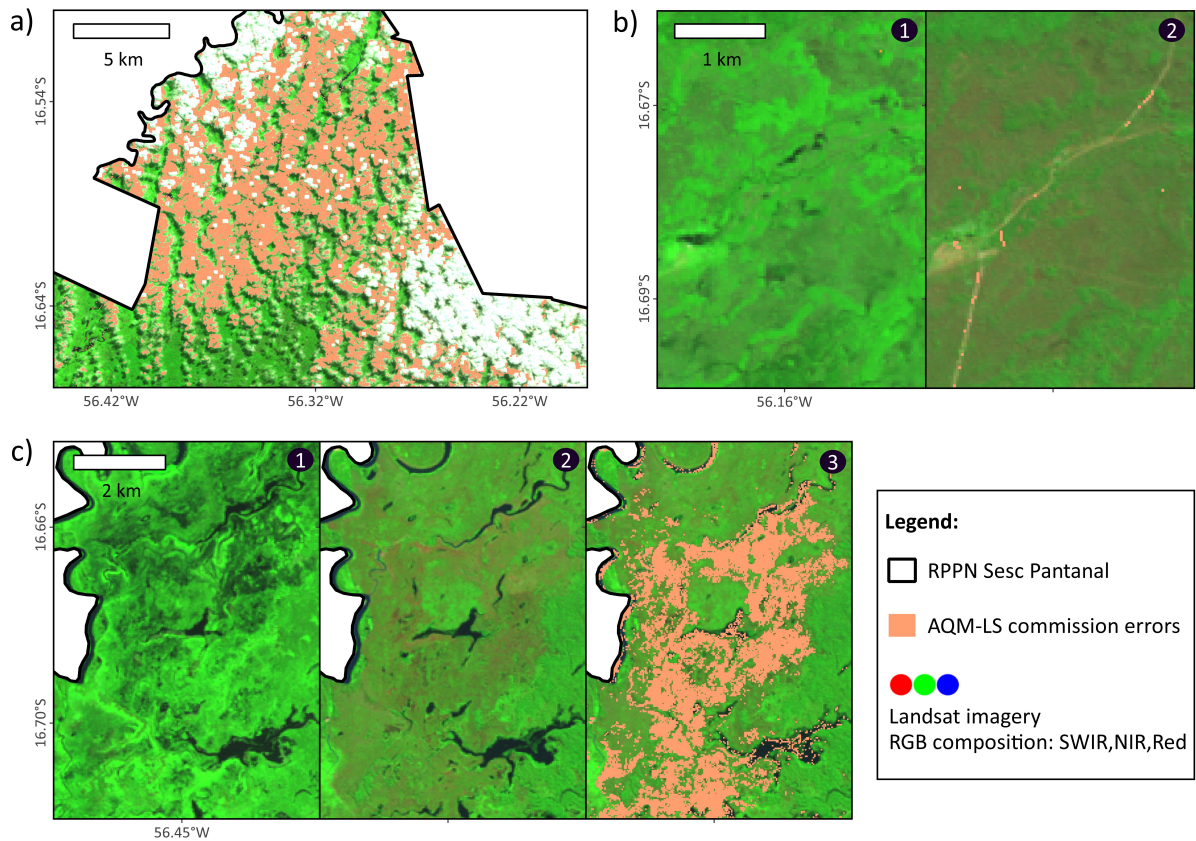


Figure 5.7: Examples of misclassification by the *AQM-LS* product, due to spectral confusion from temporal changes. (a) Clouds in 2000, as through Landsat-7 imagery on June 2<sup>nd</sup> with the *AQM-LS* product superimposed in orange. (b) Paths in 2011, as seen through (1) Landsat-5 imagery on February 1<sup>st</sup> and (2) Landsat-5 imagery on August 12<sup>th</sup> with the *AQM-LS* product superimposed in orange. (c) Water bodies and seasonally flooded areas in 2011, as seen through (1) Landsat-5 imagery on February 1<sup>st</sup>, (2) Landsat-5 imagery on August 12<sup>th</sup>, and (3) Landsat-5 imagery on August 12<sup>th</sup> with the *AQM-LS* product superimposed in orange. Landsat imagery appears in colour composition (RGB) which combines the reflectance spectral bands of short-wave infrared (SWIR, in Red), near-infrared (NIR, in Green) and red (in Blue).

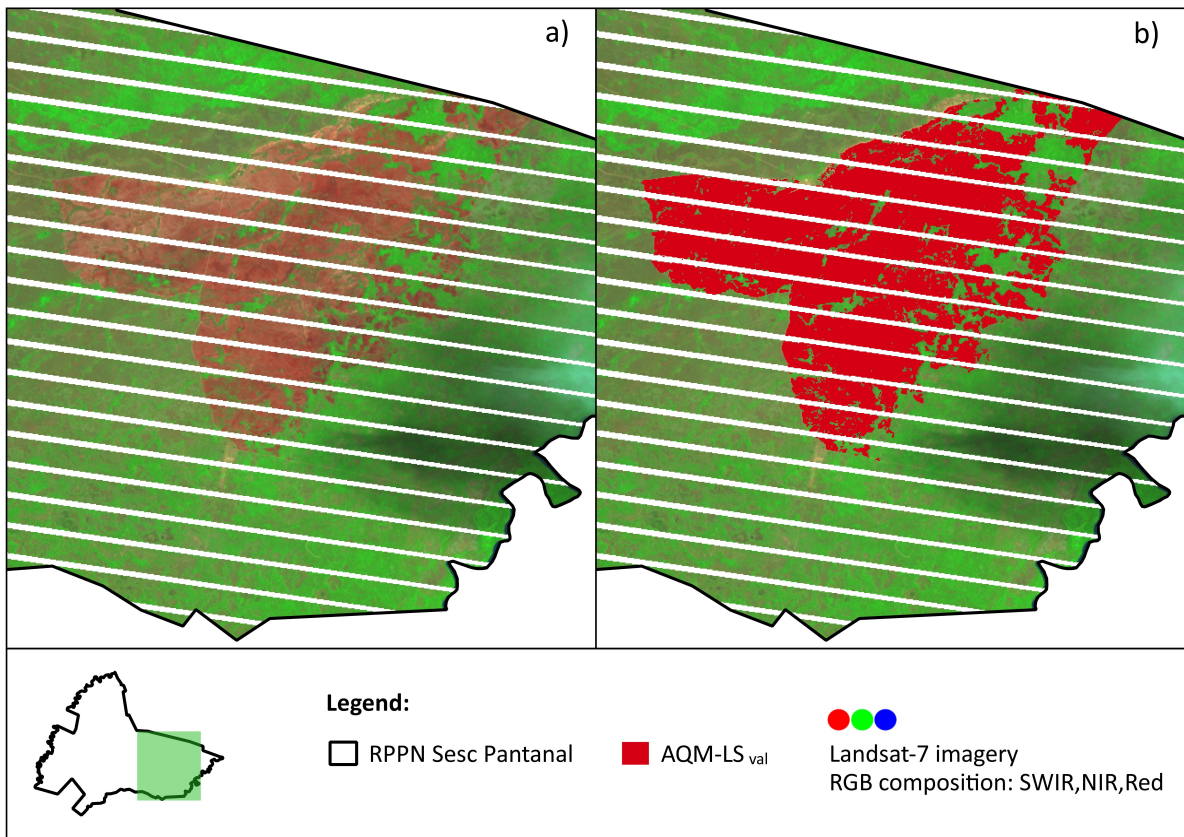


Figure 5.8: The case of the year 2003. The RPPN Sesc Pantanal is illustrated in the bottom left corner, and the section that is shown in top panels is highlighted in green. (a) Raw Landsat-7 imagery for October 1<sup>st</sup> 2003 in colour composition (RGB) which combines the reflectance spectral bands of short-wave infrared (SWIR, in Red), near-infrared (NIR, in Green) and red (in Blue). (b) as (a) but with the validated  $AQM-LS$  product ( $AQM-LS_{val}$ ) superimposed in red.

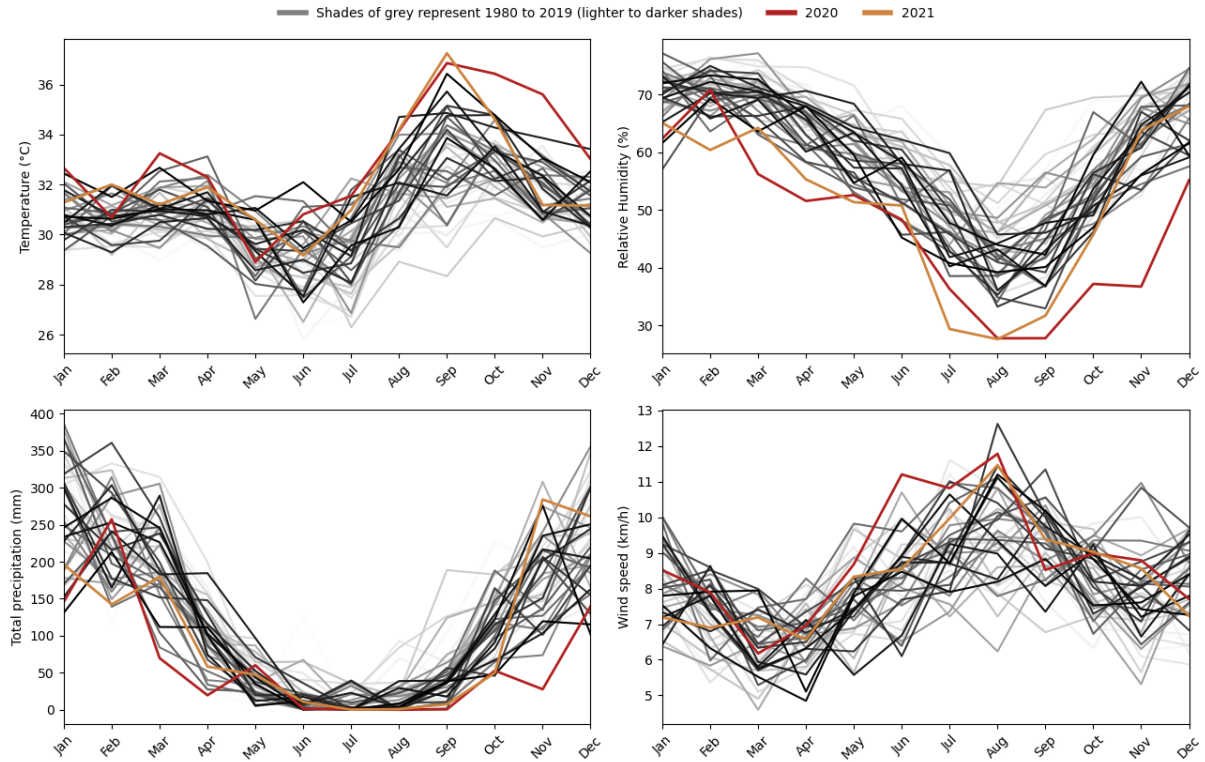


Figure 5.9: Seasonal cycles from 1980 to 2021 for: temperature ( $^{\circ}\text{C}$ , top left), relative humidity (% , top right), total precipitation (mm, bottom left) and wind speed (km/h, bottom right). Grey curves represent years 1980 to 2019, shades getting darker as the years progress; and the red and yellow curves represent 2020 and 2021, respectively. Temperature, relative humidity and wind speed, are monthly averages, whereas precipitation is accumulated over the entire month.

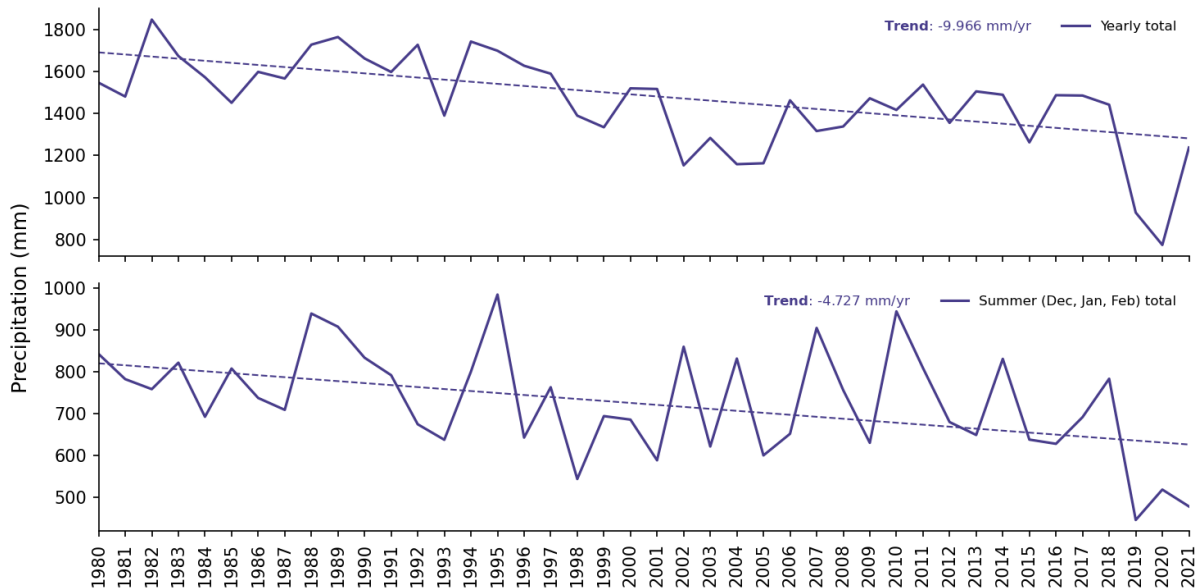


Figure 5.10: Interannual variability from 1980 to 2021 of total yearly precipitation (top panel) and total summer precipitation (bottom panel). Summer is defined as December of the previous year, and January and February from the current year (e.g. the 1980 summer total is the sum of precipitation from December 1979 and January and February from 1980). Dotted lines represent trends, estimated using the Mann-Kendall non-parametric test, and, if significant below the 5% level, the trend slope is printed on the graph.

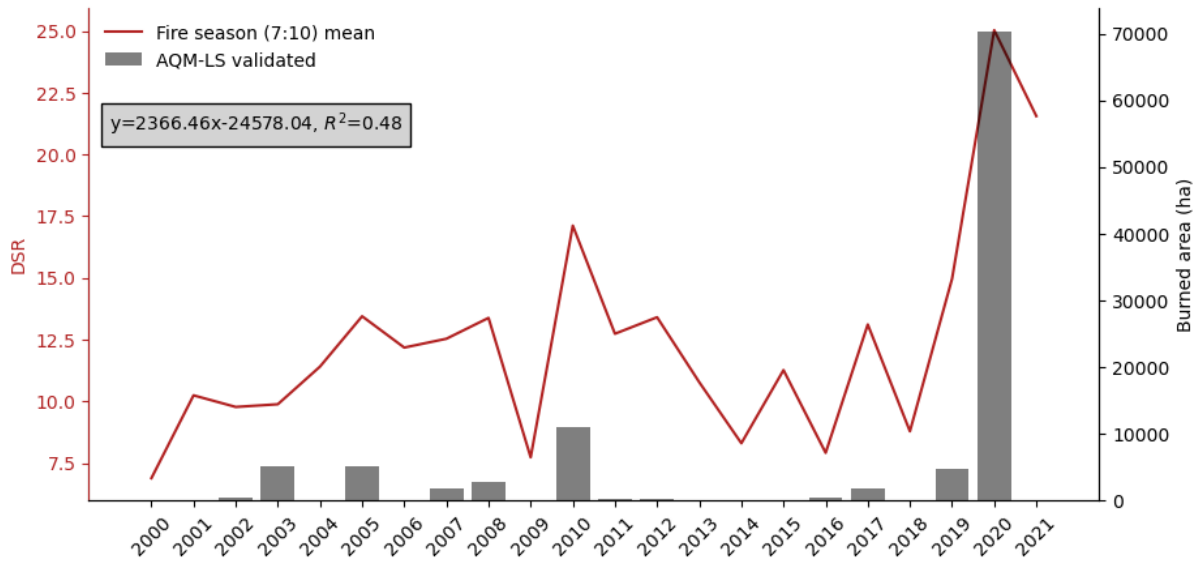


Figure 5.11: Interannual values of yearly burned area as estimated using the validated *AQM-LS* product (*AQM-LS<sub>val</sub>*, grey bars in both top and bottom panels corresponding to the right y-axis), and yearly averages of the Daily Severity Rating (DSR, bottom panel, red curve corresponding to the left y-axis), from 2000 to 2021. Grey box in both plots shows the resulting linear regression models, using the fire danger indexes as predictors of interannual burned area, and the corresponding coefficient of determination ( $R^2$ ).

Table 5.1: Comparison of the  $AQM-LS$  product ( $AQM-LS$ ) and its validated version ( $AQM-LS_{val}$ ), both values in thousands of hectares (ha). Column “ $AQM-LS - AQM-LS_{val}$ ” shows the absolute difference, in thousands of ha, and “Difference to  $AQM-LS$  (%)” shows the relative difference from  $AQM-LS_{val}$  to  $AQM-LS$ , estimated as  $(AQM-LS - AQM-LS_{val})/AQM-LS \times 100$ .

	$AQM-LS$ ( $\times 1000$ ha)	$AQM-LS_{val}$ ( $\times 1000$ ha)	$AQM-LS - AQM-LS_{val}$ ( $\times 1000$ ha)	Difference to $AQM-LS$ (%)
<b>2000</b>	12.331	0	12.331	100
<b>2001</b>	0.095	0	0.095	100
<b>2002</b>	0.885	0.386	0.499	56.4
<b>2003</b>	5.239	5.087	0.152	2.9
<b>2004</b>	1.772	0.031	1.741	98.2
<b>2005</b>	5.484	5.167	0.317	5.8
<b>2006</b>	0.332	0.005	0.327	98.6
<b>2007</b>	2.017	1.742	0.275	13.7
<b>2008</b>	3.009	2.790	0.219	7.3
<b>2009</b>	0.361	0	0.361	100
<b>2010</b>	11.204	11.056	0.148	1.3
<b>2011</b>	2.903	0.171	2.732	94.1
<b>2012</b>	0.442	0.236	0.206	46.5
<b>2013</b>	0.213	0.012	0.201	94.4
<b>2014</b>	1.442	0.020	1.422	98.6
<b>2015</b>	0.236	0.146	0.090	38.0
<b>2016</b>	1.018	0.402	0.616	60.5
<b>2017</b>	1.794	1.729	0.065	3.6
<b>2018</b>	0.281	0	0.281	100
<b>2019</b>	5.199	4.726	0.473	9.1
<b>2020</b>	70.421	70.352	0.069	0.1
<b>2021</b>	0.488	0.003	0.485	99.3

## **Author contribution**

**Patrícia S. Silva:** Writing - original draft, Visualization, Methodology, Formal analysis, Conceptualization. **Julia A. Rodrigues:** Writing - original draft, Visualization, Methodology, Formal analysis, Conceptualization. **Joana Nogueira:** Writing - original draft, Methodology, Conceptualization. **Livia C. Moura:** Writing - original draft, Conceptualization. **Alexandre Enout:** Writing - original draft, Conceptualization. **Cristina Cuiabália:** Writing - original draft, Conceptualization. **Carlos C. DaCamara:** Conceptualization. **Allan A. Pereira:** Software, Data curation. **Renata Libonati:** Writing - original draft, Supervision, Methodology, Conceptualization.



## 5.2 Synergy between heatwaves and fire in the Pantanal biome

*This section is based in the following scientific article: Silva, P. S., Geirinhas, J. L., Lapere, R., Laura, W., Cassain, D., Alegría, A., and Campbell, J. (2022). Heatwaves and fire in Pantanal: Historical and future perspectives from CORDEX-CORE. Journal of Environmental Management, 323:116193*

The Pantanal biome, at the confluence of Brazil, Bolivia and Paraguay, is the largest continental wetland on the planet and an invaluable reserve of biodiversity. The exceptional 2020 fire season in Pantanal drew particular attention due to the severe wildfires and the catastrophic natural and socio-economic impacts witnessed within the biome. So far, little progress has been made in order to better understand the influence of climate extremes on fire occurrence in Pantanal. Here, we evaluate how extreme hot conditions, through heatwave events, are related to the occurrence and the exacerbation of fires in this region. A historical analysis using a statistical regression model found that heatwaves during the dry season explained 82% of the interannual variability of burned area during the fire season. In a future perspective, an ensemble of CORDEX-CORE simulations assuming different Representative Concentration Pathways (RCP2.6 and RCP8.5), reveal a significant increasing trend in heatwave occurrence over Pantanal. Compared to historical levels, the RCP2.6 scenario leads to more than a doubling in the Pantanal heatwave incidence during the dry season by the second half of the 21<sup>st</sup> century, followed by a plateauing. Alternatively, RCP8.5 projects a steady increase of heatwave incidence until the end of the century, pointing to a very severe scenario in which heatwave conditions would be observed nearly over all the Pantanal area and during practically all the days of the dry season. Accordingly, favorable conditions for fire spread and consequent large burned areas are expected to occur more often in the future, posing a dramatic short-term threat to the ecosystem if no preservation action is undertaken.

### 5.2.1 Introduction

The Pantanal biome is the largest continental wetland in the world, extending over parts of Brazil (Bergier and Assine, 2016). This World Heritage Site (UNESCO, 2021) is home

to a wide variety of plants (Pott et al., 2011) and animals (Alho, 2008), including several endangered species (Tomas et al., 2019). In 2020, Pantanal faced the most devastating fires in the last two decades. Satellite-derived estimates showed that around a third of the Brazilian section of Pantanal was affected (Libonati et al., 2020), including several indigenous territories and conservation units being completely burnt.

Fire activity and climate have been shown to be closely linked (Mariani et al., 2018; Abatzoglou et al., 2019; Ruffault et al., 2020; Sutanto et al., 2020) and the 2020 Pantanal fires resulted from an interplay between extreme hot and dry conditions (Libonati et al., 2022b) associated with the negligent use of fire (Mataveli et al., 2021). Leading up to the 2020 fire season, Pantanal had been under severe drought conditions since 2019 (Marengo et al., 2021b), which severely impacted vegetation flammability. Soil desiccation conditions concurred with several heatwave episodes, leading to the establishment of strong soil moisture–temperature coupling regimes (water-limited) that triggered a temperature escalation through enhanced sensible heat fluxes from the surface to the atmosphere (Libonati et al., 2022b). As a result of this, the compound dry and hot conditions observed during 2020 over Pantanal, essentially drove fire danger to levels not seen since 1980 (Libonati et al., 2020).

The future dynamics and intensity of global fires is uncertain under climate change scenarios, and highly depends on the climate zone and local human drivers (Moritz et al., 2012; Williams and Abatzoglou, 2016). For South America however, an increasing trend in fire risk and extent is projected under a range of likely scenarios (Cochrane and Barber, 2009; Liu et al., 2010; Silva et al., 2019; Burton et al., 2021; de Oliveira-Júnior et al., 2021; Oliveira et al., 2022). In parallel, the number of heatwaves associated with record-breaking temperatures have been increasing over Pantanal (Marengo et al., 2021b; Libonati et al., 2022b). Such a growing trend in the number of extreme hot spells is expected to continue in most regions including South America (Dosio, 2016; Baker et al., 2018; Feron et al., 2019; Luca et al., 2020; Molina et al., 2020; Coppola et al., 2021). Feron et al. (2019) found for South America that the magnitude of this increase would not be spatially homogeneous, although by 2050, the tropical areas, including Pantanal, would witness extremely warm temperatures during at least half the days of the year. By the end of the century, annual average temperatures in Pantanal can increase by up to 7 °C relative to the 1961–1990 period (Marengo et al., 2015; Llopart et al., 2020). Additionally,

daily maximum temperature in Pantanal will likely increase by several degrees over the period 2050–2080 under different scenarios (Reboita et al., 2021b). Although the effects of climate change on Pantanal remain by far uncertain and are probably outweighed by human development and wetland destruction (Junk, 2013), the possible trends can induce changes in the dynamics and properties of the fire season, possibly jeopardizing even more of Pantanal’s ecosystems.

This work aims to evaluate the connection between heatwaves and fire in the Pantanal biome during the 2002–2020 period, and assess future trends under two climate change scenarios. Historical COordinated Regional Climate Downscaling EXperiment-COMmon Regional Experiment (CORDEX-CORE) simulations are then evaluated and compared to reanalysis data, evidencing the need for bias-correction. Accordingly, we compute bias-corrected future projections of heatwaves using the CORDEX-CORE ensemble and interpret the results in light of future climate change and what it might mean for fires in Pantanal.

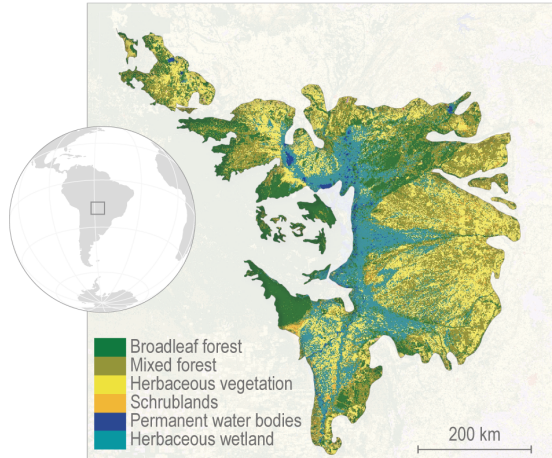
## 5.2.2 Data and methods

### 5.2.2.1 Data

The region of interest is the Pantanal biome as defined by the Terrestrial Ecoregions of the World (Figure 5.12; Olson et al., 2001). Burned area was derived from the Moderate Resolution Imaging Spectroradiometer (MODIS) MCD64A1 Collection 6 product (Giglio et al., 2018), developed by the National Atmospheric Space Agency (NASA). Derived from the MODIS sensors aboard Terra and Aqua satellites, MCD64A1 is a monthly burned area product at a 500 m spatial resolution from 2001 to 2020. Re-projected GeoTIFF data for South America was obtained from the University of Maryland’s fuoco SFTP Server (fuoco.geog.umd.edu). Burned area totals were computed for the Pantanal and 2001 was dropped as it only includes data from the MODIS sensor aboard Terra.

Daily maximum surface air temperature (Tmax) values from 1980 to present were obtained for Pantanal by computing the daily maximum of hourly surface temperatures retrieved from the European Centre for Medium-Range Weather Forecasts (ECMWF) ERA5 reanalysis dataset (Hersbach et al., 2020), at a gridded  $0.25^\circ \times 0.25^\circ$  spatial resolution.

(a) Location of the Pantanal biome.



(b) Pantanal's seasonal patterns.

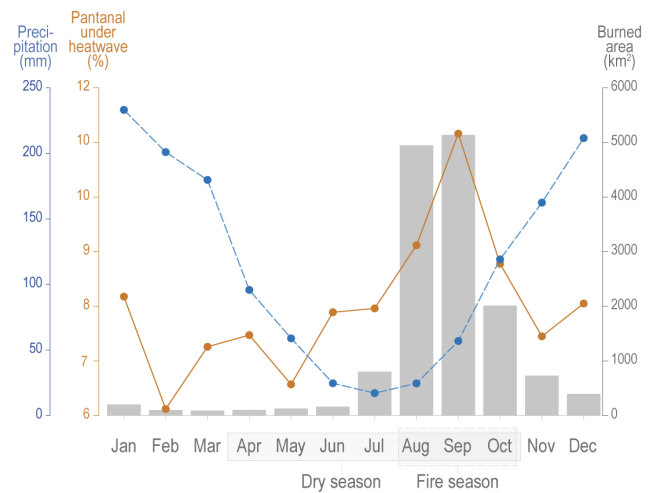


Figure 5.12: The Pantanal biome with land cover information for 2019 from the Copernicus Global Land Service (Buchhorn et al., 2020). (b) Pantanal's monthly averages of burned area (gray bars) as estimated by the MCD64A1 Collection 6 product over 2002–2020, and seasonal precipitation (blue line) and heatwave incidence (orange line) patterns in ERA5 reanalysis for the period 1981–2020.

Using data available from the Earth System Grid Federation (ESGF) platform (Cinquini et al., 2014), simulated daily maximum temperature for the historical period (spanning 1981 to 2005) and Representative Concentration Pathways (RCP) 2.6 and 8.5 were extracted from CORDEX-CORE runs on the South American domain at a  $0.22^\circ$  spatial resolution (Gutowski Jr. et al., 2016; Giorgi et al., 2022). This work relies on three realizations (historical, RCP2.6 and RCP8.5) from two Regional Climate Models - RCMs (REMO2015, RegCM4-7), each one forced by three different Global Climate Models - GCMs (HadGEM2-ES, MPI-ESM, NorESM1) as described in Table 5.2. RCP represent possible trajectories of future greenhouse gas and air pollutants emissions: the low-emission RCP2.6 scenario limits additional radiative forcing to  $2.6 \text{ W/m}^2$  by 2100 (van Vuuren et al., 2011) whereas the high-emission RCP8.5 scenario corresponds to a  $8.5 \text{ W/m}^2$  radiative forcing (Riahi et al., 2011).

### 5.2.2.2 Heatwave definition

Using a relative threshold index (Perkins and Alexander, 2013; Geirinhas et al., 2021) heatwaves were defined as periods of three or more consecutive days featuring  $T_{\text{max}}$  values above the climatological (1981–2010 in the case of data computation with ERA5, and 1981–2005 with the historical CORDEX-CORE simulations) calendar day 90<sup>th</sup> percentile (P90) of  $T_{\text{max}}$  (centered on a 15-day window). Based on this definition, a single

Table 5.2: RCM considered in this study: runs for the South American domain at  $0.22^\circ \times 0.22^\circ$  spatial resolution (SAM-22) available within the CORDEX-CORE (Giorgi et al., 2022).

RCM	Experiment	Time period	Forced by
REMO2015	Historical	1981/01/01–2005/12/31	MOHC-HadGEM2-ES
	RCP2.6	2006/01/01–2099/12/31	MPI-M-MPI-ESM-LR
	RCP8.5	2006/01/01–2099/12/31	NCC-NorESM1-M
RegCM4-7	Historical	1981/01/01–2005/12/31	MOHC-HadGEM2-ES
	RCP2.6	2006/01/01–2099/12/31	MPI-M-MPI-ESM-MR
	RCP8.5	2006/01/01–2099/12/31	NCC-NorESM1-M

one dimensional variable accounting for the time and spatial incidence of heatwaves over Pantanal was defined: the percentage of the total Pantanal domain under heatwave conditions ( $\%Pantanal_{HW}$ ). This metric was already used in previous studies conducted for regions within the USA (Mazdiyasni and AghaKouchak, 2015) and Brazil (Geirinhas et al., 2021), and consists in determining the percentage of the total Pantanal cells (in space and time,  $cellsPAN_{total}$ ) that experience heatwave conditions ( $cellsPAN_{HW}$ ), as expressed in Equation 5.1.

$$\%Pantanal_{HW} = \frac{cellsPAN_{HW}}{cellsPAN_{total}} \times 100 \quad (5.1)$$

The number of total Pantanal cells ( $cellsPAN_{total}$ ) is obtained by considering the total number of grid-points within the Pantanal region ( $cellsPAN_{region}$ ) and the total number of days of the dry season (April through October - Figure 5.12b -  $cellsPAN_{time}$ ) as in Equation 5.2.

$$cellsPAN_{total} = cellsPAN_{region} \times cellsPAN_{time} \quad (5.2)$$

The number of total Pantanal cells under heatwave ( $cellsPAN_{HW}$ ) is computed in the exact same way as  $cellsPAN_{total}$ , however it only considers the number of days and grid-points that are under heatwave conditions (as defined earlier in this section). As an example of application, a percentage of 100% indicates that every single grid point in the Pantanal domain witnessed heatwave conditions for every day of the dry season, and so,

$cellsPAN_{HW}$  equals  $cellsPAN_{total}$ .

### 5.2.2.3 Statistical analysis

The statistical relationship between burned area and heatwaves was evaluated using a simple linear regression model. Interannual variations of burned area (predictand, BA) were correlated with variations of the percentage of the total Pantanal domain under heatwave conditions (predictor,  $\%Pantanal_{HW}$ ) as in Equation 5.3.

$$BA = m \times \%Pantanal_{HW} + b \quad (5.3)$$

where  $m$  and  $b$  are the slope and intercept of the model, respectively. The goodness of fit was analyzed and assessed through the resulting coefficient of determination and  $p$ -value. To further test the robustness of the statistical model, and given the short length of the time series, a leave-one-out cross-validation scheme was performed (Wilks, 2011) and the Spearman's rank correlation coefficient computed.

Throughout this work, monotonic trends were estimated using the non-parametric Mann-Kendall two-tailed test (Mann, 1945; Kendall, 1975; Gilbert, 1987), and the Theil-Sen slope (Theil, 1950; Sen, 1968).

### 5.2.2.4 Bias correction

Bias correction was performed using a Quantile Delta Mapping (QDM) approach, in order to match Tmax distribution in the RCM realizations to that of ERA5, despite the discrepancies initially observed. The correction is applied both to historical and future scenario runs. QDM is known to perform well when it comes to preserving raw signals, trends and extremes (Cannon et al., 2015; Casanueva et al., 2020). QDM relies on the computation of the cumulative distribution functions CDF of the variable of interest, in the dataset of reference (here ERA5), and in the model to be adjusted on the historical and future periods (here CORDEX-CORE historical and RCPs). Based on these statistical distributions, the transformation applied can be summarized in Equation 5.4. Using this approach, the bias corrected Tmax obtained with Equation 5.4, referred to as  $Tmax_{FUT_{QDM}}$ , will incorporate the climate change signals present in the original CORDEX-CORE RCP runs.

$$Tmax_{FUT_{QDM}} = Tmax_{FUT} \times \frac{CDF_{ERA5}^{-1}(CDF_{FUT}(Tmax_{FUT}))}{CDF_{HIST}^{-1}(CDF_{FUT}(Tmax_{FUT}))} \quad (5.4)$$

QDM can be performed either in a parametric or empirical approach to compute the CDF. Here, the choice of a parametric (thus continuous) rather than empirical (thus discrete) approach is made so as to be able to capture future extreme values that may not be reached in the historical period distribution. For well-chosen parametric distribution forms, the performance is similar for parametric and empirical approaches (Enayati et al., 2021). Further details on QDM and its suitability and performance for our purpose can be found in Supplementary Material: Figures 5.18 and 5.19.

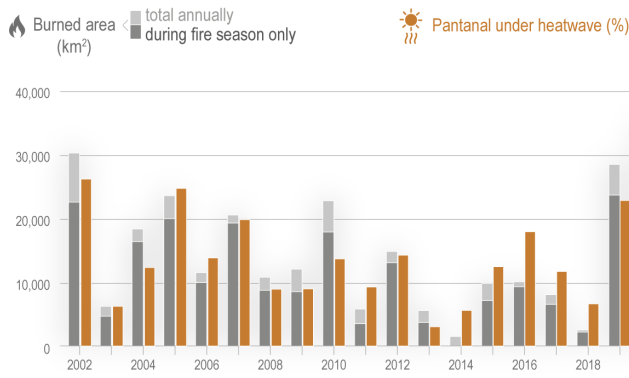
## 5.2.3 Results

### 5.2.3.1 Fire-heatwave connection

Pantanal burns quite frequently and mostly during the period from August to October, henceforth referred to as the fire season (Figure 5.12b; Damasceno-Junior, 2021). These months account, on average, for 79% of the annual burned area over the study period and coincide with low rainfall levels. Heatwaves also occur more often and over larger areas during these three months, with the maximum value of  $\%Pantanal_{HW}$  in September concurrent with the yearly peak in burned area. Heatwaves taking place in the austral summer (December, January, February) and during the transition from wet to dry season (March–April) are not associated with high burned areas as the vegetation is growing and moisture levels are high, which constrains the spread and extent of fires (Ivory et al., 2019). Accordingly, in the upcoming analysis we evaluate heatwave conditions over the months from April to October, considered here as the biome’s dry season (Figure 5.12b; de Oliveira et al., 2014; Ivory et al., 2019), to account for the effects of heatwaves on fuel moisture levels prior to the fire season.

The biome averages  $14,439 \pm 9649$  km<sup>2</sup> burned area ( $8.5 \pm 5.7\%$  of Pantanal’s area) per year over the 2002–2020 time series, with high interannual variability (Figure 5.13a). The years of 2002, 2019 and 2020, stand out as the most dramatic, with the latter burning a record-shattering amount unseen in Pantanal over the last two decades.

(a) Pantanal's interannual variability of burned area and area under heatwave.



(b) Relationship between Pantanal's area under heatwave during dry season and burned area during fire season from 2002 to 2020.

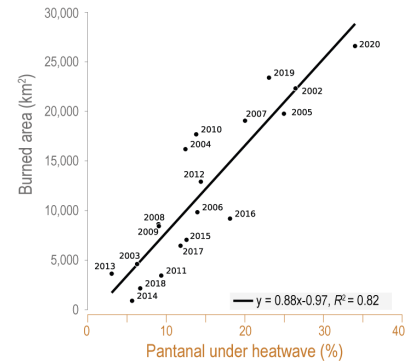


Figure 5.13: Interannual variability of annual burned area (light gray bars) and fire season burned area (August to October; dark gray bars), using the MODIS MCD64A1 product, and the percentage of Pantanal under heatwave ( $\%Pantanal_{HW}$ ) over the dry season (April to October; orange bars), from 2002 to 2020. (b) Relationship between  $\%Pantanal_{HW}$  over the dry season and the fire season burned area, estimated using ERA5 reanalysis, from 2002 to 2020, evaluated using a simple linear regression model. Black line indicates the resulting regression line and on the bottom right corner is the corresponding equation and goodness-of-fit ( $R^2$ ).

The interannual variability of burned area over the fire season seems to be closely related to the percentage of Pantanal that is under heatwave over the dry season (Figure 5.13a). Years with the highest (lowest) burned area correspond with higher (lower) percentages of heatwave incidence over Pantanal ( $\%Pantanal_{HW}$ ), with the exception of 2007, when the  $\%Pantanal_{HW}$  reached its maximum value over the 2002–2019 period while burned area values were below the time series 75<sup>th</sup> percentile.

A simple linear regression model between annual values of these two variables obtained a Pearson coefficient of 0.90 ( $p$ -value < 0.001). Hence, the linear model described in Equation 5.5 based on  $\%Pantanal_{HW}$  significantly explains 82% of the variance of burned area over the 2002–2020 period (Figure 5.13b). It is worth noting here that causality is not assumed in this relationship. It only constitutes a purely statistical conception that holds for values of  $\%Pantanal_{HW}$  varying between approximately 3% to 34%, which is the historically observed range.

$$BA = 0.88 \times \%Pantanal_{HW} - 0.97 \quad (5.5)$$

with burned area in 1,000 km<sup>2</sup> and  $\%Pantanal_{HW}$  in percentage.

The leave-one-out cross-validation scheme (Supplementary Material: Figure 5.20) resulted



in a coefficient of determination of 0.78 between the observed and the predicted burned area values, and a Spearman's correlation  $\rho$  of 0.90 ( $p$ -value  $< 0.001$ ), which confirms that the linear model is robust and indeed the best approach to correlate these variables.

### 5.2.3.2 Model evaluation

There is a large variability in the outcomes of each of the six members of the CORDEX-CORE ensemble considered. The comparison of Tmax between the six historical runs and the ERA5 reanalysis, for the Pantanal region, during the dry season and for the period 1981–2005, shows correlations on the time series of monthly averages of daily Tmax ranging from 0.42 to 0.67, and correlations on monthly P90 of Tmax between 0.60 and 0.84 (Figure 5.14a). Mean biases on these variables are between 0.4 °C to 5.3 °C and 0.28 °C to 4.4 °C, for monthly averages and P90, respectively. REMO2015 forced by HadGEM2-ES shows the best agreement with ERA5, contrary to RegCM4-7 forced by NorESM1 that features the largest discrepancies with the ERA5 reanalysis. The remaining models show intermediate values and, for all models, lower mean biases and higher correlations are found when looking at the monthly P90. This large inter-model spread is commonly observed in multi-model analyses of RCMs, in particular in the CORDEX framework for South America (e.g. Feron et al., 2019). The ensemble is also shown to have a mean bias of 2.72 °C and 3.76 °C, and a Pearson correlation coefficient of 0.68 and 0.79, for the mean and P90 of Tmax, respectively. For impact studies, the ensemble mean is usually able to properly reproduce the main climatological features of the region, notwithstanding the large variability across individual members (Teichmann et al., 2021; Coppola et al., 2021).

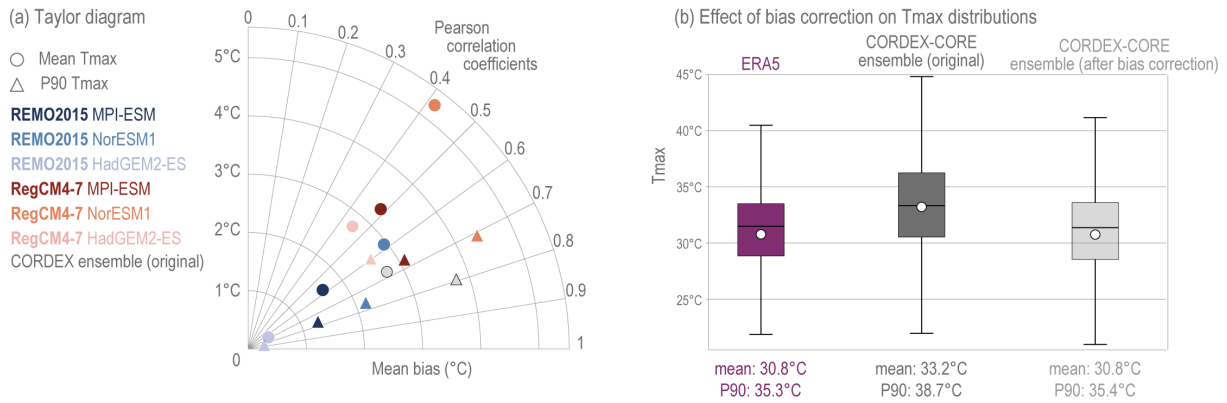


Figure 5.14: (a) Taylor diagram of raw CORDEX-CORE historical simulations compared to ERA5. T<sub>max</sub> monthly mean (circles) and monthly P90 (triangles) during dry season months (April–October) over Pantanal for the period 1981–2005, for each simulation (color range) and for the ensemble mean (gray). All Pearson correlation coefficients presented here are statistically significant at the 99.9% level. (b) T<sub>max</sub> distribution over Pantanal for dry season months of the historical period in ERA5 (purple), CORDEX-CORE original (gray) and CORDEX-CORE after bias correction (light gray).

Considering this inter-model variability and discrepancies compared to ERA5, T<sub>max</sub> datasets from the CORDEX-CORE runs were bias-corrected towards the distribution of T<sub>max</sub> in ERA5. Supplementary Material: Figure 5.18 shows the time series for T<sub>max</sub> of raw CORDEX-CORE historical data and both RCP runs over the 1981–2099 period, and the result after bias-correction. A clear shift is observed towards ERA5 values after bias correction, while keeping the trends intact. The performance of the bias correction is also illustrated in Figure 5.14b, which shows that the bias between CORDEX-CORE and ERA5 ensemble mean (P90) T<sub>max</sub> goes from 2.4 °C (3.4 °C) before correction to less than 0.1 °C after. QDM therefore seems to be successful in approximating the CORDEX-CORE ensemble mean distribution to that of ERA5, as also evidenced in Supplementary Material: Figure 5.19. The bias-corrected results are now in the same range as those of the reanalysis: the historical mean of T<sub>max</sub> is now equal for CORDEX-CORE after QDM and the ERA5 reanalysis, at 30.8 °C (Figure 5.14b). Moreover, Supplementary Material: Figure 5.18 confirms the above-mentioned large inter-model variability, with large shaded areas representing the maximum and minimum values simulated by CORDEX-CORE runs after bias-correction.

Figures 5.15 and 5.16 further highlight this inter-model variability, which is found also in future projections. Under RCP8.5 scenario (Figure 5.15), for the near future period (2026–2050, top line in the Figure), T<sub>max</sub> during the dry season increases on average between 0 to 2 °C approximately, depending on the considered GCM/RCM combination.

For the mid-term (2051–2075) and long-term (2076–2099) periods, the spread increases, with Tmax warming between 1.5 to 5 °C and 3 to 9 °C, respectively. The trajectory under RCP2.6 assumptions suggests a lesser warming of Pantanal, along with a smaller inter-model spread, in absolute value, as compared with RCP8.5 (Figure 5.16). For that scenario, all runs feature an increase in Tmax between 0 to 4 °C without a clear temporal evolution, with Tmax departure from its historical values in the short-term being similar to the mid- and long-term periods ones. In both scenarios, the expected warming is spatially quite homogeneous over the Pantanal region, except for its southernmost part, which seems to be slightly less affected in most runs, as opposed to the northeastern part that might suffer from even warmer conditions by up to 1 °C according to several runs.

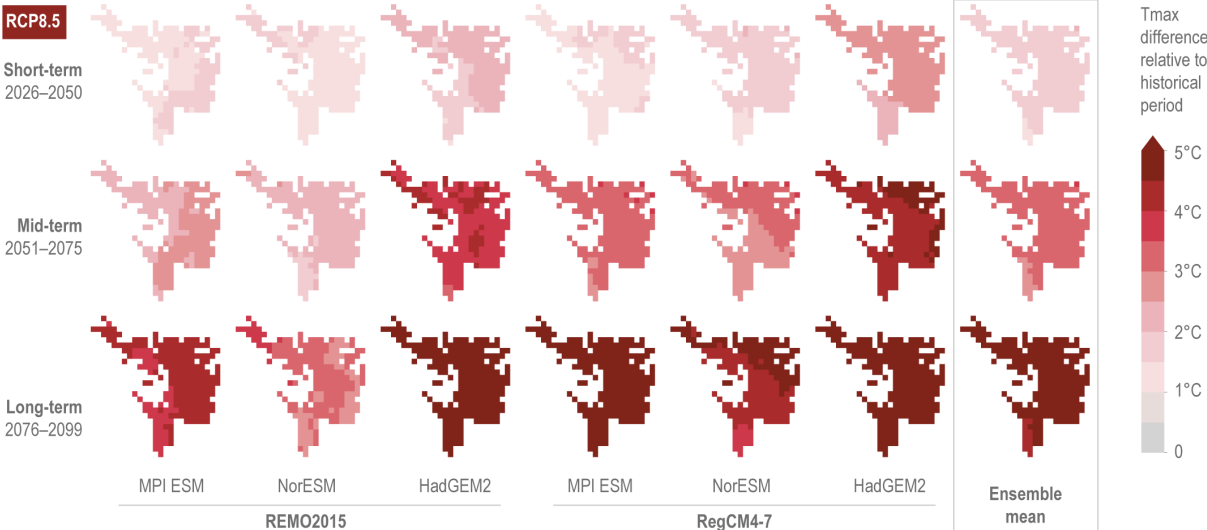


Figure 5.15: Average difference on Tmax over the Pantanal region for April to October between the historical period and three projected RCP8.5 periods (2026–2050 as short term; 2051–2075 as mid term; and 2076–2099 as long term), for the six CORDEX-CORE simulations considered and the ensemble mean (rightmost panel). All data is from the bias-corrected simulations.

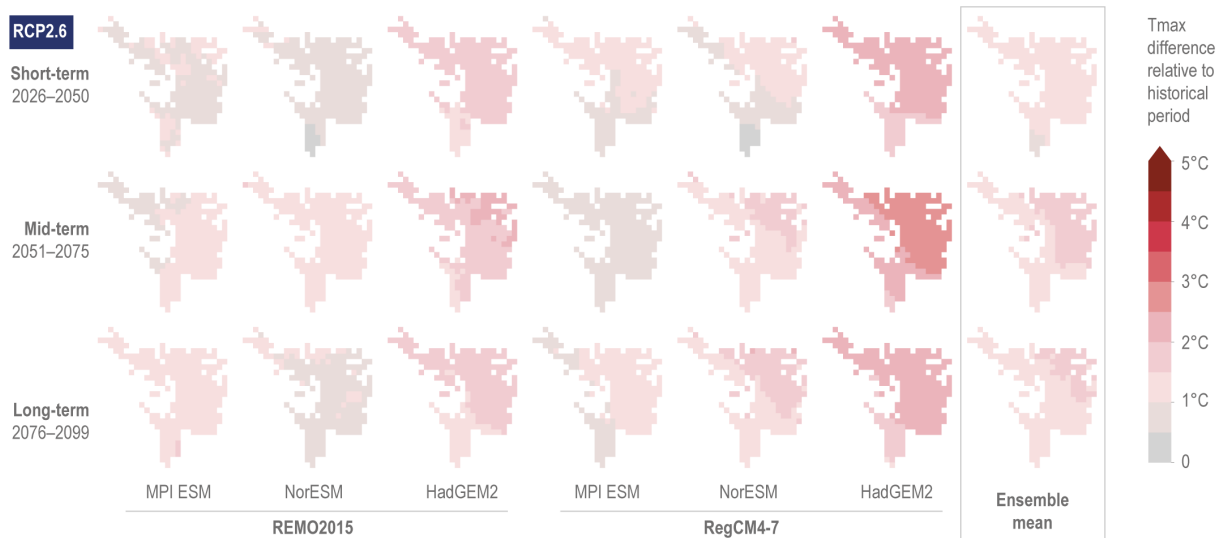


Figure 5.16: Same as Figure 4 for RCP2.6.

### 5.2.3.3 Future trends in heatwaves

We analyzed the simulated evolution of heatwaves over Pantanal from 1981 to the end of the 21<sup>st</sup> century, under scenarios RCP2.6 and RCP8.5, using CORDEX-CORE bias-corrected ensemble mean. Under both scenarios, the  $\%Pantanal_{HW}$  is expected to increase by 2100 (Figure 5.17), albeit with distinct growing patterns. Considering the optimistic emission scenario RCP2.6, the average  $\%Pantanal_{HW}$  is expected to increase up to 36.4% over the mid-term period, followed by a decrease to 35.2% in the long-term period (Table 5.3). When compared to the historical average (12.5%), this represents a relative increase of 191% and 182% of the  $\%Pantanal_{HW}$  for mid and long-term, respectively. Extremes, evaluated by the P90, reach 43.4% over mid-term and more than double the historical value with relative increases above 140% in all three time periods. However, no significant trend was found in either period, consistent with RCP2.6 assumptions of peaking emissions mid-century followed by a steady decrease afterwards (van Vuuren et al., 2011).

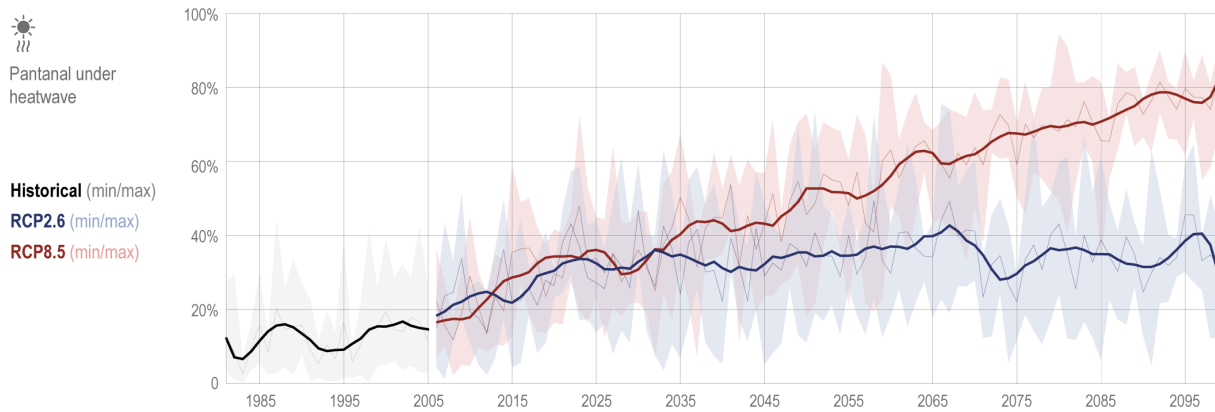


Figure 5.17: Percentage of Pantanal under heatwave from 1981 to 2099. Evolution for historical (black line), RCP2.6 (blue line), and RCP8.5 (red line) bias-corrected CORDEX-CORE runs. The gray, blue and red shaded regions show the maximum range between individual model runs. Solid lines represent the ensemble mean and those that are thicker show a smoothed time series for better visualization. The smoothing is performed by applying a Savitzky–Golay filter with a window length of 19 years and a polynomial order 5.

Alternatively, under the high-emission scenario RCP8.5 there is a statistically significant monotonic increase, clearly departing from the RCP2.6 scenario after the mid-term period, leading to a  $\%Pantanal_{HW}$  level of 80% by the end of the 21<sup>st</sup> century (Figure 5.17). Average (and P90) values of  $\%Pantanal_{HW}$  differ considerably over the three time periods (Table 5.3): from 39.9% (51%) in the short-term period, slightly above the corresponding values in RCP2.6, to 73.3% (78.4%) in the long-term period. In this scenario, departures from the mean (and P90) historical values are dramatic, with relative increases of 219% (193%), 368% (287%) and 486% (351%), for the short, mid and long-term periods, respectively.

Table 5.3: Future evolution of heatwave index ( $\%Pantanal_{HW}$ ) under RCP2.6 and RCP8.5 scenarios for three time periods: short-term from 2026 to 2050; mid-term from 2051 to 2075; and long-term from 2076 to 2099. For comparison, we further show values for the historical run from 1981 to 2005. Average values are calculated as ensemble mean from all RCM realizations. Std corresponds to the standard deviation, over time, of the ensemble mean for the considered period. Values between parentheses indicate relative change compared to the historical value. The presence of a trend is evaluated through the Mann–Kendall test at a 5% significance level. Upwards arrows indicate a significant positive trend. The average inter-model spread corresponds to the average, over each period, of the difference between the highest and lowest individual member values every year.

		Average	Std	P90	Trend	Inter-model spread
<b>Historical</b>		12.5	4.5	17.4	-	23.2
<b>RCP2.6</b>	Short-term	32.9 (163%)	6.6	41.8 (140%)	-	35.1
	Mid-term	36.4 (191%)	6.4	43.4 (149%)	-	32.8
	Long-term	35.2 (182%)	5.4	42.5 (144%)	-	33.9
<b>RCP8.5</b>	Short-term	39.9 (219%)	8.3	51 (193%)	↑	30.6
	Mid-term	58.5 (368%)	7.6	67.3 (287%)	↑	31.5
	Long-term	73.3 (486%)	4.6	78.4 (351%)	↑	24.1

Nevertheless, in both scenarios, inter-model variability is relatively large (Table 5.3). In particular, the spread of  $\%Pantanal_{HW}$  between the minimum and maximum individual members from the ensemble for each projection year is around 32%, on average. In RCP2.6 scenario, this inter-model spread remains relatively stable, from 35% in the short-term period to 34% in the long-term, pointing to a moderate climate signal in Pantanal in that scenario. Contrarily, RCP8.5 leads to a decrease in the spread between models, from 31% in the short-term down to 24% in the last 25 years of the century. This indicates that under the stronger climate forcing of the RCP8.5 scenario, models tend to agree more on the long-term pathway as all of them foresee extreme heatwave conditions in Pantanal at the end of the century. For the RCP2.6 scenario, although the mean is clearly higher than historical values, the ensemble member with the lowest warming projection is indistinguishable from the historical envelope for all the time periods considered. On the other hand, the lowest warming projection for RCP8.5 is well above the maximum of the historical envelope despite a relatively large inter-model spread. In the first half of the century, individual simulations from both RCPs overlap (shaded areas in Figure 5.17), however, after 2050 there is a clear distinction between the maximum and minimum simulated values obtained for each RCP. By the end of the century, although the maximum

simulated value of  $\%Pantanal_{HW}$  under RCP2.6 is higher than that of the historical run, the historical simulations that achieved the highest  $\%Pantanal_{HW}$  are in the same range of values as RCP2.6  $\%Pantanal_{HW}$  ensemble means. This is not the case with RCP8.5, where, by 2100, the minimum value of simulated  $\%Pantanal_{HW}$  far exceeds the maximum value obtained in any historical simulation, highlighting how RCP8.5 is a much more severe scenario.

For both RCPs, inter-model variability seems to decrease over the 21<sup>st</sup> century, with model predictions converging towards the end of the simulation period. This is particularly sharp in RCP8.5 where there is a decrease in inter-model spread and standard deviations (Table 5.3), due to a threshold effect on the heatwave index computation, which is based on a comparison between Tmax and the fixed historical P90 of Tmax (see Methods). In the case of RCP8.5 the significant increase in Tmax is such that, even though the inter-model variability in Tmax is large, all individual members are mostly above the historical heatwave threshold. Consequently, even the member with the lowest warming trajectory still generates a high heatwave index value, thereby dampening the variability observed in  $\%Pantanal_{HW}$ .

#### 5.2.4 Discussion

The linear regression model developed in this study showed that 82% of the annual variance in Pantanal’s burned area is related to annual variations in heatwave incidence. This strong connection between fire events and heatwaves is in agreement with previous analyses conducted worldwide (Chuvieco et al., 2021) and for Pantanal in particular (da Gama Viganó et al., 2018; Libonati et al., 2022b). The occurrence of heatwaves over the dry season triggers large evaporation rates and thus soil desiccation that, ultimately, may influence the level of vegetation dryness and increase flammability. On the other hand, during the fire season heatwaves promote favorable conditions for larger burned areas if an ignition source is provided (which in the case of Pantanal is mostly human; Menezes et al., 2022). Recent heatwave episodes in this region have been associated with the establishment of quasi-stationary anticyclonic circulation anomalies over central South America as a response of large-scale Rossby wave patterns forced by remote warm sea surface temperatures in Indian and Pacific oceans (e.g. ENSO, MJO, IOD) (Taschetto and Ambrizzi, 2011; Marengo et al., 2021a; Reboita et al., 2021a; Libonati et al., 2022b).

These mid-atmospheric high pressure systems are responsible for strong subsidence and large amounts of incoming shortwave radiative energy at surface (Marengo et al., 2021a; Libonati et al., 2022b; Geirinhas et al., 2022). On the other hand, they can induce large disturbances in the South Atlantic Convergence Zone (Nielsen et al., 2019) and/or in the South American Low-Level Jet (Montini et al., 2019) suppressing the passage of frontal systems and promoting the occurrence of large deficits in the water vapor transport from the Amazon basin towards Pantanal. A long-term shortage of moisture being advected from the Amazon basin coupled with a lower than normal atmospheric convergence in the region leverages large precipitation deficits and evaporation rates that, ultimately, promote a sharp decrease in soil moisture levels. In fact, Libonati et al. (2022b) showed that during the 2020 fire season due to pronounced drought conditions over Pantanal, a strong soil moisture–temperature coupling (water-limited) was established allowing a re-amplification of the already established surface hot temperature anomalies during several heatwave episodes (Coronato et al., 2020; Geirinhas et al., 2022). As such, fire activity in Pantanal is also inevitably linked to drought and flood (Mataveli et al., 2021; Libonati et al., 2021; Marengo et al., 2021a). However, precipitation estimates show large inter-model discrepancies over South America (Solman et al., 2013; Falco et al., 2019; Solman and Blázquez, 2019) due to the commonly acknowledged shortcoming of RCMs when it comes to capturing precipitation. Accordingly, here the focus was made exclusively on the heatwave–fire connection.

Still, large biases were found in temperature estimates by the RCMs and, in order to legitimate the analysis of future heatwaves, the bias observed in CORDEX-CORE historical Tmax data with respect to ERA5 was corrected through QDM. Such an adjustment is required in order to obtain more plausible climate change projections, especially when it comes to extreme temperature-related phenomena (Iturbide et al., 2021). Although in this work the bias correction showed a good performance as evidenced in Supplementary Material: Table 5.4 and Supplementary Material: Figure 5.18, such approaches to adjust simulation data towards a better match with observations have known limitations and shortcomings. In particular, they can be considered statistical artifacts that do not provide clues on the credibility of the physical processes represented in the model (Maraun, 2016; Maraun et al., 2017). However, Maraun et al. (2017) recognize that for reasonably well captured physical processes, such as the ones driving the spatio-temporal variability



of Tmax, usual bias correction methods work adequately. This is arguably the case here since the distribution of Tmax from ERA5 and from all the CORDEX-CORE models could be successfully fitted to the same class of theoretical distribution. These elements indicate that the underlying physical processes are consistently represented in the reanalysis and in the RCMs demonstrating that bias correction can be applied confidently. The choice of the bias correction technique is also known to condition the results obtained. Casanueva et al. (2020) and Iturbide et al. (2021) show that there are differences in the outputs of bias corrected models when different methods are applied to the same data, including Tmax in CMIP or CORDEX simulations, resulting in slightly different future projection scenarios. Nevertheless, the QDM applied here shows good performance to steer CORDEX-CORE data towards ERA5 values, and consistency in the climate signal between original and adjusted time series (Supplementary Material: Figure 5.18), which gives confidence in the conclusions of this study.

In particular, the climate change signal displaying increasing heatwave importance, and comparatively larger increase in RCP8.5 than in other scenarios, is consistent with previous studies investigating future trends in hot extremes. Despite differences in the projections, RCP4.5 and RCP8.5 scenarios are both known to lead to an increase in extreme temperature events, with larger changes over lower latitudes (Russo et al., 2014; Perkins-Kirkpatrick and Gibson, 2017; Feron et al., 2019). They also evidence, consistent with our findings, that heatwave future trends and levels are much worse under RCP8.5 scenario, across all of South America. Global warming will likely impose in Pantanal the occurrence of more intense and prolonged heatwaves due to linear increases of the mean surface temperature and non-linear feedbacks triggered by deep changes in precipitation, evaporation and radiative regimes (Donat et al., 2017; King, 2019). This raises new challenges not just for the ecosystems but also for human health and for other socio-economic sectors (e.g. agriculture and energy production). These threats are expected to be particularly relevant in low-income developing countries such as the ones that share the Pantanal biome (Brazil, Paraguay and Bolivia), where the public health services are fragile and where there is still a lack of investment in environmental protection policies. The heatwave projections highlighted here for Pantanal suggest that the heat-stress levels witnessed by the population of Pantanal will increase, leveraging the number of heat-related deaths to dramatic levels (Gasparrini et al., 2015; Guo et al., 2018).

Our results also suggest that such an increase in heatwave conditions could lead to higher burned areas, as favorable conditions for fire occurrence will occur more frequently and widespread over the region (Libonati et al., 2022b). This could also trigger other cascading impacts of heatwaves in public health through the occurrence of more and widespread fires: a higher exposure to wildfire smoke is likely to lead to an increase in the number of respiratory illnesses and in birth defects not just for the living population of Pantanal but also for the inhabitants of downwind regions (Aguilera et al., 2021; Requia et al., 2021).

Nevertheless, such an increase in the heatwave index over the 21<sup>st</sup> century, and thus fire activity, would inevitably translate to changes in vegetation cover and climate–vegetation dynamics. Studies have found that fire influences the forest-savanna threshold (Hoffmann et al., 2012a; de L. Dantas et al., 2013) which means that such dramatic changes in fire activity could put several areas of Pantanal at risk of biome transition. As a result, these climate-fire-vegetation dynamics could change entirely the shape of the correlation between  $\%Pantanal_{HW}$  and burned area for more intense heatwaves, which are not taken into account here as RCMs consider a static vegetation cover. For both scenarios, in addition, nonlinear vegetation-atmosphere and/or land–atmosphere feedback induced by climate change could also corrupt the climate assumptions on which our statistical regression model is based. Considering that the model assumes a climate stationarity, in that case the relation between heatwaves and fires would need to be adjusted and the model would need to be calibrated according to new climate conditions.

### 5.2.5 Conclusion

This study aimed at evaluating and modeling the connection between fire and heatwaves in Pantanal, and employed, for the first time, the CORDEX-CORE regional climate simulations at 0.22° spatial resolution, to project future heatwave estimates over the Pantanal biome. A robust connection was found between a heatwave index and burned area. A simple linear model based on  $\%Pantanal_{HW}$  significantly explains 82% of the variance of burned area over the 2002–2020 period.

When looking at bias-corrected future projections of heatwaves by CORDEX-CORE model runs, we find that results differ considerably between scenarios, with RCP2.6, the low-emission scenario, reaching close to 40% of Pantanal under heatwave by mid-century

to then stabilize to around 35% in 2100, whereas RCP8.5, the most severe scenario, shows a steady increase up to 80% by the end of the century.

The aforementioned ensemble means are associated with a large inter-model spread and therefore uncertainty. This spread is much smaller in RCP8.5 scenario indicating a stronger shift in heatwaves, with a significantly increasing trend. The lesser inter-model variability in heatwaves observed in the long-term in RCP8.5 compared to RCP2.6 reveals how extreme the former scenario is. In this trajectory, every model predicts maximum temperature occurrence and therefore heatwave frequency well above past values, thereby saturating the historical thresholds. Possible changes in climate mechanisms and dynamics in the future (e.g. surface–atmosphere feedbacks) prevent the application of the statistical link between heatwaves and burned area that was evidenced in this study. However, this model can serve as a basis for educated guesses and qualitative assessments on possible future burned area, and suggests that under any scenario, even the more optimistic RCP2.6, burned area will likely increase, and the exceptional 2020 fire season in Pantanal could possibly compare as moderate with events in the near future.

Both fire (Alho et al., 2019) and climate change (Thielen et al., 2020) are major threats to the Pantanal biome, and the 2020 fire events were illustrative of the severe consequences it can have in biodiversity (Tomas et al., 2021), economy, and human health (Machado-Silva et al., 2020). The increased frequency of these fires is among the most visible results of human-induced climate change, posing a serious threat to biodiversity conservation, as the cumulative impact of widespread burning would be catastrophic if the situation of 2020 becomes common in the coming decades. Climate change may considerably alter the ecological properties of the Pantanal (de Oliveira Aparecido et al., 2021) which, associated with changes in land use and cover (de Souza Miranda et al., 2018; Colman et al., 2019; Marques et al., 2021), further contribute to a disturbed landscape and pave the way to increased fire activity (Kumar et al., 2022). Fire and land management are thus imperative within the Pantanal wetlands, to avoid further degradation to this unique ecosystem (Garcia et al., 2021; Berlinck et al., 2022).

As to the authors' knowledge this is the first study evaluating fire and heatwaves over the Pantanal biome, employing a set of regional climate simulations of relatively-high spatial resolution to project future trends. Very little research has been done in climate

Table 5.4: Kolmogorov-Smirnov test p-values against Mielke beta-kappa distribution for Tmax in ERA5 and the historical CORDEX-CORE simulations, for months April through October during the period 1981–2005.

Model	ERA5	REMO			RegCM		
		HADGEM	MPI	NCC	HADGEM	MPI	NCC
p-value	0.36	0.37	0.36	0.33	0.28	0.44	0.41

extremes over this region and more so is needed to properly understand the physical mechanisms associated with the found heatwave–fire relationship. These results provide useful information for fire activity in the biome in light of future climate change, and may also assist with regional information of the connection between fire and heatwaves in Pantanal to improve statistical or physical models.

## 5.2.6 Supplementary Material

### 5.2.6.1 Bias correction

The parametric Quantile Delta Mapping (QDM) bias correction method applied in this work uses Mielke beta-kappa distribution function for the description of CORDEX-CORE and ERA5 Tmax distributions. The formula of the associated cumulative distribution function is given in Equation 5.6, where parameters  $\kappa$  and  $\theta$  are optimized through a least squares regression to best fit the models’ empirical distributions.

$$CDF(x; \kappa, \theta) = \frac{x^\kappa}{(1 + x^\theta)^{\kappa/\theta}} \quad (5.6)$$

The adequacy of the choice of this theoretical form is assessed in Table 5.4 where a Kolmogorov-Smirnov (KS) for goodness of fit is performed for each dataset. These tests reveal that we cannot reject the hypothesis that the samples fit a Mielke beta-kappa distribution at least at the 25% level for all the historical models and ERA5. Although not shown here, Tmax in RCP future scenarios also complies with a KS test against Mielke beta-kappa distribution, at the 5% level, despite a decreasing goodness of fit for periods farther in the future.

For the sake of consistency, QDM was applied on future Tmax values separately for different time windows, with a duration similar to the historical period. Namely, QDM

was performed independently for the future periods 2006–2025, 2026–2050, 2051–2075 and 2076–2099. The bias corrected time series of yearly mean and P90 Tmax is shown in Figure 5.18, along with the original data and ERA5 time series for the historical period. The effect of the bias correction can also be observed in the shift in distributions before and after correction shown in Figure 5.19.

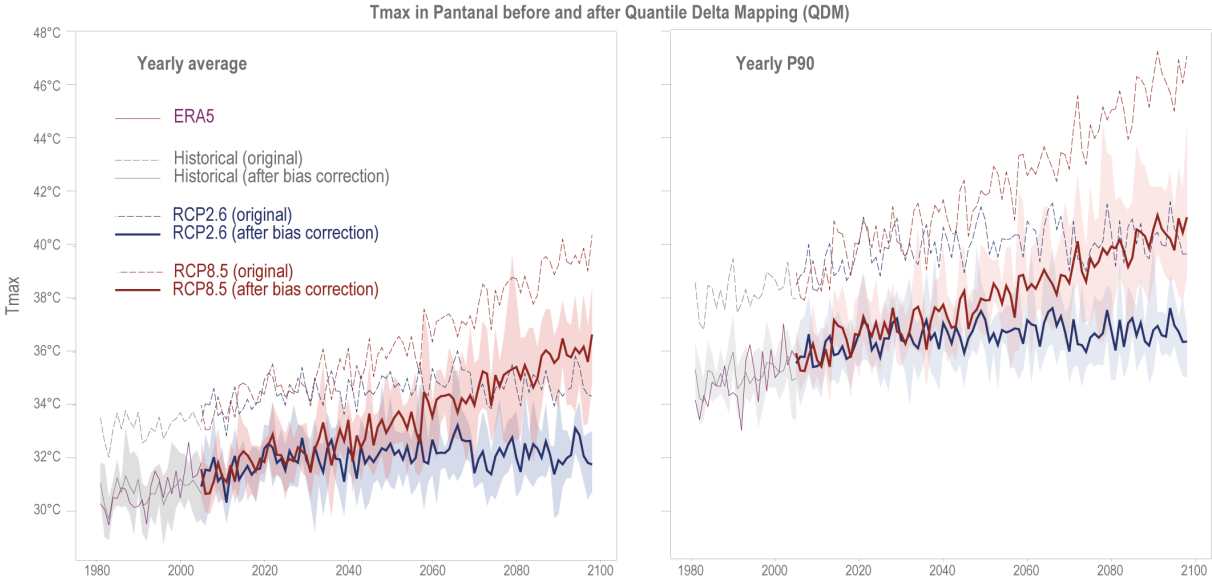


Figure 5.18: Yearly average of Tmax (left) and P90 Tmax (right) over Pantanal during the 1981–2099 period, in ERA5 (solid purple line), and for CORDEX-CORE RCP scenarios ensemble means before (dashed blue and red lines) and after (solid blue and red lines) bias correction. For CORDEX-CORE corrected, ensemble means are shown in solid lines, and the minimum and maximum of each single realization is shown in shades for the bias corrected time series.

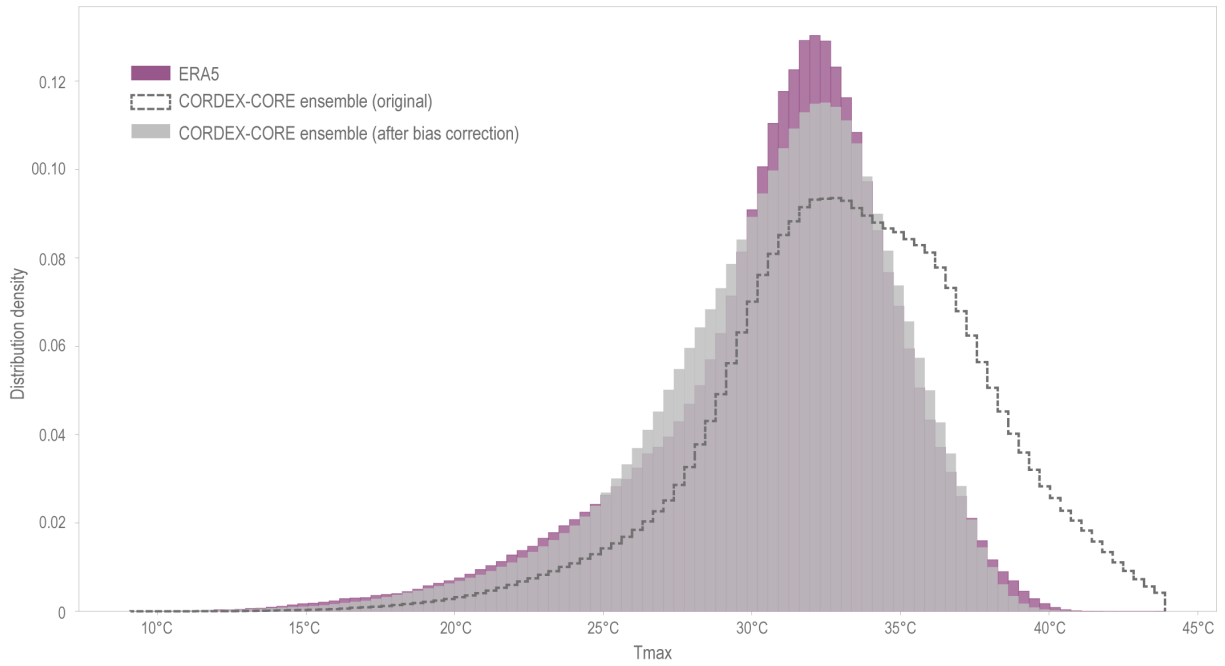


Figure 5.19: Distribution of hourly Tmax in ERA5 (purple bars) and in the ensemble of CORDEX-CORE historical runs before (black line) and after (gray bars) bias correction. Period 1981–2005.

### 5.2.6.2 Cross-validation

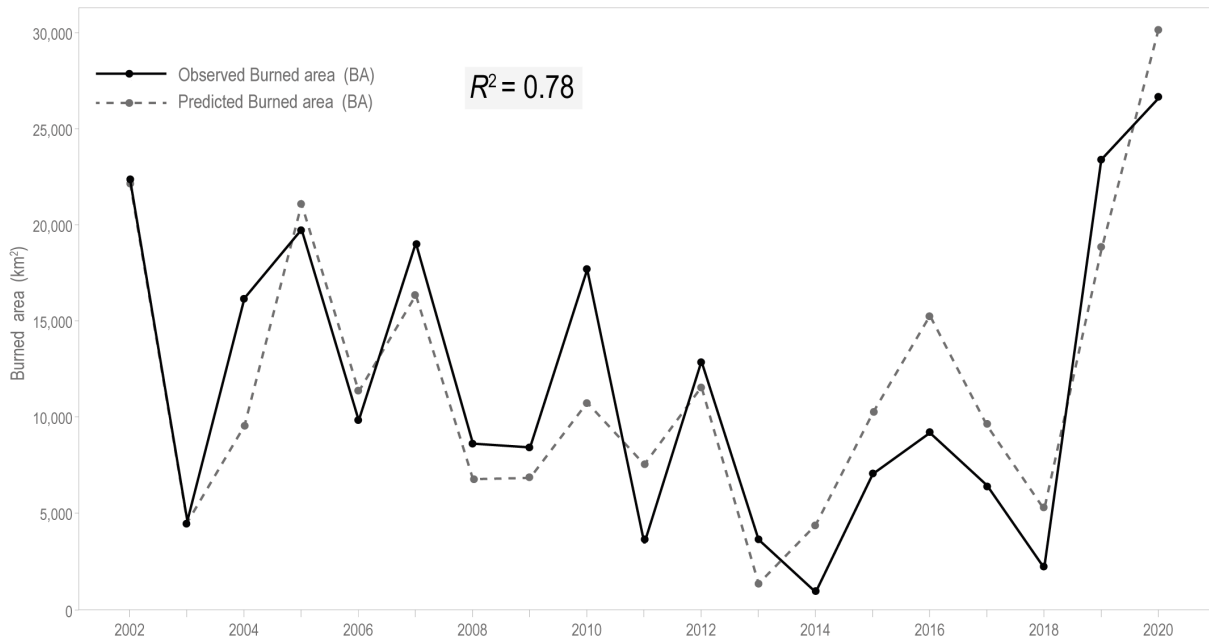


Figure 5.20: Leave-One-Out Cross-Validation (LOOCV) scheme performed from 2002 to 2020: observed burned area values (from MODIS MCD64A1) are shown in a solid black line, whereas the LOOCV predicted values for burned area are shown in a dashed black line. The resulting coefficient of determination from the observed and the predicted burned area values is also shown in red.

## **Author contribution**

**Patrícia S. Silva:** Conceptualization, Methodology, Formal analysis, Writing - original draft, Visualization, Supervision. **João L. Geirinhas:** Conceptualization, Methodology, Formal analysis, Writing - original draft. **Rémy Lapere:** Conceptualization, Formal analysis, Data curation, Writing - original draft, Visualization. **Wil Laura:** Formal analysis, Data curation, Writing - original draft, Visualization. **Domingo Cassain:** Data curation, Writing - original draft. **Andrés Alegría:** Data visualization. **Jayaka Campbell:** Writing - original draft.

## Chapter 6

### Final remarks



The main goal of this thesis was to assess regional fire patterns and their climatic and anthropogenic drivers in the Brazilian savannas. The main focus was on the Cerrado biome, but novel studies were also performed for Pantanal.

Given Cerrado's ecological and socio-economic importance for Brazil, and the role of fire in maintaining this unique ecosystem, it is essential to better understand the spatial variability in current fire behaviour. **Chapter 2** provides detailed information on regional fire parameters, including burned area, fire intensity, number and size of individual fire scars. This study employed three different remote sensing datasets to evaluate the spatial heterogeneity within Cerrado's ecoregions over the last two decades, and developed a classification based on the evaluated parameters to complete the ecoregional map with information on regional fire characteristics. To the best of the authors' knowledge, this is the first study that provides a comprehensive regional analysis of fire behaviour in Cerrado, that is not limited to the use of a single and generalized fire estimate (such as burned area or fire intensity). It is also the first study to use an individual fire events dataset to study fire in Cerrado, providing crucial information that directly informs landscape and fire management.

It is equally important to understand why there is such a variety in fire behaviours and what drives these patterns. **Chapter 3** partly answers this question, by analysing the climatic influence in regional burned areas. Using temperature and precipitation from a state-of-the-art reanalysis dataset and burned areas, this study explores the several climate modes, including pre-conditioned and concurrent climate, that influence extreme fire seasons in Cerrado. The findings suggest that extreme fire seasons are influenced by climate during both the austral autumn and during the fire season months. Through the mediating effect of vegetation, early fire season burned areas are linked to pre-conditioned climate, whereas late fire season burned areas rely on concurrent climate conditions. This information is crucial for fire management, especially in the scope of IFM practices that encompass controlling fuel availability. Given ongoing and future climate change, the understanding of the climatic controls of burned areas is essential for adaptations strategies and policy making.

As a severely disturbed biome, where most ignitions are of human origin, it is not possible to dissociate fires with human activity in Cerrado. Home to Brazil's historical and cur-

rent agricultural frontiers, and part of the Arc of Deforestation, Cerrado's socio-economic context is key to understanding current fire patterns. **Chapter 4** explores these fire-climate-human dynamics on a regional level: firstly, by studying the relationship between fire, climate and land use in Cerrado's current agricultural frontier, MATOPIBA; and secondly, by evaluating fire-climate models in Cerrado's ecoregions against several anthropogenic variables, including land use, deforestation, and population. These analysis allowed a better understanding of how humans influence fire, and reflect on the spatial scales at which these drivers act. In line with previous work presented in this thesis, Section 4.2 proposes a novel approach based on individual fire events, that leverages the information on individual fire characteristics, to show that the fire-climate-human relationships are different based on fire size.

Finally, **Chapter 5** shifts the attention to the Pantanal wetlands. This chapter includes two studies: a case study of fire, climate and fire management practices in the largest RPPN in Brazil; and an assessment of the historical fire-heatwave connection, along with future projections, for the trinational Pantanal biome. These studies provided new information for the Pantanal, which is much needed for decision-making in the aftermath of the 2020 fire events. In particular, the case study of the RPPN Sesc Pantanal directly informed the management team of the reserve in regards to historical fire and climate patterns, which in turn assisted in shifting from a zero-fire policy to Integrated Fire Management. Section 5.2 found a very tight link between heatwave incidence and burned areas, and then informed on future pathways for heatwave occurrence under several climate change scenarios.

In summary, this thesis contributes to advance fire science in both the Cerrado and Pantanal biomes with various studies focused on different aspects of regional fire patterns and fire-climate-human relationships. In light of ongoing discussions and recent policies in Brazil, these findings may assist in drafting better and more regionally-tailored fire management practices.

## 6.1 Scientific outcomes

The analysis performed in the scope of this thesis resulted in several scientific publications. Most have been cited in the text, either in the beginning of each Chapter/Section or in

#### Section 1.4.

Nonetheless, not all publications that are a direct result of this Doctoral thesis are fully transcribed in the text, due to either repetition or lack of consistency with the thesis structure. In this case is a book chapter that includes a literature review on fire activity and its drivers in Cerrado, along with novel results on historical trends of wildfires and its hypothesized environmental and anthropogenic drivers (Silva et al., 2024a), and my contribution to the UNEP report (UNEP, 2022). These scientific outcomes are shown in full in Appendix A and B, respectively.

Below is a list of all scientific outcomes directly in the scope of this Doctoral thesis.

Three published peer-reviewed scientific articles:

- Silva, P. S., Nogueira, J., Rodrigues, J. A., Santos, F. L., Pereira, J. M., DaCamara, C. C., Daldegan, G. A., Pereira, A. A., Peres, L. F., Schmidt, I. B., and Libonati, R. (2021). Putting fire on the map of Brazilian savanna ecoregions. *Journal of Environmental Management*, 296:113098
- Silva, P. S., Geirinhas, J. L., Lapere, R., Laura, W., Cassain, D., Alegría, A., and Campbell, J. (2022). Heatwaves and fire in Pantanal: Historical and future perspectives from CORDEX-CORE. *Journal of Environmental Management*, 323:116193
- Silva, P. S., Rodrigues, J. A., Nogueira, J., Moura, L. C., Enout, A., Cuiabália, C., DaCamara, C. C., Pereira, A. A., and Libonati, R. (2024b). Joining forces to fight wildfires: Science and management in a protected area of Pantanal, Brazil. *Environmental Science & Policy*, 159:103818

One published peer-reviewed conference proceeding:

- Silva, P., Rodrigues, J., Santos, F., Pereira, A., Nogueira, J., DaCamara, C., and Libonati, R. (2020). Drivers Of Burned Area Patterns In Cerrado: The Case Of Matopiba Region. *2020 IEEE Latin American GRSS & ISPRS Remote Sensing Conference (LAGIRS)*

One published peer-reviewed report:

- UNEP (2022). Spreading like Wildfire: The Rising Threat of Extraordinary Landscape Fires. Technical report, United Nations Environment Programme (UNEP),

Nairobi

One published book chapter:

- Silva, P. S., Libonati, R., Schmidt, I. B., Nogueira, J., and DaCamara, C. C. (2024a). Climate Change and Fire: The Case of Cerrado, the Brazilian Savanna. In Mishra, M., de Lucena, A. J., and Maharaj, B., editors, *Climate Change and Regional Socio-Economic Systems in the Global South*, chapter 6, pages 87–105. Springer Nature Singapore, 1st edition

And several abstracts in conferences, including:

- EGU General Assembly 2020, 2021 and 2022
- AGU Fall Meeting 2020
- 2020 IEEE Latin American GRSS & ISPRS Remote Sensing Conference (LAGIRS)
- Reunión Anual de la Unión Geofísica Mexicana de 2021 (RAUGM2021)
- 8<sup>th</sup> International Wildland Fire Conference 2023 (Wildfire)

Moreover, albeit not directly associated to this thesis and its goals, I contributed to several research outcomes that are related to fire activity in Brazilian savannas.

I participated in two peer-reviewed publications that investigated the influence of compound drought-heatwave events in fire activity over Brazilian biomes (shown in full in the Appendix C and D). These publications were published in *Environmental Research Letters* and the *Annals of the New York Academy of Sciences*, where I was third and second author (shared with two co-authors), respectively:

- Libonati, R., Geirinhas, J. L., Silva, P. S., dos Santos, D. M., Rodrigues, J. A., Russo, A., Peres, L. F., Narcizo, L., Gomes, M. E. R., Rodrigues, A. P., DaCamara, C. C., Pereira, J. M. C., and Trigo, R. M. (2022a). Drought–heatwave nexus in Brazil and related impacts on health and fires: A comprehensive review. *Annals of the New York Academy of Sciences*, 1517:44–62
- Libonati, R., Geirinhas, J. L., Silva, P. S., Russo, A., Rodrigues, J. A., Belém, L. B. C., Nogueira, J., Roque, F. O., DaCamara, C. C., Nunes, A. M. B., Marengo, J. A., and Trigo, R. M. (2022b). Assessing the role of compound drought and

heatwave events on unprecedented 2020 wildfires in the Pantanal. *Environmental Research Letters*, 17(1):015005

I also authored a book chapter regarding fire in the Anthropocene, where we review current literature on fire activity in South America and its link to anthropogenic activity and climate change, and further showcase novel results on historical fire occurrence and trends in fire danger over all countries of the sub-continent:

- Silva, P. S., Libonati, R., Marengo, J., Costa, M. C., Alves, L., and Schmidt, I. (in press). Fire in the Anthropocene. In Vânia Pivelo and Alessandra Tomaselli Fidelis, editor, *Fire in South American ecosystems*, chapter 13. Springer Nature

I was also on the organizing committee of two workshops promoted by LASA/UFRJ:

- "*Curso de capacitação em monitoramento de fogo por satélite no Cerrado*" (freely translated to English as "Workshop on remote sensed fire monitoring in Cerrado"): <https://cursolasa.com.br/2021>
- "*Curso de capacitação em monitoramento de fogo por satélite no Pantanal*" (freely translated to English as "Workshop on remote sensed fire monitoring in Pantanal"): <https://cursolasa.com.br/2022>

And contributed to two educational materials directed to the general public:

- Damasceno-Junior, G. A., Guerra, A., de Matos Martins Pereira, A., Berlinck, C. N., de Oliveira Roque, F., Ebert, A., Rocha, A. R., Nunes, A. V., Pott, A., Oliveira, B., da Cunha, C. N., Ribeiro, D. B., Bolzan, F. P., Bao, F., Fernandes, G. W., Anderson, L. O., Oliveira, M., Silva, P., Libonati, R., da Silva, R. H., and Santos, S. (2024). *Manejo Integrado do Fogo no Pantanal - Um roteiro para o fogo bom*
- Araújo, Y., de Oliveira Pismel, G., dos Reis, J. B. C., and Anderson, L. O. (2024). *É Fogo! Pantanal: guia de atividades*. Ed. dos Autores, São José dos Campos, SP

Moreover, I contributed to the development of an online course about fire in Pantanal, entitled "*Compreendendo o fogo no Pantanal através do monitoramento por satélite*" (freely translated to English as "Understanding fire in Pantanal through remote sensing"), a collaboration between LASA/UFRJ and Wetlands International Brazil. The course is to be announced during 2024.

Finally, outside of the scope of my current work, I also co-authored a paper on the influence of winter climate in vegetation productivity over the Northern Hemisphere. This paper is a result of the DAMOCLES Training School on Compound Events in 2022:

- Anand, M., Hamed, R., Linscheid, N., Silva, P. S., Andre, J., Zscheischler, J., Garry, F. K., and Bastos, A. (2024). Winter climate preconditioning of summer vegetation extremes in the Northern Hemisphere. *Environmental Research Letters*, 19:094045

# References

- Abatzoglou, J. T., Williams, A. P., and Barbero, R. (2019). Global Emergence of Anthropogenic Climate Change in Fire Weather Indices. *Geophysical Research Letters*, 46:326–336.
- Abram, N. J., Henley, B. J., Sen Gupta, A., Lippmann, T. J. R., Clarke, H., Dowdy, A. J., Sharples, J. J., Nolan, R. H., Zhang, T., Wooster, M. J., Wurtzel, J. B., Meissner, K. J., Pitman, A. J., Ukkola, A. M., Murphy, B. P., Tapper, N. J., and Boer, M. M. (2021). Connections of climate change and variability to large and extreme forest fires in southeast Australia. *Communications Earth & Environment*, 2(1):8.
- Abreu, R. C. R., Hoffmann, W. A., Vasconcelos, H. L., Pilon, N. A., Rossatto, D. R., and Durigan, G. (2017). The biodiversity cost of carbon sequestration in tropical savanna. *Science Advances*, 3.
- Aguilera, R., Corringham, T., Gershunov, A., and Benmarhnia, T. (2021). Wildfire smoke impacts respiratory health more than fine particles from other sources: observational evidence from Southern California. *Nature Communications*, 12:Not available.
- Aldersley, A., Murray, S. J., and Cornell, S. E. (2011). Global and regional analysis of climate and human drivers of wildfire. *Science of The Total Environment*, 409:3472–3481.
- Alencar, A., Shimbo, J. Z., Lenti, F., Marques, C. B., Zimbres, B., Rosa, M., Arruda, V., Castro, I., Ribeiro, J. F. M., Varela, V., Alencar, I., Piontekowski, V., Ribeiro, V., Bustamante, M. M. C., Sano, E. E., and Barroso, M. (2020). Mapping Three Decades of Changes in the Brazilian Savanna Native Vegetation Using Landsat Data Processed in the Google Earth Engine Platform. *Remote Sensing*, 12:924.

- Alencar, A. A. C., Arruda, V. L. S., da Silva, W. V., Conciani, D. E., Costa, D. P., Crusco, N., Duverger, S. G., Ferreira, N. C., Franca-Rocha, W., Hasenack, H., Martenexen, L. F. M., Piontekowski, V. J., Ribeiro, N. V., Rosa, E. R., Rosa, M. R., dos Santos, S. M. B., Shimbo, J. Z., and Vélez-Martin, E. (2022). Long-Term Landsat-Based Monthly Burned Area Dataset for the Brazilian Biomes Using Deep Learning. *Remote Sensing*, 14(11).
- Alho, C. (2008). Biodiversity of the Pantanal: response to seasonal flooding regime and to environmental degradation. *Brazilian Journal of Biology*, 68:957–966.
- Alho, C. J. R., Mamede, S. B., Benites, M., Andrade, B. S., and Sepúlveda, J. J. O. (2019). Threats to the biodiversity of the Brazilian Pantanal due to land use and occupation. *Ambiente & Sociedade*, 22:Not available.
- Alho, C. J. R. and Silva, J. S. V. (2012). Effects of Severe Floods and Droughts on Wildlife of the Pantanal Wetland (Brazil) — A Review. *Animals*, 2(4):591–610.
- Alvarado, S. T., Andela, N., Silva, T. S. F., and Archibald, S. (2020). Thresholds of fire response to moisture and fuel load differ between tropical savannas and grasslands across continents. *Global Ecology and Biogeography*, 29:331–344.
- Alvarado, S. T., Fornazari, T., Cóstola, A., Morellato, L. P. C., and Silva, T. S. F. (2017). Drivers of fire occurrence in a mountainous Brazilian cerrado savanna: Tracking long-term fire regimes using remote sensing. *Ecological Indicators*, 78:270–281.
- Anand, M., Hamed, R., Linscheid, N., Silva, P. S., Andre, J., Zscheischler, J., Garry, F. K., and Bastos, A. (2024). Winter climate preconditioning of summer vegetation extremes in the Northern Hemisphere. *Environmental Research Letters*, 19:094045.
- Andela, N., Morton, D. C., Giglio, L., Chen, Y., van der Werf, G. R., Kasibhatla, P. S., DeFries, R. S., Collatz, G. J., Hantson, S., Kloster, S., Bachelet, D., Forrest, M., Lasslop, G., Li, F., Mangeon, S., Melton, J. R., Yue, C., and Randerson, J. T. (2017). A human-driven decline in global burned area. *Science*, 356:1356–1362.
- Andela, N., Morton, D. C., Giglio, L., Paugam, R., Chen, Y., Hantson, S., van der Werf, G. R., and Randerson, J. T. (2019). The global fire atlas of individual fire size, duration, speed and direction. *Earth System Science Data*, 11:529–552.



- Andela, N., Morton, D. C., Schroeder, W., Chen, Y., Brando, P. M., and Randerson, J. T. (2022). Tracking and classifying Amazon fire events in near real time. *Science Advances*, 8.
- Andreoli, R. V., de Oliveira, S. S., Kayano, M. T., Viegas, J., de Souza, R. A. F., and Candido, L. A. (2017). The influence of different El Niño types on the South American rainfall. *International Journal of Climatology*, 37:1374–1390.
- Arantes, A. E., Ferreira, L. G., and Coe, M. T. (2016). The seasonal carbon and water balances of the Cerrado environment of Brazil: Past, present, and future influences of land cover and land use. *ISPRS Journal of Photogrammetry and Remote Sensing*, 117:66–78.
- Araújo, Y., de Oliveira Pismel, G., dos Reis, J. B. C., and Anderson, L. O. (2024). *É Fogo! Pantanal: guia de atividades*. Ed. dos Autores, São José dos Campos, SP.
- Archibald, S. (2016). Managing the human component of fire regimes: lessons from Africa. *Philosophical Transactions of the Royal Society B: Biological Sciences*, 371:20150346.
- Archibald, S., Lehmann, C. E. R., Gómez-Dans, J. L., and Bradstock, R. A. (2013). Defining pyromes and global syndromes of fire regimes. *Proceedings of the National Academy of Sciences*, 110:6442–6447.
- Archibald, S. and Roy, D. P. (2009). Identifying individual fires from satellite-derived burned area data. *2009 IEEE International Geoscience and Remote Sensing Symposium*.
- Artés, T., Oom, D., de Rigo, D., Durrant, T. H., Maianti, P., Libertà, G., and San-Miguel-Ayanz, J. (2019). A global wildfire dataset for the analysis of fire regimes and fire behaviour. *Scientific Data*, 6.
- Assis, L. F. F. G., Ferreira, K. R., Vinhas, L., Maurano, L., Almeida, C., Carvalho, A., Rodrigues, J., Maciel, A., and Camargo, C. (2019). TerraBrasilis: A Spatial Data Analytics Infrastructure for Large-Scale Thematic Mapping. *ISPRS International Journal of Geo-Information*, 8:513.
- Baker, H. S., Millar, R. J., Karoly, D. J., Beyerle, U., Guillod, B. P., Mitchell, D., Shiogama, H., Sparrow, S., Woollings, T., and Allen, M. R. (2018). Higher CO2

- concentrations increase extreme event risk in a 1.5 °C world. *Nature Climate Change*, 8:604–608.
- Balch, J. K., Bradley, B. A., Abatzoglou, J. T., Nagy, R. C., Fusco, E. J., and Mahood, A. L. (2017). Human-started wildfires expand the fire niche across the United States. *Proceedings of the National Academy of Sciences*, 114:2946–2951.
- Balch, J. K., Denis, L. A. S., Mahood, A. L., Mietkiewicz, N. P., Williams, T. M., McGlinchy, J., and Cook, M. C. (2020). FIRED (Fire Events Delineation): An Open, Flexible Algorithm and Database of US Fire Events Derived from the MODIS Burned Area Product (2001–2019). *Remote Sensing*, 12:3498.
- Barbosa, M. L. F., Haddad, I., da Silva Nascimento, A. L., da Silva, G. M., da Veiga, R. M., Hoffmann, T. B., de Souza, A. R., Dalagnol, R., Streher, A. S., Pereira, F. R. S., e Cruz de Aragão, L. E. O., and Anderson, L. O. (2022). Compound impact of land use and extreme climate on the 2020 fire record of the Brazilian Pantanal. *Global Ecology and Biogeography*, 31:1960–1975.
- Barlow, J., Berenguer, E., Carmenta, R., and França, F. (2019). Clarifying Amazonia’s burning crisis. *Global Change Biology*, 26:319–321.
- Bastarrika, A., Chuvieco, E., and Martín, M. P. (2011). Mapping burned areas from Landsat TM/ETM+ data with a two-phase algorithm: Balancing omission and commission errors. *Remote Sensing of Environment*, 115:1003–1012.
- Bedia, J., Herrera, S., Gutiérrez, J. M., Benali, A., Brands, S., Mota, B., and Moreno, J. M. (2015). Global patterns in the sensitivity of burned area to fire-weather: Implications for climate change. *Agricultural and Forest Meteorology*, 214-215:369–379.
- Bergier, I. and Assine, M. L. (2016). *Dynamics of the Pantanal Wetland in South America*. Springer International Publishing.
- Bergier, I., Assine, M. L., McGlue, M. M., Alho, C. J., Silva, A., Guerreiro, R. L., and Carvalho, J. C. (2018). Amazon rainforest modulation of water security in the Pantanal wetland. *Science of The Total Environment*, 619-620:1116–1125.
- Berlinck, C. N., Lima, L. H. A., Pereira, A. M. M., Jr, E. A. R. C., Paula, R. C., Thomas,

- W. M., and Morato, R. G. (2022). The Pantanal is on fire and only a sustainable agenda can save the largest wetland in the world. *Brazilian Journal of Biology*, 82.
- Bevan, S. L., North, P. R. J., Grey, W. M. F., Los, S. O., and Plummer, S. E. (2009). Impact of atmospheric aerosol from biomass burning on Amazon dry-season drought. *Journal of Geophysical Research: Atmospheres*, 114.
- Bilbao, B., Steil, L., Urbieto, I., Anderson, L., Pinto, C., González, M., Millán, A., Falleiro, R., Morici, E., Ibarregaray, V., Pérez-Salicrup, D., Pereira, J., and Moreno, J. (2020). Wildfires. In J.M., M., Laguna-Defi, C., Barros, V., Buendía, E. C., Marengo, J., and Spring, U. O., editors, *Adaptation to Climate Change Risks in Ibero-American Countries — RIOCCADAPT Report*, pages 435–496. McGraw Hill, Madrid, Spain.
- Bird, R. B., Bird, D. W., and Coddling, B. F. (2016). People, El Niño southern oscillation and fire in Australia: fire regimes and climate controls in hummock grasslands. *Philosophical Transactions of the Royal Society B: Biological Sciences*, 371:20150343.
- Blunden, J. and Arndt, D. S. (2019). State of the Climate in 2018. *Bulletin of the American Meteorological Society*, 100:Si–S306.
- Blázquez, J. and Silvina, A. S. (2020). Multiscale precipitation variability and extremes over South America: analysis of future changes from a set of CORDEX regional climate model simulations. *Climate Dynamics*, 55:2089–2106.
- Bolfe, E. L., Victoria, D. C., Contini, E., Bayma-Silva, G., Spinelli-Araujo, L., and Gomes, D. (2017). MATOPIBA: análise do uso da terra e a produção agrícola. In *XVIII Simpósio Brasileiro de Sensoriamento Remoto - SBSR*, pages 1676–1684, Santos, Brazil.
- Bond, W. J., Woodward, F. I., and Midgley, G. F. (2005). The global distribution of ecosystems in a world without fire. *New Phytologist*, 165:525–538.
- Boschetti, L., Flasse, S. P., and Brivio, P. A. (2004). Analysis of the conflict between omission and commission in low spatial resolution dichotomic thematic products: The Pareto Boundary. *Remote Sensing of Environment*, 91:280–292.
- Boschetti, L., Roy, D. P., Giglio, L., Huang, H., Zubkova, M., and Humber, M. L. (2019).

- Global validation of the collection 6 MODIS burned area product. *Remote Sensing of Environment*, 235:111490.
- Bowman, D. M. J. S., Balch, J., Artaxo, P., Bond, W. J., Cochrane, M. A., D'Antonio, C. M., DeFries, R., Johnston, F. H., Keeley, J. E., Krawchuk, M. A., Kull, C. A., Mack, M., Moritz, M. A., Pyne, S., Roos, C. I., Scott, A. C., Sodhi, N. S., and Swetnam, T. W. (2011). The human dimension of fire regimes on Earth. *Journal of Biogeography*, 38:2223–2236.
- Bowman, D. M. J. S., Balch, J. K., Artaxo, P., Bond, W. J., Carlson, J. M., Cochrane, M. A., D'Antonio, C. M., DeFries, R. S., Doyle, J. C., Harrison, S. P., Johnston, F. H., Keeley, J. E., Krawchuk, M. A., Kull, C. A., Marston, J. B., Moritz, M. A., Prentice, I. C., Roos, C. I., Scott, A. C., Swetnam, T. W., van der Werf, G. R., and Pyne, S. J. (2009). Fire in the Earth System. *Science*, 324(5926):481–484.
- Bowman, D. M. J. S., Kolden, C. A., Abatzoglou, J. T., Johnston, F. H., van der Werf, G. R., and Flannigan, M. (2020). Vegetation fires in the Anthropocene. *Nature Reviews Earth & Environment*, 1:500–515.
- Bowman, D. M. J. S., Williamson, G. J., Abatzoglou, J. T., Kolden, C. A., Cochrane, M. A., and Smith, A. M. S. (2017). Human exposure and sensitivity to globally extreme wildfire events. *Nature Ecology & Evolution*, 1.
- Bowman, D. M. J. S., Zhang, Y., Walsh, A., and Williams, R. J. (2003). Experimental comparison of four remote sensing techniques to map tropical savanna fire-scars using Landsat-TM imagery. *International Journal of Wildland Fire*, 12:341.
- Brando, P. M., Balch, J. K., Nepstad, D. C., Morton, D. C., Putz, F. E., Coe, M. T., Silvério, D., Macedo, M. N., Davidson, E. A., Nóbrega, C. C., Alencar, A., and Soares-Filho, B. S. (2014). Abrupt increases in Amazonian tree mortality due to drought–fire interactions. *Proceedings of the National Academy of Sciences*, 111:6347–6352.
- Brandão, L., Antas, P. d. T., Oliveira, L. d., Pádua, M., Pereira, N. d. C., and Valutky, W. (2011). Plano de Manejo da Reserva Particular do Patrimônio Natural do SESC Pantanal (2nd edition). Technical report, Reserva Particular do Patrimônio Natural do SESC Pantanal.

- Buchhorn, M., Smets, B., Bertels, L., Roo, B. D., Lesiv, M., Tsendbazar, N.-E., Herold, M., and Fritz, S. (2020). Copernicus Global Land Service: Land Cover 100 M: Collection 3: Epoch 2015: Globe. <https://zenodo.org/records/3939038>.
- Burton, C., Kelley, D. I., Jones, C. D., Betts, R. A., Cardoso, M., and Anderson, L. (2021). South American fires and their impacts on ecosystems increase with continued emissions. *Climate Resilience and Sustainability*, 1.
- C3S (2017). ERA5: Fifth generation of ECMWF atmospheric reanalyses of the global climate. <https://cds.climate.copernicus.eu>.
- Campagnolo, M., Libonati, R., Rodrigues, J., and Pereira, J. (2021). A comprehensive characterization of MODIS daily burned area mapping accuracy across fire sizes in tropical savannas. *Remote Sensing of Environment*, 252:112115.
- Campagnolo, M., Oom, D., Padilla, M., and Pereira, J. (2019). A patch-based algorithm for global and daily burned area mapping. *Remote Sensing of Environment*, 232:111288.
- Cannon, A. J., Sobie, S. R., and Murdock, T. Q. (2015). Bias Correction of GCM Precipitation by Quantile Mapping: How Well Do Methods Preserve Changes in Quantiles and Extremes? *Journal of Climate*, 28:6938–6959.
- Casanueva, A., Herrera, S., Iturbide, M., Lange, S., Jury, M., Dosio, A., Maraun, D., and Gutiérrez, J. M. (2020). Testing bias adjustment methods for regional climate change applications under observational uncertainty and resolution mismatch. *Atmospheric Science Letters*, 21.
- Chen, Y., Morton, D. C., Jin, Y., Collatz, G. J., Kasibhatla, P. S., van der Werf, G. R., DeFries, R. S., and Randerson, J. T. (2013). Long-term trends and interannual variability of forest, savanna and agricultural fires in South America. *Carbon Management*, 4:617–638.
- Chuvieco, E., Giglio, L., and Justice, C. (2008). Global characterization of fire activity: toward defining fire regimes from Earth observation data. *Global Change Biology*, 14:1488–1502.
- Chuvieco, E., Pettinari, M. L., Koutsias, N., Forkel, M., Hantson, S., and Turco, M.

- (2021). Human and climate drivers of global biomass burning variability. *Science of The Total Environment*, 779:146361.
- Cinquini, L., Crichton, D., Mattmann, C., Harney, J., Shipman, G., Wang, F., Ananthakrishnan, R., Miller, N., Denvil, S., Morgan, M., Pobre, Z., Bell, G. M., Doutriaux, C., Drach, R., Williams, D., Kershaw, P., Pascoe, S., Gonzalez, E., Fiore, S., and Schweitzer, R. (2014). The Earth System Grid Federation: An open infrastructure for access to distributed geospatial data. *Future Generation Computer Systems*, 36:400–417. Special Section: Intelligent Big Data Processing Special Section: Behavior Data Security Issues in Network Information Propagation Special Section: Energy-efficiency in Large Distributed Computing Architectures Special Section: eScience Infrastructure and Applications.
- Clarke, H., Nolan, R. H., Dios, V. R. D., Bradstock, R., Griebel, A., Khanal, S., and Boer, M. M. (2022). Forest fire threatens global carbon sinks and population centres under rising atmospheric water demand. *Nature Communications*, 13.
- Cochrane, M. A. and Barber, C. P. (2009). Climate change, human land use and future fires in the Amazon. *Global Change Biology*, 15:601–612.
- Colli, G. R., Vieira, C. R., and Dianese, J. C. (2020). Biodiversity and conservation of the Cerrado: recent advances and old challenges. *Biodiversity and Conservation*, 29:1465–1475.
- Colman, C., Oliveira, P., Almagro, A., Soares-Filho, B., and Rodrigues, D. (2019). Effects of Climate and Land-Cover Changes on Soil Erosion in Brazilian Pantanal. *Sustainability*, 11:7053.
- Conciani, D. E., dos Santos, L. P., Silva, T. S. F., Durigan, G., and Alvarado, S. T. (2021). Human-climate interactions shape fire regimes in the Cerrado of São Paulo state, Brazil. *Journal for Nature Conservation*, 61:126006.
- Copernicus Climate Change Service, C. D. S. (2019). Fire danger indices historical data from the Copernicus Emergency Management Service. Accessed: 01-05-2024.
- Coppola, E., Raffaele, F., Giorgi, F., Giuliani, G., Xuejie, G., Ciarlo, J. M., Sines, T. R., Torres-Alavez, J. A., Das, S., di Sante, F., Pichelli, E., Glazer, R., Müller, S. K., Abba Omar, S., Ashfaq, M., Bukovsky, M., Im, E.-S., Jacob, D., Teichmann, C.,

- Remedio, A., Remke, T., Kriegsmann, A., Bülow, K., Weber, T., Buntemeyer, L., Sieck, K., and Rechid, D. (2021). Climate hazard indices projections based on CORDEX-CORE, CMIP5 and CMIP6 ensemble. *Climate Dynamics*, 57(5):1293–1383.
- Coronato, T., Carril, A. F., Zaninelli, P. G., Giles, J., Ruscica, R., Falco, M., Sörensson, A. A., Fita, L., Li, L. Z. X., and Menéndez, C. G. (2020). The impact of soil moisture–atmosphere coupling on daily maximum surface temperatures in Southeastern South America. *Climate Dynamics*, 55:2543–2556.
- Correa, D. B., Alcântara, E., Libonati, R., Massi, K. G., and Park, E. (2022). Increased burned area in the Pantanal over the past two decades. *Science of The Total Environment*, 835:155386.
- Coutinho, L. M. (1990). Fire in the Ecology of the Brazilian Cerrado. *Ecological Studies, Fire in the Tropical Biota*, pages 82–105.
- Cox, P. M., Harris, P. P., Huntingford, C., Betts, R. A., Collins, M., Jones, C. D., Jupp, T. E., Marengo, J. A., and Nobre, C. A. (2008). Increasing risk of Amazonian drought due to decreasing aerosol pollution. *Nature*, 453:212–215.
- Crawshaw, D., Oliveira, G., Cordeiro, J., Kindel, Trierveiler, F., and Oliveira, L. (2020). Relatório Parcial Ações Emergenciais Pós-fogo RPPN Sesc Pantanal Parte I. Technical report, Reserva Particular do Patrimônio Natural do SESC Pantanal.
- Cunha, A. P. M. A., Zeri, M., Leal, K. D., Costa, L., Cuartas, L. A., Marengo, J. A., Tomasella, J., Vieira, R. M., Barbosa, A. A., Cunningham, C., Garcia, J. V. C., Broedel, E., Alvalá, R., and Ribeiro-Neto, G. (2019). Extreme Drought Events over Brazil from 2011 to 2019. *Atmosphere*, 10:642.
- Cunha, C. N. d., Bergier, I., Tomas, Santos, Sartori, Â. L. B., Pott, A., de Arruda, E. C., da Silva Garcia, A., Nicola, R. D., and Junk, W. J. (2021). Hydrology and Vegetation Base for Classification of Macrohabitats of the Brazilian Pantanal for Policy-Making and Management. In Damasceno-Junior, G. A. and Pott, A., editors, *Flora and Vegetation of the Pantanal Wetland*, pages 365–391. Springer International Publishing, Cham.
- da Gama Viganó, H. H., de Souza, C. C., Neto, J. F. R., Cristaldo, M. F., and de Jesus,

- L. (2018). Previsão e Modelagem das Ocorrências de Incêndios no Pantanal. *Revista Brasileira de Meteorologia*, 33:306–316.
- da Rosa, L., Fernandes, V. B., Simiqueli, R. R., Bueno, A. P., and Reydon, B. (2016). Aspectos históricos da ocupação em Mato Grosso. In *Coletânea do II Seminário Internacional Governança de Terras e Desenvolvimento Econômico*, Campinas.
- da Silva Junior, C. A., Teodoro, P. E., Delgado, R. C., Teodoro, L. P. R., Lima, M., de Andréa Pantaleão, A., Baio, F. H. R., de Azevedo, G. B., de Oliveira Sousa Azevedo, G. T., Capristo-Silva, G. F., Arvor, D., and Facco, C. U. (2020). Persistent fire foci in all biomes undermine the Paris Agreement in Brazil. *Scientific Reports*, 10.
- Daldegan, G., Carvalho, O. D., Guimarães, R., Gomes, R., Ribeiro, F., and McManus, C. (2014). Spatial Patterns of Fire Recurrence Using Remote Sensing and GIS in the Brazilian Savanna: Serra do Tombador Nature Reserve, Brazil. *Remote Sensing*, 6:9873–9894.
- Daldegan, G. A., Roberts, D. A., and de Figueiredo Ribeiro, F. (2019). Spectral mixture analysis in Google Earth Engine to model and delineate fire scars over a large extent and a long time-series in a rainforest-savanna transition zone. *Remote Sensing of Environment*, 232:111340.
- Damasceno-Junior, G. (2021). Lessons to be Learned from the Wildfire Catastrophe of 2020 in the Pantanal Wetland. *Wetland Science & Practice*, 38:107–115.
- Damasceno-Junior, G. A., Guerra, A., de Matos Martins Pereira, A., Berlinck, C. N., de Oliveira Roque, F., Ebert, A., Rocha, A. R., Nunes, A. V., Pott, A., Oliveira, B., da Cunha, C. N., Ribeiro, D. B., Bolzan, F. P., Bao, F., Fernandes, G. W., Anderson, L. O., Oliveira, M., Silva, P., Libonati, R., da Silva, R. H., and Santos, S. (2024). *Manejo Integrado do Fogo no Pantanal - Um roteiro para o fogo bom*.
- de Andrade, A. S. R., Ramos, R. M., Sano, E. E., Libonati, R., Santos, F. L. M., Rodrigues, J. A., Giongo, M., da Franca, R. R., and de Paula Laranja, R. E. (2021). Implementation of Fire Policies in Brazil: An Assessment of Fire Dynamics in Brazilian Savanna. *Sustainability*, 13:11532.
- de Andrade, C. F., Delgado, R. C., Barbosa, M. L. F., Teodoro, P. E., da Silva Junior,



- C. A., Wanderley, H. S., and Capristo-Silva, G. F. (2020). Fire regime in Southern Brazil driven by atmospheric variation and vegetation cover. *Agricultural and Forest Meteorology*, 295:108194.
- de Aplicações de Satélites Ambientais do Departamento de Meteorologia da UFRJ, L. (2024). ALARMES. <https://alarmes.lasa.ufrj.br/>. Accessed: 2024-04-15.
- de Araújo, F. M., Ferreira, L. G., and Arantes, A. E. (2012). Distribution Patterns of Burned Areas in the Brazilian Biomes: An Analysis Based on Satellite Data for the 2002–2010 Period. *Remote Sensing*, 4:1929–1946.
- de Araújo, M. L. S., Sano, E. E., Édson Luis Bolfe, Santos, J. R. N., dos Santos, J. S., and Silva, F. B. (2019). Spatiotemporal dynamics of soybean crop in the Matopiba region, Brazil (1990–2015). *Land Use Policy*, 80:57–67.
- de Arruda, F. V., de Sousa, D. G., Teresa, F. B., do Prado, V. H. M., da Cunha, H. F., and Izzo, T. J. (2018). Trends and gaps of the scientific literature about the effects of fire on Brazilian Cerrado. *Biota Neotropica*, 18.
- de Azevedo, G. B., Rezende, A. V., de Oliveira Sousa Azevedo, G. T., Miguel, E. P., de Gois Aquino, F., Bruzinga, J. S. C., de Oliveira, L. S. C., Pereira, R. S., and Teodoro, P. E. (2020). Woody biomass accumulation in a Cerrado of Central Brazil monitored for 27 years after the implementation of silvicultural systems. *Forest Ecology and Management*, 455:117718.
- de Barros Soares, D., Lee, H., Loikith, P. C., Barkhordarian, A., and Mechoso, C. R. (2017). Can significant trends be detected in surface air temperature and precipitation over South America in recent decades? *International Journal of Climatology*, 37:1483–1493.
- de L. Dantas, V., Batalha, M. A., and Pausas, J. G. (2013). Fire drives functional thresholds on the savanna–forest transition. *Ecology*, 94:2454–2463.
- de Miranda, E. E., Magalhães, L. A., and de. Carvalho, C. A. (2014). Proposta de delimitação territorial do MATOPIBA. Technical report, Grupo de Inteligência Territorial Estratégica (GITE) - Embrapa.
- de Moraes Falleiro, R., Santana, M. T., and Berni, C. R. (2016). As contribuições

- do Manejo Integrado do Fogo para o controle dos incêndios florestais nas Terras Indígenas do Brasil. *Biodiversidade Brasileira - BioBrasil*, 6(2):88–105.
- de Oliveira, M. T., Damasceno-Junior, G. A., Pott, A., Filho, A. C. P., Suarez, Y. R., and Parolin, P. (2014). Regeneration of riparian forests of the Brazilian Pantanal under flood and fire influence. *Forest Ecology and Management*, 331:256–263.
- de Oliveira, S. N., de Carvalho Júnior, O. A., Gomes, R. A. T., Guimarães, R. F., and McManus, C. M. (2017). Landscape-fragmentation change due to recent agricultural expansion in the Brazilian Savanna, Western Bahia, Brazil. *Regional Environmental Change*, 17:411–423.
- de Oliveira Aparecido, L. E., Lorençone, P. A., Lorençone, J. A., de Meneses, K. C., and da Silva Cabral de Moraes, J. R. (2021). Climate changes and their influences in water balance of Pantanal biome. *Theoretical and Applied Climatology*, 143:659–674.
- de Oliveira-Júnior, J. F., Mendes, D., Filho, W. L. F. C., da Silva Junior, C. A., de Gois, G., da Rosa Ferraz Jardim, A. M., da Silva, M. V., Lyra, G. B., Teodoro, P. E., Pimentel, L. C. G., Lima, M., de Barros Santiago, D., Rogério, J. P., and Marinho, A. A. R. (2021). Fire foci in South America: Impact and causes, fire hazard and future scenarios. *Journal of South American Earth Sciences*, 112:103623.
- de Souza Miranda, C., Filho, A. C. P., and Pott, A. (2018). Changes in vegetation cover of the Pantanal wetland detected by Vegetation Index: a strategy for conservation. *Biota Neotropica*, 18.
- de Sá Arruda, W., Oldeland, J., Filho, A. C. P., Pott, A., Cunha, N. L., Ishii, I. H., and Damasceno-Junior, G. A. (2016). Inundation and Fire Shape the Structure of Riparian Forests in the Pantanal, Brazil. *PLOS ONE*, 11:e0156825.
- Deb, P., Moradkhani, H., Abbaszadeh, P., Kiem, A. S., Engström, J., Keellings, D., and Sharma, A. (2020). Causes of the Widespread 2019–2020 Australian Bushfire Season. *Earth's Future*, 8:Not available.
- Dionizio, E. A., Costa, M. H., de Almeida Castanho, A. D., Pires, G. F., Marimon, B. S., Marimon-Junior, B. H., Lenza, E., Pimenta, F. M., Yang, X., and Jain, A. K. (2018). Influence of climate variability, fire and phosphorus limitation on vegetation structure and dynamics of the Amazon–Cerrado border. *Biogeosciences*, 15:919–936.

- do Couto de Miranda, S., Bustamante, M., Palace, M., Hagen, S., Keller, M., and Ferreira, L. G. (2014). Regional Variations in Biomass Distribution in Brazilian Savanna Woodland. *Biotropica*, 46:125–138.
- Donat, M. G., Pitman, A. J., and Seneviratne, S. I. (2017). Regional warming of hot extremes accelerated by surface energy fluxes. *Geophysical Research Letters*, 44:7011–7019.
- dos Santos, A. C., da Rocha Montenegro, S., Ferreira, M. C., Barradas, A. C. S., and Schmidt, I. B. (2021). Managing fires in a changing world: Fuel and weather determine fire behavior and safety in the neotropical savannas. *Journal of Environmental Management*, 289:112508.
- Dosio, A. (2016). Projection of temperature and heat waves for Africa with an ensemble of CORDEX Regional Climate Models. *Climate Dynamics*, 49:493–519.
- Durigan, G. (2020). Zero-fire: Not possible nor desirable in the Cerrado of Brazil. *Flora*, 268:151612.
- Durigan, G. and Ratter, J. A. (2016). The need for a consistent fire policy for Cerrado conservation. *Journal of Applied Ecology*, 53:11–15.
- Dwyer, J. and Schmidt, G. (2006). Earth Science Satellite Remote Sensing. In Qu, J., Gao, W., Murphy, M. K. R., and Salomonson, V., editors, *The MODIS Reprojection Tool*, pages 162–177. Springer, Berlin, Heidelberg.
- ECMWF (2024). ERA5: How to calculate wind speed and wind direction from u and v components of the wind? <https://confluence.ecmwf.int/pages/viewpage.action?pageId=133262398>. Accessed: 2024-04-06.
- Eloy, L., Schmidt, I. B., Borges, S. L., Ferreira, M. C., and dos Santos, T. A. (2019). Seasonal fire management by traditional cattle ranchers prevents the spread of wildfire in the Brazilian Cerrado. *Ambio*, 48:890–899.
- Enayati, M., Bozorg-Haddad, O., Bazrafshan, J., Hejabi, S., and Chu, X. (2021). Bias correction capabilities of quantile mapping methods for rainfall and temperature variables. *Journal of Water and Climate Change*, 12:401–419.
- Falco, M., Carril, A. F., Menéndez, C. G., Zaninelli, P. G., and Li, L. Z. X. (2019).

- Assessment of CORDEX simulations over South America: added value on seasonal climatology and resolution considerations. *Climate Dynamics*, 52:4771–4786.
- Feron, S., Cordero, R. R., Damiani, A., Llanillo, P. J., Jorquera, J., Sepulveda, E., Asencio, V., Laroze, D., Labbe, F., Carrasco, J., and Torres, G. (2019). Observations and Projections of Heat Waves in South America. *Scientific Reports*, 9.
- Ferreira, G. B., Collen, B., Newbold, T., Oliveira, M. J. R., Pinheiro, M. S., de Pinho, F. F., Rowcliffe, M., and Carbone, C. (2020). Strict protected areas are essential for the conservation of larger and threatened mammals in a priority region of the Brazilian Cerrado. *Biological Conservation*, 251:108762.
- Fidelis, A. and Blanco, C. (2014). Does fire induce flowering in Brazilian subtropical grasslands? *Applied Vegetation Science*, 17:690–699.
- Fidelis, A., Zironi, H. L., Rossatto, D. R., and Zanzarini, V. (2022). Fire stimulates grass flowering in the Cerrado independent of season. *Journal of Vegetation Science*, 33.
- Field, R. D., van der Werf, G. R., Fanin, T., Fetzer, E. J., Fuller, R., Jethva, H., Levy, R., Livesey, N. J., Luo, M., Torres, O., and Worden, H. M. (2016). Indonesian fire activity and smoke pollution in 2015 show persistent nonlinear sensitivity to El Niño-induced drought. *Proceedings of the National Academy of Sciences*, 113:9204–9209.
- FIRMS (2020). Fire information for resource management System (FIRMS). <https://firms.modaps.eosdis.nasa.gov/>. Accessed: 2020-07-11.
- Flannigan, M., Cantin, A. S., de Groot, W. J., Wotton, M., Newbery, A., and Gowman, L. M. (2013). Global wildland fire season severity in the 21st century. *Forest Ecology and Management*, 294:54–61.
- Flores, B. M., de Sá Dechoum, M., Schmidt, I. B., Hirota, M., Abrahão, A., Verona, L., Pecoral, L. L. F., Cure, M. B., Giles, A. L., de Britto Costa, P., Pamplona, M. B., Mazzochini, G. G., Groenendijk, P., Minski, G. L., Wolfsdorf, G., Sampaio, A. B., Piccolo, F., Melo, L., de Lima, R. F., and Oliveira, R. S. (2020). Tropical riparian forests in danger from large savanna wildfires. *Journal of Applied Ecology*, 58(2):419–430.

- Ford, A. E. S., Harrison, S. P., Kountouris, Y., Millington, J. D. A., Mistry, J., Perkins, O., Rabin, S. S., Rein, G., Schreckenber, K., Smith, C., Smith, T. E. L., and Yadav, K. (2021). Modelling Human-Fire Interactions: Combining Alternative Perspectives and Approaches. *Frontiers in Environmental Science*, 9.
- Forkel, M., Dorigo, W., Lasslop, G., Chuvieco, E., Hantson, S., Heil, A., Teubner, I., Thonicke, K., and Harrison, S. P. (2019). Recent global and regional trends in burned area and their compensating environmental controls. *Environmental Research Communications*, 1:051005.
- Françoso, R. D., Brandão, R., Nogueira, C. C., Salmons, Y. B., Machado, R. B., and Colli, G. R. (2015). Habitat loss and the effectiveness of protected areas in the Cerrado Biodiversity Hotspot. *Natureza & Conservação*, 13:35–40.
- Ganteaume, A. and Syphard, A. D. (2018). Ignition Sources. *Encyclopedia of Wildfires and Wildland-Urban Interface (WUI) Fires*, pages 1–17.
- Garcia, J. R. and Filho, J. E. R. V. (2018). O papel da dimensão ambiental na ocupação do MATOPIBA. *Número 35, Confins*, 35.
- Garcia, L. C., Szabo, J. K., de Oliveira Roque, F., de Matos Martins Pereira, A., da Cunha, C. N., Damasceno-Júnior, G. A., Morato, R. G., Tomas, W. M., Libonati, R., and Ribeiro, D. B. (2021). Record-breaking wildfires in the world’s largest continuous tropical wetland: Integrative fire management is urgently needed for both biodiversity and humans. *Journal of Environmental Management*, 293:112870.
- Gasparri, A., Guo, Y., Hashizume, M., Lavigne, E., Zanobetti, A., et al. (2015). Mortality risk attributable to high and low ambient temperature: a multicountry observational study. *The Lancet*, 386(9991):369–375.
- Geirinhas, J. L., Russo, A., Libonati, R., Sousa, P. M., Miralles, D. G., and Trigo, R. M. (2021). Recent increasing frequency of compound summer drought and heatwaves in Southeast Brazil. *Environmental Research Letters*, 16:034036.
- Geirinhas, J. L., Russo, A. C., Libonati, R., Miralles, D. G., Ramos, A. M., Gimeno, L., and Trigo, R. M. (2023). Combined large-scale tropical and subtropical forcing on the severe 2019–2022 drought in South America. *npj Climate and Atmospheric Science*, 6.

- Geirinhas, J. L., Russo, A. C., Libonati, R., Miralles, D. G., Sousa, P. M., Wouters, H., and Trigo, R. M. (2022). The influence of soil dry-out on the record-breaking hot 2013/2014 summer in Southeast Brazil. *Scientific Reports*, 12.
- Giglio, L. (2007). Characterization of the tropical diurnal fire cycle using VIRS and MODIS observations. *Remote Sensing of Environment*, 108:407–421.
- Giglio, L., Boschetti, L., Roy, D. P., Humber, M. L., and Justice, C. O. (2018). The Collection 6 MODIS burned area mapping algorithm and product. *Remote Sensing of Environment*, 217:72–85.
- Giglio, L., Schroeder, W., and Justice, C. O. (2016). The collection 6 MODIS active fire detection algorithm and fire products. *Remote Sensing of Environment*, 178:31–41.
- Gilbert, R. O. (1987). *Statistical Methods for Environmental Pollution Monitoring*, chapter Sen’s nonparametric estimator of slope, pages 217–219. John Wiley & Sons.
- Gillson, L., Whitlock, C., and Humphrey, G. (2019). Resilience and fire management in the Anthropocene. *Ecology and Society*, 24.
- Giorgi, F., Coppola, E., Jacob, D., Teichmann, C., Omar, S. A., Ashfaq, M., Ban, N., Bülow, K., Bukovsky, M., Bunttemeyer, L., Cavazos, T., Ciarlo, J., da Rocha, R. P., Das, S., di Sante, F., Evans, J. P., Gao, X., Giuliani, G., Glazer, R. H., Hoffmann, P., Im, E.-S., Langendijk, G., Lierhammer, L., Llopart, M., Mueller, S., Luna-Nino, R., Nogherotto, R., Pichelli, E., Raffaele, F., Reboita, M., Rechid, D., Remedio, A., Remke, T., Sawadogo, W., Sieck, K., Torres-Alavez, J. A., and Weber, T. (2022). The CORDEX-CORE EXP-I Initiative: Description and Highlight Results from the Initial Analysis. *Bulletin of the American Meteorological Society*, 103(2):E293 – E310.
- Glikson, A. (2013). Fire and human evolution: The deep-time blueprints of the Anthropocene. *Anthropocene*, 3:89–92.
- Gomes, L., Miranda, H. S., and da Cunha Bustamante, M. M. (2018). How can we advance the knowledge on the behavior and effects of fire in the Cerrado biome? *Forest Ecology and Management*, 417:281–290.
- Gomes, L., Miranda, H. S., Silvério, D. V., and Bustamante, M. M. (2020). Effects and

- behaviour of experimental fires in grasslands, savannas, and forests of the Brazilian Cerrado. *Forest Ecology and Management*, 458:117804.
- Grimm, A. M. (2011). Interannual climate variability in South America: impacts on seasonal precipitation, extreme events, and possible effects of climate change. *Stochastic Environmental Research and Risk Assessment*, 25:537–554.
- Grégoire, J.-M., Eva, H. D., Belward, A. S., Palumbo, I., Simonetti, D., and Brink, A. (2013). Effect of land-cover change on Africa’s burnt area. *International Journal of Wildland Fire*, 22:107.
- Guerra, A., de Oliveira Roque, F., Garcia, L. C., Ochoa-Quintero, J. M., de Oliveira, P. T. S., Guariento, R. D., and Rosa, I. M. (2020). Drivers and projections of vegetation loss in the Pantanal and surrounding ecosystems. *Land Use Policy*, 91:104388.
- Guo, Y., Gasparrini, A., Li, S., Sera, F., Vicedo-Cabrera, A. M., de Sousa Zanotti Stagliorio Coelho, M., Saldiva, P. H. N., Lavigne, E., Tawatsupa, B., Punnasiri, K., Overcenco, A., Correa, P. M., Ortega, N. V., Kan, H., Osorio, S., Jaakkola, J. J. K., Rytty, N. R. I., Goodman, P. G., Zeka, A., Michelozzi, P., Scortichini, M., Hashizume, M., Honda, Y., Seposo, X., Kim, H., Tobias, A., Íñiguez, C., Forsberg, B., Åström, D. O., Guo, Y. L., Chen, B.-Y., Zanobetti, A., Schwartz, J., Dang, T. N., Van, D. D., Bell, M. L., Armstrong, B., Ebi, K. L., and Tong, S. (2018). Quantifying excess deaths related to heatwaves under climate change scenarios: A multicountry time series modelling study. *PLOS Medicine*, 15(7):1–17.
- Gutowski Jr., W. J., Giorgi, F., Timbal, B., Frigon, A., Jacob, D., Kang, H.-S., Raghavan, K., Lee, B., Lennard, C., Nikulin, G., O’Rourke, E., Rixen, M., Solman, S., Stephenson, T., and Tangang, F. (2016). WCRP COordinated Regional Downscaling EXperiment (CORDEX): a diagnostic MIP for CMIP6. *Geoscientific Model Development*, 9:4087–4095.
- Hamed, K. H. and Rao, A. R. (1998). A modified Mann-Kendall trend test for autocorrelated data. *Journal of Hydrology*, 204:182–196.
- Hantson, S., Andela, N., Goulden, M. L., and Randerson, J. T. (2022). Human-ignited fires result in more extreme fire behavior and ecosystem impacts. *Nature Communications*, 13.

- Hantson, S., Pueyo, S., and Chuvieco, E. (2015). Global fire size distribution is driven by human impact and climate. *Global Ecology and Biogeography*, 24:77–86.
- Hardesty, J., Myers, R., and Fulks, W. (2005). Fire ecosystems and people: a preliminary assessment of fire as a global conservation issue. *Fire Management*, 22(4):78–87.
- Hernandez, C., Keribin, C., Drobinski, P., and Turquety, S. (2015). Statistical modelling of wildfire size and intensity: a step toward meteorological forecasting of summer extreme fire risk. *Annales Geophysicae*, 33:1495–1506.
- Hersbach, H., Bell, B., Berrisford, P., Hirahara, Muñoz-Sabater, J., Nicolas, J., Peubey, C., Radu, R., Schepers, D., Simmons, A., Soci, C., Abdalla, S., Abellan, X., Balsamo, Biavati, G., Bidlot, J., Bonavita, M., De Chiara, G., Dahlgren, P., Dee, D., Diamantakis, M., Dragani, R., Flemming, J., Forbes, Geer, A., Haimberger, L., Healy, S., Hogan, R. J., Hólm, E., Janisková, M., Keeley, S., Laloyaux, P., Lopez, P., Lupu, C., Radnoti, G., de Rosnay, P., Rozum, I., Vamborg, F., Villaume, S., and Thépaut, J.-N. (2020). The ERA5 global reanalysis. *Quarterly Journal of the Royal Meteorological Society*, 146(730):1999–2049.
- Higuera, P. E. (2015). Taking time to consider the causes and consequences of large wildfires. *Proceedings of the National Academy of Sciences*, 112:13137–13138.
- Hoffmann, W. A., Geiger, E. L., Gotsch, S. G., Rossatto, D. R., Silva, L. C. R., Lau, O. L., Haridasan, M., and Franco, A. C. (2012a). Ecological thresholds at the savanna-forest boundary: how plant traits, resources and fire govern the distribution of tropical biomes. *Ecology Letters*, 15:759–768.
- Hoffmann, W. A., Jaconis, S. Y., Mckinley, K. L., Geiger, E. L., Gotsch, S. G., and Franco, A. C. (2012b). Fuels or microclimate? Understanding the drivers of fire feedbacks at savanna–forest boundaries. *Austral Ecology*, 37(6):634–643.
- Hofmann, G., Hasenack, H., Oliveira, L., and Cordeiro, L. (2010). O clima na Reserva Particular do Patrimônio Natural SESC Pantanal. Technical report, Serviço Social do Comércio.
- Hofmann, G. S., Cardoso, M. F., Alves, R. J. V., Weber, E. J., Barbosa, A. A., de Toledo, P. M., Pontual, F. B., de O. Salles, L., Hasenack, H., Cordeiro, J. L. P., Aquino, F. E.,



- and de Oliveira, L. F. B. (2021). The Brazilian Cerrado is becoming hotter and drier. *Global Change Biology*, 27:4060–4073.
- Ibama (2018). Relatório da compilação dos resgates do conhecimento tradicional sobre o uso do fogo em Terras Indígenas Brasileiras. Technical report, Instituto Brasileiro do Meio Ambiente e dos Recursos Naturais Renováveis (Ibama).
- IBGE (2019). Estimativas de População. Tabela 6579 - População residente estimada. <https://sidra.ibge.gov.br/tabela/6579>. Accessed: 01-05-2019.
- IMAFLOA (2018). Atlas da Agropecuária Brasileira. <http://atlasagropecuario.imaflora.org>. Accessed: 12-07-2020.
- INPE (2024). Programa de Monitoramento da Amazônia e demais Biomas. Desmatamento - Cerrado. Accessed: 01-05-2024.
- IPCC (2021). *Climate Change 2021: The Physical Science Basis. Contribution of Working Group I to the Sixth Assessment Report of the Intergovernmental Panel on Climate Change*. Cambridge University Press, Cambridge, UK and New York, NY, USA.
- IPCC (2022). *Climate Change 2022: Impacts, Adaptation and Vulnerability, Summary for Policymakers*. Cambridge University Press, Cambridge, UK and New York, USA.
- Iturbide, M., Casanueva, A., Bedia, J., Herrera, S., Milovac, J., and Gutiérrez, J. M. (2021). On the need of bias adjustment for more plausible climate change projections of extreme heat. *Atmospheric Science Letters*, 23.
- Ivory, S. J., McGlue, M. M., Spera, S., Silva, A., and Bergier, I. (2019). Vegetation, rainfall, and pulsing hydrology in the Pantanal, the world’s largest tropical wetland. *Environmental Research Letters*, 14:124017.
- Jain, P., Castellanos-Acuna, D., Coogan, S. C. P., Abatzoglou, J. T., and Flannigan, M. D. (2021). Observed increases in extreme fire weather driven by atmospheric humidity and temperature. *Nature Climate Change*, 12:63–70.
- Jimenez, J. C., Marengo, J. A., Alves, L. M., Sulca, J. C., Takahashi, K., Ferrett, S., and Collins, M. (2019). The role of ENSO flavours and TNA on recent droughts over Amazon forests and the Northeast Brazil region. *International Journal of Climatology*, 41:3761–3780.

- Jolly, W. M., Cochrane, M. A., Freeborn, P. H., Holden, Z. A., Brown, T. J., Williamson, G. J., and Bowman, D. M. J. S. (2015). [climate-induced variations in global wildfire danger from 1979 to 2013]. *Nature Communications*, 6:Not available.
- Jones, M. W., Abatzoglou, J. T., Veraverbeke, S., Andela, N., Lasslop, G., Forkel, M., Smith, A. J. P., Burton, C., Betts, R. A., van der Werf, G. R., Sitch, S., Canadell, J. G., Santín, C., Kolden, C., Doerr, S. H., and Quéré, C. L. (2022). Global and Regional Trends and Drivers of Fire Under Climate Change. *Reviews of Geophysics*, 60:Not available.
- Junk, W. J. (2013). Current state of knowledge regarding South America wetlands and their future under global climate change. *Aquatic Sciences*, 75:113–131.
- Junk, W. J., da Silva, C. J., da Cunha, C. N., and Wantzen, K. M. (2011). *The Pantanal: Ecology, Biodiversity and Sustainable Management of a Large Neotropical Seasonal Wetland*. Pensoft.
- Junk, W. J., Piedade, M. T. F., Lourival, R., Wittmann, F., Kandus, P., Lacerda, L. D., Bozelli, R. L., Esteves, F. A., da Cunha, C. N., Maltchik, L., Schöngart, J., Schaeffer-Novelli, Y., and Agostinho, A. A. (2014). Brazilian wetlands: their definition, delineation, and classification for research, sustainable management, and protection. *Aquatic Conservation: Marine and Freshwater Ecosystems*, 24:5–22.
- Kauffman, J. B. and Uhl, C. (1990). Interactions of Anthropogenic Activities, Fire, and Rain Forests in the Amazon Basin. *Ecological Studies, Fire in the Tropical Biota*, pages 117–134.
- Keeley, J. E. and Pausas, J. G. (2019). Distinguishing disturbance from perturbations in fire-prone ecosystems. *International Journal of Wildland Fire*, 28:282.
- Kelley, D. I., Bistinas, I., Whitley, R., Burton, C., Marthews, T. R., and Dong, N. (2019). How contemporary bioclimatic and human controls change global fire regimes. *Nature Climate Change*, 9:690–696.
- Kelly, L. T., Fletcher, M.-S., Menor, I. O., Pellegrini, A. F., Plumanns-Pouton, E. S., Pons, P., Williamson, G. J., and Bowman, D. M. (2023). Understanding Fire Regimes for a Better Anthropocene. *Annual Review of Environment and Resources*, 48:207–235.

- Kelly, L. T., Giljohann, K. M., Duane, A., Aquilué, N., Archibald, S., Batllori, E., Bennett, A. F., Buckland, S. T., Canelles, Q., Clarke, M. F., Fortin, M.-J., Hermoso, V., Herrando, S., Keane, R. E., Lake, F. K., McCarthy, M. A., Morán-Ordóñez, A., Parr, C. L., Pausas, J. G., Penman, T. D., Regos, A., Rumpff, L., Santos, J. L., Smith, A. L., Syphard, A. D., Tingley, M. W., and Brotons, L. (2020). Fire and biodiversity in the Anthropocene. *Science*, 370(6519):eabb0355.
- Kendall, M. (1975). *Rank correlation methods (4th ed)*. Griffin, London.
- King, A. D. (2019). The drivers of nonlinear local temperature change under global warming. *Environmental Research Letters*, 14:064005.
- Klink, C. A. and Machado, R. B. (2005). A conservação do Cerrado brasileiro. *Megadiversidade*, 1:147–155.
- Krawchuk, M. A. and Moritz, M. A. (2011). Constraints on global fire activity vary across a resource gradient. *Ecology*, 92:121–132.
- Krawchuk, M. A., Moritz, M. A., Parisien, M.-A., Dorn, J. V., and Hayhoe, K. (2009). Global Pyrogeography: the Current and Future Distribution of Wildfire. *PLoS ONE*, 4:e5102.
- Kruskal, W. H. and Wallis, W. A. (1952). Use of Ranks in One-Criterion Variance Analysis. *Journal of the American Statistical Association*, 47:583–621.
- Kumar, S., Getirana, A., Libonati, R., Hain, C., Mahanama, S., and Andela, N. (2022). Changes in land use enhance the sensitivity of tropical ecosystems to fire-climate extremes. *Scientific Reports*, 12.
- Lahsen, M., Bustamante, M. M. C., and Dalla-Nora, E. L. (2016). Undervaluing and Overexploiting the Brazilian Cerrado at Our Peril. *Environment: Science and Policy for Sustainable Development*, 58:4–15.
- Lapola, D. M., Martinelli, L. A., Peres, C. A., Ometto, J. P. H. B., Ferreira, M. E., Nobre, C. A., Aguiar, A. P. D., Bustamante, M. M. C., Cardoso, M. F., Costa, M. H., Joly, C. A., Leite, C. C., Moutinho, P., Sampaio, G., Strassburg, B. B. N., and Vieira, I. C. G. (2014). Pervasive transition of the Brazilian land-use system. *Nature Climate Change*, 4:27–35.

- Lapola, D. M., Oyama, M. D., and Nobre, C. A. (2009). Exploring the range of climate biome projections for tropical South America: The role of CO<sub>2</sub> fertilization and seasonality. *Global Biogeochemical Cycles*, 23.
- Lasslop, G. and Kloster, S. (2017). Human impact on wildfires varies between regions and with vegetation productivity. *Environmental Research Letters*, 12:115011.
- Laurent, P., Mouillot, F., Moreno, M. V., Yue, C., and Ciais, P. (2019). Varying relationships between fire radiative power and fire size at a global scale. *Biogeosciences*, 16:275–288.
- Laurent, P., Mouillot, F., Yue, C., Ciais, P., Moreno, M. V., and Nogueira, J. M. P. (2018). FRY, a global database of fire patch functional traits derived from spaceborne burned area products. *Scientific Data*, 5.
- Lawrence, M. G. (2005). The Relationship between Relative Humidity and the Dewpoint Temperature in Moist Air: A Simple Conversion and Applications. *Bulletin of the American Meteorological Society*, 86:225–234.
- Lehmann, C. E. R., Anderson, T. M., Sankaran, M., Higgins, S. I., Archibald, S., Hoffmann, W. A., Hanan, N. P., Williams, R. J., Fensham, R. J., Felfli, J., Hutley, L. B., Ratnam, J., Jose, J. S., Montes, R., Franklin, D., Russell-Smith, J., Ryan, C. M., Durigan, G., Hiernaux, P., Haidar, R., Bowman, D. M. J. S., and Bond, W. J. (2014). Savanna Vegetation-Fire-Climate Relationships Differ Among Continents. *Science*, 343(6170):548–552.
- Li, S., Rifai, S., Anderson, L. O., and Sparrow, S. (2021a). Identifying local-scale meteorological conditions favorable to large fires in Brazil. *Climate Resilience and Sustainability*, 1.
- Li, S., Sparrow, S. N., Otto, F. E. L., Rifai, S. W., Oliveras, I., Krikken, F., Anderson, L. O., Malhi, Y., and Wallom, D. (2021b). Anthropogenic climate change contribution to wildfire-prone weather conditions in the Cerrado and Arc of deforestation. *Environmental Research Letters*, 16:094051.
- Libonati, R., DaCamara, C., Setzer, A., Morelli, F., and Melchiori, A. (2015). An Algorithm for Burned Area Detection in the Brazilian Cerrado Using 4  $\mu$ m MODIS Imagery. *Remote Sensing*, 7:15782–15803.

- Libonati, R., DaCamara, C. C., Peres, L. F., de Carvalho, L. A. S., and Garcia, L. C. (2020). Rescue Brazil’s burning Pantanal wetlands. *Nature*, 588:217–219.
- Libonati, R., Geirinhas, J. L., Silva, P. S., dos Santos, D. M., Rodrigues, J. A., Russo, A., Peres, L. F., Narcizo, L., Gomes, M. E. R., Rodrigues, A. P., DaCamara, C. C., Pereira, J. M. C., and Trigo, R. M. (2022a). Drought–heatwave nexus in Brazil and related impacts on health and fires: A comprehensive review. *Annals of the New York Academy of Sciences*, 1517:44–62.
- Libonati, R., Geirinhas, J. L., Silva, P. S., Russo, A., Rodrigues, J. A., Belém, L. B. C., Nogueira, J., Roque, F. O., DaCamara, C. C., Nunes, A. M. B., Marengo, J. A., and Trigo, R. M. (2022b). Assessing the role of compound drought and heatwave events on unprecedented 2020 wildfires in the Pantanal. *Environmental Research Letters*, 17(1):015005.
- Libonati, R., Pereira, J. M. C., Camara, C. C. D., Peres, L. F., Oom, D., Rodrigues, J. A., Santos, F. L. M., Trigo, R. M., Gouveia, C. M. P., Machado-Silva, F., Enrich-Prast, A., and Silva, J. M. N. (2021). Twenty-first century droughts have not increasingly exacerbated fire season severity in the Brazilian Amazon. *Scientific Reports*, 11.
- Liu, Y., Stanturf, J., and Goodrick, S. (2010). Trends in global wildfire potential in a changing climate. *Forest Ecology and Management*, 259:685–697.
- Liu, Z., Eden, J. M., Dieppois, B., and Blackett, M. (2022). A global view of observed changes in fire weather extremes: uncertainties and attribution to climate change. *Climatic Change*, 173.
- Lizundia-Loiola, J., Otón, G., Ramo, R., and Chuvieco, E. (2020). A spatio-temporal active-fire clustering approach for global burned area mapping at 250 m from MODIS data. *Remote Sensing of Environment*, 236:111493.
- Llopart, M., Reboita, M. S., and da Rocha, R. P. (2020). Assessment of multi-model climate projections of water resources over South America CORDEX domain. *Climate Dynamics*, 54:99–116.
- Loarie, S. R., Lobell, D. B., Asner, G. P., Mu, Q., and Field, C. B. (2011). Direct impacts on local climate of sugar-cane expansion in Brazil. *Nature Climate Change*, 1:105–109.

- Lorensini, C. L., Victoria, D. C., Vicente, L. E., and Maçorano, R. P. (2015). Mapeamento e identificação da época de desmatamento das áreas de expansão da agricultura no MATOPIBA. In *XVII Simpósio Brasileiro de Sensoriamento Remoto - SBSR*.
- Luca, A. D., de Elía, R., Bador, M., and Argüeso, D. (2020). Contribution of mean climate to hot temperature extremes for present and future climates. *Weather and Climate Extremes*, 28:100255.
- Luo, R., Hui, D., Miao, N., Liang, C., and Wells, N. (2017). Global relationship of fire occurrence and fire intensity: A test of intermediate fire occurrence-intensity hypothesis. *Journal of Geophysical Research: Biogeosciences*, 122:1123–1136.
- Lázaro, W. L., Oliveira-Júnior, E. S., da Silva, C. J., Castrillon, S. K. I., and Muniz, C. C. (2020). Climate change reflected in one of the largest wetlands in the world: an overview of the Northern Pantanal water regime. *Acta Limnologica Brasiliensia*, 32.
- Machado-Silva, F., Libonati, R., de Lima, T. F. M., Peixoto, R. B., de Almeida França, J. R., de Avelar Figueiredo Mafra Magalhães, M., Santos, F. L. M., Rodrigues, J. A., and DaCamara, C. C. (2020). Drought and fires influence the respiratory diseases hospitalizations in the Amazon. *Ecological Indicators*, 109:105817.
- Magalhães, I. B., de Paula Pereira, A. S. A., Calijuri, M. L., do Carmo Alves, S., dos Santos, V. J., and Lorentz, J. F. (2020). Brazilian Cerrado and Soy moratorium: Effects on biome preservation and consequences on grain production. *Land Use Policy*, 99:105030.
- Mann, H. B. (1945). Nonparametric Tests Against Trend. *Econometrica*, 13:245.
- Manrique-Pineda, D. A., de Souza, E. B., Filho, A. C. P., Encina, C. C. C., and Damasceno-Junior, G. A. (2021). Fire, flood and monodominance of *Tabebuia aurea* in Pantanal. *Forest Ecology and Management*, 479:118599.
- MapBiomias (2019). Collection 3.1 of Brazil's Annual Land cover and Land Use Mapping. <https://mapbiomas.org>.
- MapBiomias (2020). Collection 5 of Brazilian Land Cover & Use Map Series. <https://mapbiomas.org/>. Accessed: 31-10-2020.

- MapBiomas (2023). MapBiomas Project - Collection 7 of the Annual Series of Land Use and Land Cover Maps of Brazil. <https://brasil.mapbiomas.org>. Accessed: 2023-02-03.
- Maraun, D. (2016). Bias Correcting Climate Change Simulations - a Critical Review. *Current Climate Change Reports*, 2:211–220.
- Maraun, D., Shepherd, T. G., Widmann, M., Zappa, G., Walton, D., Gutiérrez, J. M., Hagemann, S., Richter, I., Soares, P. M. M., Hall, A., and Mearns, L. O. (2017). Towards process-informed bias correction of climate change simulations. *Nature Climate Change*, 7:764–773.
- Marengo, J., Alves, L., and Torres, R. (2016). Regional climate change scenarios in the Brazilian Pantanal watershed. *Climate Research*, 68:201–213.
- Marengo, J. A., Alves, L. M., Soares, W. R., Rodriguez, D. A., Camargo, H., Riveros, M. P., and Pabló, A. D. (2013). Two Contrasting Severe Seasonal Extremes in Tropical South America in 2012: Flood in Amazonia and Drought in Northeast Brazil. *Journal of Climate*, 26:9137–9154.
- Marengo, J. A., Ambrizzi, T., Barreto, N., Cunha, A. P., Ramos, A. M., Skansi, M., Carpio, J. M., and Salinas, R. (2021a). The heat wave of October 2020 in central South America. *International Journal of Climatology*, 42:2281–2298.
- Marengo, J. A., Cunha, A. P., Cuartas, L. A., Leal, K. R. D., Broedel, E., Seluchi, M. E., Michelin, C. M., Baião, C. F. D. P., Angulo, E. C., Almeida, E. K., Kazmierczak, M. L., Mateus, N. P. A., Silva, R. C., and Bender, F. (2021b). Extreme Drought in the Brazilian Pantanal in 2019–2020: Characterization, Causes, and Impacts. *Frontiers in Water*, 3.
- Marengo, J. A., Jimenez, J. C., Espinoza, J.-C., Cunha, A. P., and Aragão, L. E. O. (2022). Increased climate pressure on the agricultural frontier in the Eastern Amazonia–Cerrado transition zone. *Scientific Reports*, 12.
- Marengo, J. A., Oliveira, G. S., and Alves, L. M. (2015). Climate Change Scenarios in the Pantanal. *The Handbook of Environmental Chemistry, Dynamics of the Pantanal Wetland in South America*, pages 227–238.

- Marengo, J. A., Tomasella, J., Alves, L. M., Soares, W. R., and Rodriguez, D. A. (2011). The drought of 2010 in the context of historical droughts in the Amazon region. *Geophysical Research Letters*, 38.
- Marengo, J. A., Tomasella, J., Soares, W. R., Alves, L. M., and Nobre, C. A. (2012). Extreme climatic events in the Amazon basin. *Theoretical and Applied Climatology*, 107:73–85.
- Marengo, J. A., Torres, R. R., and Alves, L. M. (2017). Drought in Northeast Brazil—past, present, and future. *Theoretical and Applied Climatology*, 129:1189–1200.
- Mariani, M., Holz, A., Veblen, T. T., Williamson, G., Fletcher, M., and Bowman, D. M. J. S. (2018). Climate Change Amplifications of Climate-Fire Teleconnections in the Southern Hemisphere. *Geophysical Research Letters*, 45:5071–5081.
- Marinho, K. F. S., de Melo Barbosa Andrade, L., Spyrides, M. H. C., e Silva, C. M. S., de Oliveira, C. P., Bezerra, B. G., and Mutti, P. R. (2020). Climate Profiles in Brazilian Microregions. *Atmosphere*, 11:1217.
- Marques, E. Q., Marimon-Junior, B. H., Marimon, B. S., Matricardi, E. A. T., Mews, H. A., and Colli, G. R. (2020). Redefining the Cerrado–Amazonia transition: implications for conservation. *Biodiversity and Conservation*, 29:1501–1517.
- Marques, J. F., Alves, M. B., Silveira, C. F., e Silva, A. A., Silva, T. A., dos Santos, V. J., and Calijuri, M. L. (2021). Fires dynamics in the Pantanal: Impacts of anthropogenic activities and climate change. *Journal of Environmental Management*, 299:113586.
- Martins, P. I., Belém, L. B. C., Szabo, J. K., Libonati, R., and Garcia, L. C. (2022). Prioritising areas for wildfire prevention and post-fire restoration in the Brazilian Pantanal. *Ecological Engineering*, 176:106517.
- Mataveli, G. A. V., Pereira, G., de Oliveira, G., Seixas, H. T., da S. Cardozo, F., Shimabukuro, Y. E., Kawakubo, F. S., and Brunsell, N. A. (2021). 2020 Pantanal’s widespread fire: short- and long-term implications for biodiversity and conservation. *Biodiversity and Conservation*, 30:3299–3303.
- Mataveli, G. A. V., Silva, M. E. S., Pereira, G., da Silva Cardozo, F., Kawakubo, F. S., Bertani, G., Costa, J. C., de Cássia Ramos, R., and da Silva, V. V. (2018). Satel-



- lite observations for describing fire patterns and climate-related fire drivers in the Brazilian savannas. *Natural Hazards and Earth System Sciences*, 18:125–144.
- Mazdiyasnı, O. and AghaKouchak, A. (2015). Substantial increase in concurrent droughts and heatwaves in the United States. *Proceedings of the National Academy of Sciences*, 112:11484–11489.
- McRae, R. H. D., Sharples, J. J., and Fromm, M. (2015). Linking local wildfire dynamics to pyroCb development. *Natural Hazards and Earth System Sciences*, 15:417–428.
- Menezes, L. S., de Oliveira, A. M., Santos, F. L., Russo, A., de Souza, R. A., Roque, F. O., and Libonati, R. (2022). Lightning patterns in the Pantanal: Untangling natural and anthropogenic-induced wildfires. *Science of The Total Environment*, 820:153021.
- Mingoti, R., Brasco, M. A., Holler, W. A., Filho, E. L., and Spadotto, C. A. (2014). Matopiba: caracterização das áreas com grande produção de culturas anuais. Technical report, Embrapa Gestão Territorial, Campinas.
- Mistry, J. (1998). Fire in the cerrado (savannas) of Brazil: an ecological review. *Progress in Physical Geography: Earth and Environment*, 22:425–448.
- Mistry, J., Schmidt, I. B., Eloy, L., and Bilbao, B. (2019). New perspectives in fire management in South American savannas: The importance of intercultural governance. *Ambio*, 48:172–179.
- MMA (2020). O Bioma Cerrado. <https://www.mma.gov.br/biomas/cerrado>. Accessed 19-10-2020.
- Molina, M. O., Sánchez, E., and Gutiérrez, C. (2020). Future heat waves over the Mediterranean from an Euro-CORDEX regional climate model ensemble. *Scientific Reports*, 10.
- Montgomery, D. C., Peck, E. A., and Vining, G. G. (2012). *Introduction to Linear Regression Analysis*. John Wiley & Sons.
- Montini, T. L., Jones, C., and Carvalho, L. M. V. (2019). The South American Low-Level Jet: A New Climatology, Variability, and Changes. *Journal of Geophysical Research: Atmospheres*, 124:1200–1218.
- Moritz, M. A., Morais, M. E., Summerell, L. A., Carlson, J. M., and Doyle, J. (2005).

- Wildfires, complexity, and highly optimized tolerance. *Proceedings of the National Academy of Sciences*, 102:17912–17917.
- Moritz, M. A., Parisien, M.-A., Batllori, E., Krawchuk, M. A., Dorn, J. V., Ganz, D. J., and Hayhoe, K. (2012). Climate change and disruptions to global fire activity. *Ecosphere*, 3:1–22.
- Morton, D. C., Page, Y. L., DeFries, R., Collatz, G. J., and Hurtt, G. C. (2013). Understorey fire frequency and the fate of burned forests in southern Amazonia. *Philosophical Transactions of the Royal Society B: Biological Sciences*, 368:20120163.
- Mouillot, F. and Field, C. B. (2005). Fire history and the global carbon budget: a  $1^\circ \times 1^\circ$  fire history reconstruction for the 20th century. *Global Change Biology*, 11:398–420.
- Moura, L. C., Scariot, A. O., Schmidt, I. B., Beatty, R., and Russell-Smith, J. (2019). The legacy of colonial fire management policies on traditional livelihoods and ecological sustainability in savannas: Impacts, consequences, new directions. *Journal of Environmental Management*, 232:600–606.
- Myers, N., Mittermeier, R. A., Mittermeier, C. G., da Fonseca, G. A. B., and Kent, J. (2000). Biodiversity hotspots for conservation priorities. *Nature*, 403:853–858.
- Myers, R. L. (2006). Living with Fire - Sustaining Ecosystems & Livelihoods Through Integrated Fire Management. Technical report, The Nature Conservancy.
- Nardoto, G. B., da Cunha Bustamante, M. M., Pinto, A. S., and Klink, C. A. (2006). Nutrient use efficiency at ecosystem and species level in savanna areas of Central Brazil and impacts of fire. *Journal of Tropical Ecology*, 22:191–201.
- Neves, C. C. R. P. (2015). *Vulnerabilidade da paisagem pantaneira: estudo de caso da Reserva Particular do Patrimônio Natural Sesc Pantanal e entorno*. PhD thesis, Instituto de Energia e Ambiente, University of São Paulo.
- Nielsen, D. M., Belém, A. L., Marton, E., and Cataldi, M. (2019). Dynamics-based regression models for the South Atlantic Convergence Zone. *Climate Dynamics*, 52:5527–5553.
- Nogueira, J., Rambal, S., Barbosa, J., and Mouillot, F. (2017a). Spatial Pattern of the

- Seasonal Drought/Burned Area Relationship across Brazilian Biomes: Sensitivity to Drought Metrics and Global Remote-Sensing Fire Products. *Climate*, 5:42.
- Nogueira, J., Ruffault, J., Chuvieco, E., and Mouillot, F. (2017b). Can We Go Beyond Burned Area in the Assessment of Global Remote Sensing Products with Fire Patch Metrics? *Remote Sensing*, 9:7.
- Oliveira, S. L. J., Maier, S. W., Pereira, J. M. C., and Russell-Smith, J. (2015). Seasonal differences in fire activity and intensity in tropical savannas of northern Australia using satellite measurements of fire radiative power. *International Journal of Wildland Fire*, 24:249.
- Oliveira, U., Soares-Filho, B., Bustamante, M., Gomes, L., Ometto, J. P., and Rajão, R. (2022). Determinants of Fire Impact in the Brazilian Biomes. *Frontiers in Forests and Global Change*, 5.
- Oliveira, U., Soares-Filho, B., de Souza Costa, W. L., Gomes, L., Bustamante, M., and Miranda, H. (2021). Modeling fuel loads dynamics and fire spread probability in the Brazilian Cerrado. *Forest Ecology and Management*, 482:118889.
- Olson, D. M., Dinerstein, E., Wikramanayake, E. D., Burgess, N. D., Powell, G. V. N., Underwood, E. C., D'amico, J. A., Itoua, I., Strand, H. E., Morrison, J. C., Loucks, C. J., Allnutt, T. F., Ricketts, T. H., Kura, Y., Lamoreux, J. F., Wettengel, W. W., Hedao, P., and Kassem, K. R. (2001). Terrestrial Ecoregions of the World: A New Map of Life on Earth: A new global map of terrestrial ecoregions provides an innovative tool for conserving biodiversity. *BioScience*, 51(11):933–938.
- Oom, D., Silva, P., Bistinas, I., and Pereira, J. (2016). Highlighting Biome-Specific Sensitivity of Fire Size Distributions to Time-Gap Parameter Using a New Algorithm for Fire Event Individuation. *Remote Sensing*, 8:663.
- Overbeck, G. E., Vélez-Martin, E., Scarano, F. R., Lewinsohn, T. M., Fonseca, C. R., Meyer, S. T., Müller, S. C., Ceotto, P., Dadalt, L., Durigan, G., Ganade, G., Gossner, M. M., Guadagnin, D. L., Lorenzen, K., Jacobi, C. M., Weisser, W. W., and Pillar, V. D. (2015). Conservation in Brazil needs to include non-forest ecosystems. *Diversity and Distributions*, 21:1455–1460.

- Oyama, M. D. and Nobre, C. A. (2003). A new climate-vegetation equilibrium state for Tropical South America. *Geophysical Research Letters*, 30.
- Page, Y. L., Morton, D., Hartin, C., Bond-Lamberty, B., Pereira, J. M. C., Hurtt, G., and Asrar, G. (2017). Synergy between land use and climate change increases future fire risk in Amazon forests. *Earth System Dynamics*, 8:1237–1246.
- Pausas, J. G. and Ribeiro, E. (2013). The global fire-productivity relationship. *Global Ecology and Biogeography*, 22:728–736.
- Pechony, O. and Shindell, D. T. (2010). Driving forces of global wildfires over the past millennium and the forthcoming century. *Proceedings of the National Academy of Sciences*, 107:19167–19170.
- Pereira, A., Pereira, J., Libonati, R., Oom, D., Setzer, A., Morelli, F., Machado-Silva, F., and Carvalho, L. D. (2017). Burned Area Mapping in the Brazilian Savanna Using a One-Class Support Vector Machine Trained by Active Fires. *Remote Sensing*, 9:1161.
- Pereira, A. A., Libonati, R., Rodrigues, J. A., Nogueira, J., Santos, F. L. M., Oom, D., Sanches, W., Alvarado, S. T., and Pereira, J. M. C. (2021). Multi-Sensor, Active Fire-Supervised, One-Class Burned Area Mapping in the Brazilian Savanna. *Remote Sensing*, 13:4005.
- Pereira, J. M. C. (2003). Remote sensing of burned areas in tropical savannas. *International Journal of Wildland Fire*, 12:259.
- Pereira, J. M. C., Oom, D., Silva, P. C., and Benali, A. (2022). Wild, tamed, and domesticated: Three fire macroregimes for global pyrogeography in the Anthropocene. *Ecological Applications*, 32.
- Pereira, J. M. C., Sá, A. C. L., Sousa, A. M. O., Silva, J. M. N., Santos, T. N., and Carreiras, J. M. B. (1999). Spectral characterisation and discrimination of burnt areas. *Remote Sensing of Large Wildfires*, Not available:123–138.
- Pereira, L. I. and Pauli, L. (2016). O processo de estrangeirização da terra e expansão do agronegócio na região do Matopiba. *Revista Campo-Território*, 11(23).
- Pereira, M., Calado, T., DaCamara, C., and Calheiros, T. (2013). Effects of regional climate change on rural fires in Portugal. *Climate Research*, 57:187–200.

- Perkins, S. E. and Alexander, L. V. (2013). On the Measurement of Heat Waves. *Journal of Climate*, 26:4500–4517.
- Perkins-Kirkpatrick, S. E. and Gibson, P. B. (2017). Changes in regional heatwave characteristics as a function of increasing global temperature. *Scientific Reports*, 7.
- Peterson, D. A., Campbell, J. R., Hyer, E. J., Fromm, M. D., Kablick, G. P., Cossuth, J. H., and DeLand, M. T. (2018). Wildfire-driven thunderstorms cause a volcano-like stratospheric injection of smoke. *npj Climate and Atmospheric Science*, 1.
- Pinto, M. M., DaCamara, C. C., Trigo, I. F., Trigo, R. M., and Turkman, K. F. (2018). Fire danger rating over Mediterranean Europe based on fire radiative power derived from Meteosat. *Natural Hazards and Earth System Sciences*, 18:515–529.
- Pinto, M. M., Trigo, R. M., Trigo, I. F., and DaCamara, C. C. (2021). A Practical Method for High-Resolution Burned Area Monitoring Using Sentinel-2 and VIIRS. *Remote Sensing*, 13:1608.
- Pitta, F. T. and Vega, G. C. (2017). Impacts of Agribusiness Expansion in the Matopiba Region: Communities and the Environment. Technical report, ActionAid, Rio de Janeiro.
- Pivello, V. R. (2011). The Use of Fire in the Cerrado and Amazonian Rainforests of Brazil: Past and Present. *Fire Ecology*, 7:24–39.
- Pivello, V. R., Vieira, I., Christianini, A. V., Ribeiro, D. B., da Silva Menezes, L., Berlinck, C. N., Melo, F. P., Marengo, J. A., Tornquist, C. G., Tomas, W. M., and Overbeck, G. E. (2021). Understanding Brazil’s catastrophic fires: Causes, consequences and policy needed to prevent future tragedies. *Perspectives in Ecology and Conservation*, 19:233–255.
- Pope, R. J., Arnold, S. R., Chipperfield, M. P., Reddington, C. L. S., Butt, E. W., Keslake, T. D., Feng, W., Latter, B. G., Kerridge, B. J., Siddans, R., Rizzo, L., Artaxo, P., Sadiq, M., and Tai, A. P. K. (2020). Substantial Increases in Eastern Amazon and Cerrado Biomass Burning-Sourced Tropospheric Ozone. *Geophysical Research Letters*, 47.

- Pott, A., Oliveira, A., Damasceno-Junior, G., and Silva, J. (2011). Plant diversity of the Pantanal wetland. *Brazilian Journal of Biology*, 71:265–273.
- Pott, A. and Pott, V. J. (2004). Features and conservation of the Brazilian Pantanal wetland. *Wetlands Ecology and Management*, 12:547–552.
- PPCDAm and PPCerrado (2020). Balanço de Execução 2018. Technical report, Plano de Ação para Prevenção e Controle do Desmatamento na Amazônia Legal (PPCDAm) and Plano de Ação para Prevenção e Controle do Desmatamento no Bioma Cerrado (PPCerrado).
- Pyne, S. J., Andrews, P. L., and Laven, R. D. (1996). *Introduction to Wildland Fire*. John Wiley and Sons, Inc, New York, NY, 2nd edition.
- Quilcaille, Y., Batibeniz, F., Ribeiro, A. F. S., Padrón, R. S., and Seneviratne, S. I. (2023). Fire weather index data under historical and shared socioeconomic pathway projections in the 6th phase of the Coupled Model Intercomparison Project from 1850 to 2100. *Earth System Science Data*, 15:2153–2177.
- Rabin, S. S., Melton, J. R., Lasslop, G., Bachelet, D., Forrest, M., Hantson, S., Kaplan, J. O., Li, F., Mangeon, S., Ward, D. S., Yue, C., Arora, V. K., Hickler, T., Kloster, S., Knorr, W., Nieradzick, L., Spessa, A., Folberth, G. A., Sheehan, Kelley, D. I., Prentice, I. C., Sitch, and Arneth, A. (2017). The Fire Modeling Intercomparison Project (FireMIP), phase 1: experimental and analytical protocols with detailed model descriptions. *Geoscientific Model Development*, 10(3):1175–1197.
- Ramo, R., Roteta, E., Bistinas, I., van Wees, D., Bastarrika, A., Chuvieco, E., and van der Werf, G. R. (2021). African burned area and fire carbon emissions are strongly impacted by small fires undetected by coarse resolution satellite data. *Proceedings of the National Academy of Sciences*, 118.
- Ramos, A. M., Russo, A., DaCamara, C. C., Nunes, S., Sousa, P., Soares, P., Lima, M. M., Hurduc, A., and Trigo, R. M. (2023). The compound event that triggered the destructive fires of October 2017 in Portugal. *iScience*, 26:106141.
- Ramos-Neto, M. B. and Pivello, V. R. (2000). Lightning Fires in a Brazilian Savanna National Park: Rethinking Management Strategies. *Environmental Management*, 26:675–684.

- Ramsar (2023). About the Convention on Wetlands. <https://www.ramsar.org/about-convention-wetlands>.
- Randerson, J. T., Chen, Y., van der Werf, G. R., Rogers, B. M., and Morton, D. C. (2012). Global burned area and biomass burning emissions from small fires. *Journal of Geophysical Research: Biogeosciences*, 117.
- Ratter, J. (1997). The Brazilian Cerrado Vegetation and Threats to its Biodiversity. *Annals of Botany*, 80:223–230.
- Reboita, M. S., Ambrizzi, T., Crespo, N. M., Dutra, L. M. M., de S. Ferreira, G. W., Rehbein, A., Drumond, A., da Rocha, R. P., and de Souza, C. A. (2021a). Impacts of teleconnection patterns on South America climate. *Annals of the New York Academy of Sciences*, 1504:116–153.
- Reboita, M. S., Kuki, C. A. C., Marrafon, V. H., de Souza, C. A., Ferreira, G. W. S., Teodoro, T., and Lima, J. W. M. (2021b). South America climate change revealed through climate indices projected by GCMs and Eta-RCM ensembles. *Climate Dynamics*, 58:459–485.
- Reddington, C. L., Butt, E. W., Ridley, D. A., Artaxo, P., Morgan, W. T., Coe, H., and Spracklen, D. V. (2015). Air quality and human health improvements from reductions in deforestation-related fire in Brazil. *Nature Geoscience*, 8:768–771.
- Rego, F. C., Morgan, P., Fernandes, P., and Hoffman, C. (2021). Integrated Fire Management. *Fire Science, Springer Textbooks in Earth Sciences, Geography and Environment*, Not available:509–597.
- Requia, W. J., Kill, E., Papatheodorou, S., Koutrakis, P., and Schwartz, J. D. (2021). Prenatal exposure to wildfire-related air pollution and birth defects in Brazil. *Journal of Exposure Science & Environmental Epidemiology*, 32:596–603.
- Riahi, K., Rao, S., Krey, V., Cho, C., Chirkov, V., Fischer, G., Kindermann, G., Nakicenovic, N., and Rafaj, P. (2011). RCP 8.5 - A scenario of comparatively high greenhouse gas emissions. *Climatic Change*, 109:33–57.
- Ribeiro, A. F. S., Brando, P. M., Santos, L., Rattis, L., Hirschi, M., Hauser, M., Seneviratne, S. I., and Zscheischler, J. (2022). A compound event-oriented framework to

- tropical fire risk assessment in a changing climate. *Environmental Research Letters*, 17:065015.
- Ribeiro, A. F. S., Santos, L., Randerson, J. T., Uribe, M. R., Alencar, A. A. C., Macedo, M. N., Morton, D. C., Zscheischler, J., Silvestrini, R. A., Rattis, L., Seneviratne, S. I., and Brando, P. M. (2024). The time since land-use transition drives changes in fire activity in the Amazon-Cerrado region. *Communications Earth & Environment*, 5.
- Ribeiro, D. and Pereira, A. M. (2023). Solving the problem of wildfires in the Pantanal Wetlands. *Perspectives in Ecology and Conservation*, 21:271–273.
- Ribeiro, J. F. and Walter, B. M. T. (1998). Fitofisionomias do bioma cerrado. In Sano, S. M. and de Almeida, S. P., editors, *Cerrado: ambiente e flora*, pages 89–166. Planaltina: EMBRAPA-CPAC.
- Ribeiro, J. F. and Walter, B. M. T. (2008). As principais fitofisionomias do bioma Cerrado. In Sano, S. M., de Almeida, S. P., and Ribeiro, J. F., editors, *Cerrado: ecologia e flora*, chapter 6, pages 153–212. Embrapa Cerrados/Embrapa Informação Tecnológica.
- Richardson, D., Black, A. S., Irving, D., Matear, R. J., Monselesan, D. P., Risbey, J. S., Squire, D. T., and Tozer, C. R. (2022). Global increase in wildfire potential from compound fire weather and drought. *npj Climate and Atmospheric Science*, 5.
- Rissi, M. N., Baeza, M. J., Gorgone-Barbosa, E., Zupo, T., and Fidelis, A. (2017). Does season affect fire behaviour in the Cerrado? *International Journal of Wildland Fire*, 26:427.
- Rodrigues, C. A., Zironi, H. L., and Fidelis, A. (2021). Fire frequency affects fire behavior in open savannas of the Cerrado. *Forest Ecology and Management*, 482:118850.
- Rodrigues, J. A., Libonati, R., Pereira, A. A., Nogueira, J. M., Santos, F. L., Peres, L. F., Santa Rosa, A., Schroeder, W., Pereira, J. M., Giglio, L., Trigo, I. F., and Setzer, A. W. (2019). How well do global burned area products represent fire patterns in the Brazilian Savannas biome? An accuracy assessment of the MCD64 collections. *International Journal of Applied Earth Observation and Geoinformation*, 78:318–331.
- Rosan, T. M., Aragão, L. E., Oliveras, I., Phillips, O. L., Malhi, Y., Gloor, E., and Wagner,



- F. H. (2019). Extensive 21st-Century Woody Encroachment in South America's Savanna. *Geophysical Research Letters*, 46:6594–6603.
- Rosan, T. M., Sitch, S., Mercado, L. M., Heinrich, V., Friedlingstein, P., and Aragão, L. E. O. C. (2022). Fragmentation-Driven Divergent Trends in Burned Area in Amazonia and Cerrado. *Frontiers in Forests and Global Change*, 5.
- Rosenfeld, D. (1999). TRMM observed first direct evidence of smoke from forest fires inhibiting rainfall. *Geophysical Research Letters*, 26:3105–3108.
- Ruffault, J., Curt, T., Moron, V., Trigo, R. M., Mouillot, F., Koutsias, N., Pimont, F., Martin-StPaul, N., Barbero, R., Dupuy, J.-L., Russo, A., and Belhadj-Khedher, C. (2020). Increased likelihood of heat-induced large wildfires in the Mediterranean Basin. *Scientific Reports*, 10.
- Russo, S., Dosio, A., Graversen, R. G., Sillmann, J., Carrao, H., Dunbar, M. B., Singleton, A., Montagna, P., Barbola, P., and Vogt, J. V. (2014). Magnitude of extreme heat waves in present climate and their projection in a warming world. *Journal of Geophysical Research: Atmospheres*, 119.
- Sano, E. E., Bettioli, G. M., de Souza Martins, E., Júnior, A. F. C., Vasconcelos, V., Édson Luis Bolfe, and de Castro Victoria, D. (2020). Características gerais da paisagem do Cerrado. In Bolfe, E. L., Sano, E. E., and Campos, S. K., editors, *Dinâmica agrícola no cerrado: análises e projeções*, chapter 1, pages 21–37. Embrapa, Brasília, DF.
- Sano, E. E., Rodrigues, A. A., Martins, E. S., Bettioli, G. M., Bustamante, M. M., Bezerra, A. S., Couto, A. F., Vasconcelos, V., Schüler, J., and Bolfe, E. L. (2019). Cerrado ecoregions: A spatial framework to assess and prioritize Brazilian savanna environmental diversity for conservation. *Journal of Environmental Management*, 232:818–828.
- Sano, E. E., Rosa, R., Brito, J. L. S., and Ferreira, L. G. (2010). Land cover mapping of the tropical savanna region in Brazil. *Environmental Monitoring and Assessment*, 166:113–124.
- Santana, N. C., de Carvalho Júnior, O. A., Gomes, R. A. T., and Guimarães, R. F. (2020). Comparison of Post-fire Patterns in Brazilian Savanna and Tropical Forest

- from Remote Sensing Time Series. *ISPRS International Journal of Geo-Information*, 9:659.
- Santos, F. L., Libonati, R., Peres, L. F., Pereira, A. A., Narcizo, L. C., Rodrigues, J. A., Oom, D., Pereira, J. M. C., Schroeder, W., and Setzer, A. W. (2020). Assessing VIIRS capabilities to improve burned area mapping over the Brazilian Cerrado. *International Journal of Remote Sensing*, 41:8300–8327.
- Santos, F. L., Nogueira, J., de Souza, R. A. F., Falleiro, R. M., Schmidt, I. B., and Libonati, R. (2021). Prescribed Burning Reduces Large, High-Intensity Wildfires and Emissions in the Brazilian Savanna. *Fire*, 4:56.
- Schmidt, I. B. and Eloy, L. (2020). Fire regime in the Brazilian Savanna: Recent changes, policy and management. *Flora*, 268:151613.
- Schmidt, I. B., Figueiredo, I. B., and Scariot, A. (2007). Ethnobotany and Effects of Harvesting on the Population Ecology of *Syngonanthus nitens* (Bong.) Ruhland (Eriocaulaceae), a NTFP from Jalapão Region, Central Brazil. *Economic Botany*, 61:73–85.
- Schmidt, I. B., Fonseca, C. B., Ferreira, M. C., and Sato, M. N. (2016). Implementação do programa piloto de manejo integrado do fogo em três unidades de conservação do Cerrado. *Biodiversidade Brasileira - BioBrasil*, 6(2).
- Schmidt, I. B., Moura, L. C., Ferreira, M. C., Eloy, L., Sampaio, A. B., Dias, P. A., and Berlinck, C. N. (2018). Fire management in the Brazilian savanna: First steps and the way forward. *Journal of Applied Ecology*, 55:2094–2101.
- Schroeder, M. J., Buck, C. C., and Buck, C. C. (1970). *Fire Weather: A Guide for Application of Meteorological Information to Forest Fire Control Operations*. U.S. Department of Agriculture, Forest Service.
- Schroeder, W., Csiszar, I., Giglio, L., and Schmidt, C. C. (2010). On the use of fire radiative power, area, and temperature estimates to characterize biomass burning via moderate to coarse spatial resolution remote sensing data in the Brazilian Amazon. *Journal of Geophysical Research: Atmospheres*, 115.
- Schulz, C., Whitney, B. S., , Rossetto, O. C., Neves, D. M., Crabb, L., de Oliveira, E. C.,

- Lima, P. L. T., Afzal, M., Laing, A. F., de Souza Fernandes, L. C., da Silva, C. A., Steinke, V. A., Steinke, E. T., and Saito, C. H. (2019). Physical, ecological and human dimensions of environmental change in Brazil's Pantanal wetland: Synthesis and research agenda. *Science of The Total Environment*, 687:1011–1027.
- Schumacher, V., Setzer, A., Saba, M. M., Naccarato, K. P., Mattos, E., and Justino, F. (2022). Characteristics of lightning-caused wildfires in central Brazil in relation to cloud-ground and dry lightning. *Agricultural and Forest Meteorology*, 312:108723.
- Segura-Garcia, C., Bauman, D., Arruda, V. L. S., Alencar, A. A. C., and Menor, I. O. (2024). Human land occupation regulates the effect of the climate on the burned area of the Brazilian Cerrado. *Communications Earth & Environment*, 5.
- Sen, P. K. (1968). Estimates of the Regression Coefficient Based on Kendall's Tau. *Journal of the American Statistical Association*, 63:1379–1389.
- Senande-Rivera, M., Insua-Costa, D., and Miguez-Macho, G. (2022). Spatial and temporal expansion of global wildland fire activity in response to climate change. *Nature Communications*, 13.
- Sesc (2023). Plano de Manejo Integrado do Fogo da RPPN Sesc Pantanal. Technical report, Serviço Social do Comércio (Sesc).
- Shlisky, A., Meyer, R., Waugh, J., and Blankenship, K. (2008). Fire, Nature, and Humans: Global Challenges for Conservation. *Fire Management Today*, 68(4):36–42.
- Shuman, J. K., Balch, J. K., Barnes, R. T., Higuera, P. E., Roos, C. I., Schwilk, D. W., Stavros, E. N., Banerjee, T., Bela, M. M., Bendix, J., Bertolino, S., Bililign, S., Bladon, K. D., Brando, P., Breidenthal, R. E., Buma, B., Calhoun, D., Carvalho, L. M. V., Cattau, M. E., Cawley, K. M., Chandra, S., Chipman, M. L., Cobian-Iñiguez, J., Conlisk, E., Coop, J. D., Cullen, A., Davis, K. T., Dayalu, A., De Sales, F., Dolman, M., Ellsworth, L. M., Franklin, S., Guiterman, C. H., Hamilton, M., Hanan, E. J., Hansen, W. D., Hantson, S., Harvey, B. J., Holz, A., Huang, T., Hurteau, M. D., Ilangakoon, N. T., Jennings, M., Jones, C., Klimaszewski-Patterson, A., Kobziar, L. N., Kominoski, J., Kosovic, B., Krawchuk, M. A., Laris, P., Leonard, J., Loria-Salazar, S. M., Lucash, M., Mahmoud, H., Margolis, E., Maxwell, T., McCarty, J. L., McWethy, D. B., Meyer, R. S., Miesel, J. R., Moser, W. K., Nagy, R. C., Niyogi, D.,

- Palmer, H. M., Pellegrini, A., Poulter, B., Robertson, K., Rocha, A. V., Sadegh, M., Santos, F., Scordo, F., Sexton, J. O., Sharma, A. S., Smith, A. M. S., Soja, A. J., Still, C., Swetnam, T., Syphard, A. D., Tingley, M. W., Tohidi, A., Trugman, A. T., Turetsky, M., Varner, J. M., Wang, Y., Whitman, T., Yelenik, S., and Zhang, X. (2022). Reimagine fire science for the anthropocene. *PNAS Nexus*, 1(3):pgac115.
- Siefert, C. A. C., Netto, N. D., Marangon, F. H. S., Schultz, G. B., dos Reis Silva, L. M., Fontenelle, T. H., and dos Santos, I. (2021). Avaliação de Séries de Velocidade do Vento de Produtos de Reanálises Climáticas para o Brasil. *Revista Brasileira de Meteorologia*, 36:689–701.
- Silva, J. M. C. D. and Bates, J. M. (2002). Biogeographic Patterns and Conservation in the South American Cerrado: A Tropical Savanna Hotspot: The Cerrado, which includes both forest and savanna habitats, is the second largest South American biome, and among the most threatened on the continent. *BioScience*, 52(3):225–234.
- Silva, P., Bastos, A., DaCamara, C. C., and Libonati, R. (2016). Future Projections of Fire Occurrence in Brazil Using EC-Earth Climate Model. *Revista Brasileira de Meteorologia*, 31:288–297.
- Silva, P., Rodrigues, J., Santos, F., Pereira, A., Nogueira, J., DaCamara, C., and Libonati, R. (2020). Drivers Of Burned Area Patterns In Cerrado: The Case Of Matopiba Region. *2020 IEEE Latin American GRSS & ISPRS Remote Sensing Conference (LAGIRS)*.
- Silva, P. S., Bastos, A., Libonati, R., Rodrigues, J. A., and DaCamara, C. C. (2019). Impacts of the 1.5 °C global warming target on future burned area in the Brazilian Cerrado. *Forest Ecology and Management*, 446:193–203.
- Silva, P. S., Geirinhas, J. L., Lapere, R., Laura, W., Cassain, D., Alegría, A., and Campbell, J. (2022). Heatwaves and fire in Pantanal: Historical and future perspectives from CORDEX-CORE. *Journal of Environmental Management*, 323:116193.
- Silva, P. S., Libonati, R., Marengo, J., Costa, M. C., Alves, L., and Schmidt, I. (in press). Fire in the Anthropocene. In Vânia Pivelo and Alessandra Tomaselli Fidelis, editor, *Fire in South American ecosystems*, chapter 13. Springer Nature.
- Silva, P. S., Libonati, R., Schmidt, I. B., Nogueira, J., and DaCamara, C. C. (2024a).

- Climate Change and Fire: The Case of Cerrado, the Brazilian Savanna. In Mishra, M., de Lucena, A. J., and Maharaj, B., editors, *Climate Change and Regional Socio-Economic Systems in the Global South*, chapter 6, pages 87–105. Springer Nature Singapore, 1st edition.
- Silva, P. S., Nogueira, J., Rodrigues, J. A., Santos, F. L., Pereira, J. M., DaCamara, C. C., Daldegan, G. A., Pereira, A. A., Peres, L. F., Schmidt, I. B., and Libonati, R. (2021). Putting fire on the map of Brazilian savanna ecoregions. *Journal of Environmental Management*, 296:113098.
- Silva, P. S., Rodrigues, J. A., Nogueira, J., Moura, L. C., Enout, A., Cuiabáia, C., DaCamara, C. C., Pereira, A. A., and Libonati, R. (2024b). Joining forces to fight wildfires: Science and management in a protected area of Pantanal, Brazil. *Environmental Science & Policy*, 159:103818.
- Silveira, M. V. F., Petri, C. A., Broggio, I. S., Chagas, G. O., Macul, M. S., Leite, C. C. S. S., Ferrari, E. M. M., Amim, C. G. V., Freitas, A. L. R., Motta, A. Z. V., Carvalho, L. M. E., Junior, C. H. L. S., Anderson, L. O., and Aragão, L. E. O. C. (2020). Drivers of Fire Anomalies in the Brazilian Amazon: Lessons Learned from the 2019 Fire Crisis. *Land*, 9:516.
- Simon, M. F., Grether, R., de Queiroz, L. P., Skema, C., Pennington, R. T., and Hughes, C. E. (2009). Recent assembly of the Cerrado, a neotropical plant diversity hotspot, by in situ evolution of adaptations to fire. *Proceedings of the National Academy of Sciences*, 106:20359–20364.
- Simon, M. F. and Pennington, T. (2012). Evidence for Adaptation to Fire Regimes in the Tropical Savannas of the Brazilian Cerrado. *International Journal of Plant Sciences*, 173:711–723.
- Skiles, S. M., Flanner, M., Cook, J. M., Dumont, M., and Painter, T. H. (2018). Radiative forcing by light-absorbing particles in snow. *Nature Climate Change*, 8:964–971.
- Soares-Filho, B., Rajão, R., Macedo, M., Carneiro, A., Costa, W., Coe, M., Rodrigues, H., and Alencar, A. (2014). Cracking Brazil's Forest Code. *Science*, 344:363–364.
- Solman, S. A. and Blázquez, J. (2019). Multiscale precipitation variability over South

- America: Analysis of the added value of CORDEX RCM simulations. *Climate Dynamics*, 53:1547–1565.
- Solman, S. A., Sanchez, E., Samuelsson, P., da Rocha, R. P., Li, L., Marengo, J., Pessacg, N. L., Remedio, A. R. C., Chou, S. C., Berbery, H., Treut, H. L., de Castro, M., and Jacob, D. (2013). Evaluation of an ensemble of regional climate model simulations over South America driven by the ERA-Interim reanalysis: model performance and uncertainties. *Climate Dynamics*, 41:1139–1157.
- Song, X.-P., Hansen, M. C., Stehman, S. V., Potapov, P. V., Tyukavina, A., Vermote, E. F., and Townshend, J. R. (2018). Global land change from 1982 to 2016. *Nature*, 560:639–643.
- Soterroni, A. C., Ramos, F. M., Mosnier, A., Fargione, J., Andrade, P. R., Baumgarten, L., Pirker, J., Obersteiner, M., Kraxner, F., Câmara, G., Carvalho, A. X. Y., and Polasky, S. (2019). Expanding the Soy Moratorium to Brazil’s Cerrado. *Science Advances*, 5:Not available.
- Sousa, P. M., Trigo, R. M., Pereira, M. G., Bedia, J., and Gutiérrez, J. M. (2015). Different approaches to model future burnt area in the Iberian Peninsula. *Agricultural and Forest Meteorology*, 202:11–25.
- Souza, C. M., Z. Shimbo, J., Rosa, M. R., Parente, L. L., A. Alencar, A., Rudorff, B. F. T., Hasenack, H., Matsumoto, M., G. Ferreira, L., Souza-Filho, P. W. M., de Oliveira, S. W., Rocha, W. F., Fonseca, A. V., Marques, C. B., Diniz, C. G., Costa, Rosa, E. R., Vélez-Martin, E., Weber, E. J., Lenti, F. E. B., Paternost, F. F., Pareyn, F. G. C., Siqueira, J. V., Viera, J. L., Neto, L. C. F., Saraiva, Salgado, M. P. G., Vasconcelos, and Mesquita (2020). Reconstructing Three Decades of Land Use and Land Cover Changes in Brazilian Biomes with Landsat Archive and Earth Engine. *Remote Sensing*, 12(17).
- Spera, S. A., Galford, G. L., Coe, M. T., Macedo, M. N., and Mustard, J. F. (2016). Land-use change affects water recycling in Brazil’s last agricultural frontier. *Global Change Biology*, 22:3405–3413.
- Sperling, S., Wooster, M. J., and Malamud, B. D. (2020). Influence of Satellite Sensor Pixel Size and Overpass Time on Undercounting of Cerrado/Savannah Landscape-

- Scale Fire Radiative Power (FRP): An Assessment Using the MODIS Airborne Simulator. *Fire*, 3:11.
- Squire, D. T., Richardson, D., Risbey, J. S., Black, A. S., Kitsios, V., Matear, R. J., Monselesan, D., Moore, T. S., and Tozer, C. R. (2021). Likelihood of unprecedented drought and fire weather during Australia’s 2019 megafires. *npj Climate and Atmospheric Science*, 4.
- Staver, A. C., Archibald, S., and Levin, S. A. (2011). The Global Extent and Determinants of Savanna and Forest as Alternative Biome States. *Science*, 334:230–232.
- Stoof, C. R. and Kettridge, N. (2022). Living With Fire and the Need for Diversity. *Earth’s Future*, 10:Not available.
- Stradic, S. L., Hernandez, P., Fernandes, G., and Buisson, E. (2018). Regeneration after fire in campo rupestre: Short- and long-term vegetation dynamics. *Flora*, 238:191–200.
- Strassburg, B. B. N., Brooks, T., Feltran-Barbieri, R., Iribarrem, A., Crouzeilles, R., Loyola, R., Latawiec, A. E., Filho, F. J. B. O., de M. Scaramuzza, C. A., Scarano, F. R., Soares-Filho, B., and Balmford, A. (2017). Moment of truth for the Cerrado hotspot. *Nature Ecology & Evolution*, 1:Not available.
- Strassburg, B. B. N., Latawiec, A., and Balmford, A. (2016). Urgent action on Cerrado extinctions. *Nature*, 540:199–199.
- Sutanto, S. J., Vitolo, C., Napoli, C. D., D’Andrea, M., and Lanen, H. A. V. (2020). Heatwaves, droughts, and fires: Exploring compound and cascading dry hazards at the pan-European scale. *Environment International*, 134:105276.
- Syphard, A. D., Keeley, J. E., Pfaff, A. H., and Ferschweiler, K. (2017). Human presence diminishes the importance of climate in driving fire activity across the United States. *Proceedings of the National Academy of Sciences*, 114:13750–13755.
- Sá, A. C. L., Pereira, J. M. C., Vasconcelos, M. J. P., Silva, J. M. N., Ribeiro, N., and Awasse, A. (2003). Assessing the feasibility of sub-pixel burned area mapping in miombo woodlands of northern mozambique using modis imagery. *International Journal of Remote Sensing*, 24:1783–1796.

- Taschetto, A. S. and Ambrizzi, T. (2011). Can Indian Ocean SST anomalies influence South American rainfall? *Climate Dynamics*, 38:1615–1628.
- Taylor, A. H., Trouet, V., Skinner, C. N., and Stephens, S. (2016). Socioecological transitions trigger fire regime shifts and modulate fire–climate interactions in the Sierra Nevada, USA, 1600–2015 CE. *Proceedings of the National Academy of Sciences*, 113:13684–13689.
- Teichmann, C., Jacob, D., Remedio, A. R., Remke, T., Buntemeyer, L., Hoffmann, P., Kriegsmann, A., Lierhammer, L., Bülow, K., Weber, T., Sieck, K., Rechid, D., Langendijk, G. S., Coppola, E., Giorgi, F., Ciarlo, J. M., Raffaele, F., Giuliani, G., Xuejie, G., Sines, T. R., Torres-Alavez, J. A., Das, S., Di Sante, F., Pichelli, E., Glazer, R., Ashfaq, M., Bukovsky, M., and Im, E.-S. (2021). Assessing mean climate change signals in the global CORDEX-CORE ensemble. *Climate Dynamics*, 57(5):1269–1292.
- Theil, H. (1950). A rank-invariant method of linear and polynomial regression analysis. *Proceedings of the Royal Netherlands Academy of Sciences*, 53:467–482.
- Thielen, D., Schuchmann, K.-L., Ramoni-Perazzi, P., Marquez, M., Rojas, W., Quintero, J. I., and Marques, M. I. (2020). Quo vadis Pantanal? Expected precipitation extremes and drought dynamics from changing sea surface temperature. *PLOS ONE*, 15:e0227437.
- Thomas, J. L., Polashenski, C. M., Soja, A. J., Marelle, L., Casey, K. A., Choi, H. D., Raut, J., Wiedinmyer, C., Emmons, L. K., Fast, J. D., Pelon, J., Law, K. S., Flanner, M. G., and Dibb, J. E. (2017). Quantifying black carbon deposition over the Greenland ice sheet from forest fires in Canada. *Geophysical Research Letters*, 44:7965–7974.
- Tomas, W. M., Berlinck, C. N., Chiaravalloti, R. M., Faggioni, G. P., Strüssmann, Abrahão, C. R., do Valle Alvarenga, G., de Faria Bacellar, A. E., de Queiroz Batista, F. R., Bornato, T. S., Camilo, A. R., Castedo, J., Fernando, A. M. E., de Freitas, G. O., Garcia, C. M., Gonçalves, H. S., de Freitas Guilherme, M. B., Layme, De Oliveira, A. C., da Rosa Oliveira, M., de Matos Martins Pereira, A., Rodrigues, J. A., Semedo, T. B. F., de Souza, R. A. D., Tortato, F. R., Viana, D. F. P., Vicente-



Silva, L., and Morato, R. (2021). Distance sampling surveys reveal 17 million vertebrates directly killed by the 2020's wildfires in the Pantanal, Brazil. *Scientific Reports*, 11(1):23547.

Tomas, W. M., de Oliveira Roque, F., Morato, R. G., Medici, P. E., Chiaravalloti, R. M., Tortato, F. R., Penha, J. M. F., Izzo, T. J., Garcia, L. C., Lourival, R. F. F., Girard, P., Albuquerque, N. R., Almeida-Gomes, M., da Silva Andrade, M. H., Araujo, F. A. S., Araujo, A. C., de Arruda, E. C., Assunção, V. A., Battirola, L. D., Benites, M., Bolzan, F. P., Boock, J. C., Bortolotto, I. M., da Silva Brasil, M., Camilo, A. R., Campos, Z., Carniello, M. A., Catella, A. C., Cheida, C. C., Peter G. Crawshaw, J., Crispim, S. M. A., Junior, G. A. D., Desbiez, A. L. J., Dias, F. A., Eaton, D. P., Faggioni, G. P., Farinaccio, M. A., Fernandes, J. F. A., Ferreira, V. L., Fischer, E. A., Fragoso, C. E., Freitas, G. O., Galvani, F., Garcia, A. S., Garcia, C. M., Graciolli, G., Guariento, R. D., Guedes, N. M. R., Guerra, A., Herrera, H. M., Hoogesteijn, R., Ikeda, S. C., Juliano, R. S., Kantek, D. L. Z. K., Keuroghlian, A., Lacerda, A. C. R., Lacerda, A. L. R., Landeiro, V. L., Laps, R. R., Layme, V., Leimgruber, P., Rocha, F. L., Mamede, S., Marques, D. K. S., Marques, M. I., Mateus, L. A. F., Moraes, R. N., Moreira, T. A., Mourão, G. M., Nicola, R. D., Nogueira, D. G., Nunes, A. P., da Nunes da Cunha, C., Oliveira, M. D., Oliveira, M. R., Paggi, G. M., Pellegrin, A. O., Pereira, G. M. F., Peres, I. A. H. F. S., Pinho, J. B., Pinto, J. O. P., Pott, A., Proвете, D. B., dos Reis, V. D. A., dos Reis, L. K., Renaud, P.-C., Ribeiro, D. B., Rossetto, O. C., Sabino, J., Rumiz, D., Salis, S. M., Santana, D. J., Santos, S. A., Ângela L. Sartori, Sato, M., Schuchmann, K.-L., Scremin-Dias, E., Seixas, G. H. F., Severo-Neto, F., Sigrist, M. R., Silva, A., Silva, C. J., Siqueira, A. L., Soriano, B. M. A., Sousa, L. M., Souza, F. L., Strussmann, C., Sugai, L. S. M., Tocantins, N., Urbanetz, C., Valente-Neto, F., Viana, D. P., Yanosky, A., and Junk, W. J. (2019). Sustainability Agenda for the Pantanal Wetland: Perspectives on a Collaborative Interface for Science, Policy, and Decision-Making. *Tropical Conservation Science*, 12:1940082919872634.

Touma, D., Stevenson, S., Lehner, F., and Coats, S. (2021). Human-driven greenhouse gas and aerosol emissions cause distinct regional impacts on extreme fire weather. *Nature Communications*, 12.

- Trigueiro, W. R., Nabout, J. C., and Tessarolo, G. (2020). Uncovering the spatial variability of recent deforestation drivers in the Brazilian Cerrado. *Journal of Environmental Management*, 275:111243.
- UNEP (2022). Spreading like Wildfire: The Rising Threat of Extraordinary Landscape Fires. Technical report, United Nations Environment Programme (UNEP), Nairobi.
- UNEP (2023). Emissions Gap Report 2023: Broken Record – Temperatures hit new highs, yet world fails to cut emissions (again). Technical report, United Nations Environment Programme.
- UNESCO (2021). UNESCO world heritage centre - world heritage list. <https://whc.unesco.org/en/list/>.
- UNESCO (2023). Fires in the Pantanal ecoregion. <https://www.unesco.org/en/articles/fires-pantanal-ecoregion>. Accessed: 2024-04-15.
- UNESCO (2024). El Chaco. <https://www.unesco.org/en/mab/el-chaco?hub=66369>. Accessed: 2024-04-15.
- UNESCO (2024a). Pantanal. <https://www.unesco.org/en/mab/pantanal>. Accessed: 2024-04-15.
- UNESCO (2024b). Pantanal Conservation Area. <https://whc.unesco.org/en/list/999>. Accessed: 2024-04-15.
- USGS (2024). Landsat 7. <https://www.usgs.gov/landsat-missions/landsat-7>. Accessed: 2024-04-15.
- van der Werf, G. R., Randerson, J. T., Giglio, L., van Leeuwen, T. T., Chen, Y., Rogers, B. M., Mu, M., van Marle, M. J. E., Morton, D. C., Collatz, G. J., Yokelson, R. J., and Kasibhatla, P. S. (2017). Global fire emissions estimates during 1997–2016. *Earth System Science Data*, 9:697–720.
- van Vuuren, D. P., Stehfest, E., den Elzen, M. G. J., Kram, T., van Vliet, J., Deetman, S., Isaac, M., Goldewijk, K. K., Hof, A., Beltran, A. M., Oostenrijk, R., and van Ruijven, B. (2011). RCP2.6: exploring the possibility to keep global mean temperature increase below 2°C. *Climatic Change*, 109:95–116.

- van Wagner, C. E. (1987). Development and structure of the Canadian Forest Fire Weather Index System. Technical report, Canadian Forestry Service.
- Vitolo, C., Giuseppe, F. D., Barnard, C., Coughlan, R., San-Miguel-Ayanz, J., Libertá, G., and Krzeminski, B. (2020). ERA5-based global meteorological wildfire danger maps. *Scientific Data*, 7:Not available.
- Wang, X., Thompson, D. K., Marshall, G. A., Tymstra, C., Carr, R., and Flannigan, M. D. (2015). Increasing frequency of extreme fire weather in Canada with climate change. *Climatic Change*, 130:573–586.
- Wilks, D. S. (2011). *Statistical Methods in the Atmospheric Sciences*. Academic Press.
- Williams, A. P. and Abatzoglou, J. T. (2016). Recent Advances and Remaining Uncertainties in Resolving Past and Future Climate Effects on Global Fire Activity. *Current Climate Change Reports*, 2:1–14.
- Wooster, M. J., Roberts, G., Perry, G. L. W., and Kaufman, Y. J. (2005). Retrieval of biomass combustion rates and totals from fire radiative power observations: FRP derivation and calibration relationships between biomass consumption and fire radiative energy release. *Journal of Geophysical Research: Atmospheres*, 110:Not available.
- Wu, C., Venevsky, S., Sitch, S., Mercado, L. M., Huntingford, C., and Staver, A. C. (2021). Historical and future global burned area with changing climate and human demography. *One Earth*, 4:517–530.
- Zalles, V., Hansen, M. C., Potapov, P. V., Stehman, S. V., Tyukavina, A., Pickens, A., Song, X.-P., Adusei, B., Okpa, C., Aguilar, R., John, N., and Chavez, S. (2019). Near doubling of Brazil’s intensive row crop area since 2000. *Proceedings of the National Academy of Sciences*, 116:428–435.
- Zappa, G., Bevacqua, E., and Shepherd, T. G. (2021). Communicating potentially large but non-robust changes in multi-model projections of future climate. *International Journal of Climatology*, 41:3657–3669.
- Zscheischler, J. and Seneviratne, S. I. (2017). Dependence of drivers affects risks associated with compound events. *Science Advances*, 3:Not available.
- Zubkova, M., Boschetti, L., Abatzoglou, J. T., and Giglio, L. (2019). Changes in Fire Ac-

tivity in Africa from 2002 to 2016 and Their Potential Drivers. *Geophysical Research Letters*, 46:7643–7653.

# Annex A

Silva et al. (2024a)

# Chapter 6

## Climate Change and Fire: The Case of Cerrado, the Brazilian Savanna



Patrícia S. Silva , Renata Libonati , Isabel B. Schmidt ,  
Joana Nogueira , and Carlos C. DaCamara 

**Abstract** Stretching across central Brazil, Cerrado, harbours the most floristically diverse savannas in the world. Over the last decades, this biodiversity hotspot has undergone severe changes in land use and currently, less than 20% of its native vegetation cover remains undisturbed. One such disturbance is fire. As a fire-dependent ecosystem, Cerrado's plant and animal species have developed adaptations to fire, and its occurrence is paramount to the biome's ecological functioning. Cerrado presents a variety of fire dynamics over its 2 million km<sup>2</sup>, and thus its drivers and constraints are also diverse and highly dependent on regional context. However, changes in historical fire patterns and the increasing occurrence of wildfires severely damage the biome and risk ecosystem services. Future changes in climate will further promote favourable meteorological conditions for severe and out-of-season wildfires. In this chapter, we discuss these topics with a comprehensive literature review and contribute to understanding fire in Cerrado with novel results regarding seasonal occurrence, trends, and drivers.

**Keywords** Brazil · Brazilian savannas · Wildfires · Fire drivers · Remote sensing · Regional approach

---

P. S. Silva (✉) · R. Libonati · C. C. DaCamara  
Universidade de Lisboa, Faculdade de Ciências, Instituto Dom Luiz, Lisboa, Portugal  
e-mail: [pssilva@fc.ul.pt](mailto:pssilva@fc.ul.pt)

R. Libonati · J. Nogueira  
Departamento de Meteorologia, Universidade Federal Do Rio de Janeiro, Rio de Janeiro,  
RJ 21941–916, Brazil

I. B. Schmidt  
Departamento de Ecologia, Instituto de Ciências Biológicas, Campus Universitário Darcy  
Ribeiro, Brasília, DF 70910–900, Brazil

### 6.1 The Brazilian Savannas

Brazil houses several unique ecosystems, including some of the most important phytogeographical domains in South America (Dionizio et al., 2018). The most well-known is the Amazon rainforest, but Brazil is also home to Cerrado, the most floristically diverse savanna in the world (Klink & Machado, 2005; Myers et al., 2000). As the second largest biome in South America, Cerrado originally covered around 2 million km<sup>2</sup> in central Brazil (Fig. 6.1) and has over 13 137 plant species, on par with the 13 214 plant species reported for the Amazon region (Overbeck et al., 2015). A high degree of endemism has been observed for plants and animals of Cerrado (Cardoso Da Silva & Bates, 2002), with around 4 800 species of plants and vertebrates unique to the biome (Strassburg et al., 2016). The climate in Cerrado is markedly seasonal, with an extended dry season from May to September (Pivello, 2011). According to the Köppen climate classification, the prevailing climate type is tropical seasonal (Aw), supporting a dry winter and rainy summer (Junior et al., 2020). Cerrado is a highly heterogeneous landscape with 11 main phytophysiognomic types (Embrapa, 2022): grasslands (campo sujo, campo limpo, campo rupestre); savanna formations (cerrado sensu stricto, parque de cerrado, palmeiral, vereda); and forest formations (mata ciliar, mata de galeria, mata seca, cerradão).

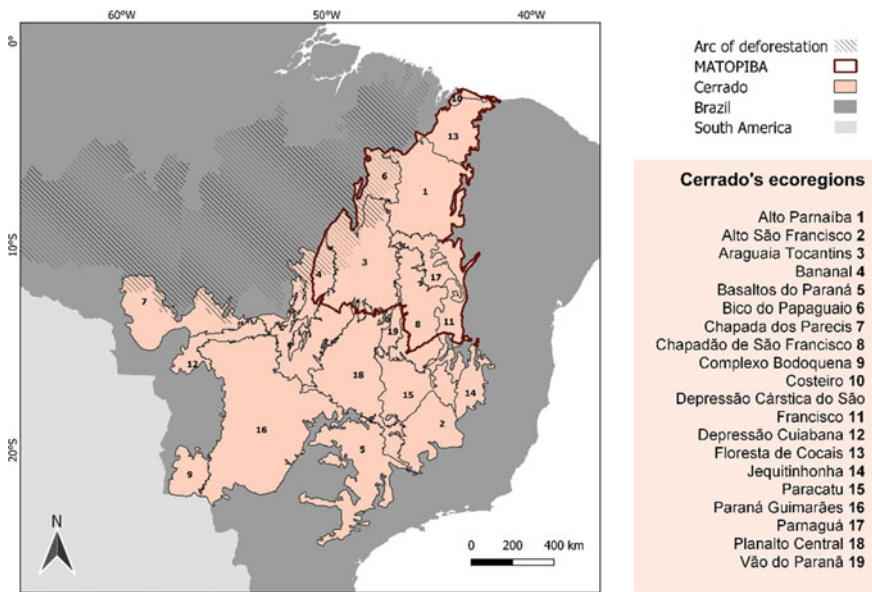


**Fig. 6.1** Cerrado's location within Brazil and South America (Source Prepared by the authors). [Note The transition zone between the Cerrado and Amazon biomes, the Arc of Deforestation, is hatched and MATOPIBA, defined here as the intersection of states Maranhão, Tocantins, Piauí and Bahia, with Cerrado, is marked by a solid brown line. Cerrado's 19 ecoregions (Sano et al., 2019) are also shown and numbered, with the respective names listed in the column on the right]

Recent studies, however, point to a very degraded biome with 46% of Cerrado's native vegetation cover having been lost (88 Mha) and only 19.8% remaining undisturbed (Strassburg et al., 2017). Despite falling annual deforestation rates since the 2000s (Lapola et al., 2014), around 93 000 km<sup>2</sup> of natural vegetation cover have been converted into agricultural lands from 2002 to 2009, an indication that current deforestation rates are still high and increasingly leading to landscape fragmentation and loss of ecosystem function (Overbeck et al., 2015). Southern Cerrado has most of its territory now deprived of native vegetation as a result of historical land conversion into agriculture and pasture lands since the 1960s (Sano et al., 2020). Continuous stretches of intact and undisturbed Cerrado are mostly located within the transitional area between Cerrado and the Amazon, commonly referred to as the Arc of Deforestation (Marques et al., 2020), or within Brazil's latest agricultural frontier, the MATOPIBA (the confluence of states Maranhão—MA, Tocantins—TO, Piauí—PI, and Bahia—BA; Fig. 6.1). Both these regions have seen high conversion rates over the last few decades, and during 2013–2017, the mean deforestation rate in MATOPIBA was 241% higher than any other region in the biome (Trigueiro et al., 2020). Land conversion in Cerrado is mainly associated with human activities as a result of the dramatic changes in land use promoted by large-scale agriculture (soybean, rice, corn, and cotton monocultures), livestock ranging, and mineral extraction (Klink & Moreira, 2002; Overbeck et al., 2015). In an effort to properly characterize the spatial heterogeneity of Cerrado, Sano et al. (2019) defined 19 ecoregions (Fig. 6.1) which were based on physical attributes (elevation, rainfall, and soil), patterns of human occupation (land use and land cover), and level of biodiversity conservation (conservation units and indigenous lands), so that they represent unique landscapes within the biome.

## 6.2 A Burning Case

In the global context, Brazil is a major fire hotspot, along with northern Australia, central and southern Africa, and Eurasia (Bowman et al., 2020). Amongst all Brazilian biomes, Cerrado burns the most and is responsible for half of Brazil's burned area (United Nations Environment Programme, 2022). Fire influences vegetation structure, climate, and the carbon cycle, and contrary to common belief, it is not always harmful to the biome. Cerrado is considered a fire-dependent biome (Hardisty et al., 2005), where fire has been a frequent and natural disturbance for millions of years (Mistry, 1998; Simon et al., 2009). Fire is thus a key component in defining the biome's physiognomy and structure, influencing species abundance and diversity (Simon & Pennington, 2012; Simon et al., 2009). Many species from Cerrado grasslands and savannas are fire-resistant, which makes this biome very resilient to fire activity (Pivello, 2011): several plant species have belowground woody organs that promote quick leaf and flower sprout after fire; Cerrado's typical twisted trees and shrubs have developed thick bark layers and fruit walls that protect their tissues and seeds from high temperatures; and belowground biomass is at least two times



higher than aboveground biomass. Fire further contributes to trait variability in plants (Hoffmann et al., 2012a; 2012b; Dantas et al., 2013), and affects their reproductive success by influencing seed germination and flowering (Fidelis & Blanco, 2014; Fidelis et al., 2022). It modifies competition amongst trees and herbaceous plants such as grasses, shrubs, and lianas (Dionizio et al., 2018), and affects the dynamics of nutrients (Nardoto et al., 2006). Frequently burned sites in Cerrado tend to become grassy and open, as most trees are killed or maintained in short stature by fire, and ash deposition brings nutrients to the surface soil (Pivello, 2011). Accordingly, along with rain seasonality and soil features, fire acts as one of the vegetation determinants in Cerrado (Lehmann et al., 2014).

Fire activity in Cerrado is characterized by a set of parameters, such as seasonality, intensity, recurrence, and extent. These parameters, however, do not behave the same within the biome (Rodrigues et al., 2019; Silva et al., 2021), as fire patterns change significantly along its 19 ecoregions (Fig. 6.1). Silva et al. (2021) showed that northern ecoregions, including MATOPIBA, present higher fire activity compared to those in southern Cerrado, and ecoregions bordering other biomes (namely, Amazon or Caatinga) burn more intensely. Larger scars are usually located in central and northern Cerrado, where there are still large stretches of natural vegetation cover, while small fire occurrences are more evenly spread out. In general, smaller scars are more frequent but contribute to lower amounts of total burned area, whereas rare and few big scars, those above 50 km<sup>2</sup>, are responsible for 90% of the total burned area of the biome. A noteworthy case is that of Bananal (ecoregion number 4 in Fig. 6.1), which encompasses the Araguaia National Park and Indigenous Land, where 7% of fire scars comprise 70% of the total burned area. These wildfires, defined as “unusual or extraordinary free-burning vegetation fires”, pose a significant risk to social, economic, or environmental values (United Nations Environment Programme, 2022). Along with the Amazon, Cerrado has the highest amount of wildfires in Brazil and the years 2007 and 2010 stand out as the most severe over the last two decades (Li et al., 2022; Silva et al., 2021).

Fire seasonality, however, is similar across Cerrado’s ecoregions. Silva et al. (2021) found that fire occurrence is mainly restricted to the dry season which accounts for more than 90% of the annual burned area in almost all ecoregions, and the months of August to October account for at least 64%. In general, smaller scars begin earlier in the season and may extend after the dry season, whereas larger scars are concentrated over a 3-month period. Higher fire intensities occur towards the end of the dry season when vegetation stress is at its peak. These patterns, however, seem to be changing. Figure 6.2 shows how Cerrado’s fire season seems to be shifting towards later in the year. Months from June to August have been systematically lowering their total contribution, whereas October accounts for a higher percentage over the last decade (2011–2020) when compared to the beginning of the century (2001–2010). Wildfires show a similar pattern, with October doubling its contribution in 2015–2018 when compared to 2003–2006.

Regional discrepancies are a product of a variety of factors that drive and constrain fire activity, both natural and anthropogenic. This includes meteorological conditions, topography, fuel availability and continuity, and the human factor. In the case of

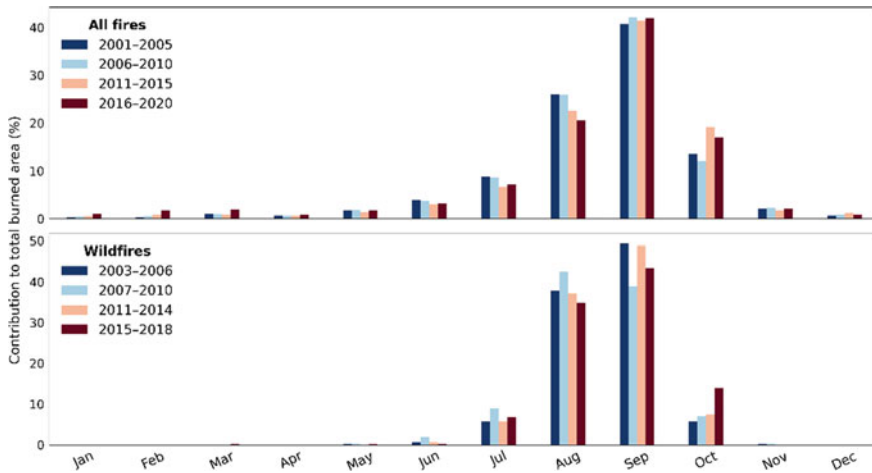


**Fig. 6.2** Monthly contribution (%) to total burned area in the Cerrado (Prepared by the authors). [Note The top panel shows results for all fires (regardless of scar size) using the MODIS MCD64A1 collection 6 (Giglio et al., 2018) and considering four periods: 2001–2005, 2006–2010, 2011–2015, and 2016–2020. Bottom panel restricts to wildfires (defined here as fire scars above 50 km<sup>2</sup>) using data from the Global Fire Atlas (Andela et al., 2019) over four periods: 2003–2006, 2007–2010, 2011–2014, and 2015–2018]

Cerrado, studies have shown that there is a strong connection between fire activity and precipitation (Libonati et al., 2015; Mataveli et al., 2018) and vapour pressure deficit (Gomes et al., 2018). Fire occurrence within Cerrado is moisture-dependent, as high precipitation rates increase primary productivity and lead to fast biomass recovery and fuel availability (Alvarado et al., 2017). Wildfires in Cerrado have been shown to be mainly driven by strong wind speeds and compounded hot and dry conditions (Li et al., 2022), and extreme events such as drought are also associated with increases in fire activity (Alvarado et al., 2017; Li et al., 2021), which are in turn related to large-scale mechanisms such as El Niño and sea surface temperatures (Jimenez et al., 2019). Fire weather conditions (i.e., weather conditions favourable to fire activity, which generally include high air temperature, low soil moisture and air humidity, and strong wind; IPCC, 2021) are usually characterized by means of indexes of meteorological fire danger. Meteorological fire danger has been increasing in Brazil (Jolly et al., 2015; Nogueira et al., 2017; Silva et al., 2016) and, in Cerrado, the year-to-year variability of burned area (i.e. the extent of fire) can be accounted for using the Fire Weather Index (FWI), a commonly used index of meteorological fire danger (Silva et al., 2019). In an intercomparison of meteorological fire danger indexes for Brazil, Nogueira et al. (2017), observed that the burned area in Cerrado was most correlated with indexes that consider precipitation effects on the topsoil moisture layer and the moisture content of the surface litter and fine fuels, suggesting that seasonal fire activity increases with a rapid drying of grasses or herbaceous fuel.

Land cover also influences fuel flammability, fire spread, and intensity. The high susceptibility of savannas to fire has been attributed to a predominance of grassy fuel

loads (Hoffmann et al., 2012a; 2012b) that become dry and very flammable during the dry season (Pivello, 2011). Savanna and grassland formations are known to burn more intensely than forests due to the continuous grassy layer (Gomes et al., 2018), and wet grasslands in Cerrado present regular burning, even if associated with lower temperatures and intensities (Schmidt et al., 2017). Lands with high fragmentation levels, e.g., due to large-scale agriculture, experience smaller fires as there is no fuel continuity on the landscape (Archibald et al., 2012). A recent study has found that increased land fragmentation and agricultural expansion in Cerrado lead to smaller burned areas of native vegetation by limiting the spread of fires between fragments (Rosan et al., 2022).

In the case of Brazil, land use and population density are also linked with fire occurrence and ignitions. Anthropogenic fire mostly occurs within Cerrado's dry season, whereas natural fires take place during the rainy season or in the dry-rainy season transition (Menezes et al., 2022; Schumacher et al., 2022). The latter tend to be smaller and less severe, constrained by soil and fuel moisture (Alvarado et al., 2020; Ramos-Neto & Pivello, 2000), contrary to anthropogenic fires, which tend to be larger and more intense, triggering changes to the floristic composition and community structure of vegetation, favouring fire-resistant species, and negatively impacting fire-sensitive species (de Azevedo et al., 2020). In areas with native vegetation cover, fire is usually used as an inexpensive tool to clean up deforested or degraded areas (Junior et al., 2020), whereas, in small-scale agricultural areas, fire serves a diversity of purposes, such as the management of species and landscapes, cattle raising upon native or exotic pasturelands, and subsistence agriculture (Eloy et al., 2019; Schmidt, Figueiredo & Scariot, 2007). However, contrary to the Amazon (de Oliveira et al., 2020; Libonati et al., 2021), fire emissions are not correlated with deforestation in Cerrado (Mataveli et al., 2021), and relationships between land use and fire have been shown to be quite complex and highly dependable on regional context (Silva et al., 2020). Similarly, the relationship between population density and fire activity may also vary locally. Lower population densities have been shown to lead to shorter fire seasons, whereas proximity to densely populated areas reveals recurring fire activity and longer fire seasons (Chuvienco et al., 2008), due to increased ignitions.

Human influence has been shown to be disrupting fire regimes in savannas worldwide (Archibald, 2016; Shlisky et al., 2008) and, in the particular case of Cerrado, severely weakened the biome by limiting regeneration capabilities (Rosan et al., 2019; Santana et al., 2020), further compromising Brazil's pledges to the Paris Agreement (Junior et al., 2020). In the period 1999 to 2018, Cerrado was responsible for emitting more than 2 500 Tg of carbon into the atmosphere, second only to the Amazon, and these rates are not expected to decrease (Junior et al., 2020). Moreover, a reduction in the biomass of fire-sensitive species may transform Cerrado from a carbon sink into a source of carbon emissions (de Azevedo et al., 2020). According to a study covering the period from 2005 to 2016, ozone emissions have also been rising in Cerrado, reducing air quality and increasing regional health risks (Pope et al., 2020).

### 6.3 Under Climate Change

Brazil is already showing significant changes in its historical record (Dubreuil et al., 2019). In Cerrado, maximum and minimum temperatures have increased by 2.2–4.0 and 2.4–2.8 °C, respectively, since 1961 (Hofmann et al., 2021), particularly in the central and northern regions. MATOPIBA presents temperature increases at a rate of 0.3 °C per decade since 1981, with a warming rate of 0.45 °C per decade after the turn of the twenty-first century, decreasing rainfall and an increase in dry day frequency and drought (Marengo et al., 2022). Relative humidity has also decreased in Cerrado by about 15% since 1961 (Hofmann et al., 2021). Figure 6.3 shows the historical evolution of four parameters that influence fire activity: meteorological fire danger (evaluated through FWI); farming and urban areas (i.e., land use); and population. In the last four decades, fire danger has been consistently increasing over Cerrado, with higher intensities found at the southeastern border. Favourable meteorological conditions for fire activity have thus been increasing, along with expanding agricultural areas, particularly in southwestern and northeastern Cerrado. Urban areas and population go hand-in-hand with large increases in southern ecoregions. These results point to an already disturbed fire regime over the last decades, with significant and complex interactions amongst natural and anthropogenic factors.

The Intergovernmental Panel on Climate Change (IPCC) has developed several climate change scenarios, the Representative Concentration Pathways (RCP) for its Fifth Assessment Report (AR5), and the Shared Socioeconomic Pathways for the latest Assessment Report (AR6). Each of these considers a different pathway of emissions in the twenty-first century. Temperature estimates have high confidence as surface temperatures are expected to increase under all climate change scenarios (Llopart et al., 2020; Bustos Usta et al., 2021). This leads to an increase in hot extremes and heatwave frequency and duration (Di Luca et al., 2020; Feron et al., 2019). On the other hand, precipitation estimates present much more uncertainty as models disagree on both the sign and magnitude of change. Although models show no significant change in annual precipitation (Hodnebrog et al., 2022), when looking at the dry season months of Cerrado, simulations seem to point to a drier future (Blázquez & Silvina, 2020; Zappa et al., 2021). Compounded hot and dry events will thus occur more frequently under climate change (Ridder et al., 2022; Vogel et al., 2020). Surface wind is also expected to increase over the biome (Reboita et al., 2018), and Cerrado's river basins are expected to have decreased stream flows, particularly in the dry season, and increases in the duration, intensity, and frequency of droughts (Lu et al., 2019; Rodrigues et al., 2020). Floods may also increase over Brazilian territory (Hirabayashi et al., 2021) but keeping to the threshold of 1.5 °C of warming will reduce exposure to extreme precipitation (Li et al., 2020).

The changes mentioned above in climate, particularly increased temperatures, lower relative humidity, and extended drought periods, provide aggravated conditions for fire weather. Anthropogenic climate change has been linked to the severe 2015 fire season in Cerrado (Li et al., 2021) and meteorological fire danger is expected to increase over the twenty-first century (Silva et al., 2016). Silva et al. (2019)

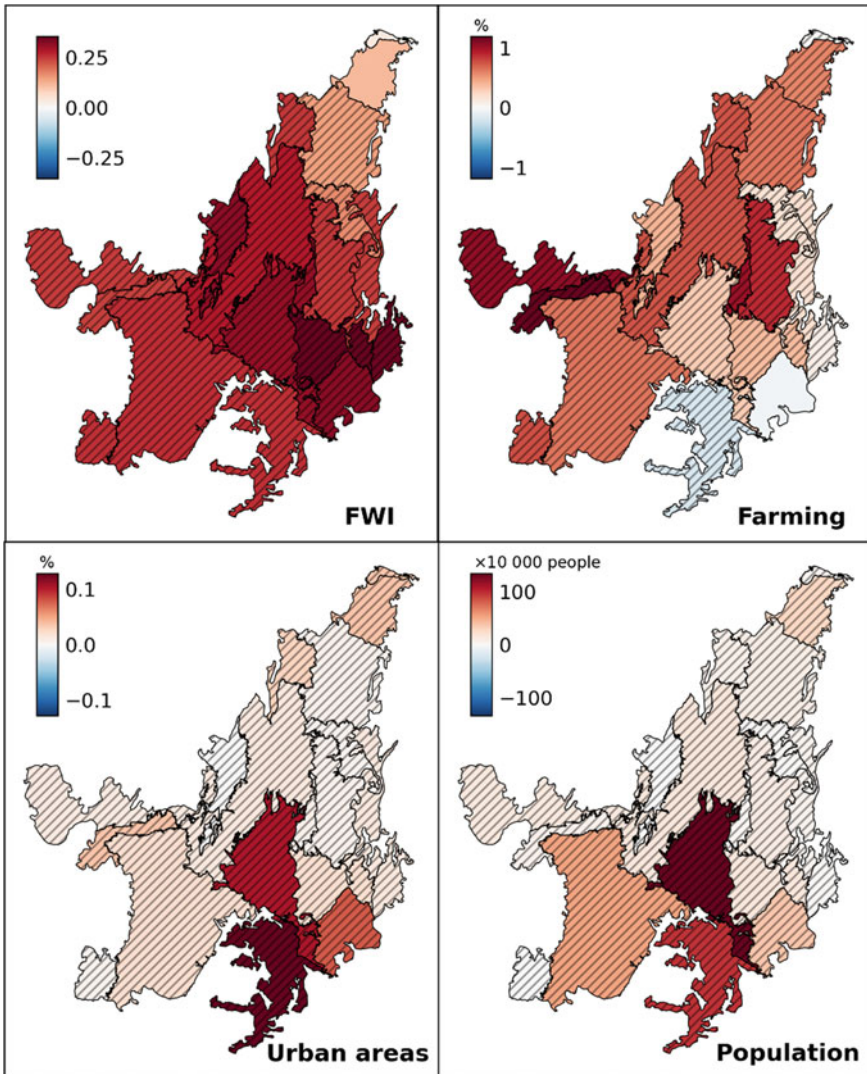


**Fig. 6.3** Historical trends of drivers and constraints of fire activity in Cerrado’s ecoregions (Source Prepared by the authors) [Note The upper left panel shows dry season (considered here as July to October) averaged Fire Weather Index (FWI), dimensionless, derived using meteorological fields from the European Centre for Medium-Range Weather Forecasts’ ERA5 reanalysis (Hersbach et al., 2020) over 1980–2018. Upper right shows Farming areas, %, normalized with each ecoregion’s area, as estimated with the MapBiomias collection 5 (Project MapBiomias, 2020) over 1985–2018. Bottom left panel uses the same dataset and methods as for Farming but for Urban areas. The bottom right panel shows the population total from the annual census of the Brazilian Institute of Geography and Statistics over 2001–2018. Trends were estimated using the Theil-Sen regression slope (Sen, 1968; Theil, 1950) and hatched regions represent significance below the 5% level using the Mann–Kendall nonparametric test (Kendall, 1975; Mann, 1945)]

found increasing burned areas in Cerrado under several climate change scenarios. RCPs 4.5 and 8.5, respectively, the moderate and severe climate change scenarios for IPCC's AR5, show a steady increase in burned area over the twenty-first century, reaching 39% and 95% by 2100, respectively. The stringent mitigation scenario, RCP 2.6, is the only scenario where the increase in burned area will decrease by the end of the century in comparison with that of the mid-century, from 22 to 11%. The most concerning result, however, regards wildfire, where extreme events are expected to increase substantially under RCPs 4.5 and 8.5. Only RCP 2.6 seems to keep climate conditions close to the present climate, which reinforces the importance of keeping to the Paris Agreement goals. Junior et al. (2020) further confirmed an increasing trend in fire foci over the 2019–2030 period.

Moreover, changes in land use further disturb regional climate. For instance, changes in Cerrado's albedo and evapotranspiration due to deforestation and replacement of native vegetation cover by agricultural lands may lead to a warming of 1.6 °C followed by a cooling of 0.9 °C when these agricultural lands are converted into sugarcane fields (Lapola et al., 2014). Land conversion to soy and maize crops may also lead to further increases in temperature and decreases in evapotranspiration (Spera et al., 2020). Increased land conversion is expected (Soterroni et al., 2019), which in turn may also lead to carbon emissions and biodiversity loss. It is expected that land use will be the most intense in the regions where the greatest species richness is harboured (Velazco et al., 2019), threatening several plant and animal species (Alves-Ferreira et al., 2022; Ferreira et al., 2021; Maciel et al., 2021). Already we are witnessing a major extinction event in Cerrado, with future plant extinctions to be a magnitude higher than all global recorded plant extinctions so far (Strassburg et al., 2016). Climate change will further determine species distribution by altering local climate conditions at such a higher rate than species are able to adapt to (Bellard et al., 2012), and by determining, according to their climatic tolerances, where they will occur (Lenoir & Svenning, 2015). Overall, species richness in Cerrado will decrease under climate change, with southern Cerrado becoming biotically homogenized by the extinction of native specialist species (Hidasi-Neto et al., 2019), further degrading the resilience of communities to environmental disturbances.

All the above-referred changes in climate are expected to have severe consequences in Cerrado, potentially causing the ecosystem to collapse (Hofmann et al., 2021), and putting at risk electric energy production and water availability (Althoff et al., 2020; Rodrigues et al., 2020; Siqueira et al., 2021), food security (Zilli et al., 2020), and the Brazilian economy (Marengo et al., 2022).

## 6.4 The Way Forward

Cerrado has been extensively altered over the last decades and is regarded as one of the most threatened biomes worldwide (Durigan & Ratter, 2016; Eloy et al., 2016; Strassburg et al., 2017). Quick and targeted efforts are needed to maintain what remains of its original cover and possibly recover disturbed regions, as the Brazilian government

has been consistently neglecting this biodiversity hotspot. Heavily contrasting with its neighbouring biome, the Amazon, public, protected areas cover less than 8% of Cerrado (Sano et al., 2019; Strassburg et al., 2017). It has been shown that the present number, area, and distribution of its Protected Areas (PA) are insufficient to guarantee the conservation of all the biome's biodiversity (Oliveira et al., 2017; Velazco et al., 2019). Worldwide, Brazil is the country with the largest tree cover loss in PAs (Wade et al., 2020), mainly due to the lack of government enforcement and the weakening of environmental policies (Rajão et al., 2020). Some PAs within Cerrado, particularly MATOPIBA, have seen a surge in deforestation in recent years (Mataveli et al., 2021), and are marked as highly vulnerable to future changes in climate (Lapola et al., 2020). Only recently, a routine deforestation surveillance programme has been established. However, due to Cerrado's topography and soils being highly suitable for large-scale agriculture, combined with a lack of legal protection and declining deforestation rates in the Amazon rainforest, all indicate that the biome will continue as a major region of land use change (Lapola et al., 2014). Moreover, contrary to the Amazon, Cerrado does not have a Soy Moratorium, and current legislation allows deforestation of 65–80% of the property (Federal law 12,651/2012). Cerrado is thus in desperate need of a zero-deforestation moratorium to conserve its last vegetation remnants in order to meet the Paris Agreement goals (Junior et al., 2020).

Future changes in the frequency, intensity, extent, and seasonality of fires, particularly in areas with native vegetation remnants, will further degrade and disturb this already fragile ecosystem. A crucial step to prevent and manage future wildfires is to rely on human-managed burning to maintain low fuel loads and avoid spreading (Ramos-Neto & Pivello, 2000). Several wildfire events were linked to the accumulation of fuels for long fire-free periods (Flores et al., 2021) and no-fire policies lead to the occurrence of periodic and severe wildfires (Ramos-Neto & Pivello, 2000; Schmidt et al., 2018). Moreover, the argument that there are no wildfires in industrial agricultural areas is commonly used to incriminate local communities that use fire to manage landscapes, omitting the fact that the use of fire might be a tool to coexist with Cerrado. The conversion of Cerrado into industrial monoculture does not cause wildfires but neither does it provide any ecosystem services such as biodiversity conservation, water cycle, or carbon stock (Eloy et al., 2016).

Integrated Fire Management (IFM) has recently been implemented in federally protected areas in the Cerrado (2014), and early evidence highlights its advantages. It has been shown that fire management does not lead to biodiversity loss in the Brazilian savannas located at the Santa Bárbara Ecological Station (Durigan et al., 2020), and Santos et al. (2021) show that prescribed burnings have reduced the average rise of burned areas and fire scars on management season, decreased wildfire season, and increased low-fire-recurrence regions in the Xerente and Araguaia Indigenous Territories. Also, for the Araguaia, de Andrade et al. (2021) showed that IFM contributed to the formation of a heterogeneous landscape composed of fire-resistant and fire-sensitive native vegetation, thus limiting the number of areas affected by fires during the late dry season. Oliveira et al. (2022) found that fire management by indigenous brigades substantially reduced fire frequency in high-fire-frequency areas and also contributed to the reduction of burned areas in the

Kadiwéu Indigenous Territory. This pattern is likely to be repeated in other PAs where IFM has been implemented (Mistry et al., 2019). However, there is a need for a more comprehensive IFM approach (Oliveira et al., 2021). So far, IFM is mostly restricted to federal PAs, and there is still large room for expansion and improvement. Uncertainty will necessarily be part of the process since scientific knowledge is and will be limited, especially considering the high local and regional social and biological diversity of the Cerrado. Fire management has been implemented considering local and traditional ecological knowledge (Falleiro et al., 2021), and using the adaptive management perspective, i.e., planning, implementation, and monitoring of all management actions performed in one year are used to improve activities in the following year (Schmidt et al., 2018). Applied research is important to assist managers and policymakers and put new management practices in place. However, it is important to acknowledge that management and research commonly have different time perspectives and demands. The learning environment resulting from the collaboration between researchers, managers, and local communities might be very effective in improving knowledge and management practices (Christensen, 2005; Wilgen et al., 2007). For fire management to effectively contribute to Cerrado conservation and climate change mitigation, it is essential that IFM practices and prescribed burns are implemented in state PA as well as in private land, which represents the majority of the land in the biome.

Conserving forests in Cerrado will help mitigate future climate change as forested areas maintain lower surface temperatures and relatively high precipitation (Coe et al., 2017). Old-growth savannas and grasslands within the Cerrado are also important to mitigate climate change, especially due to their large underground root systems (Veldman et al., 2015, 2019). Protecting these ecosystems from conversions and managing them with prescribed fires helps to conserve both their biodiversity and their ability to mitigate future climate change.

**Acknowledgements** The authors would like to thank Niels Andela for providing Global Fire Atlas data from 2017 to 2018, and Edson E. Sano for Cerrado ecoregion shapefiles. We would also like to acknowledge Filipe L. M. Santos' contribution in processing the Global Fire Atlas data to Cerrado's ecoregions.

**Funding** P.S.S. was supported by Fundação para a Ciência e a Tecnologia (FCT) [grant number SFRH/BD/146646/2019]; R.L. was supported by Conselho Nacional de Desenvolvimento Científico e Tecnológico (CNPq) [grant 311487/2021–1] and FAPERJ [grant E26/202.714/2019]; and I.B.S. was supported by CNPq [grant 441951/2018–0]. This work was funded by the Portuguese Fundação para a Ciência e a Tecnologia (FCT) I.P./MCTES through national funds (PIDDAC)—UIDB/50019/2020 (<https://doi.org/10.54499/UIDB/50019/2020>), UIDP/50019/2020 (<https://doi.org/10.54499/UIDP/50019/2020>) and LA/P/0068/2020 (<https://doi.org/10.54499/LA/P/0068/2020>).



## References

- Althoff, D., Rodrigues, L. N., & da Silva, D. D. (2020). Impacts of climate change on the evaporation and availability of water in small reservoirs in the Brazilian Savannah. *Climatic Change*, *159*(2), 215–232. Springer. <https://doi.org/10.1007/s10584-020-02656-y>
- Alvarado, S. T., et al. (2017). Drivers of fire occurrence in a mountainous Brazilian cerrado Savanna: Tracking long-term fire regimes using remote sensing. *Ecological Indicators*, *78*, 270–281. Elsevier. <https://doi.org/10.1016/J.ECOLIND.2017.02.037>.
- Alvarado, S. T., et al. (2020). Thresholds of fire response to moisture and fuel load differ between tropical Savannas and grasslands across continents. *Global Ecology and Biogeography*, *29*(2), 331–344. Blackwell Publishing Ltd. <https://doi.org/10.1111/geb.13034>
- Alves-Ferreira, G., et al. (2022). Projected responses of Cerrado anurans to climate change are mediated by biogeographic character. *Perspectives in Ecology and Conservation*. Elsevier. <https://doi.org/10.1016/J.PECON.2021.12.001>.
- Andela, N., et al. (2019). The global fire atlas of individual fire size, duration, speed, and direction. *Earth System Science Data Discussions*, *11*(2), 1–28. Copernicus GmbH. <https://doi.org/10.5194/essd-2018-89>
- Archibald, S., Staver, A. C., & Levin, S. A. (2012). Evolution of human-driven fire regimes in Africa. *Proceedings of the National Academy of Sciences*, *109*(3), 847–852. <https://doi.org/10.1073/pnas.1118648109>
- Archibald, S. (2016). Managing the human component of fire regimes: Lessons from Africa. *Philosophical Transactions of the Royal Society B: Biological Sciences*, *371*(1696), 20150346. Royal Society of London. <https://doi.org/10.1098/rstb.2015.0346>
- Bellard, C., et al. (2012). Impacts of climate change on the future of biodiversity. *Ecology Letters*, *15*(4), 365–377. John Wiley & Sons Ltd. <https://doi.org/10.1111/J.1461-0248.2011.01736.X>
- Blázquez, J., & Silvina, A. S. (2020). Multiscale precipitation variability and extremes over South America: Analysis of future changes from a set of CORDEX regional climate model simulations. *Climate Dynamics*, *55*(7–8), 2089–2106. Springer. <https://doi.org/10.1007/s00382-020-05370-8>
- Bowman, D. M. J. S., et al. (2020). Vegetation fires in the Anthropocene. *Nature Reviews Earth & Environment*, *1*(10), 500–515. Springer Science and Business Media LLC. <https://doi.org/10.1038/s43017-020-0085-3>
- Bustos Usta, D. F., Teymouri, M., & Chatterjee, U. (2021). Projections of temperature changes over South America during the twenty-first century using CMIP6 models. *GeoJournal*, 1–25. Springer Science and Business Media Deutschland GmbH. <https://doi.org/10.1007/s10708-021-10531-1>
- Cardoso Da Silva, J. M., & Bates, J. M. (2002). Biogeographic patterns and conservation in the South American Cerrado: A tropical Savanna hotspot. *BioScience*, *52*(3), 225–234. Oxford University Press. [https://doi.org/10.1641/0006-3568\(2002\)052\[0225:bpacit\]2.0.co;2](https://doi.org/10.1641/0006-3568(2002)052[0225:bpacit]2.0.co;2)
- Christensen, N. L. (2005). Fire in the parks: A case study for change management. *The George Wright Forum*, *22*(4), 12–31. <https://www.jstor.org/stable/43597963>
- Chuvieco, E., Giglio, L., & Justice, C. (2008). Global characterization of fire activity: Toward defining fire regimes from earth observation data. *Global Change Biology*, *14*(7), 1488–1502. <https://doi.org/10.1111/j.1365-2486.2008.01585.x>
- Coe, M. T., et al. (2017). The forests of the Amazon and Cerrado moderate regional climate and are the key to the future tropical conservation science. *SAGE Publications*, *10*. <https://doi.org/10.1177/1940082917720671>
- de Dantas, V. L., et al. (2013). The role of fire in structuring trait variability in Neotropical Savannas. *Oecologia*, *171*(2), 487–494. Springer-Verlag. <https://doi.org/10.1007/s00442-012-2431-8>
- de Andrade, A. S. R., et al. (2021). Implementation of fire policies in Brazil: An assessment of fire dynamics in Brazilian Savanna. *Sustainability*, *13*(20), 11532. Multidisciplinary Digital Publishing Institute. <https://doi.org/10.3390/SU132011532>

- de Azevedo, G. B., et al. (2020). Woody biomass accumulation in a Cerrado of central Brazil monitored for 27 years after the implementation of silvicultural systems. *Forest Ecology and Management*, 455, 117718. Elsevier. <https://doi.org/10.1016/J.FORECO.2019.117718>
- de Falleiro, R. M., et al. (2021). Histórico, Avaliação, Oportunidades e Desafios do Manejo Integrado do Fogo nas Terras Indígenas Brasileiras. *Biodiversidade Brasileira-BioBrasil*, 11(2), 75–98. <https://doi.org/10.37002/biobrasil.v11i2>
- da Junior, C. A. S., et al. (2020). Persistent fire foci in all biomes undermine the Paris agreement in Brazil. *Scientific Reports. Nature Research*, 10(1), 16246. <https://doi.org/10.1038/s41598-020-72571-w>
- de Oliveira, G., et al. (2020). Rapid recent deforestation incursion in a vulnerable indigenous land in the Brazilian amazon and fire-driven emissions of fine particulate aerosol pollutants. *Forests*, 11(8), 829. Multidisciplinary Digital Publishing Institute. <https://doi.org/10.3390/f11080829>
- Dionizio, E. A., et al. (2018). Influence of climate variability, fire and phosphorus limitation on vegetation structure and dynamics of the Amazon-Cerrado border. *Biogeosciences*, 15(3), 919–936. European Geosciences Union. <https://doi.org/10.5194/BG-15-919-2018>
- Di Luca, A., et al. (2020). Contribution of mean climate to hot temperature extremes for present and future climates. *Weather and Climate Extremes*, 28, 100255. Elsevier. <https://doi.org/10.1016/J.WACE.2020.100255>
- Dubreuil, V., et al. (2019). Climate change evidence in Brazil from Köppen's climate annual types frequency. *International Journal of Climatology*, 39(3), 1446–1456. John Wiley & Sons Ltd. <https://doi.org/10.1002/JOC.5893>
- Durigan, G., & Ratter, J. A. (2016). The need for a consistent fire policy for Cerrado conservation. In J. James (Ed.), John Wiley & Sons, Ltd (10.1111). *Journal of Applied Ecology*, 53(1), 11–15. <https://doi.org/10.1111/1365-2664.12559>
- Durigan, G., et al. (2020). No net loss of species diversity after prescribed fires in the Brazilian Savanna. *Frontiers in Forests and Global Change*, 3(13), 13. Frontiers Media SA. <https://doi.org/10.3389/ffgc.2020.00013>
- Eloy, L., et al. (2016). On the margins of soy farms: Traditional populations and selective environmental policies in the Brazilian Cerrado. *The Journal of Peasant Studies*, 43(2), 494–516. Routledge. <https://doi.org/10.1080/03066150.2015.1013099>
- Eloy, L., et al. (2019). Seasonal fire management by traditional cattle ranchers prevents the spread of wildfire in the Brazilian Cerrado. *Ambio*, 48(8), 890–899. Springer, Netherlands. <https://doi.org/10.1007/s13280-018-1118-8>
- Embrapa. (2022). Bioma Cerrado. Retrieved April 28, 2022, from <https://www.embrapa.br/cerrados/colecao-entomologica/bioma-cerrado>
- Feron, S., et al. (2019). Observations and projections of heat waves in South America. *Scientific Reports*, 9(1). Nature Publishing Group. <https://doi.org/10.1038/s41598-019-44614-4>
- Ferreira, R. B., Pereira, M. R., & Nabout, J. C. (2021). The impact of global climate change on the number and replacement of provisioning ecosystem services of Brazilian Cerrado plants. *Environmental Monitoring and Assessment*, 193(11), 731. Springer Science and Business Media Deutschland GmbH. <https://doi.org/10.1007/s10661-021-09529-6>
- Fidelis, A., & Blanco, C. (2014). Does fire induce flowering in Brazilian subtropical grasslands? *Applied Vegetation Science*, 17(4), 690–699. John Wiley & Sons Ltd. <https://doi.org/10.1111/AVSC.12098>
- Fidelis, A., et al. (2022). Fire stimulates grass flowering in the Cerrado independent of season. *Journal of Vegetation Science*, 33(2), e13125. John Wiley & Sons Ltd. <https://doi.org/10.1111/JVS.13125>
- Flores, B. M., et al. (2021). Tropical riparian forests in danger from large Savanna wildfires. *Journal of Applied Ecology*, 58(2). In C. Remy (Ed.), Blackwell Publishing Ltd. <https://doi.org/10.1111/1365-2664.13794>
- Giglio, L., et al. (2018). The collection 6 MODIS burned area mapping algorithm and product. *Remote Sensing of Environment*, 217, 72–85. Elsevier. <https://doi.org/10.1016/J.RSE.2018.08.005>

- Gomes, L., Miranda, H. S., & da Bustamante, M. M. C. (2018). How can we advance the knowledge on the behavior and effects of fire in the Cerrado biome? *Forest Ecology and Management*, 417, 281–290. Elsevier. <https://doi.org/10.1016/j.foreco.2018.02.032>
- Hardesty, J., Myers, R., & Fulks, W. (2005). Fire, ecosystems and people: A preliminary assessment of fire as a global conservation issue. *Fire Management*, 22(4), 78–87. <https://doi.org/10.1177/0146167209351886>
- Hersbach, H., et al. (2020). The ERA5 global reanalysis. *Quarterly Journal of the Royal Meteorological Society*, 146(730), 1999–2049. John Wiley & Sons Ltd. <https://doi.org/10.1002/QJ.3803>
- Hidasi-Neto, J., et al. (2019). Climate change will drive mammal species loss and biotic homogenization in the Cerrado biodiversity hotspot. *Perspectives in Ecology and Conservation*, 17(2), 57–63. Elsevier. <https://doi.org/10.1016/J.PECON.2019.02.001>
- Hirabayashi, Y., et al. (2021). Global exposure to flooding from the new CMIP6 climate model projections. *Scientific Reports*, 11(1), 1–7. Nature Publishing Group. <https://doi.org/10.1038/s41598-021-83279-w>
- Hodnebrog, Ø., et al. (2022). Understanding model diversity in future precipitation projections for South America. *Climate Dynamics*, 58(5–6), 1329–1347. Springer Science and Business Media Deutschland GmbH. <https://doi.org/10.1007/s00382-021-05964-w>
- Hoffmann, W. A., Geiger, E. L., et al. (2012). Ecological thresholds at the Savanna-forest boundary: How plant traits, resources and fire govern the distribution of tropical biomes. *Ecology Letters*, 15(7), 759–768. In F. Lloret (Eds.), John Wiley & Sons, Ltd (10.1111). <https://doi.org/10.1111/j.1461-0248.2012.01789.x>
- Hoffmann, W. A., Jaconis, S. Y., et al. (2012). Fuels or microclimate? Understanding the drivers of fire feedbacks at Savanna-forest boundaries. *Austral Ecology*, 37(6), 634–643. John Wiley & Sons, Ltd (10.1111). <https://doi.org/10.1111/j.1442-9993.2011.02324.x>
- Hofmann, G. S., et al. (2021). The Brazilian Cerrado is becoming hotter and drier. *Global Change Biology*, 27(17), 4060–4073. John Wiley & Sons Ltd. <https://doi.org/10.1111/GCB.15712>
- IPCC. (2021). Climate change 2021: The physical science basis. Contribution of working group I to the sixth assessment report of the intergovernmental panel on climate change. In V. Masson-Delmotte (Ed.), Cambridge University Press. <https://www.ipcc.ch/>
- Jimenez, J. C., et al. (2019) The role of ENSO flavours and TNA on recent droughts over Amazon forests and the Northeast Brazil region. *International Journal of Climatology*, joc.6453. John Wiley and Sons Ltd. <https://doi.org/10.1002/joc.6453>
- Jolly, W. M., et al. (2015). Climate-induced variations in global wildfire danger from 1979 to 2013. *Nature Communications*, 6(1), 7537. Nature Publishing Group. <https://doi.org/10.1038/ncomms8537>
- Kendall, M. G. (1975). *Rank correlation methods* (4th ed.). Griffin.
- Klink, C. A., & Moreira, A. G. (2002). 5. Past and current human occupation, and land use. In C. U. Press (Ed.), *The Cerrados of Brazil* (pp. 69–88). Columbia University Press. <https://doi.org/10.7312/oliv12042-006>.
- Klink, C. A., & Machado, R. B. (2005). A conservação do Cerrado brasileiro. *Megadiversidade*, 1(1), 147–155.
- Lapola, D. M., et al. (2014). Pervasive transition of the Brazilian land-use system. *Nature Climate Change*, 4(1), 27–35. Nature Publishing Group. <https://doi.org/10.1038/nclimate2056>
- Lapola, D. M., et al. (2020). A climate-change vulnerability and adaptation assessment for Brazil's protected areas. *Conservation Biology*, 34(2), 427–437. John Wiley & Sons Ltd. <https://doi.org/10.1111/COBI.13405>
- Lehmann, C. E. R., et al. (2014). Savanna vegetation-fire-climate relationships differ among continents. *Science*, 343(6170), 548–552. American Association for the Advancement of Science. <https://doi.org/10.1126/science.1247355>
- Lenoir, J., & Svenning, J. C. (2015). Climate-related range shifts—a global multidimensional synthesis and new research directions. *Ecography*, 38(1), 15–28. John Wiley & Sons Ltd. <https://doi.org/10.1111/ECOG.00967>

- Li, S., et al. (2020). A pan-South-America assessment of avoided exposure to dangerous extreme precipitation by limiting to 1.5 °C warming. *Environmental Research Letters*, 15(5), 054005. IOP Publishing. <https://doi.org/10.1088/1748-9326/AB50A2>
- Li, S., et al. (2021). Anthropogenic climate change contribution to wildfire-prone weather conditions in the Cerrado and Arc of deforestation. *Environmental Research Letters*, 16(9), 094051. IOP Publishing. <https://doi.org/10.1088/1748-9326/AC1E3A>
- Li, S., et al. (2022). Identifying local-scale meteorological conditions favorable to large fires in Brazil. *Climate Resilience and Sustainability*. 1(1), e11. John Wiley & Sons Ltd. <https://doi.org/10.1002/CLJ2.11>
- Libonati, R., et al. (2021). Twenty-first century droughts have not increasingly exacerbated fire season severity in the Brazilian Amazon. *Scientific Reports*, 11(1), 4400. <https://doi.org/10.1038/s41598-021-82158-8>
- Libonati, R., et al. (2015). An algorithm for burned area detection in the Brazilian Cerrado using 4 μm MODIS imagery. *Remote Sensing*, 7(11), 15782–15803. Multidisciplinary Digital Publishing Institute. <https://doi.org/10.3390/rs71115782>
- Llopart, M., Simões Reboita, M., & Porfírio da Rocha, R. (2020). Assessment of multi-model climate projections of water resources over South America CORDEX domain. *Climate Dynamics*. 54(1–2), 99–116. Springer Verlag. <https://doi.org/10.1007/s00382-019-04990-z>
- Lu, J., Carbone, G. J., & Grego, J. M. (2019). Uncertainty and hotspots in 21st century projections of agricultural drought from CMIP5 models. *Scientific Reports* 2019 9:1. 9(1), 1–12. Nature Publishing Group. <https://doi.org/10.1038/s41598-019-41196-z>
- Maciel, E. A., et al. (2021). Climate change forecasts suggest that the conservation area network in the Cerrado-Amazon transition zone needs to be expanded. *Acta Oecologica*, 112, 103764. Elsevier Masson. <https://doi.org/10.1016/j.actao.2021.103764>
- Mann, H. B. (1945). Nonparametric tests against trend. *Econometrica*, 13(3), 245. <https://doi.org/10.2307/1907187>
- Marengo, J. A., et al. (2022). Increased climate pressure on the agricultural frontier in the Eastern Amazonia-Cerrado transition zone. *Scientific Reports* 2022 12:1, 12(1), 1–10. Nature Publishing Group. <https://doi.org/10.1038/s41598-021-04241-4>
- Marques, E. Q., et al. (2020). Redefining the Cerrado-Amazonia transition: Implications for conservation. *Biodiversity and Conservation*, 29(5), 1501–1517. Springer. <https://doi.org/10.1007/s10531-019-01720-z>
- Mataveli, G. A. V., et al. (2018). Satellite observations for describing fire patterns and climate-related fire drivers in the Brazilian Savannas. *Natural Hazards and Earth System Sciences*. 18(1), 125–144. Copernicus GmbH. <https://doi.org/10.5194/nhess-18-125-2018>.
- Mataveli, G. A. V., et al. (2021). Deforestation and land use and land cover changes in protected areas of the Brazilian Cerrado: Impacts on the fire-driven emissions of fine particulate aerosols pollutants. *Remote Sensing Letters*, 12(1), 79–92. Taylor and Francis Ltd. <https://doi.org/10.1080/2150704X.2021.1875147>
- Menezes, L. S., et al. (2022). Lightning patterns in the Pantanal: Untangling natural and anthropogenic-induced wildfires. *Science of the Total Environment*, 820, 153021. Elsevier. <https://doi.org/10.1016/j.scitotenv.2022.153021>
- Mistry, J., et al. (2019). New perspectives in fire management in South American Savannas: The importance of intercultural governance. *Ambio*, 48(2), 172–179. Springer, Netherlands. <https://doi.org/10.1007/s13280-018-1054-7>
- Mistry, J. (1998). Fire in the cerrado (Savannas) of Brazil: An ecological review. *Progress in Physical Geography: Earth and Environment*, 22(4), 425–448. SAGE Publications. <https://doi.org/10.1177/030913339802200401>
- Myers, N., et al. (2000). Biodiversity hotspots for conservation priorities. *Nature*, 403(6772), 853–858. Nature Publishing Group. <https://doi.org/10.1038/35002501>
- Nardoto, G. B., et al. (2006). Nutrient use efficiency at ecosystem and species level in Savanna areas of central Brazil and impacts of fire. *Journal of Tropical Ecology*, 22(2), 191–201. Cambridge University Press. <https://doi.org/10.1017/S0266467405002865>

- Nogueira, J., et al. (2017). Spatial pattern of the seasonal drought/burned area relationship across Brazilian Biomes: Sensitivity to drought metrics and global remote-sensing fire products. *Climate*, 5(2), 42. Multidisciplinary Digital Publishing Institute. <https://doi.org/10.3390/cli5020042>
- Oliveira, U., et al. (2017). Biodiversity conservation gaps in the Brazilian protected areas. *Scientific Reports*, 7(1), 9141. Nature Publishing Group. <https://doi.org/10.1038/s41598-017-08707-2>
- Oliveira, A. S., et al. (2021). Costs and effectiveness of public and private fire management programs in the Brazilian Amazon and Cerrado. *Forest Policy and Economics*, 127, 102447. Elsevier. <https://doi.org/10.1016/J.FORPOL.2021.102447>
- Oliveira, M. R., et al. (2022). Indigenous brigades change the spatial patterns of wildfires, and the influence of climate on fire regimes. *Journal of Applied Ecology*. John Wiley & Sons, Ltd. <https://doi.org/10.1111/1365-2664.14139>
- Overbeck, G. E., et al. (2015). Conservation in Brazil needs to include non-forest ecosystems. *Diversity and Distributions*, 21(12), 1455–1460. In R. Loyola (Ed.), John Wiley & Sons, Ltd (10.1111). <https://doi.org/10.1111/ddi.12380>
- Pivello, V. R. (2011). The use of fire in the Cerrado and Amazonian rainforests of Brazil: Past and present. *Fire Ecology*, 7(1), 24–39. Springer International Publishing. <https://doi.org/10.4996/fireecology.0701024>
- Pope, R. J., et al. (2020). Substantial increases in eastern Amazon and Cerrado biomass burning-sourced tropospheric ozone. *Geophysical Research Letters*. 47(3), e2019GL084143. John Wiley & Sons, Ltd. <https://doi.org/10.1029/2019GL084143>
- Project MapBiomias. (2020). Collection 5 of Brazilian land cover & use map series. Retrieved October 31, 2020, from <https://mapbiomas.org/>
- Rajão, R., et al. (2020). The rotten apples of Brazil's agribusiness. *Science*. 369(6501), 246–248. American Association for the Advancement of Science. <https://doi.org/10.1126/science.aba6646>
- Ramos-Neto, M. B., & Pivello, V. R. (2000). Lightning fires in a Brazilian Savanna national park rethinking management strategies. *Environmental Management*, 26(6), 675–684. Springer-Verlag, New York. <https://doi.org/10.1007/s002670010124>
- Reboita, M. S., Amaro, T. R., & de Souza, M. R. (2018). Winds: Intensity and power density simulated by RegCM4 over South America in present and future climate. *Climate Dynamics*, 51(1–2), 187–205. Springer Verlag. <https://doi.org/10.1007/s00382-017-3913-5>
- Ridder, N. N., et al. (2022). Increased occurrence of high impact compound events under climate change. *NPJ Climate and Atmospheric Science*, 5(1), 3. Nature Publishing Group. <https://doi.org/10.1038/s41612-021-00224-4>
- Rodrigues, J. A., et al. (2019). How well do global burned area products represent fire patterns in the Brazilian Savannas biome? An accuracy assessment of the MCD64 collections. *International Journal of Applied Earth Observation and Geoinformation*, 78, 318–331. Elsevier. <https://doi.org/10.1016/J.JAG.2019.02.010>
- Rodrigues, J. A. M., et al. (2020). Climate change impacts under representative concentration pathway scenarios on streamflow and droughts of basins in the Brazilian Cerrado biome. *International Journal of Climatology*, 40(5), 2511–2526. John Wiley & Sons Ltd. <https://doi.org/10.1002/JOC.6347>
- Rosan, T. M., et al. (2019). Extensive 21st-century woody encroachment in South America's Savanna. *Geophysical Research Letters*, 46(12), 6594–6603. Blackwell Publishing Ltd. <https://doi.org/10.1029/2019GL082327>
- Rosan, T. M., et al. (2022). Fragmentation-driven divergent trends in burned area in Amazonia and Cerrad. *Frontiers in Forests and Global Change*, 5, 15. Frontiers. <https://doi.org/10.3389/ffgc.2022.801408>
- Sano, E. E., et al. (2019). Cerrado ecoregions: A spatial framework to assess and prioritize Brazilian Savanna environmental diversity for conservation. *Journal of Environmental Management*, 232, 818–828. Academic Press. <https://doi.org/10.1016/j.jenvman.2018.11.108>

- Sano, E. E., et al. (2020). 'Características gerais da paisagem do Cerrado', in Dinâmica agrícola no cerrado: análises e projeções. Brasília, DF: Embrapa, pp. 21–37. Retrieved April 28, 2022, from <http://www.infoteca.cnptia.embrapa.br/handle/doc/1124107>.
- Santana, N. C., et al. (2020). Comparison of post-fire patterns in Brazilian Savanna and tropical forest from remote sensing time series. *ISPRS International Journal of Geo-Information*, 9(11), 659. MDPI AG. <https://doi.org/10.3390/ijgi9110659>
- Santos, F. L. M., et al. (2021). Prescribed burning reduces large, high-intensity wildfires and emissions in the Brazilian Savanna. *Fire*, 4(3), 56. Multidisciplinary Digital Publishing Institute. <https://doi.org/10.3390/fire4030056>
- Schmidt, I. B., Figueiredo, I. B., & Scariot, A. (2007). Ethnobotany and effects of harvesting on the population ecology of *Syngonanthus nitens* (Bong.) Ruhland (Eriocaulaceae), a NTFP from Jalapao region, central Brazil. *Economic Botany*, 61(1), 73–85. New York Botanical Garden Press. [https://doi.org/10.1663/0013-0001\(2007\)61\[73:EAEOHO\]2.0.CO;2](https://doi.org/10.1663/0013-0001(2007)61[73:EAEOHO]2.0.CO;2)
- Schmidt, I. B., et al. (2017). How do the wets burn? Fire behavior and intensity in wet grasslands in the Brazilian Savanna. *Brazilian Journal of Botany*, 40(1), 167–175. Springer International Publishing. <https://doi.org/10.1007/s40415-016-0330-7>
- Schmidt, I. B., et al. (2018). Fire management in the Brazilian Savanna: First steps and the way forward. *Journal of Applied Ecology*, 55(5), 2094–2101. In R. Zenni (Ed.), Blackwell Publishing Ltd. <https://doi.org/10.1111/1365-2664.13118>.
- Schumacher, V., et al. (2022). Characteristics of lightning-caused wildfires in central Brazil in relation to cloud-ground and dry lightning. *Agricultural and Forest Meteorology*, 312, 108723. Elsevier. <https://doi.org/10.1016/J.AGRFORMET.2021.108723>
- Sen, P. K. (1968). Estimates of the regression coefficient based on Kendall's Tau. *Journal of the American Statistical Association*, 63(324), 1379–1389. <https://doi.org/10.1080/01621459.1968.10480934>
- Shlisky, A., et al. (2008). Fire, nature, and humans: Global challenges for conservation. *Fire management today*, 68(4), 36–42. Retrieved April 28, 2022 <http://agris.fao.org/agris-search/search.do?recordID=US201301637384>
- Silva, P., et al. (2016). 'Future Projections of Fire Occurrence in Brazil Using EC-Earth Climate Model', Revista Brasileira de Meteorologia. *Revista Brasileira De Meteorologia*, 31(3), 288–297. <https://doi.org/10.1590/0102-778631320150142>
- Silva, P. S., et al. (2019). Impacts of the 1.5°C global warming target on future burned area in the Brazilian Cerrado. *Forest Ecology and Management*, 446, 193–203. Elsevier. <https://doi.org/10.1016/j.foreco.2019.05.047>
- Silva, P. S., et al. (2021). Putting fire on the map of Brazilian Savanna ecoregions. *Journal of Environmental Management*, 296, 113098. Academic Press. <https://doi.org/10.1016/j.jenvman.2021.113098>
- Silva, P. S., et al. (2020). Drivers of burned area patterns in Cerrado: The case of Matopiba region. *The International Archives of the Photogrammetry, Remote Sensing and Spatial Information Sciences*, XLII-3/W12, 135–140. Copernicus GmbH. <https://doi.org/10.5194/isprs-archives-XLII-3-W12-2020-135-2020>.
- Simon, M. F., et al. (2009). Recent assembly of the Cerrado, a neotropical plant diversity hotspot, by in situ evolution of adaptations to fire. *Proceedings of the National Academy of Sciences*, 106(48), 20359–20364. <https://doi.org/10.1073/pnas.0903410106>
- Simon, M. F., Pennington, T. (2012). Evidence for adaptation to fire regimes in the tropical Savannas of the Brazilian Cerrado. *International Journal of Plant Sciences*, 173(6), 711–723. University of Chicago Press Chicago, IL. <https://doi.org/10.1086/665973>
- Siqueira, P. P., et al. (2021). Effects of climate and land cover changes on water availability in a Brazilian Cerrado basin. *Journal of Hydrology: Regional Studies*, 37, 100931. Elsevier. <https://doi.org/10.1016/J.EJRH.2021.100931>
- Soterroni, A. C., et al. (2019). Expanding the soy moratorium to Brazil's Cerrado. *Science Advances*, 5(7), 7336–7353. American Association for the Advancement of Science. <https://doi.org/10.1126/sciadv.aav7336>

- Spera, S. A., Winter, J. M., & Partridge, T. F. (2020). Brazilian maize yields negatively affected by climate after land clearing. *Nature Sustainability*, 3(10), 845–852. Nature Publishing Group. <https://doi.org/10.1038/s41893-020-0560-3>
- Strassburg, B. B. N., Latawiec, A., & Balmford, A. (2016). Brazil: Urgent action on Cerrado extinctions. *Nature*, 540(7632), 199–199. <https://doi.org/10.1038/540199A>
- Strassburg, B. B. N., et al. (2017). Moment of truth for the Cerrado hotspot. *Nature Ecology & Evolution*, 1(4), 0099. <https://doi.org/10.1038/s41559-017-0099>
- Theil, H. (1950). A rank-invariant method of linear and polynomial regression analysis, 3; confidence regions for the parameters of polynomial regression equations. *Indagationes Mathematicae*, 1(2), 467–482.
- Trigueiro, W. R., Nabout, J. C., & Tessarolo, G. (2020). Uncovering the spatial variability of recent deforestation drivers in the Brazilian Cerrado. *Journal of Environmental Management*, 275, 111243. Academic Press. <https://doi.org/10.1016/j.jenvman.2020.111243>
- United Nations Environment Programme. (2022). Spreading like wildfire: The rising threat of extraordinary landscape fires. Nairobi. <https://www.unep.org/resources/report/spreading-wildfire-rising-threat-extraordinary-landscape-fires>
- Van Wilgen, B. W., et al. (2007). The contribution of fire research to fire management: A critical review of a long-term experiment in the Kruger national park, South Africa. *International Journal of Wildland Fire*, 16(5), 519–530. CSIRO Publishing. <https://doi.org/10.1071/WF06115>
- Velazco, S. J. E., et al. (2019). A dark scenario for Cerrado plant species: Effects of future climate, land use and protected areas ineffectiveness. *Diversity and Distributions*, 25(4), 660–673. John Wiley & Sons Ltd. <https://doi.org/10.1111/DDI.12886>
- Veldman, J. W., et al. (2015). Tyranny of trees in grassy biomes. *Science*, 347(6221), 484–485. American Association for the Advancement of Science. <https://doi.org/10.1126/science.347.6221.484-c>
- Veldman, J. W., et al. (2019). Comment on “The global tree restoration potential”. *Science*, 366(6463). American Association for the Advancement of Science. <https://doi.org/10.1126/SCIENCE.AAY7976>
- Vogel, M. M., Hauser, M., & Seneviratne, S. I. (2020). Projected changes in hot, dry and wet extreme events’ clusters in CMIP6 multi-model ensemble. *Environmental Research Letters*, 15(9), 094021. IOP Publishing. <https://doi.org/10.1088/1748-9326/AB90A7>
- Wade, C. M., et al. (2020). What is threatening forests in protected areas? A global assessment of deforestation in protected areas, 2001–2018. *Forests*, 11(5), 539. Multidisciplinary Digital Publishing Institute. <https://doi.org/10.3390/f11050539>
- Zappa, G., Bevacqua, E., & Shepherd, T. G. (2021). Communicating potentially large but non-robust changes in multi-model projections of future climate. *International Journal of Climatology*, 41(6), 3657–3669. John Wiley & Sons Ltd. <https://doi.org/10.1002/JOC.7041>
- Zilli, M. et al., (2020). The impact of climate change on Brazil’s agriculture. *Science of the Total Environment*, 740, 139384. Elsevier. <https://doi.org/10.1016/J.SCITOTENV.2020.139384>

**Patrícia S. Silva** is a Ph.D. student at the Faculty of Sciences, University of Lisbon. She graduated in Energy and Environmental Engineering and has been doing research on fire activity in the Brazilian savannas for more than nine years. This resulted in four scientific papers she has authored on the Cerrado biome, and a contribution to the United Nations Environmental Programme’s report “Spreading like Wildfire: The Rising Threat of Extraordinary Landscape Fires”.

**Dr. Renata Libonati** received her B.Sc. and Ph.D. degrees in Geophysics from the University of Lisbon, in 2005 and 2011, respectively and is currently an Assistant Professor with the Department of Meteorology, Federal University of Rio de Janeiro, and also part of the research team of the Forest Ecology Group from the Institute of Agronomy (Portugal) and of the Instituto Dom

Luiz, University of Lisbon. She is currently core member of the WMO Expert Team on Climate Monitoring and Assessment (ET-CMA) and an Associate Member of WMO Inter-Programme Expert Team on Satellite Utilization and Products (IPET-SUP). Her research activities focus on remote sensing of active fires and burned areas by satellite, the recovery of vegetation after large wildfires, the meteorological conditions associated with extreme events (droughts, heatwaves) and how these phenomena are related to impacts on human health and vegetation fires. She is currently funded by FAPERJ Young Scientist Fellowship and by CNPQ Productivity Grant.

**Dr. Isabel B. Schmidt** is a Biologist with Master and Ph.D. in Plant Ecology, and Associate Professor at the Ecology Department of the University of Brasília. Has worked as an environmental manager for the Brazilian environmental agency and has help the implementation of fire management in the Brazilian savanna.

**Dr. Joana Nogueira** Ph.D. in Ecology and Biodiversity from the University of Montpellier, France, working with Landscape Ecology, Remote Sensing and Fire Ecology in tropical savannas. Bachelor in Biology and Master in Plant Ecophysiology from the Federal University of Lavras, Brazil, and Postdoctoral Researcher from the University of Münster, Germany. Currently she is a scientific collaborator at the Laboratory of Environmental Satellite Applications (LASA) at the Federal University of Rio de Janeiro - UFRJ, Brazil, and works as Geodata Analyst in a sustainable energy company in Germany.

**Dr. Carlos C. DaCamara** BSc in Physics (1979) by the University of Lisbon (FCUL), License in Geophysics (1981) by the University of Lisbon (FCUL), PhD in Atmospheric Science (1991) by the University of Missouri-Columbia (USA). He is an Associate Professor at the Department of Geographic Engineering, Geophysics and Energy at the Faculty of Sciences of the University of Lisbon (DEGGE-FCUL), where he has been lecturing a wide range of subjects in the fields of Meteorology, Climatology, Remote Sensing, Physics (Continuum and Fluid Mechanics, Thermodynamics, Radiation) and Numerical Modelling. His research has been dedicated to climate dynamics, climate extremes, fire meteorology, meteorological fire danger, burned area monitoring from space and land surface temperature and emissivity retrieval from satellite data.



# Annex B

## Contribution to UNEP (2022)



UN  
environment  
programme

5  
1972-2022



GRID  
ARENAL

A UNEP Partner



A RAPID RESPONSE ASSESSMENT

# SPREADING LIKE WILDFIRE

## THE RISING THREAT OF EXTRAORDINARY LANDSCAPE FIRES





Ministry for Foreign  
Affairs of Finland



NICFI Norway's  
International Climate  
and Forest Initiative

© 2022 United Nations Environment Programme

ISBN:

This publication may be reproduced in whole or in part and in any form for educational or nonprofit services without special permission from the copyright holders, provided acknowledgement of the source is made. The United Nations Environment Programme would appreciate receiving a copy of any publication that uses this publication as a source.

No use of this publication may be made for resale or any other commercial purpose whatsoever without prior permission in writing from the United Nations Environment Programme. Applications for such permission, with a statement of the purpose and extent of the reproduction, should be addressed to the Director, Communication Division, United Nations Environment Programme, P. O. Box 30552, Nairobi 00100, Kenya.

#### Disclaimers

The designations employed and the presentation of the material in this publication do not imply the expression of any opinion whatsoever on the part of the Secretariat of the United Nations concerning the legal status of

any country, territory or city or area or its authorities, or concerning the delimitation of its frontiers or boundaries. For general guidance on matters relating to the use of maps in publications please go to <http://www.un.org/Depts/Cartographic/english/htmain.htm>

Mention of a commercial company or product in this document does not imply endorsement by the United Nations Environment Programme or GRID-Arendal. The use of information from this document for publicity or advertising is not permitted. Trademark names and symbols are used in an editorial fashion with no intention on infringement of trademark or copyright laws.

The views expressed in this publication are those of the authors and do not necessarily reflect the views of the United Nations Environment Programme or GRID-Arendal. We regret any errors or omissions that may have been unwittingly made.

© Maps, photos and illustrations as specified

Suggested citation: United Nations Environment Programme (2022). *Spreading like Wildfire – The Rising Threat of Extraordinary Landscape Fires*. A UNEP Rapid Response Assessment. Nairobi.



# **SPREADING LIKE WILDFIRE**

## **THE RISING THREAT OF EXTRAORDINARY LANDSCAPE FIRES**

A RAPID RESPONSE ASSESSMENT

### **Contents**

Foreword .....	6
Summary .....	8
Recommendations .....	13
Chapter 1 – Our planet on fire .....	19
Chapter 2 – The changing pattern of wildfires .....	29
Chapter 3 – Impacts of wildfires on people .....	55
Chapter 4 – Impacts of wildfires on the environment .....	67
Chapter 5 – Risk mitigation and wildfire management .....	81
Appendix .....	96
References .....	97

## Editors

Andrew Sullivan, Commonwealth Scientific and Industrial Research Organisation (CSIRO), Canberra  
Elaine Baker, GRID-Arendal at The University of Sydney  
Tiina Kurvits, GRID-Arendal

## Contributing authors (alphabetical order)

Alexandra Popescu, United Nations Environment Programme (UNEP)  
Alison K. Paulson, University of California, Davis  
Amy Cardinal Christianson, Canadian Forest Service (Natural Resources Canada)  
Andrew Sullivan, Commonwealth Scientific and Industrial Research Organisation (CSIRO), Canberra  
Ayesha Tulloch, University of Sydney  
Bibiana Bilbao, Universidad Simón Bolívar, Caracas  
Camilla Mathison, Met Office, UK  
Catherine Robinson, Commonwealth Scientific and Industrial Research Organisation (CSIRO), Brisbane  
Chantelle Burton, Met Office, UK  
David Ganz, RECOFTC  
David Nangoma, African Parks  
David Saah, University of San Francisco  
Dolors Armenteras, National University of Colombia  
Don A. Driscoll, Deakin University  
Don L. Hankins, California State University  
Douglas I. Kelley, UK Centre for Ecology and Hydrology  
E.R. (Lisa) Langer, Scion (New Zealand Forest Research Institute)  
Elaine Baker, GRID-Arendal at The University of Sydney  
Fabienne Reisen, Commonwealth Scientific and Industrial Research Organisation (CSIRO), Melbourne  
François-Nicolas Robinne, Canadian Forest Service  
Gamma Galudra, RECOFTC  
Glynis Humphrey, University of Cape Town  
Hugh Safford, Vibrant Planet, University of California, Davis, and US Forest Service (retired)  
Ian G. Baird, University of Wisconsin  
Imma Oliveras, University of Oxford  
Jeremy Littell, US Geological Survey  
Johan Kieft, United Nations Environment Programme (UNEP)  
Joshua Chew, The University of Sydney  
Kirsten Maclean, Commonwealth Scientific and Industrial Research Organisation (CSIRO), Brisbane  
Lea Wittenberg, University of Haifa  
Liana O. Anderson, National Center for Monitoring and Early Warning of Natural Disasters  
Lindsey Gillson, University of Cape Town  
Matt Plucinski, Commonwealth Scientific and Industrial Research Organisation (CSIRO), Canberra  
Max Moritz, University of California, Santa Barbara  
Megan Brown, Open University, UK  
Miguel Castillo Soto, University of Chile  
Mike Flannigan, University of Alberta and The Canadian Partnership for Wildland Fire Science, currently at Thompsons Rivers University  
Oliver Costello, Jagun Alliance Aboriginal Corporation, Australia  
Patrícia S. Silva, University of Lisbon  
Paulo Fernandes, Universidade de Trás-os-Montes e Alto Douro and ForestWISE – Collaborative Laboratory for Integrated Forest & Fire Management  
Peter Moore, Food and Agriculture Organization (FAO) of the United Nations  
Randi Jandt, Alaska Fire Science Consortium  
Raphaela Bianchi, Commonwealth Scientific and Industrial Research Organisation (CSIRO), Melbourne  
Renata Libonati, Universidade Federal do Rio de Janeiro  
Sally Archibald, University of the Witwatersrand  
Sarah Dunlop, University of Western Australia  
Sarah McCaffrey, US Forest Service  
Susan Page, University of Leicester

Tania Marisol González Delgado, National University of Colombia  
Tiina Kurvits, GRID-Arendal  
Tol Sokchea, RECOFTC  
Val Charlton, LandWorks

### **Lead data analyst**

Douglas I. Kelley, UK Centre for Ecology and Hydrology

### **Project coordinators**

Tiina Kurvits, GRID-Arendal  
Sam Barratt, United Nations Environment Programme (UNEP)

### **Reviewers**

Adam Leavesley, Bushfire and Natural Hazards Cooperative Research Centre, Australian Capital Territory  
Andrea Hinwood, United Nations Environment Programme (UNEP)  
Julian Blanc, United Nations Environment Programme (UNEP)  
David Bowman, University of Tasmania  
Dianna Kopansky, United Nations Environment Programme (UNEP)  
Elizabeth Sellwood, United Nations Environment Programme (UNEP)  
Gabriel Labbate, United Nations Environment Programme (UNEP)  
Jay Mistry, Leverhulme Centre for Wildfires, Environment and Society, Imperial College of London  
Jessica L. McCarty, Miami University  
Jon Keeley, US Geological Survey  
Julian Blanc, United Nations Environment Programme (UNEP)  
Lachie McCaw, Department of Biodiversity, Conservation and Attractions, Government of Western Australia  
Matthew Thompson, US Forest Service  
Petina Pert, Commonwealth Scientific and Industrial Research Organisation (CSIRO), Townsville  
Stefan Doerr, University of Swansea  
Tom Smith, London School of Economics

### **Cartographers**

Federico Labanti, Studio Atlantis  
Kristina Thygesen, GRID-Arendal  
Nieves López Izquierdo, Studio Atlantis

## Case study: The changing fire regime in the Brazilian Cerrado



The Cerrado is a Brazilian tropical savanna – a fire-prone biome that covers almost 2 million km<sup>2</sup> of which less than 60 per cent remains as natural vegetation (Strassburg et al. 2017). Only 3 per cent of the original area

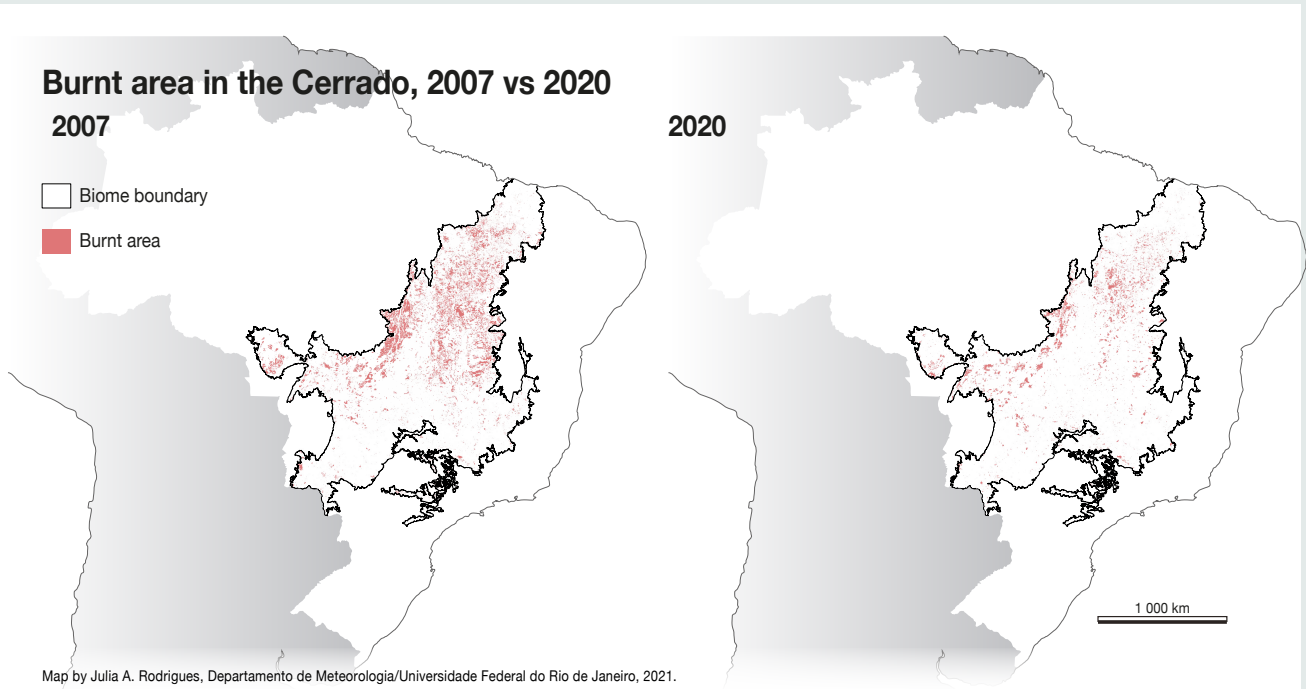
is currently protected (Ferreira et al. 2020), although the Cerrado is considered the most botanically diverse savanna and is recognised as a biodiversity hotspot. The region experiences increased fire activity from August to October and has historically accounted for more than half of Brazil's annual burnt area (Figure 2.5). The use of fire for land conversion is common, and the highest fire activity is observed in regions where most of the biome's natural vegetation cover remains, along the new agricultural frontier ("MATOPIBA", the region comprising the Brazilian state of Tocantins and some parts of the states of Maranhão, Piauí and Bahia) and in the transitional area between the Cerrado and Amazonia biomes (also known as the Arc of Deforestation) (Silva et al. 2021).

In recent years, increased deforestation for agriculture, fire suppression policies, and regional climate changes have

led to an increasingly altered fire regime (Pivello 2011). Late dry season fires have become more frequent in many regions of the Cerrado, with extreme wildfires occurring every two to three years, burning both fire-resistant and fire-sensitive vegetation (Schmidt and Eloy 2020).

The Cerrado is projected to experience increasing temperatures, lower relative humidity, and altered precipitation regimes for the remainder of the century (Silva et al. 2016). A recent study suggests that weather factors are responsible for more than two-thirds of inter-annual variability in the Cerrado burnt area (Silva et al. 2019). Using IPCC's climate change scenarios (RCP2.6, RCP4.5, and RCP8.5), the burnt area is expected to increase in the Cerrado, associated with a higher probability of extreme events (see Figure 2.6 for an explanation of the RCPs). The medium CO<sub>2</sub> stabilization scenario, RCP4.5, indicated a 39 per cent increase in the burnt area by 2100, while the most ambitious CO<sub>2</sub> mitigation scenario, RCP2.6, resulted in a 22 per cent increase by 2050 compared with the historical period, followed by a decrease to 11 per cent by 2100. The conditions predicted under RCP2.6 show the importance of limiting global warming to 1.5°C by the end of the century to minimise the environmental and social costs associated with wildfires in the Cerrado.





### Contribution of the Cerrado to Brazil's annual burnt area, 2001–2019

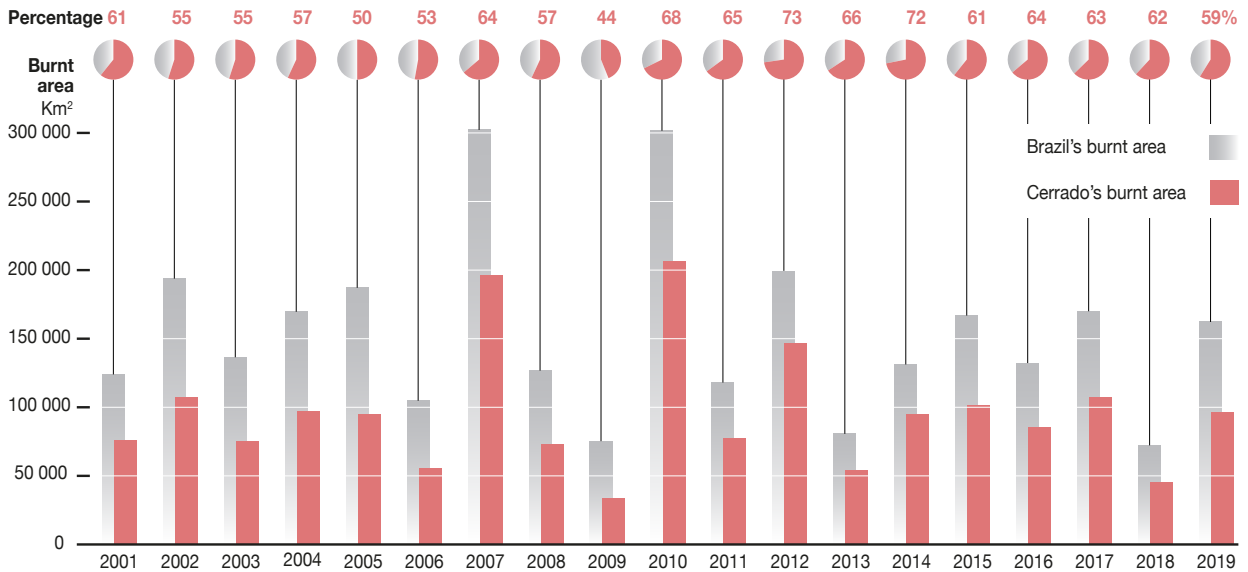


Illustration by Patrícia S. Silva, Instituto Dom Luiz/Universidade de Lisboa, 2021.

Source: MODIS Collection 6 MCD64A1 Burned Area product (Giglio et al. 2018).

GRID-Arendal/Studio Atlantis, 2021

**Figure 2.5.** Top: Difference in fire activity in an ordinary (2020) and extraordinary (2007) year in the Cerrado. Changes in the burnt area reflect the occurrence of wildfires in 2007. Bottom: The inter-annual variability of burnt area in Brazil from 2001–2019 is shown in grey and the corresponding percentage from the Cerrado is shown in red. All panels use the MCD64A1 500m product.



## Case study: Burning a wetland – the Pantanal



Stretching across Brazil and parts of Bolivia and Paraguay, the Pantanal is the world's largest tropical wetland, covering around 15 million hectares. Parts of the Pantanal have been designated a biosphere

conservation area and recognised as a United Nations Educational, Scientific and Cultural Organization (UNESCO) World Heritage site. The area is home to thousands of endangered species such as the jaguar (*Panthera onca*), the giant otter (*Pteronura brasiliensis*), the marsh deer (*Blastocerus dichotomus*), and the hyacinth macaws (*Anodorhynchus hyacinthinus*), and has the greatest concentration of wildlife in South America. The Pantanal is also a key migratory route of terrestrial and aquatic bird species.

Since 2019, the Pantanal has experienced a severe drought (Marengo et al. 2021). In 2020, the coincidence of hot and dry conditions pushed vegetation combustibility thresholds to their highest since 1980 (Libonati et al. 2020a). These conditions, combined with a lack of appropriate management, resulted in the intense and widespread fires of 2020 – the highest fire year recorded between 2001 and 2020 (Garcia et al. 2021). The fires, which in most cases were deliberately lit, consumed almost one-third of the biome – approximately 4 million hectares (Figure 4.3; Libonati et al. 2020a). Large areas of Indigenous lands and converted areas were extensively burnt, devastating the habitat of many endangered species. Protected areas such as the “Encontro das Águas” (the Meeting of Waters) State Park, an area with the highest feline density in the world, burnt entirely (Libonati et al. 2020b). It will take several months to assess the total extent of plant and animal loss across the area, but already there are indications that the impact will be extensive and long-lasting, giving rise to concerns that this biodiversity hotspot may not be able to fully recover from these extreme fires (Mega 2020).



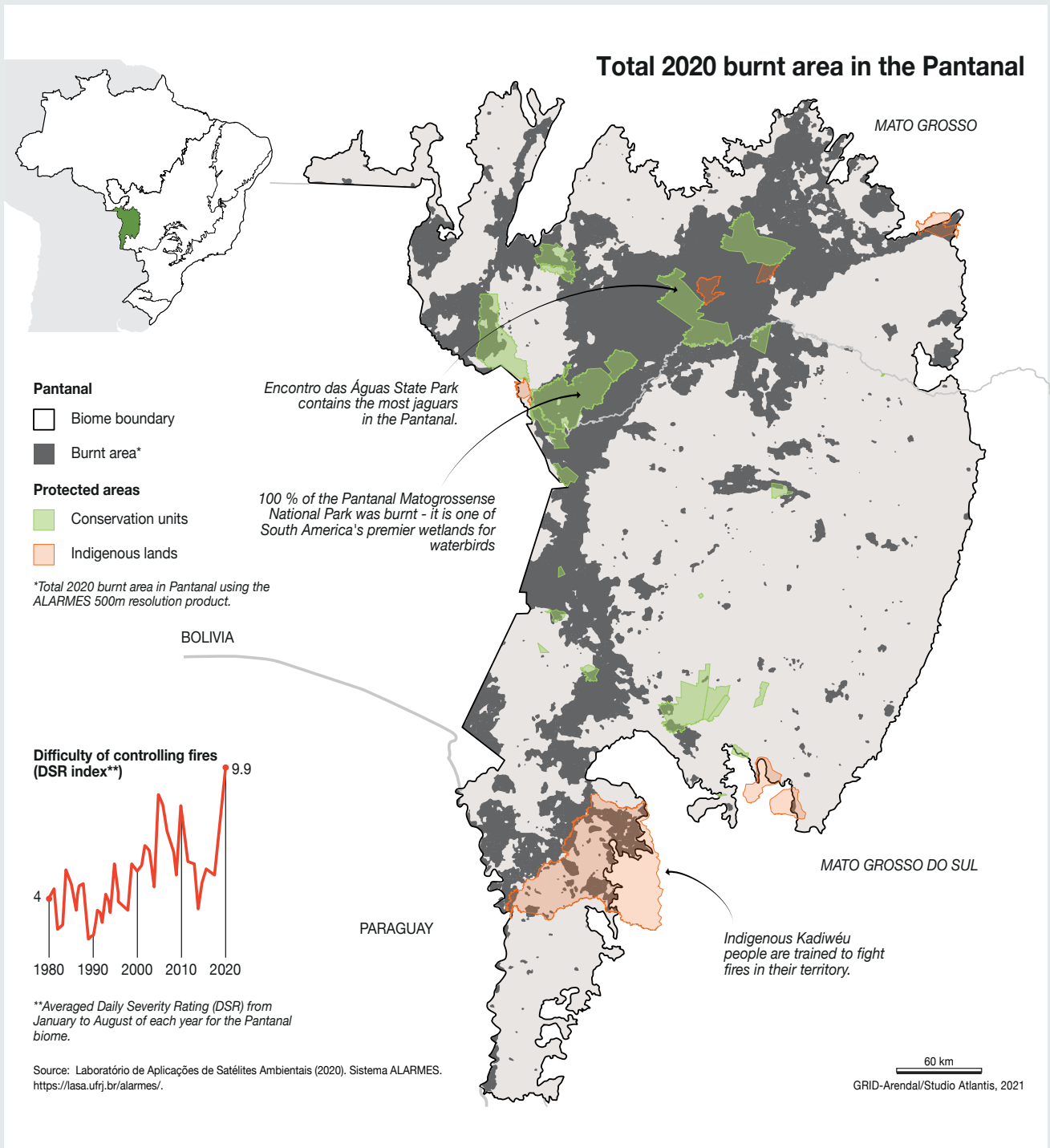










**Figure 4.3.** Total 2020 burnt area in the Pantanal using the ALARMES 500m resolution product. Conservation units and Indigenous lands are shown in green and orange, respectively. The bottom left graph shows Pantanal's average Daily Severity Rating (DSR) from January to August each year, estimated using the ERA5 reanalysis product (Libonati et al. 2020a). DSR is a numeric rating of the difficulty of controlling fires.

## Annex C

Libonati et al. (2022a)

## REVIEW

# Drought–heatwave nexus in Brazil and related impacts on health and fires: A comprehensive review

Renata Libonati<sup>1,2,3</sup>  | João L. Geirinhas<sup>2,#</sup>  | Patrícia S. Silva<sup>2,#</sup>  |  
 Djacinto Monteiro dos Santos<sup>1,#</sup> | Julia A. Rodrigues<sup>1</sup> | Ana Russo<sup>2</sup>  |  
 Leonardo F. Peres<sup>1</sup>  | Luiza Narcizo<sup>1</sup> | Monique E. R. Gomes<sup>1</sup> |  
 Andreza P. Rodrigues<sup>4</sup> | Carlos C. DaCamara<sup>2</sup>  | José Miguel C. Pereira<sup>3,5</sup>  |  
 Ricardo M. Trigo<sup>1,2</sup> 

<sup>1</sup>Departamento de Meteorologia, Universidade Federal do Rio de Janeiro, Rio de Janeiro, Brazil

<sup>2</sup>Instituto Dom Luiz, Faculdade de Ciências, Universidade de Lisboa, Lisbon, Portugal

<sup>3</sup>Forest Research Centre, School of Agriculture, University of Lisbon, Lisbon, Portugal

<sup>4</sup>Escola de Enfermagem Anna Nery, Universidade Federal do Rio de Janeiro, Rio de Janeiro, Brazil

<sup>5</sup>TERRA Associate Laboratory, Tapada da Ajuda, Portugal

## Correspondence

Renata Libonati, Universidade Federal do Rio de Janeiro – Meteorology, Cidade Universitária, Rio de Janeiro 21941-901, Brazil.  
 Email: [renata.libonati@igeo.ufrj.br](mailto:renata.libonati@igeo.ufrj.br)

#These authors contributed equally to this work.

## Funding information

Fundação Oswaldo Cruz, Grant/Award Number: VPPCB-003-FIO-19; Fundação Carlos Chagas Filho de Amparo à Pesquisa do Estado do Rio de Janeiro, Grant/Award Number: E26/202.714/2019; Conselho Nacional de Desenvolvimento Científico e Tecnológico, Grant/Award Number: 311487/2021-1; Fundação para a Ciência e a Tecnologia, Grant/Award Numbers: 2020.05198.BD, JPIOCEANS/0001/2019, PTDC/CTA-CLI/28902/2017, SFRH/BD/146646/2019, UIDB/50019/2020

## Abstract

Climate change is drastically altering the frequency, duration, and severity of compound drought-heatwave (CDHW) episodes, which present a new challenge in environmental and socioeconomic sectors. These threats are of particular importance in low-income regions with growing populations, fragile infrastructure, and threatened ecosystems. This review synthesizes emerging progress in the understanding of CDHW patterns in Brazil while providing insights about the impacts on fire occurrence and public health. Evidence is mounting that heatwaves are becoming increasingly linked with droughts in northeastern and southeastern Brazil, the Amazonia, and the Pantanal. In those regions, recent studies have begun to build a better understanding of the physical mechanisms behind CDHW events, such as the soil moisture–atmosphere coupling, promoted by exceptional atmospheric blocking conditions. Results hint at a synergy between CDHW events and high fire activity in the country over the last decades, with the most recent example being the catastrophic 2020 fires in the Pantanal. Moreover, we show that HWs were responsible for increasing mortality and preterm births during record-breaking droughts in southeastern Brazil. This work paves the way for a more in-depth understanding on CDHW events and their impacts, which is crucial to enhance the adaptive capacity of different Brazilian sectors.

## KEYWORDS

compound events, droughts, fires, health, heatwaves

## INTRODUCTION

Heatwave (HW) events are typically defined as prolonged periods where temperatures are substantially hotter than a specific climatological threshold.<sup>1</sup> The frequency, duration, and severity of such extreme climate events have substantially risen since the middle of the 20th century due to the observed global warming.<sup>2</sup> The intensity of heat-related extremes significantly increased during the last four decades globally, with the fastest rates being observed in the tropical and polar zones.<sup>3</sup> Prolonged periods of excessive heat pose a serious challenge for public health,<sup>4,5</sup> the economy,<sup>6</sup> and terrestrial and marine ecosystems.<sup>7,8</sup> Studies show evidence of the impact of temperature on health, especially in hospitalizations and mortality.<sup>9–14</sup> The effects on society may vary according to the vulnerability of individuals or social groups due to factors, such as the social, economic, and political scenario, in addition to age, gender, and pre-existing diseases.<sup>15</sup> Recent HW episodes have affected billions of people worldwide, particularly in densely populated urban settlements located in both tropical and mid-latitude regions.<sup>16,17</sup> Excessive heat can impact the human body, leading to death,<sup>18,19</sup> with more vulnerable people, such as the elderly, the poorest, and those suffering from additional comorbidity factors, such as cardiovascular, respiratory, or diabetic diseases,<sup>20,21</sup> at higher risk. Even low-intensity HW episodes may increase mortality, particularly in regions with hot and humid summers.<sup>22</sup> In addition to deaths, extreme heat is known to influence human cognitive performance,<sup>23</sup> mental health and suicide rates,<sup>24</sup> work-related injuries and illnesses,<sup>25</sup> the normal gestational period,<sup>26</sup> and the number of premature births.<sup>27</sup> Recent evidence also links HW episodes with the dynamics of dengue mosquito outbreaks in tropical regions,<sup>28,29</sup> and with the intensification of urban heat islands.<sup>30</sup> HWs are often associated with a lack of rainfall and large evaporation rates, which can increase vegetation flammability and favor the occurrence of vegetation fires.<sup>31–33</sup> A large amount of particulate matter and gases released into the atmosphere during vegetation fires increases the levels of air pollution which, in turn, contributes to an increase in mortality and hospitalizations due to respiratory diseases,<sup>34,35</sup> evidencing a cascade effect of HW episodes on human health. There are several other heat-related effects on terrestrial and marine ecosystems, such as long-lasting changes in forest productivity<sup>36</sup> and increases in harmful algal blooms<sup>37</sup> and coral bleaching.<sup>38</sup> Economic heat-related impacts include increases in electricity demand,<sup>39</sup> vulnerability of electricity supply,<sup>40</sup> crop losses,<sup>41,42</sup> weakening of the tourism sector,<sup>43</sup> and water scarcity.<sup>44</sup>

Evidence is mounting that HWs are becoming increasingly linked with drought episodes in many parts of the world, particularly in transition zones between wet and dry climates.<sup>45–50</sup> Independently of their temporal and spatial scales, the occurrence of both events in a compound manner is usually linked to local land–atmospheric interactions triggered by large-scale atmospheric circulation anomalies responsible for persistent clear sky conditions and strong subsidence and advection of warm air.<sup>51–53</sup> Recent results point out that over the last two decades, many regions in Europe and the Americas had over 2/3 of their areas under increased susceptibility to HWs during drought episodes.<sup>54</sup> In accordance with the Intergovernmental

Panel on Climate Change (IPCC), which considers compound events as “the combination of multiple drivers and/or hazards that contribute to societal or environmental risk,”<sup>55</sup> the periods characterized by simultaneous extreme hot and dry conditions were defined here as compound drought-heatwave (CDHW) events. Those CDHW events are shown to cause considerably more impacts than those related to the occurrence of an isolated event.<sup>56</sup> The last IPCC report<sup>55</sup> states that CDHW episodes have been more frequent over the last century and that there is high confidence that this trend will persist with higher global warming. Several studies also reveal the enhanced impacts of CDHW events on vegetation productivity,<sup>57,58</sup> tree mortality,<sup>59</sup> food and water supply,<sup>60</sup> health,<sup>61</sup> vegetation fires, and air pollution,<sup>62</sup> among others. Compound extremes and their associated impacts occur in a complex chain of interactions shaped not only by physical and environmental drivers, but also dependent on population exposure, governance, and infrastructure.<sup>63</sup> In contrast to single-hazard analyses, the investigation of multiple hazards poses additional challenges due to the diversity of processes and spatial-temporal scales involved.<sup>56,64</sup> Given the complexity of the such interplay between events, a multidisciplinary approach is required, involving the understanding of societal or environmental impacts, climate-related hazards, drivers of these hazards, and, finally, the modulators of the drivers.<sup>56,65</sup>

Over the course of the last two decades, evidence of CDHW events has been well documented regionally, mainly for the northern hemisphere, and their impacts on vegetation, vegetation fires, and human health have been studied extensively in North America,<sup>66–70</sup> Asia,<sup>71–75</sup> and Europe.<sup>76–83</sup> Although CDHW occurrences have been amplified considerably during the 21st century in both hemispheres,<sup>54,84</sup> compound events analysis in the southern hemisphere is still underexplored and poorly understood, despite the recent efforts conducted for Australia<sup>85,86</sup> and some sectors of Brazil.<sup>33,87,88</sup> Accordingly, few studies have been devoted to the characterization, modeling, and impact evaluation of these compound events over South America (SA), despite its size (i.e., larger than Europe or Australia) and a large number of densely populated regions. Nevertheless, in the past decade, the number of studies focusing on individual extreme climate events of high temperature and low precipitation in different regions of Brazil has increased notably. For instance, studies have analyzed the observed changes in both the temperature and precipitation extremes over Brazil, although employing a single and separate hazard perspective.<sup>89,90</sup>

Among them, drought studies are generally the main topic considered. For instance, in the last two decades, droughts over Amazonia,<sup>91–93</sup> Northeast<sup>94,95</sup> and Southeast Brazil,<sup>96–98</sup> and the Pantanal<sup>99,100</sup> have been thoroughly analyzed from an individual perspective of drivers and impacts. More recently, a number of studies regarding drought-related events have also reported direct and indirect harmful impacts on the environment, economy, and society. For example, fires in the Brazilian Amazonia increased dramatically during the strong drought years of 2005, 2007, and 2010,<sup>101,102</sup> as well as in the Pantanal during 2020.<sup>103,104</sup> Reduction in tree growth and forest productivity are connected with recurrent drought episodes in Amazonia, leading to the reduction in biomass carbon uptake.<sup>105,106</sup>

From a health impact perspective, drought is considered as one of the most far-reaching natural disasters that threaten the Brazilian population, mainly linked to food and water scarcity, vector-borne infectious diseases, and respiratory health effects.<sup>107,108</sup> From 2001 to 2016, there was an increase of 27% in hospital admissions for respiratory diseases affecting children and the elderly related to drought and fire in southern Amazonia.<sup>34</sup> Fire smoke is also associated with birth defects, including cleft lip/cleft palate and congenital anomalies of both respiratory and nervous systems.<sup>109,110</sup> In addition, adverse birth outcomes were recently related to dry periods in the Amazonia,<sup>111</sup> and a positive association between drought exposure and mortality was evidenced in the population of the main Brazilian metropolitan regions between 2000 and 2019.<sup>112</sup> Recent studies show that crop production from the Amazonia-Cerrado region, which is one of the largest agricultural regions in the world, is highly vulnerable to droughts.<sup>113,114</sup> The recurrent, intense, and severe drought events during the last decade have also critically impacted hydroelectricity generation in almost all Brazilian regions.<sup>115</sup>

Compared to drought events, relatively few studies in Brazil have focused on HW modeling and interpretation, with the majority of these published since 2011.<sup>116–122</sup> By contrast, most of the HW-related studies in Brazil mainly focus on public health impacts.<sup>21,119,123–133</sup> Besides health-related studies in the country, a few studies show HW impacts on agriculture,<sup>134</sup> food production,<sup>135</sup> and fires.<sup>33</sup> The overwhelming majority of health-related assessments address HWs and excess deaths, although the results are mainly limited to the southeastern Brazilian states of São Paulo and Rio de Janeiro. Regardless of the HW definition used, all those studies suggest an excess of deaths due to extreme heat in both cities, highlighting the elderly and the least educated as the most vulnerable groups. The highest mortality rates during HW events are mainly linked to circulatory illnesses and diabetes.<sup>128,129</sup> Rural and urban populations also show different susceptibility to high-temperature events in those regions, suggesting the role of the heat-island effect in exacerbating HW impacts.<sup>136</sup> Comprehensive country-level analyses showed that the risk of hospitalization during HW events is mainly for children, the elderly, and pregnant women.<sup>126</sup> It has also been shown that the effects on mortality risk last for almost 3–4 days after the end of an HW event.<sup>125</sup> By the end of this century, Brazil will experience a more than doubling of heat-related health stress, due to the increased severity of natural hazards and ongoing population growth.<sup>137</sup>

Although the response of compound weather and climate events to climate change is challenging, recent studies point out that the entire globe will experience increased occurrences of CDHW episodes,<sup>138</sup> mainly driven by regional precipitation trends.<sup>139</sup> Globally, the future frequency of such events is estimated to increase by 37%, with an increase in warming from 1.5 to 2°C.<sup>140</sup> By the end of this century, between 1/3 and half of the global land area, depending on the mitigation scenario, is estimated to be exposed to deadly temperatures and drought conditions for more than 20 days per year, exposing around half to two-thirds of the world's human population.<sup>141</sup> Depending on the rates of warming and population growth over the coming 50 years, around 1–3 billion people are expected to find themselves in areas

outside the range of climatic conditions acceptable for humans.<sup>142</sup> By mid-century, CDHW impacts on the economy may increase drastically, compared to current estimates.<sup>6</sup> However, these future changes may be underestimated in tropical and subtropical regions,<sup>138,143</sup> suggesting that the risk for developing tropical countries, like Brazil, will likely be worse than previously assessed. Due to the strong impacts of drought and heat extremes, the lack of adaptive capacity will become critical in regions where growing population, poor infrastructure, fragile public health systems, and threatened natural ecosystems are extensively exposed to extreme events,<sup>2</sup> particularly the extreme heat ones.<sup>141</sup> Therefore, improving knowledge about the joint occurrence of drought and HW events in tropical regions, particular in SA and specifically in Brazil, is an important prerequisite for the development and maintenance of strong strategies to predict and mitigate the associated impacts.

By recognizing and addressing current knowledge gaps, here we provide a comprehensive compilation of the most recent assessments of CDHW events in Brazil. On the one hand, we pinpoint the most vulnerable areas within this very large country and its wide range of ecosystems; additionally, we contribute to the assessment and quantification of the impacts on public health and on vegetation fires of record-breaking CDHW events around the country. Fire outbreaks triggered by 21st-century CDHW episodes are highlighted in three main ecosystems: the Amazonia rainforest, the Pantanal wetlands, and the Cerrado savannas. The impact of recent persistent CDHW conditions on human mortality and premature births is analyzed for the most populated region, southeastern Brazil.

## EMERGING EVIDENCE AND PHYSICAL MECHANISMS OF CDHW EVENTS IN BRAZIL

In this section, we first analyze studies that highlight Brazil in their global analysis regarding the occurrence of CDHW events. Then, we present and discuss the available recent few regional studies which have begun to look at the physical mechanisms connecting the occurrence of hot and dry conditions in different regions of Brazil.

Emerging global studies highlight SA, including Brazil, as a potential hotspot for the occurrence of compound events, particularly those linked to droughts and HWs.<sup>84,144</sup> For instance, two recent global assessments on the impact of anthropogenic warming and natural climate variability in the occurrence of CDHWs concluded that northeastern and southeastern Brazil and central Amazonia were some of the regions with an increase in the frequency, duration, and magnitude of CDHW events per year since 2000.<sup>45,54</sup> Another global survey revealed a strong relationship between the occurrence of CDHW conditions and the phase of the El Niño–Southern Oscillation (ENSO), particularly during the warm season in the northern region of Brazil.<sup>145</sup> Agricultural regions, namely those dominated by rice, maize, and soybean production in Brazil, have been increasingly exposed to CDHW events.<sup>60,144</sup> Regional increases in the frequency of CDHW conditions from the present to the time when mean global temperature increases by 1.5°C (2°C) above the preindustrial levels are projected to span

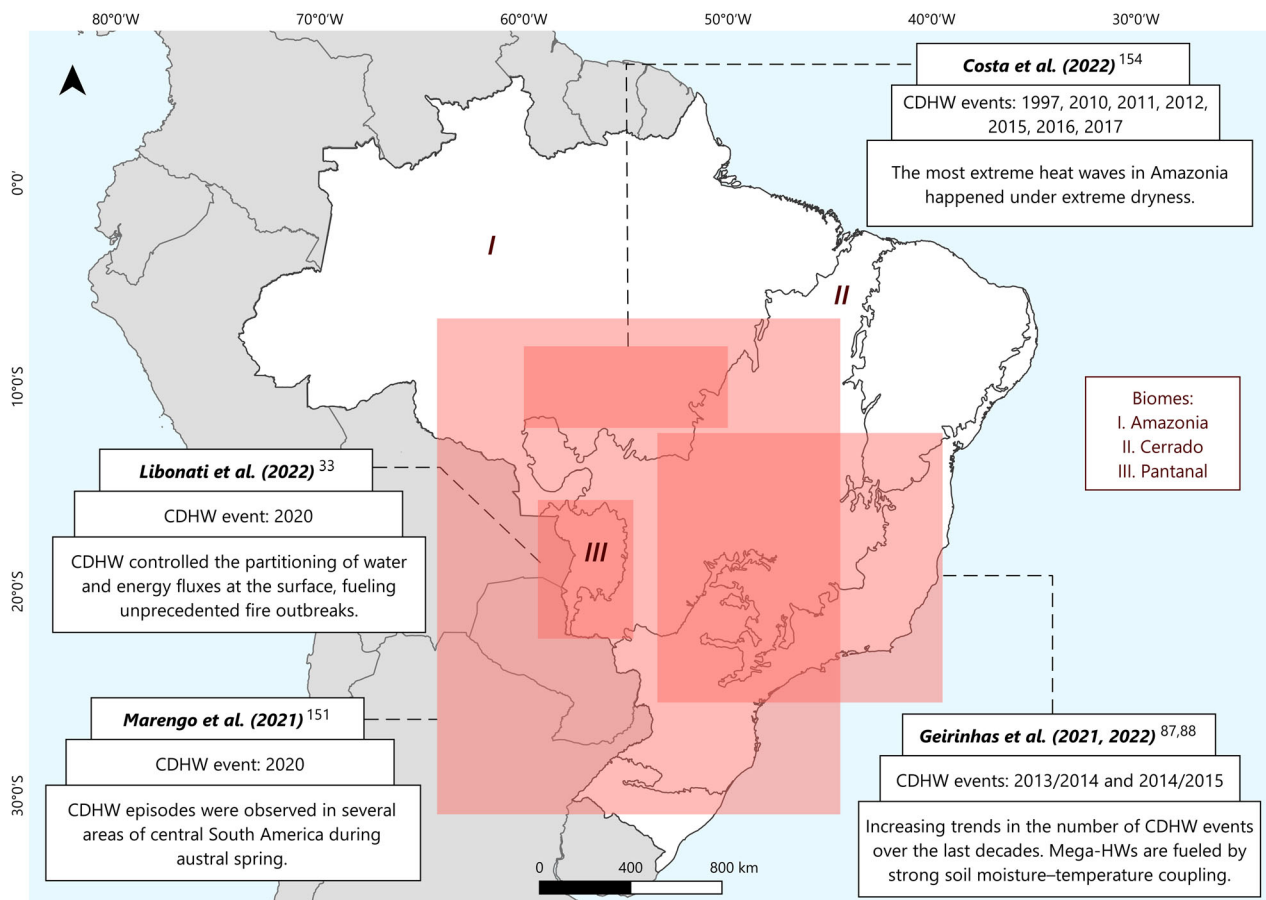


**FIGURE 1** Main regions targeted (red squares) by the first emerging studies<sup>33,87,88,151,154</sup> of the patterns, trends, and physical mechanisms triggering the occurrence of CDHW events in different regions of Brazil over the last decade. The main biomes used here to illustrate the impacts on vegetation fires are depicted in the figure.

between 140% and 200% in many parts of SA, including Brazil.<sup>140</sup> As projected for other parts of the globe, continuous warming of the South American continent will inflict dire impacts on the well-being of the populations. Global warming between 1.5 and 3°C is estimated to imply an increment in the population exposure to CDHW events over southeastern SA (2–6 million people), the Amazonia (1–5 million people), northeastern Brazil (1–5 million people), and over the west coast of SA (1–4 million people).<sup>146</sup> Bevacqua et al.<sup>139</sup> suggested that improving the representation of the physical processes controlling the mean precipitation trends over the Amazonia rainforest is essential for enhancing the robustness of risk estimates of future CDHW events. These authors estimate that the frequency of compound events will increase between 20% and 42%, according to wet and dry future scenarios for the region, respectively.

Regional efforts by the Brazilian academic community to understand extreme CDHW events are slowly refocusing toward a compound perspective, aiming to help to close the gap between climate science and risk assessment (Figure 1). This joint effort has been encapsulated in a recent editorial in the journal “Nature,” where more than 95 national and international water and climate scientists cosigned a letter regarding the 2021 Brazilian water crisis, recom-

mending, among other points, that compound event studies should be a research priority in the country to best inform policymakers and managers.<sup>98</sup> Here, we introduce existing literature on understanding the general patterns and physical mechanisms associated with multivariate climate extreme episodes consisting of drought and HW events co-occurring in space and time, in distinct regions of Brazil.

### Southeastern Brazil

The first effort to evaluate changes in the occurrence of CDHW events in Brazil was undertaken by Geirinhas et al.<sup>87</sup> They found that during the last two decades the number of summer CDHW events has increased substantially over parts of southeastern Brazil, namely, the central section of the state of Minas Gerais, the state of Rio de Janeiro, and the eastern and northeastern parts of the state of São Paulo. For these particular regions, increasing levels ranged from 50% to 100% during the second half of the analysis period (2000–2018), when compared with the first half (1980–1999). The period that contributed the most to these positive changes were the two consecutive summers of 2013/2014 and 2014/2015 when southeastern Brazil

witnessed severe CDHW conditions. During 2013/2014 summer, the incidence of compound conditions was more noticeable over the state of São Paulo, while during 2014/2015 summer, the states of Minas Gerais and Rio de Janeiro recorded the severest concurrence incidence. This study also explored the atmospheric and surface conditions that triggered such a high incidence of CDHW episodes in the region. Geirinhas et al.<sup>87</sup> found that surface dryness and hot temperature anomalies were promoted by a higher-than-normal number of summer days defined by atmospheric blocking conditions affecting southeastern Brazil.<sup>147</sup> These quasi-stationary anticyclonic patterns were embedded in a large-scale Rossby wave train that spanned from the western South Pacific to the South Atlantic and offered the ideal conditions for the occurrence of persistent precipitation deficits throughout the 2013/2014 and 2014/2015 summer seasons.<sup>96,97</sup> At a synoptic time-scale, large diabatic heating rates and strong subsidence conditions enhanced temperature escalation and the occurrence of high evaporation rates, triggering the development of HW episodes and the reamplification of the already established drought conditions. The maintenance of these atmospheric conditions throughout both summer seasons promoted a steady soil moisture decrease into exceptionally low levels. Consequently, a strong soil moisture–atmosphere coupling (water-limited) regime was leveraged and the surface lost its capability to meet the atmospheric water demand, starting to disproportionately dissipate the extra incoming shortwave radiative energy back to the atmosphere as sensible heat, allowing a reamplification of HW episodes. This study unraveled for the first time the relationship between CDHW extremes over southeastern Brazil, demonstrating that, at the first stage, HWs are important for soil desiccation, while during the second stage, under a strong soil moisture imbalance, drought conditions can play a crucial role in temperature escalation and HW amplification through the establishment of strong soil moisture–atmosphere coupling regimes.

Several studies have provided an analysis of the atmospheric causes for the drought event recorded over southeastern Brazil and during the abovementioned two summer periods.<sup>96,97,148–150</sup> However, the assessment and quantification of the simultaneous hot temperature anomalies and land–atmosphere interactions have been receiving much less attention. Accordingly, Geirinhas et al.<sup>88</sup> proposed to fill this gap by presenting at several temporal (from yearly to daily) and spatial (from large to mesoscale) scales a detailed analysis of the extreme temperature anomalies induced during 2013/2014 summer over southeast Brazil, with a special focus on the metropolitan regions of São Paulo and Curitiba. This study shows the exceptionality of the hot conditions that were observed, particularly over the state of São Paulo, where the surface temperature anomalies reached values of 8°C, exceeding the mean by four standard deviations. These massive temperature extremes led to record-breaking temperature levels corresponding, in some cases, to values 5°C higher than the previous record. Another signature of this severe hot summer season was the occurrence of several hot spells over the two metropolitan regions of São Paulo and Curitiba. In fact, the 2013/2014 season witnessed the highest ever recorded number of summer days under HW conditions in both cities, with the occurrence of an unprecedented mega-HW episode<sup>88</sup> that lasted for around 20 days. Some of these hot spells, including this

mega-HW, were fueled by a combined effect of strong diabatic heating, low entrainment of cooler air masses caused by a suppression of mesoscale sea-breeze circulation mechanisms, and the establishment of strong soil moisture–temperature coupling that resulted in enhanced sensible heat fluxes from the surface to the atmosphere. In fact, the authors found a close parallel in what concerns the magnitude and spatial extent of this exceptional HW episode and also the major role played by the land–atmosphere interactions in temperature escalation with the remarkable and well-known 2003 European and 2010 Russian mega-HWs.<sup>51</sup> This clearly underlines the massive amplitude and persistence of temperature extremes throughout 2013/2014 summer, showing that such temperature escalation was not explained by atmospheric circulation anomalies alone and that the combined effect of soil dryness with atmospheric heating due to radiative processes and other mesoscale temperature advection processes was crucial.

## The Pantanal wetlands

Recently, Libonati et al.<sup>33</sup> and Marengo et al.<sup>151</sup> identified the occurrence of outstanding CDHW conditions in central SA during 2020. Several countries, including Brazil, Argentina, Peru, Paraguay, and Bolivia, have recorded a large number of HW events, with record-breaking temperatures reaching up to 10°C above the 1981–2010 climatology. Those HWs occurred in the middle of an unprecedented drought that affected that region since 2018 linked to the warming trends in sea surface temperature of the Pacific and Atlantic Oceans.<sup>99,100,152</sup> On the other hand, the persistent atmospheric blocking conditions in the region fueled by a stationary Rossby wave train in the middle and upper atmosphere coming from the Indian Ocean region<sup>151</sup> were crucial for temperature escalation and large evaporation rates that resulted in pronounced soil moisture deficit during these HW episodes.<sup>38</sup> This drought-HW configuration was supported by enhanced land–atmosphere interactions, thus influencing the persistence of more warm and dry days. CDHW conditions in 2020 were particularly widespread over the Pantanal, located in central-southern Brazil.<sup>38</sup> The 2020 dry season (July–November) was hotter and drier than any other corresponding dry season period in the Pantanal, since at least 1980.<sup>103</sup> During these exceptional CDHW conditions, a pronounced decrease in the evaporative fraction values was observed, indicating the establishment of a strong soil moisture–temperature coupling regime (water-limited) characterized by a near-zero evaporative cooling and a large flux of sensible heat from the surface to the atmosphere.<sup>38</sup>

## The Amazon rainforest

During the dry season, the southern part of the Amazonia rainforest faced a warming trend of 0.49°C/decade over the 1979–2012 period, with a sharper trend of 1.12°C/decade since the year 2000.<sup>153</sup> In addition, this region has been recording an increasing frequency in the number of hot days since 1961<sup>89</sup> as well as in the number of HW events.<sup>120</sup> The synoptic conditions associated with HWs in this



region are linked to the northward displacement of the Intertropical Convergence Zone<sup>120</sup> and to the intensification of the northerly South Atlantic Anticyclone, which reduces the influx of moisture to southeast Amazonia linked to the South American Low-Level Jet.<sup>154</sup> Concurrent with this warming, the region has experienced three major droughts in the short span of 10 years, namely, in 2005, 2010, and 2015. These extreme drought episodes were triggered by large-scale teleconnections patterns forced by warm anomalies in the sea surface temperatures of both the Pacific and Atlantic oceans.<sup>91,155,156</sup> Recent studies have pointed out that the hottest years in the biome were coincident with those extreme droughts.<sup>106,153</sup> The area stricken by precipitation deficits (high temperatures) has increased from 37.9% (10.3%) in 2005 to 42.9% (42%) in 2010, reaching 80.1% (90%) of the Amazonia basin in 2015.<sup>92</sup> In particular, long-term records suggest that 2015 was likely the hottest and driest year over the region in a century.<sup>157</sup> Recently, it was shown that drought conditions over the southeast of Amazonia have a critical impact on the amplification of surface temperature, with the most extreme HW episodes co-occurring during extreme dry years.<sup>154</sup> During these drought events, warm temperature anomalies were concurrent with anomalously high amounts of incoming solar radiation,<sup>92</sup> reduction in cloud cover,<sup>93</sup> and soil moisture deficits.<sup>158</sup> These compound conditions probably led to enhanced land-atmosphere feedbacks that caused a reamplification of the already established conditions of soil dryness and extreme hot temperatures.<sup>51,52,88,159,160</sup>

## IMPACTS OF CDHW EVENTS ON THE ENVIRONMENT AND SOCIETY: EARLY EVIDENCE

In the above sections, we highlighted current knowledge regarding individual hot and dry extremes in Brazil and their associated impacts, as well as the emerging evidence about the occurrence and physical processes associated with CDHW episodes, based on global and regional studies over the last decades. Although each individual type of extreme (hot or dry) is known to trigger severe impacts over the affected region, the implications of the co-occurrence of both extremes over the country are still not well understood. Taking into account the increasing role played by the abovementioned CDHW events in the region, we present a first overview of the associated impacts at a country level. The focus is to evaluate the associated impacts on human health and fire occurrence, in a top-down approach. Using early published case studies representative of main CDHW events that affected diverse areas of the country (Figure 1), we present a first-hand interpretation of potential impacts. In each of the following two subsections, we first introduce some aspects associated with general research available on the topic and then identify the individual case study from the second main section, and then the analysis of the impacts is carried out separately for threats to human health and vegetation fires. The aim is not to exhaustively analyze the results but instead to introduce research questions and methods to be further explored in the future. The key databases and methods used to formally address the impacts are described in the [Supporting Information](#).

## Threats to public health

The understanding of the potential impacts of CDHW events on public health in Brazil is still far from satisfactory, despite the widespread efforts to quantify the impacts of droughts<sup>34,107,108,112</sup> and HWs<sup>21,119,123–133</sup> from the perspective of a single climate extreme.

To first address this knowledge gap, here we analyze the impacts of the CDHW events during the 2013/2014 and 2014/2015 summer seasons<sup>87,88</sup> on human mortality and preterm births in southeastern Brazil. We follow the methods used in previous work on the region,<sup>119,129</sup> to analyze daily mortality for all-natural death causes (nonaccidental or nonviolent) and total births/preterm births (<37 gestational weeks) for the metropolitan region of Rio de Janeiro (MRRJ), based on the Brazilian Health System database (DATASUS) for 2000–2018 and 2011–2017, respectively (see [Supporting Information](#)). With around 12 million inhabitants, the MRRJ is one of the most densely populated urban areas in SA, and the second most populated metropolitan region in Brazil, surpassed only by the metropolitan region of São Paulo.

## Human mortality

The existing literature has investigated the impacts of HW events on human mortality across the entire country over the last decades. Particularly for the MRRJ, according to Geirinhas et al.,<sup>119</sup> during an intense HW that took place in February 2010, 737 excess deaths occurred, with a greater impact on women (44% higher than expected) than on men (21% higher than expected). In terms of age, the elderly were the most affected, with a higher excess of deaths for elderly women (56% higher than expected). Geirinhas et al.<sup>129</sup> expanded the previous analysis to four major HW events, highlighting an excess of 1748 fatalities regarding the expected mortality, with women and the elderly being the most affected. The effects of different levels of drought severity on mortality rates were analyzed by Salvador et al.<sup>112</sup> from 2000 to 2019 for the main metropolitan regions of Brazil, including MRRJ. Evidence of positive association was found, mainly for females, children, and the elderly, and the effects were exacerbated as the drought severity increased. Furthermore, this study found that the excess mortality risk due to extreme drought exposure was greater than that observed due to heat stress in Brazil.

To illustrate the joint impacts of both hot and dry events on excess mortality, we analyzed the 2013/2014 and 2014/2015 summer compound conditions recorded in Rio de Janeiro.<sup>87,88</sup> Over these two record-breaking dry summer periods, the excess heat factor (EHF)<sup>161</sup> allowed identifying several HW events. The EHF quantifies the heat stress levels considering not only the actual hot conditions but also taking into account the previous 30 days, thus considering, to some extent, the human body's acclimatization.<sup>161</sup> Therefore, this index is recommended to describe the impacts of HW events on human mortality and morbidity.<sup>162</sup> A total of four and six HW events occurred during the 2013/2014 and 2014/2015 summer compound conditions, respectively (Table 1). From all CDHW events, seven presented excess

**TABLE 1** Heatwaves identified during the 2013/2014 and 2014/2015 summer CDHW conditions in MRRJ

Summer season	Start of HW	HW duration (days)	O/E (95% CI) for total number of deaths
2013/2014	2013-12-29	4	1.18 (1.09–1.29)
	2014-01-03	3	1.33 (1.21–1.45)
	2014-01-23	3	1.07 (0.98–1.18)
	2014-02-06	5	1.25 (1.17–1.34)
2014/2015	2014-12-20	4	1.04 (0.96–1.13)
	2014-12-28	8	1.09 (1.03–1.16)
	2015-01-07	26	1.08 (1.04–1.11)
	2015-02-09	7	0.97 (0.91–1.04)
	2015-02-17	6	1.00 (0.93–1.07)
	2015-02-25	4	1.00 (0.92–1.08)

Note: Start, duration, and intensity of heatwaves were derived from EHF. Observed to expected (O/E) ratio for total number of deaths during the CDHW is also presented, including the 95% confidence interval.

mortality (O/E > 1), five of them statistically significant ( $p$ -value < 0.05) (Table 1). The highest increase in the observed number of deaths was 33% (O/E = 1.33, CI: 1.21–1.45), which corresponds to an estimated 269 excess deaths during the event of January 3, 2014. Since this event occurred shortly after the previous one (December 29, 2013), with an O/E = 1.18 (CI: 1.09–1.28) and excess mortality estimated at 195 deaths, their combined effect on mortality (464 excess deaths) can be interpreted as a single and longer HW. During the largest HW (26 days during January 2015), with an O/E of 1.08 (CI: 1.04–1.11), 567 excess deaths were estimated. Considering only the CDHW conditions in which O/E ratio was statistically significant and higher than unity, the estimate of the total excess mortality during 2013/2014 and 2014/2015 reaches 828 and 759 deaths, respectively. Several factors, such as gender, age, social inequalities, and pre-existing diseases, influence the population vulnerability to CDHWs,<sup>163</sup> which need to be better investigated in the MRRJ and other Brazilian metropolitan regions. Future population aging is expected to amplify climate-related excess deaths, thus representing a particular challenge for Brazil, in a scenario where population aging has been rapid and marked by socioeconomic and regional disparities.<sup>164</sup>

### Gestational health effects under CDHW conditions

Studies have shown that temperature extremes can affect gestational health and promote an increase in preterm births.<sup>26,27,165</sup> For instance, maternal exposure to extreme temperatures was linked to an increased risk of preterm birth in Australia,<sup>166</sup> Europe,<sup>167</sup> the United States,<sup>168</sup> and China.<sup>169</sup> Although most preterm babies survive, maternal exposure to extreme temperature has been pointed out as a leading cause of child mortality, long-term neurological disabilities, and increased risk of respiratory and gastrointestinal complications.<sup>170,171</sup> Consequently, the occurrence of premature births also leads to an increase in the demand for long-term care, which puts pressure on the public health system.<sup>172</sup>

Drought can affect pregnancy health by limiting water and food availability, disrupting infrastructures, and facilitating the dissemina-

tion of water-related diseases.<sup>173</sup> Studies about the direct impact of extreme droughts on human pregnancy are still limited worldwide.<sup>174</sup> Nevertheless, Gitau et al.<sup>175</sup> showed that the Southern African drought of 2001–2002 led to the increase in food prices and consequently to poor maternal nutrition status, culminating in decreased infant length. These results indicate that drought can have long-term effects on the population and public health services.<sup>176</sup> In Brazil, the studies of health risks of droughts highlight that social and economic vulnerabilities aggravate the associated health impacts.<sup>107,112</sup>

Despite evidence in the literature about the impacts of isolated HW and drought events, little is known about the magnitude of the association between CDHW episodes and preterm birth in Brazil, and the factors that influence this relationship, mainly due to regional differences. Here, we evaluated the impact of CDHW conditions on gestational health by analyzing the increase in total births and preterm births during the already discussed 2013/2014 and 2014/2015 summers (Table 1). For this purpose, some HW events from Table 1, consecutive and in close proximity, were concatenated, resulting in five longer periods (Table 2).

For both the 2013/2014 and 2014/2015 summer seasons, a statistically significant increase (O/E > 1) in total and preterm births was observed in all CDHW events (Figure 2). For preterm births, CDHW conditions were associated with an increase varying from 10% (O/E = 1.10, CI: 1.01–1.19) to 23% (O/E = 1.23, CI: 1.09–1.39). The increase in the O/E ratio obtained here is within the same range reported by Chersich et al.<sup>177</sup> in their systematic review of 70 studies in 27 countries (1.16; 95% CI: 1.10–1.23). Overall, a small increment of the O/E ratio was observed for total births, with an increase observed from 5% (O/E = 1.05; CI: 1.01–1.09) to 13% (O/E = 1.13; CI: 1.08–1.19). No clear links between the HW duration and intensity and birth rates were observed here, despite previous studies suggesting that such factors can be positively associated with an increase in early-term births.<sup>165</sup> A possible explanation for this is the fact that the Brazilian birth certificates record the gestational time in weeks. This could be a confounder for the daily analysis of HW events conducted here, which motivates further long-term analysis in Brazil.

**TABLE 2** Classification of periods composed of sequential CDHWs

Summer season	Period label	Start of period	Period duration (days)	Number of sequential HW included in this period (from Table 1)
2013/2014	P1	2013-12-29	8	2
	P2	2014-01-23	3	1
	P3	2014-02-06	5	1
2014/2015	P4	2014-12-20	44	3
	P5	2015-02-09	20	3

Note: The duration of each period was calculated by adding the duration of each sequential HW from Table 1.

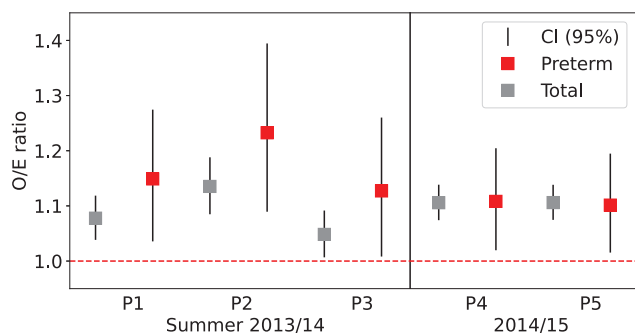


**FIGURE 2** Observed to expected (O/E) ratio for total (gray squares) and preterm births (red squares) in the metropolitan area of Rio de Janeiro during CDHW periods in the summers of 2013/2014 and 2014/2015. Error bars indicate the 95% confidence intervals (CIs). Values greater than unity (red dotted line) represent a statistically significant increase in birth rates during compound events. The vertical line visually separates the 2013/2014 and 2014/2015 periods.

### Vegetation fire response to the simultaneous occurrence of hot and dry events

The link between fire activity and climate has been extensively covered worldwide, with the IPCC defining fire weather as “weather conditions favorable to fire activity, which generally includes temperature, soil moisture, humidity, and wind.”<sup>55,178</sup> In general, fire activity is linked to concurrent high temperatures, low relative humidity and precipitation, and windy conditions, although meteorological conditions during the growing season also play a major role in modulating both vegetation and fuel levels.<sup>179,180</sup> In the case of Brazil, there are several studies evaluating the relationship between fire and meteorological parameters; however, due to the extent of the country and the variety of ecosystems, these relationships differ among biomes and even at a regional scale. Moreover, regarding the impact of CDHW events in Brazilian biomes, there is very little research. In fact, to the best of our knowledge, the only explicit joint assessment on the present-day impact of CDHW events on vegetation fires was a recent study for the 2020 fire season in the Pantanal region.<sup>33</sup> In addition, future fire danger forced by dry and hot conditions under climate change scenarios was only recently evaluated for two Brazilian regions, namely the Xingu Basin and the Pantanal.<sup>181</sup> Here, we attempt to go a few steps further, summarizing the efforts developed by the academic research com-

munity to describe these fire–CDHW relationships over the Pantanal wetlands, the Amazonia rainforest, and the Cerrado savannas. We further provide novel results covering both the Amazonia rainforest and the savannas of Cerrado, where we followed the methods used in Libonati et al.<sup>33</sup> based on well-consolidated satellite-derived active fire and burned area datasets. More information on these datasets and the methods employed here may be found in the [Supporting Information](#).

### The Pantanal wetlands

Up until the catastrophic 2020 wildfire event, there was very little literature on vegetation fires over Pantanal and their connection to meteorological conditions and climate change. When roughly 4 million hectares (1/3 of the biome) burned down in 2020,<sup>103</sup> including long stretches of wetlands and forest formations,<sup>182</sup> and around 17 million vertebrates were killed,<sup>183</sup> attention shifted to understanding why and how this fire-sensitive biome was burning. The 2020 fire season in Pantanal was marked by anomalous meteorological conditions associated with unprecedented meteorological danger<sup>103</sup> and severe drought.<sup>99</sup> Libonati et al.<sup>33</sup> developed this analysis further, linking CDHW conditions to daily variations of the burned area within Pantanal and its hydrological subregions. Most burned areas occurred within a 4-month period from July to October (henceforth the Pantanal’s fire season), with record values of hot and dry conditions. The percentage of Pantanal under CDHW conditions ( $\%Pantanal_{CDHW}$ ), a single metric that illustrates the temporal and spatial occurrence of CDHW conditions during the fire season,<sup>87</sup> reached its maximum during 2020 (Figure 3). From August 26th to October 15th, three consecutive CDHW events were recorded (see orange shaded areas in Figure 3), where maximum temperatures rose almost 6°C above the climatological mean, reaching a staggering 41°C on the third CDHW event that lasted more than 20 consecutive days. Long-term precipitation deficits coupled with a large evaporative demand leveraged by the occurrence of several hot spells since the beginning of 2020 promoted a steady and sharp decrease of soil moisture values during the Pantanal’s wet season, culminating in pronounced soil desiccation during the fire season. Accordingly, the HW conditions triggered during the Pantanal’s fire season concurred with a near-zero evaporative cooling evidenced by the sharp decreases observed in the evaporative fraction values (see blue lines in Figure 3). This highlights the establishment of strong soil moisture–temperature

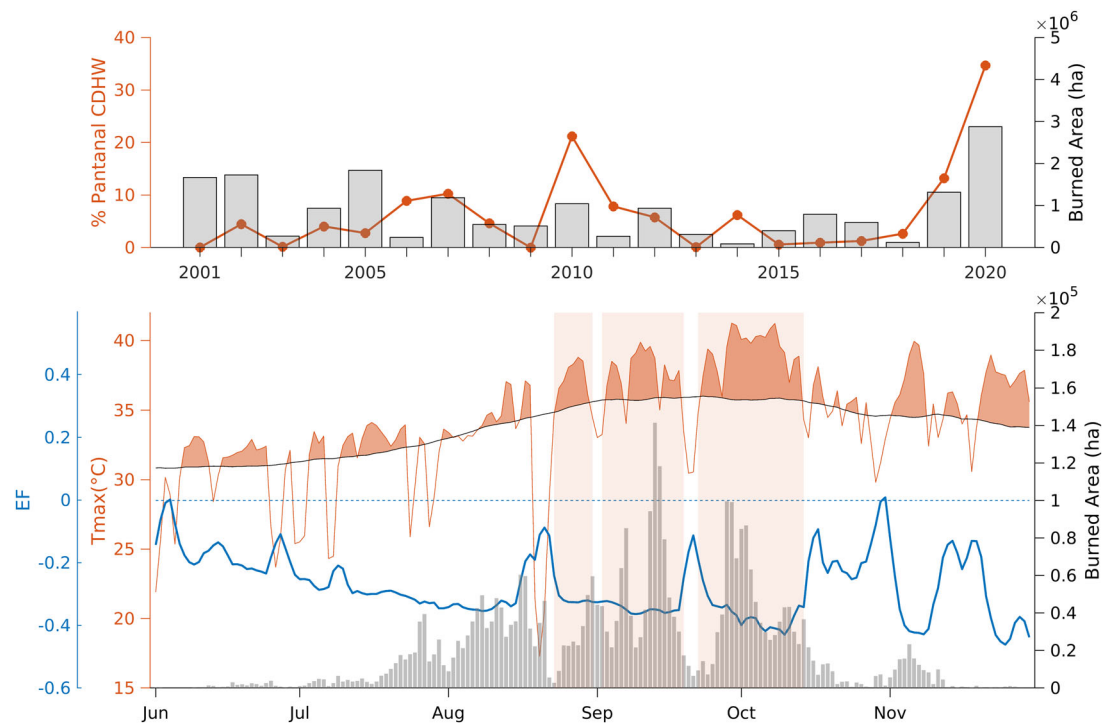


**FIGURE 3** Vegetation fire response to the simultaneous occurrence of hot and dry events during the Pantanal fire crisis in 2020. Top panel: Interannual variability from 2001 to 2020 of the percentage of Pantanal under CDHW conditions (orange line, left y-axis) and of total annual burned area (gray bars, right y-axis) computed for the Pantanal's fire season period (July–October). Bottom panel: Time series from June to November 2020 (bottom panel) of daily area-averaged values of maximum temperatures ( $T_{\max}$ , orange line, left y-axis), the respective calendar day climatological (1981–2010 base period) 90th percentile (black line), and of evaporative fraction anomalies over Pantanal (EF, blue line, left y-axis); gray bars indicate daily total burned area recorded over Pantanal (right y-axis); the orange shaded rectangles highlight periods marked by the occurrence of consecutive HW episodes followed by a pronounced decrease in the EF values.

coupling regime (water-limited) in which the surface started to disproportionately dissipate the incoming radiation as sensible heat, instead of latent heat (evaporation), allowing a reamplification of the HW episodes and thus fostering the ideal conditions for fire propagation. In fact, the highest levels of vegetation flammability thresholds ever recorded over the last 4 decades were observed during 2020. Although the number of days during the three abovementioned CDHW periods represented circa 37% of the total fire season days, they accounted disproportionately for 71% of the total burned area of that period. Contrary to previous years,<sup>184</sup> most of these fires were located over northern Pantanal in forested areas.<sup>33</sup> These regions, where fuel is not a limiting factor, are more vulnerable to CDHW events and their effects are greater in years that experience less flooding, as is the case of 2019 and 2020. They also found that, in the Pantanal, conditions for the occurrence of CDHW episodes are becoming more frequent, with temperatures rising at a rate four times that of the global average, and negative precipitation anomalies occurring more frequently since the turn of the 21st century. Although models do not fully agree on future precipitation trends, state-of-the-art projections agree on a warmer future for the biome.<sup>185</sup> A recent study highlights that limiting global warming to 1.5°C instead of 3°C is likely to reduce the expected increase in CDHW-related fire danger by 11.4% in the Pantanal.<sup>181</sup>

It is worth mentioning that intense fire seasons in the Pantanal, like in most other regions around the globe, result from the inter-

play of the appropriate conditions for fire triggering and maintenance, that is, availability of fuels, appropriate extreme meteorological conditions, and frequency of ignitions. Therefore, the existence of intense drought and HW conditions such as the ones that took place in 2010 (Figure 3) represents a necessary (but not sufficient) condition, to ensure a higher-than-usual fire season. The condition of the fuels, and particularly the number of ignitions (natural or anthropogenic), also play a critical role. In the case of the Pantanal, human activities are the main source of vegetation fire ignitions, accounting for 84% of the annual burned area.<sup>186</sup>

### The Amazonia rainforest

Over the past few decades, human activities and climate variability contributed to periodic spikes in forest fire activity in the Amazonia rainforest.<sup>101,102</sup> Since natural fires are uncommon in Amazonia, the fire regime is mainly shaped by anthropogenic activities. Nevertheless, the role of climate has to be considered, especially during extreme droughts, which have been shown to exacerbate fire incidence, intensity, and severity in the region.<sup>101,187</sup> From 2000 to 2015, drought frequency in Amazonia was almost three times higher than the decadal incidence of the last century,<sup>92</sup> which represents a major threat to the forest ecosystem.<sup>106</sup> During the drought event of

1997–1998, which was related to one of the most intense episodes of the ENSO ever recorded, 1/3 of the Amazonia became susceptible to fire, and approximately 40,000 km<sup>2</sup> burned.<sup>188</sup> In 2005, the lack of precipitation induced by the warming tropical North Atlantic Ocean affected mainly the western Amazonia, promoting an extended and extreme fire season in this region.<sup>178</sup> In 2010, the co-occurrence of positive phases of both the ENSO and the Atlantic Multidecadal Oscillation (AMO) led to record drought and fire activity over western and southern Amazonia.<sup>187</sup> In the face of the observed extreme values of temperature and precipitation that were exacerbated by the strong El Niño event of 2015,<sup>157</sup> new record-breaking drought conditions occurred in the rainforest during that year but resulted in a relatively low level of fire activity due to decreasing levels of deforestation.<sup>101,102</sup> Climate anomalies triggered by ENSO and AMO-related activity are expected to continue impacting Amazonia through a higher frequency of extreme droughts.<sup>189</sup> Such an increase in hydroclimatic extremes, coupled with anthropogenic land cover changes, are expected to further promote fire activity in this region.<sup>62</sup> In addition, the observed warming trends<sup>89,120</sup> may increase evapotranspiration, leading to a decrease in soil moisture,<sup>190</sup> thus enhancing vegetation flammability.

The ongoing intensification of the hydrological cycle is linked to the amplification of surface temperature,<sup>93</sup> with the most extreme HW episodes co-occurring during extreme dry years,<sup>154</sup> and presents a showcase to explore the responses of Amazonia fires under CDHW conditions. Here, we show preliminary results on the synergy between fire activity and CDHW events that further confirm that these hot and dry conditions favor the occurrence of fire. Figure 4 shows the spatial distribution of CDHW conditions (see [Supporting Information](#)) in Amazonia over 2005 (June–August), 2010 (June–August), and 2015 (October–December), along with active fire anomalies and deforestation patterns. CDHW conditions increased in duration and extent over the considered periods, and in 2015, almost the entire Amazonia was affected. In comparison, the periods of 2005 and 2010 experienced fewer days under CDHW conditions, and these occurred mainly in the western and southern parts of the biome. Fire anomalies, on the other hand, seem to have decreased from 2005 onward and show fewer regional fire hotspots. At first glance, there appears to be no spatial concurrence of CDHW conditions and increased active fire anomalies. However, as pointed out before, the anthropogenic disturbance has a preponderant role in fire activity over the Amazonia. The period considered for 2005 saw more than double the extent of deforestation compared to both 2010 and 2015.<sup>101</sup> In 2005 and 2010, higher fire anomalies were found in areas that experienced increased CDHW conditions and high deforestation, whereas in 2015, despite extreme hot and dry conditions, the biome saw lower deforestation and consequently, less fire activity. These preliminary results demonstrate that, given anthropogenic ignitions, CDHW conditions exacerbate fire activity in Amazonia.

Other factors can also influence fire activity and may contribute to some of the variability that is not explained by climate extremes, for instance, anthropogenic factors, including political and economic drivers,<sup>191</sup> but also natural factors, such as soil moisture content,<sup>188</sup>

and positive fire–climate<sup>192</sup> and deforestation–climate<sup>193</sup> feedbacks. In particular, the influence of deforestation-induced feedback on the occurrence, intensity, and frequency of CDHW events should be further investigated, given the observed influence of Amazonia land cover changes on surface temperature, the energy budget, and the hydrological cycle.<sup>194</sup> Additionally, the direct impacts of hot and dry compound events on the forest ecosystem are not yet documented over the region, although studies have reported changes in Amazonia forest productivity related to drought frequencies and warming trends.<sup>105,106,188</sup>

## The Cerrado savannas

By contrast to the other biomes referred to in this section, the Cerrado is no stranger to fire. This fire-prone biome sees high fire activity every year as the largest contributor to Brazil's annual burned area and a major fire hotspot worldwide.<sup>195</sup> Fires in Cerrado have been shown to be linked with meteorological conditions, in particular rainfall and temperature.<sup>196,197</sup> For instance, the Daily Severity Rating (DSR in short, an extension of the Canadian Forest Fire Weather Index System) explains 71% of the interannual variability of burned area in Cerrado.<sup>198</sup> Here, we show further evidence for the Cerrado's fire seasons (defined here as August–October) from 2001 to 2019 of a link between CDHW conditions with fire activity over four Cerrado ecoregions (Figure 5): Bico do Papagaio, Araguaia Tocantins, Bananal, and Alto Parnaíba. These ecoregions<sup>199</sup> are located in the central and northern Cerrado and are the highest annual contributors to the total burned area in the biome, burning more than 8% of their respective areas every year, on average.<sup>200</sup> Indeed, there seems to be a link between CDHW conditions and fire as, for all ecoregions, the top three years with higher burned areas fall into the lower right quadrant of Figure 5, except for the year 2010 for Alto Parnaíba. The years of 2007 and 2010 are associated with La Niña events that, as usual, induced widespread drought conditions over the Cerrado,<sup>155</sup> confirmed by low soil moisture values and associated with a %Cerrado<sub>HW</sub> incidence (a single metric that illustrates the temporal and spatial occurrence of HW conditions during the fire season above the historical series 75th percentile<sup>33,87</sup>). These two years witnessed the most severe fire seasons within the Cerrado over the last two decades, with all four ecoregions showing positive burned area anomalies.<sup>200</sup> The year of 2012 saw moderate to severe drought over Alto Parnaíba and Araguaia Tocantins,<sup>201</sup> and are here associated with a high percentage of HW incidence in both ecoregions. Noteworthy is the case of Bananal in 2017, and to a lesser extent, Bico do Papagaio, with the highest ever-recorded value of HW incidence in the region and corresponding peak in burned area values. These results hint at a possible synergy between CDHW events and fire activity in the Cerrado, but additional research is needed to properly characterize these relationships and explain the associated physical mechanisms. Nevertheless, fire activity in this biome is linked to meteorological conditions and the Cerrado seems to be heading for a hotter and drier future<sup>122,198</sup> where CDHW events are bound to occur more often.

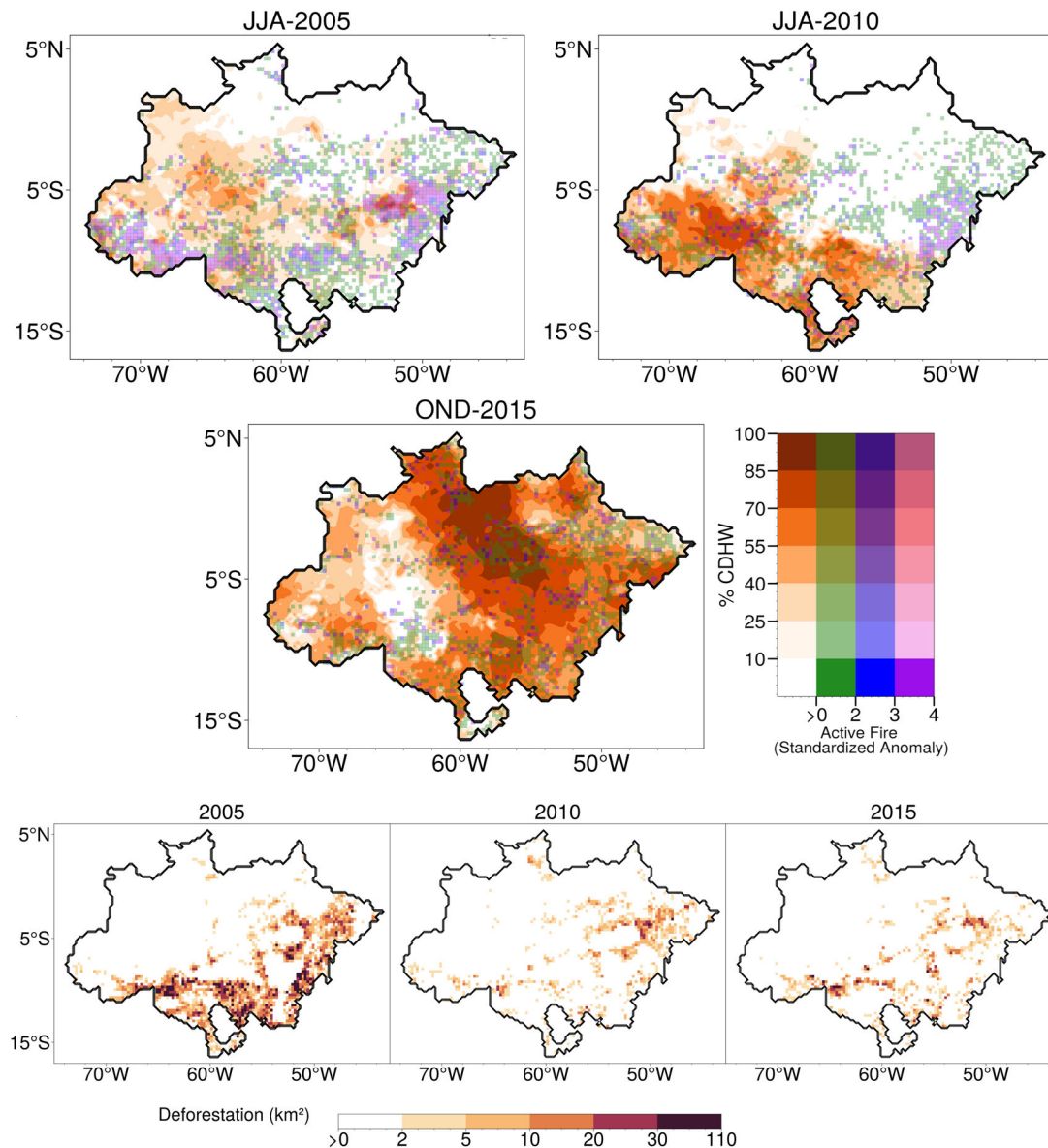


**FIGURE 4** The spatial distribution of CDHW conditions in the Amazonia in 2005, 2010, and 2015, along with active fire anomalies and deforestation patterns. Top panels: Spatial distribution over Amazon of the percentage of days affected by CDHW conditions (%; top color bar) and of active fire standardized anomalies (bottom color bar) during the periods of June–August 2005 (left panel), June–August 2010 (right panel), and October–December 2015 (bottom panel).

## FUTURE PERSPECTIVES AND RECOMMENDATIONS

Extreme climate events, such as intense, prolonged, and frequent CDHW episodes, present a new challenge for human health, the economy, and ecosystems around the world. These threats are of particular importance in low-income regions with limited public health resources, low environmental protection investments, and a growing urban population, such as Brazil.<sup>202</sup> Therefore, it is crucial that the country acknowledges this multiple hazard framework and becomes more engaged internationally as part of a global network of research on CDHW events. This is particularly relevant for Brazilian public agencies, with oversight attributions in different socioeconomic sectors (e.g., agriculture, energy, or health), that aim to provide rigorous and

useful information for decision-makers to mitigate the impacts of current and future extreme climatic episodes linked to HW and drought. As described in this work, some studies have begun to build a better understanding of the physical mechanisms connecting the occurrence of persistent hot and dry conditions in Brazil. However, to the best of our knowledge, and with the exception of the recent works of Libonati et al.<sup>33</sup> and Ribeiro et al.,<sup>181</sup> there is a clear gap in the identification and quantification of the spatial pattern and temporal evolution of impacts associated with CDHW in the country. We are confident that obtaining a better understanding of the coupled phenomena of HWs and droughts in the country is crucial to enhance the adaptive capacity of different sectors, such as public health, civil defense, agriculture, tourism, and public policy management. In this context, we would like

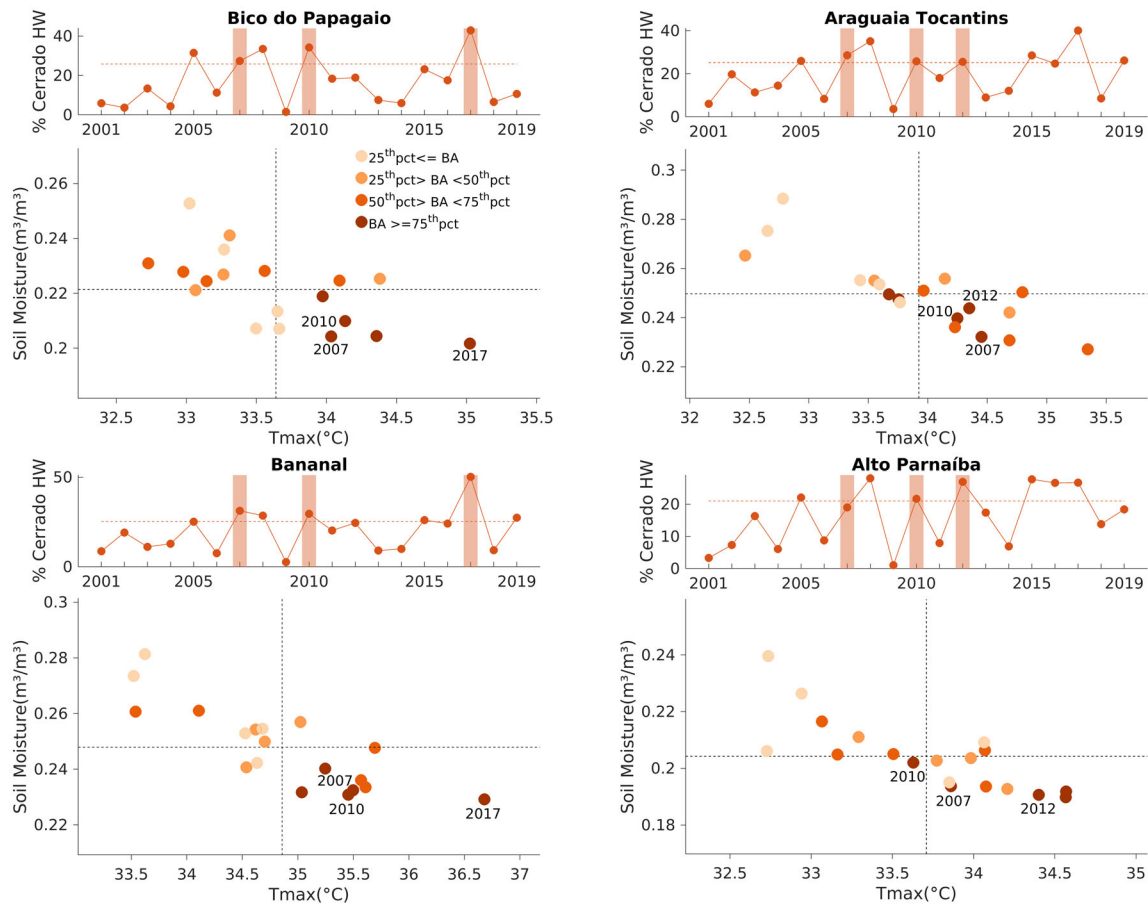


**FIGURE 5** The impact of soil moisture deficits and HW events during the Cerrado fire season (August–October) on burned areas in distinct ecoregions of the Cerrado. The upper panels represent the year-to-year variability of the percentage of HW incidence over each ecoregion; the dashed line is the 75th percentile over the time series (2001–2019) and the years highlighted in orange are the top three years with higher burned areas. The bottom panels show the yearly average of maximum temperature  $T_{\max}$  ( $^{\circ}\text{C}$ ) and soil moisture ( $\text{m}^3/\text{m}^3$ ): dot colors represent the burned area in a given year; finally, dashed lines indicate the medians of  $T_{\max}$  and soil moisture during 2001–2019.

to highlight below some recommendations for the development of this research field in Brazil:

- **Disentangling the physical mechanisms and atmospheric patterns associated with CDHW events.** Given the complexity involved, accurately forecasting CDHW events is a major challenge for climate scientists. It requires a deep understanding of the various physical processes involved, including the associated soil–atmosphere feedback. If the research community aims to improve the CDHW forecasting field, it is mandatory to have a better understanding of the large-scale meteorological conditions that trigger hot and dry conditions observed in past events and how remote forcing factors, such as sea surface temperature anomalies, influence these patterns. With this information in hand, researchers can then develop monitoring systems and even early warning systems that can predict the evolution of these events. To this end, it is urgent to guarantee high-quality and long-term *in situ* observational datasets around the country as well as refined satellite-derived information covering land-related, meteorological, and hydrological variables, an area where Brazil suffers serious deficiencies.<sup>98</sup> Moreover, the

enhancement of regional physical models as climate and hydrological modeling is also crucial for studying the current and future dynamics of such compound events. For instance, a recent study pointed out that, for the Amazonia rainforest, improving the representation of the processes driving precipitation trends, such as forest productivity response to global warming and shifts in the Atlantic meridional overturning circulation, is crucial for better estimates of future compound risk.<sup>139</sup> In this context, the exploitation of new techniques, such as machine learning, aiming to circumvent current uncertainties and missing processes in Earth system models is a promising field of research.

- **Quantitative mapping of high-intensity and high-frequency CDHW areas.** As more information is gathered across different Brazilian regions, the understanding of spatial and temporal patterns (duration, frequency, and intensity) and trends of CDHW events will move beyond a general approach and toward a region-specific one based on the intrinsic characteristics of each ecosystem (e.g., geographical, climatic, urbanization, and degree of degradation). This would allow the identification of still-unknown important climatic and anthropogenic drivers of CDHW events in hotspot areas.<sup>45,54</sup>

Such an approach may serve to determine the effects of these extreme events on different environmental and socioeconomic sectors, allowing the adoption of more local strategies for better management and prediction. Besides, regionalized climate projections can be applied in the assessment of CDHW events in such vulnerable areas to identify changes between the present and future regime and assess the impacts of regional climate changes.<sup>139</sup>

- **Quantification of the impacts and identification of regions/populations with the highest vulnerability.** The continuous exposure of the country to CDHW episodes provides strong motivation to explore adaptation strategies to increase societal and environmental resilience. In this context, multidisciplinary scientific research is essential to provide robust knowledge about the impacts of CDHW events. Accordingly, impacts can be correlated with auxiliary economic or demographic data, such as population density, average income, land cover and land use changes, social conditions, and other factors that reflect the conditions of human life and natural ecosystems. In this way, and considering the likely increase in frequency and amplitude of CDHWs in Brazil,<sup>84,144</sup> there is a strong need for work that provides clear guidelines for public health and environmental policies related to CDHW events, contributing to change the purely reactive response of historical basis and avoiding the escalation of socioeconomic inequalities. As we have outlined above, most of the current impact analysis on the country relies on isolated droughts and HWs events. Accordingly, progress in impact analysis may be accelerated if these extreme events are considered combined instead of separately.

## ACKNOWLEDGMENTS

R.L. was supported by CNPq (grant 311487/2021-1) and FAPERJ (grant E26/202.714/2019). J.L.G. and P.S.S. acknowledge FCT (Fundação para a Ciência e a Tecnologia) for the PhD grants 2020.05198.BD and SFRH/BD/146646/2019, respectively. A.R. and R.M.T. acknowledge FCT under projects FIRECAST (PTDC/CTA-CLI/28902/2017) and ROADMAP (JPIOCEANS/0001/2019). D.M.S. was supported by FIOCRUZ (grant VPPCB-003-FIO-19). L.N. and M.E.R.G. were supported by PIBIC-UFRJ grants. FCT also supports IDL (project UIDB/50019/2020) and CEF (UIDB/00239/2020).

## AUTHOR CONTRIBUTIONS

Conceptualization, R.L., R.M.T., C.C.D.C., J.L.G., and P.S.S.; methodology and formal analysis, R.L., J.L.G., P.S.S., D.M.S., J.A.R., L.N., M.E.R.G., A.P.R., A.R., L.F.P., R.M.T., and J.M.C.P.; writing-review and editing, R.L., J.L.G., P.S.S., D.M.S., A.R., L.F.P., R.M.T., and J.M.C.P.; funding acquisition, R.L. All authors have read and agreed to the published version of the manuscript.

## COMPETING INTERESTS

The authors declare no competing interests.

## ORCID

Renata Libonati  <https://orcid.org/0000-0001-7570-1993>

João L. Geirinhas  <https://orcid.org/0000-0002-2110-4891>

Patricia S. Silva  <https://orcid.org/0000-0003-0410-2971>

Ana Russo  <https://orcid.org/0000-0003-0042-2441>

Leonardo F. Peres  <https://orcid.org/0000-0001-6820-6935>

Carlos C. DaCamara  <https://orcid.org/0000-0003-1699-9886>

José Miguel C. Pereira  <https://orcid.org/0000-0003-2583-3669>

Ricardo M. Trigo  <https://orcid.org/0000-0002-4183-9852>

## REFERENCES

- Perkins, S. E., & Alexander, L. V. (2013). On the measurement of heat waves. *Journal of Climate*, *26*, 4500–4517.
- Perkins-Kirkpatrick, S. E., & Lewis, S. C. (2020). Increasing trends in regional heatwaves. *Nature Communications*, *11*, 1–8.
- Zhang, Y., Li, Q., Ge, Y., Du, X., & Wang, H. (2022). Growing prevalence of heat over cold extremes with overall milder extremes and multiple successive events. *Communications Earth & Environment*, *3*, 1–13.
- Chambers, J. (2020). Global and cross-country analysis of exposure of vulnerable populations to heatwaves from 1980 to 2018. *Climatic Change*, *163*, 539–558.
- Vicedo-Cabrera, A. M., Scovronick, N., & Sera, F. (2021). The burden of heat-related mortality attributable to recent human-induced climate change. *Nature Climate Change*, *11*, 492–500.
- García-León, D., Casanueva, A., Standardi, G., Burgstall, A., Flouris, A. D., & Nybo, L. (2021). Current and projected regional economic impacts of heatwaves in Europe. *Nature Communications*, *12*, 1–10.
- Wohlfahrt, G., Gerdel, K., Migliavacca, M., Rotenberg, E., Tatarinov, F., Müller, J., Hammerle, A., Julitta, T., Spielmann, F. M., & Yakir, D. (2018). Sun-induced fluorescence and gross primary productivity during a heat wave. *Scientific Reports*, *8*, 14169.
- Sen Gupta, A., Thomsen, M., Benthuyzen, J. A., Hobday, A. J., Oliver, E., Alexander, L. V., Burrows, M. T., Donat, M. G., Feng, M., Holbrook, N. J., Perkins-Kirkpatrick, S., Moore, P. J., Rodrigues, R. R., Scannell, H. A., Taschetto, A. S., Ummenhofer, C. C., Wernberg, T., & Smale, D. A. (2020). Drivers and impacts of the most extreme marine heatwave events. *Scientific Reports*, *10*, 19359.
- Cheng, J., Xu, Z., Bambrick, H., Su, H., Tong, S., & Hu, W. (2018). Heat-wave and elderly mortality: An evaluation of death burden and health costs considering short-term mortality displacement. *Environment International*, *115*, 334–342.
- Guo, Y., Gasparrini, A., Li, S., Sera, F., Vicedo-Cabrera, A. M., de Sousa Zanotti Stagliorio Coelho, M., Saldiva, P. H. N., Lavigne, E., Tawatsupa, B., Punnasiri, K., Overcenco, A., Correa, P. M., Ortega, N. V., Kan, H., Osorio, S., Jaakkola, J. J. K., Rytty, N. R. I., Goodman, P. G., Zeka, A., ... Tong, S. (2018). Quantifying excess deaths related to heatwaves under climate change scenarios: A multicountry time series modelling study. *PLoS Medicine*, *15*, e1002629.
- Merte, S. (2017). Estimating heat wave-related mortality in Europe using singular spectrum analysis. *Climatic Change*, *142*, 321–330.
- Rey, G., Fouillet, A., Bessemoulin, P., Frayssinet, P., Dufour, A., Jouglu, E., & Hémond, D. (2009). Heat exposure and socio-economic vulnerability as synergistic factors in heat-wave-related mortality. *European Journal of Epidemiology*, *24*, 495–502.
- Sousa, P. M., Trigo, R. M., Russo, A., Geirinhas, J. L., Rodrigues, A., Silva, S., & Torres, A. (2022). Heat-related mortality amplified during the COVID-19 pandemic. *International Journal of Biometeorology*, *66*, 457–468.
- Yan, M., Xie, Y., Zhu, H., Ban, J., Gong, J., & Li, T. (2022). The exceptional heatwaves of 2017 and all-cause mortality: An assessment of nationwide health and economic impacts in China. *Science of the Total Environment*, *812*, 152371.
- Wang, H., Abajobir, A. A., Abate, K. H., Abbafati, C., Abbas, K. M., Abd-Allah, F., Abera, S. F., Abraha, H. N., Abu-Raddad, L. J., Abu-Rmeileh, N. M. E., Adedeji, I. A., Adedoyin, R. A., Adetifa, I. M. O., Adetokunboh, O., Afshin, A., Aggarwal, R., Agrawal, A., Agrawal, S., Ahmad Kiadaliri,



- A., ... Murray, C. J. L. (2017). Global, regional, and national under-5 mortality, adult mortality, age-specific mortality, and life expectancy, 1970–2016: A systematic analysis for the Global Burden of Disease Study 2016. *Lancet*, 390, 1084–1150.
16. Herold, N., Alexander, L., Green, D., & Donat, M. (2017). Greater increases in temperature extremes in low versus high income countries. *Environmental Research Letters*, 12, 034007.
  17. Papalexioiu, S. M., AghaKouchak, A., Trenberth, K. E., & Foufoula-Georgiou, E. (2018). Global, regional, and megacity trends in the highest temperature of the year: Diagnostics and evidence for accelerating trends. *Earth's Future*, 6, 71–79.
  18. Hertig, E., Russo, A., & Trigo, R. M. (2020). Heat and ozone pollution waves in Central and South Europe—Characteristics, weather types, and association with mortality. *Atmosphere*, 11, 1271.
  19. Gasparri, A., Guo, Y., Hashizume, M., Lavigne, E., Zanobetti, A., Schwartz, J., Tobias, A., Tong, S., Rocklöv, J., Forsberg, B., Leone, M., De Sario, M., Bell, M. L., Guo, Y.-L. L., Wu, C., Kan, H., Yi, S.-M., de Sousa Zanotti Stagliorio Coelho, M., Saldiva, P. H. N., ... Armstrong, B. (2015). Mortality risk attributable to high and low ambient temperature: A multicountry observational study. *Lancet*, 386, 369–375.
  20. Patz, J. A., Campbell-Lendrum, D., Holloway, T., & Foley, J. A. (2005). Impact of regional climate change on human health. *Nature*, 438, 310–317.
  21. Péres, W. E., Ribeiro, A. F. S., Russo, A., & Nunes, B. (2020). The association between air temperature and mortality in two Brazilian health regions. *Climate*, 8, 16.
  22. Strathearn, M., Osborne, N. J., & Selvey, L. A. (2022). Impact of low-intensity heat events on mortality and morbidity in regions with hot, humid summers: A scoping literature review. *International Journal of Biometeorology*, 66, 1013–1029.
  23. Hancock, P. A., & Vasmatazidis, I. (2003). Effects of heat stress on cognitive performance: The current state of knowledge. *International Journal of Hyperthermia*, 19, 355–372.
  24. Florido Ngu, F., Kelman, I., Chambers, J., & Ayeb-Karlsson, S. (2021). Correlating heatwaves and relative humidity with suicide (fatal intentional self-harm). *Scientific Reports*, 11, 22175.
  25. Varghese, B. M., Barnett, A. G., Hansen, A. L., Bi, P., Nairn, J., Rowett, S., Nitschke, M., Hanson-Easey, S., Heyworth, J. S., Sim, M. R., & Pisaniello, D. L. (2019). Characterising the impact of heatwaves on work-related injuries and illnesses in three Australian cities using a standard heatwave definition—Excess Heat Factor (EHF). *Journal of Exposure Science & Environmental Epidemiology*, 29, 821–830.
  26. Kuehn, L., & McCormick, S. (2017). Heat exposure and maternal health in the face of climate change. *International Journal of Environmental Research and Public Health*, 14, 853.
  27. Barreca, A., & Schaller, J. (2020). The impact of high ambient temperatures on delivery timing and gestational lengths. *Nature Climate Change*, 10, 77–82.
  28. Jia, P., Liang, L., Tan, X., Chen, J., & Chen, X. (2019). Potential effects of heat waves on the population dynamics of the dengue mosquito *Aedes albopictus*. *PLoS Neglected Tropical Diseases*, 13, e0007528.
  29. Cheng, J., Bambrick, H., Yakob, L., Devine, G., Frentiu, F. D., Toan, D. T. T., Thai, P. Q., Xu, Z., & Hu, W. (2020). Heatwaves and dengue outbreaks in Hanoi. *PLoS Neglected Tropical Diseases*, 14, e0007997.
  30. He, B.-J., Wang, J., Liu, H., & Ulpiani, G. (2021). Localized synergies between heat waves and urban heat islands: Implications on human thermal comfort and urban heat management. *Environmental Research*, 193, 110584.
  31. Ruffault, J., Curt, T., Moron, V., Trigo, R. M., Mouillot, F., Koutsias, N., Pimont, F., Martin-StPaul, N., Barbero, R., Dupuy, J.-L., Russo, A., & Belhadj-Khedher, C. (2020). Increased likelihood of heat-induced large wildfires in the Mediterranean Basin. *Scientific Reports*, 10, 13790.
  32. Trigo, R. M., Pereira, J. M. C., Pereira, M. G., Mota, B., Calado, T. J., Dacamara, C. C., & Santo, F. E. (2006). Atmospheric conditions associated with the exceptional fire season of 2003 in Portugal. *International Journal of Climatology*, 26, 1741–1757.
  33. Libonati, R., Geirinhas, J. L., Silva, P. S., Russo, A., Rodrigues, J. A., Belém, L. B. C., Nogueira, J., Roque, F. O., DaCamara, C. C., Nunes, A. M. B., Marengo, J. A., & Trigo, R. M. (2022). Assessing the role of compound drought and heatwave events on unprecedented 2020 wildfires in the Pantanal. *Environmental Research Letters*, 17, 015005.
  34. Machado-Silva, F., Libonati, R., Melo de Lima, T. F., Bittencourt Peixoto, R., de Almeida França, J. R., de Avelar Figueiredo Mafra Magalhães, M., Lemos Maia Santos, F., Abrantes Rodrigues, J., & DaCamara, C. C. (2020). Drought and fires influence the respiratory diseases hospitalizations in the Amazon. *Ecological Indicators*, 109, 105817.
  35. Shaposhnikov, D., Revich, B., Bellander, T., Bedada, G. B., Bottai, M., Kharkova, T., Kvasha, E., Lezina, E., Lind, T., Semutnikova, E., & Pershagen, G. (2014). Mortality related to air pollution with the Moscow heat wave and wildfire of 2010. *Epidemiology*, 25, 359–364.
  36. Salomón, R. L., Peters, R. L., Zweifel, R., Sass-Klaassen, U. G. W., Stegehuis, A. I., Smiljanic, M., Poyatos, R., Babst, F., Cienciala, E., Fonti, P., Lerink, B. J. W., Lindner, M., Martínez-Vilalta, J., Mencuccini, M., Nabuurs, G.-J., van der Maaten, E., von Arx, G., Bär, A., Akhmetzhanov, L., ... Steppe, K. (2022). The 2018 European heatwave led to stem dehydration but not to consistent growth reductions in forests. *Nature Communications*, 13, 1–11.
  37. Jöhnk, K. D., Huisman, J., Sharples, J., Sommeijer, B., Visser, P. M., & Stroom, J. M. (2008). Summer heatwaves promote blooms of harmful cyanobacteria. *Global Change Biology*, 14, 495–512.
  38. Leggat, W. P., Camp, E. F., Suggett, D. J., Heron, S. F., Fordyce, A. J., Gardner, S., Deakin, L., Turner, M., Beeching, L. J., Kuzhiumparambil, U., Eakin, C. M., & Ainsworth, T. D. (2019). Rapid coral decay is associated with marine heatwave mortality events on reefs. *Current Biology*, 29, 2723–2730.
  39. Larcom, S., She, P.-W., & van Gevelt, T. (2019). The UK summer heatwave of 2018 and public concern over energy security. *Nature Climate Change*, 9, 370–373.
  40. van Vliet, M. T. H., Yearsley, J. R., Ludwig, F., Vögele, S., Lettenmaier, D. P., & Kabat, P. (2012). Vulnerability of US and European electricity supply to climate change. *Nature Climate Change*, 2, 676–681.
  41. Ribeiro, A. F. S., Russo, A., Gouveia, C. M., Páscoa, P., & Zscheischler, J. (2020). Risk of crop failure due to compound dry and hot extremes estimated with nested copulas. *Biogeosciences*, 17, 4815–4830.
  42. Brás, T. A., Seixas, J., Carvalhais, N., & Jägermeyr, J. (2021). Severity of drought and heatwave crop losses tripled over the last five decades in Europe. *Environmental Research Letters*, 16, 065012.
  43. Rosselló, J., Becken, S., & Santana-Gallego, M. (2020). The effects of natural disasters on international tourism: A global analysis. *Tourism Management*, 79, 104080.
  44. Larbey, R., & Weitkamp, E. (2020). Water scarcity communication in the UK: Learning from Water Company Communications following the 2018 heatwave. *Frontiers in Environmental Science*, 8, 578423.
  45. Feng, S., Wu, X., Hao, Z., Hao, Y., Zhang, X., & Hao, F. (2020). A database for characteristics and variations of global compound dry and hot events. *Weather and Climate Extremes*, 30, 100299.
  46. Wang, R., Lü, G., Ning, L., Yuan, L., & Li, L. (2021). Likelihood of compound dry and hot extremes increased with stronger dependence during warm seasons. *Atmospheric Research*, 260, 105692.
  47. Schumacher, D. L., Keune, J., van Heerwaarden, C. C., Vilà-Guerau de Arellano, J., Teuling, A. J., & Miralles, D. G. (2019). Amplification of mega-heatwaves through heat torrents fuelled by upwind drought. *Nature Geoscience*, 12, 712–717.

48. Shi, Z., Jia, G., Zhou, Y., Xu, X., & Jiang, Y. (2021). Amplified intensity and duration of heatwaves by concurrent droughts in China. *Atmospheric Research*, 261, 105743.
49. Wouters, H., Keune, J., Petrova, I. Y., van Heerwaarden, C. C., Teuling, A. J., Pal, J. S., Vilà-Guerau de Arellano, J., & Miralles, D. G. (2022). Soil drought can mitigate deadly heat stress thanks to a reduction of air humidity. *Science Advances*, 8, eabe6653.
50. He, B.-J., Wang, J., Zhu, J., & Qi, J. (2022). Beating the urban heat: Situation, background, impacts and the way forward in China. *Renewable and Sustainable Energy Reviews*, 161, 112350.
51. Miralles, D. G., Teuling, A. J., van Heerwaarden, C. C., & Vilà-Guerau de Arellano, J. (2014). Mega-heatwave temperatures due to combined soil desiccation and atmospheric heat accumulation. *Nature Geoscience*, 7, 345–349.
52. Miralles, D. G., Gentine, P., Seneviratne, S. I., & Teuling, A. J. (2019). Land–atmospheric feedbacks during droughts and heatwaves: State of the science and current challenges. *Annals of the New York Academy of Sciences*, 1436, 19–35.
53. Schumacher, D. L., Keune, J., Dirmeyer, P., & Miralles, D. G. (2022). Drought self-propagation in drylands due to land–atmosphere feedbacks. *Nature Geoscience*, 15, 262–268.
54. Mukherjee, S., Mishra, A. K., Ashfaq, M., & Kao, S.-C. (2022). Relative effect of anthropogenic warming and natural climate variability to changes in Compound drought and heatwaves. *Journal of Hydrology*, 605, 127396.
55. AR6 Climate Change. (2022). *Impacts, Adaptation and Vulnerability – IPCC*. Retrieved from <https://www.ipcc.ch/report/sixth-assessment-report-working-group-ii/>
56. Zscheischler, J., & Seneviratne, S. I. (2017). Dependence of drivers affects risks associated with compound events. *Science Advances*, 3, e1700263.
57. Wu, X., & Jiang, D. (2022). Probabilistic impacts of compound dry and hot events on global gross primary production. *Environmental Research Letters*, 17, 034049.
58. Zhou, S., Zhang, Y., Park Williams, A., & Gentine, P. (2019). Projected increases in intensity, frequency, and terrestrial carbon costs of compound drought and aridity events. *Science Advances*, 5, eaau5740.
59. Gazol, A., & Camarero, J. J. (2022). Compound climate events increase tree drought mortality across European forests. *Science of the Total Environment*, 816, 151604.
60. He, Y., Hu, X., Xu, W., Fang, J., & Shi, P. (2022). Increased probability and severity of compound dry and hot growing seasons over world's major croplands. *Science of the Total Environment*, 824, 153885.
61. Ebi, K. L., Vanos, J., Baldwin, J. W., Bell, J. E., Hondula, D. M., Errett, N. A., Hayes, K., Reid, C. E., Saha, S., Spector, J., & Berry, P. (2021). Extreme weather and climate change: Population health and health system implications. *Annual Review of Public Health*, 42, 293–315.
62. Richardson, D., Black, A. S., Irving, D., Matear, R. J., Monselesan, D. P., Risbey, J. S., Squire, D. T., & Tozer, C. R. (2022). Global increase in wildfire potential from compound fire weather and drought. *Npj Climate and Atmospheric Science*, 5, 1–12.
63. Raymond, C., Horton, R. M., Zscheischler, J., Martius, O., AghaKouchak, A., Balch, J., Bowen, S. G., Camargo, S. J., Hess, J., Kornhuber, K., Oppenheimer, M., Ruane, A. C., Wahl, T., & White, K. (2020). Understanding and managing connected extreme events. *Nature Climate Change*, 10, 611–621.
64. Kappes, M. S., Keiler, M., von Elverfeldt, K., & Glade, T. (2012). Challenges of analyzing multi-hazard risk: A review. *Natural Hazards*, 64, 1925–1958.
65. Bevacqua, E., De Michele, C., Manning, C., Couasnon, A., Ribeiro, A. F. S., Ramos, A. M., Vignotto, E., Bastos, A., Blesić, S., Durante, F., Hillier, J., Oliveira, S. C., Pinto, J. G., Ragno, E., Rivoire, P., Saunders, K., van der Wiel, K., Wu, W., Zhang, T., & Zscheischler, J. (2021). Guidelines for studying diverse types of compound weather and climate events. *Earth's Future*, 9, e2021EF002340.
66. Haqiqi, I., Grogan, D. S., Hertel, T. W., & Schlenker, W. (2021). Quantifying the impacts of compound extremes on agriculture. *Hydrology and Earth System Sciences*, 25, 551–564.
67. Khorshidi, M. S., Dennison, P. E., Nikoo, M. R., AghaKouchak, A., Luce, C. H., & Sadegh, M. (2020). Increasing concurrence of wildfire drivers tripled megafire critical danger days in Southern California between 1982 and 2018. *Environmental Research Letters*, 15, 104002.
68. Mazdiyasi, O., & AghaKouchak, A. (2015). Substantial increase in concurrent droughts and heatwaves in the United States. *Proceedings of the National Academy of Sciences of the United States of America*, 112, 11484–11489.
69. Tavakol, A., Rahmani, V., & Harrington, J. (2020). Temporal and spatial variations in the frequency of compound hot, dry, and windy events in the central United States. *Scientific Reports*, 10, 15691.
70. Alizadeh, M. R., Adamowski, J., Nikoo, M. R., AghaKouchak, A., Dennison, P., & Sadegh, M. (2020). A century of observations reveals increasing likelihood of continental-scale compound dry-hot extremes. *Science Advances*, 6, eaaz4571.
71. Flach, M., Sippel, S., Gans, F., Bastos, A., Brenning, A., Reichstein, M., & Mahecha, M. D. (2018). Contrasting biosphere responses to hydrometeorological extremes: Revisiting the 2010 western Russian heatwave. *Biogeosciences*, 15, 6067–6085.
72. Sharma, S., & Mujumdar, P. (2017). Increasing frequency and spatial extent of concurrent meteorological droughts and heatwaves in India. *Scientific Reports*, 7, 1–9.
73. Wu, X., Hao, Z., Zhang, X., Li, C., & Hao, F. (2020). Evaluation of severity changes of compound dry and hot events in China based on a multivariate multi-index approach. *Journal of Hydrology*, 583, 124580.
74. Yu, R., & Zhai, P. (2020). More frequent and widespread persistent compound drought and heat event observed in China. *Scientific Reports*, 10, 14576.
75. Kong, Q., Guerreiro, S. B., Blenkinsop, S., Li, X.-F., & Fowler, H. J. (2020). Increases in summertime concurrent drought and heatwave in Eastern China. *Weather and Climate Extremes*, 28, 100242.
76. Russo, A., Gouveia, C. M., Dutra, E., Soares, P. M. M., & Trigo, R. M. (2019). The synergy between drought and extremely hot summers in the Mediterranean. *Environmental Research Letters*, 14, 014011.
77. Manning, C., Widmann, M., Bevacqua, E., Loon, A. F. V., Maraun, D., & Vrac, M. (2019). Increased probability of compound long-duration dry and hot events in Europe during summer (1950–2013). *Environmental Research Letters*, 14, 094006.
78. Ribeiro, A. F. S., Russo, A., Gouveia, C. M., & Pires, C. A. L. (2020). Drought-related hot summers: A joint probability analysis in the Iberian Peninsula. *Weather and Climate Extremes*, 30, 100279.
79. Vogel, J., Paton, E., Aich, V., & Bronstert, A. (2021). Increasing compound warm spells and droughts in the Mediterranean Basin. *Weather and Climate Extremes*, 32, 100312.
80. Orth, R., O, S., Zscheischler, J., Mahecha, M. D., & Reichstein, M. (2022). Contrasting biophysical and societal impacts of hydro-meteorological extremes. *Environmental Research Letters*, 17, 014044.
81. Sutanto, S. J., Vitolo, C., Di Napoli, C., D'Andrea, M., & Van Lanen, H. A. J. (2020). Heatwaves, droughts, and fires: Exploring compound and cascading dry hazards at the pan-European scale. *Environment International*, 134, 105276.
82. Rammig, A., Wiedermann, M., Donges, J. F., Babst, F., von Bloh, W., Frank, D., Thonicke, K., & Mahecha, M. D. (2015). Coincidences of climate extremes and anomalous vegetation responses: Comparing tree ring patterns to simulated productivity. *Biogeosciences*, 12, 373–385.
83. Sedlmeier, K., Feldmann, H., & Schädler, G. (2018). Compound summer temperature and precipitation extremes over central Europe. *Theoretical and Applied Climatology*, 131, 1493–1501.

84. Mukherjee, S., & Mishra, A. K. (2021). Increase in compound drought and heatwaves in a warming world. *Geophysical Research Letters*, *48*, e2020GL090617.
85. Páscoa, P., Gouveia, C. M., Russo, A., & Ribeiro, A. F. S. (2022). Summer hot extremes and antecedent drought conditions in Australia. *International Journal of Climatology*, <https://doi.org/10.1002/joc.7544>
86. Reddy, P. J., Perkins-Kirkpatrick, S. E., Ridder, N. N., & Sharples, J. J. (2022). Combined role of ENSO and IOD on compound drought and heatwaves in Australia using two CMIP6 large ensembles. *Weather and Climate Extremes*, *37*, 100469.
87. Geirinhas, J. L., Russo, A., Libonati, R., Sousa, P. M., Miralles, D. G., & Trigo, R. M. (2021). Recent increasing frequency of compound summer drought and heatwaves in Southeast Brazil. *Environmental Research Letters*, *16*, 034036.
88. Geirinhas, J. L., Russo, A. C., Libonati, R., Miralles, D. G., Sousa, P. M., Wouters, H., & Trigo, R. M. (2022). The influence of soil dry-out on the record-breaking hot 2013/2014 summer in Southeast Brazil. *Scientific Reports*, *12*, 5836.
89. Regoto, P., Dereczynski, C., Chou, S. C., & Bazzanella, A. C. (2021). Observed changes in air temperature and precipitation extremes over Brazil. *International Journal of Climatology*, *41*, 5125–5142.
90. De Los Milagros Skansi, M., Brunet, M., Sigró, J., Aguilar, E., Arevalo Groening, J. A., Bentancur, O. J., Castellón Geier, Y. R., Correa Amaya, R. L., Jácome, H., Malheiros Ramos, A., Oria Rojas, C., Pasten, A. M., Sallons Mitro, S., Villaroel Jiménez, C., Martínez, R., Alexander, L. V., & Jones, P. D. (2013). Warming and wetting signals emerging from analysis of changes in climate extreme indices over South America. *Global and Planetary Change*, *100*, 295–307.
91. Marengo, J. A., & Espinoza, J. C. (2016). Extreme seasonal droughts and floods in Amazonia: Causes, trends and impacts. *International Journal of Climatology*, *36*, 1033–1050.
92. Panisset, J. S., Libonati, R., Gouveia, C. M. P., Machado-Silva, F., França, D. A., França, J. R. A., & Peres, L. F. (2018). Contrasting patterns of the extreme drought episodes of 2005, 2010 and 2015 in the Amazon Basin. *International Journal of Climatology*, *38*, 1096–1104.
93. Jimenez, J. C., Libonati, R., & Peres, L. F. (2018). Droughts over Amazonia in 2005, 2010, and 2015: A cloud cover perspective. *Frontiers in Earth Science*, *6*, 227.
94. Jimenez, J. C., Marengo, J. A., Alves, L. M., Sulca, J. C., Takahashi, K., Ferrett, S., & Collins, M. (2021). The role of ENSO flavours and TNA on recent droughts over Amazon forests and the Northeast Brazil region. *International Journal of Climatology*, *41*, 3761–3780.
95. Marengo, J. A., Torres, R. R., & Alves, L. M. (2017). Drought in Northeast Brazil—Past, present, and future. *Theoretical and Applied Climatology*, *129*, 1189–1200.
96. Coelho, C. A. S., Cardoso, D. H. F., & Firpo, M. A. F. (2016). Precipitation diagnostics of an exceptionally dry event in São Paulo, Brazil. *Theoretical and Applied Climatology*, *125*, 769–784.
97. Coelho, C. A. S., de Oliveira, C. P., Ambrizzi, T., Reboita, M. S., Carpenedo, C. B., Campos, J. L. P. S., Tomaziello, A. C. N., Pampuch, L. A., de Souza Custódio, M., Dutra, L. M. M., Da Rocha, R. P., & Rehbein, A. (2016). The 2014 southeast Brazil austral summer drought: Regional scale mechanisms and teleconnections. *Climate Dynamics*, *46*, 3737–3752.
98. Getirana, A., Libonati, R., & Cataldi, M. (2021). Brazil is in water crisis—It needs a drought plan. *Nature*, *600*, 218–220.
99. Thielen, D., Ramoni-Perazzi, P., Puche, M. L., Márquez, M., Quintero, J. I., Rojas, W., Soto-Werschitz, A., Thielen, K., Nunes, A., & Libonati, R. (2021). The Pantanal under siege—On the origin, dynamics and forecast of the megadrought severely affecting the largest wetland in the world. *Water*, *13*, 3034.
100. Marengo, J. A., Cunha, A. P., Cuartas, L. A., Deusdará Leal, K. R., Broedel, E., Seluchi, M. E., Michelin, C. M., De Praga Baião, C. F., Chuchón Angulo, E., Almeida, E. K., Kazmierczak, M. L., Mateus, N. P. A., Silva, R. C., & Bender, F. (2021). Extreme drought in the Brazilian Pantanal in 2019–2020: Characterization, causes, and impacts. *Frontiers in Water*, *3*, 639204.
101. Libonati, R., Pereira, J. M. C., Da Camara, C. C., Peres, L. F., Oom, D., Rodrigues, J. A., Santos, F. L. M., Trigo, R. M., Gouveia, C. M. P., Machado-Silva, F., Enrich-Prast, A., & Silva, J. M. N. (2021). Twenty-first century droughts have not increasingly exacerbated fire season severity in the Brazilian Amazon. *Scientific Reports*, *11*, 4400.
102. Cano-Crespo, A., Traxl, D., & Thonicke, K. (2021). Spatio-temporal patterns of extreme fires in Amazonian forests. *European Physical Journal Special Topics*, *230*, 3033–3044.
103. Libonati, R., DaCamara, C. C., Peres, L. F., Sander de Carvalho, L. A., & Garcia, L. C. (2020). Rescue Brazil's burning Pantanal wetlands. *Nature*, *588*, 217–219.
104. Garcia, L. C., Szabo, J. K., de Oliveira Roque, F., de Matos Martins Pereira, A., da Cunha, C. N., Damasceno-Júnior, G. A., Morato, R. G., Tomas, W. M., Libonati, R., & Ribeiro, D. B. (2021). Record-breaking wildfires in the world's largest continuous tropical wetland: Integrative fire management is urgently needed for both biodiversity and humans. *Journal of Environmental Management*, *293*, 112870.
105. Feldpausch, T. R., Phillips, O. L., Brienens, R. J. W., Gloor, E., Lloyd, J., Lopez-Gonzalez, G., Monteagudo-Mendoza, A., Malhi, Y., Alarcón, A., Álvarez Dávila, E., Alvarez-Loayza, P., Andrade, A., Aragao, L. E. O. C., Arroyo, L., Aymard, C. G. A., Baker, T. R., Baraloto, C., Barroso, J., Bonal, D., ... Vos, V. A. (2016). Amazon forest response to repeated droughts. *Global Biogeochemical Cycles*, *30*, 964–982.
106. Machado-Silva, F., Peres, L. F., Gouveia, C. M., Enrich-Prast, A., Peixoto, R. B., Pereira, J. M. C., Marotta, H., Fernandes, P. J. F., & Libonati, R. (2021). Drought resilience debt drives NPP decline in the Amazon forest. *Global Biogeochemical Cycles*, *35*, e2021GB007004.
107. Sena, A., Freitas, C., Feitosa Souza, P., Carneiro, F., Alpino, T., Pedroso, M., Corvalan, C., & Barcellos, C. (2018). Drought in the semiarid region of Brazil: Exposure, vulnerabilities and health impacts from the perspectives of local actors. *PLoS Currents*, *10*, <https://doi.org/10.1371/currents.dis.c226851ebd64290e619a4d1ed79c8639>
108. Menezes, J. A., Madureira, A. P., Dos Santos, R. B., de Brito Duvs, I., Regoto, P., Margonari, C., de Lima Barata, M. M., & Confalonieri, U. (2021). Analyzing spatial patterns of health vulnerability to drought in the Brazilian semiarid region. *International Journal of Environmental Research and Public Health*, *18*, 6262.
109. Requia, W. J., Kill, E., Papatheodorou, S., Koutrakis, P., & Schwartz, J. D. (2021). Prenatal exposure to wildfire-related air pollution and birth defects in Brazil. *Journal of Exposure Science & Environmental Epidemiology*, *32*, 596–603.
110. Requia, W. J., Papatheodorou, S., Koutrakis, P., Mukherjee, R., & Roig, H. L. (2022). Increased preterm birth following maternal wildfire smoke exposure in Brazil. *International Journal of Hygiene and Environmental Health*, *240*, 113901.
111. Chacón-Montalván, E. A., Taylor, B. M., Cunha, M. G., Davies, G., Orellana, J. D. Y., & Parry, L. (2021). Rainfall variability and adverse birth outcomes in Amazonia. *Nature Sustainability*, *4*, 583–594.
112. Salvador, C., Vicedo-Cabrera, A. M., Libonati, R., Russo, A., Garcia, B. N., Belem, L. B. C., Gimeno, L., & Nieto, R. (2022). Effects of drought on mortality in macro urban areas of Brazil between 2000 and 2019. *GeoHealth*, *6*, e2021GH000534.
113. Costa, M. H., Fleck, L. C., Cohn, A. S., Abrahão, G. M., Brando, P. M., Coe, M. T., Fu, R., Lawrence, D., Pires, G. F., Pousa, R., & Soares-Filho, B. S. (2019). Climate risks to Amazon agriculture suggest a rationale to conserve local ecosystems. *Frontiers in Ecology and the Environment*, *17*, 584–590.
114. Rattis, L., Brando, P. M., Macedo, M. N., Spera, S. A., Castanho, A. D. A., Marques, E. Q., Costa, N. Q., Silverio, D. V., & Coe, M. T. (2021). Climatic limit for agriculture in Brazil. *Nature Climate Change*, *11*, 1098–1104.

115. Cuartas, L. A., Cunha, A. P. M. D. A., Alves, J. A., Parra, L. M. P., Deusdará-Leal, K., Costa, L. C. O., Molina, R. D., Amore, D., Broedel, E., Seluchi, M. E., Cunningham, C., Alvalá, R. C. D. S., & Marengo, J. A. (2022). Recent hydrological droughts in Brazil and their impact on hydropower generation. *Water*, 14, 601.
116. Carne, S. B., & Vera, C. S. (2011). Influence of the intraseasonal variability on heat waves. *Climate Dynamics*, 36, 2265–2277.
117. Rusticucci, M. (2012). Observed and simulated variability of extreme temperature events over South America. *Atmospheric Research*, 106, 1–17.
118. Ceccherini, G., Russo, S., Ameztoy, I., Romero, C. P., & Carmona-Moreno, C. (2016). Magnitude and frequency of heat and cold waves in recent decades: The case of South America. *Natural Hazards and Earth System Sciences*, 16, 821–831.
119. Geirinhas, J. L., Trigo, R. M., Libonati, R., Castro, L. C. O., Sousa, P. M., Coelho, C. A. S., Peres, L. F., & de Avelar, F. M., Magalhães, M. (2019). Characterizing the atmospheric conditions during the 2010 heat-wave in Rio de Janeiro marked by excessive mortality rates. *Science of the Total Environment*, 650, 796–808.
120. Geirinhas, J. L., Trigo, R. M., Libonati, R., Coelho, C. A. S., & Palmeira, A. C. (2018). Climatic and synoptic characterization of heat waves in Brazil. *International Journal of Climatology*, 38, 1760–1776.
121. Cordero Simões dos Reis, N., Boiaski, N. T., & Ferraz, S. E. T. (2019). Characterization and spatial coverage of heat waves in subtropical Brazil. *Atmosphere*, 10, 284.
122. Feron, S., Cordero, R. R., Damiani, A., Llanillo, P. J., Jorquera, J., Sepulveda, E., Asencio, V., Laroze, D., Labbe, F., Carrasco, J., & Torres, G. (2019). Observations and projections of heat waves in South America. *Scientific Reports*, 9, 8173.
123. Bell, M. L., O'Neill, M. S., Ranjit, N., Borja-Aburto, V. H., Cifuentes, L. A., & Gouveia, N. C. (2008). Vulnerability to heat-related mortality in Latin America: A case-crossover study in São Paulo, Brazil, Santiago, Chile and Mexico City, Mexico. *International Journal of Epidemiology*, 37, 796–804.
124. Son, J.-Y., Gouveia, N., Bravo, M. A., de Freitas, C. U., & Bell, M. L. (2016). The impact of temperature on mortality in a subtropical city: Effects of cold, heat, and heat waves in São Paulo, Brazil. *International Journal of Biometeorology*, 60, 113–121.
125. Guo, Y., Gasparrini, A., Armstrong, B. G., Tawatsupa, B., Tobias, A., Lavigne, E., de Sousa Zanotti Stagliorio Coelho, M., Pan, X., Kim, H., Hashizume, M., Honda, Y., Guo, Y.-L. L., Wu, C.-F., Zanobetti, A., Schwartz, J. D., Bell, M. L., Scortichini, M., Michelozzi, P., Punnasiri, K., ... Tong, S. (2017). Heat wave and mortality: A multicountry, multi-community study. *Environmental Health Perspectives*, 125, 087006.
126. Zhao, Q., Li, S., Coelho, M. S. Z. S., Saldiva, P. H. N., Hu, K., Huxley, R. R., Abramson, M. J., & Guo, Y. (2019). The association between heat-waves and risk of hospitalization in Brazil: A nationwide time series study between 2000 and 2015. *PLoS Medicine*, 16, e1002753.
127. Zhao, Q., Li, S., Coelho, M. S. Z. S., Saldiva, P. H. N., Hu, K., Arblaster, J. M., Nicholls, N., Huxley, R. R., Abramson, M. J., & Guo, Y. (2019). Geographic, demographic, and temporal variations in the association between heat exposure and hospitalization in Brazil: A nationwide study between 2000 and 2015. *Environmental Health Perspectives*, 127, 017001.
128. Xu, R., Zhao, Q., Coelho, M. S. Z. S., Saldiva, P. H. N., Zoungas, S., Huxley, R. R., Abramson, M. J., Guo, Y., & Li, S. (2019). Association between heat exposure and hospitalization for diabetes in Brazil during 2000–2015: A nationwide case-crossover study. *Environmental Health Perspectives*, 127, 117005.
129. Geirinhas, J. L., Russo, A., Libonati, R., Trigo, R. M., Castro, L. C. O., Peres, L. F., de Avelar, F. M., Magalhães, M., & Nunes, B. (2020). Heat-related mortality at the beginning of the twenty-first century in Rio de Janeiro, Brazil. *International Journal of Biometeorology*, 64, 1319–1332.
130. Prosdocimi, D., & Klima, K. (2020). Health effects of heat vulnerability in Rio de Janeiro: A validation model for policy applications. *SN Applied Sciences*, 2, 1948.
131. Diniz, F. R., Gonçalves, F. L. T., & Sheridan, S. (2020). Heat wave and elderly mortality: Historical analysis and future projection for metropolitan region of São Paulo, Brazil. *Atmosphere*, 11, 933.
132. Costa, I. T., Wollmann, C. A., Gobo, J. P. A., Ikefuti, P. V., Shooshtarian, S., & Matzarakis, A. (2021). Extreme weather conditions and cardiovascular hospitalizations in Southern Brazil. *Sustainability*, 13, 12194.
133. de Moraes, S. L., Almendra, R., & Barrozo, L. V. (2022). Impact of heat waves and cold spells on cause-specific mortality in the city of São Paulo, Brazil. *International Journal of Hygiene and Environmental Health*, 239, 113861.
134. Gusso, A., Ducati, J. R., Veronez, M. R., Arvor, D., & da Silveira, L. G. (2014). Monitoring the vulnerability of soybean to heat waves and their impacts in Mato Grosso state, Brazil. 2014 IEEE Geoscience and Remote Sensing Symposium, 859–862.
135. Vale, M., Moura, D., Nääs, I., & Pereira, D. (2010). Characterization of heat waves affecting mortality rates of broilers between 29 days and market age. *Brazilian Journal of Poultry Science*, 12, 279–285.
136. de Faria Peres, L., José de Lucena, A., Filho, O. C., & de Almeida Franca, J. R. (2018). The urban heat island in Rio de Janeiro, Brazil, in the last 30 years using remote sensing data. *International Journal of Applied Earth Observation and Geoinformation*, 64, 104–116.
137. Sun, Q., Miao, C., Hanel, M., Borthwick, A. G. L., Duan, Q., Ji, D., & Li, H. (2019). Global heat stress on health, wildfires, and agricultural crops under different levels of climate warming. *Environment International*, 128, 125–136.
138. Ridder, N. N., Ukkola, A. M., Pitman, A. J., & Perkins-Kirkpatrick, S. E. (2022). Increased occurrence of high impact compound events under climate change. *Npj Climate and Atmospheric Science*, 5, 1–8.
139. Bevacqua, E., Zappa, G., Lehner, F., & Zscheischler, J. (2022). Precipitation trends determine future occurrences of compound hot–dry events. *Nature Climate Change*, 12, 350–355.
140. Meng, Y., Hao, Z., Feng, S., Zhang, X., & Hao, F. (2022). Increase in compound dry-warm and wet-warm events under global warming in CMIP6 models. *Global and Planetary Change*, 210, 103773.
141. Mora, C., Dousset, B., Caldwell, I. R., Powell, F. E., Geronimo, R. C., Bielecki, C. R., Counsell, C. W. W., Dietrich, B. S., Johnston, E. T., Louis, L. V., Lucas, M. P., McKenzie, M. M., Shea, A. G., Tseng, H., Giambelluca, T. W., Leon, L. R., Hawkins, E., & Trauernicht, C. (2017). Global risk of deadly heat. *Nature Climate Change*, 7, 501–506.
142. Xu, C., Kohler, T. A., Lenton, T. M., Svenning, J.-C., & Scheffer, M. (2020). Future of the human climate niche. *Proceedings of the National Academy of Sciences of the United States of America*, 117, 11350–11355.
143. Freychet, N., Hegerl, G., Mitchell, D., & Collins, M. (2021). Future changes in the frequency of temperature extremes may be underestimated in tropical and subtropical regions. *Communications Earth & Environment*, 2, 28.
144. Raymond, C., Suarez-Gutierrez, L., Kornhuber, K., Pascolini-Campbell, M., Sillmann, J., & Waliser, D. E. (2022). Increasing spatiotemporal proximity of heat and precipitation extremes in a warming world quantified by a large model ensemble. *Environmental Research Letters*, 17, 035005.
145. Hao, Z., Hao, F., Singh, V. P., & Zhang, X. (2018). Quantifying the relationship between compound dry and hot events and El Niño–Southern Oscillation (ENSO) at the global scale. *Journal of Hydrology*, 567, 332–338.
146. Liu, W., Sun, F., Feng, Y., Li, C., Chen, J., Sang, Y.-F., & Zhang, Q. (2021). Increasing population exposure to global warm-season concurrent dry and hot extremes under different warming levels. *Environmental Research Letters*, 11, 094002.

147. Luiz Silva, W., Nascimento, M. X., & Menezes, W. F. (2015). Atmospheric blocking in the South Atlantic during the summer 2014: A synoptic analysis of the phenomenon. *Atmospheric and Climate Sciences*, 5, 386–393.
148. Finke, K., Jiménez-Esteve, B., Taschetto, A. S., Ummenhofer, C. C., Bumke, K., & Domeisen, D. I. V. (2020). Revisiting remote drivers of the 2014 drought in South-Eastern Brazil. *Climate Dynamics*, 55, 3197–3211.
149. Seth, A., Fernandes, K., & Camargo, S. J. (2015). Two summers of São Paulo drought: Origins in the western tropical Pacific. *Geophysical Research Letters*, 42, 10,816–10,823.
150. Rodrigues, R. R., Taschetto, A. S., Sen Gupta, A., & Foltz, G. R. (2019). Common cause for severe droughts in South America and marine heatwaves in the South Atlantic. *Nature Geoscience*, 12, 620–626.
151. Marengo, J. A., Ambrizzi, T., Barreto, N., Cunha, A. P., Ramos, A. M., Skansi, M., Molina Carpio, J., & Salinas, R. (2021). The heat wave of October 2020 in central South America. *International Journal of Climatology*, 42, 2281–2298.
152. Thielen, D., Schuchmann, K.-L., Ramoni-Perazzi, P., Marquez, M., Rojas, W., Quintero, J. I., & Marques, M. I. (2020). Quo vadis Pantanal? Expected precipitation extremes and drought dynamics from changing sea surface temperature. *PLoS One*, 15, e0227437.
153. Jiménez-Muñoz, J. C., Sobrino, J. A., Mattar, C., & Malhi, Y. (2013). Spatial and temporal patterns of the recent warming of the Amazon forest. *Journal of Geophysical Research: Atmospheres*, 118, 5204–5215.
154. Costa, D. F., Gomes, H. B., Silva, M. C. L., & Zhou, L. (2022). The most extreme heat waves in Amazonia happened under extreme dryness. *Climate Dynamics*, 59, 1–15.
155. Andreoli, R. V., de Oliveira, S. S., Kayano, M. T., Viegas, J., de Souza, R. A. F., & Candido, L. A. (2017). The influence of different El Niño types on the South American rainfall. *International Journal of Climatology*, 37, 1374–1390.
156. Coelho, C. A. S., Cavalcanti, I. A. F., Costa, S. M. S., Freitas, S. R., Ito, E. R., Luz, G., Santos, A. F., Nobre, C. A., Marengo, J. A., & Pezza, A. B. (2012). Climate diagnostics of three major drought events in the Amazon and illustrations of their seasonal precipitation predictions. *Meteorological Applications*, 19, 237–255.
157. Jiménez-Muñoz, J. C., Mattar, C., Barichivich, J., Santamaría-Artigas, A., Takahashi, K., Malhi, Y., Sobrino, J. A., & van der Schrier, G. (2016). Record-breaking warming and extreme drought in the Amazon rainforest during the course of El Niño 2015–2016. *Scientific Reports*, 6, 33130.
158. Garcia, B. N., Libonati, R., & Nunes, A. M. B. (2018). Extreme drought events over the Amazon Basin: The perspective from the reconstruction of South American hydroclimate. *Water*, 10, 1594.
159. Coronato, T., Carril, A. F., Zaninelli, P. G., Giles, J., Ruscica, R., Falco, M., Sörensson, A. A., Fita, L., Li, L. Z. X., & Menéndez, C. G. (2020). The impact of soil moisture–atmosphere coupling on daily maximum surface temperatures in Southeastern South America. *Climate Dynamics*, 55, 2543–2556.
160. Benson, D. O., & Dirmeyer, P. A. (2021). Characterizing the relationship between temperature and soil moisture extremes and their role in the exacerbation of heat waves over the contiguous United States. *Journal of Climate*, 34, 2175–2187.
161. Nairn, J. R., & Fawcett, R. J. B. (2015). The excess heat factor: A metric for heatwave intensity and its use in classifying heatwave severity. *International Journal of Environmental Research and Public Health*, 12, 227–253.
162. Scalley, B., Spicer, T., Jian, L., Xiao, J., Nairn, J., & Robertson, A. (2015). Responding to heatwave intensity: Excess Heat Factor is a superior predictor of health service utilisation and a trigger for heatwave plans. *Australian and New Zealand Journal of Public Health*, 36, 582–587.
163. Ellena, M., Ballester, J., Mercogliano, P., Ferracin, E., Barbato, G., Costa, G., & Ingole, V. (2020). Social inequalities in heat-attributable mortality in the city of Turin, northwest of Italy: A time series analysis from 1982 to 2018. *Environmental Health*, 19, 116.
164. Tramuja Vasconcellos Neumann, L., & Albert, S. M. (2018). Aging in Brazil. *Gerontologist*, 58, 611–617.
165. Huang, M., Strickland, M. J., Richards, M., Holmes, H. A., Newman, A. J., Garn, J. V., Liu, Y., Warren, J. L., Chang, H. H., & Darrow, L. A. (2021). Acute associations between heatwaves and preterm and early-term birth in 50 US metropolitan areas: A matched case–control study. *Environmental Health*, 20, 47.
166. Strand, L. B., Barnett, A. G., & Tong, S. (2012). Maternal exposure to ambient temperature and the risks of preterm birth and stillbirth in Brisbane, Australia. *American Journal of Epidemiology*, 175, 99–107.
167. Schifano, P., Asta, F., Dadvand, P., Davoli, M., Basagana, X., & Michelozzi, P. (2016). Heat and air pollution exposure as triggers of delivery: A survival analysis of population-based pregnancy cohorts in Rome and Barcelona. *Environment International*, 88, 153–159.
168. Basu, R., Malig, B., & Ostro, B. (2010). High ambient temperature and the risk of preterm delivery. *American Journal of Epidemiology*, 172, 1108–1117.
169. Li, C., Bloom, M. S., Lin, S., Ren, M., Hajat, S., Wang, Q., Zhang, W., Ho, H. C., Zhao, Q., Lin, Y., & Huang, C. (2021). Temperature variation and preterm birth among live singleton deliveries in Shenzhen, China: A time-to-event analysis. *Environmental Research*, 195, 110834.
170. Goldenberg, R. L., Culhane, J. F., Iams, J. D., & Romero, R. (2008). Epidemiology and causes of preterm birth. *Lancet*, 371, 75–84.
171. Villar, J., Giuliani, F., Barros, F., Roggero, P., Coronado Zanco, I. A., Rego, M. A. S., Ochieng, R., Gianni, M. L., Rao, S., Lambert, A., Ruymina, I., Britto, C., Chawla, D., Cheikh Ismail, L., Ali, S. R., Hirst, J., Teji, J. S., Abawi, K., Asibey, J., ... Kennedy, S. (2018). Monitoring the post-natal growth of preterm infants: A paradigm change. *Pediatrics*, 141, e20172467.
172. World Health Organization. (2015). *WHO recommendations on interventions to improve preterm birth outcomes: Highlights and key messages from the World Health Organization's 2015 global recommendations (WHO/RHR/15.16)*. World Health Organization.
173. Roos, N., Kovats, S., Hajat, S., Filippi, V., Chersich, M., Luchters, S., Scorgie, F., Nakstad, B., Stephansson, O., & CHAMNHA Consortium. (2021). Maternal and newborn health risks of climate change: A call for awareness and global action. *Acta Obstetrica Et Gynecologica Scandinavica*, 100, 566–570.
174. Ha, S. (2022). The changing climate and pregnancy health. *Current Environmental Health Reports*, 9, 263–275.
175. Gitau, R., Makasa, M., Kasonka, L., Sinkala, M., Tomkins, A., Chintu, C., & Filteau, S. (2005). Maternal micronutrient status and decreased growth of Zambian infants born during and after the maize price increases resulting from the southern African drought of 2001–2002. *Public Health Nutrition*, 8, 837–843.
176. Ebi, K. L., & Bowen, K. (2016). Extreme events as sources of health vulnerability: Drought as an example. *Weather and Climate Extremes*, 11, 95–102.
177. Chersich, M. F., Pham, M. D., Areal, A., Haghghi, M. M., Manyuchi, A., Swift, C. P., Wernecke, B., Robinson, M., Hetem, R., Boeckmann, M., & Hajat, S. (2020). Associations between high temperatures in pregnancy and risk of preterm birth, low birth weight, and stillbirths: Systematic review and meta-analysis. *BMJ*, 371, m3811.
178. Jolly, W. M., Cochrane, M. A., Freeborn, P. H., Holden, Z. A., Brown, T. J., Williamson, G. J., & Bowman, D. M. J. S. (2015). Climate-induced variations in global wildfire danger from 1979 to 2013. *Nature Communications*, 6, 1–11.
179. Jain, P., Castellanos-Acuna, D., Coogan, S. C. P., Abatzoglou, J. T., & Flannigan, M. D. (2022). Observed increases in extreme fire weather driven by atmospheric humidity and temperature. *Nature Climate Change*, 12, 63–70.
180. Bowman, D. M. J. S., Kolden, C. A., Abatzoglou, J. T., Johnston, F. H., van der Werf, G. R., & Flannigan, M. (2020). Vegetation

- fires in the Anthropocene. *Nature Reviews Earth & Environment*, 1, 500–515.
181. Ribeiro, A. F. S., Brando, P. M., Santos, L., Rattis, L., Hirschi, M., Hauser, M., Seneviratne, S. I., & Zscheischler, J. (2022). A compound event-oriented framework to tropical fire risk assessment in a changing climate. *Environmental Research Letters*, 17, 065015.
  182. Kumar, S., Getirana, A., Libonati, R., Hain, C., Mahanama, S., & Andela, N. (2022). Changes in land use enhance the sensitivity of tropical ecosystems to fire-climate extremes. *Scientific Reports*, 12, 964.
  183. Tomas, W. M., Berlinck, C. N., Chiaravalloti, R. M., Faggioni, G. P., Strüssmann, C., Libonati, R., Abrahão, C. R., do Valle Alvarenga, G., de Faria Bacellar, A. E., de Queiroz Batista, F. R., Bornato, T. S., Camilo, A. R., Castedo, J., Fernando, A. M. E., de Freitas, G. O., Garcia, C. M., Gonçalves, H. S., de Freitas Guilherme, M. B., Layme, V. M. G., ... Morato, R. (2021). Distance sampling surveys reveal 17 million vertebrates directly killed by the 2020's wildfires in the Pantanal, Brazil. *Scientific Reports*, 11, 23547.
  184. Correa, D. B., Alcântara, E., Libonati, R., Massi, K. G., & Park, E. (2022). Increased burned area in the Pantanal over the past two decades. *Science of the Total Environment*, 835, 155386.
  185. Marengo, J. A., Alves, L. M., & Torres, R. R. (2016). Regional climate change scenarios in the Brazilian Pantanal watershed. *Climate Research*, 68, 201–213.
  186. Menezes, L. S., de Oliveira, A. M., Santos, F. L. M., Russo, A., de Souza, R. A. F., Roque, F. O., & Libonati, R. (2022). Lightning patterns in the Pantanal: Untangling natural and anthropogenic-induced wildfires. *Science of the Total Environment*, 820, 153021.
  187. Chen, Y., Morton, D., Andela, N., Werf, G., Giglio, L., & Randerson, J. (2017). A pan-tropical cascade of fire driven by El Niño/Southern Oscillation. *Nature Climate Change*, 7, 906–911.
  188. Nepstad, D., Lefebvre, P., Lopes da Silva, U., Tomasella, J., Schlesinger, P., Solórzano, L., Moutinho, P., Ray, D., & Guerreira Benito, J. (2004). Amazon drought and its implications for forest flammability and tree growth: A basin-wide analysis. *Global Change Biology*, 10, 704–717.
  189. Duffy, P. B., Brando, P., Asner, G. P., & Field, C. B. (2015). Projections of future meteorological drought and wet periods in the Amazon. *Proceedings of the National Academy of Sciences of the United States of America*, 112, 13172–13177.
  190. Choat, B., Jansen, S., Brodribb, T. J., Cochard, H., Delzon, S., Bhaskar, R., Bucci, S. J., Feild, T. S., Gleason, S. M., Hacke, U. G., Jacobsen, A. L., Lens, F., Maherali, H., Martínez-Vilalta, J., Mayr, S., Mencuccini, M., Mitchell, P. J., Nardini, A., Pittermann, J., ... Zanne, A. E. (2012). Global convergence in the vulnerability of forests to drought. *Nature*, 491, 752–755.
  191. Rochedo, P. R. R., Soares-Filho, B., Schaeffer, R., Viola, E., Szklo, A., Lucena, A. F. P., Koberle, A., Davis, J. L., Rajão, R., & Rathmann, R. (2018). The threat of political bargaining to climate mitigation in Brazil. *Nature Climate Change*, 8, 695–698.
  192. Roux, R. L., Wagner, F., Blanc, L., Betbeder, J., Gond, V., Dessard, H., Funatsu, B., Bourgoin, C., Cornu, G., Herault, B., Montfort, F., Sist, P., Begue, A., Dubreuil, V., Laurent, F., Messner, F., Hasan, A. F., & Arvor, D. (2022). How wildfires increase sensitivity of Amazon forests to droughts. *Environmental Research Letters*, 17, 044031.
  193. Lejeune, Q., Davin, E. L., Guillod, B. P., & Seneviratne, S. I. (2015). Influence of Amazonian deforestation on the future evolution of regional surface fluxes, circulation, surface temperature and precipitation. *Climate Dynamics*, 44, 2769–2786.
  194. Jiang, Y., Wang, G., Liu, W., Erfanian, A., Peng, Q., & Fu, R. (2021). Modeled response of South American climate to three decades of deforestation. *Journal of Climate*, 34, 2189–2203.
  195. UN Environment. (2022). *Spreading like wildfire: The rising threat of extraordinary landscape fires*. UNEP - UN Environment Programme. <http://www.unep.org/resources/report/spreading-wildfire-rising-threat-extraordinary-landscape-fires>
  196. Nogueira, J. M. P., Rambal, S., Barbosa, J. P. R. A. D., & Mouillot, F. (2017). Spatial pattern of the seasonal drought/burned area relationship across Brazilian biomes: Sensitivity to drought metrics and global remote-sensing fire products. *Climate*, 5, 42.
  197. Li, S., Rifai, S., Anderson, L. O., & Sparrow, S. (2022). Identifying local-scale meteorological conditions favorable to large fires in Brazil. *Climate Resilience and Sustainability*, 1, e11.
  198. Silva, P. S., Bastos, A., Libonati, R., Rodrigues, J. A., & DaCamara, C. C. (2019). Impacts of the 1.5 °C global warming target on future burned area in the Brazilian Cerrado. *Forest Ecology and Management*, 446, 193–203.
  199. Sano, E. E., Rodrigues, A. A., Martins, E. S., Bettiol, G. M., Bustamante, M. M. C., Bezerra, A. S., Couto, A. F., Vasconcelos, V., Schüler, J., & Bolfe, E. L. (2019). Cerrado ecoregions: A spatial framework to assess and prioritize Brazilian savanna environmental diversity for conservation. *Journal of Environmental Management*, 232, 818–828.
  200. Silva, P. S., Nogueira, J., Rodrigues, J. A., Santos, F. L. M., Pereira, J. M. C., DaCamara, C. C., Daldegan, G. A., Pereira, A. A., Peres, L. F., Schmidt, I. B., & Libonati, R. (2021). Putting fire on the map of Brazilian savanna ecoregions. *Journal of Environmental Management*, 296, 113098.
  201. Cunha, A. P. M. A., Zeri, M., Deusdará Leal, K., Costa, L., Cuartas, L. A., Marengo, J. A., Tomasella, J., Vieira, R. M., Barbosa, A. A., Cunningham, C., Cal Garcia, J. V., Broedel, E., Alvalá, R., & Ribeiro-Neto, G. (2019). Extreme drought events over Brazil from 2011 to 2019. *Atmosphere*, 10, 642.
  202. Alizadeh, M. R., Abatzoglou, J. T., Adamowski, J. F., Prestemon, J. P., Chittoori, B., Akbari Asanjan, A., & Sadegh, M. (2022). Increasing heat-stress inequality in a warming climate. *Earth's Future*, 10, e2021EF002488.

## SUPPORTING INFORMATION

Additional supporting information can be found online in the Supporting Information section at the end of this article.

**How to cite this article:** Libonati, R., Geirinhas, J. L., Silva, P. S., Monteiro dos Santos, D., Rodrigues, J. A., Russo, A., Peres, L. F., Narcizo, L., Gomes, M. E. R., Rodrigues, A. P., DaCamara, C. C., Pereira, J. M. C., & Trigo, R. M. (2022). Drought–heatwave nexus in Brazil and related impacts on health and fires: A comprehensive review. *Ann NY Acad Sci.*, 1517, 44–62. <https://doi.org/10.1111/nyas.14887>

## Annex D

Libonati et al. (2022b)

ENVIRONMENTAL RESEARCH  
LETTERS

## LETTER

## OPEN ACCESS

RECEIVED  
15 August 2021REVISED  
30 November 2021ACCEPTED FOR PUBLICATION  
23 December 2021PUBLISHED  
6 January 2022

Original content from  
this work may be used  
under the terms of the  
[Creative Commons  
Attribution 4.0 licence](#).

Any further distribution  
of this work must  
maintain attribution to  
the author(s) and the title  
of the work, journal  
citation and DOI.

Assessing the role of compound drought and heatwave events on  
unprecedented 2020 wildfires in the PantanalRenata Libonati<sup>1,2,7,\*</sup> , João L Geirinhas<sup>2,7</sup> , Patrícia S Silva<sup>2</sup> , Ana Russo<sup>2</sup> , Julia A Rodrigues<sup>1</sup> ,  
Liz B C Belém<sup>1</sup> , Joana Nogueira<sup>3</sup>, Fabio O Roque<sup>4,5</sup> , Carlos C DaCamara<sup>2</sup> , Ana M B Nunes<sup>1</sup> ,  
José A Marengo<sup>6</sup> and Ricardo M Trigo<sup>1,2</sup> <sup>1</sup> Departamento de Meteorologia, Universidade Federal do Rio de Janeiro, Rio de Janeiro, Brazil<sup>2</sup> Instituto Dom Luiz (IDL), Faculdade de Ciências, Universidade de Lisboa, 1749-016 Lisboa, Portugal<sup>3</sup> Institut für Landschaftsökologie, Westfälische Wilhelms (WWU), Universität Münster, Münster, Germany<sup>4</sup> Instituto de Biociências, Universidade Federal de Mato Grosso do Sul, Campo Grande, Brazil<sup>5</sup> Centre for Tropical Environmental and Sustainability Science (TESS) and College of Science and Engineering, James Cook University, Cairns, Australia<sup>6</sup> National Center for Monitoring and Early Warning of Natural Disasters CEMADEN, São Paulo, Brazil<sup>7</sup> These authors contributed equally to this work.

\* Author to whom any correspondence should be addressed.

E-mail: [renata.libonati@igeo.ufrj.br](mailto:renata.libonati@igeo.ufrj.br)**Keywords:** Pantanal, Brazil, compound events, droughts, heatwaves, climate extremes, wildfiresSupplementary material for this article is available [online](#)**Abstract**

The year 2020 had the most catastrophic fire season over the last two decades in the Pantanal, which led to outstanding environmental impacts. Indeed, much of the Pantanal has been affected by severe dry conditions since 2019, with evidence of the 2020's drought being the most extreme and widespread ever recorded in the last 70 years. Although it is unquestionable that this mega-drought contributed significantly to the increase of fire risk, so far, the 2020's fire season has been analyzed at the univariate level of a single climate event, not considering the co-occurrence of extreme and persistent temperatures with soil dryness conditions. Here, we show that similarly to other areas of the globe, the influence of land-atmosphere feedbacks contributed decisively to the simultaneous occurrence of dry and hot spells (HPs), exacerbating fire risk. The ideal synoptic conditions for strong atmospheric heating and large evaporation rates were present, in particular during the HPs, when the maximum temperature was, on average, 6 °C above the normal. The short span of the period during those compound drought-heatwave (CDHW) events accounted for 55% of the burned area of 2020. The vulnerability in the northern forested areas was higher than in the other areas, revealing a synergistic effect between fuel availability and weather-hydrological conditions. Accordingly, where fuel is not a limiting factor, fire activity tends to be more modelled by CDHW events. Our work advances beyond an isolated event-level basis towards a compound and cascading natural hazards approach, simultaneously estimating the contribution of drought and heatwaves to fuelling extreme fire outbreaks in the Pantanal such as those in 2020. Thus, these findings are relevant within a broader context, as the driving mechanisms apply across other ecosystems, implying higher flammability conditions and further efforts for monitoring and predicting such extreme events.

**1. Introduction**

In 2020, the world witnessed one-quarter of the Brazilian Pantanal, the largest continuous tropical

wetland, on fire [1, 2]. More than 3.9 million hectares were burned, an area four times larger than the long-term average observed between 2001 and 2019 [3, 4]. The Pantanal 2020 fire (hereafter P20F) season may



have directly affected 17 million native vertebrates [5] and resulted in total national economic losses of ~USD 3.6 billion [6].

These extremely intense impacts inevitably raise the doubt: why was the P20F so exceptional? Evidence is mounting that the P20F resulted from a complex interplay of distinct contributing components, including human factors, landscape characteristics, and adverse meteorological conditions [2, 7]. Globally, the year 2020 tied with 2016 for the warmest year on record since record-keeping began in 1880 [8], with several record-breaking temperature (compounded) events taking place in different regions. The 2019/2020 mega-fires in Australia were tightly linked to record-breaking temperatures, both induced to a large extent, by widespread prolonged severe dryness [9–11]. The 2020's catastrophic fires in California were enabled by long-lasting dry conditions across much of western U.S [12]. Among the 2020's unprecedented climate conditions favoring fire activity in Oceania, Euro-Asia and North America, South America (SA) was not an exception [13]. Extreme dry conditions were reported in countries across central-south SA, reaching Argentina, Brazil, Bolivia and Paraguay [14–16]. Much of SA has been in drought since 2019, influenced by a warming trend in the sea surface temperature of Pacific and Atlantic Oceans [14–17].

The extremely dry conditions across central-south SA were accompanied by heatwave (HW) episodes throughout the austral spring which triggered record-breaking daily maximum temperatures [18]. In Brazil, between the end of September and early November, when anomalies were persistently above 5 °C in the central and southeastern regions, including the Pantanal [18, 19], several warnings of the HWs' risk were issued.

Previous studies suggest that the P20Fs were strongly influenced by the most extreme drought recorded in the region since 1950 [2, 7, 18] which was accompanied by the occurrence of several prolonged periods of extremely high temperatures. Compound drought-HW (CDHW) events usually cause more severe wildfires than single events of drought or HW alone [20] and are being routinely reported worldwide [21–26], including in Brazil [27]. Although understanding the factors that influence the regional occurrence of a CDHW event is imperative, so far, its characterization and association with fire outbreaks have not been fully explored in wetlands such as the Pantanal. Thus, this study aims to assess, for the first time, the severe CDHW conditions and the land-atmosphere feedbacks associated with the P20Fs. A detailed analysis of the exceptional P20F season is provided together with the spatial and temporal analysis of surface conditions and the associated synoptic patterns. The present approach provides a more comprehensive understanding of the physical land-atmosphere coupling mechanisms associated with

this extreme climate event, highlighting its dominant role in the observed record-breaking fires.

## 2. Data and methods

### 2.1. Datasets

Burned area (BA) was obtained from two main sources. Monthly values were obtained from the MCD64A1 collection 6 derived from the MODIS (moderate resolution imaging spectroradiometer) sensor at 500 m spatial resolution from 2001 to 2020 [28]. For improved accuracy on day-to-day variability of BA [29], daily values for 2020 were obtained through the ALARMES dataset with a 500 m spatial resolution using images from the visible infrared imaging suite imager sensor [29].

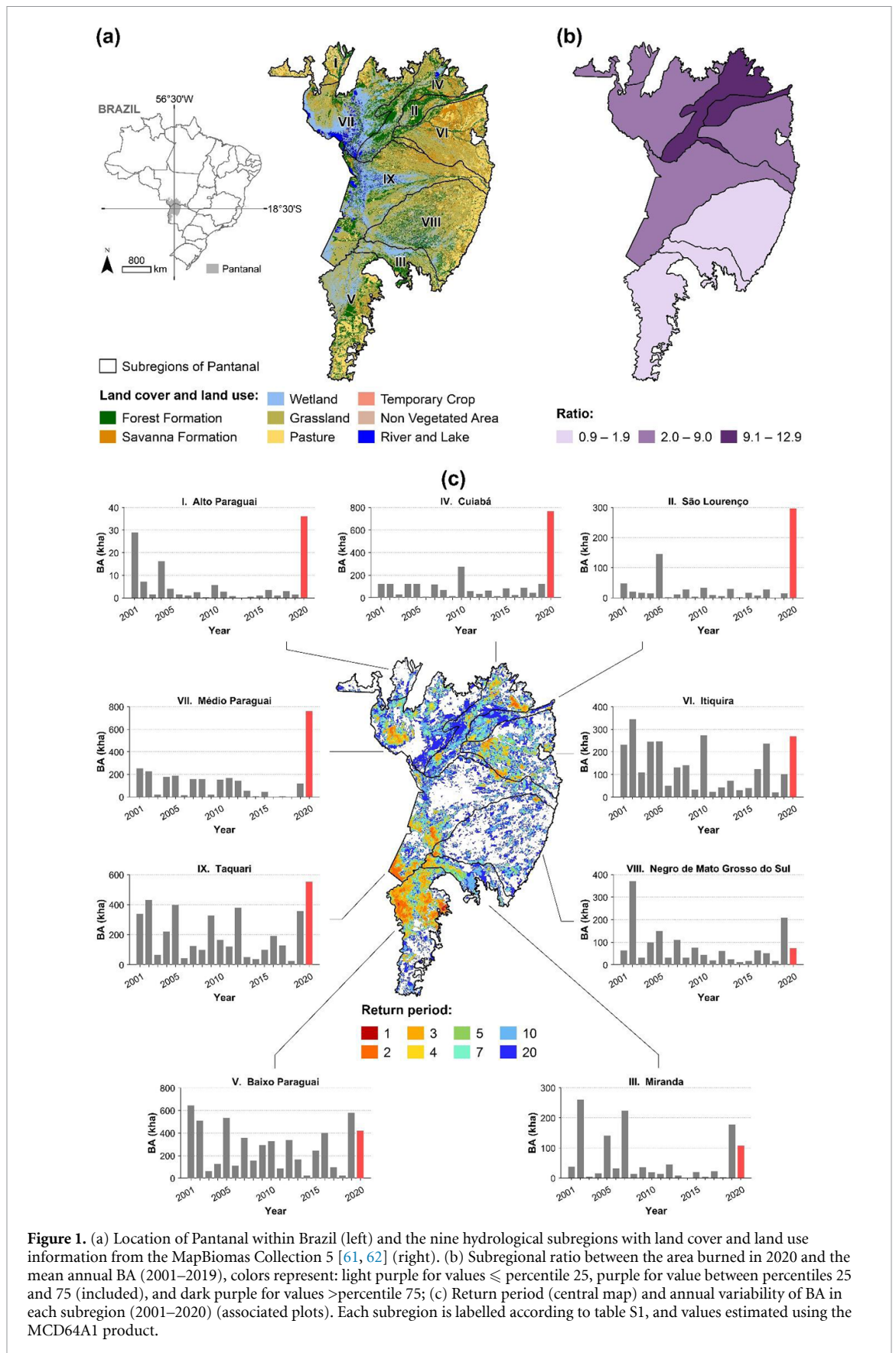
Meteorological parameters, including maximum temperature ( $T_{max}$ ), precipitation, surface net solar radiation, geopotential height and temperature at several levels of the atmosphere were extracted, at daily scale, from the European Centre of Medium-range Weather Forecast ERA-5 reanalysis dataset [30]. Soil moisture, evaporation and potential evaporation, at daily scale, were obtained from the Global Land Evaporation Amsterdam Model (GLEAM v3.5a) [31, 32]. All variables were retrieved at a gridded  $0.25^\circ \times 0.25^\circ$  spatial resolution and the composite anomalies were computed with respect to the climatological seasonal cycle (1981–2010).

Surface meteorological fire danger conditions were evaluated using the fire weather index (FWI) [33], allowing summarizing the chances of a fire to ignite and propagate and to foresee hazardous fire conditions [34]. The FWI product is provided by the Copernicus Emergency Management Service [35], computed with meteorological fields from the ERA5 reanalysis [36]. Daily values were obtained for the historical period (1980–2020) on a regular grid of  $0.25^\circ \times 0.25^\circ$  resolution [37]. All analyses were carried out for the Brazilian sector of the Pantanal wetland.

### 2.2. Methodology

#### 2.2.1. Fire analysis

To assess the exceptionality of the P20Fs we considered the ratio between the total BA in 2020 and the respective mean BA for the 2001–2019 period. We also estimated the fire return period, defined as the ratio between the 20 years that encompass our study period (2001–2020) and the annual recurrence. Finally, we computed the 75th percentile (P75) of the 2001–2019 period and the percentage of the 2020 BA with no fire and low recurrence (1–2 years). The above-mentioned metrics were computed for each of the nine hydrological subregions of Pantanal [38], to evaluate regional discrepancies within the biome (figure 1(a)).



2.2.2. Heat wave identification

HW was defined as a period of three or more consecutive days with daily  $T_{max}$  values above predefined climatological (1981–2010 base period) percentiles

(80th, 90th and 95th) of  $T_{max}$  for each calendar day (on a 15 day moving window). Based on this definition, a secondary metric was computed: the percentage of the Pantanal domain under HW conditions

(% Pantanal<sub>HW</sub>). This method was already used in previous studies conducted for the USA [39] and Brazil [27] and consists of determining the yearly percentage of the total Pantanal cells (cellsPAN<sub>total</sub>) that experienced HW conditions:

$$\%Pantanal_{HW} = \frac{cellsPAN_{HW}}{cellsPAN_{total}} \times 100. \quad (1)$$

Per year, the number of total cells (cellsPAN<sub>total</sub>) is obtained by considering the total number of grid-points within the region (cellsPAN<sub>region</sub>) and the hypothetical total number of days that could experience HW conditions (cellsPAN<sub>time</sub>):

$$cellsPAN_{total} = cellsPAN_{region} \times cellsPAN_{time}. \quad (2)$$

In our particular case, the cellsPAN<sub>time</sub> corresponds to the total number of days of the fire season in the Pantanal (July to October [3]). For instance, for a particular year, a percentage of 100% indicates that all the Pantanal experienced HW conditions during all the fire season days.

### 2.2.3. Drought conditions

Drought conditions were assessed by analyzing soil moisture anomaly composites and monthly standardized precipitation index (SPI) values [40] from 1980 to 2020, using a 6 month accumulation timescale (SPI-6) and precipitation from ERA5 reanalysis as input data. SPI is widely used to characterize drought conditions using a purely meteorological perspective: it indicates the number of standard deviations by which the observed precipitation anomaly deviates from the long-term mean in a particular location. To better assess the long-term tendencies (quantified by applying a 1st-degree polynomial regression) and interannual variability, we further analyze the temporal evolution of key average meteorological parameters over the fire seasons between 1980 and 2020.

### 2.2.4. Relating fires with the heatwave/drought conditions

We first identified the temporal evolution of each hazard (fire, HW and drought) at the daily scale for the entire Pantanal allowing the identification of concurrent behaviour, i.e. co-occurrence of two or even three of these hazards. Since the Brazilian Pantanal is quite large, we also analyzed the co-occurrence of the multiple hazards for each one of the nine hydrological subregions. During the fire season, we calculated, at the subregional level, the percentage of the BA during the identified hot periods (HPs), defined here as consecutive HWs separated by days with a short heat-stress relief and under drought conditions.

## 3. Results

### 3.1. The 2020 fire season in perspective

The P20Fs show an increase in BA for almost all subregions ranging from ~60% to 1190% of the historical mean value (figure 1(b)). Higher ratios are found in the northern subregions, namely São Lourenço (II) and Cuiabá (IV), which burned ~65% and 55% of their area in 2020 (table S1 available online at [stacks.iop.org/ERL/17/015005/mmedia](https://stacks.iop.org/ERL/17/015005/mmedia)), respectively. These values were absolute outliers within the historical series (figure 1(c)), as so far these subregions had burned a yearly average of ~5.1% and 5.8% (table S1), respectively. In the P20Fs only one subregion burned less than its annual average over the 2001–2019 period: Negro de Mato Grosso do Sul (VIII); which, along with Miranda (III) and Baixo Paraguai (V), obtained the lowest ratios to historical mean values (figure 1(b)). Historically, the northern regions are characterized by lower return periods, whereas the southern regions burn more regularly (figure 1(c)). However, this historical tendency was reversed in 2020, when most of the BA was in forested areas of northern Pantanal. Conversely, southern and south-eastern subregions, characterized by large extents of pasture and grasslands (figure 1(a)), burned considerably in 2020 but did not reach record levels. Nevertheless, with the exception of Negro de Mato Grosso do Sul (VIII), the BA from the P20Fs went above P75 of the historical time series for all southern subregions (table S1).

Most subregions in the Pantanal burn within a 4 month period from July to October (figure S1) and, in this regard, 2020 kept as expected: a steady BA increase from July to September is seen in Pantanal, with a peak on 12 September (116 605 ha) and a secondary observed on 27 September (95 478 ha; figure S1). Médio Paraguai (VII) and Taquari (IX) showed the earliest signs of burning in July, while the remaining subregions burned over August to October, and solely Baixo Paraguai (V) and Médio Paraguai (VII) showed considerable BA in the earlier weeks of November. The latter subregion burned consistently over a period of 5 months, severely contrasting with its historical series where BAs mainly occur in September and October. It is also worth noting how Médio Paraguai (VII) burned very little in previous years (2016–2018; figure 1(c)).

Around a third of the BAs in the P20Fs had been undisturbed since 2001, and another 31% burned only once or twice over the entire study period (table S1). Of the entire P20Fs, 64% of BAs were areas not accustomed to regular and systematic burning. Noteworthy are the cases of Cuiabá (IV) and Médio Paraguai (VII) with ~18% and 19%, respectively, of areas that had not or barely burned within the last 19 years.

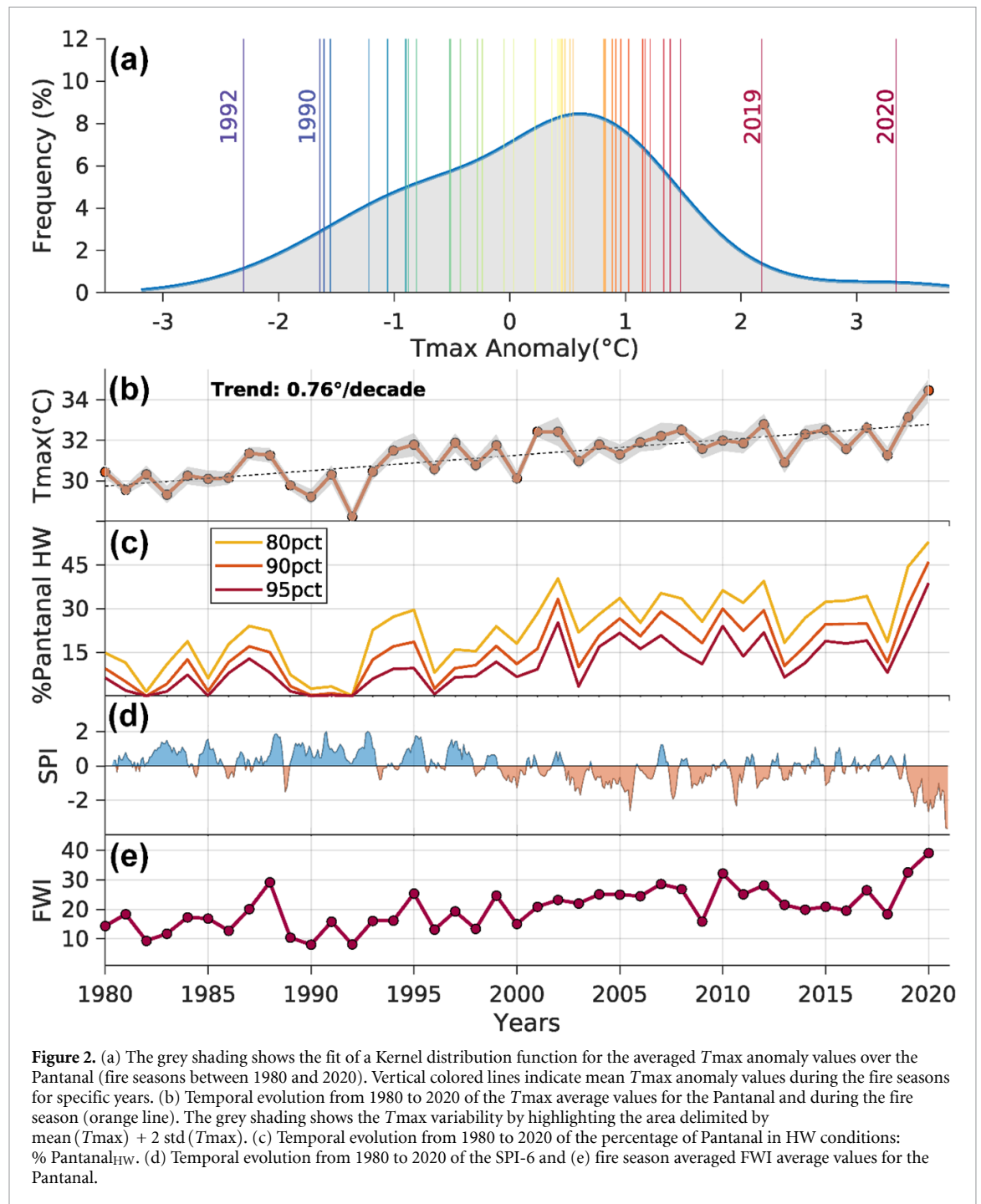


**Figure 2.** (a) The grey shading shows the fit of a Kernel distribution function for the averaged  $T_{max}$  anomaly values over the Pantanal (fire seasons between 1980 and 2020). Vertical colored lines indicate mean  $T_{max}$  anomaly values during the fire seasons for specific years. (b) Temporal evolution from 1980 to 2020 of the  $T_{max}$  average values for the Pantanal and during the fire season (orange line). The grey shading shows the  $T_{max}$  variability by highlighting the area delimited by mean ( $T_{max}$ ) + 2 std ( $T_{max}$ ). (c) Temporal evolution from 1980 to 2020 of the percentage of Pantanal in HW conditions: %Pantanal<sub>HW</sub>. (d) Temporal evolution from 1980 to 2020 of the SPI-6 and (e) fire season averaged FWI average values for the Pantanal.

### 3.2. Compound drought and heatwaves

Results show unprecedented extreme heat conditions, with  $T_{max}$  anomalies for the last two fire seasons over the Pantanal (2019 and 2020) positioned in the high-end tail of the empirical distribution of average  $T_{max}$  anomalies (figure 2(a)). By contrast, the years 1992, 1990, 1984 are in the low-end tail, as in general, the years within the first half of the analysis period. The time series of  $T_{max}$  (figure 2(b)) is characterized by a pronounced and statistically significant positive trend of  $0.76^{\circ}\text{C}$  per decade, responsible for warming throughout the last four decades of  $\sim 3^{\circ}\text{C}$ . Accordingly, the spatially averaged  $T_{max}$  level during the P20F season was  $34^{\circ}\text{C}$ , roughly  $4^{\circ}\text{C}$  higher

than the average for the first decade in the 1980s. The percentage of the Pantanal under HW conditions (figure 2(c)) followed, closely, the  $T_{max}$  evolution (figure 2(b)). Because of this sharp warming trend, the spatial and temporal signature of HWs had marked increase, with unprecedented extreme heat conditions in 2020 as well. Analyzing the monthly SPI-6 values from 1980 and 2020 (figure 2(d)), one concludes that during the 21st century most of the fire seasons were preceded by the occurrence of precipitation deficits. As previously described, this period also marks a sharp increase in the Pantanal under HW conditions (figure 2(b)), indicating that after the turn of the century the CDHW conditions became more

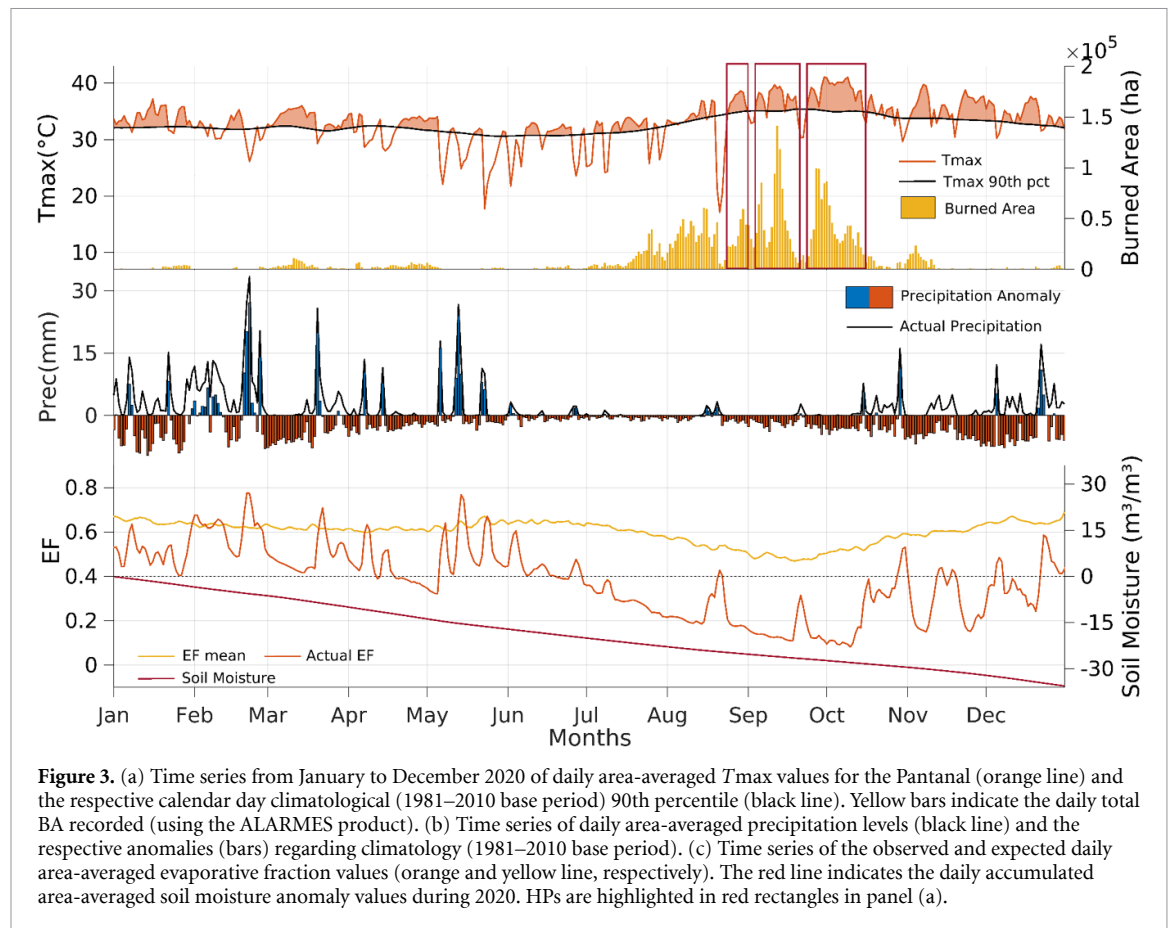


**Figure 3.** (a) Time series from January to December 2020 of daily area-averaged  $T_{\max}$  values for the Pantanal (orange line) and the respective calendar day climatological (1981–2010 base period) 90th percentile (black line). Yellow bars indicate the daily total BA recorded (using the ALARMES product). (b) Time series of daily area-averaged precipitation levels (black line) and the respective anomalies (bars) regarding climatology (1981–2010 base period). (c) Time series of the observed and expected daily area-averaged evaporative fraction values (orange and yellow line, respectively). The red line indicates the daily accumulated area-averaged soil moisture anomaly values during 2020. HPs are highlighted in red rectangles in panel (a).

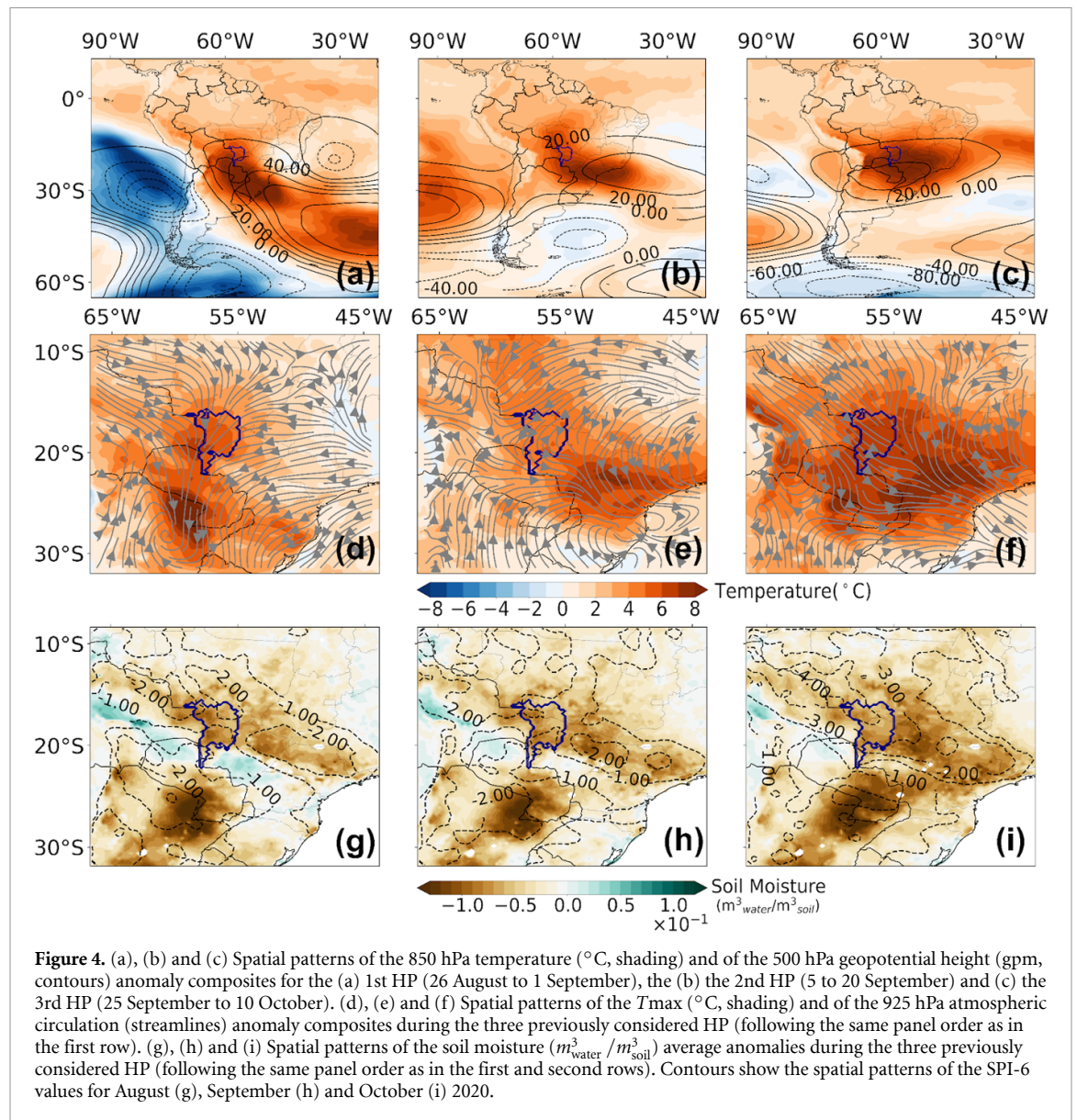
frequent, in particular for 2020. Accordingly, 2020 was also marked by record fire danger (figure 2(e)): fire season averaged FWI reached values above 30 for the second year in a row. Previously, 2010 held the highest value, consistent with widespread drought conditions in neighboring biomes [41, 42]. Higher fire danger values over the last two decades strongly contrast with those of the 20th century, with a significant positive trend over the last 40 years.

In general, 2020 was marked by the occurrence of numerous HW episodes over the Pantanal when the daily area-averaged  $T_{\max}$  values were considerably above the expected levels for several periods of three or more consecutive days (figures 3(a) and S2). Thus, several HPs were also observed, particularly during the fire season. The first HP occurred from 26 August to 1 September, the second from 5 to 20 September and the third from 25 September to 15 October (red boxes in figure 3(a)).

Throughout 2020, a temporal match between the occurrence of HPs and increasing values of BA (figures 3(a) and S2) was observed. However, it was during the austral winter and the three considered HPs that this temporal correspondence was more pronounced, indicating a close relationship between the induced atmospheric heat-stress conditions and the occurrence of fires. On average, the  $T_{\max}$  value for the three HPs was  $38.5\text{ }^{\circ}\text{C}$ , representing a staggering temperature anomaly of about  $5.8\text{ }^{\circ}\text{C}$ . In fact, on

1 October (the 6th day of the third HP) the mean  $T_{\max}$  value reached  $41\text{ }^{\circ}\text{C}$ , establishing a new record-breaking level for the region. A very similar value was observed nine days later on 10 October, defining this as a period of outstanding extreme heat stress conditions. During this HP of 21 d, the  $T_{\max}$  values were on average  $6.5\text{ }^{\circ}\text{C}$  higher than the expected mean levels and a total of 983 900 ha burned, a value that accounts for 25% of the total BA recorded during 2020 in Pantanal. The BA recorded over the entire Pantanal during these three massive HPs accounted for 55% (60%) of the total 2020 (fire season) BA. In all subregions, with the exception of Baixo Paraguai, the BA observed during the three HPs accounted for more than 50% of the amount from the fire season. Moreover, in six of the nine subregions, this BA amount corresponds to more than two-thirds of the fire season, reaching 95% in Miranda (figure S2).

The months preceding the 2020 fire season were marked by large deficits in precipitation (figure 2(d)), within the drought period. During the P20F season, precipitation levels were lower than expected, reaching zero or near-zero values for most of the days (figure 3(b)). Thus, the drought pattern and soil desiccation that initiated during the first months due to a drier wet season substantially amplified throughout the following months, leading to extreme negative anomalies of accumulated soil moisture (figure 3(c)). These precipitation deficits



combined with clear sky conditions that were linked to large amounts of incoming shortwave radiative energy at the surface and enhanced diabatic processes (figure 3(a)), induced large evaporation rates from the surface to satisfy the high atmospheric demand for water. This combined process was crucial for the establishment of the pronounced soil moisture deficits and evaporative stress observed during the P20F season.

Concurring warm and dry conditions controlled the partitioning of water and energy fluxes at the surface. The evaporative fraction observed during 2020 followed very closely the precipitation and temperature regimes (figures 3(c) and S2). Several periods marked by a sharp decrease in the evaporative fraction values were clearly paired with dry episodes combined with extremely hot conditions. Thus, negative anomalies of the evaporative fraction were a constant presence during 2020 (figures 3(c) and S2). However, it was during the fire season that the values reached

their minima indicating the presence of a strong soil moisture-temperature coupling regime (water-limited) in which disproportional surface losses in the incoming shortwave radiation through upward sensible heat flux allowed a re-amplification of the near-surface (air) temperatures. The atmospheric cooling through latent heat flux was then suppressed as well as the capacity of the surface to mitigate the low atmospheric humidity levels.

Finally, we evaluate the synoptic conditions that triggered the development of such CDHW events (figure 4). The spatial pattern of the 500 hPa geopotential height anomaly field indicates the presence of concentric positive anomalies during the second and third HPs over the Pantanal (figures 4 (b) and (c)). During the first HP, positive anomalies were also observed. However, they resulted from a north-west extension of the high-pressure system located over the South Atlantic Ocean (figure 4(a)). Exceptional low-tropospheric heating was also recorded

as it can be observed by analyzing the 850 hPa temperature anomaly field. These conditions represent an enhanced anomalous anticyclonic circulation pattern over the Pantanal. This continental high-pressure anomaly was widespread and responsible for the air subsidence, causing pronounced adiabatic heating at the surface, through air compression, as well as the persistent clear sky conditions that promoted enhanced diabatic heating at surface (figure S3), low levels of humidity and the absence of precipitation episodes. Therefore, the ideal synoptic conditions for strong atmospheric heating and large evaporation rates were present throughout the P20F season, in particular during the third HP, when the  $T_{\max}$  values were, on average, 6 °C above the expected levels (figure 4(f)). Changes in the low tropospheric wind configuration were also observed, showing the signature, close to the surface, of this anticyclonic circulation pattern. During the two first HPs, it can be observed that the wind pattern presented a higher-than-normal northeast-southwest orientation (figures 4(d) and (e)). This anomalous wind pattern was marked by a confluence throughout a north-south oriented asymptote towards south Paraguay (during the first HP), and throughout a northwest-southeast oriented asymptote towards southeastern Brazil (during the second HP). In fact, by analyzing the mean of the observed wind configuration recorded during these two periods (figures S3(a) and (b)) one may conclude that air masses predominantly from the northeastern regions moved towards the Pantanal. During the third HP the 925 hPa wind pattern was substantially different (figures 4(f) and S3), showing an anomalous northwest-southeast orientation over the Pantanal. Nevertheless, a pronounced confluence similar to the one observed during the second HP was present. In fact, the asymptotes marking these regions of strong confluence were, for all the analyzed HP's, oriented towards the regions where the anomalies of  $T_{\max}$  were higher. This could indicate that the intense daytime heating in the low troposphere over these regions caused the lifting of air, imposing pronounced changes in the normal near-surface wind configuration.

Therefore, during three HPs, the ideal synoptic conditions, triggering high rates of potential evaporation from the occurrence of clear sky conditions linked to atmospheric subsidence (figure S3), were observed over central SA, particularly in the Pantanal. However, due to the desiccated soil already observed at the time (figure 3(b)), the surface could not meet such atmospheric water demand. This led to low rates of actual evaporation and, consequently, to pronounced evaporative stress in the region (figure 3(c)) when extreme low levels of evaporative fraction were observed during these periods. The spatial pattern of the SPI-6 values, computed from the months when these HPs occurred, confirms severe meteorological

drought conditions (figures 4(g)–(i)). An approximately northwest-southeast oriented broad region extending from northern Bolivia to southeastern Brazil, with Pantanal in its center, endured pronounced negative SPI-6 levels from August to October (ranging from  $-1$  to  $-4$ ). The soil moisture deficits during the three HPs (figures 4(g)–(i)) confirm this situation and are spatially consistent with the analysis of figure S2 by showing the high potential of soil desiccation in inducing low levels of evaporative fraction. A similar situation was also observed southwards, particularly over southern Paraguay and over northern Argentina. It is noteworthy the spatial match between the regions with strong positive  $T_{\max}$  anomalies and areas with negative soil moisture anomalies, emphasizing CDHW conditions, unequivocally associated with the land-atmosphere feedbacks over these SA regions and particularly over all subregions of the Pantanal (figure S2).

#### 4. Discussion and conclusion

Previous studies for several regions in the globe, markedly Europe, the Mediterranean, the USA and Australia, highlighted the key role played by land-atmosphere feedbacks in the amplification of fire episodes [43–46]. However, to the best of our knowledge, the inter-links played by CDHW and fires in Brazil remained practically unknown, particularly in wetlands. Here, we provide evidence that the unprecedented P20Fs were favored by the joint effect of the observed drought and hot conditions. In fact, most of the P20Fs occurred simultaneously to CDHW episodes, which have fuelled fires through two distinct mechanisms, in a cascading effect. First, long-term precipitation deficits and large evaporation rates were essential to dry out the soil and vegetation and to reduce the flood pulse, providing unusual amounts of fuel to fires. In parallel, soil desiccation also played a key role in boosting the concurrence of extremely hot conditions through the establishment of a water-limited regime and an increase in the sensible heat flux between the surface and the atmosphere, increasing flammability thresholds.

High-pressure systems are known to favor CDHW conditions [47], particularly in the Pantanal [18] and also over surrounding regions such as Southeast Brazil [27]. These high-pressure (anticyclonic) anomalies are linked to large-scale teleconnections induced by perturbations of inter-tropical oceanic modes such as the Madden-Julian oscillation [45] and the El Niño-Southern oscillation [48]. In the analyzed CDHW events, positive anomalies of the 500 hPa geopotential heights associated with higher surface pressure over Central SA contributed to pronounced diabatic heating rates at the surface and strong atmospheric subsidence, allowing the escalation of temperatures and leveraging high evaporation rates until the soil dry out.

The occurrence of concurrent hazards (CDHW-fires) is widespread over Pantanal, showing however a great spatial variability in the amount of area affected by fire in each subregion. The P20F occurred mainly in forested zones (in the north) and areas that experienced no flooding and, consequently, had a huge amount of biomass as fuel, mainly as histosols [3], while the fires during the 2001–2019 fire seasons tended to occur in savanna environments (mainly in the south). This fact reinforces the relative contribution of climate and fuel as drivers of fire activity [43, 49]. Accordingly, in regions where fuel was not a limiting factor, fire activity tended to be more vulnerable to CDHW, increasing flammability and the probability of high fire spread.

Previous studies have shown that differences in hydrology modulate nexus between large-scale climatic or geomorphic drivers and vegetation (fuel availability) in the Pantanal [50]. Therefore, it is fundamental to consider the hydrological variability to understand fire dynamics, through the influence of the seasonal north-to-south flood-pulse wave of the Paraguay River, as noted before for Amazonia floodplains [51]. In general, summer rainfall in surrounding areas of the Pantanal results in a slow-moving flood pulse from north to south. Due to complex processes of water retention and flow through floodplain, inundation of the central and southern Pantanal may occur several months after the rainfall peaks [48]. Under these circumstances, areas in the northern Pantanal and areas away from floodplains, vegetation biomass respond synchronically to rainfall [50]. Moreover, as we showed here these areas have spatial matches between strong positive  $T_{max}$  and negative soil moisture anomalies, particularly in some hydrological regions in the north. On the other hand, in flooded areas, rainfall and vegetation productivity are not clearly correlated [50]. This dynamic suggests that land-atmosphere physical mechanisms responsible for triggering the amplification of fires as we showed here seem to operate more strongly in the years without large floods, as in 2019 and 2020. It is likely that these mechanisms do not have the same importance and synchronicity across the different regions of the Pantanal, nor during years of large floods.

Climate change scenarios from state-of-the-art models, project significant warming in the Pantanal, and although changes in the precipitation pattern are less clear cut than those expected for temperature [52, 53], projected changes in SA monsoon have shown a reduction in the length of the rainy season by the end of the century [54]. Indeed, our results highlight that the current trend in the Pantanal temperature since 1980 is approximately four times greater than the average global warming [8]. The fact that CDHW events are expected to become more frequent and intense worldwide under future climate scenarios [55] may reinforce the occurrence of large fires as also

shown for other regions [20, 41, 43, 44, 56, 57]. We are confident that our findings are relevant for other regions of the world, as some of the driving physical mechanisms described here, namely those responsible for the CDHWs, also apply across other ecosystems, implying higher flammability conditions and further efforts for monitoring and predicting such events.

It is worth mentioning that fire is also influenced by drivers beyond those directly associated with weather conditions, namely fuel availability and socio-economic factors. As stated by previous authors [2, 4, 58], the P20F outbreak is not attributable to just a single factor, but rather results from a complex interplay among several contributing factors, including weather conditions, availability of fuel (vegetation), and human ignition sources (both accidental and intended) [2]. A recent study showed that human-caused fires exacerbated drought effects on natural ecosystem during the P20F season, with more BAs primarily over natural areas [59].

Accordingly, any strategy to mitigate the effects of wildfires in the Pantanal needs to consider a combination of these factors and the different characteristics of each one. Accordingly, integrative fire strategies should require adaptive and social transformative perspectives [4, 60]. Thus, our results may improve the assessment of potential high-impact hazards, like the P20F, helping stakeholders to act upon these complex events.

### Data availability statement

The data that support the findings of this study are available upon reasonable request from the authors.

### Acknowledgments

This work was developed under the scope of Project Andura (CNPq Grant No. 441971/2018–0) and partially funded by Project Rede Pantanal from the Ministry of Science, Technology and Innovations of Brazil (FINEP Grant No. 01.20.0201.00). R L was supported by CNPq (Grant No. 305159/2018–6) and FAPERJ (Grant No. E26/202.714/2019); J L G and P S S were supported by FCT (Grant Nos. 2020.05198.BD and SFRH/BD/146646/2019); A R and R T were supported by FCT (IMPECAF, PTDC CTA-CLI28902 2017); J N was supported by the ‘Women in Research’-fellowship program, Westfälische Wilhelms-Universität Münster (WWU Münster); J A R was supported by CNPq (Grant No. 380779/2019–6); L B C B was supported by FAPERJ (Grant No. E-26/202.118/2020); F O R was supported by CNPq (Grant No. 302755/2018–7); J A M was supported by CNPq (Grant No. 465501/2014–1), FAPESP (Grant Nos. 2014/50848–9 and 2017/09659–6) and CAPES (Grant No. 88887.136402/2017–00). FCT supports IDL (Project No. UIDB/50019/2020).



We thank Ivan Bergier for his helpful suggestions about the hydrological dynamics of the Pantanal in an earlier version of the manuscript.

## ORCID iDs

Renata Libonati  <https://orcid.org/0000-0001-7570-1993>

João L Geirinhas  <https://orcid.org/0000-0002-2110-4891>

Patrícia S Silva  <https://orcid.org/0000-0003-0410-2971>

Ana Russo  <https://orcid.org/0000-0003-0042-2441>

Julia A Rodrigues  <https://orcid.org/0000-0003-0525-9516>

Liz B C Belém  <https://orcid.org/0000-0002-0319-1784>

Fabio O Roque  <https://orcid.org/0000-0001-5635-0622>

Carlos C DaCamara  <https://orcid.org/0000-0003-1699-9886>

Ana M B Nunes  <https://orcid.org/0000-0002-1877-2688>

Ricardo M Trigo  <https://orcid.org/0000-0002-4183-9852>

## References

- Junk W J, Nunes Da Cunha C, Da Silva C J and Wantzen K M 2011 The Pantanal: a large South American wetland and its position in limnological theory *The Pantanal: Ecology, Biodiversity and Sustainable Management of a Large Neotropical Seasonal Wetland* (Bulgaria: Pensoft) ed W J Junk, C J Da Silva, C N Da Cunha and K M Wantzen pp 23–44
- Libonati R, DaCamara C C, Peres L F, Sander de Carvalho L A and Garcia L C 2020 Rescue Brazil's burning Pantanal wetlands *Nature* **588** 217–9
- Damasceno-Junior G A et al 2021 Lessons to be learned from the wildfire catastrophe of 2020 in the Pantanal wetland *Wetland Sci. Pract.* **38** 107–15
- Garcia L C et al 2021 Record-breaking wildfires in the world's largest continuous tropical wetland: integrative fire management is urgently needed for both biodiversity and humans *J. Environ. Manage.* **293** 112870
- Tomas W M, Berlink C N, Chiaravalloti R M, Faggioni G P, Strussmann C, Libonati R and Morato R 2021 Counting the dead: 17 million vertebrates directly killed by the 2020's wildfires in the Pantanal wetland, Brazil *Sci. Rep.* **11** 23547
- Podlaha A, Lörinc M, Srivastava G, Bowen S and Kerschner B 2020 *Weather, Climate & Catastrophe Insight 2020 Annual Report* AON 78
- Marengo J A et al 2021 Extreme drought in the Brazilian Pantanal in 2019–2020: characterization, causes, and impacts *Front. Water* **3** 13
- NASA's Jet Propulsion Laboratory 2021 Global temperature | vital signs—climate change: vital signs of the planet (available at: <https://climate.nasa.gov/vital-signs/global-temperature/>) (Accessed 5 August 2021)
- King A D, Pitman A J, Henley B J, Ukkola A M and Brown J R 2020 The role of climate variability in Australian drought *Nat. Clim. Change* **10** 177–9
- Boer M M, Resco de Dios V and Bradstock R A 2020 Unprecedented burn area of Australian mega forest fires *Nat. Clim. Change* **10** 171–2
- Collins L, Bradstock R A, Clarke H, Clarke M F, Nolan R H and Penman T D 2021 The 2019/2020 mega-fires exposed Australian ecosystems to an unprecedented extent of high-severity fire *Environ. Res. Lett.* **16** 044029
- Higuera P E and Abatzoglou J T 2021 Record-setting climate enabled the extraordinary 2020 fire season in the western United States *Glob. Change Biol.* **27** 1–2
- Mishra A, Bruno E and Zilberman D 2021 Compound natural and human disasters: managing drought and COVID-19 to sustain global agriculture and food sectors *Sci. Total Environ.* **754** 142210
- Thielen D, Ramoni-Perazzi P, Puche M L, Márquez M, Quintero J I, Rojas W and Libonati R 2021 The Pantanal under siege—on the origin, dynamics and forecast of the megadrought severely affecting the largest wetland in the world *Water* **13** 3034
- Rivera J A, Otta S, Lauro C and Zazulie N 2021 A decade of hydrological drought in central-Western Argentina *Front. Water* **28** 3
- Marengo J A, Espinoza J C, Alves L M, Ronchail J, Lavado-Casimiro W, Ramos A M, Molina-Carpio J, Correa K, Baez J and Salinas R 2020 Central South America. Regional climates, central South America *Bull. Am. Meteorol. Soc.* **101** S321–420
- Thielen D, Schuchmann K-L, Ramoni-Perazzi P, Marques M, Rojas W, Quintero J I and Marques M I 2020 Quo vadis Pantanal? Expected precipitation extremes and drought dynamics from changing sea surface temperature *PLoS One* **15** e0227437
- Marengo J A et al 2021 The heat wave of October 2020 in central South America *Int. J. Clim.* **1**–18
- WMO 2021 State of the climate in latin America and the caribbean 2020 (Geneve) 37 (available at: [https://library.wmo.int/index.php?lvl=notice\\_display%26id=21926#.YXAvuRrMI2x](https://library.wmo.int/index.php?lvl=notice_display%26id=21926#.YXAvuRrMI2x)) (Accessed 5 November 2021)
- Sutanto S J, Vitolo C, Di Napoli C, D'Andrea M and Van Lanen H A J 2020 Heatwaves, droughts, and fires: exploring compound and cascading dry hazards at the pan-European scale *Environ. Int.* **134** 105276
- Dirmeyer P A, Balsamo G, Blyth E M, Morrison R and Cooper H M 2021 Land-atmosphere interactions exacerbated the drought and heatwave over Northern Europe during summer 2018 *AGU Adv.* **2** e2020AV000283
- Sousa P M, Barriopedro D, García-Herrera R, Ordóñez C, Soares P M M and Trigo R M 2020 Distinct influences of large-scale circulation and regional feedbacks in two exceptional 2019 European heatwaves *Commun. Earth Environ.* **1** 1–13
- Miralles D G et al 2012 Soil moisture-temperature coupling: a multiscale observational analysis *Geophys. Res. Lett.* **39** 21
- Miralles D G et al 2014 Mega-heatwave temperatures due to combined soil desiccation and atmospheric heat accumulation *Nat. Geosci.* **7** 345–9
- Schumacher D L et al 2019 Amplification of mega-heatwaves through heat torrents fuelled by upwind drought *Nat. Geosci.* **12** 712–7
- Mukherjee S and Mishra A K 2021 Increase in compound drought and heatwaves in a warming world *Geophys. Res. Lett.* **48** 1
- Geirinhas J L, Russo A, Libonati R, Sousa P M, Miralles D G and Trigo R M 2021 Recent increasing frequency of compound summer drought and heatwaves in Southeast Brazil *Environ. Res. Lett.* **16** 034036
- Giglio L, Boschetti L, Roy D P, Humber M L and Justice C O 2018 The collection 6 MODIS burned area mapping algorithm and product *Remote Sens. Environ.* **217** 72–85
- Pinto M M, Libonati R, Trigo R M, Trigo I F and DaCamara C C 2020 A deep learning approach for mapping and dating burned areas using temporal sequences of satellite images *ISPRS J. Photogramm. Remote Sens.* **160** 260–74
- Avila-Diaz A, Benezoli V, Justino F, Torres R and Wilson A 2020 Assessing current and future trends of climate extremes

- across Brazil based on reanalyses and earth system model projections *Clim. Dyn.* **55** 1403–26
- [31] Martens B, Miralles D G, Lievens H, Van Der Schalie R, De Jeu R A M, Fernández-Prieto D, Beck H E, Dorigo W A and Verhoest N E C 2017 GLEAM v3: satellite-based land evaporation and root-zone soil moisture *Geosci. Model Dev.* **10** 1903–25
- [32] Miralles D G, Holmes T R H, De Jeu R A M, Gash J H, Meesters A G C A and Dolman A J 2011 Global land-surface evaporation estimated from satellite-based observations *Hydrol. Earth Syst. Sci.* **15** 453–69
- [33] Van Wagner C E 1987 *Development and Structure of the Canadian Forest Fire Weather Index System* (Ottawa: Canadian Forestry Service)
- [34] Rodrigues M, Peña-Angulo D, Russo A, Zúñiga-Antón M and Cardil A 2021 Do climate teleconnections modulate wildfire-prone conditions over the Iberian peninsula? *Environ. Res. Lett.* **16** 044050
- [35] Vitolo C, Di Giuseppe F, Barnard C, Coughlan R, San-Miguel-Ayaz J, Libertá G and Krzeminski B 2020 ERA5-based global meteorological wildfire danger maps *Scientific Data* **7** 216
- [36] Hersbach H et al 2020 The ERA5 global reanalysis *Q. J. R. Meteorol. Soc.* **146** 1999–2049
- [37] Di G F et al 2016 The potential predictability of fire danger provided by numerical weather prediction *J. Appl. Meteorol. Climatol.* **55** 2469–91
- [38] Agência Nacional das Águas Bacias Hidrográficas (available at: [www.gov.br/ana/pt-br](http://www.gov.br/ana/pt-br)) (Accessed 28 July 2021)
- [39] Mazdiyasi O and AghaKouchak A 2015 Substantial increase in concurrent droughts and heatwaves in the United States *Proc. Natl Acad. Sci.* **112** 11484–9
- [40] Svoboda M, Svoboda M, Hayes M and Wood D A 2012 *Standardized Precipitation Index User Guide* ISBN 978-92-63-11091-6 (Geneva: WMO)
- [41] Ribeiro I O, Andreoli R V, Kayano M T, Sousa T R, Medeiros A S, Godoi R H M, Godoi A F L, Duvoisin S, Martin S T and Souza R A F 2018 Biomass burning and carbon monoxide patterns in Brazil during the extreme drought years of 2005, 2010, and 2015 *Environ. Pollut.* **243** 1008–14
- [42] Panisset J S, Libonati R, Gouveia C M P, Machado-Silva F, França D A, França J R A and Peres L F 2018 Contrasting patterns of the extreme drought episodes of 2005, 2010 and 2015 in the Amazon basin *Int. J. Climatol.* **38** 1096–104
- [43] Gouveia C M, Bistinas I, Liberato M L R, Bastos A, Koutsias N and Trigo R 2016 The outstanding synergy between drought, heatwaves and fuel on the 2007 Southern Greece exceptional fire season *Agric. For. Meteorol.* **218–219** 135–45
- [44] Ruffault J et al 2020 Increased likelihood of heat-induced large wildfires in the Mediterranean basin *Sci. Rep.* **10** 13790
- [45] Jyoteeshkumar Reddy P et al 2021 Modulating influence of drought on the synergy between heatwaves and dead fine fuel moisture content of bushfire fuels in the Southeast Australian region *Weather Clim. Extrem.* **31** 100300
- [46] Schiermeier Q 2021 Climate change made North America's deadly heatwave 150 times more likely *Nature* (<https://doi.org/10.1038/D41586-021-01869-0>)
- [47] Pendergrass A G et al 2020 Flash droughts present a new challenge for subseasonal-to-seasonal prediction *Nat. Clim. Change* **10** 191–9
- [48] Cai W et al 2020 Climate impacts of the El Niño–Southern Oscillation on South America *Nat. Rev. Earth Environ.* **1** 215–31
- [49] Pausas J G and Ribeiro E 2013 The global fire–productivity relationship *Glob. Ecol. Biogeogr.* **22** 728–36
- [50] Ivory S J, McGlue M M, Spera S, Silva A and Bergier I 2019 Vegetation, rainfall, and pulsing hydrology in the Pantanal, the world's largest tropical wetland *Environ. Res. Lett.* **14** 124017
- [51] Schöngart J, Wittmann F, Junk W J and Piedade M T F 2017 Vulnerability of Amazonian floodplains to wildfires differs according to their typologies impeding generalizations *Proc. Natl Acad. Sci.* **114** E8550–8551
- [52] Llopart M, Simões Reboita M and Porfírio Da Rocha R 2019 Assessment of multi-model climate projections of water resources over South America CORDEX domain *Clim. Dyn.* **54** 99–116
- [53] Marengo J A, Alves L M and Torres R R 2016 Regional climate change scenarios in the Brazilian Pantanal watershed *Clim. Res.* **68** 201–13
- [54] Gomes G D, Nunes A M B, Libonati R and Ambrizzi T 2021 Projections of subcontinental changes in seasonal precipitation over the two major river basins in South America under an extreme climate scenario *Clim. Dyn.* **1–23**
- [55] Zscheischler J et al 2018 Future climate risk from compound events *Nat. Clim. Change* **8** 469–77
- [56] Turco M, Marcos-Matamoros R, Castro X, Canyameras E and Llasat M C 2019 Seasonal prediction of climate-driven fire risk for decision-making and operational applications in a Mediterranean region *Sci. Total Environ.* **676** 577–83
- [57] Xi Y, Peng S, Ciais P and Chen Y 2020 Future impacts of climate change on inland Ramsar wetlands *Nat. Clim. Change* **11** 45–51
- [58] Leal Filho W, Azeiteiro U M, Salvia A L, Fritzen B and Libonati R 2021 Fire in paradise: why the Pantanal is burning *Environ. Sci. Policy* **123** 31–34
- [59] Kumar S, Getirana A, Libonati R, Hain C, Mahanama S and Andela N 2022 Changes in land use enhance the sensitivity of tropical ecosystems to fire-climate extremes *Sci. Rep.* accepted
- [60] McWethy D B et al 2019 Rethinking resilience to wildfire *Nat. Sustain.* **2** 797–804
- [61] MapBiomass Project 2020 Collection 5 of Brazilian land cover & use map series [WWW document] (available at: <https://mapbiomas.org/>) (Accessed 8 July 2021)
- [62] Souza C M et al 2020 Reconstructing three decades of land use and land cover changes in Brazilian biomes with Landsat archive and Earth Engine *Remote Sens.* **12** 2735